Stony Brook University

Part I. Design, synthesis and biological evaluation of novel 2,5,6-trisubstituted benzimidazoles targeting FtsZ as antitubercular agents

Part II. Development of novel taxoid-based drug conjugates and theranostic imaging agents towards tumor-targeted chemotherapy

A Dissertation Presented

by

Bora Park

to

The Graduate School

in Partial Fulfillment of the

Requirements

for the Degree of

Doctor of Philosophy

in

Chemistry

Stony Brook University

December 2014

Stony Brook University

The Graduate School

Bora Park

We, the dissertation committee for the above candidate for the

Doctor of Philosophy degree, hereby recommend

acceptance of this dissertation.

Iwao Ojima
Dissertation Advisor
Distinguished Professor, Department of Chemistry

Frank W. Fowler
Chairperson of Defense
Professor, Department of Chemistry

Peter J. Tonge
Third Member
Professor, Department of Chemistry

James B. Bliska
Outside Member
Professor, Department of Molecular Pharmacology

This dissertation is accepted by the Graduate School

Charles Taber
Dean of the Graduate School

Abstract of the Dissertation

Part I. Design, synthesis and biological evaluation of novel 2,5,6-trisubstituted benzimidazoles targeting FtsZ as antitubercular agents

Part II. Development of novel taxoid-based drug conjugates and theranostic imaging agents towards tumor-targeted chemotherapy

by

Bora Park

Doctor of Philosophy

in

Chemistry

Stony Brook University

2014

Part I. Design, synthesis and biological evaluation of novel 2,5,6-trisubstituted benzimidazoles targeting FtsZ as antitubercular agents

Filamenting temperature-sensitive protein Z (FtsZ), an essential cell division protein, is a promising target for the drug discovery of new-generation antibacterial agents against various bacterial pathogens. As a part of SAR studies on benzimidazoles, we have synthesized a library of 376 novel 2,5,6-trisubstituted benzimidazoles, bearing ether or thioether linkage at the 6-position. In a preliminary HTP screening against *Mtb* H37Rv, 108 compounds were identified as hits at a cut off values of 5 μg/mL. Among those hits, 10 compounds exhibited MIC values in the range of 0.63-12.5 μg/mL. Light scattering assay and TEM analysis with the most potent compound clearly indicate that its molecular target is *Mtb* FtsZ. In addition, we have identified number of hits against *M. Smeg.* Further optimization of the lead compound is currently on going in our lab based on rational drug design.

Part II. Development of novel taxoid-based drug conjugates and theranostic imaging agents towards tumor-targeted chemotherapy

The second part of my dissertation pertains to development of new generation of taxoids and taxoid-based imaging probes for tumor-targeted drug delivery. The folate-linker-taxoid (FLT) conjugate which contains spacers to promote aqueous solubility and promote tumor-specific uptake and a mechanism-based self-immolative disulfide linker for site-specific prodrug activation was designed and synthesized. The conjugate was evaluated *in vitro* against a series of FR-positive cancer cell lines, L1210FR, MX-1, and ID8 and FR-negative cell line, WI-38. Folate conjugate demonstrated almost equally high potency against FR-positive cell lines as the parent taxoid, indicating rapid internalization and efficient drug release. However, against FR- normal lung fibroblast cell line WI-38, the folate conjugate was virtually non-toxic (IC50 > 5 μM).

In addition, we have identified a novel class of 3'-vinyliodo taxoids to develop a better understanding of their biodistribution and PK profiles since radioactive isotopes of ^{123}I and ^{124}I can be used for PET and SPECT studies. 3'-Vinyliodo taxoid has been evaluated *in vitro* against various cancer cell lines, ID8, NCI/ADR-RES, HCT-116, MX-1 and MCF-7 with high potency. We also have developed conditions for their synthesis via site-specific iodination amenable to radiolabeling.

Furthermore, we have been exploring synergistic combinations between new-generation taxoids and other drugs, i.e. CMC2.24, EGCG, MMP inhibitors, against various cell lines including cancer stem cells (CSCs). Preliminary screening showed very promising results.

Dedicated to my parents and sisters

Table of Contents

List of Figures……..... xi
List of Tables……...…… xiv
List of Schemes..…….……..... xvi
List of Abbreviations……..… xvii
List of Acknowledgements……..... xxii
Vita, Publications, Selected Presentations, and Honors and Awards.....…… ..xxv

Chapter 1 Design and Synthesis of Novel 2,5,6-Trisubstitued Bezimidazoles

§ 1.1 Introduction 2
§ 1.1.1 Tuberculosis..... 2
§ 1.1.2 Current Treatments of TB..... 4
§ 1.1.3 FtsZ: A Novel TB Drug Target 8
§ 1.1.4 Drug Design..... 9
§ 1.2 Results and discussion 18
§ 1.2.1 Synthesis of 2,5,6-Trisubstituted Benzimidazole Library 18
§ 1.2.2 Preliminary Screening Result 19
§ 1.2.3 Re-synthesis of Hit Compounds for Their Accurate MIC determination 20
§ 1.3 Conclusion 23
§ 1.4 Experimental Section 24
§ 1.4.1 General Methods..... 24
§ 1.4.2 Materials 24
§ 1.4.3 Experimental Procedures 24
§ 1.4.4 Bacterial Strains and Growth..... 40
§ 1.4.5 Antibacterial Activity Determination 41
§ 1.5 References..... 42

Chapter 2 Target Confirmation and Biological Evaluation of Lead Compounds

§ 2.1 Introduction 47

§ 2.2 Results and discussion 49
§ 2.2.1 Inhibition of FtsZ polymerization 49
§ 2.2.2 Transmission Electron Microscopy (TEM) of FtsZ assembly 51
§ 2.2.3 Dissociation Constant 52
§ 2.2.4 Cytotoxicity Assay against Vero Cells 53
§ 2.2.5 Early Metabolism Study on compound 2-1 54
§ 2.3 Conclusion 55
§ 2.4 Experimental Section 56
§ 2.4.1 General Methods 56
§ 2.4.2 Materials 56
§ 2.4.3 Experimental Procedures 56
§ 2.4.4 Protein Purification 62
§ 2.4.5 FtsZ Inhibitory Polymerization Assay 64
§ 2.4.6 TEM Analysis 64
§ 2.4.7 MTT assay for Cytotoxicity 64
§ 2.5 References 66

Chapter 3 Synthesis and Biological Evaluation of New Series of Benzimidazoles

§ 3.1 Introduction 68
§ 3.2 Results and discussion 69
§ 3.2.1 Synthesis of Novel 2,5,6-Trisubstituted Benzimidazole 69
§ 3.2.2 MIC Determination of Selected Compounds 70
§ 3.2.3 Metabolism Results 71
§ 3.3 Conclusion 72
§ 3.4 Experimental Section 73
§ 3.4.1 General Methods 73
§ 3.4.2 Materials 73
§ 3.4.3 Experimental Procedures 73
§ 3.5 References 80

Chapter 4 Biological Evaluation of 2,5,6-TrisubstituedBenzimidazoles against *M. Smeg*

§ 4.1 Introduction 82

§ 4.2 Results and discussion 84

§ 4.2.1 *M. Smeg* Assay 84

§ 4.2.2 Optimizing *M. Smeg* Assay 84

§ 4.2.3 Introducing the automatic system to *M. Smeg* assay 85

§ 4.3 Conclusion 88

§ 4.4 Experimental Section 89

§ 4.4.1 General Methods 89

§ 4.4.2 Materials 89

§ 4.4.3 Experimental Procedures 89

§ 4.4.4 *M. Smegmatis* Assay with Alamar Blue 94

§ 4.4.5 *M. Smegmatis* Assay based on the Clarity 94

§ 4.5 References 96

Chapter 5 Biological Evaluation of Folate-Linker-Taxoid

§ 5.1 Introduction 101

§ 5.1.1 Cancer 101

§ 5.1.2 Chemotherapy 102

§ 5.1.3 Paclitaxel and Taxanes 102

§ 5.1.4 Next Generation Taxoid 103

§ 5.1.5 Folic Acid as Tumor Targeting Drug Conjugate 105

§ 5.1.6 Disulfide Linkers 107

§ 5.2 Results and discussion 111

§ 5.2.1 Biological Evaluation of Folate Linker Taxoid 111

§ 5.3 Conclusion 113

§ 5.4 Experimental Section 114

§ 5.4.1 Caution 114

§ 5.4.2 Materials 114

§ 5.4.3 Cell culture system for MTT assay 114
§ 5.4.4 Single drug MTT assay 115
§ 5.4.5 Data analysis for MTT assay 115
§ 5.5 References 117

Chapter 6 3'-Vinyliodo Taxoids for PET- and SPECT-Based Theranostics

§ 6.1 Introduction 122
§ 6.1.1 Positron Emission Tomograpy 122
§ 6.1.2 Radiolabeling of Taxanes in Clinical Use 123
§ 6.1.3 Radiolabeling with Iodine 124
§ 6.1.4 Biotin as Tumor Targeting Moiety 124
§ 6.1.5 3'-Vinyliodo taxoids for PET- and SPECT-Based Theranostics 125
§ 6.2 Results and discussion 127
§ 6.2.1 Biological Evaluation of 3'-vinyliodo taxoid 127
§ 6.2.2 Cold Labeling of 3'-Vinyliodo taxoid 128
§ 6.3 Conclusion 133
§ 6.4 Experimental Section 134
§ 6.4.1 Caution 134
§ 6.4.2 Materials 134
§ 6.4.3 Cell culture system for MTT assay 134
§ 6.4.4 Single drug MTT assay 135
§ 6.4.5 Data analysis for MTT assay 135

Chapter 7 Combination Chemotherapy

§ 7.1 Introduction 139
§ 7.1.1 Cancer Stem Cells 139
§ 7.1.2 Combination Chemotherapy with SB-T-1214 140
§ 7.1.3 Camptothecin (CPT) 141
§ 7.1.4 CMC2.24 142
§ 7.1.5 Epigallocatechin Gallate (EGCG) 143

§ 7.1.6 MMP inhibitors..... 145
§ 7.2 Results and discussion..... 147
§ 7.2.1 Synthesis of MMP inhibitors..... 147
§ 7.2.2 Biological Evaluation of combination therapy..... 147
§ 7.3 Conclusion..... 151
§ 7.4 Experimental Section..... 152
§ 7.4.1 General Methods..... 152
§ 7.4.2 Materials..... 152
§ 7.4.3 Experimental Procedures..... 152
§ 7.4.4 Cell culture system for MTT assay..... 154
§ 7.4.5 Drug Treatment for MTT assay..... 154
§ 7.4.6 Data analysis for MTT assay..... 155
§ 7.5 References..... 156

References……. **160**

Appendices

Appendix Chapter 1……..... 177

Appendix Chapter 2……..... 246

Appendix Chapter 3……..... 267

Appendix Chapter 4……..... 290

Appendix Chapter 7…...……..... 307

List of Figures

Chapter 1

Figure 1- 1: Tuberculosis in humans (adapted from [5]) 2
Figure 1- 2: Estimated TB incidence rates, 2012 (adapted from [1]) 3
Figure 1- 3: Estimated HIV prevalence in new TB cases, 2012 (adapted from [1]) 4
Figure 1- 4: Treatment algorithm for active, culture-negative pulmonary tuberculosis and inactive tuberculosis (adapted from [3]) 5
Figure 1- 5: First-line treatment of TB for drug-sensitive TB (adapted from [3]) and modified ... 6
Figure 1- 6: Current drugs and their target (adapted from [21]) 7
Figure 1- 7: Self-assembly of FtsZ to form Z-ring (adapted from [27]) 8
Figure 1- 8: Inhibitor of *Mtb* FtsZ 9
Figure 1- 9: Chemical structures of *Mtb* FtsZ inhibitors, taxanes 11
Figure 1- 10: SEM images of *Mtb* cells 10
Figure 1- 11: Further chemical structures of *Mtb* FtsZ inhibitors, taxanes 12
Figure 1- 12: Inhibition of FtsZ polymerization .....
Figure 1- 13: Structures of 2,5,6- and 2,5,7-trisubsituted benzimidazoles 13
Figure 1- 14: Previously reported anti-TB 2,5,6-trisubstituted benzimidazoles 14
Figure 1- 15: Effect of bezimidazoles on FtsZ polymerization .....
Figure 1- 16: SEM images of *Mtb* cells treated with SB-P8B2 16
Figure 1- 17: Novel 2,5,6-trisubstituted benzimidazoles bearing an ether or thioether substituent at the 6-position 17
Figure 1- 18: List of 47 reagents for creation of a library of 376 novel 2,5,6-trisubstituted benzimidazoles 19

Chapter 2

Figure 2- 1 Bacterial cell division (adapted from [4]) 44
Figure 2- 2: Chemical structure of 10 lead compounds and their accurate MIC values 48
Figure 2- 3: Chemical structure of compound 2-1 and 2-4 49
Figure 2- 4: Polymerization assay of (A) compound 2-1 and (B) compound 2-2 50
Figure 2- 5: TEM images of FtsZ 51

Figure 2- 6: Determination of binding parameter of 2-1 with *Mtb* FtsZ 50

Chapter 3

Figure 3- 1: Preliminary SAR studies and optimization of the 6-position 68
Figure 3- 2: Accurate MIC values and their chemical structures 70

Chapter 4

Figure 4- 1: The bacterial division cycle 82
Figure 4- 2: Chemical structures and their MIC values 84
Figure 4- 3: Chemical structure of lead compound and its MIC values 85
Figure 4- 4: Chemical structures of lead compounds and their MIC values 86

Chapter 5

Figure 5- 1: Worldwide cancer statistics (Adapted from [2]) 101
Figure 5- 2: Examples of traditional chemotherapeutics 102
Figure 5- 3: Summary of SAR studies of paclitaxel 103
Figure 5- 4: Chemical structure of folic acid 106
Figure 5- 5: FR-mediated endocytosis (adapted from [22]) 107
Figure 5- 6: Second-generation self- immolative disulfide linkers and their drug-release mechanism (adapted from [14]) 108
Figure 5- 7: Chemical Structures of paclitaxel, SB-T-1214 and FLT (5-1) 110

Chapter 6

Figure 6- 1: β+ decay and positron/electron annihilation (adapted from [1]) 122
Figure 6- 2: Examples of clinical use of paclitaxel and docetaxel 124
Figure 6- 3: Chemical Structure of Biotin 125
Figure 6- 4: Chemical Structures of 125
Figure 6- 5: Compound 6-1 and 6-2confirmation by mass chromatogram 128
Figure 6- 6: Confirmation of desired product by LC/HRMS 129
Figure 6- 7: Full HPLC trace of iodination 130
Figure 6- 8: Confirmation of desired product by LC/HRMS of the reaction mixture 131

Figure 6- 9: Compound 6-3 confirmation by mass chromatogram..... 131
Figure 6- 10: Target confirmation..... 132

Chapter 7

Figure 7- 1: The cancer stem cell hypothesis (adapted from [7])..... 139
Figure 7- 2: Chemical structures of camptothecin (CPT), topotecan, and irinotecan (CPT-11) 141
Figure 7- 3: Chemical structure of curcumin and CMC2.24..... 142
Figure 7- 4: Cytotoxic effects of the SBT-1214/CMC2.24 combination against prostate CD133+ cells (adapted from [20])..... 143
Figure 7- 5: Chemical Structure of Epigallocatechin Gallate (EGCG)..... 144
Figure 7- 6: Percent apoptosis by PC-3ML cells (adapted from [22])..... 144
Figure 7- 7: Development of novel MMP-9 inhibitory compounds..... 145

List of Tables

Chapter 1

Table 1- 1: Antimicrobial activities of taxanes 10
Table 1- 2: Hit compounds from the preliminary screening against Mtb H37Rv strain at 1.0 μg/mL concentration (adapted from [28]) 20
Table 1- 3: MIC values of selected hit compounds against Mtb H37Rv strain 22

Chapter 2

Table 2- 1: Cytotoxicity of 10 Lead Compounds against Vero Cells 53
Table 2- 2: Metabolism Result 54

Chapter 3

Table 3- 1: Metabolism result 71

Chapter 4

Table 4- 1: Reference values 85

Chapter 5

Table 5- 1: Selected new-generation taxoids 104
Table 5- 2: Cytotoxicity (IC_{50}; nM) of new-generation taxoids against selected cancer cell lines 105
Table 5- 4: The Internalization of Vitamin-Targeted Rhodamine-Labeled 106
Table 5- 5: Cytotoxicities (IC_{50}, nM) of Paclitaxel, SB-T-1214, and Folate Linker Taxoid (FLT) in the Presence of GSH-OEt or GSH Following Internalization. 111

Chapter 6

Table 6- 1: The properties of radionuclides (adapted from [2]) 123
Table 6- 2: Cytotoxicities (IC_{50}, nM) of paclitaxel, SB-T-1214, and 3'-vinyliodotaxoid (6-2). 127

Chapter 7

Table 7- 1: Biological evaluation of chemotherapeutic agents against CSC-enriched cancer cells (adapted from [10]) 140
Table 7- 2: Preliminary screening against CICs 148
Table 7- 3: Cytotoxicities (IC_{50}) of single and combination administration 149

List of Schemes

Chapter 1

Scheme 1- 1: Synthesis of 2,5,6-trisubstituted benzimidazole library..... 18
Scheme 1- 2: Re-synthesis of 2,5,6-trisubstituted benzimidazoles..... 21

Chapter 3

Scheme 3- 1: First synthesis of 2,5,6-trisubstituted benzimidazoles..... 69
Scheme 3- 2: synthesis of 2,5,6-trisubstituted benzimidazoles 69

Chapter 6

Scheme 6- 1: Cold iodination to form 3'-vinyliodo taxoid (6-2)..... 130

Chapter 7

Scheme 7- 1: Synthetic route for MMP inhibitor, 7-4..... 147

List of Abbreviations

℃	Degrees Celsius
Ac	Acetyl
AIDS	Acquired immune deficiency syndrome
ATP	Adenosine triphosphate
BCG	Bacillus Calmette-Gu
BLT	Biotin-linker-taxoid
BMS	Bristol-Myers Squibb
Bn	Benzyl
Boc	Butoxycarbonyl
BR	Biotin Receptor
Bu	Butyl
C	Centigrade; Carbon
Cbz	Carboxybenzyl
CDC	Center for disease control and prevention
CDI	Carbonyldiimidazole
CFM	Confocal fluorescence microscopy
CFU	Colony forming unit
CPT	Camptothecin
d	Day, doublet
DAB	10-deacetylbaccatin III
dd	Doublet of doublets
DIC	*N,N'*-diisopropylcarbodiimide
DIPEA	*N*,*N*-diisoproylethylamine
DMAP	4-(dimethylamino)pyridine
DMEM	Dulbecco's Modified Eagle medium
DMF	*N*,*N*-dimethylformamide
DMSO	Dimethyl sulfoxide
DNA	Deoxyribonucleic acid

DPBS	Dulbecco's Phosphate buffered saline
dt	Doublet of triplets
E. coli	*Escherichia coli*
EDC	1-Ethyl-3-(3-dimethylaminopropyl)carbodiimide
EM	Electron microscopy
ESI	Electrospray ionization
Et	Ethyl
EtOH	Ethanol
F. tularensis	*Fransicella tularensis*
FA	Folic acid
FBS	Fetal Bovine Serum
FDA	Food and drug administration
FLT	Folate-linker-taxoid
FR	Folate receptor
FtsZ	Filamenting temperature-sensitive protein Z
g	Gram
GDP	Guanosine diphosphatase
GSH	Glutathion reduced form
GSH-OEt	Glutathion ethyl ester
GTP	Guanoside-5'-triphosphate
GTPase	Guanosine triphosphate
h	Hour
H37Rv	*M. tuberculosis representing virulent*
HCl	Hydrochloric acid
His	histitine
HIV	Human immunodeficiency virus
HNMR	Proton nuclear magnetic resonance
HPLC	High-performance liquid chromatography
HRMS	High-resolution mass spectrometry
HT-29	Human colon cancer cell line
HTP	High throughput

Hz	Hertz
IC_{50}	Half-maximum inhibiory concentration
ID8	Murine ovarian cancer cell line
INH	Isoniazid
IPA	Osopropanol
J	Coupling constant
k	Kilo- (scale)
K_2CO_3	Potassium carbonate
KOH	Potassium hydroxide
L	Liter
L1210	Murine leukemia cell line
L1210-FR	Murine leukemia cell line
LC	Liquid chromatography
M	Mega- (scale); molar
m	Milli- (scale); multiplet (NMR)
M. Smeg	Mycobacterium smegmatis
m.p.	Melting point
m/z	Mass-to-charge ratio
MABA	Microplate Alamar Blue Assa
MCF-7	Human breast carcinoma cell line
MDR	Multidrug resistant
MDR-TB	Multi-drug resistant tuberculosis
Me	Methyl
MeOH	Methanol
mg	Milligram
MHz	Megahertz
MIC	Minimum inhibitory concentration
min	Minute
mL	Milliliter
mmol	Millimole
mol	Mole

MRI	Magnetic resonance imaging
Mtb	*Mycobacterium tuberculosis*
MTT	3-(4,5-dimethylthiazol-2-yl)-2,5-diphenyltetrazolium bromide
MX-1	Human breast carcinoma cell line
n	Nano- (scale)
NCI	National Cancer Institute
NCI/ADR-RES	Platinum-resistant metastatic ovarian cancer cell line
NHS	*N*-hydroxysuccinimide
NIAID	National institute of allergy and infectious diseases
nM	Nanomolar
NMR	Nuclear magnetic resonance
OD	Optical density
p	Para
PBS	Phosphate buffered saline
PEG	Polyethylene glycol
PET	Positron emission tomography
Ph	Phenyl
pM	Picomolar
PMP	*p*-Methoxyphenyl
ppm	Parts per million
Pr	Propyl
q	Quartet
Rf	Retention factor
RIF	Rifampicin
RME	Receptor-mediated endocytosis
RNA	Ribonucleic acid
RPMI	Roswell Park Memorial Institute medium
s	Singlet
S. aureus	*Staphylococcus aureus*
SAR	structure-activity relationship
SB-P	Stony Brook Plate

SB-T	Stony Brook taxoid
SEM	Scanning electron microscopy
SPECT	Single-photon emission computed tomography
SRI	Southern Research Institute
SS	Disulfide bond
t	time; triplet (NMR)
t	*tert*
TB	Tuberculosis
TEM	Transmission electron microscopy
TFA	Trifluoroacetic acid
THF	Tetrahydrofuran
TLC	Thin-layer chromatography
TOF	Time-of-flight
topo I	Topoisomerase I
TTDDS	Tumor-targeted drug system
TTM	Tumor-targeted module
UV	Ultraviolet
WHO	World Health Organization
WI-38	Normal human lung fibroblast
XDR	Extensively drug resistant
XDR-TB	Extremely drug-resistant tuberculosis
Y. pestis	*Yersinia pestis*
δ	Chemical shift
Δ	Difference
λ	Wavelength
μ	Micro- (scale)
μM	Micromolar

Acknowledgments

First and foremost, I would like to thank my advisor, Distinguished Professor Iwao Ojima for welcoming and giving me the opportunity to work in his research laboratory. I am grateful for his guidance, endless support, willingness to teach me, share his extensive knowledge of chemistry, and always provide advice in my research. He has provided me in both synthetic and medicinal chemistry that I aim to carry on in my future journeys. In addition, I would like to thank Mrs. Yoko Ojima for generous hospitality during the annual 4th of July BBQ and Thanksgiving Eve parties over the years.

Also, I would like to show my appreciation my dissertation committee members, Professor Frank W. Fowler, Professor Peter J. Tonge for their participation in constructive discussions, and sharing their experiences and a passion for chemistry with me throughout my graduate school career. I would also like to extend my appreciation to Professor James B. Bliska for taking time out of his busy schedule to be the outside member of my dissertation committee.

I would also like to express gratitude to our collaborators who have made significant contribution to my research. I wish to thank Professor Richard A. Slayden and Dr. Susan Knudson at Colorado State University, for performing anti-bacterial assays and determine the activity for our compounds. I would like to sincerely thank Sanofi-Aventis for sharing their knowledge and determining ADMET properties of our benzimidazoles.

When I applied for a degree in Chemistry, I never thought that I would have done so much cellular biology. This part of my research would not be possible without the help of Dr. Galina Botchkina, Rebecca Rowehl and Dr. Anne Savitt. I would like to thank her let me work in her lab and her valuable help in cancer stem cell research. Also, Rebecca and Anne for teaching me the basics of cell culture and their extremely helpful and encouraging advice.

I would like to acknowledge and thank the many members of the Department of Chemistry. Dr. Béla Ruzsicska, for mass spectrometry; Susan Van Horn for TEM Facility; Dr. Jim Marecek and Dr. Francis Picart, for NMR spectrometry; Mrs. Roxanne Brockner, for playing an integral part in helping and supporting the Ojima group. I am also grateful for the help of the chemistry department office staff, especially Heidi Ciolfi, Liz Perez, Norma Reyes, Charmine

Yapchin, Barbara Schimmenti, Kimberly Toell, and Katherine Hughes. I would also like to thank our building managers and directors of labs, Dr. Al Silverstein, Mike Teta, and Dr. Deborah Stoner-Ma.

The Ojima lab would not be able to function without Mrs. Patricia Marinaccio, "the Ojima Group Mom". I would like to utmost thank Pat for her support, the laughs, love, advice and hugs.

I want to especially thank Daisy, Wen, Josh, Jacob and Edison for being a wonderful friend in my Stony Brook "Chemistry" life. Also, it has been my pleasure to have worked with the many members of the Ojima research group. The "benzo" team: Lucy Li, Dr. Eduard Melief, Dr. Kunal Kumar, Dr. Divya Awasthi, Dr. Soumya Chowdhury, Simon Tong, Krupa Haranahalli and Edwin "Ricky" Lazo. Also, the cancer team members: Dr. Edison S. Zuniga, Dr. Joshua D. Seitz, Dr. Jacob G. Vineberg, Dr. William Berger, Dr. Anushree Kamath, Dr. Siyeon Lee, Tao Wang, Longfei Wei, Chanwei Wang, Xin Wang, Brendan Lichtenthal, Yao Zong, Yaozhong Zhang, Su Yan, Ying-Jen Chen, Wen Chen and Winnie Situ. In addition, organometallic team members: Dr. Gary Teng, Dr. Chi-Feng Lin, Dr. Chih-Wei Chien, Dr. Dr. Alex "Daisy" A. Athan, , Dr. Yang Zang. Dr. Tadashi Honda, Dr. Suqing Zheng, It has also been a pleasure knowing Dr. Honda and working with the members of the Honda group: Dr. Hiroki Moriwaki, Dr. Motohiro Takahashi, Dr. Akiro Saito, and Dr. Wei Li. I would like to thank all of the 6th and 7th floor chemistry groups, the members of Chem Masters Int. It was a great pleasure working with them.

My journey through graduate school was made much more enjoyable with the support and friendship of people outside of the Ojima group as well. I would like to extend a special thanks to the "Choo" and "Lee" families for being my "America family". Jiiyeon Kim, Soyoung Park, Dr. Jayon Lim, A ram Kim, Sujung Han, Dr. Hyejin Ryu, Dr. Hee Nam Lim, Dr. Jungyong Lee, Dr. Gunwoo Kim, Hyeyoung Kim, Dr. Jusang Lee, Dr. Brian Choi, Dr. Sungchan Pack, Andy Khoo and Sonam Shah for sharing not only the happy moments but also being true friend throughout my tough time here in Stony Brook. Also, my friends in Korea, Jwayoung Kim, Inhye Kim, Pilsang Ryu, Jinho Jeon, Yongjun Cho, Hyeyeon An, Sujung "Crystal" Kwon, Yeonmi Park, Jihye Park, Hyojoo Lee, Hyokyung Lee, Jihye "Sidney: Ahn and Minkyung "MK" Lee for their kind support and love even from the distance.

Most importantly and needless to say, I would like to thank my parents, my sisters, brother-in-laws, and nephew and nieces for all their continuous love and support throughout my entire life.

Vita

EDUCATION

Stony Brook University, Stony Brook, NY
PhD. In Organic Chemistry- Professor Iwao Ojima
Stony Brook University, Stony Brook, NY
B.S. in chemistry- Professor Joanna Fowler
Konkuk University, Seoul, South Korea
B.S. in Chemistry- Professor Sueng-Un Park
(Note: Dual-degree undergraduate program between Stony Brook University and Konkuk University.)

LAB EXPERIENCE

08/2009 – present Stony Brook University
Teaching Assistant, Research Assistant
Institute of Chemical Biology and Drug Discovery
Graduate Assistant
12/2011 – present Sanofi-Aventis R&D, Infectious Disease (Toulouse, France) Collaboration
01/2008 – 12/2008 Brookhaven National Laboratory (Medical Department)
Research Program
10/2006 – 08/2007 The Organic chemistry Lab., Konkuk University
Research Assistant
03/2006 – 08/2006 The Biochemistry Lab., Konkuk University
Research Assistant

RESEARCH EXPERIENCE

- Multistep synthesis on milligram to decagram scales
- Reaction scheme optimization for scale up synthesis
- Contributing to SAR of 2,5,6-trisubstituted benzimidazoles
- Synthesis, purification and characterization of drug candidates for biological testing
- Automated system developing for bioassays
- Design and synthesis of chemical tools to facilitate pharmacological studies
- Active agent formulation and stability profiling
- Compounds purified by recrystallization, distillation and flash chromatography
- Compound identification by ^{1}H, ^{13}C and ^{19}F NMR, melting point analysis, mass spectrometry: FIA and LCMS, IR, and HRMS

- Cell based biological evaluation of new generation of taxoids *in vitro* utilizing MTT assay
- Management of multiple collaborative projects involving cell biologists, polymer chemists and biochemists
- Exploration of synergistic combinations with new-generation taxoids against various cancer cell lines including cancer stem cells (CSCs)

PUBLICATIONS

Bora Park, Divya Awasthi, Soumya R. Chowdhury, Eduard Melief, Kunal Kumar, Susan E. Knudson, Richard A. Slayden, and Iwao Ojima, Design, Synthesis and Evaluation of Novel 2,5,6-Trisubstituted Benzimidazoles Targeting FtsZ as Antitubercular Agents, *Bioorganic & medicinal chemistry*, 2014, *22* (9), 2602–2612

SELECTED POSTERS AND PRESENTATIONS

- Bora Park, Divya Awasthi, Soumy R. Chowdhury, Eduard Melief, Kunal Kumar, Susan E. Knudson, Richard A. Slayden, and Iwao Ojima, A New Series of 2,5,6-Trisubstituted Benzimidazoles for Tuberculosis Drug Discovery Targeting FtsZ, The New York Academy of Sciences: World TB Day Symposium: Countdown to 2015, 2014, NY.
- Bora Park, Kunal Kumar, Divya Awasthi, Eduard Melief, Susan Knudson, Richard A. Slayden, Iwao Ojima, Design, synthesis, and evaluation of novel trisubstituted benzimidazoles targeting FtsZ as antimicrobial agents, 245th ACS National Meeting and Exposition. 2013, New Orleans, LA.
- Bora Park; Kunal Kumar; Divya Awasthi; Edward Melief; Jason Cummings; Richard A Slayden; Iwao Ojima. Synthesis and Evaluation of Novel Trisubstituted Benzimidazoles Targeting FtsZ as Antimicrobial Agents, 243rd ACS National Meeting & Exposition, 2012, San Diego, CA.
- Bora Park, Joshua D. Seitz, Jacob G. Vineberg, Iwao Ojima, Next-Generation Taxoids as Potent Theranostic Agents for Targeted Cancer Therapy, ICB&DD 8th Annual Symposium, 2014, Stony Brook University, NY

TEACHING EXPERIENCE

08/2009 – 12/2010 Stony Brook University- General Chemistry Lab, Organic Chemistry Lab

Chapter 1

Design and Synthesis of Novel 2,5,6-Trisubstitued Bezimidazoles

Chapter Contents

§ 1.1 Introduction 2

§ 1.1.1 Tuberculosis 2

§ 1.1.2 Current Treatments of TB 4

§ 1.1.3 FtsZ: A Novel TB Drug Target 8

§ 1.1.4 Drug Design 9

§ 1.2 Results and discussion 18

§ 1.2.1 Synthesis of 2,5,6-Trisubstituted Benzimidazole Library 18

§ 1.2.2 Preliminary Screening Result 19

§ 1.2.3 Re-synthesis of Hit Compounds for Their Accurate MIC determination 20

§ 1.3 Conclusion 23

§ 1.4 Experimental Section 24

§ 1.4.1 General Methods 24

§ 1.4.2 Materials 24

§ 1.4.3 Experimental Procedures 24

§ 1.4.4 Bacterial Strains and Growth 40

§ 1.4.5 Antibacterial Activity Determination 41

§ 1.5 References 42

§ 1.1 Introduction

§ 1.1.1 Tuberculosis

Tuberculosis (TB) is a contagious bacterial infection which is caused by mycobacteria of the "tuberculosis complex", including *Mycobacterium bovis*, *Mycobacterium africanum* and mailnly *Mycobacterium tuberculosis* (*Mtb*).[1, 2] This bacteria typically attacks the lungs, but it can also damage almost any organ of the body such as the kidney, spine, and brain.[3] It spreads by the air when people have an active TB infection. People who are infected by TB may not notice any symptoms of illness until the disease is advanced since the symptoms are very common. The symptoms of TB are somewhat similar to such as loss of weight, fever, cough, and night sweats except severe coughing up of blood.

When *Mtb* enters the human body via the respiratory track through the inhalation of respiratory droplet, the host and pathogen can have any of the four outcomes.[4]

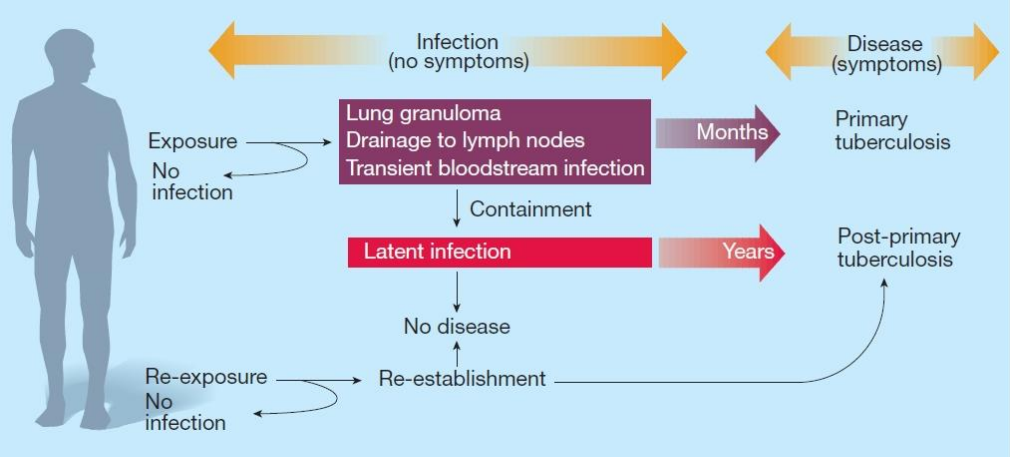

Figure 1- 1: Tuberculosis in humans (adapted from [5])

First, the initial host response may be completely effective and kill the bacilli; Second, the organisms can grow and multiply immediately after infection, resulting in primary TB; Third, the bacilli may become dormant state, this is called latent TB infection[3] and in this state, the body does not realize sickness or any other symptoms; and last, the latent bacilli can eventually become active and progress to fully grown disease condition. Possible outcomes of disease are described in **Figure 1- 1**.[5]

TB is curable and preventable disease, however, it is still a challenging disease for clinical researchers for over 50 years due to poor chemotherapeutics and inadequate local-control programs.[6] It has been estimated that about two billion people, almost one-third of the world's total population, are infected with TB.[1] World Health Organization (WHO) estimated that there were 8.6 million new cases of TB globally (13% co-infected with HIV) resulting in 1.3 million deaths in 2013 alone.[1] The five countries with the largest number of incident cases in 2012 are showing in **Figure 1-2**. The disease is particular interest to India (2.0 million - 2.4 million), followed by China (0.9 million - 1.1 million), South Africa (0.4 million - 0.6 million), Indonesia (0.4 million - 0.5 million) and Pakistan (0.3 million - 0.5 million).[1]

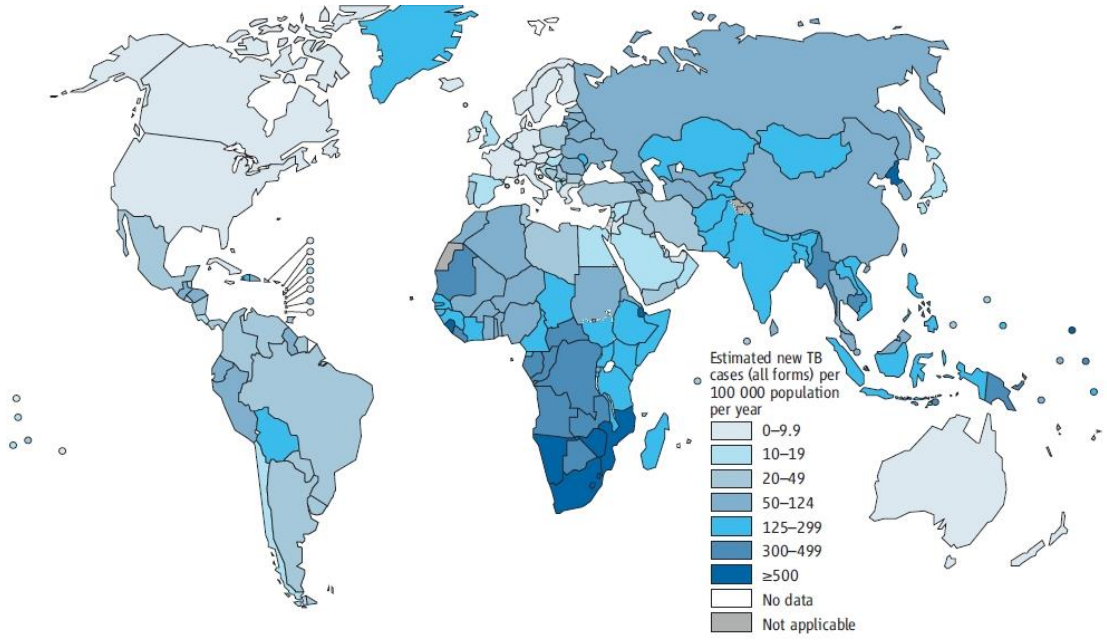

Figure 1- 2 Estimated TB incidence rates, 2012 (adapted from [1])

TB is especially the huge problem among those people who are weakened their immune systems such as in case of human immunodeficiency virus (HIV), aging, or other medical conditions.[3] Thus, co-infection with HIV has added to the seriousness of TB as global pandemic. As the immune system is compromised, the probability of developing TB increases by up to 30 times for those who are HIV-positive people and co-infected with TB.[2] The proportion of TB

cases co-infected with HIV was highest in countries in the African Region (**Figure 1-3**). Overall, 37% of TB cases were estimated to be co-infected with HIV in this region, which accounted for 75% of TB cases among people living with HIV worldwide. In parts of southern Africa, more than 50% of TB cases were co-infected with HIV.[1]

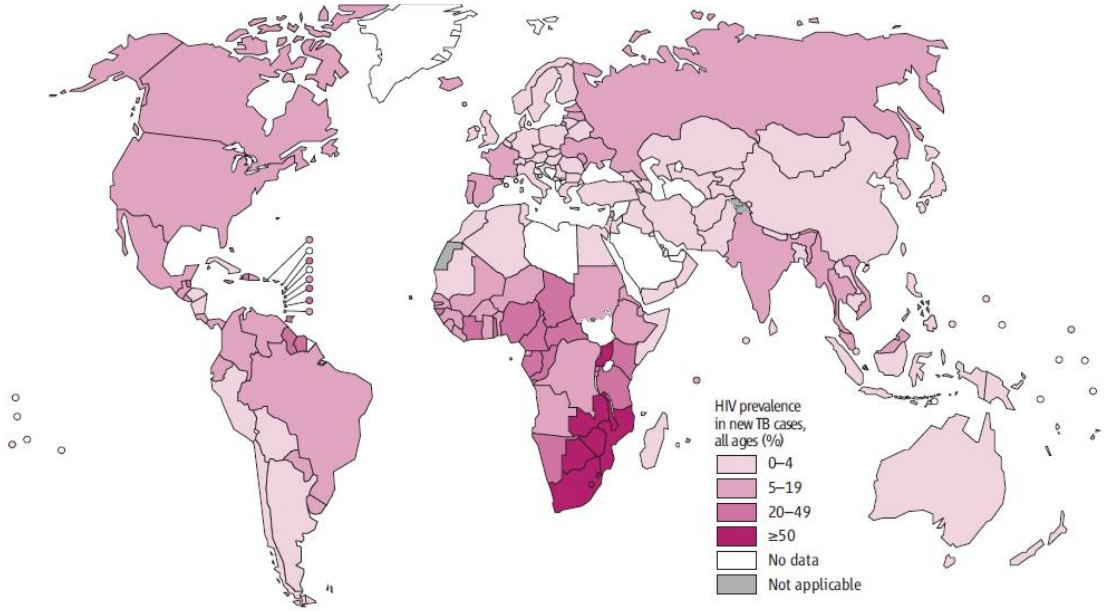

Figure 1- 3: Estimated HIV prevalence in new TB cases, 2012 (adapted from [1])

In addition to co-infection with other health condition, multidrug-resistant (MDR-TB) and extensively drug resistant TB (XDR-TB) are contributing to the rise in TB and responsible for a significant public health threat for TB control efforts.[7, 8]

§ 1.1.2 Current Treatments of TB

Despite the availability of several drugs and the Bacillus Calmette-Guérin (BCG) vaccine,[9] TB still remains a major health concern worldwide, warranting the identification of new drug targets for the design of more effective drugs. BCG is currently the only available vaccine against TB, and it is widely administered within the WHO expanded program for immunization.

The protective efficacy of BCG has been shown to be highly variable across different populations.[9]

There are 10 drugs currently approved by the U.S. Food and Drug Administration (FDA) for treating TB.[3] Current therapy for TB is dependent on a combination of various potent antibiotics, such as isoniazid (INH), rifampicin (RIF) and pyrazinamide, in a treatment of six months' duration. Treatment completion is determined by the number of doses ingested over a given period of time (**Figure 1-4**).[3] It may be necessary to add other first-line drugs such as ethambutol and streptomycin to the treatment, if initial resistance to INH is observed.

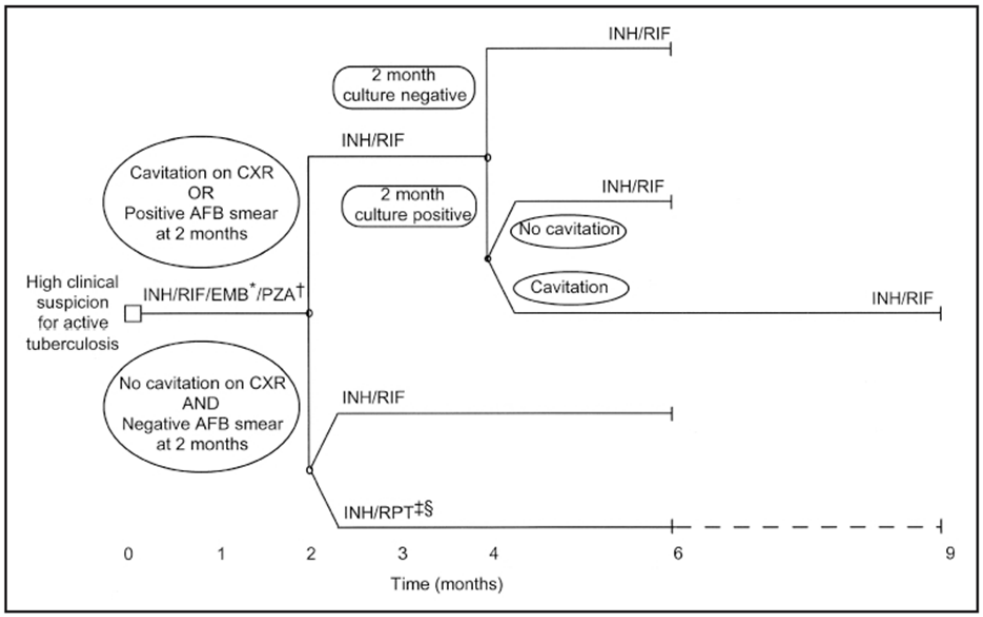

Figure 1- 4: Treatment algorithm for active, culture-negative pulmonary tuberculosis and inactive tuberculosis (adapted from [3])

Patients who proved or strongly suspected has TB are should treat with first-line anti-TB agents for the initial 2 months. When 2 months of treatment has been completed, INH and RIF are given daily or twice weekly for 4 months to complete a total of 6 months of treatment.[3] Patients receiving INH and RIF, and whose 2-month cultures are positive, should have treatment extended by an additional 3 months (total of 9 months).[3]

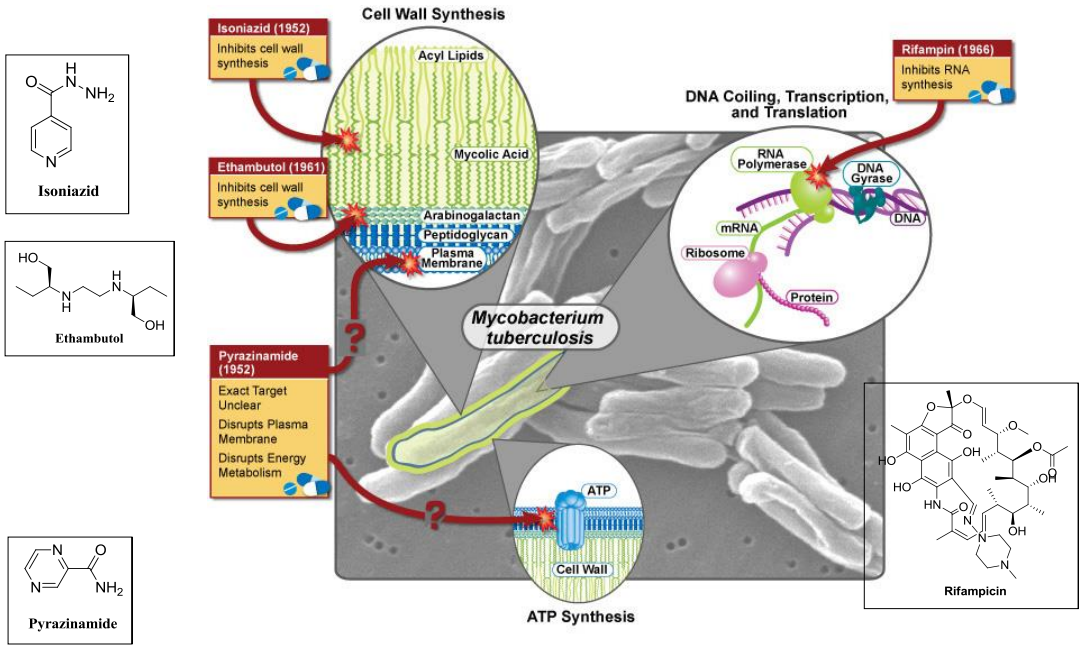

Figure 1- 5: First-line treatment of TB for drug-sensitive TB (adapted from [3]) and modified

When there is resistant to two or more of the first line antibiotics, such as INH, and RIF it is defined as MDR-TB. It is necessary to extend of the treatment period and frequent the use of second and/or third-line drugs despite their increased toxicity.[10] Typical MDR-TB treatment duration is about 18 to 24 months. Furthermore, when TB disease is resistant to any fluoroquinolone and at least one of the three injectable drugs, kanamycin, capreomycin, and amikacin, used to treat TB is classified as extensively drug resistant TB, XDR-TB. XDR-TB is widespread, including occurrence in the developed countries such as United States of America, where TB had been considered to be under control.

Drug-resistant TB is arising from a combination of physician error and patient non-compliance during treatment.[11] In order to figure out the mechanisms of resistance to the main anti-TB drugs, many advances in genome sequence of *Mtb* were developed.[12] Studies showed that specific gene mutations were associated with drug resistance.[13] Traditionally, intrinsic drug resistance of *Mtb* is known to the unusual structure of its mycolic acid-containing cell wall that gives the bacteria a low permeability for many antibiotics.[14]

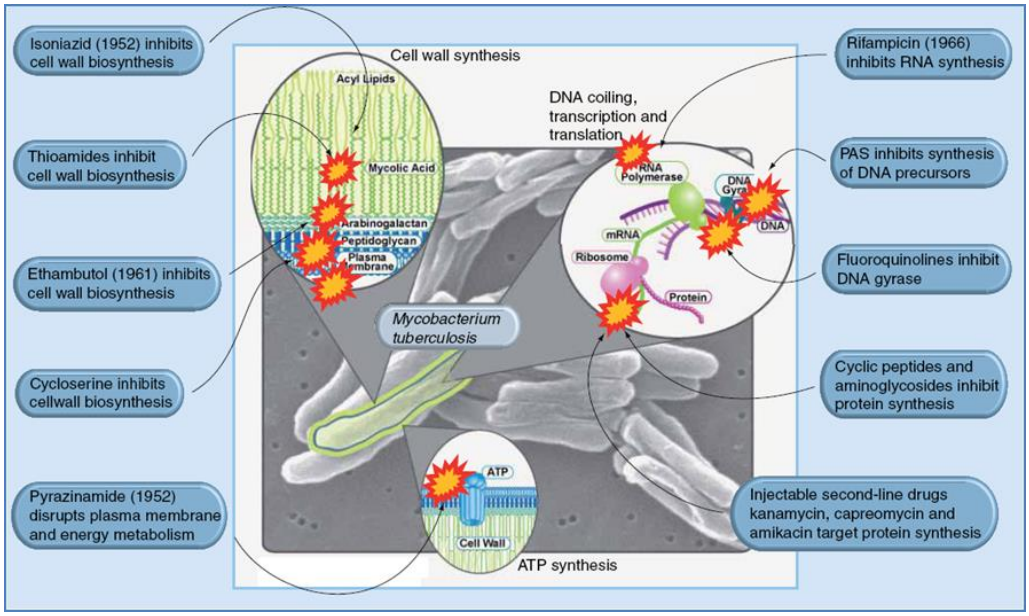

Figure 1- 6: Current drugs and their target (adapted from [21])

Unlike other bacteria, *Mtb* acquired drug resistance is caused by spontaneous mutation in chromosomal genes at a low rate of 0.0033 per replication.[12, 15] The majority of *Mtb* resistant to INH is a complex process including several genes, *katG*, *ahpC*, *inhA*, *kasA* and *ndh*.[16, 17] Resistance to RIF is due to mutation in the gene *rpoB* that encodes the β–subunit of RNA polymerase resulting in conformational changes.[18] Resistance to fluoroquinolones is associated with nutations with *gryA* and *gyrB*.[19] The other second line drugs, kanamycin and amikacin, their mutations are associated with an A1201G mutation in the *rrs* gene coding for 16S rRNA. The mutation of gene *tlyA* is involved in the resistance to capreomycin and viomycin.[20]

Despite efforts in last 50 years, development of new TB treatments (**Figure 1-6**) have been limited to drug targets like cell wall biosynthesis, ATP synthesis, RNA synthesis etc., leading to resistance in these areas.[21] Emergence of drug resistant strains of *Mtb* makes many of the currently available anti-TB drugs much less effective.[7] Therefore, there is an urgent necessity to discover novel drugs that target other bacterial processes in order to counter the developed bacterial resistance.[6, 21]

§ 1.1.3 FtsZ: A Novel TB Drug Target

Identification of a novel drug target is the first step in the development of new series of anti TB drugs. Filamenting temperature-sensitive protein Z (FtsZ) is not only crucial and the most abundant protein which acts early in bacterial cell division,[22] but it also shares also several similarities with tubulin.[23] Although the primary sequence homology is limited and mainly centered around the GTP-binding motif, the crystal structures of FtsZ and tubulin demonstrate extensive similarities.[24] In addition to structural similarities, FtsZ, like tubulin, it can bind and hydrolyze GTP and it can assemble into protofilaments.[24]

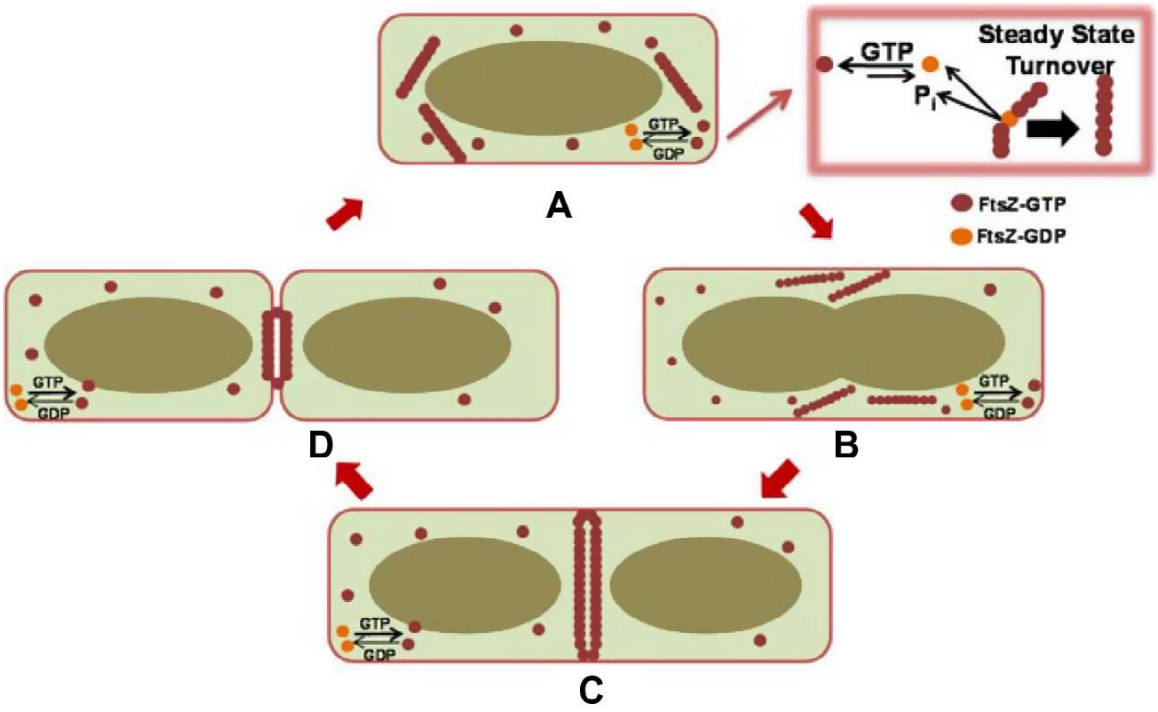

Figure 1- 7: Self-assembly of FtsZ to form Z-ring (adapted from [27])

FtsZ polymerizes in the presence of GTP to form a highly dynamic structure, the Z-ring at the cell division site.[22, 25] With the recruitment of several other cell division proteins, Z-ring constriction proceeds resulting in septum formation and subsequent cell division[26] (**Figure 1-7**).[27] Due to the crucial role of FtsZ in bacterial cytokinesis, inactivation of FtsZ is an attractive target for novel drug discovery.[28, 29] Since FtsZ is a homologue of tubulin with less than 10-18%

sequence identity,[30] known tubulin inhibitors could be a good starting point for developing FtsZ specific inhibitor.

§ 1.1.4 Drug Design

Previously, the researchers at the Southern Research Institute (SRI) studied about known tubulin inhibitors based on the premise that they can inhibit FtsZ assembly.[31] They screened their library of 200 2-alkoxycarbonylaminopyridines for antimicrobial activity against *Mtb*.[32] They found out that SRI-3072 and SRI-7614 (**Figure 1-8**) inhibited *Mtb* FtsZ polymerization in a dose-dependent manner. [32, 33] These two compounds also inhibited the GTPase activity by 20-25 % at 100 μM concentration.

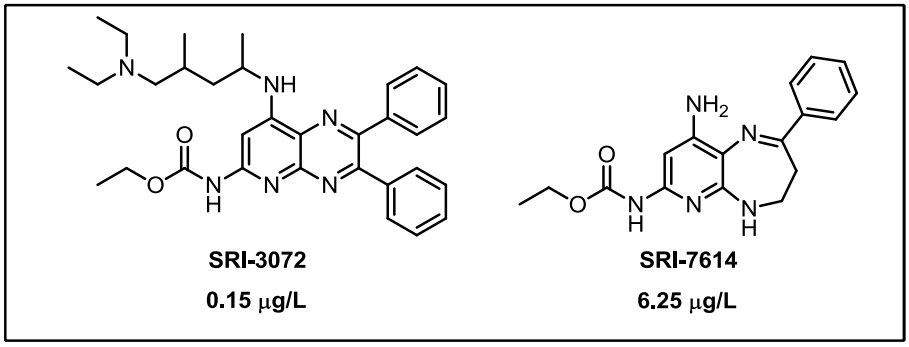

Figure 1- 8: Inhibitor of *Mtb* FtsZ

Moreover, Taxanes were first screened against *Mtb* FtsZ with the same hypothesis that known tubulin inhibitor could also affect bacterial cell division.[6] Since taxanes were known as microtubules stabilizing agent, 120 taxanes were synthesized in Ojima's lab and screened against drug-sensitive and drug-resistent *Mtb* strains.[6] Several compounds were found to be a highly promising non-cytotoxic anti-TB activity against drug-resistant along with drug sensitive *Mtb* strains from the MIC_{99} values and IC_{50} values (**Table 1-1**).

Table 1- 1: Antimicrobial activities of taxanes

Entry	Taxane	MIC (μM)		Cytotoxicity (IC_{50}, μM)	
		Mtb H37Rv[a]	*Mtb* IMCJ946.K2[b]	MCF-7[c]	A549[d]
1	Paclitaxel	40	40	0.019	0.028
2	SB-T-0032	5	1.25	0.65	0.065
3	SB-RA-2001	5	2.5	4.5	15.7
4	SB-RA-5001	2.5	1.25	> 80	> 80
5	SB-RA-5001MeO6	2.5	2.5	> 80	> 80
6	SB-RA-5011	2.5	1.25	> 80	> 80
7	SB-RA-5012	2.5	1.25	> 80	> 80

[a] drug-sensitive strain; [b] drug sensitive strain; [c] human breast cancer cell line; [d] non-small-cell lung cancer cell lines

SB-T-0032 and SB-RA-2001 were chosen for further optimization and also a new library of taxanes with modification of 10-deacetylbaccatin III (DAB).[6] Moreover, it has been proven that novel and effective anti-angiogenic taxoid with C-seco-baccatin moiety has less cytotoxicity than paclitaxel. Therefore, C-seco taxanes (**Figure 1-9**) were designed and synthesized in our lab.

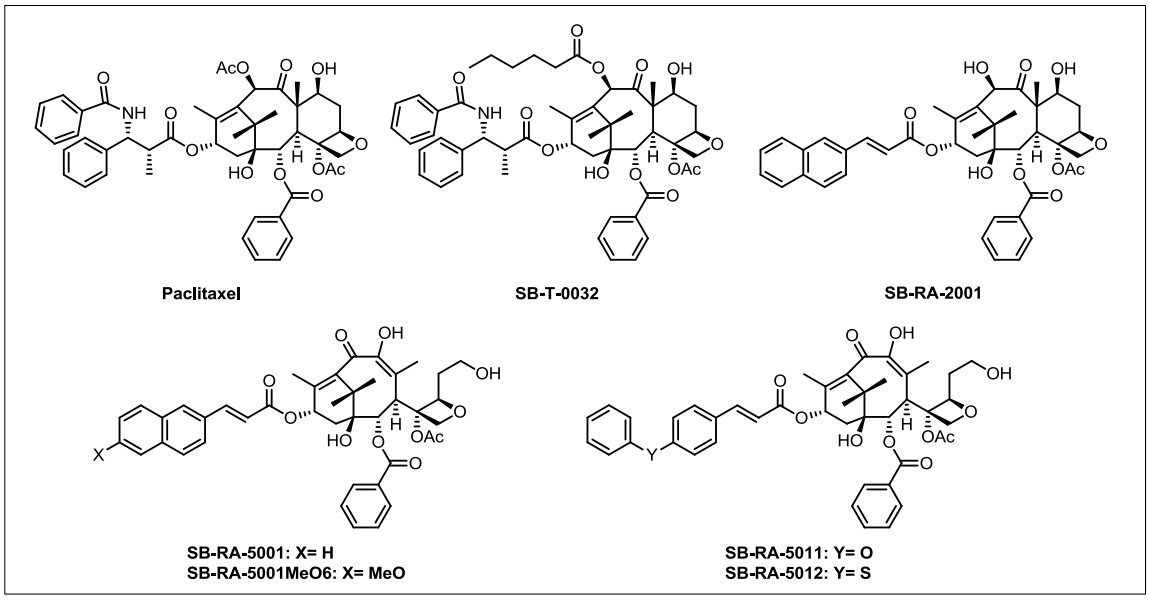

Figure 1- 9: Chemical structures of *Mtb* FtsZ inhibitors, taxanes

In addition, the scanning electron microscopy (SEM) images (**Figure 1-10**) of *Mtb* cells treated with SB-RA-20018 and SB-RA-5001 (**Figure 1-11**) showed that cell elongation and filamentation which is a phenotypic response to FtsZ inactivation.

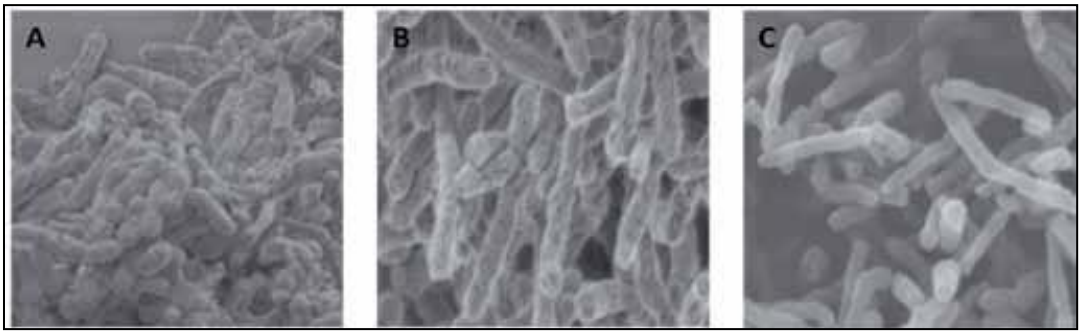

Figure 1- 10: SEM images of *Mtb* cells

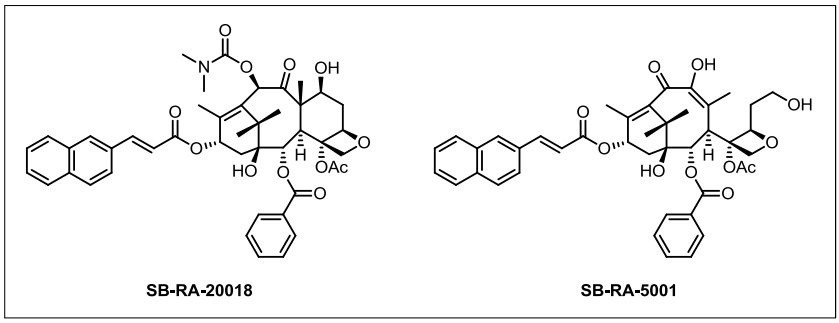

Figure 1- 11: Further chemical structures of *Mtb* FtsZ inhibitors, taxanes

In addition, various groups have explored known tubulin inhibitors based on the importance of FtsZ assembly in cell division to identify their ability to inhibit FtsZ polymerization or de-polymerization.[28, 32, 33] Following on this principle, albendazole and thiabendazole (**Figure 1-12**) , fungicide and parasiticide, were tested for their anti-TB activities.[34] The main mechanism of action of these two compounds was known to cause degenerative alterations in the intestinal cells of worms by binding to the colchicine-sensitive site of tubulin and inhibiting its polymerization or assembly into microtubules. Slayden and co-workers found that these two compounds inhibit FtsZ polymerization that led to the absence of septum formation based on ultra-structural analysis and gene expression profiling. MIC_{99} values of albendazole and thiabendazole were determined to be 61 μM and 80 μM, respectively.

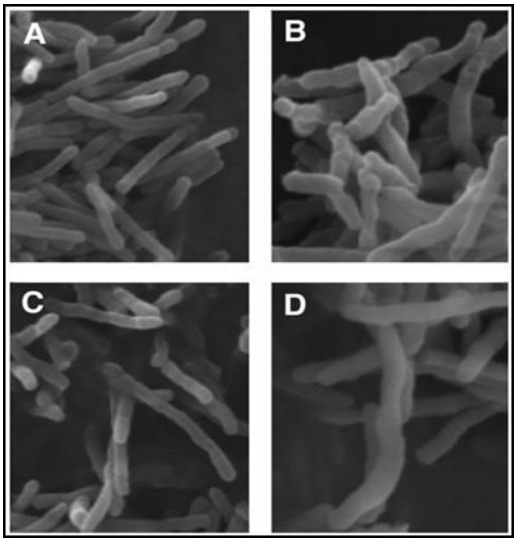

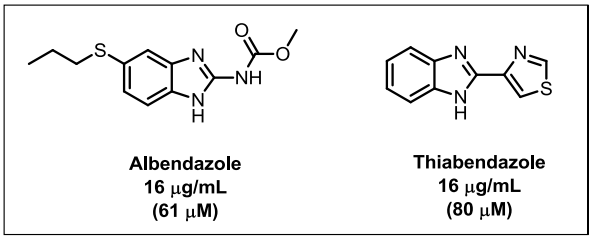

A .with 60 μM albendazole for 3 days;

B. with 60 μM albendazole for 5 days;

C. with 80 μM thiabendazole for 3 days;

D. with 80 μM thiabendazole for 5 days

Figure 1- 12: Inhibition of FtsZ polymerization

Since both of these compounds share a common benzimidazole moiety, we chose benzimidazole as the scaffold for development of novel anti-TB agents. In our previous work,[35-37] based on rational drug design, libraries of 2,5,6- and 2,5,7-trisubstituted benzimidazoles (**Figure 1-13**) were synthesized and evaluated for anti-TB activities

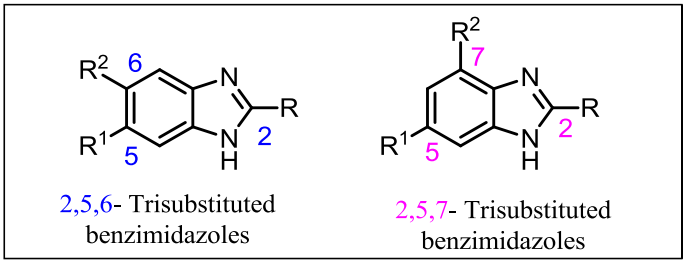

Figure 1- 13: Structures of 2,5,6- and 2,5,7-trisubsituted benzimidazoles

A large number of compounds were identified with MICs in the range of 0.39-6.2 μg/mL against drug sensitive as well as drug resistant *Mtb* strains (**Figure 1-14**).

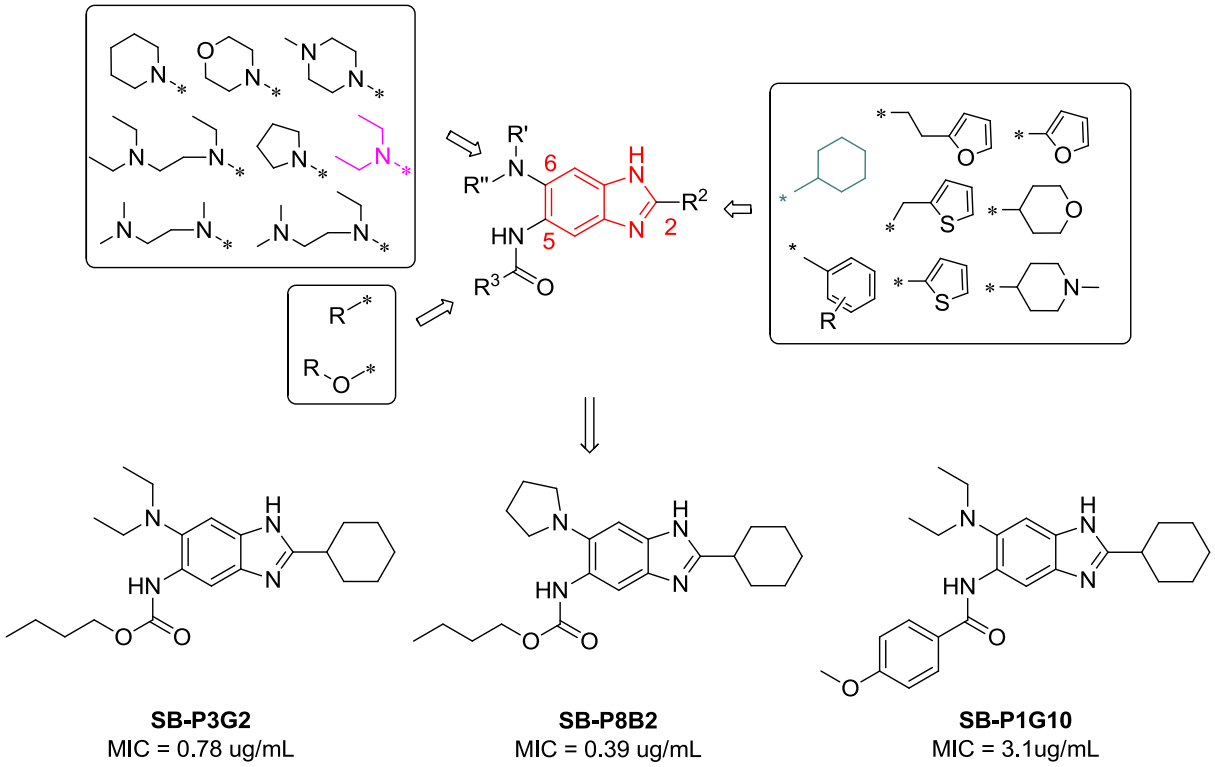

Figure 1- 14: Previously reported anti-TB 2,5,6-trisubstituted benzimidazoles

Previously, FtsZ polymerization assay[38] was carried out to validate the hypothesis that the lead compounds exhibit antibacterial activity by interacting with FtsZ. In the light scattering experiment (**Figure 1-15**), some of these novel lead compounds, **SB-P3G2** and **SB-P1G8** exhibited inhibition of FtsZ assembly in a dose dependent manner while enhancing the GTPase activity[36] of *Mtb* FtsZ. These results confirmed the hypothesis that the lead benzimidazoles target FtsZ.

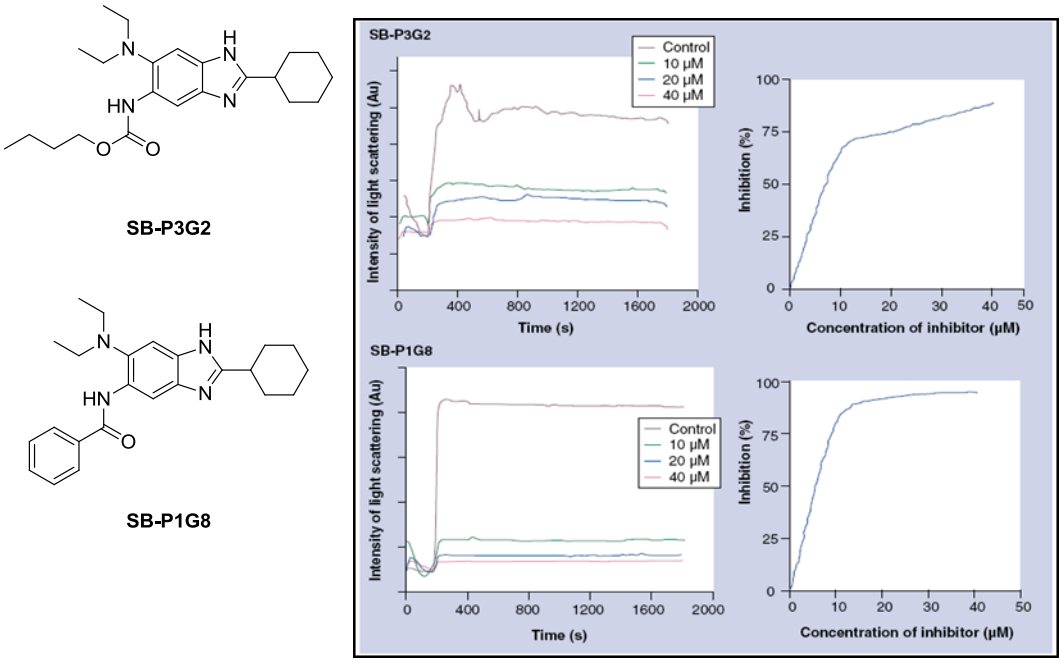

Figure 1- 15: Effect of bezimidazoles on FtsZ polymerization

Moreover, the scanning electron microscopy (SEM) images (**Figure 1-16**) of *Mtb* cells treated with **SB-P8B2** clearly show that cell elongation and filamentation which indicates that cell division was inhibited.

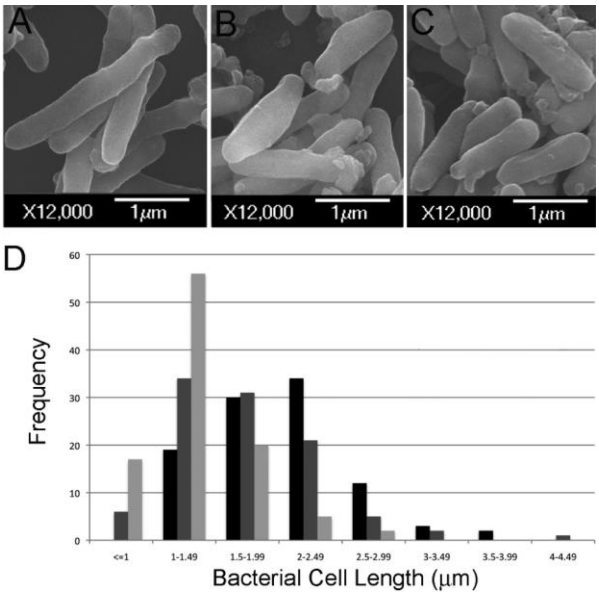

Figure 1- 16: SEM images of *Mtb* cells treated with SB-P8B2

The SEM images showed inhibition of FtsZ leading to disruption in septum formation and recruitment of septum associated proteins involved in later steps of division and septum resolution.

The preliminary SAR studies of lead compounds indicate that cyclohexyl group at the 2-position and diethyl amino/dimethyl amino group at the 6-position play important role for antibacterial activity.[36, 37] Building upon three representative compounds bearing alkyl carbamate or benzamide at the 5-position, we planned to expand our novel trisubstituted benzimidazole libraries with a substitution pattern different from the previous series for high throughput (HTP) screening.[39] [Note: In the 6-amino series, we have very recently found that the 6-dimethylamino series exhibit excellent activities up to the MIC value of 0.06 μg/mL.[37]]

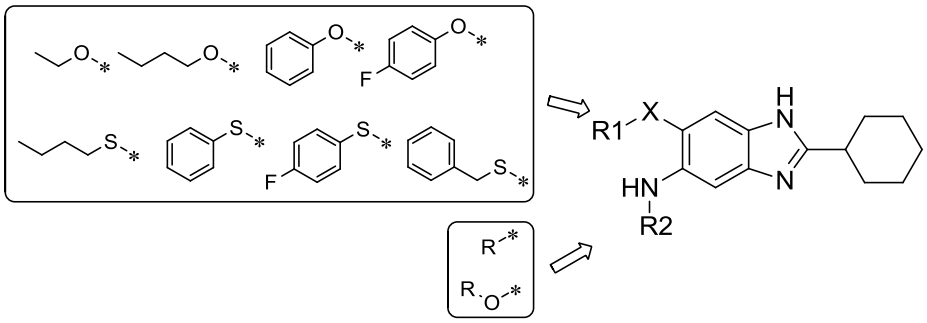

Figure 1- 17: Novel 2,5,6-trisubstituted benzimidazoles bearing an ether or thioether substituent at the 6-position

In order to investigate the effect of substituents other than amines at the 6-postion on antibacterial activity, a new series of 2,5,6-trisubstituted benzimidazole library was designed and synthesized with ether/thioether groups at the 6-position (**Figure 1-17**). Based on previous SAR studies, the cyclohexyl group at the 2-positon was fixed and various substituents at the 5-position were examined.

§ 1.2 Results and discussion

§ 1.2.1 Synthesis of 2,5,6-Trisubstituted Benzimidazole Library

General procedure for the synthesis of 2,5,6-trisubstituted benzimidazoles bearing an ether/thioether moiety at the 6-position is illustrated in **Scheme 1-1**.[6]

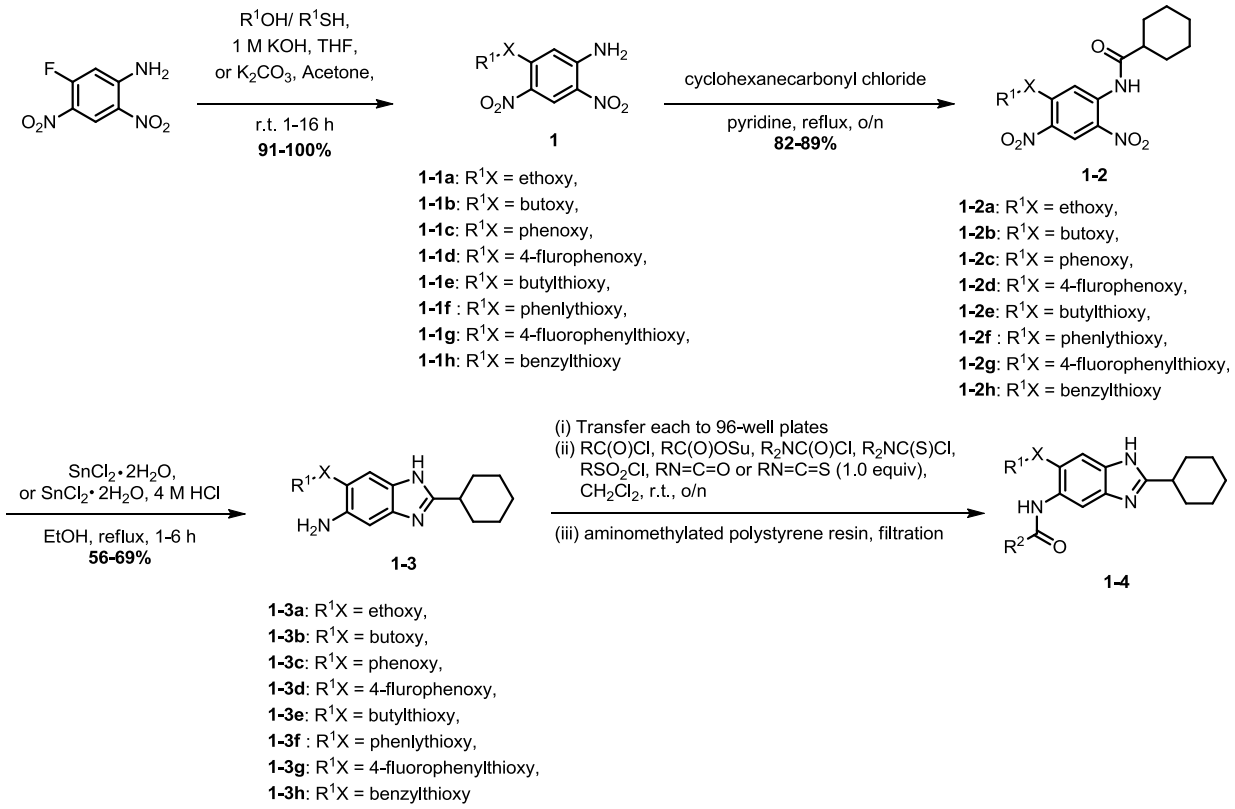

Scheme 1- 1: Synthesis of 2,5,6-trisubstituted benzimidazole library

The first step was the nucleophilic aromatic substitution of commercially available 2,4-dinitro-5-fluoroaniline with various alkyl or aryl alcohol/thiols. Compounds **1-1a**, **1-1b** and **1-1e** were prepared by using 1 M KOH while **1-1c**, **1-1d** and **1-1f** ~ **1-1h** were obtained by using 1 M K_2CO_3 to afford compounds **1-1a** ~ **1-1h** in 91–100 % yields. The acylation of compounds **1-1a** ~ **1-1h** with the cyclohexanecarbonyl chloride gave **1-2a** ~ **1-2h** in 82–89 % yields. Compounds **1-2a** ~ **1-2d** were treated with tin(II) chloride dihydrate while **1-2e** ~ **1-2h** were reacted with tin(II) chloride dihydrate and 4 M HCl to afford benzimidazoles **1-3a** ~ **1-3h** in 56–69 % yields.

5-Aminobenzimidazoles **1-3a** ~ **1-3h** (0.01 mM) were dissolved in dichloromethane and transferred into 96 well plates. Then, 47 different acyl chlorides, hydroxysuccinimide esters of chloroformates, isocyanates, isothiocyanates and sulfonyl chlorides (1.0 equiv) in dichloromethane were added to the individual wells. These 47 different reagents are shown in **Figure 1-18**. The plates were gently shaken for a day. Then, aminomethylated polystyrene resin EHL/2% DVB (200–400 mesh) (10 equiv) was added to scavenge excess or unreacted acyl chloride, isocyanates, isothiocyanate and sulfonyl chlorides. After reacting for 24 h, the resin was filtered to afford a library of 376 novel 2,5,6-tribsustituted benzimidazoles **1-4**.

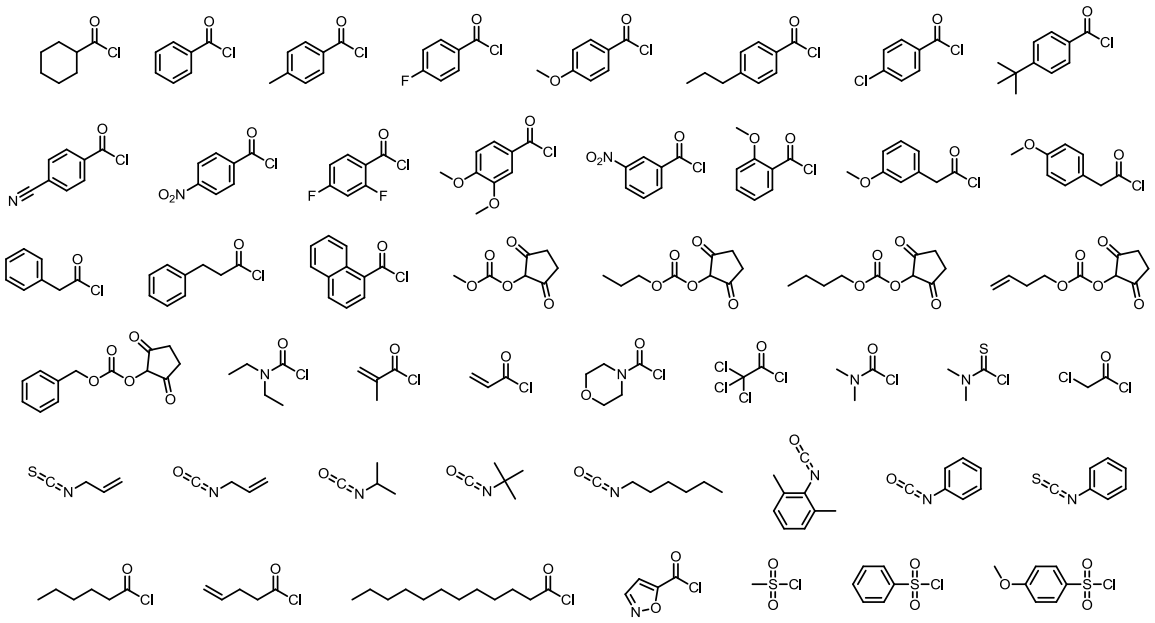

Figure 1- 18: List of 47 reagents for creation of a library of 376 novel 2,5,6-trisubstituted benzimidazoles

§ 1.2.2 Preliminary Screening Result

The library of 2,5,6-trisubstituted benzimidazoles **1-4** (376 compounds) was screened against drug sensitive *Mtb* H37Rv strain using 'Microplate Alamar Blue Assay' (MABA) and then, growth inhibition was measured in percentage. Among these compounds, 108 compounds were identified to inhibit the growth of *Mtb* H37Rv by 22–79% at 5 μg/mL concentration and 22 compounds (**Table 1-2**) exhibited 28-65% growth inhibition at 1.0 μg/mL concentration.[40] From

the preliminary screening, the butylthio group, followed by the benzylthio group at the 6-position appeared to be rather preferred, but 4-fluorophenoxy, 4-fluorophenylthio, and phenylthio groups did not seem to be much different. However, no compounds with a phenoxy group at the 6-position were included in the hit list. Also, no benzimidazoles bearing sulfoxide, urea or thiourea groups at the 5-position were found in the hit list. Thus, only amide or carbamate groups appear to be preferred at this position.

Table 1- 2: Hit compounds from the preliminary screening against Mtb H37Rv strain at 1.0 µg/mL concentration (adapted from [40])

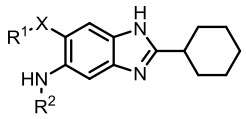

Compound	R^1X	R^2	% Growth inhibition	Compound	R^1X	R^2	% Growth inhibition
1	EtO	4-MeC_6H_4CO	65	**12**	BuS	$Ph(CH_2)_2CO$	33
2	BuO	$CH_2=CH(CH_2)_2CO$	28	**13**	PhS	4-MeC_6H_4CO	31
3	4-FC_6H_4O	2,4-$F_2C_6H_3CO$	44	**14**	PhS	4-*t*-BuC_6H_4CO	42
4	4-FC_6H_4O	4-MeC_6H_4CO	36	**15**	PhS	$CH_2=CH(CH_2)_2CO$	56
5	4-FC_6H_4O	$CH_2=CH(CH_2)_2CO$	54	**16**	4-FC_6H_4S	$CH_3(CH_2)_2OCO$	46
6	BuS	2,4-$F_2C_6H_3CO$	51	**17**	4-FC_6H_4S	$PhSO_2$	30
7	BuS	$CH_3(CH_2)_2OCO$	38	**18**	4-FC_6H_4S	$CH_2=CH(CH_2)_2CO$	41
8	BuS	$PhSO_2$	42	**19**	$PhCH_2S$	$CH_3(CH_2)_2OCO$	28
9	BuS	4-*t*-BuC_6H_4CO	45	**20**	$PhCH_2S$	$PhSO_2$	30
10	BuS	4-MeC_6H_4CO	53	**21**	$PhCH_2S$	4-*t*-BuC_6H_4CO	52
11	BuS	$CH_2=CH(CH_2)_2CO$	52	**22**	$PhCH_2S$	$CH_2=CH(CH_2)_2CO$	64

§ 1.2.3 Re-synthesis of Hit Compounds for Their Accurate MIC determination

These hit compounds were resynthesized (**Scheme 1-2**) in analytically pure form and examined for their accurate MIC values.

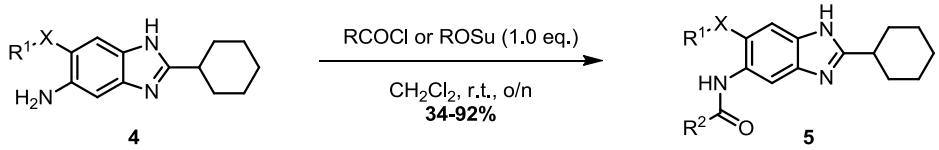

4

5

1-3a: R^1X = ethoxy,
1-3b: R^1X = butoxy,
1-3c: R^1X = phenoxy,
1-3d: R^1X = 4-flurophenoxy,
1-3e: R^1X = butylthioxy,
1-3f : R^1X = phenlythioxy,
1-3g: R^1X = 4-fluorophenylthioxy,
1-3h: R^1X = benzylthioxy

1-4a: R^1X = 4-flurophenoxy, R^2 = butoxy,
1-4b: R^1X = 4-flurophenoxy, R^2 = 4-methoxybenzyl,
1-4c: R^1X = 4-flurophenoxy, R^2 = 4-methylbenzyl,
1-4d: R^1X = 4-flurophenoxy, R^2 = 2,4-difluorobenzyl,
1-4e: R^1X = 4-flurophenoxy, R^2 = 4-pentenoyl,
1-4f: R^1X = phenlythioxy, R^2 = 4-methylbeozyl,
1-4g: R^1X = benzylthioxy, R^2 = 4-*tert*-butylbenzyl,
1-4h: R^1X = butylthioxy, R^2 = 2,4-difluorobenzyl,
1-4i: R^1X = butylthioxy, R^2 = 4-methylbenzyl,
1-4j: R^1X = butylthioxy, R^2 = propoxy

Scheme 1- 2: Re-synthesis of 2,5,6-trisubstituted benzimidazoles

Then, it turned out that the MIC values did not necessarily correlate with the percent inhibition at the fixed concentration of the test compounds, as anticipated. This would be due to, for example, inaccuracy in the actual weight and purity of a test compound in a 96-well plate, as well as false positives in the HTP screening. As **Table 1-3** shows, some of the hit compounds with a 4-fluorophenoxy or buthylthio group exhibit promising activities, but those with a 6-phenylthio or 6-benzylthio group appear to be less potent among the compounds examined so far.

Table 1- 3: MIC values of selected hit compounds against *Mtb* H37Rv[a] strain

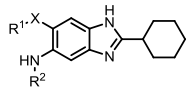

compound	R^1X	R^2	MIC (µg/mL) *Mtb* H37Rv	cytotocicity (µM) Vero Cells	compound	R^1X	R^2	MIC (µg/mL) *Mtb* H37Rv	cytotocicity (µM) Vero Cells
1-4a		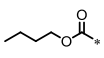	0.63	60 ± 7.2	**1-4f**		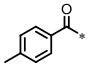	6.25	> 200
1-4b		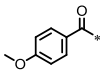	3.13	40 ± 8.5	**1-4g**		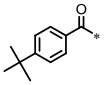	12.5	> 200
1-4c			1.56	26 ± 9.5	**1-4h**			1.25	> 200
1-4d			12.5	> 200	**1-4i**		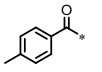	1.25	> 200
1-4e			12.5	> 200	**1-4j**			1.25	75 ± 21

[a] Mtb H37Rv: drug-sensitive strain

Although **1-4a**, bearing a n-butoxycarbonylamino group at the 5-position, was not among the 22 hit compounds, we added this compound for the MIC determination, since this carbamate group gave the best potency in the 6-dialkyamino series of 2,5,6-trisubstituted benzimidazoles in our another study, Indeed, **1-4a** exhibited the best potency (MIC 0.63 µg mL) against *Mtb* H37Rv in this series (**Table x**). The cytotoxicity of **1-4a** ~ **1-4j** was evaluated in vitro against Vero cells using the MTT assay. Compounds **1-4a**, **1-4b**, **1-4c** and **1-4j** showed cytotoxicity with IC_{50} values in the range of 26-75 µM. However, most of the analytically pure compounds did not show appreciable cytotoxicity against Vero cells.

§ 1.3 Conclusion

New library of 2,5,6-trisubstituted benzimidazoles bearing sulfide and ether linkage at the 6-position have been synthesized. Among 376 compounds from preliminary HTP screening, 108 benzimidazoles were active at 5 μg/mL concentration and 22 compounds were identified at less than 1 μg/mL concentration. A number of hit compounds have been identified against *Mtb* H37Rv strain with good MIC values in the range of 0.63-12.5 μg/mL. Further SAR study is necessary to obtain more detailed information for the substituent effects at 5 and 6-positions of the 2,5,6-trisubstituted benzimidazoles in this series. Nevertheless, 4-fluorophenoxy and butylthio groups were found to be preferred substituents at the 6-position. For the compounds, bearing a 4-fluorophenoxy group at the 6-position, a carbamate group at the 5-position gave the most potent compound (**1-4a**), but there is no difference between a carbamate group and benzamide groups for their potency (**1-4j** vs **1-4h** and **1-4i**) for the compounds, bearing a butylthio group at the 6-position. This is a unique feature in this series of benzimidazoles since a carbamate group at the 5-position provides, in general, more potent compounds than the corresponding 5- amidobenzimidazoles in the 5-dialkylamino-benzimidazole series. Further optimization and biological evaluation of the lead compounds will be carried out to investigate pathogen specific as well as broad spectrum antibacterial activities.

§ 1.4 Experimental Section

§ 1.4.1 General Methods

^{1}H and ^{13}C NMR spectra were measured on a Brucker 400 or 500 MHz NMR spectrometer. Melting points were measured on a Thomas Hoover Capillary melting point apparatus and are uncorrected. TLC was performed on Sorbtech with UV254 and column chromatography was carried out on silica gel 60 (Merck; 230-400 mesh ASTM). High-resolution mass spectra were obtained on Agilent-TOF instrument.

§ 1.4.2 Materials

The chemicals were purchased from Sigma Aldrich Co., Synquest Inc., Alfa Aesar and purified before use by standard methods. Tetrahydrofuran was freshly distilled from sodium metal and benzophenone. Dichloromethane was also distilled immediately prior to use under nitrogen from calcium hydride. Aminomethylated polystyrene resine EHL (200-400 mesh) 2 % DVB was purchased from Novagen Biochem.

§ 1.4.3 Experimental Procedures

2,4-Dinitro-5-ethoxyaniline (1-1a)

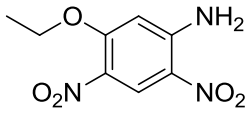

To a magnetically stirred solution of 2,4-dinitro-5-fluoroaniline (4.0 g, 19.9 mmol) in 50 mL of THF and excess ethanol was added 1 M KOH aqueous solution drop wise until a yellow precipitate appeared. The reaction mixture was stirred for additional 1 h. The solution was extracted with ethyl acetate. The organic layer was collected, dried over anhydrous magnesium sulfate and concentrated *in vacuo* to give **1-1a** as a yellow solid (4.8 g, 100 % yield): mp 162-165 °C; ^{1}H NMR (500 MHz, $CDCl_3$) δ1.53 (t, 3 H, *J* = 7.0 Hz), 4.18 (q, 2 H, *J* = 7.0 Hz), 6.23 (s, 1 H), 8.95 (s, 1 H); ^{13}C NMR (125 MHz, $CDCl_3$) δ 14.3, 66.1, 99.7, 127.2, 148.8, 158.1; HRMS (ESI) m/z calcd for $C_8H_{10}N_3O_5^+$ 228.0615 Found: 228.0615 (Δ = 0.0 ppm)

In a similar manner, intermediate **1-1b** and **1-1e** were synthesized and characterized.

5-Butoxy-2,4-dinitroaniline (1-1b)

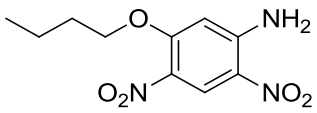

Yellow solid; 76 % yield; mp 176-178 °C; ^{1}H NMR (500 MHz, $CDCl_3$) δ 0.99 (t, 3 H, *J* = 7.4 Hz), 1.21-1.33 (m, 3 H), 1.41-1.46 (m, 2 H), 1.53 (dd, 2 H, *J* = 15.1, 7.5 Hz), 1.63-1.66 (m, 2 H), 1.75-1.78 (m, 2 H), 1.86 (t, 2 H, *J* = 7.6 Hz), 1.92-1.95 (m, 2 H), 2.32-2.36 (m, 1 H), 4.10 (t, 2 H, *J* = 6.4 Hz), 6.24 (s, 1 H), 8.95 (s, 1 H); ^{13}C NMR (125 MHz, $CDCl_3$) δ 13.7, 19.0, 25.3, 25.7, 28.8, 30.6, 42.8, 70.0, 99.7, 124.5, 127.2, 130.2, 148.8, 158.2; HRMS (ESI) m/z calcd for $C_{10}H_{14}N_3O_5^+$ 256.0928 Found: 256.0931 (Δ = 1.17 ppm).

2,4-Dinitro-5-phenoxyaniline (1-1c)

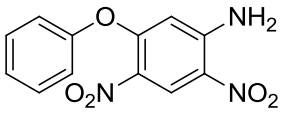

To a magnetically stirred solution of 2,4-dinitro-5-fluoroaniline 1 (3.0 g, 14.9 mmol) in 45 mL of acetone were phenol (1.68 g, 17.9 mmol) and anhydrous K_2CO_3 (4.12 g, 29.8 mmol). The reaction mixture was stirred mechanically at room temperature for at least 16 h until the total disappearance of 1 by MS (FIA) analysis. The solution was extracted with ethyl acetate. The organic layer was collected, dried over anhydrous magnesium sulfate, and concentrated in vacuo to give 2c as a yellow solid (3.7 g, 91 % yield): mp 148-150 °C; ^{1}H NMR (500 MHz, $CDCl_3$) δ 5.97 (s, 1 H), 7.56 (m, 3 H), 7.60 (dd, 2 H, *J* = 7.57, 1.83 Hz), 9.05 (s, 1 H); ^{13}C NMR (125 MHz, $CDCl_3$) δ 114.6, 126.4, 128.4, 129.7, 130.5, 130.9, 134.7, 136.2, 146.3, 148.7; HRMS (ESI) m/z calcd for $C_{12}H_{10}N_3O_5^+$ 276.0615 Found: 276.0622 (Δ = 2.54 ppm).

In a similar manner, intermediate **1-1d**, **1-1f**, **1-1g**, and **1-1h** were synthesized and characterized.

2,4-Dinitro-5-(4-fluorophenoxy)aniline (1-1d)

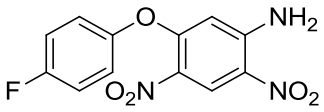

Yellow solid; 93% yield; mp 164- 165.5 ℃; ^{1}H NMR (500 MHz, $CDCl_3$) δ 6.01 (s, 1 H), δ 7.11-7.19 (m, 4 H), δ 9.05 (s, 1 H); ^{13}C NMR (125 MHz, $CDCl_3$) δ 103.7, 117.2, 117.4, 122.5, 122.6, 127.6, 148.5, 149.2, 157.8, 159.5, 161.5; HRMS (ESI) m/z calcd for $C_{12}H_9FN_3O_5^+$ 294.0521 Found: 294.0521 (Δ = 0.0 ppm)

5-(Butylthio)-2,4-dinitroaniline (1-1e)

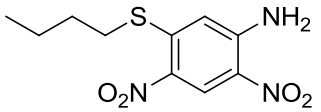

Yellow solid; 99% yield; mp 148- 149 ℃; ^{1}H NMR (400 MHz, $CDCl_3$) δ 0.99 (t, 3 H, *J* = 7.5 Hz), 1.53-1.57 (m, 2 H), 1.74-2.05 (m, 2 H), 2.01 (t, 2 H, *J* = 7.5 Hz), 6.55 (s, 1 H), 9.18 (s, 1 H); ^{13}C NMR (100 MHz, $CDCl_3$) δ 13.7, 22.3, 29.2, 32.4, 112.6, 126.6, 127.8, 135.4, 146.3, 147.8; HRMS (ESI) m/z calcd for $C_{10}H_{14}N_3O_4S^+$ 272.0700 Found: 272.0701 (Δ = 0.35 ppm)

2,4-Dinitro-5-(phenylthio)aniline (1-1f)

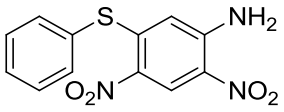

Yellow solid; 100% yield; mp 214-217 ℃; ^{1}H NMR (400 MHz, $CDCl_3$) δ 5.97 (s, 1 H), 7.21-7.24 (m, 3 H), 7.28-7.32 (m, 2 H), 9.02 (s, 1 H); ^{13}C NMR (100 MHz, $CDCl_3$) δ 126.4, 127.2, 127.5, 129.1, 130.5, 130.8, 136.2, 137.0; HRMS (ESI) m/z calcd for $C_{12}H_{10}N_3O_4S^+$ 292.0387 Found: 292.0387 (Δ = 0.0 ppm).

2,4-Dinitro-5-(4-fluorophenylthio)aniline (1-1g)

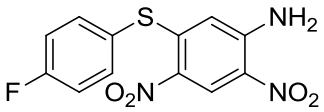

Yellow solid; 100 % yield; m,p 217-219 ℃; ^{1}H NMR (500 MHz, $CDCl_3$) δ 5.96 (s, 1 H), 7.04 (t, 1 H, *J* = 8.6 Hz), 7.27 (d, 1 H, *J* = 8.53), 7.49-7.46 (m, 1 H), 7.62 (dd, 1 H, *J* = 8.5, 5.3 Hz), 9.23 (s, 1 H); ^{13}C NMR (125 MHz, $CDCl_3$) δ 114.4, 116.2, 116.4, 117.8, 118.0, 126.5, 131.2, 131.3, 138.3, 138.4, 146.3; HRMS (ESI) m/z calcd for $C_{12}H_9FN_3O_4S^+$ 310.0292 Found: 310.0292 (Δ = 0.0 ppm).

5-(Benzylthio)-2,4-dinitroaniline (1-1h)

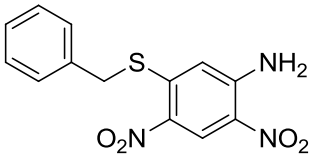

Yellow solid; 100 % yield; mp 188.5-190 ℃; ^{1}H NMR (400 MHz, $CDCl_3$) δ 4.17 (s, 2 H), δ 6.62 (s, 1 H), δ 7.36-7.44 (m, 5 H), 9.19 (s, 1 H); ^{13}C NMR (100 MHz, CDCl3) δ 37.8, 113.0, 126.5, 128.2, 129.0, 129.1, 133.7; HRMS (ESI) m/z calcd for $C_{12}H_{12}N_3O_4S^+$ 306.0543 Found: 306.0543 (Δ = 0.0 ppm).

1-(Cyclohexanecarboxamido)-5-ethoxy-2,4-dinitro-benzene (1-2a)

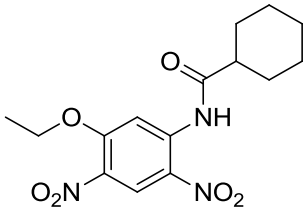

To a solution of **1-1a** (0.71 g, 3.13 mmol) in 12 mL of pyridine was added cyclohexanecarbonyl chloride (0.54 mL, 1.3 eq.), and the mixture was magnetically stirred and refluxed overnight. After completion of the reaction by TLC analysis, the reaction mixture was concentrated under reduced pressure and then washed with $CuSO_4$ solution twice to get rid of the leftover pyridine.

The reaction mixture was washed with brine and then diluted with ethyl acetate and dichloromethane, and washed with water three times. The organic layers were dried over sodium sulfate, filtered, and concentrated to afford **1-2a** as a yellow solid (0.9 g, 89 % yield): mp 109-109.5 ℃; ^{1}H NMR (400 MHz, $CDCl_3$) δ 1.28-1.31 (m, 1 H), 1.38-1.42 (m, 2 H), 1.51 (t, 3 H, *J* = 7.41 Hz), 1.59-1.60 (m, 2 H), 1.76-1.79 (m, 1 H), 1.88-1.93 (m, 2 H), 2.05-2.09 (m, 2 H), 2.44 (tt, 1 H, *J* = 11.6, 3.5 Hz), 3.12 (q, 2 H, *J* = 7.44 Hz), 9.19 (s, 1 H), 9.24 (s, 1 H), 10.9 (s, 1 H); ^{13}C NMR (100 MHz, $CDCl_3$) δ 12.2, 25.4, 25.5, 27.1, 29.4, 47.4, 116.9, 124.9, 130.7, 138.1, 149.7, 176.0; HRMS (ESI) m/z calcd for $C_{15}H_{20}N_3O_6^+$ 338.1347 Found: 338.1351 (Δ = 1.18 ppm).

In a similar manner, compounds **1-2b ~ 1-2h** were synthesized and characterized.

1-(Cyclohexanecarboxamido)-5-butoxy-2,4-dinitro-benzene (1-2b)

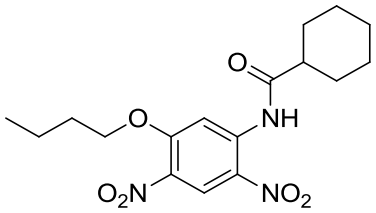

Yellow solid; 100 % yield; mp 187.5-189℃; ^{1}H NMR (500 MHz, $CDCl_3$) δ 0.99 (t, 3 H, *J* = 7.4 Hz), 1.21-1.33 (m, 3 H), 1.45 (d, 2 H, *J* = 11.5 Hz), 1.50-1.56 (m, 2 H), 1.6401.66 (m, 1 H), 1.75-1.78 (m, 2 H), 1.86 (dd, 2 H, *J* = 8.4, 6.8 Hz), 1.93 (d, 2 H, *J* = 12.8 Hz), 2.32-2.36 (m, 1 H), 4.09 (t, 2 H, J = 6.4 Hz), 6.24 (s, 1 H), 8.95 (s, 1 H);^{13}C NMR (125 MHz, $CDCl_3$) δ 13.7, 19.0, 25.3, 25.3, 28.8, 30.6, 42.8, 70.0, 99.7, 124.5, 127.2, 130.2, 148.8, 158.2; MS (ESI) *m/z* 366.1 (M+1).

1-(Cyclohexanecarboxamido)-5-phenoxyphenyl-2,4-dinitro-benzene (1-2c)

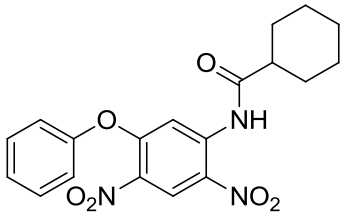

Yellow solid; 97 % yield; mp 150.5-152 ℃; ^{1}H NMR (400 MHz, $CDCl_3$) δ 1.21 (tt, 1 H, *J* = 12.3, 3.2 Hz), 1.26-1.35 (m, 2 H), 1.43 (qd, 2 H, *J* = 12.3, 3.1), 1.68-1.72 (m, 1 H), 1.81 (dt, 2 H, *J* = 13.1, 3.3 Hz), 1.95 (dd, 2 H, *J* = 13.5, 1.9 Hz), 2.23-2.33 (m, 1 H), 7.15-7.17 (m, 2 H), 7.35 (t, 1 H, *J* = 7.5 Hz), 7.49-7.52 (m, 2 H), 8.53 (s, 1 H), 9.06 (s, 1 H), 10.8 (s, 1 H); ^{13}C NMR (125 MHz, $CDCl_3$) δ 25.5, 29.3, 47.3, 108.8, 120.6, 121.6, 125.6, 126.7, 128.8, 129.4, 130.6, 133.2, 140.4, 153.2, 157.7, 175.4; HRMS (ESI) m/z calcd for $C_{19}H_{20}N_3O_6^+$ 386.1347 Found: 386.1345 (Δ = -0.52 ppm).

1-(Cyclohexanecarboxamido)-5-(4-fluorophenoxy)-2,4-dinitrobenzene (1-2d)

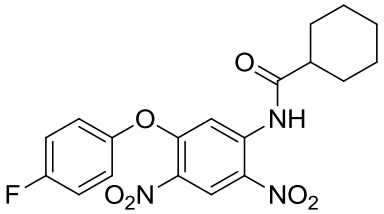

Yellow solid; mp 147-149 ℃; ^{1}H NMR (500 MHz, $CDCl_3$) δ 1.18-1.20 (m, 1 H), 1.27-1.32 (m, 2 H), 1.40 (d, 2 H, *J* = 11.6 Hz), 1.71 (dd, 1 H, *J* = 1.69, 1.42 Hz), 1.78-1.83 (m, 2 H), 1.90-1.94 (m , 2 H), 2.22-2.30 (m, 1 H), 7.23-2.30 (m, 2 H), 7.58-7.62 (m, 2 H), 8.47 (s, 1 H), δ 9.21 (s, 1 H), δ 10.6 (s, 1 H) ; ^{13}C NMR (125 MHz, $CDCl_3$) δ 25.2, 25.4, 29.1, 29.3, 47.2, 117.9, 118.1, 119.0, 123.9, 124.1, 124.7, 138.1, 138.2,150.4, 165.8, 174.8; MS (ESI) *m/z* 404.0 $(M+1)^+$.

1-(Cyclohexanecarboxamido)-5-(butylthio)-2,4-dinitro-benzene (1-2e)

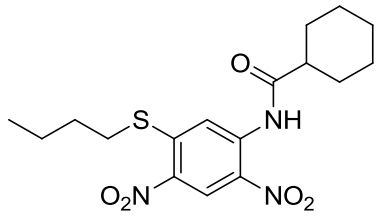

Yellow solid; 100 % yield; mp 118-119 ℃; ^{1}H NMR (500 MHz, $CDCl_3$) δ 0.99 (t, 3 H, *J* = 7.3 Hz), 1.25-1.32 (m, 1 H), 1.33-1.42 (m, 2 H), 1.55-1.59 (m, 4 H), 1.74-1.78 (m, 1 H), 1.80-1.83 (m, 2 H), 1.88 (dt, 2 H, *J* = 13.3, 3.4 Hz), 2.05 (dd, 2 H, *J* = 13.4, 2.2 Hz), 2.42 (tt, 1 H, *J* = 11.7,

3.5 Hz), 3.07 (t, 2 H, J = 7.3 Hz), 9.16 (s, 1 H), 9.21 (s, 1 H), 10.9 (s, 1 H); ^{13}C NMR (125 MHz, $CDCl_3$) δ 13.7, 22.1, 25.5, 29.5, 32.7, 47.5, 117.0, 124.9, 138.1, 150.0, 175.9; MS (ESI) *m/z* 382.1 $(M+1)^+$.

1-(Cyclohexanecarboxamido)-5-(phenylthio)phenyl-2,4-dinitrobenzene (1-2f)

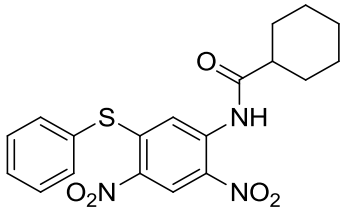

Yellow solid; 100 % yield; mp 217-218 ℃; ^{1}H NMR (400 MHz, $CDCl_3$) δ 1.18-1.22 (m, 2 H), 1.24-1.32 (m, 2 H), 1.37(qd, 2 H, *J* = 12.2, 2.8 Hz), 1.67 (dd, 1 H, *J* = 12.8, 0.8 Hz), 1.78-1.82 (m, 2 H), 1.89-1.92 (m, 2 H), 2.24 (tt, 1 H, *J* = 11.7, 3.5 Hz), 7.60 (q, 5 H, *J* = 6.1 Hz), 8.46 (s, 1 H), 9.22 (s, 1 H), 10.6 (s, 1 H); ^{13}C NMR (100 MHz, CDCl3) δ 25.4, 29.3, 30.9, 47.3, 119.1, 124.7, 128.6, 130.6, 131.1, 135.9, 137.5, 138.0, 150.7, 174.8; MS (ESI) *m/z* 402.1 $(M+1)^+$.

1-(Cyclohexanecarboxamido)-5-(4-fluorophenylthio)-2,4-dinitrobenzene (1-2g)

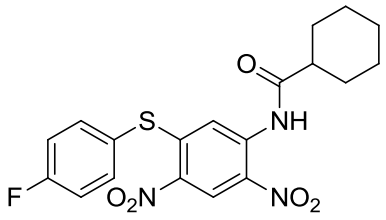

Yellow solid; 96 % yield; mp 186-189 ℃; ^{1}H NMR (400 MHz, $CDCl_3$) δ 1.16-1.23 (m, 1 H), 1.25-1.31 (m, 2 H), 1.34-1.42 (m, 2 H), 1.68-1.74 (m, 1 H), 1.79-1.83 (m, 2 H), 1.94 (dd, 2 H, *J* = 12.9, 2.1 Hz), 2.25-2.31 (m, 1 H), 7.25-7.29 (m, 2 H), 7.62 (dd, 2 H, *J* = 8.8, 5.2 Hz), 8.49 (s, 1 H), 9.24 (s, 1 H), 10.6 (s, 1 H); ^{13}C NMR (100 MHz, $CDCl_3$) δ 25.5, 29.3, 31.0, 47.3, 119.1, 124.7, 128.7, 130.6, 131.1, 131.5, 135.9, 137.6, 138.1, 150.8, 174.8; MS (ESI) *m/z* 420.1 $(M+1)^+$.

1-(Cyclohexanecarboxamido)-5-(benzylthio)-2,4-dinitro-benzene (1-2h)

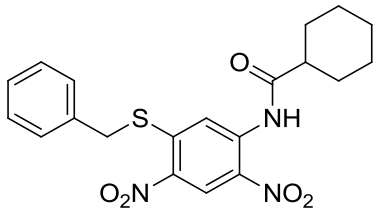

Yellow solid; 96 % yield: mp 150-153 °C; ^{1}H NMR (500 MHz, $CDCl_3$) δ 1.27-1.30 (m, 1 H), 1.37-1.44 (m, 2 H), 1.52-1.62 (m, 2 H), 1.74-1.77 (m, 1 H), 1.87-1.90 (m, 2 H), 2.04-2.07 (m, 2 H), 2.39-2.47 (m, 1 H), 4.30 (s, 2 H), 7.26-7.37 (m, 3 H), 7.45 (d, 2 H, *J* = 6.8 Hz), 9.21 (s, 1 H), 9.29 (s, 1 H), 10.9 (s, 1 H); ^{13}C NMR (125 MHz, $CDCl_3$) δ 25.4, 25.5, 29.4, 38.1, 43.3, 47.4, 117.1, 124.8, 127.4, 128.2, 128.5, 128.8, 129.4, 129.6, 130.9, 133.5, 137.4, 138.1, 138.2, 149.1, 175.9; MS (ESI) *m/z* 416.0 $(M+1)^+$.

5-Amino-6-ethoxy-2-cyclohexyl-1H-benzo[d]imidazol (1-3a)

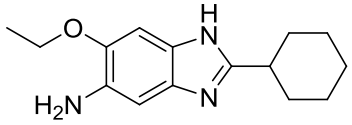

A solution of **1-2a** (100 mg, 0.30 mmol), tin(II) chloride dihydrate (0.47 g, 2.1 mmol) in 10 mL of EtOH was magnetically stirred and refluxed at 90 ^{o}C under nitrogen for 1 h. The reaction mixture was cooled, quenched with 30 % KOH, and pH adjusted to ~13. The solution was diluted with dichloromethane and washed with water three times. The organic layers were dried over sodium sulfate, filtered, and concentrated. The residue was purified by flash chromatography on silica gel (gradient 20-40 % EtOAc/hexanes) to afford compound **1-3a** as a pale red color solid (69 g, 89 % yield): mp 89-90 °C; ^{1}H NMR (500 MHz, $CDCl_3$) δ 1.23 (ddd, 1 H, *J* = 14.2, 10.8, 3.3 Hz), 1.32 (ddd, 2 H, *J* = 14.2, 11.1, 3.1 Hz), 1.37-1.42 (m, 3 H), 1.60 (qd, 2 H, *J* = 12.4, 3.1 Hz), 1.69-1.71 (m, 1 H), 1.79-1.81 (m, 2 H), 2.08 (d, 2 H, *J* = 12.4 Hz), 2.80 (tt, 1 H, *J* = 11.8, 3.51 Hz), 3.79 (br, 2 H), 3.99 (dd, 2 H, *J* = 8.3, 3.3 Hz), 6.78 (s, 1 H), 6.96 (s, 1 H); ^{13}C NMR (125 MHz, $CDCl_3$) δ 15.0, 25.9, 26.1, 32.0, 38.5, 64.4, 132.9, 133.0, 144.5, 157.0; HRMS (ESI) m/z calcd for $C_{15}H_{22}N_3O^+$ 260.1757 Found: 260.1758 (Δ = 0.38 ppm).

In a similar manner, compounds **1-3b** ~ **1-3d** were synthesized and characterized.

5-Amino-6-butoxy-2-cyclohexyl-1H-benzo[d]imidazol (1-3b)

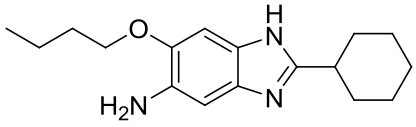

Reddish solid; 69 % yield; mp 113-115 ℃; ^{1}H NMR (400 MHz, $CDCl_3$) δ 0.97 (t, 3 H, *J* = 7.4 Hz), 1.23-1.28 (m, 1 H), 1.35-1.40 (m, 2 H), 1.50 (dd, 2 H, *J* = 15.0, 7.5 Hz), 1.60 (qd, 2 H, *J* = 12.4, 3.2 Hz), 1.70-1.75 (m, 1 H), 1.76-1.86 (m, 4 H), 2.08-2.12 (m, 2 H), 2.78-2.84 (m, 1 H), 3.76 (br, 2 H), 3.98 (t, 2 H, *J* = 6.5 Hz), 6.80 (s, 1 H), 7.00 (s, 1 H); ^{13}C NMR (100 MHz, $CDCl_3$) δ 13.9, 19.4, 25.9, 26.1, 31.4, 32.0, 38.4, 68.6, 133.1, 144.6, 156.7; HRMS (ESI) m/z calcd for $C_{17}H_{26}N_3O^+$ 288.2070 Found: 288.2071 (Δ = 0.35 ppm).

5-Amino-6-phenoxy-2-cyclohexyl-1H-benzo[d]imidazol (1-3c)

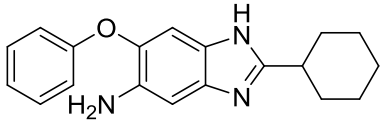

Pale yellow solid; 46 % yield; mp 136-138 ℃; ^{1}H NMR (400 MHz, $CDCl_3$) δ 1.25-1.32 (m, 1 H), 1.35-1.44 (m, 2 H), 1.56-1.66 (m, 2 H), 1.72-1.77 (m, 1 H), 1.83-1.88 (m, 2 H), 2.09-2.14 (m, 2 H), 2.80-2.86 (m, 1 H), 3.73 (br, 2 H), 6.93-6.97 (m, 2 H), 7.01-7.05 (m, 1 H), 7.12 (s, 1 H), 7.26-7.29 (m, 2 H); ^{13}C NMR (100 MHz, $CDCl_3$) δ 25.9, 26.0, 31.9, 38.5, 116.7, 122.4, 129.7, 135.3, 140.3, 158.1; HRMS (ESI) m/z calcd for $C_{19}H_{22}N_3O^+$ 308.1757 Found: 308.1758 (Δ = 0.32 ppm).

5-Amino-6-(4-fluorophenoxy)-2-cyclohexyl-1H-benzo-[d]imidazol (1-3d)

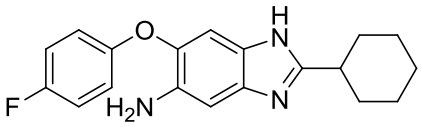

Beige solid; 70 % yield; mp 195-196 ℃; ^{1}H NMR (400 MHz, $CDCl_3$) δ 1.26-2.30 (m, 1 H), 1.38-1.43 (m, 2 H), 1.61 (dd, 2 H, *J* = 12.4, 3.1 Hz), 1.72-1.77(m, 1 H), 1.86 (dt, 2 H, *J* = 13.1, 3.3 Hz), 2.12 (dd, 2 H, *J* = 13.6, 2.0 Hz), 2.83 (tt, 1 H, *J* = 11.8, 3.6 Hz), 3.74 (br, 2 H), 6.95 (m, 5 H), 8.89 (s, 1 H); ^{13}C NMR (100 MHz, $CDCl_3$) δ 25.8, 26.0, 31.8, 38.5, 116.0, 116.2, 118.1, 118.2, 154.0, 157.1, 159.5; HRMS (ESI) m/z calcd for $C_{19}H_{23}FN_3O^+$ 326.1663 Found: 326.1667 (Δ = 1.2 ppm).

5-Amino-6-(butylthio)-2-cyclohexyl-1H-benzo[d]-imidazol (1-3e)

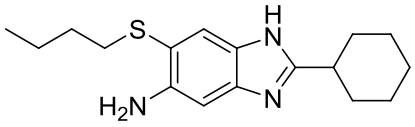

A solution of **1-2e** (1.97 g, 5.16 mmol), tin(II) chloride dihydrate (15.5 g, 36.1 mmol), and 4 M HCl (80 mL) in 200 mL of EtOH was magnetically stirred and refluxed for 4 h. The reaction mixture was cooled, quenched with 1M NaOH, and pH was adjusted to ~10. Tin salts precipitated in solution upon addition of 1 M NaOH. The reaction mixture was filtered to remove the tin salts. The solution was diluted with ethyl acetate and washed with water three times. The organic layers were dried over magnesium sulfate, filtered, and concentrated in vacuo. The residue was purified by flash chromatography on silica gel (gradient 20-40 % EtOAc/hexanes) to afford compound **4e** as a pale greenish gray solid (0.413g): 71 % yield; mp 110-112 ℃; ^{1}H NMR 500 MHz, $CDCl_3$) δ 0.88 (t, 3 H, J = 7.3 Hz), 1.25-1.30 (m, 1 H), 1.36-1.42 (m, 4 H), 1.55 (dt, 2 H, *J* = 14.0, 7.4 Hz), 1.64 (qd, 2 H, *J* = 12.4, 3.2 Hz), 1.72-1.76 (m, 1 H), 1.85 (dt, 2 H, *J* = 13.2, 3.3 Hz), 2.13 (dd, 2 H, *J* = 13.7, 1.9 Hz), 2.72 (t, *J* = 7.4 Hz), 2.86 (tt, 1 H, *J* = 11.8, 3.5 Hz), 4.35 (br, 2 H), 6.83 (s, 1 H), 7.66 (s, 1 H); ^{13}C NMR (100 MHz, $CDCl_3$) δ 13.7, 21.9, 25.8, 26.0, 31.6, 31.9, 35.5, 38.5, 114.5, 144.0, 158.8; HRMS (ESI) m/z calcd for $C_{17}H_{26}N_3S$+ 304.1842 Found: 304.1842 (Δ = 0.0 ppm).

In a similar manner, compounds **1-3f** ~ **1-3h** were synthesized and characterized.

5-Amino-6-(phenylthio)-2-cyclohexyl-1H-benzo[d]-imidazol (1-3f)

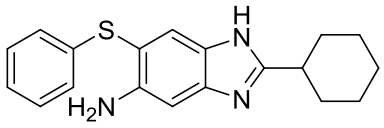

Brownish solid; 57 % yield; mp 116-118 ℃; ^{1}H NMR (500 MHz, $CDCl_3$) δ 1.27-1.35 (m, 1 H), 1.42 (qt, 2 H, *J* = 12.79, 3.29 Hz), 1.66 (qd, 2 H, *J* = 12.4, 3.29 Hz), 1.76-1.80 (m, 1 H), 1.89 (dt, 2 H, *J* = 13.3, 3.38 Hz), 2.16 (dd, 2 H, *J* = 13.7, 2.01 Hz), 2.88 (tt, 1 H, *J* = 11.8, 3.55 Hz), 4.22 (br, 2 H), 6.92 (s, 1 H), δ 7.08-7.13 (m, 3 H), δ 7.20-7.23 (m, 2 H), δ 7.67 (s, 1 H); ^{13}C NMR (125 MHz, $CDCl_3$) δ 25.8, 26.0, 31.8, 38.5, 110.6, 125.3, 126.1, 128.9, 137.6, 144.6; HRMS (ESI) m/z calcd for $C_{19}H_{22}N_3S^+$ 324.1529 Found: 324.1529 (Δ = 0.0 ppm).

5-Amino-6-(4-fluorophenylthio)-2-cyclohexyl-1H-benzo[d]-imidazol (1-3g)

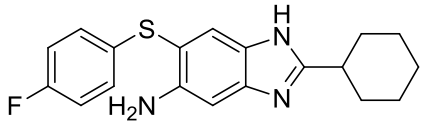

Pale green solid; 61 % yield; mp 107-108 ℃; ; ^{1}H NMR (500 MHz, $CDCl_3$) δ 1.25 (ddd, 1 H, *J* = 13.8, 7.1, 3.6 Hz), 1.33-1.40 (m, 2 H), 1.62 (qd, 2 H, *J* = 12.4, 3.1 Hz), 1.71-1.74 (m, 1 H), 1.82-1.84 (m, 2 H), 2.85 (tt, 1 H, *J* = 11.8, 3.5 Hz), 6.86-6.89 (m, 3 H), 7.02-7.05 (m, 2 H), 7.70 (s, 1 H); ^{13}C NMR (125 MHz, $CDCl_3$) δ 25.8, 26.0, 31.8, 38.5, 98.8, 111.2, 115.9, 116.1, 124.2, 128.2, 132.4, 144.4, 159.3, 160.2, 162.1; HRMS (ESI) m/z calcd for $C_{19}H_{22}N_3S^+$ 342.1435 Found: 342.1435 (Δ = 0.0 ppm).

5-Amino-6-(benzylthio)-2-cyclohexyl-1H-benzo[d]-imidazol (1-3h)

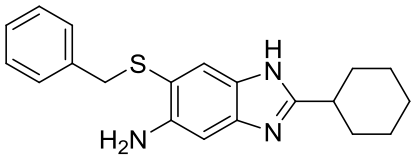

Pale beige solid; 56 % yield; mp 129.5-131 °C; ^{1}H NMR (500 MHz, $CDCl_3$) δ 1.18-1.23 (m, 1 H), 1.27-1.35 (m, 2 H), 1.60 (qd, 2 H, *J* = 12.4, 3.2 Hz), 1.69 (d, 1 H, *J* = 12.7 Hz), 1.78 (dt, 2 H, J = 13.1, 3.0 Hz), 2.07 (dd, 2 H, *J* = 14.2, 2.5 Hz), 2.80-1.85 (m, 1 H), 3.86 (s, 2 H), 6.77 (s, 1 H), 7.10-7.12 (m, 2 H), 7.17 (td, 3 H, *J* = 6.5, 2.8 Hz), 7.49 (s, 1 H); ^{13}C NMR (125 MHz, $CDCl_3$) δ 25.7, 26.0, 31.7, 38.4, 40.7, 64.4, 98.4, 114.0, 123.1, 126.9, 128.3, 128.7, 132.8, 138.2, 139.1, 144.2, 159.1, 176.3; HRMS (ESI) m/z calcd for $C_{20}H_{24}N_3S^+$ 338.1685 Found: 338.1686 (Δ = 0.3 ppm).

5-Butoxycarbonylamino-2-cyclohexyl-6-(4-fluorophenoxy)-1H-benzo[d]imidazole (1-4a)

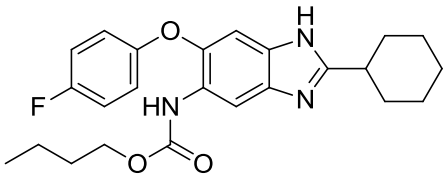

To a solution of **1-3a** (100 mg, 0.31 mmol) in 6 mL of dichloromethane was added *N*-butoxycarbonyloxysuccinimide (68 mg, 0.31 mmol) in 6 mL of dichloromethane and the mixture was magnetically stirred under nitrogen atmosphere in an ice bath. The reaction mixture was slowly warmed up to room temperature and stirred for 16 h. The solution was diluted with dichloromethane and basified with $NaHCO_3$ and then washed with water three times. The organic layers were dried over sodium sulfate, filtered, and concentrated. The residue was purified by flash chromatography on silica gel (gradient 20-40 % EtOAc/hexanes) to afford compound **1-4a** as an off-white solid (54 mg, 47 % yield): mp 91-92 °C; ^{1}H NMR (400 MHz, $CDCl_3$) 0.97 (t, 3 H, *J* = 7.4 Hz), 1.28-1.30 (m, 1 H), 1.39-1.45 (m, 4 H), 1.61-1.65 (m, 2 H), 1.67 (t, 2 H, *J* = 7.5 Hz), 1.76 (d, 1 H, *J* = 12.5 Hz), 1.85-1.88 (m, 2 H), 2.12 (d, 2 H, *J* = 12.5 Hz), 2.83-2.88 (m, 1 H), 4.19 (t, 2 H, *J* = 6.7 Hz), 6.96-7.05 (m, 4 H), 7.13 (s, 1 H), 8.23 (s, 1 H); ^{13}C NMR (100 MHz, $CDCl_3$) δ 13.8, 19.1, 25.8, 26.0, 31.0, 31.8, 38.5, 65.3, 116.5, 119.5, 125.6, 142.3, 153.1, 154.0, 157.8, 159.5, 159.6, 159.7; HRMS (ESI) m/z calcd for $C_{24}H_{29}FN_3O_3^+$ 426.2187 Found: 426.2187 (Δ = 0.0 ppm).

In a similar manner, compound **1-4j** was synthesized and characterized.

6-(Butylthio)-2-cyclohexyl-5-propoxycarbonylamino-1H-benzo[d]imidazole (1-4j)

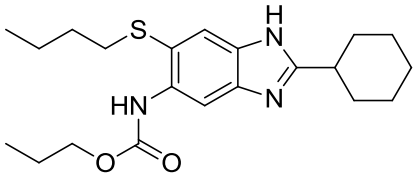

Off-white solid; 62 % yield; mp 133-134.5 °C; ^{1}H NMR (500 MHz, $CDCl_3$) δ 0.87 (t, 3 H, *J* = 7.32 Hz), 1.00 (t, 3 H, *J* = 7.43 Hz), 1.30 (dt, 1 H, *J* = 3.51, 12.5 Hz), 1.38-1.43 (m, 3 H), 1.50-1.53 (m, 2 H), 1.59-1.67 (m, 4 H), 1.74 (q, 2 H, *J* = 7.11 Hz), 1.88 (dt, 2 H, *J* = 3.41, 13.3 Hz), 2.13 (dd, 2 H, *J* = 2.29, 13.4 Hz), 2.69 (t, 2 H, *J* = 7.35 Hz), 2.84-2.89 (m, 1 H), 4.26 (t, 2 H, *J* = 6.74 Hz), 7.88 (s, 1 H), 8.20 (s, 1 H), 8.27 (s, 1 H), 8.95 (s, 1 H); ^{13}C NMR (125 MHz, $CDCl_3$) δ 10.4, 13.6, 21.8, 22.3, 25.8, 26.0, 29.7, 31.4, 31.7, 36.9, 38.4, 66.8, 98.5, 100.2, 126.5, 126.6, 134.9, 153.9; HRMS (ESI) m/z calcd for $C_{21}H_{32}N_3O_2S^+$ 390.2210 Found: 390.2214 (Δ = 1.0 ppm).

2-Cyclohexyl-6-(4-fluorophenoxy)-5-(4-methoxy-benzamido)-1H-benzo[d]imidazole (1-4b)

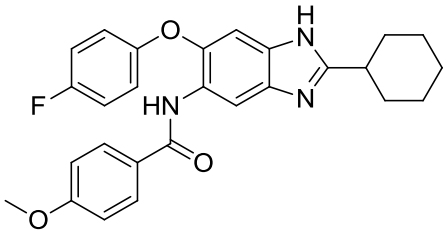

To a solution of **1-3d** (100 mg, 0.31 mmol) in 6 mL of dichloromethane was added 4-methoxybenzoyl chloride (42 μL, 0.31 mmol) in 6 mL of dichloromethane, and magnetically stirred in the ice bath. The reaction mixture was slowly warmed up to room temperature and stirred for 16 h. The solution was diluted with dichloromethane, basified with $NaHCO_3$ and then washed with water three times. The organic layers were dried over sodium sulfate, filtered, and concentrated. The residue was purified by flash chromatography on silica gel (gradient 20-40 % EtOAc/hexanes) to afford compound **1-4b** as an off-white solid (152 mg, 92 % yield): mp > 230 °C; ^{1}H NMR (400 MHz, $CDCl_3$) δ 1.22-1.33 (m, 3 H), 1.59 (dd, 2 H, *J* = 12.1, 2.9 Hz), 1.68-1.71 (m, 1 H), 1.78-1.81 (m, 2 H), 2.01-2.08 (m, 2 H), 2.76-2.82 (m, 1 H), 3.87 (s, 3 H), 6.96 (d,

2 H, *J* = 8.8 Hz), 7.03 (d, 3 H, *J* = 6.3 Hz), 7.78 (d, 2 H, *J* = 8.8 Hz), 8.55 (s, 1 H), 8.83 (s, 1 H), 9.81 (s, 1 H); ^{13}C NMR (100 MHz, $CDCl_3$) δ 13.8, 19.1, 25.8, 26.0, 31.0, 31.8, 38.5, 65.3, 116.5, 119.5, 125.6, 142.3, 153.1, 154.0, 157.8, 159.5, 159.6, 159.8; HRMS (ESI) m/z calcd for $C_{27}H_{27}FN_3O_3^+$ 460.2031 Found: 460.2028 (Δ = -0.7 ppm).

In a similar manner, compounds **1-4c ~ 1-4g** were synthesized and characterized.

2-Cyclohexyl-6-(4-fluorophenoxy)-5-(4-methxyl-benzamido)-1H-benzo[d]imidazole (1-4c)

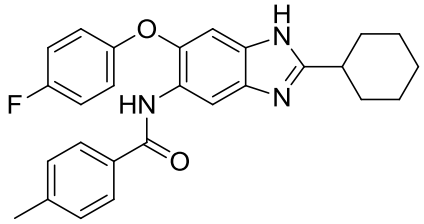

Off-white solid; 47 % yield; mp 166-168 ℃; ^{1}H NMR (500 MHz, $CDCl_3$) δ 1.81-1.23 (m, 1 H), 1.26-1.34 (m, 2 H), 1.56-1.64 (qd, 2 H, *J* = 12.4, 2.6 Hz), 1.71 (m, 1 H), 1.78-1.81 (d, 2 H, *J* = 12.8 Hz), 2.01 (dd, 2 H, *J* = 12.5, 0.6 Hz), 2.45 (t, 3 H), 2.79 (t, 1 H, *J* = 11.5 Hz), 7.05 (d, 3 H, *J* = 6.4 Hz), 7.24 (s, 1 H), 7.31 (d, 2 H, *J* = 7.8 Hz), 7.74 (d, 2 H, *J* = 8.1 Hz), 8.63 (s, 1 H), 8.90 (s, 1H), 10.2 (s, 1 H); ^{13}C NMR (100 MHz, $CDCl_3$) δ 21.5, 25.7, 25.9, 29.7, 31.7, 38.5, 116.4, 116.6, 119.4, 119.5, 125.3, 126.9, 132.2, 142.6, 153.0, 153.1, 137.9, 159.9, 160.2, 165.8; HRMS (ESI) m/z calcd for $C_{27}H_{27}FN_3O_2^+$ 442.2082 Found: 442.2082 (Δ = 0.0 ppm).

2-Cyclohexyl-5-(2,4-difluorobenzamido)-6-(4-fluorophenoxy)-1H-benzo[d]imidazole (1-4d)

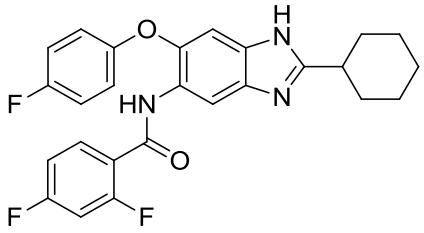

Off-white solid; 92 % yield; mp 184-185 ℃; ^{1}H NMR (500 MHz, $CDCl_3$) 0.83-0.88 (m, 1 H), 1.25-1.32 (m, 2 H), 1.59 (dd, 2 H, *J* = 12.3, 3.0 Hz), 1.68-1.70 (m, 1 H), 1.78-1.80 (m, 2 H), 2.07

(d, 2 H, *J* = 12.8 Hz), 2.80-2.84 (m, 1 H), 6.90 (ddd, 1 H, *J* = 11.7, 8.8, 2.6 Hz), 6.99 (d, 3 H, *J* = 6.3 Hz), 7.02-7.06 (m, 1 H), 7.21 (s, 1 H), 8.21 (td, 1 H, *J* = 8.9, 6.6 Hz), 8.81 (s, 1 H), 9.26 (d, 1 H, *J* = 15.7 Hz); ^{13}C NMR (100 MHz, $CDCl_3$) δ 25.9, 26.2, 31.9, 38.2, 101.1, 105.2, 112.5, 112.6, 112.7, 116.5, 116.7, 120.8 120.9, 126.4, 128.8, 138.4, 144.8, 151.7, 158.4, 161.0, 163.1; HRMS (ESI) m/z calcd for $C_{26}H_{23}F_3N_3O_2^+$ 466.1737 Found: 466.1743 (Δ = 1.29 ppm).

2-Cyclohexyl-6-(4-fluorophenoxy)-5-(pent-4-enimido)- 1H-benzo[d]imidazole (1-4e)

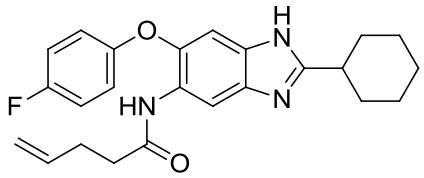

White solid; 63 % yield; mp 180.5-181.5 ℃; ^{1}H NMR (500 MHz, $CDCl_3$) δ 1.24-1.30 (m, 2 H), 1.36-1.44 (m, 2 H), 1.59-1.64 (m, 2 H), 1.73-1.76 (m, 1 H), 1.86 (dq, 2 H, *J* = 3.34, 9.98 Hz), 2.11 (dd, 2 H, *J* = 2.28, 13.3 Hz), 2.48 (dt, 3 H, *J* = 5.88, 11.7 Hz), 2.82-2.87 (m, 1 H), 4.99 (d, 1 H, *J* = 10.2 Hz), 5.07 (d, 1 H, *J* = 16.1 Hz), 5.82 (ddt, 1 H, *J* = 6.27, 10.5, 16.9 Hz), 6.95-7.04 (m, 3 H), 7.17 (s, 1 H), 7.87 (s, 1 H), 8.58 (s, 1 H), 9.58 (s, 1 H); ^{13}C NMR (125 MHz, $CDCl_3$) δ 14.2, 25.8, 26.0, 29.5, 31.7, 37.3, 38.5, 60.4, 102.7, 108.0, 116.1, 116.3, 116.5, 119.5, 125.2, 136.4, 142.4,157.9, 159.8, 170.7; HRMS (ESI) m/z calcd for $C_{24}H_{26}FN_3O_2^+$ 408.2082 Found: 408.2090 (Δ = 1.96 ppm).

2-Cyclohexyl-5-(4-methxylbenzamido)-6-(phenylthio)-1H-benzo[d]imidazole (1-4f)

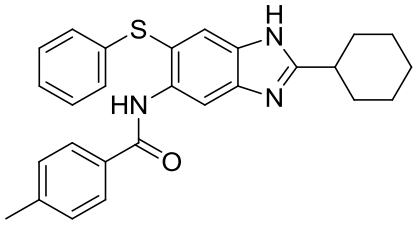

Off-white solid; 79 % yield; mp 184.5-186 ℃; ^{1}H NMR (500 MHz, $CDCl_3$) δ 1.06-1.20 (m, 3 H), 1.53-1.63 (m, 3 H), 1.70 (d, 2 H, *J* = 9.5 Hz), 2.00 (d, 2 H, *J* = 11.3 Hz), 2.44 (s, 3 H), 2.73 (t, 1

H, *J* = 9.6 Hz), 7.14 (t, 2 H, *J* = 7.62 Hz), 7.22-7.27 (m, 4 H), 7.59 (d, 2 H, *J* = 8.0 Hz), 8.06 (s, 1 H), 9.01 (s, 1 H), 9.39 (s, 1 H), 11.0 (s, 1 H);^{13}C NMR (125 MHz, $CDCl_3$) δ 21.5, 25.6, 25.9, 29.7, 31.6, 38.5, 103.3, 113.6, 126.0, 126.3, 126.4, 126.9, 129.0, 129.3, 129.6, 132.2, 134.2, 136.6, 142.6, 160.9, 166.1; HRMS (ESI) m/z calcd for $C_{26}H_{34}N_3OS^+$ 436.2417 Found: 436.2417 (Δ = 0.0 ppm).

6-(Benzylthio)-2-cyclohexyl-5-(4-(*tert*-butyl)benzamido)-1H-benzo[d]imidazole (1-4g)

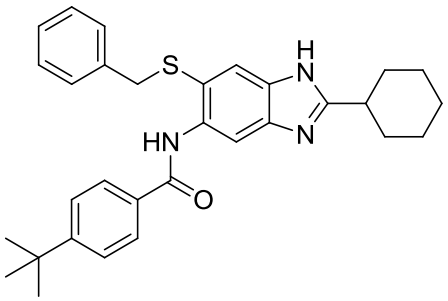

Off-white solid; 92 % yield; mp 173-173.5 °C; ^{1}H NMR (500 MHz, $CDCl_3$) δ 1.06-1.23 (m, 3 H), 1.40 (s, 9 H), 1.51-1.59 (m, 3 H), 1.68 (d, 2 H, *J* = 11.3 Hz), 1.97 (d, 2 H, *J* = 11.8 Hz), 2.67-2.72 (m, 1 H), 3.90 (s, 2 H), 6.98 (dd, 2 H, *J* = 7.1, 2.3 Hz), 7.04 (dd, 3 H, *J* = 5.0, 1.9 Hz), 7.52 (d, 2 H, *J* = 8.4 Hz), 7.70 (d, 2 H, *J* = 8.4 Hz), 7.96 (s, 1 H), 8.93 (s, 1 H), 9.38 (s, 1 H), 11.1 (s, 1 H); ^{13}C NMR (125 MHz, $CDCl_3$) δ 25.6, 25.9, 31.2, 31.7, 35.1, 38.5, 43.4, 102.2, 116.4, 125.8, 126.9, 127.1, 127.3, 128.5, 132.3, 135.3, 138.0, 140.2, 155.5, 160.8, 165.8; HRMS (ESI) m/z calcd for $C_{31}H_{36}N_3OS^+$ 498.2574 Found: 498.2574 (Δ = 0.0 ppm).

6-(Butylthio)-5-(2,4-difluorobenzamido)-2-cyclohexyl-1H-benzo[d]imidazole (1-4h)

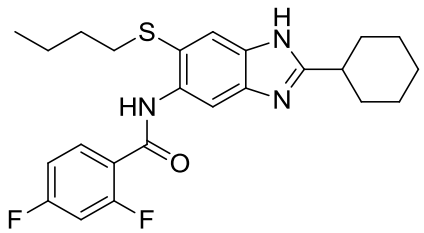

Off-white solid; 93 % yield; mp 170-170.5 °C; ^{1}H NMR (400 MHz, $CDCl_3$) δ 0.83 (t, 3 H, *J* = 7.33 Hz), 1.17-1.29 (m, 3 H), 1.36 (dd, 2 H, *J* = 15.0, 7.37 Hz), 1.49-1.60 (m, 4 H), 1.67 (d, 1 H, *J* = 12.1 Hz), 1.77 (d, 2 H, *J* = 12.3 Hz), 2.06 (d, 2 H, *J* = 11.9 Hz), 2.73 (t, 2 H, *J* = 7.42 Hz), 2.79 (m, 1 H), 6.96-7.09 (m, 2 H), 7.93 (s, 1 H), 8.23 (td, 1 H, *J* = 8.85, 6.54 Hz), 8.87 (s, 1 H), 10.1 (s, 1 H), 10.3 (s, 1 H); ^{13}C NMR (100 MHz, $CDCl_3$) δ 13.6, 21.7, 25.7, 25.9, 31.3, 31.7, 37.0, 38.5, 104.7, 112.5, 112.7, 117.8, 118.3, 118.4, 133.8, 134.3, 160.5; HRMS (ESI) m/z calcd for $C_{24}H_{28}F_2N_3OS^+$ 444.1916 Found: 444.1922 (Δ = 1.35 ppm).

6-(Butylthio)-5-(4-metylbenzamido)-2-cyclohexyl-1H-benzo[d]imidazole (1-4i)

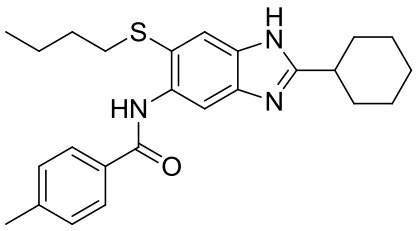

Off-white solid; 34 % yield; mp 155-156 °C; ^{1}H NMR (400 MHz, $CDCl_3$) δ 0.81 (t, 3 H, *J* = 7.38 Hz), 1.05-1.15 (m, 3 H), 1.24 (s, 1 H), 1.34 (q, 2 H, *J* = 7.34 Hz), 1.49-1.60 (m, 4 H), 1.66 (d, 2 H, *J* = 12.1 Hz), 1.97 (d, 2 H, 11.9 Hz), 2.46 (s, 3 H), 2.71-2.75 (m, 3 H), 7.36 (d, 2 H, *J* = 7.79 Hz), 7.92 (d, 3 H, *J* = 7.73 Hz), 8.99 (s, 1 H), 9.84 (s, 1 H), 11.4 (s, 1 H); ^{13}C NMR (100 MHz, $CDCl_3$) δ; 13.5, 21.5, 21.8, 25.5, 25.8, 29.6, 31.4, 31.6, 37.2, 38.4, 102.7, 117.1, 126.2, 127.0, 129.7, 132.3, 133.8, 135.2, 140.1, 142.6, 160.7, 165.7; HRMS (ESI) m/z calcd for $C_{25}H_{32}N_3OS^+$ 422.2261 Found: 422.2265 (Δ = 0.9 ppm).

§ 1.4.4 Bacterial Strains and Growth

For evaluation of drug sensitivity, *Mtb* H37Rv was grown in 7H9 media containing 10% oleic acid/albumin/catalase (OADC) enrichment and 0.05% Tween-80 and assessed at mid log phase growth.

§ 1.4.5 Antibacterial Activity Determination

The minimum inhibitory concentration (MIC) was determined by the microplate Alamar Blue assay (MABA)[39] as described previously. Briefly, stock solutions of the compounds were prepared in DMSO and were serially diluted 2-fold in 96-well microtiter plates, and *Mtb* H37Rv strain was added to each well to an OD600 of 0.005. Plates were incubated for 6 days at 37 ℃. Alamar Blue (Invitrogen) was added to the plates, and the plates were incubated for an additional 24 h at 37 ℃. Plates were monitored for color change, and MIC_{99} was determined in triplicate.

§ 1.5 References

1. Global tuberculosis report 2013, World Health Organization. *http://apps.who.int/iris/bitstream/10665/75938/10661/9789241564502_eng.pdf*, **2013**.
2. Pasqualoto, K. F.; Ferreira, E. I., An approach for the rational design of new antituberculosis agents. *Current drug targets,* **2001,** *2* (4), 427-437.
3. Gill, W. P.; Harik, N. S.; Whiddon, M. R.; Liao, R. P.; Mittler, J. E.; Sherman, D. R., A replication clock for Mycobacterium tuberculosis. *Nature medicine,* **2009,** *15* (2), 211-214.
4. Schluger, N. W.; Rom, W. N., The host immune response to tuberculosis. *American journal of respiratory and critical care medicine,* **1998,** *157* (3 Pt 1), 679-691.
5. Bishai, W., Lipid lunch for persistent pathogen. *Nature,* **2000,** *406* (6797), 683-685.
6. Huang, Q.; Tonge, P. J.; Slayden, R. A.; Kirikae, T.; Ojima, I., FtsZ: a novel target for tuberculosis drug discovery. *Curr. Top. Med. Chem.,* **2007,** *7* (5), 527-543.
7. Gandhi, N. R.; Moll, A.; Sturm, A. W.; Pawinski, R.; Govender, T.; Lalloo, U.; Zeller, K.; Andrews, J.; Friedland, G., Extensively drug-resistant tuberculosis as a cause of death in patients co-infected with tuberculosis and HIV in a rural area of South Africa. *Lancet,* **2006,** *368* (9547), 1575-1580.
8. Raviglione, M. C., Issues facing TB control (7). Multiple drug-resistant tuberculosis. *Scott. Med. J.,* **2000,** *45*, 52-55.
9. Haile, M.; Kallenius, G., Recent developments in tuberculosis vaccines. *Current opinion in infectious diseases,* **2005,** *18* (3), 211-215.
10. Ducati, R. G.; Ruffino-Netto, A.; Basso, L. A.; Santos, D. S., The resumption of consumption -- a review on tuberculosis. *Memorias do Instituto Oswaldo Cruz,* **2006,** *101* (7), 697-714.
11. Ormerod, L. P., Multidrug-resistant tuberculosis (MDR-TB): epidemiology, prevention and treatment. *British medical bulletin,* **2005,** *73-74*, 17-24.
12. Almeida Da Silva, P. E.; Palomino, J. C., Molecular basis and mechanisms of drug resistance in Mycobacterium tuberculosis: classical and new drugs. *The Journal of antimicrobial chemotherapy,* **2011,** *66* (7), 1417-1430.
13. Ramaswamy, S.; Musser, J. M., Molecular genetic basis of antimicrobial agent resistance in Mycobacterium tuberculosis: 1998 update. *Tubercle and lung disease : the official*

journal of the International Union against Tuberculosis and Lung Disease, **1998,** *79* (1), 3-29.

14. Jarlier, V.; Nikaido, H., Mycobacterial cell wall: structure and role in natural resistance to antibiotics. *FEMS microbiology letters,* **1994,** *123* (1-2), 11-18.
15. Kochi, A.; Vareldzis, B.; Styblo, K., Multidrug-resistant tuberculosis and its control. *Research in microbiology,* **1993,** *144* (2), 104-110.
16. Rawat, R.; Whitty, A.; Tonge, P. J., The isoniazid-NAD adduct is a slow, tight-binding inhibitor of InhA, the Mycobacterium tuberculosis enoyl reductase: adduct affinity and drug resistance. *Proceedings of the National Academy of Sciences of the United States of America,* **2003,** *100* (24), 13881-13886.
17. Zhang, Y.; Heym, B.; Allen, B.; Young, D.; Cole, S., The catalase-peroxidase gene and isoniazid resistance of Mycobacterium tuberculosis. *Nature,* **1992,** *358* (6387), 591-593.
18. Telenti, A.; Imboden, P.; Marchesi, F.; Schmidheini, T.; Bodmer, T., Direct, automated detection of rifampin-resistant Mycobacterium tuberculosis by polymerase chain reaction and single-strand conformation polymorphism analysis. *Antimicrobial agents and chemotherapy,* **1993,** *37* (10), 2054-2058.
19. Takiff, H. E.; Salazar, L.; Guerrero, C.; Philipp, W.; Huang, W. M.; Kreiswirth, B.; Cole, S. T.; Jacobs, W. R., Jr.; Telenti, A., Cloning and nucleotide sequence of Mycobacterium tuberculosis gyrA and gyrB genes and detection of quinolone resistance mutations. *Antimicrobial agents and chemotherapy,* **1994,** *38* (4), 773-780.
20. Johansen, S. K.; Maus, C. E.; Plikaytis, B. B.; Douthwaite, S., Capreomycin binds across the ribosomal subunit interface using tlyA-encoded 2'-O-methylations in 16S and 23S rRNAs. *Molecular cell,* **2006,** *23* (2), 173-182.
21. Kumar, K.; Awasthi, D.; Berger, W. T.; Tonge, P. J.; Slayden, R. A.; Ojima, I., Discovery of anti-TB agents that target the cell-division protein FtsZ. *Future medicinal chemistry,* **2010,** *2* (8), 1305-1323.
22. Bi, E. F.; Lutkenhaus, J., FtsZ ring structure associated with division in Escherichia coli. *Nature,* **1991,** *354* (6349), 161-164.
23. van den Ent, F.; Amos, L.; Lowe, J., Bacterial ancestry of actin and tubulin. *Current opinion in microbiology,* **2001,** *4* (6), 634-638.

24. Oliva, M. A.; Cordell, S. C.; Lowe, J., Structural insights into FtsZ protofilament formation. *Nature structural & molecular biology,* **2004,** *11* (12), 1243-1250.
25. Ben-Yehuda, S.; Losick, R., Asymmetric cell division in B. subtilis involves a spiral-like intermediate of the cytokinetic protein FtsZ. *Cell,* **2002,** *109* (2), 257-266.
26. Errington, J.; Daniel, R. A.; Scheffers, D. J., Cytokinesis in bacteria. *Microbiology and molecular biology reviews : MMBR,* **2003,** *67* (1), 52-65, table of contents.
27. Ojima, I.; Kumar, K.; Awasthi, D.; Vineberg, J. G., Drug discovery targeting cell division proteins, microtubules and FtsZ. *Bioorganic & medicinal chemistry,* **2014,** *22* (18), 5060-5077.
28. Slayden, R. A.; Knudson, D. L.; Belisle, J. T., Identification of cell cycle regulators in Mycobacterium tuberculosis by inhibition of septum formation and global transcriptional analysis. *Microbiology,* **2006,** *152* (Pt 6), 1789-1797.
29. Respicio, L.; Nair, P. A.; Huang, Q.; Anil, B.; Tracz, S.; Truglio, J. J.; Kisker, C.; Raleigh, D. P.; Ojima, I.; Knudson, D. L.; Tonge, P. J.; Slayden, R. A., Characterizing septum inhibition in Mycobacterium tuberculosis for novel drug discovery. *Tuberculosis,* **2008,** *88* (5), 420-429.
30. Romberg, L.; Levin, P. A., Assembly dynamics of the bacterial cell division protein FTSZ: poised at the edge of stability. *Annual review of microbiology,* **2003,** *57*, 125-154.
31. de Pereda, J. M.; Leynadier, D.; Evangelio, J. A.; Chacon, P.; Andreu, J. M., Tubulin secondary structure analysis, limited proteolysis sites, and homology to FtsZ. *Biochemistry,* **1996,** *35* (45), 14203-14215.
32. Reynolds, R. C.; Srivastava, S.; Ross, L. J.; Suling, W. J.; White, E. L., A new 2-carbamoyl pteridine that inhibits mycobacterial FtsZ. *Bioorganic & medicinal chemistry letters,* **2004,** *14* (12), 3161-3164.
33. White, E. L.; Suling, W. J.; Ross, L. J.; Seitz, L. E.; Reynolds, R. C., 2-Alkoxycarbonylaminopyridines: inhibitors of Mycobacterium tuberculosis FtsZ. *The Journal of antimicrobial chemotherapy,* **2002,** *50* (1), 111-114.
34. Sarcina, M.; Mullineaux, C. W., Effects of tubulin assembly inhibitors on cell division in prokaryotes in vivo. *FEMS microbiology letters,* **2000,** *191* (1), 25-29.
35. Awasthi, D.; Kumar, K.; Ojima, I., Therapeutic potential of FtsZ inhibition: a patent perspective. *Expert opinion on therapeutic patents,* **2011,** *21* (5), 657-679.

36. Kumar, K.; Awasthi, D.; Lee, S. Y.; Zanardi, I.; Ruzsicska, B.; Knudson, S.; Tonge, P. J.; Slayden, R. A.; Ojima, I., Novel trisubstituted benzimidazoles, targeting Mtb FtsZ, as a new class of antitubercular agents. *Journal of medicinal chemistry*, **2011,** *54* (1), 374-381.
37. Awasthi, D.; Kumar, K.; Knudson, S. E.; Slayden, R. A.; Ojima, I., SAR studies on trisubstituted benzimidazoles as inhibitors of Mtb FtsZ for the development of novel antitubercular agents. *Journal of medicinal chemistry*, **2013,** *56* (23), 9756-9770.
38. Mukherjee, A.; Lutkenhaus, J., Analysis of FtsZ assembly by light scattering and determination of the role of divalent metal cations. *Journal of bacteriology*, **1999,** *181* (3), 823-832.
39. Collins, L.; Franzblau, S. G., Microplate alamar blue assay versus BACTEC 460 system for high-throughput screening of compounds against Mycobacterium tuberculosis and Mycobacterium avium. *Antimicrobial agents and chemotherapy*, **1997,** *41* (5), 1004-1009.
40. Park, B.; Awasthi, D.; Chowdhury, S. R.; Melief, E. H.; Kumar, K.; Knudson, S. E.; Slayden, R. A.; Ojima, I., Design, synthesis and evaluation of novel 2,5,6-trisubstituted benzimidazoles targeting FtsZ as antitubercular agents. *Bioorganic & medicinal chemistry*, **2014,** *22* (9), 2602-2612.

Chapter 2

Target Confirmation and Biological Evaluation of Lead Compounds

Chapter Contents

§ 2.1 Introduction 47
§ 2.2 Results and discussion 49
§ 2.2.1 Inhibition of FtsZ polymerization 49
§ 2.2.2 Transmission Electron Microscopy (TEM) of FtsZ assembly 51
§ 2.2.3 Dissociation Constant 52
§ 2.2.4 Cytotoxicity Assay against Vero Cells 53
§ 2.2.5 Early Metabolism Study on compound 2-1 54
§ 2.3 Conclusion 55
§ 2.4 Experimental Section 56
§ 2.4.1 General Methods 56
§ 2.4.2 Materials 56
§ 2.4.3 Experimental Procedures 56
§ 2.4.4 Protein Purification 62
§ 2.4.5 FtsZ Inhibitory Polymerization Assay 64
§ 2.4.6 TEM Analysis 64
§ 2.4.7 MTT assay for Cytotoxicity 64
§ 2.5 References 66

§ 2.1 Introduction

As previously discussed, FtsZ is a cell division protein which forms the cytokinetic Z-ring at the division site (**Figure 2-1**).[1, 2] Once a normal cell is ready to divide, GTP-FtsZ initiates polymerization with recruitment of several non-essential accessory proteins such as FtsA, ZapA, EzrA and SepF at mid-cell.[3] Then, Z-ring starts forming when steady-state turnover equilibrium reached with GTP-FtsZ in the cytoplasm.[4]

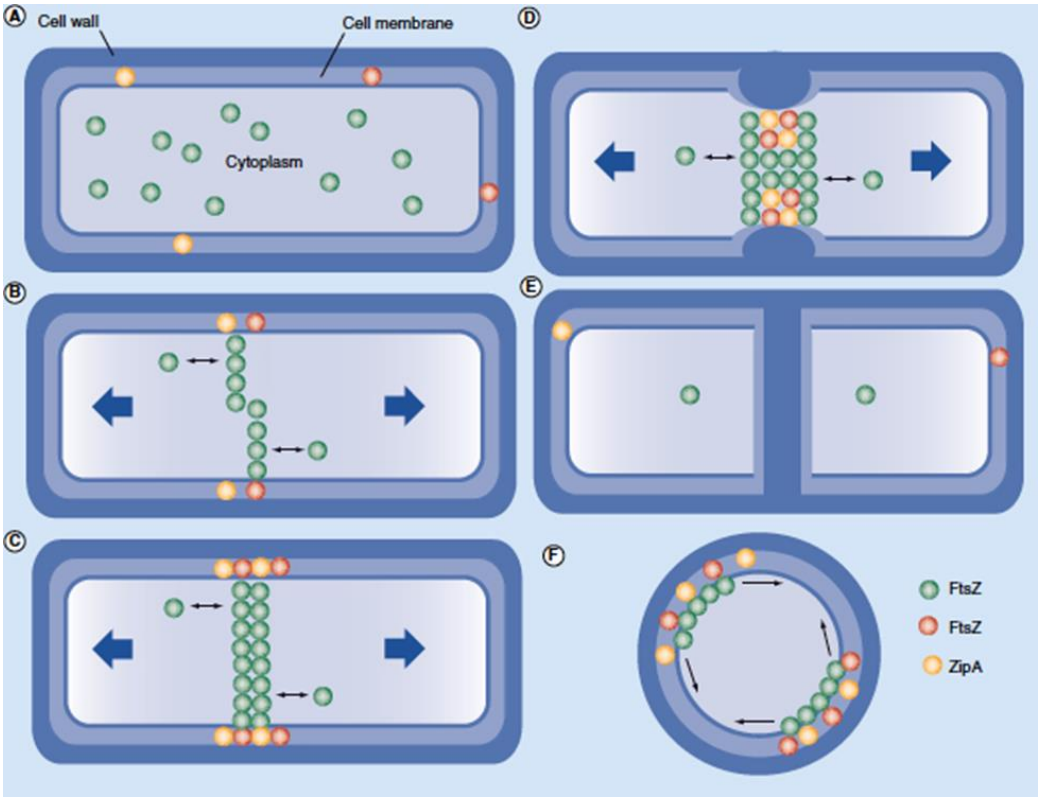

Figure 2- 1: Bacterial cell division (adapted from [4])

Construction of the Z-ring results in septum formation and gives two daughter cells, as well as depolymerization of the Z-ring. The FtsZ ring behaves dynamically during the cell division and remains attached to the leading edge of the constricting septum.[5] It has been suggested that FtsZ polymers generate the membrane constriction force through iterative cycles of GTP hydrolysis, depolymerization, and polymerization again.[6] Therefore, we hypothesized that inhibiting FtsZ polymerization or depolymerizaiton could prevent septum formation resulting in cell death.

To validate the hypothesis, a library of 2,5,6-trisubstituted benzmidazoles was synthesized as described in the previous chapter. Among 376 preliminary screened compounds 108 compounds had activity at the 5 µg/mL and 22 compounds had activity at the 1 µg/mL concentration.

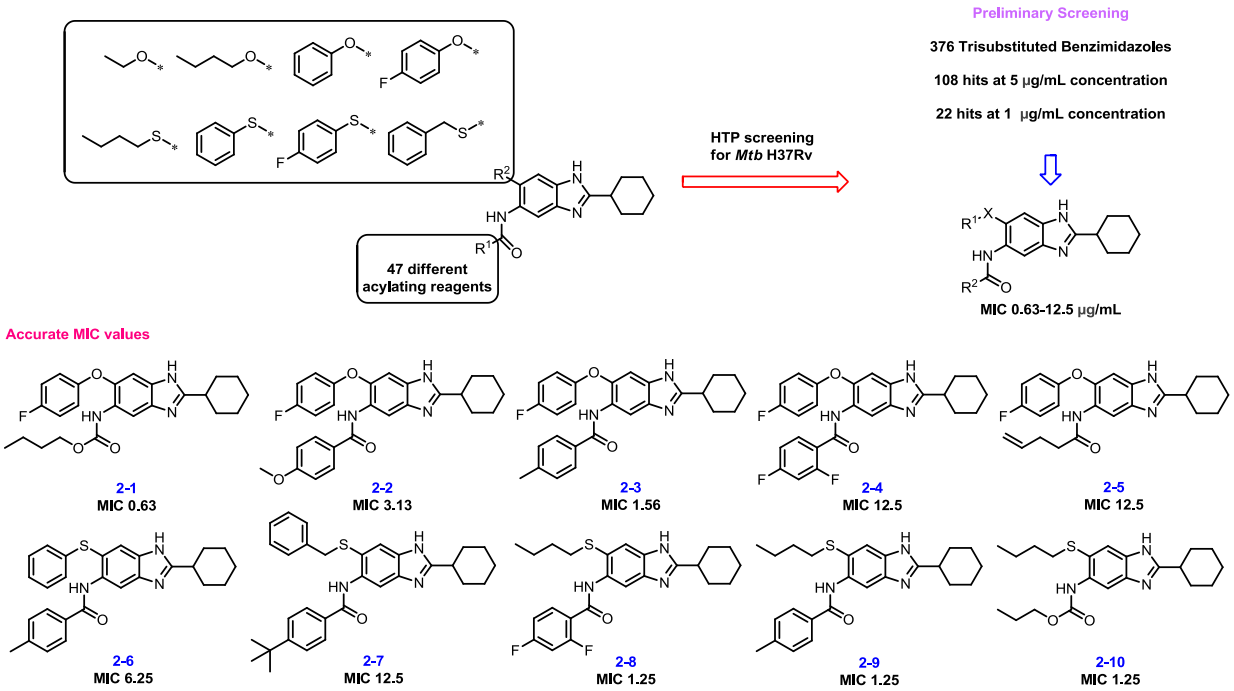

Figure 2- 2: Chemical structure of 10 lead compounds and their accurate MIC values

These hit compounds were resynthesized in analytically pure form and examined for their accurate MIC values and the structure of 10 lead compounds are described in **Figure 2-2**. In order to validate lead compounds inhibit bacterial growth by interfering with FtsZ assembly, light scattering assay based on FtsZ polymerization and TEM images of FtsZ upon compound treatment was measures.

§ 2.2 Results and discussion

§ 2.2.1 Inhibition of FtsZ polymerization

Two benzimidazoles **2-1** and **2-2** (**Figure 2-3**) were evaluated for their ability to inhibit the *Mtb* FtsZ polymerization. A light scattering assay was carried out to examine the effect of these compounds on inhibition of the FtsZ polymerization. The amount of the FtsZ polymer formed after addition of GTP was monitored by the intensity of light scattered by the sample. As **Figure 2-4** illustrates, **2-1** (MIC = 0.63 µg/mL; 1.2µM) and **2-4** (MIC = 12.5 µg/mL; 12.2 µM) inhibited FtsZ polymerization in a dose-dependent manner.

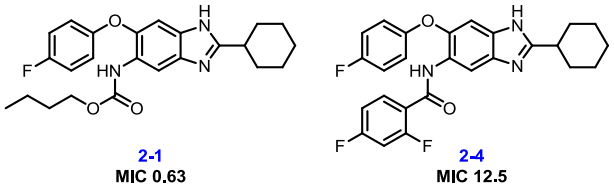

Figure 2- 3: Chemical structure of compound 2-1 and 2-4

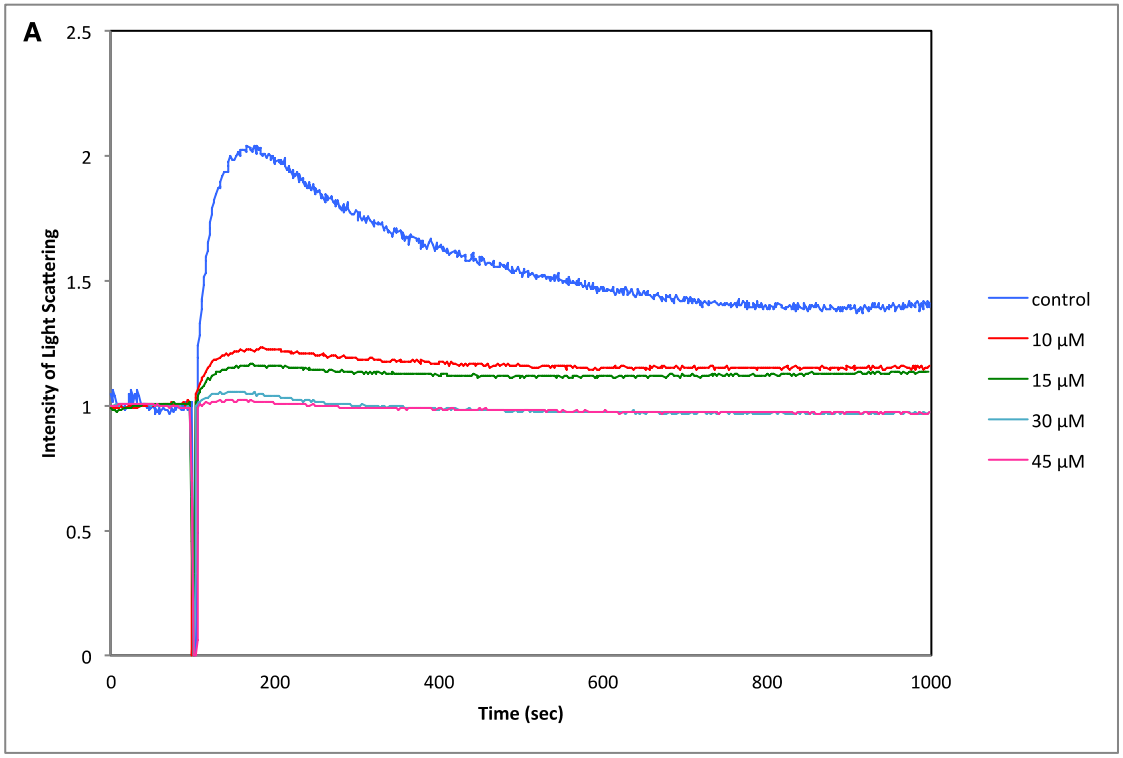

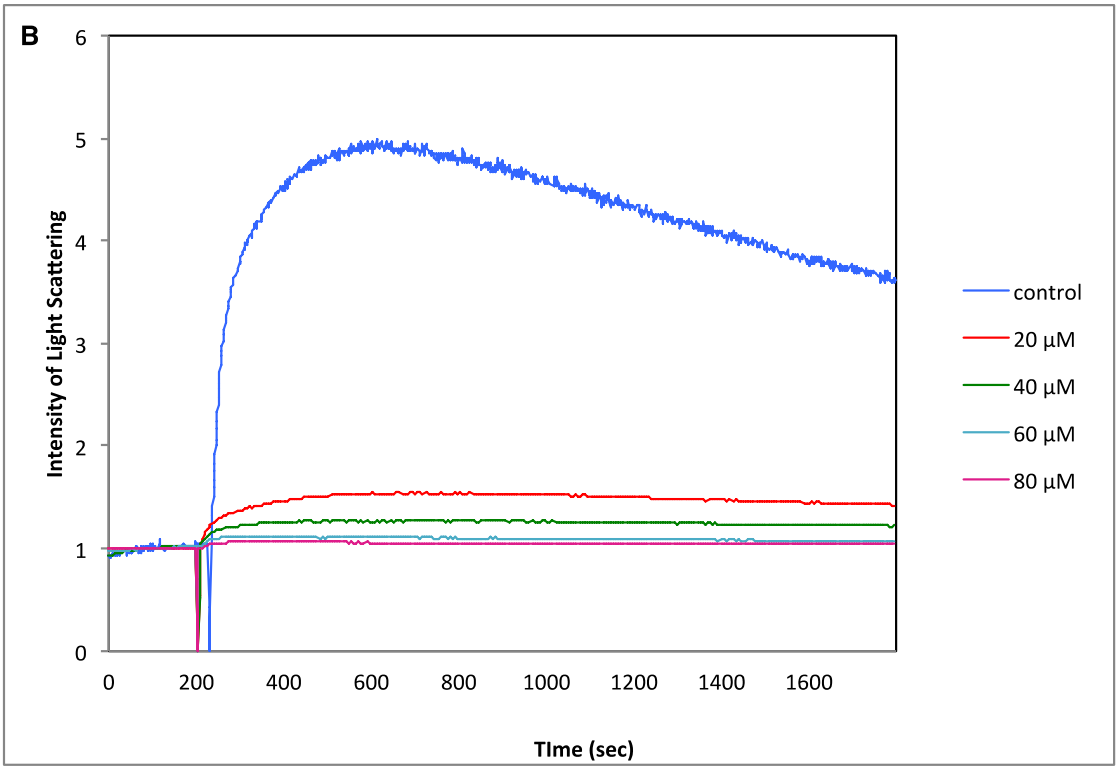

Figure 2- 4: Polymerization assay of (A) compound 2-1 and (B) compound 2-2

The inhibitory activity of two lead benzimidazoles **2-1** and **2-4** for *Mtb* FtsZ polymerization was determined by means of light scattering on a PTI-QM4 Fluorescence Master system. The 90° light scattering was measured at 30 ℃, using excitation and emission wavelength of 400 nm with slit width of 2 nm. The gain was set at 875 V. *Mtb* FtsZ (15 µM) was incubated in the polymerization buffer (50 mM MES pH 6.5, 100 mM KCl, 5mM MgC_{l2}) for up to 300 sec. Polymerization was initiated with 100 µM GTP and monitored for up to 30 min. Benzimidazole stocks were prepared in DMSO and incubated with FtsZ enzyme prior to initiation of polymerization with GTP.

This light scattering assay confirmed that two lead benzimidazoles inhibited polymerizaiton of FtsZ in a dose dependent manner as anticipated. A reduction in the intensity of light scattering was observed as the concentration of compound was increased. In the case of compound **2-1**, almost no FtsZ polymerization was observed at 30 µM concentration. For compound **2-4**, a significant reduction of FtsZ formation and similar patterns in inhibition of FtsZ polymerization were observed.

§ 2.2.2 Transmission Electron Microscopy (TEM) of FtsZ assembly

Transmission electron microscopy (TEM) imaging of *Mtb* FtsZ treated with **2-1** demonstrated in **Figure 2-5** showed the ability of the compound to inhibit FtsZ polymerization and aggregation.

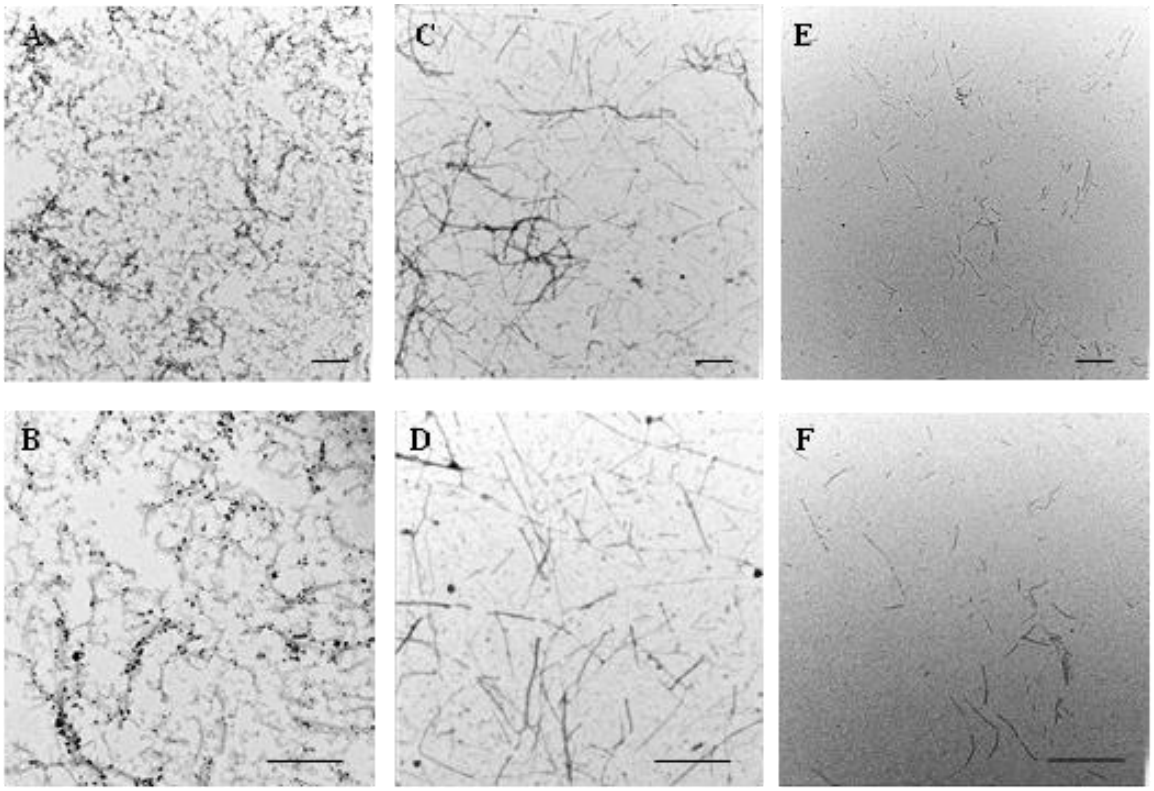

Figure 2- 5: TEM images of FtsZ

FtsZ (5 µM) was polymerized by GTP (25 µM) in the absence (A, B) and presence of **2-1** at 40 µM (C, D) and 80 µM (E, F). Images (A, C, E) are at 23,000 x magnification (scale bar 500 nm) and (B, D, F) are at 49,000 x magnification (scale bar 500 nm). Stock solution of compound **2-1** was prepared in ethanol. *Mtb* FtsZ (5 µM) was incubated with 40 or 80 µM of 5a in the polymerization buffer (50 mM MES, 5 mM MgCl2, 100 mM KCl, pH 6.5) for 15 min on ice. To each solution was added GTP to the final concentration of 25 µM. The resulting solution was incubated at 37 ^{o}C for 30 min. The incubated solution was diluted 2 times with the polymerization buffer and immediately transferred to carbon coated 300 mesh formvar copper grid and negatively stained with 1% uranyl acetate. The samples were viewed with a FEI

Tecnai12 BioTwinG transmission electron microscope at 80 kV. Digital images were acquired with an AMT XR-60 CCD digital camera system.[7] *Mtb* FtsZ (5 µM) incubated with **2-1** at 40 µM and 80 µM concentration on addition of GTP (25 µM) formed shorter and thinner FtsZ polymers when compared to the untreated polymerized *Mtb* FtsZ. In the absence of inhibitor, *Mtb* FtsZ formed a dense network of long polymers which tend to aggregate (**Figure 2-5**: **A**, **B**) while in the presence of **2-1** (40 µM), the length, density and aggregation was visibly reduced (**Figure 2-5**: **C**, **D**). The effect was more apparent at 80 µM treatment where very short and dispersed FtsZ polymers were observed (**Figure 2-5**: **E**, **F**).

In combination with the light scattering assay, TEM images confirm the target of compound **2-1** as *Mtb* FtsZ and gives insight into the mode of action of these new series of trisubstituted benzimidazoles bearing an ether or thioether linkage at 6-postion.

§ 2.2.3 Dissociation Constant

The binding study was performed by our former group member, Dr. Soumya R. Chowdhury. The fluorescence intensity of the compound was measured in the presence of increasing FtsZ concentrations, in 50 mM MES, 100 mM KCl, 5 mM $MgCl_2$ in absence of GTP by exciting the compound at 316nm and monitoring the change of fluorescence at 427.9 nm using a PTI-QM4 spectrofluorometry. The change in fluorescence (ΔF) at 427.9 nm was fitted into the equation $\Delta F = (\Delta Fmax \times L)/(Kd + L)$.[8] Results are shown in **Figure 2-6**.

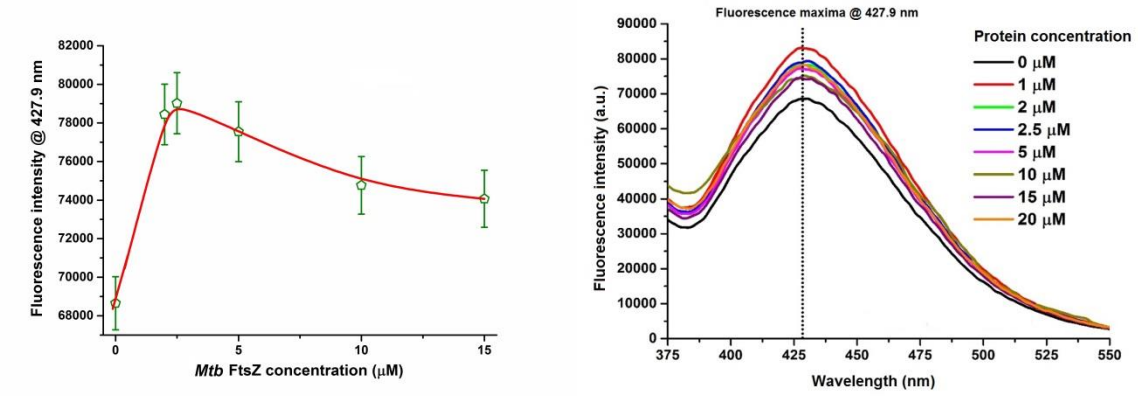

Figure 2- 6: Determination of binding parameter of 2-1 with *Mtb* FtsZ

The fluorescence intensity of **2-1**, the most active compound, was used to determine its dissociation constant (K*d*) with the *Mtb* FtsZ.[8] Compound **2-1** has an emission maximum at 427.9 nm with the excitation maximum at 316 nm. A Fixed concentration of **2-1** (100 µM) was excited at 316 nm with varying concentration of *Mtb* FtsZ (as shown in the graph) and fluorescence monitored at 427.9 nm and plotted against wavelength. Increase in fluorescence intensity observed on addition of increasing concentration of protein. Fluorescence profiles of emission intensity at 427 nm for the titration of *Mtb* FtsZ. The peak saturation was observed at 2.5 µM and then there is a progressive decrease in fluorescence emotion. The K*d* of **2-1** was calculated to be 1.32 ±0.5 µM

§ 2.2.4 Cytotoxicity Assay against Vero Cells

The cytotoxicity of the compounds was tested against Vero cells utilizing MTT assay showed in **Table 2-1**.[9, 10]

Table 2- 1: Cytotoxicity of 10 Lead Compounds against Vero[a] Cells

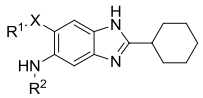

compound	R^1X	R^2	MIC (µg/mL) *Mtb* H37Rv	cytotocicity (µM) Vero Cells	compound	R^1X	R^2	MIC (µg/mL) *Mtb* H37Rv	cytotocicity (µM) Vero Cells
2-1		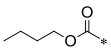	0.63	60 ± 7.2	**2-6**			6.25	> 200
2-2		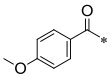	3.13	40 ± 8.5	**2-7**		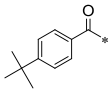	12.5	> 200
2-3			1.56	26 ± 9.5	**2-8**		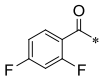	1.25	> 200
2-4			12.5	> 200	**2-9**			1.25	> 200
2-5	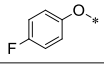	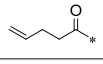	12.5	> 200	**2-10**	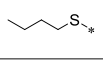	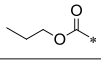	1.25	75 ± 21

[a] kidney epithelial cells

The cells were grown in DMEM media supplemented with 5 % Calf Bovine Serum and 1 % Penn Strip and incubated at 37 ℃ with 5 % CO_2. 5,000 cells added to each well of a 96-well

plate in 200 µM aliquots. The cells were incubated at 37 ℃ for 1-2 days until 50 % cell confluency. A serial dilution of benzimidazoles dissolved in sterile DMSO was added to the 96-well plates in 200 µM aliquots. The plates were incubated at 37 ℃ for 3 days. The medium was aspirated and then 40 µL of 0.5 mg/mL MTT in DPBS was added to each well. The plates were then incubated at 37 ℃ for 3 hours. Then, 40 µL of 0.8 M HCl solution were added to dissolve the remaining crystals. Each experiment was run in triplicate. The optical density data was used to calculate IC_{50} values using the Hill slope equation. The IC_{50} values and their standard errors were calculated from the viability-concentration curve using the Four Parameter Logistic Model of Sigmaplot.

Compounds **2-1**, **2-2**, **2-3** and **2-10** showed cytotoxicity in the range of 26-75 µM. However, most of the analytically pure compounds did not show appreciable cytotoxicity against Vero cells.

§ 2.2.5 Early Metabolism Study on compound 2-1

The metabolism study on compound **2-1** was carried out in our collaboration, Sanofi, and the result is shown in **Table 2-2**.

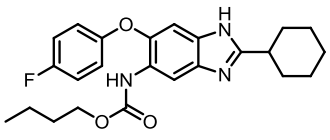

2-1
MIC 0.63
SB code: SB-P26D2
Sanofi code: SAR429567

Table 2- 2: Metabolism Result

	EME (% lability in liver microsomes)
Human	77% (61% without NADPH)
	49% + Ketoconazole (3A4)
	74% + Quinidine (2D6)
Rat	88% (0% without NADPH)
Mouse	100% (97% without NADPH)

In vivo activity of the compound is low due to fast hydrolysis of the carbamate at 5-postion. Systematic modification of the carbamate will be required to the identification of compounds with relatively improved stability.

§ 2.3 Conclusion

Compound **2-1** and **2-2** were chosen for FtsZ polymerization assays and compound **2-1** was used for TEM images for target validation. These results showed that the two selected compounds inhibit FtsZ assembly in a dose dependent manner. Further optimization of the lead compounds for their anti-TB activities is actively underway in our laboratory. Also biological evaluations of the hit/lead compounds of this series against various other pathogens will be carried out to investigate their pathogen specific as well as broad spectrum antibacterial activities. For the metabolism study of compound **2-1** revealed that the further optimization at the 5-position needed to improve stability.

To clearly see the effects of the compounds on FtsZ protein, higher concentration of compounds were used for the target validation compared to that of MIC determination. Even though we cannot exclude the fact that there is possible other mechanism of action for our compounds to show the activity in terms of MIC determination, FtsZ polymerization and TEM studies showed that the two selected compounds inhibit FtsZ assembly in a dose dependent manner. The polymerization assay and TEM imaging conditions used 40-80 uM of these FtsZ-inhibitors, but MIC values are submicro M concentration, which may look strange at a glance. However, we must be aware of a huge difference between the enzymatic assay and the polymerization/depolymerization assay of cell-division proteins. The in vitro conditions with proteins are very different from cells (antibacterial effect) and tubulin/microtubules or FtsZ-monomer/FtsZ-polymer (clear structural changes). Thus, the conditions that we used are norm to see the clear effects on the structure of the protein. These compounds, however, exert antibacterial effect (or cytotoxicity effect of taxane drugs for microtubules) at much lower concentrations. Nevertheless, it is true that these FtsZ-inhibitors may have secondary target(s) in bacterial cells. Thus, we need further investigation into the target validation and identification of possible additional molecular target(s).

§ 2.4 Experimental Section

§ 2.4.1 General Methods

^{1}H and 13C NMR spectra were measured on a Brucker 400 or 500 MHz NMR spectrometer. Melting points were measured on a Thomas Hoover Capillary melting point apparatus and are uncorrected. TLC was performed on Sorbtech with UV254 and column chromatography was carried out on silica gel 60 (Merck; 230-400 mesh ASTM). High-resolution mass spectra were obtained on Agilent-TOF instrument.

§ 2.4.2 Materials

The chemicals were purchased from Sigma Aldrich Co., Synquest Inc., Alfa Aesar and purified before use by standard methods. Tetrahydrofuran was freshly distilled from sodium metal and benzophenone. Dichloromethane was also distilled immediately prior to use under nitrogen from calcium hydride. Aminomethylated polystyrene resine EHL (200-400 mesh) 2 % DVB was purchased from Novagen Biochem.

§ 2.4.3 Experimental Procedures

5-Butoxycarbonylamino-2-cyclohexyl-6-(4-fluorophenoxy)-1H-benzo[d]imidazole (2-1)

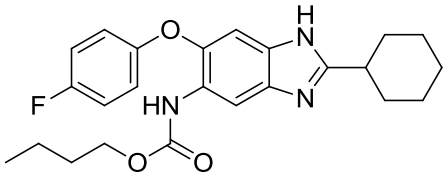

To a solution of **1-3a** (100 mg, 0.31 mmol) in 6 mL of dichloromethane was added *N*-butoxycarbonyloxysuccinimide (68 mg, 0.31 mmol) in 6 mL of dichloromethane and the mixture was magnetically stirred under nitrogen atmosphere in an ice bath. The reaction mixture was slowly warmed up to room temperature and stirred for 16 h. The solution was diluted with dichloromethane and basified with $NaHCO_3$ and then washed with water three times. The organic layers were dried over sodium sulfate, filtered, and concentrated. The residue was purified by flash chromatography on silica gel (gradient 20-40 % EtOAc/hexanes) to afford compound **2-1** as an off-white solid (54 mg, 47 % yield): mp 91-92 °C; ^{1}H NMR (400 MHz,

$CDCl_3$) 0.97 (t, 3 H, *J* = 7.4 Hz), 1.28-1.30 (m, 1 H), 1.39-1.45 (m, 4 H), 1.61-1.65 (m, 2 H), 1.67 (t, 2 H, *J* = 7.5 Hz), 1.76 (d, 1 H, *J* = 12.5 Hz), 1.85-1.88 (m, 2 H), 2.12 (d, 2 H, *J* = 12.5 Hz), 2.83-2.88 (m, 1 H), 4.19 (t, 2 H, *J* = 6.7 Hz), 6.96-7.05 (m, 4 H), 7.13 (s, 1 H), 8.23 (s, 1 H); ^{13}C NMR (100 MHz, $CDCl_3$) δ 13.8, 19.1, 25.8, 26.0, 31.0, 31.8, 38.5, 65.3, 116.5, 119.5, 125.6, 142.3, 153.1, 154.0, 157.8, 159.5, 159.6, 159.7; HRMS (ESI) m/z calcd for $C_{24}H_{29}FN_3O_3^+$ 426.2187 Found: 426.2187 (Δ = 0.0 ppm).

In a similar manner, compound **2-10** was synthesized and characterized.

6-(Butylthio)-2-cyclohexyl-5-propoxycarbonylamino-1H-benzo[d]imidazole (2-10)

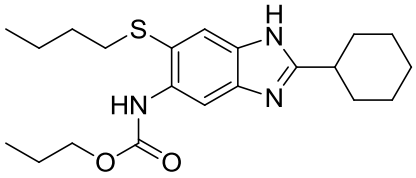

Off-white solid; 62 % yield; mp 133-134.5 °C; ^{1}H NMR (500 MHz, $CDCl_3$) δ 0.87 (t, 3 H, *J* = 7.32 Hz), 1.00 (t, 3 H, *J* = 7.43 Hz), 1.30 (dt, 1 H, *J* = 3.51, 12.5 Hz), 1.38-1.43 (m, 3 H), 1.50-1.53 (m, 2 H), 1.59-1.67 (m, 4 H), 1.74 (q, 2 H, *J* = 7.11 Hz), 1.88 (dt, 2 H, *J* = 3.41, 13.3 Hz), 2.13 (dd, 2 H, *J* = 2.29, 13.4 Hz), 2.69 (t, 2 H, *J* = 7.35 Hz), 2.84-2.89 (m, 1 H), 4.26 (t, 2 H, *J* = 6.74 Hz), 7.88 (s, 1 H), 8.20 (s, 1 H), 8.27 (s, 1 H), 8.95 (s, 1 H); ^{13}C NMR (125 MHz, $CDCl_3$) δ 10.4, 13.6, 21.8, 22.3, 25.8, 26.0, 29.7, 31.4, 31.7, 36.9, 38.4, 66.8, 98.5, 100.2, 126.5, 126.6, 134.9, 153.9; HRMS (ESI) m/z calcd for $C_{21}H_{32}N_3O_2S^+$ 390.2210 Found: 390.2214 (Δ = 1.0 ppm).

2-Cyclohexyl-6-(4-fluorophenoxy)-5-(4-methoxy-benzamido)-1H-benzo[d]imidazole (2-2)

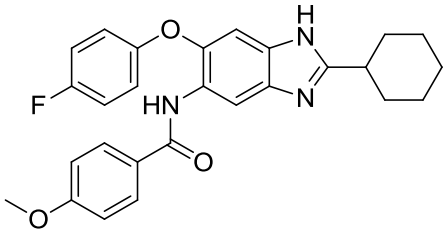

To a solution of **1-3d** (100 mg, 0.31 mmol) in 6 mL of dichloromethane was added 4-methoxybenzoyl chloride (42 μL, 0.31 mmol) in 6 mL of dichloromethane, and magnetically stirred in the ice bath. The reaction mixture was slowly warmed up to room temperature and stirred for 16 h. The solution was diluted with dichloromethane, basified with $NaHCO_3$ and then washed with water three times. The organic layers were dried over sodium sulfate, filtered, and concentrated. The residue was purified by flash chromatography on silica gel (gradient 20-40 % EtOAc/hexanes) to afford compound **2-2** as an off-white solid (152 mg, 92 % yield): mp > 230 ℃; ^{1}H NMR (400 MHz, $CDCl_3$) δ 1.22-1.33 (m, 3 H), 1.59 (dd, 2 H, *J* = 12.1, 2.9 Hz), 1.68-1.71 (m, 1 H), 1.78-1.81 (m, 2 H), 2.01-2.08 (m, 2 H), 2.76-2.82 (m, 1 H), 3.87 (s, 3 H), 6.96 (d, 2 H, *J* = 8.8 Hz), 7.03 (d, 3 H, *J* = 6.3 Hz), 7.78 (d, 2 H, *J* = 8.8 Hz), 8.55 (s, 1 H), 8.83 (s, 1 H), 9.81 (s, 1 H); ^{13}C NMR (100 MHz, $CDCl_3$) δ 13.8, 19.1, 25.8, 26.0, 31.0, 31.8, 38.5, 65.3, 116.5, 119.5, 125.6, 142.3, 153.1, 154.0, 157.8, 159.5, 159.6, 159.8; HRMS (ESI) m/z calcd for $C_{27}H_{27}FN_3O_3^+$ 460.2031 Found: 460.2028 (Δ = -0.7 ppm).

In a similar manner, compounds **2-3 ~ 2-9** were synthesized and characterized.

2-Cyclohexyl-6-(4-fluorophenoxy)-5-(4-methxyl-benzamido)-1H-benzo[d]imidazole (2-3)

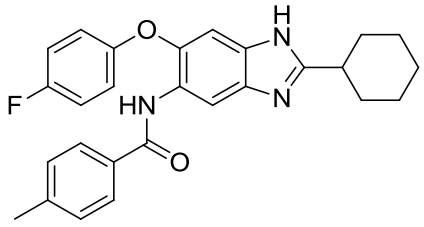

Off-white solid; 47 % yield; mp 166-168 ℃; ^{1}H NMR (500 MHz, $CDCl_3$) δ 1.81-1.23 (m, 1 H), 1.26-1.34 (m, 2 H), 1.56-1.64 (qd, 2 H, *J* = 12.4, 2.6 Hz), 1.71 (m, 1 H), 1.78-1.81 (d, 2 H, *J* = 12.8 Hz), 2.01 (dd, 2 H, *J* = 12.5, 0.6 Hz), 2.45 (t, 3 H), 2.79 (t, 1 H, *J* = 11.5 Hz), 7.05 (d, 3 H, *J* = 6.4 Hz), 7.24 (s, 1 H), 7.31 (d, 2 H, *J* = 7.8 Hz), 7.74 (d, 2 H, *J* = 8.1 Hz), 8.63 (s, 1 H), 8.90 (s, 1H), 10.2 (s, 1 H); ^{13}C NMR (100 MHz, $CDCl_3$) δ 21.5, 25.7, 25.9, 29.7, 31.7, 38.5, 116.4, 116.6, 119.4, 119.5, 125.3, 126.9, 132.2, 142.6, 153.0, 153.1, 137.9, 159.9, 160.2, 165.8; HRMS (ESI) m/z calcd for $C_{27}H_{27}FN_3O_2^+$ 442.2082 Found: 442.2082 (Δ = 0.0 ppm).

2-Cyclohexyl-5-(2,4-difluorobenzamido)-6-(4-fluorophenoxy)-1H-benzo[d]imidazole (2-4)

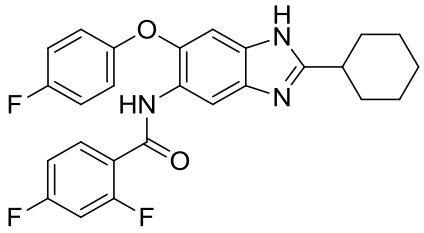

Off-white solid; 92 % yield; mp 184-185 ℃; ^{1}H NMR (500 MHz, $CDCl_3$) 0.83-0.88 (m, 1 H), 1.25-1.32 (m, 2 H), 1.59 (dd, 2 H, *J* = 12.3, 3.0 Hz), 1.68-1.70 (m, 1 H), 1.78-1.80 (m, 2 H), 2.07 (d, 2 H, *J* = 12.8 Hz), 2.80-2.84 (m, 1 H), 6.90 (ddd, 1 H, *J* = 11.7, 8.8, 2.6 Hz), 6.99 (d, 3 H, *J* = 6.3 Hz), 7.02-7.06 (m, 1 H), 7.21 (s, 1 H), 8.21 (td, 1 H, *J* = 8.9, 6.6 Hz), 8.81 (s, 1 H), 9.26 (d, 1 H, *J* = 15.7 Hz); ^{13}C NMR (100 MHz, $CDCl_3$) δ 25.9, 26.2, 31.9, 38.2, 101.1, 105.2, 112.5, 112.6, 112.7, 116.5, 116.7, 120.8 120.9, 126.4, 128.8, 138.4, 144.8, 151.7, 158.4, 161.0, 163.1; HRMS (ESI) m/z calcd for $C_{26}H_{23}F_3N_3O_2^+$ 466.1737 Found: 466.1743 (Δ = 1.29 ppm).

2-Cyclohexyl-6-(4-fluorophenoxy)-5-(pent-4-enimido)- 1H-benzo[d]imidazole (2-5)

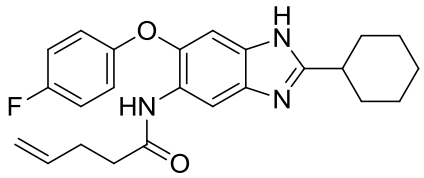

White solid; 63 % yield; mp 180.5-181.5 ℃; ^{1}H NMR (500 MHz, $CDCl_3$) δ 1.24-1.30 (m, 2 H), 1.36-1.44 (m, 2 H), 1.59-1.64 (m, 2 H), 1.73-1.76 (m, 1 H), 1.86 (dq, 2 H, *J* = 3.34, 9.98 Hz), 2.11 (dd, 2 H, *J* = 2.28, 13.3 Hz), 2.48 (dt, 3 H, *J* = 5.88, 11.7 Hz), 2.82-2.87 (m, 1 H), 4.99 (d, 1 H, *J* = 10.2 Hz), 5.07 (d, 1 H, *J* = 16.1 Hz), 5.82 (ddt, 1 H, *J* = 6.27, 10.5, 16.9 Hz), 6.95-7.04 (m, 3 H), 7.17 (s, 1 H), 7.87 (s, 1 H), 8.58 (s, 1 H), 9.58 (s, 1 H); ^{13}C NMR (125 MHz, $CDCl_3$) δ 14.2, 25.8, 26.0, 29.5, 31.7, 37.3, 38.5, 60.4, 102.7, 108.0, 116.1, 116.3, 116.5, 119.5, 125.2, 136.4, 142.4,157.9, 159.8, 170.7; HRMS (ESI) m/z calcd for $C_{24}H_{26}FN_3O_2^+$ 408.2082 Found: 408.2090 (Δ = 1.96 ppm).

2-Cyclohexyl-5-(4-methxylbenzamido)-6-(phenylthio)-1H-benzo[d]imidazole (2-6)

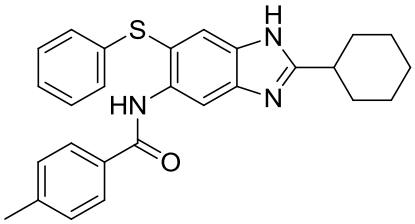

Off-white solid; 79 % yield; mp 184.5-186 °C; ^{1}H NMR (500 MHz, $CDCl_3$) δ 1.06-1.20 (m, 3 H), 1.53-1.63 (m, 3 H), 1.70 (d, 2 H, *J* = 9.5 Hz), 2.00 (d, 2 H, *J* = 11.3 Hz), 2.44 (s, 3 H), 2.73 (t, 1 H, *J* = 9.6 Hz), 7.14 (t, 2 H, *J* = 7.62 Hz), 7.22-7.27 (m, 4 H), 7.59 (d, 2 H, *J* = 8.0 Hz), 8.06 (s, 1 H), 9.01 (s, 1 H), 9.39 (s, 1 H), 11.0 (s, 1 H);^{13}C NMR (125 MHz, $CDCl_3$) δ 21.5, 25.6, 25.9, 29.7, 31.6, 38.5, 103.3, 113.6, 126.0, 126.3, 126.4, 126.9, 129.0, 129.3, 129.6, 132.2, 134.2, 136.6, 142.6, 160.9, 166.1; HRMS (ESI) m/z calcd for $C_{26}H_{34}N_3OS^+$ 436.2417 Found: 436.2417 (Δ = 0.0 ppm).

6-(Benzylthio)-2-cyclohexyl-5-(4-(*tert*-butyl)benzamido)-1H-benzo[d]imidazole (2-7)

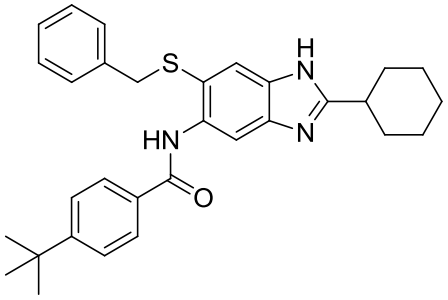

Off-white solid; 92 % yield; mp 173-173.5 °C; ^{1}H NMR (500 MHz, $CDCl_3$) δ 1.06-1.23 (m, 3 H), 1.40 (s, 9 H), 1.51-1.59 (m, 3 H), 1.68 (d, 2 H, *J* = 11.3 Hz), 1.97 (d, 2 H, *J* = 11.8 Hz), 2.67-2.72 (m, 1 H), 3.90 (s, 2 H), 6.98 (dd, 2 H, *J* = 7.1, 2.3 Hz), 7.04 (dd, 3 H, *J* = 5.0, 1.9 Hz), 7.52 (d, 2 H, *J* = 8.4 Hz), 7.70 (d, 2 H, *J* = 8.4 Hz), 7.96 (s, 1 H), 8.93 (s, 1 H), 9.38 (s, 1 H), 11.1 (s, 1 H); ^{13}C NMR (125 MHz, $CDCl_3$) δ 25.6, 25.9, 31.2, 31.7, 35.1, 38.5, 43.4, 102.2, 116.4, 125.8, 126.9, 127.1, 127.3, 128.5, 132.3, 135.3, 138.0, 140.2, 155.5, 160.8, 165.8; HRMS (ESI) m/z calcd for $C_{31}H_{36}N_3OS^+$ 498.2574 Found: 498.2574 (Δ = 0.0 ppm).

6-(Butylthio)-5-(2,4-difluorobenzamido)-2-cyclohexyl-1H-benzo[d]imidazole (2-8)

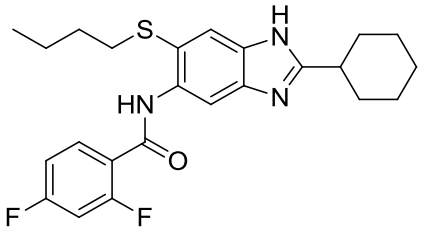

Off-white solid; 93 % yield; mp 170-170.5 ℃; ^{1}H NMR (400 MHz, $CDCl_3$) δ 0.83 (t, 3 H, *J* = 7.33 Hz), 1.17-1.29 (m, 3 H), 1.36 (dd, 2 H, *J* = 15.0, 7.37 Hz), 1.49-1.60 (m, 4 H), 1.67 (d, 1 H, *J* = 12.1 Hz), 1.77 (d, 2 H, *J* = 12.3 Hz), 2.06 (d, 2 H, *J* = 11.9 Hz), 2.73 (t, 2 H, *J* = 7.42 Hz), 2.79 (m, 1 H), 6.96-7.09 (m, 2 H), 7.93 (s, 1 H), 8.23 (td, 1 H, *J* = 8.85, 6.54 Hz), 8.87 (s, 1 H), 10.1 (s, 1 H), 10.3 (s, 1 H); ^{13}C NMR (100 MHz, $CDCl_3$) δ 13.6, 21.7, 25.7, 25.9, 31.3, 31.7, 37.0, 38.5, 104.7, 112.5, 112.7, 117.8, 118.3, 118.4, 133.8, 134.3, 160.5; HRMS (ESI) m/z calcd for $C_{24}H_{28}F_2N_3OS^+$ 444.1916 Found: 444.1922 (Δ = 1.35 ppm).

6-(Butylthio)-5-(4-metylbenzamido)-2-cyclohexyl-1H-benzo[d]imidazole (2-9)

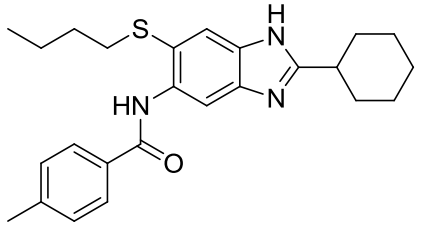

Off-white solid; 34 % yield; mp 155-156 ℃; ^{1}H NMR (400 MHz, $CDCl_3$) δ 0.81 (t, 3 H, *J* = 7.38 Hz), 1.05-1.15 (m, 3 H), 1.24 (s, 1 H), 1.34 (q, 2 H, *J* = 7.34 Hz), 1.49-1.60 (m, 4 H), 1.66 (d, 2 H, *J* = 12.1 Hz), 1.97 (d, 2 H, 11.9 Hz), 2.46 (s, 3 H), 2.71-2.75 (m, 3 H), 7.36 (d, 2 H, *J* = 7.79 Hz), 7.92 (d, 3 H, *J* = 7.73 Hz), 8.99 (s, 1 H), 9.84 (s, 1 H), 11.4 (s, 1 H); ^{13}C NMR (100 MHz, $CDCl_3$) δ; 13.5, 21.5, 21.8, 25.5, 25.8, 29.6, 31.4, 31.6, 37.2, 38.4, 102.7, 117.1, 126.2, 127.0, 129.7, 132.3, 133.8, 135.2, 140.1, 142.6, 160.7, 165.7; HRMS (ESI) m/z calcd for $C_{25}H_{32}N_3OS^+$ 422.2261 Found: 422.2265 (Δ = 0.9 ppm).

§ 2.4.4 Protein Purification

A. Protein Purification for Inhibitory Assay

E.coli expression plasmid encoding the *ftsz* gene (pET 15b vector) was transformed into 100 µL of BL21 (DE3) cells. The transformed cells were plated onto LB plates, containing 100 µg/mL ampicilin. The antibiotic concentration was kept the same for the following steps. The plates were incubated overnight at 37 ℃. The colonies were picked and grown in 10 mL of LB media at 37 ℃ at 250 rpm shake rate. The inoculum was transferred to 1 L of LB media in a 4 L flask and grown to an OD of 0.6 at A600. Then, 1 mM IPTG was added to induce protein expression overnight at 20 ℃ at 250 rpm shake rate. Cells were then pelleted by centrifugation at 3000 x *g*, flash frozen in liquid nitrogen, and stored at -80 ℃ until further purification steps.Thawed cells were suspended in 40 mL 50 mM Tris pH 7.5, 500 mM NaCl, 100 mM KCl, 0.1% NP-40 per liter cell culture growth and passed through 3 rounds of cell disrupter (French press) at 27 psi to disrupt cells. Lysed cells were centrifuged at 27,000 x *g* for 20 min to clear insoluble cellular components and cell wall fractions. Thawed cells were re-suspended in 40mL 50mM sodium phosphate pH 7.5, 300 mM sodium chloride, 10mM imidazole, per liter cell culture growth and sonicated at 15 W 6 times for 30 seconds each with 1 minute pauses in between to disrupt cells. Lysed cells were centrifuged at 44,000 *x g* for one hour to clear insoluble cellular components. Cleared lysate was applied to Ni+2 charged His-bind resin and washed with double the volume of resuspension buffer of 50 mM sodium phosphate pH 7.5, 300 mM sodium chloride, then double the volume of re-suspension buffer of 50 mM sodium phosphate pH 7.5, 300 mM sodium chloride, 60 mM imidazole. FtsZ protein was eluted with 4 x 5 mL portions of 50 mM sodium phosphate pH 7.5, 300 mM NaCl, 500 mM imidazole. Protein was loaded onto a Sephadex G25 size exclusion column to remove excess imidazole and to exchange protein into 25 mM HEPES pH 7.2, 1mM DTT, 0.1 mM EDTA, 10% glycerol (or other buffer as indicated). Resulting protein fractions were pooled and the N-terminal 6xHis affinity tag was removed by biotin tagged thrombin treatment overnight at 4 ℃ (0.25 Units biotinylated thrombin per mg tagged FtsZ protein). Successive passes through streptavidin agarose and fresh Ni+2 charged His-bind resin removed biotinylated thrombin, uncut FtsZ protein, and free cut off affinity tag. A final cleanup was performed through an Akta driven Sephadex 200 60/16 size exclusion column in 25mM HEPES pH 7.2, 1 mM DTT, 0.1 mM EDTA, 10% glycerol or other buffer as indicated. Protein was then concentrated to 10 mg/mL

(~250 µM) with centrifugal 30 kDa molecular weight cutoff filters, aliquoted 150 µL, flash frozen in liquid nitrogen, and stored at -80℃.

B. Protein Purification for TEM Analysis

For TEM analysis the following procedure was followed for protein purification. The cells were suspended in approximately 20-30 mL binding buffer (500 mM NaCl, 20 mM sodium phosphate, pH 7.8) and lysed using cell disruptor. The lysate was centrifuged in an ultracentrifuge at 126603 × *g*, 4 ^{o}C for 90 min. The supernatant was filtered and loaded onto Ni2+-NTA column washed with 50 mL of binding buffer and eluted using a gradient of binding buffer with 30-500 mM imidazole. The eluted protein was dialyzed against buffer containing 50 mM Tris, 5mM $MgCl_2$, 50 mM KCl, pH 7.2 followed by buffer containing 10 % v/v glycerol. The protein after dialysis was concentrated and stored at -80 ℃ for further use. Since the number of aromatic residues in *Mtb* FtsZ protein are low (Tyr: 1, Trp: 0), it is not reliable to follow concentration of protein by scanning at A280. The concentration of protein was therefore ascertained using the Bradford kit from Sigma.

C. Protein Purification for Binding Studies

For Kd studies the protein was purified as follows. Cleared lysate was applied to Ni^{+2} charged His-bind resin and made to equilibrate for one hour followed by washing in two volumes of wash buffer (50 mM Tris pH 7.5, 300 mM NaCl, 100 mM KCl, 0.1% NP-40, and 10 mM Imidazole). Bound protein was eluted with 10 mL of Elution buffer (50 mM Tris pH 7.5, 500 mM NaCl, 100 mM KCl, and 500 mM imidazole). The eluted protein was first dialyased against 2 L Storage buffer (50 mM Tris pH 7.8, 200 mM NaCl, 100 mM KCl,) overnight followed by 3hrs dialysis against Storage buffer with 10% glycerol. Post dialysis, the concentration of the protein was checked by Bradford assay and purity of the purified protein determined by SDS page. If necessary, protein was further concentrated to 10mg/mL (~250 µM) with centrifugal 10 kDa molecular weight cutoff filters, aliquoted 500 µL, and flash frozen in liquid nitrogen, and stored at -80 ℃ till further use.

§ 2.4.5 FtsZ Inhibitory Polymerization Assay

The inhibitory activity of lead benzamidazoles for *Mtb*-FtsZ polymerization was determined by means of light scattering on a PTI-QM4 Fluorescence Master system. The 90° light scattering was measured at 30 ℃, using excitation and emission wavelength of 400 nm with slit width of 2 nm. The gain was set at 875 V. *Mtb* FtsZ (15 μM) was incubated in the polymerization buffer (50 mM MES pH 6.5, 100 mM KCl, 5 mM $MgCl_2$) for up to 300 sec. Polymerization was initiated with 100 μM GTP and monitored for up to 30 min. Benzimidazole stocks were prepared in DMSO and incubated with FtsZ enzyme prior to initiation of polymerization with GTP.

§ 2.4.6 TEM Analysis

Stock solution of compound 5a was prepared in ethanol. *Mtb*-FtsZ (5 μM) was incubated with 40 or 80 μM of 5a in the polymerization buffer (50 mM MES, 5mM $MgCl_2$, 100 mM KCl, pH 6.5) for 15 min on ice. To each solution was added GTP to the final concentration of 25 μM. The resulting solution was incubated at 37 ^{o}C for 30 min. The incubated solution was diluted 2 times with the polymerization buffer and immediately transferred to carbon coated 300 mesh formvar copper grid and negatively stained with 1% uranyl acetate. The samples were viewed with a FEI Tecnai12 BioTwinG transmission electron microscope at 80 kV. Digital images were acquired with an AMT XR-60 CCD digital camera system.

§ 2.4.7 MTT assay for Cytotoxicity

The cytotoxicity of the compounds was tested against VERO cells using MTT assay (MTT = 3-(4,5-dimethylthiazol-2-yl)-2,5-diphenyltetrazolium bromide). Vero cells were obtained from Stony Brook University Cell Culture/Hybridoma Facility. The cells were grown in DMEM media supplemented with 5 % FBS and 1 % Penn Strip and incubated at 37 ℃ in a humidified incubator with 5 % CO_2. The cells were washed with DPBS and dissociated using TrypLe. The cells were incubated at 37 ℃ until the cells were detached from the plate, transferred to centrifuge vial and pelleted via centrifugation at 1000 rpm for 5 min. The cells were counted per 2 mL media. The desired amount of media was added to the cell solution so that 5,000 cells can be added to each well of a 96-well plate in 200 μM aliquots. After the

addition, the cells were incubated at 37 ℃ for 1-2 days. A serial dilution of the benzimidazoles dissolved in sterile DMSO was prepared by the addition of fully-supplemented DMEM. The residual medium in each well was aspirated and the different compounds concentrations were added to each well of every column of the 96-well plate in 100 μM aliquots. After the addition of the solution, the cells were incubated at 37 ℃ for 3 days. After the incubation period, the medium was aspirated and then 40 μL of 0.5 mg/mL MTT (3-(4,5-dimethylthizol-2-yl)-2,5-diphenyltetrazolium bromide) in DPBS was added to each well. The cells were then incubated at 37 ℃ for 3 hours. After the incubation period, 40 μL of 0.8 M HCl solution were added to dissolve the remaining crystals. The plates were shaken for 8 minutes to assure that all of the crystals are dissolved. The optical density was deternied from the resulting solutions using the Acsent Multiskan optical density reader. Each experiment was run in triplicate. The optical density data was used to calculate IC_{50} values for each compound on VERO cells using the Hill slope equation. The IC_{50} values and their standard errors were calculated from the viability-concentration curve using the Four Parameter Logistic Model of Sigmaplot. The concentration of DMSO per well was $\leq$ 1 % in all cases. The control experiment, i.e., adding 1 % DMSO to the cells, indicated that 1 % DMSO was not cytotoxic, and thus, all the cells treated remained virtually 100 % positive.

§ 2.5 References

1. Bi, E. F.; Lutkenhaus, J., FtsZ ring structure associated with division in Escherichia coli. *Nature* **1991,** *354* (6349), 161-164.
2. Schaffner-Barbero, C.; Martin-Fontecha, M.; Chacon, P.; Andreu, J. M., Targeting the assembly of bacterial cell division protein FtsZ with small molecules. *ACS chemical biology* **2012,** *7* (2), 269-277.
3. Adams, D. W.; Wu, L. J.; Czaplewski, L. G.; Errington, J., Multiple effects of benzamide antibiotics on FtsZ function. *Molecular microbiology* **2011,** *80* (1), 68-84.
4. Kumar, K.; Awasthi, D.; Berger, W. T.; Tonge, P. J.; Slayden, R. A.; Ojima, I., Discovery of anti-TB agents that target the cell-division protein FtsZ. *Future medicinal chemistry* **2010,** *2* (8), 1305-1323.
5. Kaur, S.; Modi, N. H.; Panda, D.; Roy, N., Probing the binding site of curcumin in Escherichia coli and Bacillus subtilis FtsZ--a structural insight to unveil antibacterial activity of curcumin. *European journal of medicinal chemistry* **2010,** *45* (9), 4209-4214.
6. Li, Z.; Trimble, M. J.; Brun, Y. V.; Jensen, G. J., The structure of FtsZ filaments in vivo suggests a force-generating role in cell division. *The EMBO journal* **2007,** *26* (22), 4694-4708.
7. Kumar, K.; Awasthi, D.; Lee, S. Y.; Zanardi, I.; Ruzsicska, B.; Knudson, S.; Tonge, P. J.; Slayden, R. A.; Ojima, I., Novel trisubstituted benzimidazoles, targeting Mtb FtsZ, as a new class of antitubercular agents. *Journal of medicinal chemistry* **2011,** *54* (1), 374-381.
8. Kelley, C.; Zhang, Y.; Parhi, A.; Kaul, M.; Pilch, D. S.; LaVoie, E. J., 3-Phenyl substituted 6,7-dimethoxyisoquinoline derivatives as FtsZ-targeting antibacterial agents. *Bioorganic & medicinal chemistry* **2012,** *20* (24), 7012-7029.
9. Chen, S.; Zhao, X.; Chen, J.; Chen, J.; Kuznetsova, L.; Wong, S. S.; Ojima, I., Mechanism-based tumor-targeting drug delivery system. Validation of efficient vitamin receptor-mediated endocytosis and drug release. *Bioconjugate chemistry* **2010,** *21* (5), 979-987.
10. Mosmann, T., Rapid colorimetric assay for cellular growth and survival: application to proliferation and cytotoxicity assays. *Journal of immunological methods* **1983,** *65* (1-2), 55-63.

Chapter 3

Synthesis and Biological Evaluation of New Series of Benzimidazoles

Chapter Contents

§ 3.1 Introduction 68

§ 3.2 Results and discussion 69

§ 3.2.1 Synthesis of Novel 2,5,6-Trisubstituted Benzimidazole 69

§ 3.2.2 MIC Determination of Selected Compounds 70

§ 3.2.3 Metabolism Results 71

§ 3.3 Conclusion 72

§ 3.4 Experimental Section 73

§ 3.4.1 General Methods 73

§ 3.4.2 Materials 73

§ 3.4.3 Experimental Procedures 73

§ 3.5 References 80

§ 3.1 Introduction

The preliminary SAR studies of lead compounds indicate that cyclohexyl group at the 2-position and diethyl amino/dimethyl amino group at the 6-position play a critical role for antibacterial activity (**Figure 3-1**).[1, 2] Building upon three representative compounds bearing alkyl carbamate or benzamide at the 5-position, we planned to expand our novel trisubstituted benzimidazole with a substitution pattern different from the previous series for high throughput (HTP) screening.[3] Especially, we have very recently found that the 6-dimethylamino series exhibit excellent activities up to the MIC value of 0.06 μg/mL. Therefore, we planned to synthesize smaller substituent, methoxy group, at the 6-position.[1]

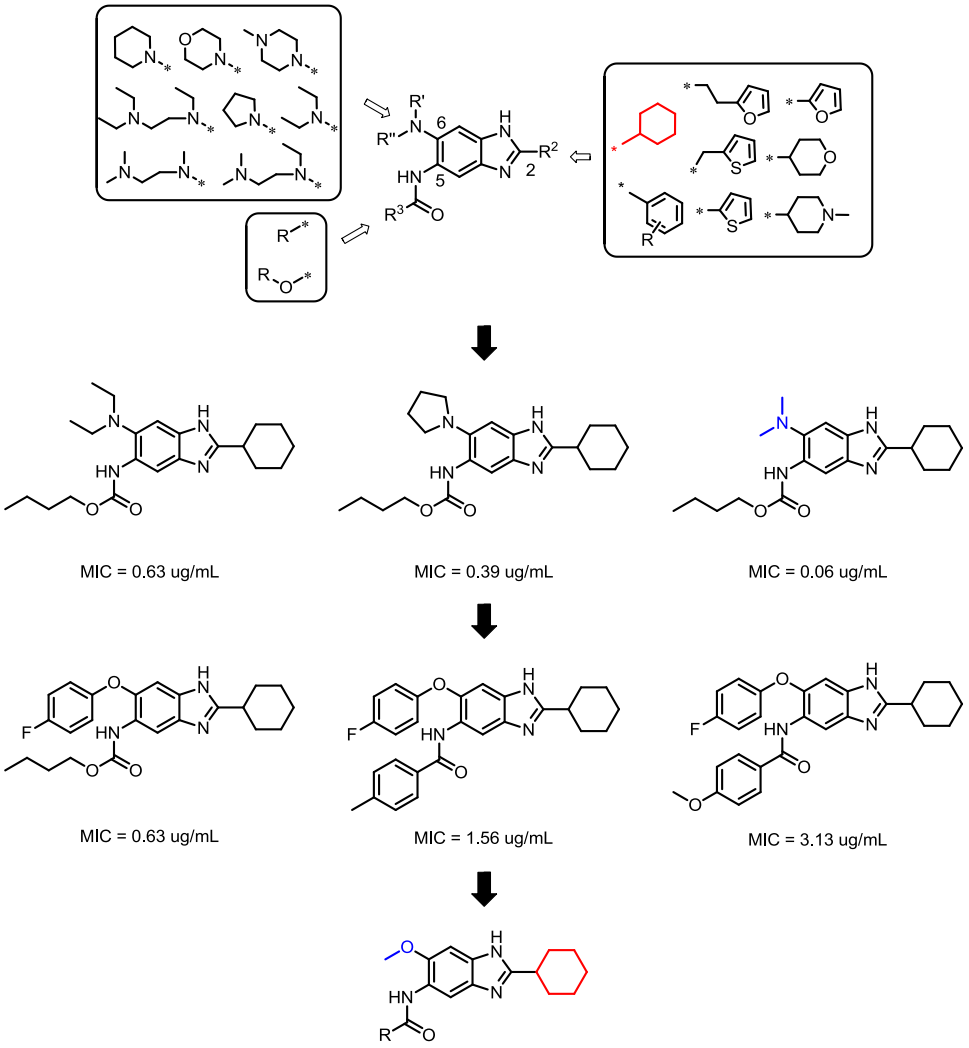

Figure 3- 1: Preliminary SAR studies and optimization of the 6-position

§ 3.2 Results and discussion

§ 3.2.1 Synthesis of Novel 2,5,6-Trisubstituted Benzimidazole

The first attempt to synthesize 2,5,6-trisubstituted benzimidazoles with methoxy group at the 6-position described in **Scheme 3-1**.

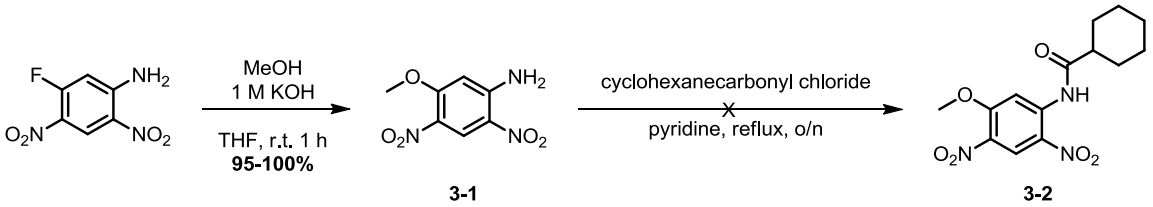

Scheme 3- 1: First synthesis of 2,5,6-trisubstituted benzimidazoles

The first step is the nucleophilic aromatic substitution of commercially available 2,4-dinitro-5-fluoroaniline with methanol. Compounds **3-1** was prepared by addition of 1 M KOH solution dropwise to afford compounds **3-1** in 95–100% yields. Earlier, the acylation of **3-1** carried out with the cyclohexanecarbonyl chloride. Unfortunately, the reaction did not proceed as expected. After overnight reaction, based on the NMR analysis, compound 3-2 was not obtained. Instead, demethoxyl acylated compound was found. Demethylation happened at the 6-position since HCl was generated When the reaction proceed. To avoid the demethylation, we set up the different route.

General procedure for the second synthesis method of 2,5,6-trisubstituted benzimidazoles bearing an methoxy moiety at the 6-position is illustrated in **Scheme 3-2**.

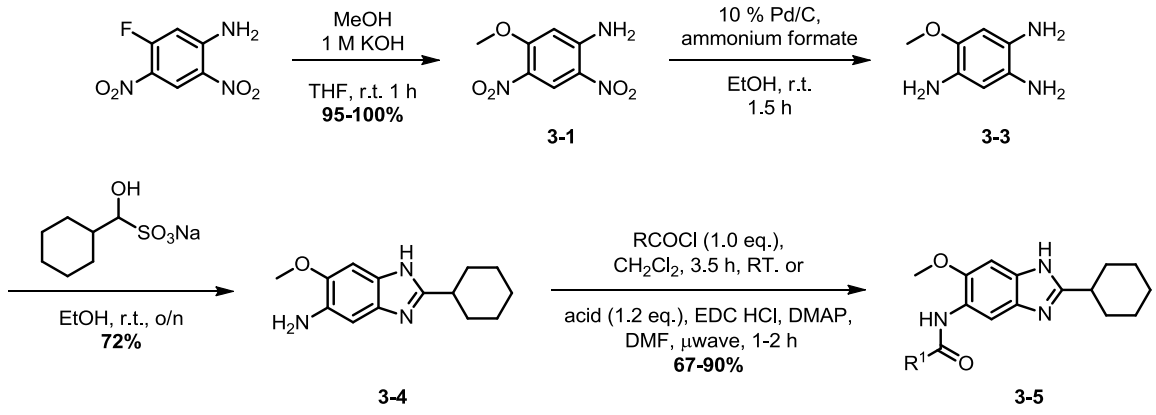

Scheme 3- 2: synthesis of 2,5,6-trisubstituted benzimidazoles

The first step is the nucleophilic aromatic substitution of commercially available 2,4-dinitro-5-fluoroaniline with methanol. Reduction of intermediate **3-3** with 10 % Pd/C and ammonium formate to afford compound **3-2**. Formation of compound **3-2** was confirmed by FIA and went to the next step without further purification. After FIA confirmation, compound **3-2** was treated with bisulfate salts of aldehyde afforded compound **3-4**. Final novel benzimidazoles **3-5** were generated with acychloride or EDC•DMAP coupling with corresponding acid in 67 -90 % yield.

§ 3.2.2 MIC Determination of Selected Compounds

To determine the accurate MIC values, 2,5,6-trisubstituted benzimidazole bearing methoxy group at the 6-position were prepared in analytically pure form (HPLC purity > 97 %). The MIC values are shown in **Figure 3-2**.

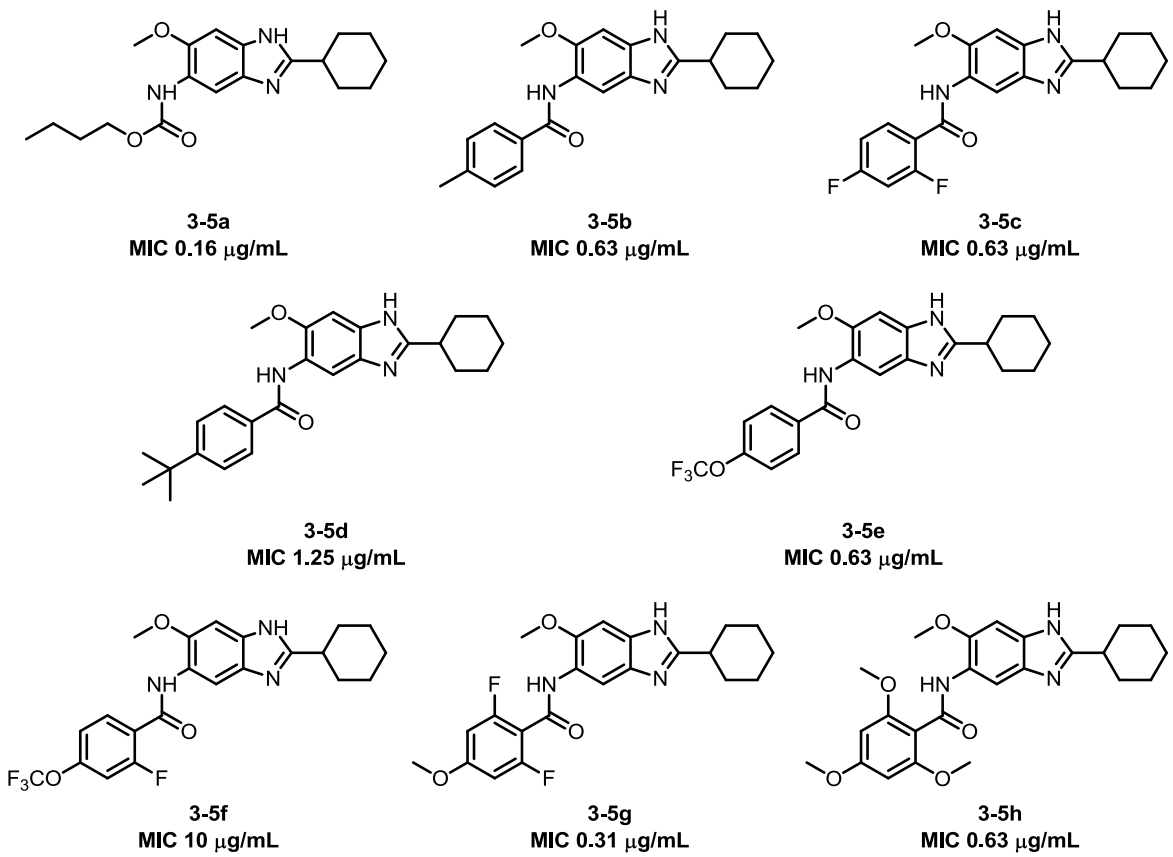

Figure 3- 2: Accurate MIC values and their chemical structures

As anticipated, butyl carbamate at the 5-position exhibited the best MIC values among this series. All the compounds which were tested showed excellent activities against drug-resistant clinical isolates of *Mtb* with MIC values in the range of 0.16-0.63 μg/mL. Accurate MIC values of more compounds in this series will be determined.

§ 3.2.3 Metabolism Results

The metabolism study on compound **3-5b**, **3-5c** and **3-5e** were carried out in our collaboration, Sanofi, and the result is shown in **Table 3-1**.

Table 3- 1: Metabolism result

Metabolism - Reference	3-5b OMe	NMe_2	3-5c OMe	NMe_2	3-5e OMe	NMe_2	3-5i F10
human (hydrolysis)	46 (29)	61 (37)	68	55 (16)	26 (28)	39 (23)	100 (100)
human +ketoconazole (3A4)	35	60	58	45	20	12	98
human + Quinidine (2D6)	44	61	65	53	27	34	100
rat (hydrolysis)	64	47	69	40	27	14	100
mouse (hydrolysis)	96 (95)	81 (73)	98 (43)	64 (18)	76 (66)	45 (33)	100 (100)

Since *in vivo* activity of among our most potent compound in terms of MIC values is low due to fast hydrolysis of the carbamate at 5-postion. Systematic modification of the carbamate was done to the identification of compounds with relatively improved stability. Three of the compounds were compared to our lead series with dimethylamino group at the 6-position. Compared to dimethylamino moiety series, methoxy group at the 6-position tends to improve human metabolism, but not rodent one. Further modification will be needed to the identification of compounds with relatively improved stability.

§ 3.3 Conclusion

Novel 2,5,6-trisubstituted benzimidazoles, which bears methoxy group at the 6-position, were synthesized with good yield and test their activity against *Mtb* H37Rv strain. All of the compounds have been tested exhibited better activity compared to previous compounds which bearing bigger sulfide and ether linkage at the 6-position. Some of the compounds were tested their metabolism and somewhat improve human metabolism, but not the rodent one. Several other compounds in this series were sent to CSU to measure the accurate MIC values. For the metabolism study in this series, methoxy group at the 6-position tends to improve human metabolism, but not rodent one compared to dimethylamino moiety series. Also, more compounds will be tested their activity *in vitro* to improve their metabolism.

§ 3.4 Experimental Section

§ 3.4.1 General Methods

^{1}H and 13C NMR spectra were measured on a Brucker 400 or 500 MHz NMR spectrometer. Melting points were measured on a Thomas Hoover Capillary melting point apparatus and are uncorrected. TLC was performed on Sorbtech with UV254 and column chromatography was carried out on silica gel 60 (Merck; 230-400 mesh ASTM). High- resolution mass spectra were obtained on Agilent-TOF instrument.

§ 3.4.2 Materials

The chemicals were purchased from Sigma Aldrich Co., Synquest Inc., Alfa Aesar and purified before use by standard methods. Tetrahydrofuran was freshly distilled from sodium metal and benzophenone. Dichloromethane was also distilled immediately prior to use under nitrogen from calcium hydride. Aminomethylated polystyrene resine EHL (200-400 mesh) 2 % DVB was purchased from Novagen Biochem.

§ 3.4.3 Experimental Procedures

5-methoxy-2,4-dinitroaniline (3-1)

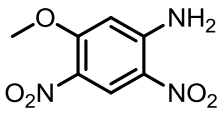

To a magnetically stirred solution of 2,4-dinitro-5-fluoroaniline (3.16 g, 15.7 mmol) in 40 mL methanol, 1 M KOH aqueous solution was added dropwise until a yellow precipitate appeared. The reaction mixture was stirred for additional 1 h. The solution was extracted with ethyl acetate. The organic layer was collected, dried over anhydrous magnesium sulfate and evaporated to give desired compound as a yellow solid in **98 %** yield; mp 200-200.5 °C; ^{1}H NMR (400 MHz, $CDCl_3$) δ 3.94 (s, 3 H), 6.22 (s, 1 H), 8.96 (s, 1H); ^{13}C NMR (100 MHz, $CDCl_3$) δ 57.0, 99.2, 127.4, 148.8

5-methoxybenzene-1,2,4-triamine (3-2)

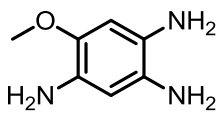

To a solution of 5-methoxy-2,4-dinitroaniline **3-1** (752 mg, 3.53 mmol) in 6 mL of ethanol, 10 % Pd/C and 1.5 eq. of ammonium formate was added magnetically stirred in room temperature. The reaction mixture turned from yellow to red and then to colorless in 1.5 hours at room temperature. The reaction was monitored by FIA analysis. The crude reaction mixture was carried out for the next step.

2-cyclohexyl-6-methoxy-1*H*-benzo[*d*]imidazol-5-amine (3-4)

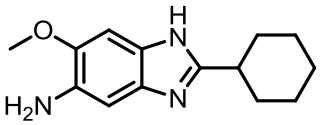

To the reaction mixture that contained compound **3-2** a solution of cyclohexylbisulfate salt in water was added directly. After stirring at room temperature overnight it had been confirmed with FIA that all the starting material had been consumed. The solution was diluted ethyl acetate and washed with water three times. The organic layers were dried with sodium sulfate, filtered, and concentrated. The residue was purified by flash chromatography on silica gel (gradient 20-40 % EtOAc/hexanes) to afford compound **3i** as off-white solid (622 mg, 72 % yield); mp 68-70 °C; ^{1}H NMR (400 MHz, $CDCl_3$) δ 1.24-1.31 (m, 1 H), 1.35-1.43 (m, 2 H), 1.61 (qd, 2 H, *J* = 12.4, 3.11 Hz), 1.74 (d, 1 H, *J* = 12.6 Hz), 1.85 (d, 2 H, *J* = 13.2 Hz), 2.11 (dd, 2 H, *J* = 13.2, 1.72 Hz), 2.81 (tt, 1 H, *J* = 11.8, 3.51 Hz), 3.86 (s, 3 H), 6.82 (s, 1 H), 7.03 (s, 1 H); ^{13}C NMR (100 MHz, $CDCl_3$) δ 14.1, 22.6, 25.9, 26.0, 31.6, 31.9, 38.4, 56.0, 132.9, 133.0, 145.3, 156.6, 156.7

Butyl (2-cyclohexyl-6-methoxy-1*H*-benzo[*d*]imidazol-5-yl)carbamate (3-5a)

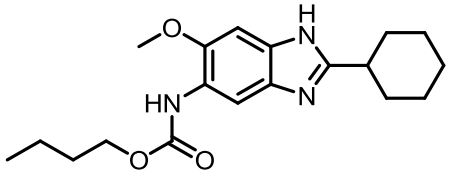

To a solution of **3e** (49 mg, 0.2 mmol) in 6 mL of DCM, 1.1 eq. of CDI was added and refluxed for 9 hours and magnetically stirred. 1-butanol (1.0 eq.) was added and stirred for 16 hours. The solution was diluted with DCM and basified with NaHCO3 and then washed with water three times. The organic layers were dried with sodium sulfate, filtered, and concentrated. The residue was purified by flash chromatography on silica gel (gradient 20-40 % EtOAc/hexanes) to afford

compound as off-white solid (46 mg, 67 % yield); mp 79-80.5 °C; ^{1}H NMR (400 MHz, $CDCl_3$) δ 0.93 (t, 3 H, *J* = 7.29 Hz), 1.25-1.48 (m, 5 H), 1.56-1.73 (m, 5 H), 1.82 (d, 2 H, *J* = 12.5 Hz), 2.09 (d, 2 H, *J* = 12.1 Hz), 2.78-2.85 (m, 1 H), 3.86 (s, 3 H), 4.18 (t, 2 H, *J* = 6.57 Hz), 7.12 (s, 1 H), 7.30 (s, 1 H), 8.19 (s, 1 H); ^{13}C NMR (100 MHz, $CDCl_3$) δ 13.7, 19.1, 25.8, 26.0, 29.7, 31.0, 31.8, 38.4, 56.1, 65.0, 123.8, 145.0, 154.0, 158.4

_N_-(2-cyclohexyl-6-methoxy-1_H_-benzo[_d_]imidazol-5-yl)-4-methylbenzamide (3-5b)

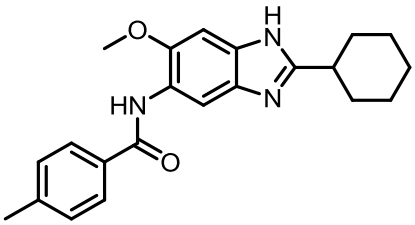

To a solution of **4i** (91 mg, 0.37 mmol) in 6 mL of DCM, *p*-toluoyl chloride (1.0 eq.) in 6 mL of DCM was added and magnetically stirred in the ice bath. The reaction mixture was slowly warmed up to room temperature and stirred for 3.5 hours. The solution was diluted with DCM and then washed with water three times. The organic layers were dried with sodium sulfate, filtered, and concentrated. The residue was purified by flash chromatography on silica gel (gradient 20-40 % EtOAc/hexanes) to afford compound as off-white solid (112 mg, 83 % yield); mp 122.5-123 °C; ^{1}H NMR (400 MHz, $CDCl_3$) δ 1.10-1.25 (m, 3 H), 1.51-1.64 (m, 3 H), 1.71 (dd, 2 H, *J* = 10.1, 2.91 Hz), 1.99 (d, 2 H, *J* = 11.9 Hz), 2.45 (s, 3 H), 2.67-2.75 (m, 1 H), 3.94 (s, 3 H), 7.22 (s, 1 H), 7.33 (d, 2 H, *J* = 8.0 Hz), 7.84 (d, 2 H, *J* = 8.15 Hz), 8.76 (s, 1 H), 8.85 (s, 1 H); ^{13}C NMR (100 MHz, $CDCl_3$) δ 21.5, 25.7, 25.9, 38.4, 56.3, 123.4, 127.0, 129.5, 132.7, 142.3, 145.3, 159.4, 165.8

_N_-(2-cyclohexyl-6-methoxy-1_H_-benzo[_d_]imidazol-5-yl)-2,4-difluorobenzamide (3-5c)

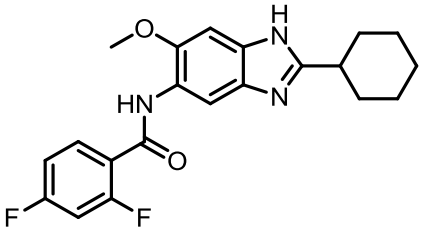

To a solution of **4i** (75 mg, 0.31 mmol) in 6 mL of DCM, 2,4-difluorobenzoyl chloride (1.0 eq.) in 6 mL of DCM was added and magnetically stirred in the ice bath. The reaction mixture was

slowly warmed up to room temperature and stirred for 4 hours. The solution was diluted with DCM and then washed with water three times. The organic layers were dried with sodium sulfate, filtered, and concentrated. The residue was purified by flash chromatography on silica gel (gradient 20-40 % EtOAc/hexanes) to afford compound as off-white solid (83 mg, 70 % yield); mp 112-112.5 °C; ^{1}H NMR (400 MHz, $CDCl_3$) δ 1.20-1.34 (m, 3 H), 1.56-1.70 (m, 3 H), 1.78 (d, 2 H, *J* = 12.95 Hz), 2.08 (d, 2 H, J = 12.3 Hz), 2.81 (tt, 1 H, *J* = 11.7, 3.26 Hz), 3.95 (s, 3 H), 6.95 (ddd, 1 H, *J* = 11.5, 8.79, 2.42 Hz), 7.05-7.09 (m, 1 H), 7.23 (s, 1 H), 8.25 (td, 1 H, *J* = 8.70, 6.83 Hz), 8.79 (s, 1 H), 9.38 (d, 1 H, *J* = 14.4 Hz); ^{13}C NMR (100 MHz, $CDCl_3$) δ 25.7, 26.0, 38.5, 56.4, 104.2, 104.5, 104.8, 112.4, 112.6, 118.2, 118.3, 118.4, 123.4, 133.6, 133.7, 145.5, 159.3, 159.4, 159.5, 160.1, 161.9, 162.0, 163.6, 163.7, 166.1, 166.3

4-(*tert*-butyl)-*N*-(2-cyclohexyl-6-methoxy-1*H*-benzo[*d*]imidazol-5-yl)benzamide (3-5d)

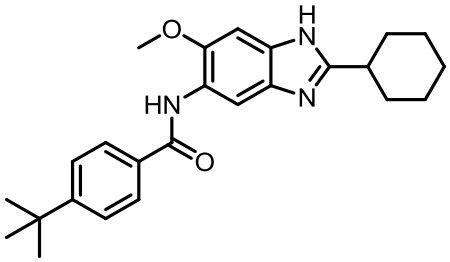

To a solution of **4i** (74 mg, 0.30 mmol) in 6 mL of DCM, *t*-butylbenzoyl chloride (1.0 eq.) in 6 mL of DCM was added and magnetically stirred in the ice bath. The reaction mixture was slowly warmed up to room temperature and stirred for 3.5 hours. The solution was diluted with DCM and then washed with water three times. The organic layers were dried with sodium sulfate, filtered, and concentrated. The residue was purified by flash chromatography on silica gel (gradient 20-40 % EtOAc/hexanes) to afford compound as off-white solid (109 mg, 90 % yield); mp > 230 °C; ^{1}H NMR (400 MHz, $CDCl_3$) δ 1.10-1.13 (m, 1 H), 1.24-1.27 (m, 2 H), 1.38 (s, 9 H), 1.53-1.60 (m, 3 H), 1.68 (d, 2 H, *J* = 12.4 Hz), 1.98 (d, 2 H, *J* = 12.3 Hz), 2.67-2.73 (m, 1 H), 3.95 (s, 3 H), 7.24 (s, 1 H), 7.56 (d, 2 H, *J* = 8.41 Hz), 7.89 (d, 2 H, *J* = 8.42 Hz), 8.81 (s, 1 H), 8.92 (s, 1 H); ^{13}C NMR (100 MHz, $CDCl_3$) δ 14.2, 21.0, 25.7, 25.9, 29.7, 31.2, 31.8, 35.0, 38.4, 56.3, 60.4, 123.4, 125.9, 126.8, 132.8, 145.2, 145.2, 155.3, 159.3, 159.5, 165.9, 171.1

***N*-(2-cyclohexyl-6-methoxy-1*H*-benzo[*d*]imidazol-5-yl)-4-(trifluoromethoxy)benzamide (3-5e)**

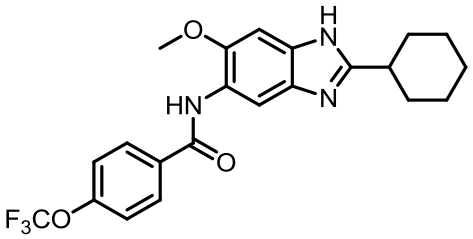

To a solution of **4i** (65 mg, 0.27 mmol) in 6 mL of DMF, 4-(trifluoromethoxy)benzoic acid (1.2 eq.), EDC (1.2 eq.) and DMAP (1.2 eq.) were added and magnetically stirred and carried in the microwave for 1 hour. The solution was diluted with EA and then washed with water three times. The organic layers were dried with sodium sulfate, filtered, and concentrated. The residue was purified by flash chromatography on silica gel (gradient 20-40 % EtOAc/hexanes) to afford compound as off-white solid (81 mg, 70 % yield); mp 175-176 °C; ^{1}H NMR (400 MHz, $CDCl_3$) δ 1.13-1.25 (m, 3 H), 1.54-1.66 (m, 3 H), 1.74 (d, 2 H, *J* = 12.1 Hz), 2.03 (d, 2 H, *J* = 11.5 Hz), 2.75 (t, 1 H, *J* = 11.4 Hz), 3.94 (s, 3 H), 7.23 (s, 1 H), 7.36 (d, 2 H, *J* = 7.95 Hz), 7.98 (d, 2 H, *J* = 8.33 Hz), 8.74 (s, 1 H), 8.77 (s, 1 H); ^{13}C NMR (100 MHz, $CDCl_3$) δ 25.7, 25.9, 29.7, 31.8, 38.5, 56.3, 119.3, 120.9, 121.3, 123.1, 128.9, 133.9, 145.4, 151.6, 159.4, 164.2

In a similar manner, compounds **3-5f** ~ **3-5h** were synthesized and characterized.

***N*-(2-cyclohexyl-6-methoxy-1*H*-benzo[*d*]imidazol-5-yl)-2-fluoro-4-(trifluoromethoxy)benzamide (3-5f)**

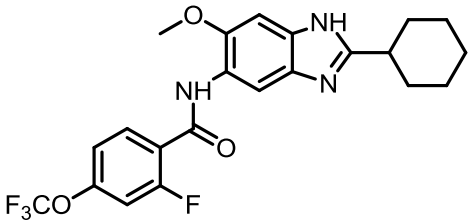

Off-white solid; 55 % yield; mp 175-176 °C; ^{1}H NMR (500 MHz, $CDCl_3$) δ 1.20-1.36 (m, 3 H), 1.57-1.65 (m, 2 H), 1.69-1.71 (m, 1 H), 1.79-1.81 (m, 2 H), 2.09-2.10 (d, 2 H, *J* = 5 Hz), 2.79-2.84 (m, 1 H), 3.95 (s, 3 H), 7.10 (d, 1 H, *J* = 10 Hz), 7.19 (d, 1 H, , *J* = 10 Hz), 8.27 (t, 1 H, , *J* = 10 Hz), 8.76 (s, 1 H), 9.37 (d, 1 H, , *J* = 10 Hz); ^{13}C NMR (125 MHz, $CDCl_3$) δ 25.8, 26.0, 31.8, 39.5, 56.4, 108.8, 109.0, 116.8, 119.1, 120.3, 120.4, 121.2, 123.4, 133.5, 145.5, 152.1, 159.3, 159.7, 161.3

***N*-(2-cyclohexyl-6-methoxy-1*H*-benzo[*d*]imidazol-5-yl)-2,6-difluoro-4-methoxybenzamide (3-5g)**

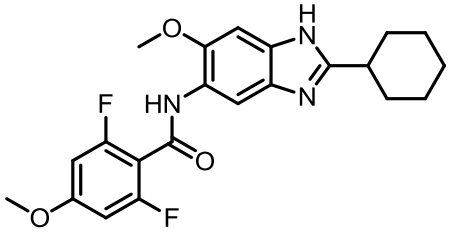

Off-white solid; 33 % yield; mp 112-112.5 ℃; ^{1}H NMR (500 MHz, $CDCl_3$) δ 1.17-1.34 (m, 3 H), 1.55-1.63 (m, 2 H), 1.69-1.70 (m, 1 H), 1.77-1.80 (m, 2 H), 2.04-2.06 (d, 2 H, *J* = 10 Hz), 2.74-2.80 (m, 1 H), 3.85 (s, 3 H), 3.91 (s, 3 H),6.55 (s, 1 H), 6.57 (s, 1 H), 7.22 (s, 1 H), 8.56 (s, 1 H), 8.79 (s, 1 H); ^{13}C NMR (125 MHz, $CDCl_3$) δ 25.8, 26.0, 29.7, 31.7, 56.1, 56.4, 99.6, 99.8, 107.2, 123.2, 145.2, 159.2, 159.3, 160.2, 162.3, 162.4, 162.5, 162.6

***N*-(2-cyclohexyl-6-methoxy-1*H*-benzo[*d*]imidazol-5-yl)-2,4,6-trimethoxybenzamide (3-5h)**

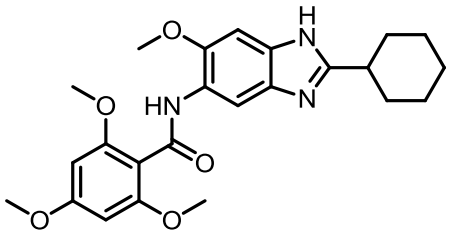

Off-white solid; mp 109-112 ℃; 73 % yield: ^{1}H NMR (500 MHz, $CDCl_3$) δ 1.20-1.32 (m, 2 H), 1.53-1.63 (m, 2 H), 1.66-1.72 (m, 1 H), 1.75-1.82 (m, 3 H), 2.01-2.07 (m, 3 H), 3.79 (s, 3 H), 3.86 (s, 3 H), 3.87 (s, 3 H), 3.90 (s, 3 H), 6.29 (s, 2 H), 7.20 (s, 2 H), 8.97 (s, 1 H); ^{13}C NMR (125 MHz, $CDCl_3$) δ 25.8, 26.0, 26.1, 38.4, 55.5, 56.0, 56.2, 56.3, 90.6, 90.8, 109.4, 122.5, 124.1, 145.0, 145.1, 157.4, 158.7, 158.8, 159.0, 161.8, 162.4, 163.7

***N*-(2-cyclohexyl-6-(phenylthio)-1*H*-benzo[*d*]imidazol-5-yl)pent-4-enamide (3-5i)**

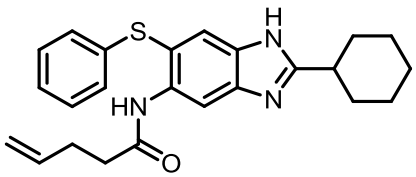

To a solution of **4f** (30 mg, 0.09 mmol) in 6 mL of DMF, 4-pentenoic acid (1.2 eq.), EDC (1.2 eq.) and DMAP (1.2 eq.) were added and magnetically stirred in the microwave for 1.5 hours.

The solution was diluted with EA and then washed with water three times. The organic layers were dried with sodium sulfate, filtered, and concentrated. The residue was purified by flash chromatography on silica gel (gradient 20-40 % EtOAc/hexanes) to afford compound as off-white solid (25 mg, 69 % yield): ^{1}H NMR (400 MHz, $CDCl_3$) δ 1.25-1.36 (m, 3 H), 1.60-1.72 (m, 3 H), 1.84 (dd, 2 H, *J* = 10.1, 3.14 Hz), 2.11 (d, 2 H, *J* = 11.6 Hz), 2.30-2.41 (m, 4 H), 2.85 (ddd, 1 H, *J* = 15.5, 8.01, 3.80 Hz), 4.92-5.01 (m, 2 H), 5.71 (ddt, 1 H, *J* = 16.9, 10.4, 6.44 Hz), 7.04 (d, 2 H, *J* = 7.53 Hz), 7.12 (t, 1 H, *J* = 7.33 Hz), 7.20 (t, 2 H, *J* = 7.57 Hz), 7.97 (s, 1 H), 8.51 (s, 1 H), 8.67 (s, 1 H); ^{13}C NMR (100 MHz, $CDCl_3$) 25.8, 26.0, 29.6, 29.7, 31.7, 37.6, 39.6, 116.1, 125.9, 126.5, 129.2, 133.9, 136.1, 136.8, 160.7, 170.9

§ 3.4.4 Bacterial Strains and Growth

For evaluation of drug sensitivity, *Mtb* H37Rv was grown in 7H9 media containing 10% oleic acid/albumin/catalase (OADC) enrichment and 0.05% Tween-80 and assessed at mid log phase growth.

§ 3.4.5 Antibacterial Activity Determination

The minimum inhibitory concentration (MIC) was determined by the microplate Alamar Blue assay (MABA)[4] as described previously. Briefly, stock solutions of the compounds were prepared in DMSO and were serially diluted 2-fold in 96-well microtiter plates, and *Mtb* H37Rv strain was added to each well to an OD600 of 0.005. Plates were incubated for 6 days at 37 ℃. Alamar Blue (Invitrogen) was added to the plates, and the plates were incubated for an additional 24 h at 37 ℃. Plates were monitored for color change, and MIC_{99} was determined in triplicate.

§ 3.5 References

1. Awasthi, D.; Kumar, K.; Knudson, S. E.; Slayden, R. A.; Ojima, I., SAR studies on trisubstituted benzimidazoles as inhibitors of Mtb FtsZ for the development of novel antitubercular agents. *Journal of medicinal chemistry* **2013,** *56* (23), 9756-9770.
2. Kumar, K.; Awasthi, D.; Lee, S. Y.; Zanardi, I.; Ruzsicska, B.; Knudson, S.; Tonge, P. J.; Slayden, R. A.; Ojima, I., Novel trisubstituted benzimidazoles, targeting Mtb FtsZ, as a new class of antitubercular agents. *Journal of medicinal chemistry* **2011,** *54* (1), 374-381.
3. Park, B.; Awasthi, D.; Chowdhury, S. R.; Melief, E. H.; Kumar, K.; Knudson, S. E.; Slayden, R. A.; Ojima, I., Design, synthesis and evaluation of novel 2,5,6-trisubstituted benzimidazoles targeting FtsZ as antitubercular agents. *Bioorganic & medicinal chemistry* **2014,** *22* (9), 2602-2612.
4. Collins, L.; Franzblau, S. G., Microplate alamar blue assay versus BACTEC 460 system for high-throughput screening of compounds against Mycobacterium tuberculosis and Mycobacterium avium. *Antimicrobial agents and chemotherapy* **1997,** *41* (5), 1004-1009.

Chapter 4

Biological Evaluation of 2,5,6-TrisubstituedBenzimidazoles against *M. Smeg*

Chapter Contents

§ 4.1 Introduction 82

§ 4.2 Results and discussion 84

§ 4.2.1 *M. Smeg* Assay 84

§ 4.2.2 Optimizing *M. Smeg* Assay 84

§ 4.2.3 Introducing the automatic system to *M. Smeg* assay 85

§ 4.3 Conclusion 88

§ 4.4 Experimental Section 89

§ 4.4.1 General Methods 89

§ 4.4.2 Materials 89

§ 4.4.3 Experimental Procedures 89

§ 4.4.4 *M. Smegmatis* Assay with Alamar Blue 94

§ 4.4.5 *M. Smegmatis* Assay based on the Clarity 94

§ 4.5 References 96

§ 4.1 Introduction

With the emergence of drug resistant bacteria (MDR-TB, XDR-TB, VRE, MRSA), co-infection with HIV-immune compromised individuals,[1-3] current available antibiotics are much less effective. Moreover, the potential of weaponizable existing pathogens (*B. pseudomallei*, *Y. pestis*, *F. tularensis*),[2-8] there is a pressing need to develop new and novel classes of drugs to combat these pathogens.

Current representative antibiotic targets include cellular mechanisms involved in fatty-acid biosynthesis for cell membrane and cell wall synthesis (Isoniazid, Ethambutol, etc), RNA polymerase (Rifampicin), ribosomal protein synthesis (Kanimycin, Capreomycin), and DNA replication/maintenance (Ciprofloxcin and other quinolones); all of which have shown levels of bacterial resistance.[9-11]

As discussed previous chapters, one possible target for new drug development is cell division. Especially, the bacterial tubulin homolog FtsZ which is a GTP-dependent, cell division protein required for bacterial survival and proliferation.[12-19]

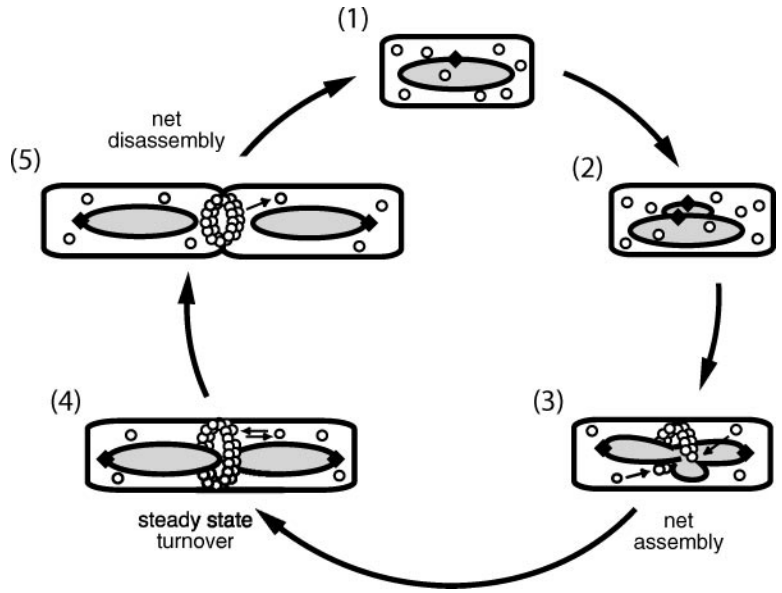

Figure 4- 1: The bacterial division cycle

Figure 4-1 illustrated the bacterial division cell cycle. FtsZ assembly is coordinated with DNA replication and segregation. Step 1: In newborn cells FtsZ (O) is unassembled. A circular chromosome with a single origin of replication (r) is located at midcell. Steps 2–4: After

chromosome replication initiates, the polymerase machinery remains at midcell, but origins of replication separate and move to opposite poles of the cell. Once replication is complete, the condensed chromosomes separate, leaving a nucleoid-free space. Step 3: Z ring formation coincides with chromosome segregation. Assembly starts from a single point at midcell and extends bidirectionally. Step 5: During cytokinesis the Z ring constricts at the leading edge of the invaginating septum. Small arrows indicate the assembly and disassembly of FtsZ subunits.[20]

Mycobacterium smegmatis (*M. Smeg.)* is recognized as a good model of *M. tuberculosis*, due to their conserved transcriptional machinery, sigma factors, and two-component systems. *M. smegmatis* was originally isolated from human smegma in 1885 and it is known to have approximately 1.7-fold larger genome than that of *M. tuberculosis.*[21, 22] Free access to the unfinished DNA sequence of *M. smegmatis* (http://www.tigr.org) has enabled *in silico* comparisons to be made between the annotated genome of *Mycobacterium tuberculosis* and the sequence of *M. smegmatis*.[23] Studies showed that 6 of 11 two-component systems and 5 of seven orphan response-regulator/histidine kinases of *M. tuberculosis* had homologues in *M. smegmatis* cut off values of 50 % identity over 90% length of the protein.[24] A recent report had cited the conservation of 10 out of 11 two-component systems and 5 out of 7 orphan response-regulator/sensor kinase proteins, however, the identity criteria for homology were not specified by the authors.[24] It is considered as good mycobacteria model since it grows fast and non-pathogenic. Even though there are several other fast growing species within the mycobacterium family has been evaluated as surrogates for *Mtb* in vitro, we *chose M. Smeg* since it was shown to respond most similarly to *Mtb*, especially MDR-TB phenotype.[5] Since it is not pathogenic, it only requires biosafety level 1 laboratory. Given the fact that *Mtb* grows slow (doubling time between 18 and 54 hours) and pathogenic, MIC determination with *M. Smeg* was employed.[1] Screen of lead compounds was carried out using established protocols via Alamar Blue assay[25] at first. Later on, we hypothesized that this dye could interact with our compounds and gave us the un-explainable random results. Therefore, we removed dye and determined the MIC result by clarity of the media.

§ 4.2 Results and discussion

§ 4.2.1 *M. Smeg* Assay

2,5,6-Trisubstituted benimidazoles were used for evaluating their MIC values. All of the compounds were dissolved in ethanol and then serially diluted. Compounds were incubated with the cells for 48 hours and evaluated for viability using Alamar Blue. Structures of intermediate compounds shown in Figure 4-2 with observed MIC values.

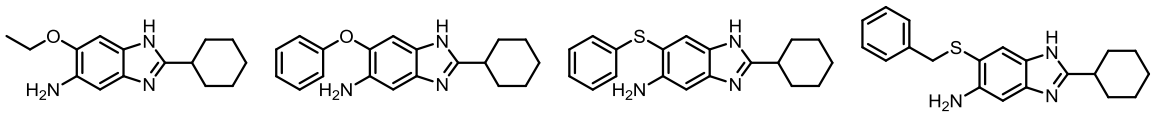

4-1 MIC 25 μg/mL | **4-2** MIC 12.5 μg/mL | **4-3** MIC 6.23 μg/mL | **4-4** MIC 3.13 μg/mL

Figure 4- 2: Chemical structures and their MIC values

Fig. 4-2 shows the MIC values with **4-1**, **4-2**, **4-3** and **4-4**. The two compounds, **4-1** and **4-2** which are bearing ether linkage at the 6-position, were determined MIC values 25 and 12.5 μg/mL, respectively. The two other benzimidazoles, which are bearing thiophenoxy, and benzylthioxy group at the 6-position, were determined their MIC values as 6.25 and 3.13 μg/mL respectively.

§ 4.2.2 Optimizing *M. Smeg* Assay

As we proceed to determine the MIC values of our lead 2,5,6-trisubstituted benzimidazoles, we found the inconsistency of the assay. There were problems with the assay such as contamination and/or possible cross reaction with Alamar blue dye. At this point, we tried to reduce the chance from the bacteria contamination. As a result, we removed the step for adding the Alamar Blue dye since it might cause the problems to reduce the inconsistency. Instead of color change, we decide to determine the MIC values by clarity of the media. When the drug is active after the drug treatment, the media remains clear. However, when the bacteria alive, then the media becomes murky and unclear since bacteria keep growing. In each experiment, we prepare the two controls which only media and only cells and media to compare

the clarity. To validate this assay condition is reliable, 5 known antibiotics were determined.

Table 4-1 shows the MIC result testing against *M. Smeg* using known inhibitors, rifampin, ampicillin, isoniazid, ethambutol, and tricolsan. As **Table 4-1** indicates this assay is reliable compared to the reference values.[5, 26-29]

Table 4- 1: Reference values

Compounds	MIC
Rifampin	**3.125 µg/µL**
Ampicilin	**> 100 µg/µL**
Isoniazid	**12.5 µg/µL**
Ethambutol	**< 0.625 µg/µL**
Tricolsan	**25 µg/µL**

After we validate the assay works with many trials and errors, the lead compound was test to determine their MIC values against *M. Smeg* along with reference compounds.

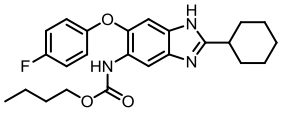

4-5
MIC 1.56 µM

Figure 4- 3: Chemical structure of lead compound and its MIC values

The compound 4-5 exhibited MIC value of 1.56 µM against *M. smegmatis* strain.

§ 4.2.3 Introducing the automatic system to *M. Smeg* assay

With the optimized condition, we tried to apply the *M. Smeg* assay into the robotic system. First, we need to confirm that this assay works since the bacteria had been frozen at -78 ℃ for about 3 months. After confirmed the bacteria strain had no issues such as contamination, we

carried forward the assay with the known antibiotics. To apply the automated system, we needed to serially dilute compounds from the most concentrated one resulting in reducing the total DMSO amount. Therefore we fixed the 1 % DMSO for the most concentrated stock solution, and serially dilute the drug concentration from there. As we expected, the results shows the same. Isoniazid determined the MIC value of 50 µM and ampicilin determined as > 100 µM as similar as literature values.

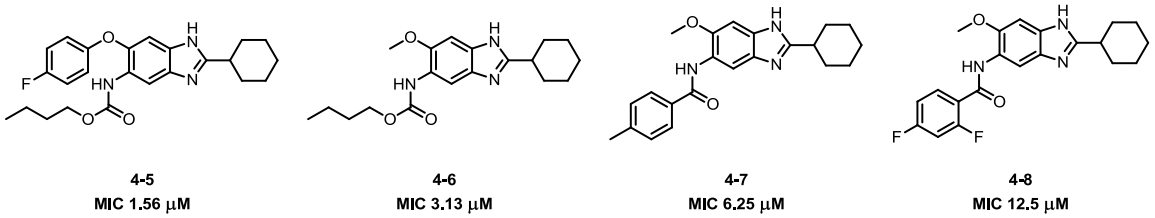

Figure 4- 4: Chemical structures of lead compounds and their MIC values

After we validated the automated system worked with the assay, we carried out our compounds to confirm their MIC values. **Figure 4-4** illustrated the chemical structures and their MIC values against *M. Smegmatis* strain. The compounds **4-6**, **4-7** and **4-8** which are bearing methoxy group at the 6-position were tested and they exhibited MIC values 3.13 to 12.5 µM. Compound **4-5** was tested as a positive control and exhibited the same value as previously reported. With significant benefit of time saving, this system will be further used with our other trisubstitued benzimidazoles not only against *M smegmatis* but also other pathogens such as *Staphylococcus aureus*.

Even though, previous evaluation of 2,5,6-trisubstituted benzimidazoles bearing amino moiety at the 6-position did not show correlation between *Mtb* and *M. Smeg*., most of our hit compounds especially bearing 6-methoxy group exhibited good MIC values against both pathogens. The lack of correlation for some of our compounds between *Mtb* and *M. smegmatis* is mainly due to their basic physiological differences between M. smegmatis and pathogenic *Mycobacterium*. *M. smegmatis* lacks properties of pathogen, and cannot enter epithelial cells and persists in professional phagocytes which are equipped with receptor molecules that are attracted to certain chemicals that signal the presence of an infection. Even though the difference and similarity in structures between *Mtb* FtsZ and *M. Smeg* FtsZ are largely unclear, there might be substantial difference in the binding site structure between *Mtb* FtsZ and *M. Smeg* FtsZ despite

the fact that those two pathogens are categorized as very close *Micobacterium* species. Underlying genetic basis for such remarkable difference remains to be determined.

§ 4.3 Conclusion

In-house libraries of trisubstituted benzimidazoles were screened against other pathogens, *M. smegmatis*, since FtsZ is a highly conserved bacteria cell division protein. Remarkably, most of our hit compounds exhibited good MIC values. To resolve the unclear problems with alamar blue assay, we developed the new method to determine MIC values. With many trials and errors, the reproducible *M. Smeg* assay was successfully introduced. Moreover, this assay can further prepared by the robotic system. Further optimaization of the lead compounds for their activity against *M. smegmatis* strain with the robotic system is actively underway in our laboratory.

§ 4.4 Experimental Section

§ 4.4.1 General Methods

^{1}H and 13C NMR spectra were measured on a Brucker 400 or 500 MHz NMR spectrometer. Melting points were measured on a Thomas Hoover Capillary melting point apparatus and are uncorrected. TLC was performed on Sorbtech with UV254 and column chromatography was carried out on silica gel 60 (Merck; 230-400 mesh ASTM). High- resolution mass spectra were obtained on Agilent-TOF instrument.

§ 4.4.2 Materials

The chemicals were purchased from Sigma Aldrich Co., Synquest Inc., Alfa Aesar and purified before use by standard methods. Tetrahydrofuran was freshly distilled from sodium metal and benzophenone. Dichloromethane was also distilled immediately prior to use under nitrogen from calcium hydride. Aminomethylated polystyrene resine EHL (200-400 mesh) 2 % DVB was purchased from Novagen Biochem.

§ 4.4.3 Experimental Procedures

5-Amino-6-ethoxy-2-cyclohexyl-1H-benzo[d]imidazol (4-1)

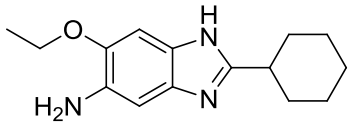

A solution of **1-2a** (100 mg, 0.30 mmol), tin(II) chloride dihydrate (0.47 g, 2.1 mmol) in 10 mL of EtOH was magnetically stirred and refluxed at 90 ^{o}C under nitrogen for 1 h. The reaction mixture was cooled, quenched with 30 % KOH, and pH adjusted to ~13. The solution was diluted with dichloromethane and washed with water three times. The organic layers were dried over sodium sulfate, filtered, and concentrated. The residue was purified by flash chromatography on silica gel (gradient 20-40 % EtOAc/hexanes) to afford compound **1-3a** as a pale red color solid (69 g, 89 % yield): mp 89-90 ℃; ^{1}H NMR (500 MHz, $CDCl_3$) δ 1.23 (ddd, 1 H, *J* = 14.2, 10.8, 3.3 Hz), 1.32 (ddd, 2 H, *J* = 14.2, 11.1, 3.1 Hz), 1.37-1.42 (m, 3 H), 1.60 (qd, 2 H, *J* = 12.4, 3.1 Hz), 1.69-1.71 (m, 1 H), 1.79-1.81 (m, 2 H), 2.08 (d, 2 H, *J* = 12.4 Hz), 2.80 (tt, 1 H, *J* = 11.8, 3.51 Hz), 3.79 (br, 2 H), 3.99 (dd, 2 H, *J* = 8.3, 3.3 Hz), 6.78 (s, 1 H), 6.96 (s, 1 H);

^{13}C NMR (125 MHz, $CDCl_3$) δ 15.0, 25.9, 26.1, 32.0, 38.5, 64.4, 132.9, 133.0, 144.5, 157.0; HRMS (ESI) m/z calcd for $C_{15}H_{22}N_3O^+$ 260.1757 Found: 260.1758 (Δ = 0.38 ppm).

In a similar manner, compounds **4-2** were synthesized and characterized.

5-Amino-6-phenoxy-2-cyclohexyl-1H-benzo[d]imidazol (4-2)

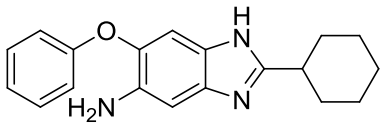

Pale yellow solid; 46 % yield; mp 136-138 °C; ^{1}H NMR (400 MHz, $CDCl_3$) δ 1.25-1.32 (m, 1 H), 1.35-1.44 (m, 2 H), 1.56-1.66 (m, 2 H), 1.72-1.77 (m, 1 H), 1.83-1.88 (m, 2 H), 2.09-2.14 (m, 2 H), 2.80-2.86 (m, 1 H), 3.73 (br, 2 H), 6.93-6.97 (m, 2 H), 7.01-7.05 (m, 1 H), 7.12 (s, 1 H), 7.26-7.29 (m, 2 H); ^{13}C NMR (100 MHz, $CDCl_3$) δ 25.9, 26.0, 31.9, 38.5, 116.7, 122.4, 129.7, 135.3, 140.3, 158.1; HRMS (ESI) m/z calcd for $C_{19}H_{22}N_3O^+$ 308.1757 Found: 308.1758 (Δ = 0.32 ppm).

5-Amino-6-(phenylthio)-2-cyclohexyl-1H-benzo[d]-imidazol (4-3)

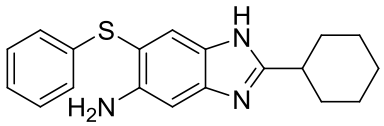

A solution of **1-2f** (1.97 g, 5.16 mmol), tin(II) chloride dihydrate (15.5 g, 36.1 mmol), and 4 M HCl (80 mL) in 200 mL of EtOH was magnetically stirred and refluxed for 4 h. The reaction mixture was cooled, quenched with 1M NaOH, and pH was adjusted to ~10. Tin salts precipitated in solution upon addition of 1 M NaOH. The reaction mixture was filtered to remove the tin salts. The solution was diluted with ethyl acetate and washed with water three times. The organic layers were dried over magnesium sulfate, filtered, and concentrated in vacuo. The residue was purified by flash chromatography on silica gel (gradient 20-40 % EtOAc/hexanes) to

afford compound **4-3** as a pale brownish solid in 57 % yield; mp 116-118 ℃; ^{1}H NMR (500 MHz, $CDCl_3$) δ 1.27-1.35 (m, 1 H), 1.42 (qt, 2 H, *J* = 12.79, 3.29 Hz), 1.66 (qd, 2 H, *J* = 12.4, 3.29 Hz), 1.76-1.80 (m, 1 H), 1.89 (dt, 2 H, *J* = 13.3, 3.38 Hz), 2.16 (dd, 2 H, *J* = 13.7, 2.01 Hz), 2.88 (tt, 1 H, *J* = 11.8, 3.55 Hz), 4.22 (br, 2 H), 6.92 (s, 1 H), δ 7.08-7.13 (m, 3 H), δ 7.20-7.23 (m, 2 H), δ 7.67 (s, 1 H); ^{13}C NMR (125 MHz, $CDCl_3$) δ 25.8, 26.0, 31.8, 38.5, 110.6, 125.3, 126.1, 128.9, 137.6, 144.6; HRMS (ESI) m/z calcd for $C_{19}H_{22}N_3S^+$ 324.1529 Found: 324.1529 (Δ = 0.0 ppm).

In a similar manner, compounds **4-4** were synthesized and characterized.

5-Amino-6-(benzylthio)-2-cyclohexyl-1H-benzo[d]-imidazol (4-4)

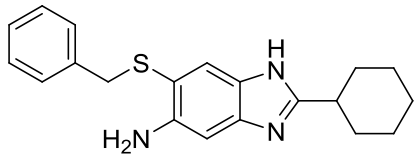

Pale beige solid; 56 % yield; mp 129.5-131 ℃; ^{1}H NMR (500 MHz, $CDCl_3$) δ 1.18-1.23 (m, 1 H), 1.27-1.35 (m, 2 H), 1.60 (qd, 2 H, *J* = 12.4, 3.2 Hz), 1.69 (d, 1 H, *J* = 12.7 Hz), 1.78 (dt, 2 H, J = 13.1, 3.0 Hz), 2.07 (dd, 2 H, *J* = 14.2, 2.5 Hz), 2.80-1.85 (m, 1 H), 3.86 (s, 2 H), 6.77 (s, 1 H), 7.10-7.12 (m, 2 H), 7.17 (td, 3 H, *J* = 6.5, 2.8 Hz), 7.49 (s, 1 H); ^{13}C NMR (125 MHz, $CDCl_3$) δ 25.7, 26.0, 31.7, 38.4, 40.7, 64.4, 98.4, 114.0, 123.1, 126.9, 128.3, 128.7, 132.8, 138.2, 139.1, 144.2, 159.1, 176.3; HRMS (ESI) m/z calcd for $C_{20}H_{24}N_3S^+$ 338.1685 Found: 338.1686 (Δ = 0.3 ppm).

5-Butoxycarbonylamino-2-cyclohexyl-6-(4-fluorophenoxy)-1H-benzo[d]imidazole (4-5)

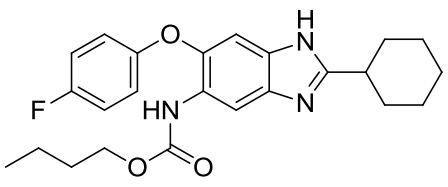

To a solution of **1-3a** (100 mg, 0.31 mmol) in 6 mL of dichloromethane was added *N*-butoxycarbonyloxysuccinimide (68 mg, 0.31 mmol) in 6 mL of dichloromethane and the mixture was magnetically stirred under nitrogen atmosphere in an ice bath. The reaction mixture was slowly warmed up to room temperature and stirred for 16 h. The solution was diluted with dichloromethane and basified with $NaHCO_3$ and then washed with water three times. The organic layers were dried over sodium sulfate, filtered, and concentrated. The residue was purified by flash chromatography on silica gel (gradient 20-40 % EtOAc/hexanes) to afford compound **4-5** as an off-white solid (54 mg, 47 % yield): mp 91-92 °C; ^{1}H NMR (400 MHz, $CDCl_3$) 0.97 (t, 3 H, *J* = 7.4 Hz), 1.28-1.30 (m, 1 H), 1.39-1.45 (m, 4 H), 1.61-1.65 (m, 2 H), 1.67 (t, 2 H, *J* = 7.5 Hz), 1.76 (d, 1 H, *J* = 12.5 Hz), 1.85-1.88 (m, 2 H), 2.12 (d, 2 H, *J* = 12.5 Hz), 2.83-2.88 (m, 1 H), 4.19 (t, 2 H, *J* = 6.7 Hz), 6.96-7.05 (m, 4 H), 7.13 (s, 1 H), 8.23 (s, 1 H); ^{13}C NMR (100 MHz, $CDCl_3$) δ 13.8, 19.1, 25.8, 26.0, 31.0, 31.8, 38.5, 65.3, 116.5, 119.5, 125.6, 142.3, 153.1, 154.0, 157.8, 159.5, 159.6, 159.7; HRMS (ESI) m/z calcd for $C_{24}H_{29}FN_3O_3^+$ 426.2187 Found: 426.2187 (Δ = 0.0 ppm).

Butyl (2-cyclohexyl-6-methoxy-1*H*-benzo[*d*]imidazol-5-yl)carbamate (4-6)

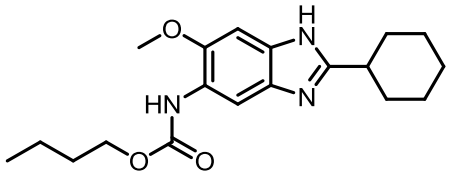

To a solution of **3e** (49 mg, 0.2 mmol) in 6 mL of DCM, 1.1 eq. of CDI was added and refluxed for 9 hours and magnetically stirred. 1-butanol (1.0 eq.) was added and stirred for 16 hours. The solution was diluted with DCM and basified with NaHCO3 and then washed with water three times. The organic layers were dried with sodium sulfate, filtered, and concentrated. The residue was purified by flash chromatography on silica gel (gradient 20-40 % EtOAc/hexanes) to afford compound as off-white solid (46 mg, 67 % yield): ^{1}H NMR (400 MHz, $CDCl_3$) δ 0.93 (t, 3 H, *J* = 7.29 Hz), 1.25-1.48 (m, 5 H), 1.56-1.73 (m, 5 H), 1.82 (d, 2 H, *J* = 12.5 Hz), 2.09 (d, 2 H, *J* = 12.1 Hz), 2.78-2.85 (m, 1 H), 3.86 (s, 3 H), 4.18 (t, 2 H, *J* = 6.57 Hz), 7.12 (s, 1 H), 7.30 (s, 1 H), 8.19 (s, 1 H); ^{13}C NMR (100 MHz, $CDCl_3$) δ 13.7, 19.1, 25.8, 26.0, 29.7, 31.0, 31.8, 38.4, 56.1, 65.0, 123.8, 145.0, 154.0, 158.4

***N*-(2-cyclohexyl-6-methoxy-1*H*-benzo[*d*]imidazol-5-yl)-4-methylbenzamide (4-7)**

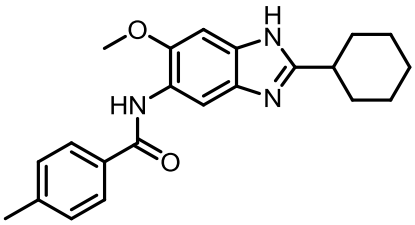

To a solution of **4i** (91 mg, 0.37 mmol) in 6 mL of DCM, *p*-toluoyl chloride (1.0 eq.) in 6 mL of DCM was added and magnetically stirred in the ice bath. The reaction mixture was slowly warmed up to room temperature and stirred for 3.5 hours. The solution was diluted with DCM and then washed with water three times. The organic layers were dried with sodium sulfate, filtered, and concentrated. The residue was purified by flash chromatography on silica gel (gradient 20-40 % EtOAc/hexanes) to afford compound as off-white solid (112 mg, 83 % yield); ^{1}H NMR (400 MHz, $CDCl_3$) δ 1.10-1.25 (m, 3 H), 1.51-1.64 (m, 3 H), 1.71 (dd, 2 H, *J* = 10.1, 2.91 Hz), 1.99 (d, 2 H, *J* = 11.9 Hz), 2.45 (s, 3 H), 2.67-2.75 (m, 1 H), 3.94 (s, 3 H), 7.22 (s, 1 H), 7.33 (d, 2 H, *J* = 8.0 Hz), 7.84 (d, 2 H, *J* = 8.15 Hz), 8.76 (s, 1 H), 8.85 (s, 1 H); ^{13}C NMR (100 MHz, $CDCl_3$) δ 21.5, 25.7, 25.9, 38.4, 56.3, 123.4, 127.0, 129.5, 132.7, 142.3, 145.3, 159.4, 165.8

***N*-(2-cyclohexyl-6-methoxy-1*H*-benzo[*d*]imidazol-5-yl)-2,4-difluorobenzamide (4-8)**

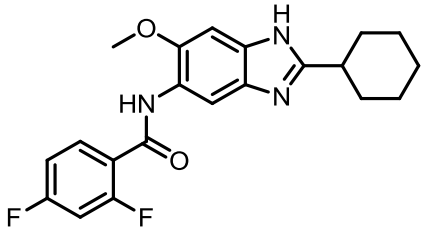

To a solution of **4i** (75 mg, 0.31 mmol) in 6 mL of DCM, 2,4-difluorobenzoyl chloride (1.0 eq.) in 6 mL of DCM was added and magnetically stirred in the ice bath. The reaction mixture was slowly warmed up to room temperature and stirred for 4 hours. The solution was diluted with DCM and then washed with water three times. The organic layers were dried with sodium sulfate, filtered, and concentrated. The residue was purified by flash chromatography on silica gel (gradient 20-40 % EtOAc/hexanes) to afford compound as off-white solid (83 mg, 70 % yield); ^{1}H NMR (400 MHz, $CDCl_3$) δ 1.20-1.34 (m, 3 H), 1.56-1.70 (m, 3 H), 1.78 (d, 2 H, *J* = 12.95 Hz), 2.08 (d, 2 H, J = 12.3 Hz), 2.81 (tt, 1 H, *J* = 11.7, 3.26 Hz), 3.95 (s, 3 H), 6.95 (ddd, 1 H, *J* =

11.5, 8.79, 2.42 Hz), 7.05-7.09 (m, 1 H), 7.23 (s, 1 H), 8.25 (td, 1 H, *J* = 8.70, 6.83 Hz), 8.79 (s, 1 H), 9.38 (d, 1 H, *J* = 14.4 Hz); ^{13}C NMR (100 MHz, $CDCl_3$) δ 25.7, 26.0, 38.5, 56.4, 104.2, 104.5, 104.8, 112.4, 112.6, 118.2, 118.3, 118.4, 123.4, 133.6, 133.7, 145.5, 159.3, 159.4, 159.5, 160.1, 161.9, 162.0, 163.6, 163.7, 166.1, 166.3

§ 4.4.4 *M. Smegmatis* Assay with Alamar Blue

M. smegmatis mc^2 155 cells (ATCC# 700084) were obtained and cultured on Middlebrook 7H10 agar supplemented with 0.5% v/v glycerol at 35.5℃ until good colonies resulted. Isolated colonies were picked and inoculated into 10 mL of Middlebrook 7H9 media supplemented with 0.05% v/v Tween 80 and 0.2% v/v glycerol (7H9-TG) and grown for 48 hours at 35.5℃ at 200-250 RPM. Cells were then diluted to OD600 of 0.15 for microplate MIC assays. Compounds under evaluation were dissolved to 4 mg/mL in ethanol and then serially diluted with 7H9-TG media across or down the microplate to make 100 μL in each well. 100 μL of diluted *M.smeg.* cells are then added to each well to make 200 μL final in each well. Final ethanol content in each well was 10% or less and did not affect cell growth. Microplates were incubated at 35.5℃ shaking 50 RPM for 24 or 48 hours as indicated, after which cells were evaluated for viability with the addition of 20 μL Alamar Blue reagent (Invitrogen) and readings were taken after another 12 to 24 hours of incubation at 35.5℃ shaking 50 RPM. MIC was recorded as the lowest concentration of inhibitor that did not show a color change in the Alamar Blue reagent from blue to pink.

§ 4.4.5 *M. Smegmatis* Assay based on the Clarity

Grow *M. smeg* on 7H10 + 0.5 % glycerol agar plates for 3-4 days until good colonies. Inoculate 10 mL 7H9-TH (supppemented with 0.05 % v/v tween 80, 0.2 % glycerol to prevent aggregation) with one colony in a sterile tube and grow until mid log phase (OD600 0.5 to 0.9: about 2 days). When cells are ready, dilute cells to OD600 0.001 with media 7H9 + tween 80 + glycerol for addition to 96 plates. Add 100 μL of the diluted cells to each well and then add media to column 2 to 11. Add 200 μL cells and 2 μL DMSO to column 1. Add 200 μL media to column 12. Add 2 μL of drug stock solution that dissolved in DMSO. Prepare the hydration

plates by filing all of the wells of 2 96 well plates with sterile water and put one on top and the other at the bottom of the plates that are used for testing.

§ 4.5 References

1. Gill, W. P.; Harik, N. S.; Whiddon, M. R.; Liao, R. P.; Mittler, J. E.; Sherman, D. R., A replication clock for Mycobacterium tuberculosis. *Nature medicine,* **2009,** *15* (2), 211-214.
2. Klevens, R. M.; Morrison, M. A.; Nadle, J.; Petit, S.; Gershman, K.; Ray, S.; Harrison, L. H.; Lynfield, R.; Dumyati, G.; Townes, J. M.; Craig, A. S.; Zell, E. R.; Fosheim, G. E.; McDougal, L. K.; Carey, R. B.; Fridkin, S. K.; Active Bacterial Core surveillance, M. I., Invasive methicillin-resistant Staphylococcus aureus infections in the United States. *Jama,* **2007,** *298* (15), 1763-1771.
3. Raviglione, M. C., Issues facing TB control (7). Multiple drug-resistant tuberculosis. *Scottish medical journal,* **2000,** *45* (5 Suppl), 52-55; discussion 56.
4. Branda, J. A.; Ruoff, K., Bioterrorism. Clinical recognition and primary management. *American journal of clinical pathology,* **2002,** *117 Suppl,* S116-123.
5. Chaturvedi, V.; Dwivedi, N.; Tripathi, R. P.; Sinha, S., Evaluation of Mycobacterium smegmatis as a possible surrogate screen for selecting molecules active against multi-drug resistant Mycobacterium tuberculosis. *The Journal of general and applied microbiology,* **2007,** *53* (6), 333-337.
6. Meyer, C. G.; May, J., [Germs employed as biological weapons]. *Anasthesiologie, Intensivmedizin, Notfallmedizin, Schmerztherapie : AINS,* **2002,** *37* (9), 538-546.
7. Pohanka, M.; Skladal, P., Bacillus anthracis, Francisella tularensis and Yersinia pestis. The most important bacterial warfare agents - review. *Folia microbiologica,* **2009,** *54* (4), 263-272.
8. Warren, D. K.; Nitin, A.; Hill, C.; Fraser, V. J.; Kollef, M. H., Occurrence of co-colonization or co-infection with vancomycin-resistant enterococci and methicillin-resistant Staphylococcus aureus in a medical intensive care unit. *Infection control and hospital epidemiology : the official journal of the Society of Hospital Epidemiologists of America,* **2004,** *25* (2), 99-104.
9. Konno, K.; Oizumi, K.; Oka, S., Mode of action of rifampin on mycobacteria. II. Biosynthetic studies on the inhibition of ribonucleic acid polymerase of Mycobacterium bovis BCG by rifampin and uptake of rifampin- 14 C by Mycobacterium phlei. *The American review of respiratory disease,* **1973,** *107* (6), 1006-1012.

10. Zhang, Y.; Dhandayuthapani, S.; Deretic, V., Molecular basis for the exquisite sensitivity of Mycobacterium tuberculosis to isoniazid. *Proceedings of the National Academy of Sciences of the United States of America*, **1996,** *93* (23), 13212-13216.
11. Birosova, L.; Mikulasova, M., The mechanism of ciprofloxacin resistance in dihydrogen peroxide-induced mutants of Salmonella enterica subsp. enterica serovar typhimurium consists mainly in mutations in gyrA gene and less in mutations affecting ciprofloxacin uptake. *Folia microbiologica*, **2008,** *53* (4), 368-372.
12. Huang, Q.; Kirikae, F.; Kirikae, T.; Pepe, A.; Amin, A.; Respicio, L.; Slayden, R. A.; Tonge, P. J.; Ojima, I., Targeting FtsZ for antituberculosis drug discovery: noncytotoxic taxanes as novel antituberculosis agents. *Journal of medicinal chemistry*, **2006,** *49* (2), 463-466.
13. Huang, Q.; Tonge, P. J.; Slayden, R. A.; Kirikae, T.; Ojima, I., FtsZ: a novel target for tuberculosis drug discovery. *Current topics in medicinal chemistry*, **2007,** *7* (5), 527-543.
14. Kumar, K.; Awasthi, D.; Berger, W. T.; Tonge, P. J.; Slayden, R. A.; Ojima, I., Discovery of anti-TB agents that target the cell-division protein FtsZ. *Future medicinal chemistry*, **2010,** *2* (8), 1305-1323.
15. Awasthi, D.; Kumar, K.; Ojima, I., Therapeutic potential of FtsZ inhibition: a patent perspective. *Expert opinion on therapeutic patents*, **2011,** *21* (5), 657-679.
16. Kumar, K.; Awasthi, D.; Lee, S. Y.; Zanardi, I.; Ruzsicska, B.; Knudson, S.; Tonge, P. J.; Slayden, R. A.; Ojima, I., Novel trisubstituted benzimidazoles, targeting Mtb FtsZ, as a new class of antitubercular agents. *Journal of medicinal chemistry*, **2011,** *54* (1), 374-381.
17. Awasthi, D.; Kumar, K.; Knudson, S. E.; Slayden, R. A.; Ojima, I., SAR studies on trisubstituted benzimidazoles as inhibitors of Mtb FtsZ for the development of novel antitubercular agents. *Journal of medicinal chemistry*, **2013,** *56* (23), 9756-9770.
18. Ojima, I.; Kumar, K.; Awasthi, D.; Vineberg, J. G., Drug discovery targeting cell division proteins, microtubules and FtsZ. *Bioorganic & medicinal chemistry*, **2014,** *22* (18), 5060-5077.
19. Park, B.; Awasthi, D.; Chowdhury, S. R.; Melief, E. H.; Kumar, K.; Knudson, S. E.; Slayden, R. A.; Ojima, I., Design, synthesis and evaluation of novel 2,5,6-trisubstituted

benzimidazoles targeting FtsZ as antitubercular agents. *Bioorganic & medicinal chemistry,* **2014,** *22* (9), 2602-2612.

20. Romberg, L.; Levin, P. A., Assembly dynamics of the bacterial cell division protein FTSZ: poised at the edge of stability. *Annual review of microbiology,* **2003,** *57,* 125-154.
21. Tyagi, J. S.; Sharma, D., Mycobacterium smegmatis and tuberculosis. *Trends in microbiology,* **2002,** *10* (2), 68-69.
22. Bercovier, H.; Vincent, V., Mycobacterial infections in domestic and wild animals due to Mycobacterium marinum, M. fortuitum, M. chelonae, M. porcinum, M. farcinogenes, M. smegmatis, M. scrofulaceum, M. xenopi, M. kansasii, M. simiae and M. genavense. *Revue scientifique et technique,* **2001,** *20* (1), 265-290.
23. Cole, S. T.; Brosch, R.; Parkhill, J.; Garnier, T.; Churcher, C.; Harris, D.; Gordon, S. V.; Eiglmeier, K.; Gas, S.; Barry, C. E., 3rd; Tekaia, F.; Badcock, K.; Basham, D.; Brown, D.; Chillingworth, T.; Connor, R.; Davies, R.; Devlin, K.; Feltwell, T.; Gentles, S.; Hamlin, N.; Holroyd, S.; Hornsby, T.; Jagels, K.; Krogh, A.; McLean, J.; Moule, S.; Murphy, L.; Oliver, K.; Osborne, J.; Quail, M. A.; Rajandream, M. A.; Rogers, J.; Rutter, S.; Seeger, K.; Skelton, J.; Squares, R.; Squares, S.; Sulston, J. E.; Taylor, K.; Whitehead, S.; Barrell, B. G., Deciphering the biology of Mycobacterium tuberculosis from the complete genome sequence. *Nature,* **1998,** *393* (6685), 537-544.
24. Zahrt, T. C.; Deretic, V., Mycobacterium tuberculosis signal transduction system required for persistent infections. *Proceedings of the National Academy of Sciences of the United States of America,* **2001,** *98* (22), 12706-12711.
25. Collins, L.; Franzblau, S. G., Microplate alamar blue assay versus BACTEC 460 system for high-throughput screening of compounds against Mycobacterium tuberculosis and Mycobacterium avium. *Antimicrobial agents and chemotherapy*, **1997,** *41* (5), 1004-1009.
26. Pasca, M. R.; Guglierame, P.; De Rossi, E.; Zara, F.; Riccardi, G., mmpL7 gene of Mycobacterium tuberculosis is responsible for isoniazid efflux in Mycobacterium smegmatis. *Antimicrobial agents and chemotherapy,* **2005,** *49* (11), 4775-4777.
27. Stephan, J.; Mailaender, C.; Etienne, G.; Daffe, M.; Niederweis, M., Multidrug resistance of a porin deletion mutant of Mycobacterium smegmatis. *Antimicrobial agents and chemotherapy,* **2004,** *48* (11), 4163-4170.

28. Alexander, D. C.; Jones, J. R.; Liu, J., A rifampin-hypersensitive mutant reveals differences between strains of Mycobacterium smegmatis and presence of a novel transposon, IS1623. *Antimicrobial agents and chemotherapy,* **2003,** *47* (10), 3208-3213.

29. Piddock, L. J.; Williams, K. J.; Ricci, V., Accumulation of rifampicin by Mycobacterium aurum, Mycobacterium smegmatis and Mycobacterium tuberculosis. *The Journal of antimicrobial chemotherapy,* **2000,** *45* (2), 159-165.

Chapter 5

Biological Evaluation of Folate-Linker-Taxoid

Chapter Contents

§ 5.1 Introduction 101

§ 5.1.1 Cancer 101

§ 5.1.2 Chemotherapy 102

§ 5.1.3 Paclitaxel and Taxanes 102

§ 5.1.4 Next Generation Taxoid 103

§ 5.1.5 Folic Acid as Tumor Targeting Drug Conjugate 105

§ 5.1.6 Disulfide Linkers 107

§ 5.2 Results and discussion 111

§ 5.2.1 Biological Evaluation of Folate Linker Taxoid 111

§ 5.3 Conclusion 113

§ 5.4 Experimental Section 114

§ 5.4.1 Caution 114

§ 5.4.2 Materials 114

§ 5.4.3 Cell culture system for MTT assay 114

§ 5.4.4 Single drug MTT assay 115

§ 5.4.5 Data analysis for MTT assay 115

§ 5.5 References 117

§ 5.1 Introduction

§ 5.1.1 Cancer

Caner is the general name for a group of more than 100 diseases. Cancer cases the second most death in the US, followed by heart disease, accounting for nearly 1 of every 4 deaths.[1] In 2014, it has been estimated about 585,720 Americans are expected to die of cancer, almost 1,600 people per day (**Figure 5-1**).[1, 2]

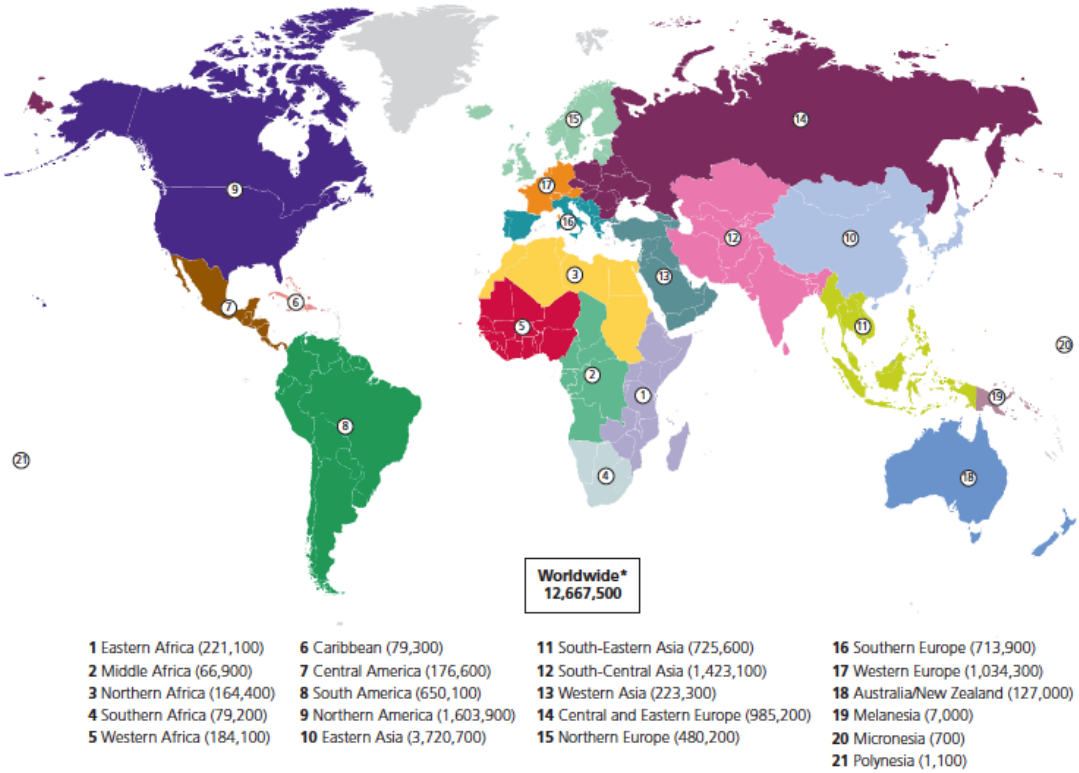

Figure 5- 1: Worldwide cancer statistics (Adapted from [2])

Even though there is an outstanding improvement in the area of anticancer research, a cure for cancer has not been found. Therefore, there is an urgent need for better anticancer treatments. Since there is no cure-all treatment, combination of treatments, are used in common such as, surgery, radiation therapy, biological therapy, gene therapy, anti-angiogenic therapy, and chemotherapy.

§ 5.1.2 Chemotherapy

Every treatment has its advantages and disadvantages. Current chemotherapy (**Figure 5-2**) uses highly potent cytotoxic agents to differentiate rapid proliferating malignant cells from normal cells. There are several classes of chemotherapeutics each with different mechanisms of action.[3-5]

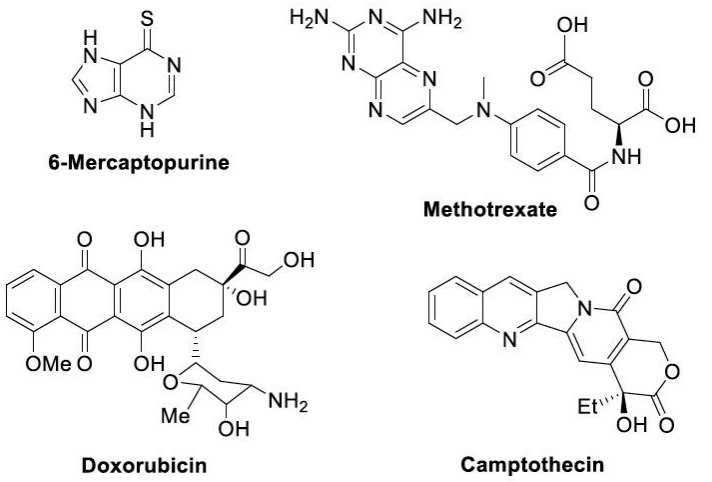

Figure 5- 2: Examples of traditional chemotherapeutics

However, the lack of specificity leads to adverse effects. In addition, the drug dosage required for effective tumor suppression is often intolerable to the patients. To conquer these problems associated with conventional chemotherapy, cytotoxic agents or their prodrugs with higher selectivity to tumors should be developed. One of the most important strategies is the tumor-specific delivery of cytotoxic agents by recognizing the differences between normal cells and cancer cells. It is conceivable that a prodrug with minimal systemic toxicity can be constructed by conjugating a cytotoxic agent to a tumor-targeting molecule.

§ 5.1.3 Paclitaxel and Taxanes

Paclitaxel (Taxol®) is a potent anticancer agent and known to inhibit cell growth and trigger significant apoptosis in various cancer cells.[6] Taxol was extracted from extracted from the bark of the pacific yew tree, Taxus brevifolia, in 1962.[7] Since then, numerous paclitaxel derivatives have been synthesized, and their effect on microtubules stabilization and cytotoxicity were investigated in terms of structure-activity relationships (SAR).[8] Extensive SAR studies have been done on paclitaxel and their analogs and it is summarized in **Figure 5-3**.

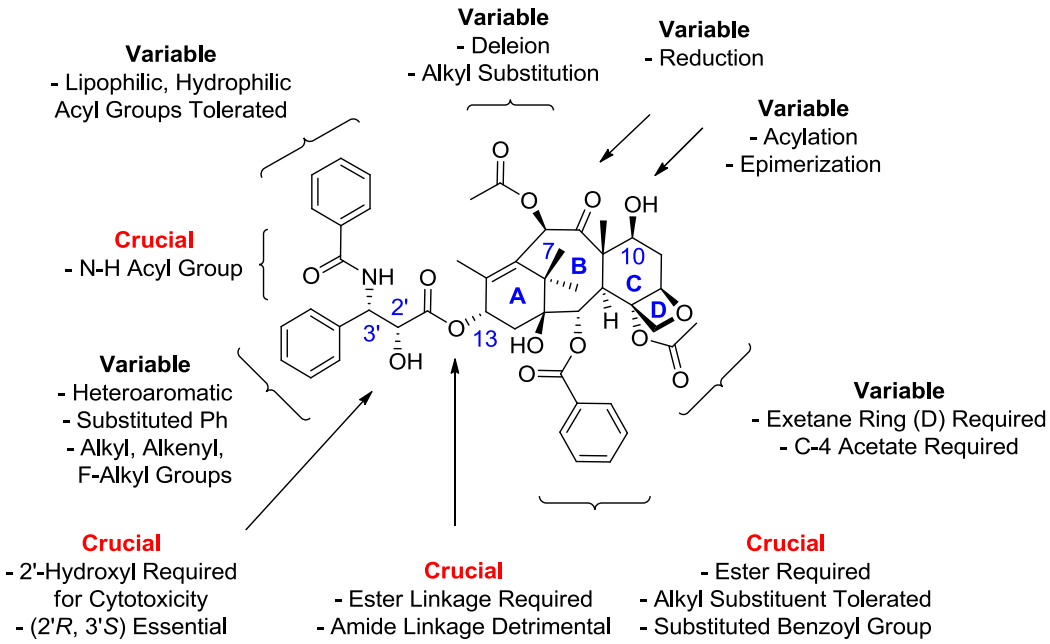

Figure 5- 3: Summary of SAR studies of paclitaxel

Throughout the years, the Ojima laboratory has developed a series of highly potent new generation taxoids through extensive SAR studies.[9-13] A number of these taxoids exhibited 1 to 2 orders of magnitude greater potencies in drug-sensitive cancer cell lines. Moreover, 2 to 3 orders of magnitude greater potencies in drug-resistant cell lines compared to that of paclitaxel and docetaxel.[13-16] It has been determined that the amide bond has been shown to be optimal at C13 position, and both primary and secondary R1 substituents have been shown to be detrimental to activity, whereas tertiary and aromatic groups at this position tend to improve efficacy. Furthermore, introducing an alkenyl or alkyl group at the C-3' position, a *t*-Boc moiety at the C-3'-N, modifications at the C-10 position and substituted phenyl rings at the C-2 benzoate increase the anticancer activity of the taxoid.

§ 5.1.4 Next Generation Taxoid

Based on our extensive SAR study of taxoids, we developed a series of highly potent new-generation toxoids (**Table 5-1**).[13] SAR studies indicated that taxoids with meta-substituted C2-benzoate modifications demonstrated remarkable potency against drug-sensitive and drug-

resistant (Pgp+) cancer cell lines. Some of these C2-benzoate modified taxoids exhibited 3 orders of magnitude higher potency than paclitaxel and docetaxel against drug-resistant cell lines. SB-T-121602, has demonstrated picomolar activity against human colon cancer cell line, HT-29, as well as excellent activity against breast and pancreatic cancer.

Multidrug resistance (MDR) is the phenomenon where the tumor cells is resistance to a cytotoxic agent and develop broad cross resistance. A number of transmembrane transporter proteins, ATP-binding cassette (ABC) transporters or efflux pumps, for involved in tumor resistance to chemotherapeutic agents.[17] MDR is usually caused by the overexpression of ATP-binding cassettes, most notably P-glycoprotein (Pgp), a broad spectrum multidrug efflux pump that has 12 transmembrane domains and two ATP-binding sites.[17] Pgp acts as an efflux pump and binds to and removes hydrophobic molecules from the cell.[18] Due to the overexpression of superfamily proteins, several types of drugs lost their efficacy.[19] Therefore, new drugs are being developed with increased efficacy against MDR cancer.

Table 5- 1: Selected new-generation toxoids

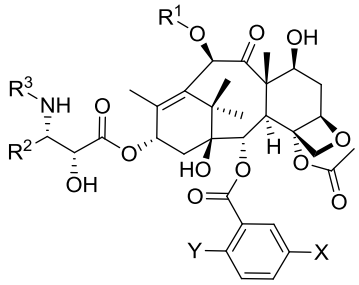

Taxane	R¹	R²	R³	X	Y
Paclitaxel	Ac	Ph	PhCO	H	H
Docetaxel	H	Ph	*t*-Boc	H	H
SB-T-1213	EtCO	*i*-butenyl	*t*-Boc	H	H
SB-T-1214	*c*-PrCO	*i*-butenyl	*t*-Boc	H	H
SB-T-1216	Me_2NCO	*i*-butenyl	*t*-Boc	H	H
SB-T-11033	EtCO	*i*-Bu	*t*-Boc	MeO	H
SB-T-121303	EtCO	*i*-butenyl	*t*-Boc	MeO	H
SB-T-121313	EtCO	*i*-butenyl	*t*-Boc	MeO	MeO
SB-T-121602	Me_2NCO	*i*-butenyl	*t*-Boc	Me	H

Table 5- 2: Cytotoxicity (IC_{50}; nM) of new-generation taxoids against selected cancer cell lines

Taxane	MCF-7[a]	NCI/ADR[b]	LCC6-MRK[c]	CFPAC-1[d]	HT-29[e]	DLD-1[f]
Paclitaxel	1.7	550	346	68	12	300
Docetaxel	1.0	723	120	-	-	-
SB-T-1213	0.18	4.0	-	4.6	0.37	3.9
SB-T-1214	0.2	3.9	-	0.38	0.73	3.8
SB-T-1216	0.13	7.4	-	0.66	0.052	5.4
SB-T-11033	0.36	0.61	0.80	-	-	-
SB-T-121303	0.36	0.79	0.90	0.89	-	-
SB-T-121313	0.30	-	-	0.025	0.56	-
SB-T-121602	0.08	-	-	0.31	0.003	0.46

[a] Human mammary cancer cell line (Pgp–); [b] Human ovarian cancer cell line (Pgp+); [c] *mdr1* transduced human breast cancer cell line (Pgp+); [d] Human pancreatic cancer cell line; [e] Human colon cancer cell line (Pgp-); [f] Human colon cancer cell line (Pgp+)

New-generation taxoids show magnitudes greater activity (**Table 5-2**) in a series of cancer cell lines compared to paclitaxel and docetaxel. In most cases, the IC_{50} of the new-generation taxoids is subnanomolar with some taxoids exhibited picomolar activity.[13] Thus, new-generation taxoids are promising candidates for possible use as chemotherapeutic agents and for use as warhead for tumortargeting drug conjugates.

§ 5.1.5 Folic Acid as Tumor Targeting Drug Conjugate

Vitamins are necessary to all living cells for survival, but the rapidly dividing cancer cells in particular need certain vitamins to sustain their rapid growth and proliferation.[14] Many tumor cells overexpress tumor-specific receptors such as biotin and folate receptors that have been used as targets to deliver the cytotoxic drug. Vitamin B12, folic acid, biotin and ribofravin are essential for cell division. Therefore, the vitamin receptors are overexpressed on the cancer cell surface for uptake of necessary vitamins.[20] Consequently, these vitamin receptors serve as appropriate targets for tumor-targeting drug delivery in addition to biomarkers for identification

and imaging of cancer cells.[14] Among various vitamin receptors, folate and biotin receptors have been identified as significant and relevant targets in numerous cancer cell lines.[7]

Folic acid (**Figure 5-4**) is important for targeted cancer therapies since it is essential for DNA synthesis, repair, and methylation, and biological reaction involving folate required vitamin B6 and B12 as cofactors.[21]

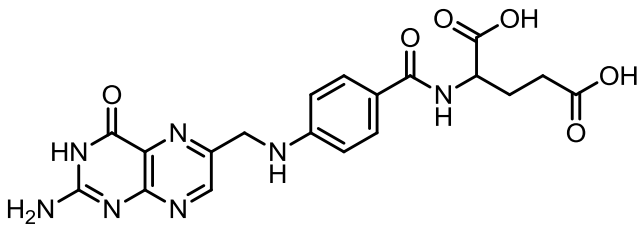

Figure 5- 4: Chemical structure of folic acid

Since the folate receptor (FR) has been known to be overexpressed in tumor cells[22] folate-drug conjugates can deliver therapeutic drugs specifically to FR-positive tumor cells. Folic acid is known to have a remarkably high affinity to the FR.[23] The cancer cell lines which are known to overexpress the FR included ovarian, lung, kidney, endometrial, breast, brain, colon carcinomas and myeloid cells (**Table 5-4**).[24]

Table 5- 3: The Internalization of Vitamin-Targeted Rhodamine-Labeled Polymers in Various Cancer Cell Lines (adapted from [17])

Tumour	Mouse	Type	Folate	Cbl	Biotin
O157	Balb/C	Bcell lymph	+/–	+/–	+/–
BW5147	AKR/J	Lymphoma	+/–	+/–	+/–
B16	C57/Bl	Melanoma	–	–	–
LL-2	C57/Bl	Lung	–	–	–
HCT-116	Balb/C-Nu	Colon	–	–	–
L1210	DBA/2	Leukemia	+/–	+/–	–
L1210FR	DBA/2	Leukemia	++	+	+++
Ov 2008	Balb/C-Nu	Ovarian	+++	–	++
ID8	C57/Bl	Ovarian	+++	–	++
Ovcar-3		Ovarian	+++	–	++
Colo-26	Balb/C	Colon	+/–	++	+++
P815	DBA/2	Mastocytoma	+/–	++	+++
M109	Balb/C	Lung	+	+++	+++
RENCA	Balb/C	Renal cell	+	+++	+++
RD995	C3H/HeJ	Renal cell	+	++	+++
4T1	Balb/C	Breast	+	++	+++
JC	Balb/C	Breast	+	++	+++
MMT060562	Balb/C	Breast	+	++	+++

Folate is a nutrient required by all living cells, and it is essential for cellular division. As illustrated in the image below (**Figure 5-5**), folate enters human cells via two distinct transport systems: (1) the reduced folate carrier pathway (RFC) which has low affinity for folate, (2) the folate receptor pathway, which has high-affinity for folate.[25]

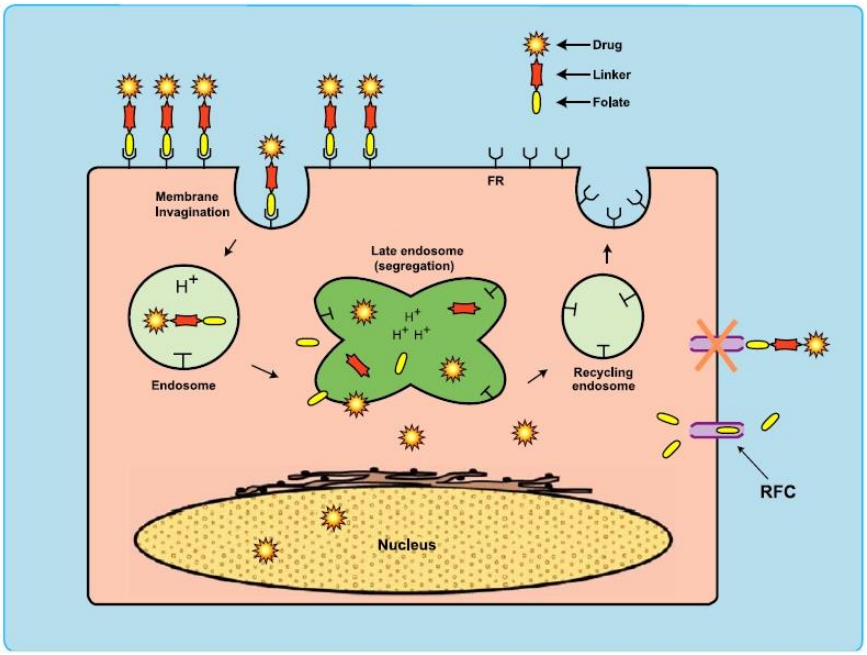

Figure 5- 5: FR-mediated endocytosis (adapted from [22])

The RFC is the major route by which normal cells access folate circulating in the body. The RFC is a transport protein that is expressed on virtually all cells in the body.[25] On the other hands, rapidly dividing cancer cells over-express the high-affinity folate receptor.[25] The folate receptor captures folate from outside the cell and transports it inside by engulfing it within a vesicle, an endosome. Once folate is internalized, the FR releases the folate and FR is then recycled back to the cell surface where it resumes its function.[25]

§ 5.1.6 Disulfide Linkers

Disulfide linkers can efficiently release a taxoid inside cancer cells when the disulfide bond is cleaved by an intracellular thiol, such as glutathione (GSH), which is 1,000 times greater in concentration in cancer cells than in blood plasma.[26] Studies suggest that antioxidant could provide a promising treatment for cancer since oxidative stress has long been concerned in

cancer development and progression.[27] Among the enzymatic systems to maintain the intracellular redox balance, GSH plays a major role, not only in antioxidant defense systems, but also in many metabolic processes.[28, 29] Elevated GSH levels are observed in several types of tumors, and this makes the neoplastic tissues more resistant to chemotherapy.[30, 31] Moreover, the content of GSH in some tumor cells is typically associated with higher levels of GSH-related enzymes, such as γ-glutamylcysteine ligase (GCL) and γ-glutamyl-transpeptidase (GGT) activities, as well as a higher expression of GSH-transporting export pumps.

There are two forms of GSH are possible: the reduced form, the majority of GSH, and the oxidized form (GSSG) that is estimated to be less than 1 % of the total GSH.[32] It has been known that the reversible thiolation of proteins regulate several metabolic processes including enzyme activity, transport activity, signal transduction and gene expression through redox-sensitive nuclear transcription factors.[32] The important GSH function is the maintenance of the intracellular redox balance and the essential thiol status of proteins.[33] The equilibrium of this balance depends on the concentrations of GSH and GSSG. Studies showed that increased GSH level in many malignant cells, i.e. 1000 times higher than that of bloodstream,[34] were found since tumor cells with high GSH content were able to survive in the presence of the nitrosative and oxidative stress.[32] Therefore, the GSH system has an attractive target for medical intervention against cancer progression and chemoresistance.[30, 35]

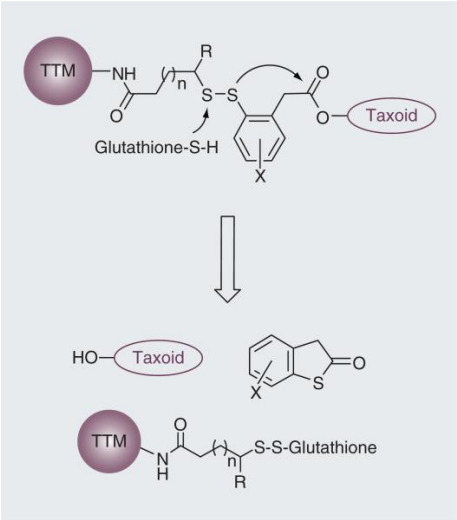

Figure 5- 6: Second-generation self- immolative disulfide linkers and their drug-release mechanism (adapted from [14])

The Ojima lab has developed a selfimmolative disulfide linker, specifically designed to release the unmodified taxoid upon linker cleavage (**Figure 5-6**), to prevent loss of potency of the active agent. Upon the disulfide exchange, the thiolate is positioned by the aromatic ring which can rapidly react with the C2' ester bond.[14, 36] After thiolactonization, the free drug is released. The second-generation disulfide linkers have been successfully incorporated into various tumor-targeting drug conjugates and their efficacy has been evaluated in vitro.[13]

§ 5.1.7 Folate-Linker-Taxoids

As previous mentioned, the FR has shown considerable promise as a therapeutic target in targeted drug delivery and has been extensively recognized as a tumor-specific biomarker. Folic acid is an attractive candidate for receptor-mediated delivery of highly potent cytotoxic agents since FA has small size, low cost, synthetic versatility, and lack of immunogenicity. Folate-based small molecule drug conjugates (SMDCs) have demonstrated excellent target specificity for the α-folate receptor and numerous drug conjugates and imaging agents have emerged in clinical trials with positive results. While significant advances in folate-based conjugates have been made, there is still need for improvements in design of the tumor-targeted drug delivery system.

A novel synthetic route to a solubilized folate-linker-taxoid conjugate was developed via solid phase pepetide synthesis and Cu-free click chemistry previously in our lab by Dr. Joshua D. Seitz.[37] This conjugate consists of second-generation taxoid (SB-T-1214), self-immolative disulfide linkers for drug release, folate as the TTM.

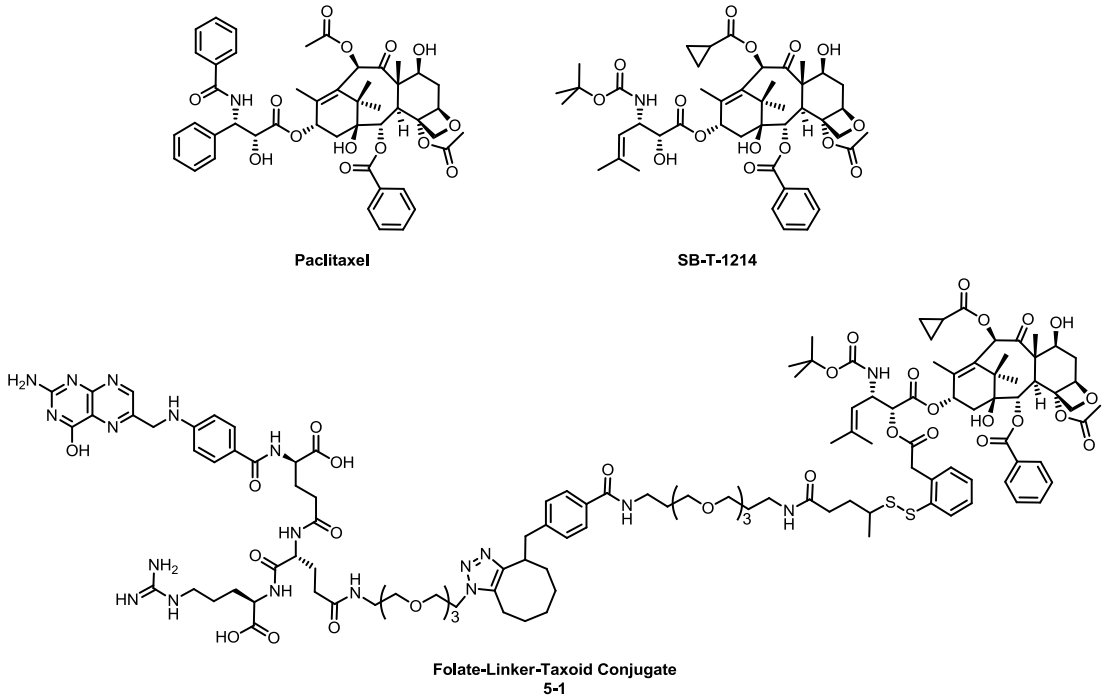

Figure 5- 7: Chemical Structures of paclitaxel, SB-T-1214 and FLT (5-1)

Chemical structure for The detailed method development for synthesis of **5-1** was described previously.[37] Compound were prepared by Dr. Seitz and used as received. Chemical structure of the compounds for evaluation of potency and efficacy of FLT are shown in **Figure 5-7**.

§ 5.2 Results and discussion

§ 5.2.1 Biological Evaluation of Folate Linker Taxoid

The potency and efficacy of FLT was evaluated in vitro against various FR+ cell lines and FR- cell line. The cytotoxicity assays of FLT against L1210FR (FR++), MX-1 (FR++), ID8 (FR+++), and WI-38 (FR-) were performed by MTT method. As controls for comparison, paclitaxel and parent taxoid SB-T-1214 were evaluated as well. The results for 72 h drug incubation with or without supplemental GSH, and GSH-OEt are given in **Table 5-5**.

Table 5- 4: Cytotoxicities (IC_{50}, nM) of Paclitaxel, SB-T-1214, and Folate Linker Taxoid (FLT) in the Presence of GSH-OEt or GSH Following Internalization.

Compound	L1210-FR[a] (FR+++)	MX-1[b] (FR++)	ID8[c] (FR+++)	WI-38[d] (FR-)
Paclitaxel[e]	27.6 ± 7.48	5.59 ± 2.12	30.2 ± 1.77	44.4 ± 21
SB-T-1214[e]	2.66 ± 1.33	1.89 ± 0.80	4.85 ± 0.62	1.20 ± 0.1
FLT[e]	3.51 ± 1.16	3.43 ± 2.33	7.73 ± 1.25	> 5000
FLT (GSH-OEt)[f]	3.35 ± 3.00	2.08 ± 1.30	7.43 ± 2.93	14.4 ± 2.20
FLT (GSH)[g]	3.87 ± 2.61	3.42 ± 2.98	7.78 ± 1.77	36.6 ± 12

[a] Murine lymphocytic leukemia cell line (FR+++); [b] Human breast carcinoma cell line (FR++); [c] Murine ovarian carcinoma cell line (FR+++); [d] normal human lung fibroblast cell line (FR-); [e] Cells were incubated with a drug for 72 h at 37 ℃; [f] Cells were incubated FLT at a given concentration for 24 h at 37 ℃. Then, 6 equiv. of GSH-OEt was added to conjugate for drug release and additional incubation for 48 h at 37 ℃; [g] Cells were incubated FLT at a given concentration for 24 h at 37 ℃. Then, 6 equiv. of GSH was added to conjugate for drug release and additional incubation for 48 h at 37 ℃ followed by addition of GSH-OEt (6 equiv. to conjugate) for drug release. Total drug or conjugate incubation was 72 h for all experiments; [a,c] the drugs were treated in FA-free RPMI media; [b,d] the drugs were treated in normal RPMI.

In the first experiment, L1210FR, MX-1, and ID8 (FR+) cancer cell lines were incubated with FLT for 72 h, and the corresponding IC_{50} values were determined. As **Table 5-5** shows, the cytotoxicity of FLT based on its IC_{50} values was determined to be in a range of 3.51 - 7.73 nM, while that against normal cell line WI38 (IC_{50} > 5000 nM) was not show appreciate cytotoxicity. The results indicate that FLT (**5-1**) was selectively internalized into FR+ cancer cells and release of the taxoid within the cancer cells. As expected, both paclitaxel and the parent taxoid, SB-T-

1214 showed nonspecific activity against FR+ and FR- cell lines in the range of 5.6 - 44 nM, and 1.2 – 4.9 nM, respectively.

In the second experiment, glutathione and glutathione ethyl ester (GSH, and GSH-OEt; 6 mole equivalents to conjugate) were added to the resuspended cancer cells after the cells were incubated with compound **5-1** for 24 h, and an additional incubation period of 48 h, i.e., 72 h total incubation. It should be noted that in this experiment the resuspended cancer cells only included conjugate internalized in the first 24 h period. As indicated in **Table 5-5**, addition of GSH or GSH-OEt did not make any appreciable difference in the cytotoxicity of these conjugates against FR+ cell lines. However, WI38 normal fibroblast cells, upon the addition of GSH or GSH-OEt, the conjugate showed slightly less cytotoxicity in the range of 14 – 37 nM compared to SB-T-1214.

§ 5.3 Conclusion

Folic acid is essential for the longevity and maintenance of rapidly dividing cells. A novel folate-based drug conjugate of next-generation taxoid SB-T-1214 was designed and synthesized previously (by Dr. Seitz) using a combination of solid-phase peptide synthesis with synthetically modified amino acids and copper-free "click" chemistry. The folate-linker-taxoid (FLT) conjugate contains spacers to promote aqueous solubility and promote tumor-specific uptake. Also, it contains a mechanism-based self-immolative disulfide linker for site-specific prodrug activation. The cleavage of disulfide linkers is attributed to the abundance of intracellular glutathione found in cancer cells. The conjugate was evaluated *in vitro* against a series of FR-positive cancer cell lines, L1210FR, MX-1, and ID8.

As anticipated, SB-T-1214 was found to be highly potent against all cell lines tested with IC_{50} values ranging from 1-5 nM. Folate conjugate demonstrated almost equally high potency against L1210FR, MX-1 and ID8 as the parent taxoid, indicating rapid internalization and efficient drug release. However, against FR- normal lung fibroblast cell line WI38, the folate conjugate was virtually non-toxic ($IC_{50} > 5$ μM). The difference in cytotoxicity of FLT against FR-positive and FR-negative cell lines was of at least three orders of magnitude. These results indicate that this folate-based conjugate **5-1** design vastly reduces non-specific internalization.

§ 5.4 Experimental Section

§ 5.4.1 Caution

Taxoids have been identified as potent cytotoxic agents. Thus, all drugs and structurally related compounds and derivatives must be considered mutagens and potential reproductive hazards for both males and females. All appropriate precautions, such as the use of gloves, goggles, labware, and fume hood, must be taken while handling the compounds at all times.

§ 5.4.2 Materials

The chemicals were purchased from Sigma-Aldrich, Fisher Scientific, and VWR International, and used as received or purified before use by standard methods. Tetrahydrofuran was freshly distilled from sodium and benzophenone. Dichloromethane was also distilled immediately prior to use under nitrogen from calcium hydride. 3-(4,5-Dimethylthiazol-2-yl)-2,5-diphenyltetrazolium bromide (MTT) was obtained from Sigma Chemical Co. Biological materials including RPMI-1640 and DMEM cell culture media, fetal bovine serum, NuSerum, PenStrep, and TrypLE were obtained from Gibco and VWR International, and used as received for cell-based assays.

§ 5.4.3 Cell culture system for MTT assay

All cell lines were obtained from ATCC unless otherwise noted. Cells were cultured in RPMI-1640 cell culture medium (Gibco) in the absence of folic acid, supplemented with 10% (v/v) heat-inactivated fetal bovine serum (FBS) and 1% (v/v) penicillin and streptomycin (PenStrep) at 37 ℃ in a humidified atmosphere with 5% CO_2. Murine leukemia cell line L1210FR (a gift from Dr. Gregory Russell-Jones, Access Pharmaceuticals Pty Ltd., Australia) was grown as a suspension in supplemented RPMI-1640. Human breast carcinoma, MX-1, murine ovarian carcinoma, ID8, and normal lung fibroblast, WI-38, cell lines were cultured as monolayers on 100 mm tissue culture dishes in a supplemented RPMI-1640 cell culture medium. Cells were harvested, collected by centrifugation at 850 rpm for 5 min, and resuspended in fresh culture medium. Cell cultures were routinely divided by treatment with trypsin (TrypLE, Gibco) as needed every 2-4 days and collected by centrifugation at 850 rpm for 5 min, and resuspended in fresh cell culture medium, containing varying cell densities for subsequent biological experiments and analysis.

§ 5.4.4 Single drug MTT assay

The cytotoxicities (IC_{50}, nM) of paclitaxel, SB-T-1214, and folate-linker- SB-T-1214 were evaluated against various cancer cell lines by means of the standard quantitative colorimetric MTT assay. The inhibitory activity of each compound is represented by the IC_{50} value, which is defined as the concentration required for inhibiting 50 % of the cell growth. Cells were harvested, collected, and resuspended in 100 μL cell culture medium (RPMI-1640, folate-free) at a concentrations ranging from 0.5-1.5 x 10^4 cells per well in a 96-well plate. For adhesive cell types, cells were allowed to descend to the bottom of the wells overnight, and appropriate fresh medium was added to each well upon removal of the old medium.

For the MTT assay of paclitaxel, SB-T-1214, and FLT, cells were resuspended in 200 μL medium with 8,000 to 10,000 cells per well of a 96-well plate and incubated at 37 ℃ for 24 h before drug treatment. In DMSO stock solutions, each drug or conjugate was diluted to a series of concentrations in cell culture medium to prepare test solutions. After removing the old medium, these test solutions were added to the wells in the 96-well plate to give the final concentrations ranging from 0.5 to 5,000 nM (100 μL), and the cells were subsequently cultured at 37 ℃ for 48 of 72 h. For the leukemia cell lines, cells were harvested, collected, and resuspended in the test solutions ranging from 0.5 to 5,000 nM (100 μL) at 0.5 to 0.8 x 10^4 cells per well in a 96-well plate and subsequently incubated at 37 ℃ for 72 h.

In another experiment, cells were incubated with FLT at 37 ℃ for 24 h, and GSH or GSH-OEt (6 equivalents) in cell culture medium (100 μL) was directly added to the wells. These cells were incubated at 37 ℃ for an additional 48 h; i.e. the total incubation time was also 72 h.

For all experiments, after removing the test medium, fresh solution of MTT in PBS (40 μL of 0.5 mg MTT/mL) was added to the wells, and the cells were incubated at 37 ℃ for 3 h. The MTT solution was then removed, and the resulting insoluble violet formazan crystals were dissolved in 0.1 N HCl in isopropanol with 10% Triton X-100 (40 μL) to give a violet solution.

§ 5.4.5 Data analysis for MTT assay

The spectrophotometric absorbance measurement of each well in the 96-well plate was run at 570 nm using a Labsystems Multiskan Ascent microplate reader. The IC_{50} values and their standard errors were calculated from the viability-concentration curve using Four Parameter

Logistic Model of Sigmaplot. The concentration of DMSO per well was ≤ 1% in all cases. Each experiment was run in triplicate.

§ 5.5 References

1. Cancer Facts & Figures 2014. *American Cancer Society* **2014**.
2. Worldwide cancer Key Facts. *Cancer Research UK*, **2012**.
3. Goodman, L. S.; Wintrobe, M. M.; et al., Nitrogen mustard therapy; use of methyl-bis (beta-chloroethyl) amine hydrochloride and tris (beta-chloroethyl) amine hydrochloride for Hodgkin's disease, lymphosarcoma, leukemia and certain allied and miscellaneous disorders. *Journal of the American Medical Association,* **1946,** *132*, 126-132.
4. Farber, S.; Diamond, L. K., Temporary remissions in acute leukemia in children produced by folic acid antagonist, 4-aminopteroyl-glutamic acid. *The New England journal of medicine,* **1948,** *238* (23), 787-793.
5. DeVita, V. T., Jr.; Chu, E., A history of cancer chemotherapy. *Cancer research,* **2008,** *68* (21), 8643-8653.
6. Park, S. J.; Wu, C. H.; Gordon, J. D.; Zhong, X.; Emami, A.; Safa, A. R., Taxol induces caspase-10-dependent apoptosis. *The Journal of biological chemistry,* **2004,** *279* (49), 51057-51067.
7. Wall, M. E.; Wani, M. C., Camptothecin and taxol: discovery to clinic--thirteenth Bruce F. Cain Memorial Award Lecture. *Cancer research,* **1995,** *55* (4), 753-760.
8. Fu, Y.; Li, S.; Zu, Y.; Yang, G.; Yang, Z.; Luo, M.; Jiang, S.; Wink, M.; Efferth, T., Medicinal chemistry of paclitaxel and its analogues. *Current medicinal chemistry,* **2009,** *16* (30), 3966-3985.
9. Ojima, I.; Duclos, O.; Zucco, M.; Bissery, M. C.; Combeau, C.; Vrignaud, P.; Riou, J. F.; Lavelle, F., Synthesis and structure-activity relationships of new antitumor taxoids. Effects of cyclohexyl substitution at the C-3' and/or C-2 of taxotere (docetaxel). *Journal of medicinal chemistry,* **1994,** *37* (16), 2602-2608.
10. Ojima, I.; Slater, J. C.; Kuduk, S. D.; Takeuchi, C. S.; Gimi, R. H.; Sun, C. M.; Park, Y. H.; Pera, P.; Veith, J. M.; Bernacki, R. J., Syntheses and structure-activity relationships of taxoids derived from 14 beta-hydroxy-10-deacetylbaccatin III. *Journal of medicinal chemistry,* **1997,** *40* (3), 267-278.
11. Ojima, I.; Geng, X.; Lin, S.; Pera, P.; Bernacki, R. J., Design, synthesis and biological activity of novel C2-C3' N-Linked macrocyclic taxoids. *Bioorganic & medicinal chemistry letters,* **2002,** *12* (3), 349-352.

12. Ojima, I.; Fumero-Oderda, C. L.; Kuduk, S. D.; Ma, Z.; Kirikae, F.; Kirikae, T., Structure-activity relationship study of taxoids for their ability to activate murine macrophages as well as inhibit the growth of macrophage-like cells. *Bioorganic & medicinal chemistry,* **2003,** *11* (13), 2867-2888.
13. Ojima, I.; Zuniga, E. S.; Berger, W. T.; Seitz, J. D., Tumor-targeting drug delivery of new-generation taxoids. *Future medicinal chemistry,* **2012,** *4* (1), 33-50.
14. Ojima, I., Guided molecular missiles for tumor-targeting chemotherapy--case studies using the second-generation taxoids as warheads. *Accounts of chemical research,* **2008,** *41* (1), 108-119.
15. Ojima, I.; Chen, J.; Sun, L.; Borella, C. P.; Wang, T.; Miller, M. L.; Lin, S.; Geng, X.; Kuznetsova, L.; Qu, C.; Gallager, D.; Zhao, X.; Zanardi, I.; Xia, S.; Horwitz, S. B.; Mallen-St Clair, J.; Guerriero, J. L.; Bar-Sagi, D.; Veith, J. M.; Pera, P.; Bernacki, R. J., Design, synthesis, and biological evaluation of new-generation taxoids. *Journal of medicinal chemistry,* **2008,** *51* (11), 3203-3221.
16. Chen, S.; Zhao, X.; Chen, J.; Chen, J.; Kuznetsova, L.; Wong, S. S.; Ojima, I., Mechanism-based tumor-targeting drug delivery system. Validation of efficient vitamin receptor-mediated endocytosis and drug release. *Bioconjugate chemistry,* **2010,** *21* (5), 979-987.
17. Wind, N. S.; Holen, I., Multidrug resistance in breast cancer: from in vitro models to clinical studies. *International journal of breast cancer,* **2011,** *2011,* 967419.
18. Gottesman, M. M.; Pastan, I., Biochemistry of multidrug resistance mediated by the multidrug transporter. *Annual review of biochemistry,* **1993,** *62,* 385-427.
19. Ferlini, C.; Distefano, M.; Pignatelli, F.; Lin, S.; Riva, A.; Bombardelli, E.; Mancuso, S.; Ojima, I.; Scambia, G., Antitumour activity of novel taxanes that act at the same time as cytotoxic agents and P-glycoprotein inhibitors. *British journal of cancer,* **2000,** *83* (12), 1762-1768.
20. Russell-Jones, G.; McTavish, K.; McEwan, J.; Rice, J.; Nowotnik, D., Vitamin-mediated targeting as a potential mechanism to increase drug uptake by tumours. *Journal of inorganic biochemistry,* **2004,** *98* (10), 1625-1633.
21. Weinstein, S. J.; Hartman, T. J.; Stolzenberg-Solomon, R.; Pietinen, P.; Barrett, M. J.; Taylor, P. R.; Virtamo, J.; Albanes, D., Null association between prostate cancer and

serum folate, vitamin B(6), vitamin B(12), and homocysteine. *Cancer epidemiology, biomarkers & prevention : a publication of the American Association for Cancer Research, cosponsored by the American Society of Preventive Oncology,* **2003,** *12* (11 Pt 1), 1271-1272.

22. Vlahov, I. R.; Leamon, C. P., Engineering folate-drug conjugates to target cancer: from chemistry to clinic. *Bioconjugate chemistry,* **2012,** *23* (7), 1357-1369.
23. Lu, Y.; Sega, E.; Leamon, C. P.; Low, P. S., Folate receptor-targeted immunotherapy of cancer: mechanism and therapeutic potential. *Advanced drug delivery reviews,* **2004,** *56* (8), 1161-1176.
24. Xia, W.; Low, P. S., Folate-targeted therapies for cancer. *Journal of medicinal chemistry,* **2010,** *53* (19), 6811-6824.
25. Leamon, C. P.; Reddy, J. A., Folate-targeted chemotherapy. *Advanced drug delivery reviews,* **2004,** *56* (8), 1127-1141.
26. Kigawa, J.; Minagawa, Y.; Kanamori, Y.; Itamochi, H.; Cheng, X.; Okada, M.; Oishi, T.; Terakawa, N., Glutathione concentration may be a useful predictor of response to second-line chemotherapy in patients with ovarian cancer. *Cancer,* **1998,** *82* (4), 697-702.
27. Hussain, S. P.; Hofseth, L. J.; Harris, C. C., Radical causes of cancer. *Nature reviews. Cancer,* **2003,** *3* (4), 276-285.
28. Sies, H., Glutathione and its role in cellular functions. *Free radical biology & medicine,* **1999,** *27* (9-10), 916-921.
29. Meister, A., Glutathione metabolism. *Methods in enzymology,* **1995,** *251*, 3-7.
30. Estrela, J. M.; Ortega, A.; Obrador, E., Glutathione in cancer biology and therapy. *Critical reviews in clinical laboratory sciences,* **2006,** *43* (2), 143-181.
31. Calvert, P.; Yao, K. S.; Hamilton, T. C.; O'Dwyer, P. J., Clinical studies of reversal of drug resistance based on glutathione. *Chemico-biological interactions,* **1998,** *111-112*, 213-224.
32. Traverso, N.; Ricciarelli, R.; Nitti, M.; Marengo, B.; Furfaro, A. L.; Pronzato, M. A.; Marinari, U. M.; Domenicotti, C., Role of glutathione in cancer progression and chemoresistance. *Oxidative medicine and cellular longevity,* **2013,** *2013*, 972913.

33. Lu, S. C., Regulation of hepatic glutathione synthesis: current concepts and controversies. *FASEB journal : official publication of the Federation of American Societies for Experimental Biology*, **1999,** *13* (10), 1169-1183.
34. Zheng, Z. B.; Zhu, G.; Tak, H.; Joseph, E.; Eiseman, J. L.; Creighton, D. J., N-(2-hydroxypropyl)methacrylamide copolymers of a glutathione (GSH)-activated glyoxalase i inhibitor and DNA alkylating agent: synthesis, reaction kinetics with GSH, and in vitro antitumor activities. *Bioconjugate chemistry*, **2005,** *16* (3), 598-607.
35. O'Brien, M. L.; Tew, K. D., Glutathione and related enzymes in multidrug resistance. *European journal of cancer*, **1996,** *32A* (6), 967-978.
36. Wu, X.; Ojima, I., Tumor specific novel taxoid-monoclonal antibody conjugates. *Current medicinal chemistry*, **2004,** *11* (4), 429-438.
37. Seitz, J. D. The design, synthesis and biological evaluation of novel taxoid anticancer agents and their tumor-targeted drug conjugates. Dortoral Dissertation State University of New York at Stony Brook, **2013**.

Chapter 6

3’-Vinyliodo Taxoids for PET- and SPECT-Based Theranostics

Chapter Contents

§ 6.1 Introduction 122

§ 6.1.1 Positron Emission Tomograpy 122

§ 6.1.2 Radiolabeling of Taxanes in Clinical Use 123

§ 6.1.3 Radiolabeling with Iodine 124

§ 6.1.4 Biotin as Tumor Targeting Moiety 124

§ 6.1.5 3’-Vinyliodo taxoids for PET- and SPECT-Based Theranostics 125

§ 6.2 Results and discussion 127

§ 6.2.1 Biological Evaluation of 3’-vinyliodo taxoid 127

§ 6.2.2 Cold Labeling of 3’-Vinyliodo taxoid 128

§ 6.3 Conclusion 133

§ 6.4 Experimental Section 134

§ 6.4.1 Caution 134

§ 6.4.2 Materials 134

§ 6.4.3 Cell culture system for MTT assay 134

§ 6.4.4 Single drug MTT assay 135

§ 6.4.5 Data analysis for MTT assay 135

§ 6.5 References 136

§ 6.1 Introduction

§ 6.1.1 Positron Emission Tomograpy

There are two nuclear imaging modalities: single-photon emission computed tomography (SPECT) and positron emission tomography (PET). PET is a powerful nuclear imaging technique that gives detailed three dimensional images of functional processes in the body. A PET radiopharmaceutical is administered to a patient and then given time (depending on the type of scan) to distribute through the body, accumulate at sites of interest. Therefore, PET is an efficient imaging technique in the area such as, oncology, cardiology and neurology for monitoring tumors or visualizing disease.

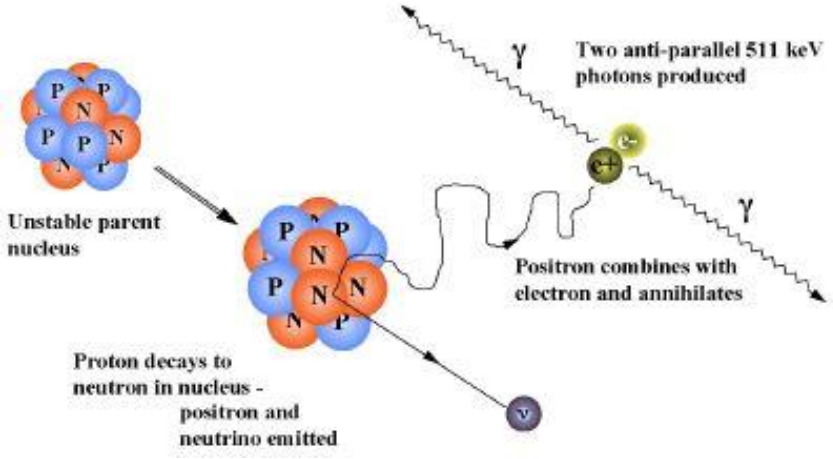

Figure 6- 1: β+ decay and positron/electron annihilation (adapted from [1])

The radionuclide has an unstable nucleus. It decays to reach a stable state by emitting positrons (an antimatter counterpart of an electron). Once it expelled from the nucleus, a positron travels a short distance (~1 mm) and collides with an electron in the surrounding tissues (**Figure 6-1**).[1] This mutual annihilation results in production of two high energy (511 KeV) photons or γ-rays, which are emitted at almost 180° to each other. The detection of two simultaneous photons by the PET scanner by a process called coincidence detection, is subsequently used to reconstruct tomographic PET images.[1]

§ 6.1.2 Radiolabeling of Taxanes in Clinical Use

The principal component of imaging with PET is the radiopharmaceutical agent (also known as a ligand or tracer). The tracer molecule is formed by incorporating a positron emitting isotope (radionuclide) into a metabolically active molecule.

Table 6- 1: The properties of radionuclides (adapted from [2])

Nuclide	Application	Decay mode	Energy (keV)	Half-life
^{18}F	PET	β+ (97%)	633.5	109 min
^{13}N	PET	β+ (100%)	1198.2	9.97 min
^{74}As	PET	β+ (26.1%)	944.61353	17.77 d
		β− (18.6%)		
^{64}Cu	PET	β+ (17.8%)	653	12.7 h
^{89}Zr	PET	β+ (23%)	2400	78.4 h
^{124}I	PET	β+ (11.7%)	1534	4.17 d
^{68}Ga	PET	β+ (88%)	1899	67.6 m
^{131}I	SPECT	β− (89.9%)	606	8.02 d
		γ (81.7%)	364	
^{90}Y	Radiotherapy	β− (99.9%)	2280	64 h
^{32}P	Radiotherapy	β− (100%)	1710	14.26 d
^{198}Au	Radiotherapy	β− (98.9%)	960.7	2.69 d
^{111}In	Radiotherapy	β− (100%)	448.3	2.8 d
^{177}Lu	Radiotherapy	β− (78.6%)	498.3	6.73 d
^{225}Ac	Radiotherapy	α (50.7%)	5830	10 d
*^{99m}Tc	SPECT	γ (89%)	140.5	6.01 h

*^{99m}Tc has shown to have no significant CR.

^{15}O, ^{13}N, ^{11}C and ^{18}F are frequently used positron-emitting isotopes.[2] The latter is often used as a substitute for hydrogen in the molecule of interest. ^{14}O, ^{64}Cu, ^{62}Cu, ^{124}I, ^{76}Br, ^{82}Rb and ^{68}Ga are also used occasionally.[2] **Table 6-1** illustrated some of radionuclides and their properties.[3]

Paclitaxel and docetaxel and have been labeled with β+ emitting nuclei for PET (**Figure 6-2**). Paclitaxel employed ^{11}C labeling at the C3'N- carbonyl and ^{18}F, ^{76}Br and ^{124}I labeling at the para position of the C3'-phenyl ring.[4, 5] In addition, ^{123}I labeling had been introduced at the C3'-phenyl ring for SPECT imaging.[6]

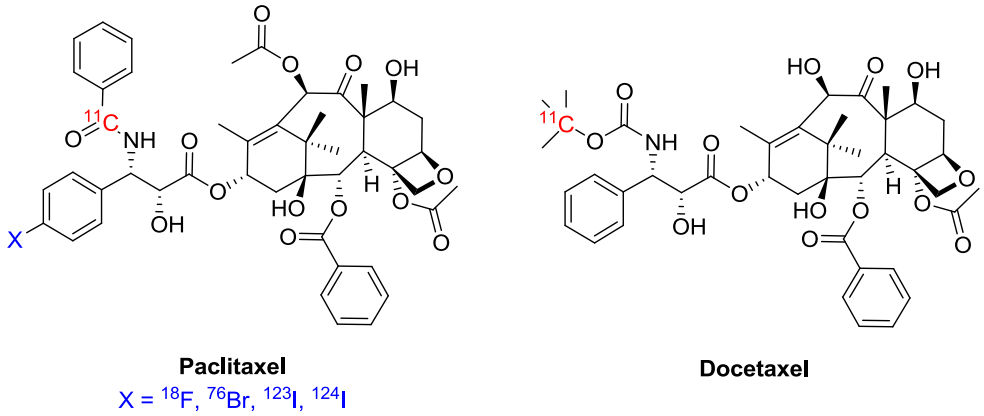

Figure 6- 2: Examples of clinical use of paclitaxel and docetaxel

Docetaxel has been labeled with ^{11}C at the quaternary carbon of the C3'N-*t*-Boc group for biodistribution in patients with advanced solid tumors.[7, 8]

§ 6.1.3 Radiolabeling with Iodine

Recently, the positron emitting halogen has become an attractive long-lived radionuclide for the design and synthesis of novel PET radiotracers.[9] Expecially, iodine has been frequently used as an imaging agent for the labeling of proteins and peptides. The two most common metastable isotopes are ^{123}I and ^{124}I since both isotopes possess long half-life (^{123}I, $t_{1/2}$ = 13 h and 4.2 days and ^{124}I, $t_{1/2}$ = 4.2 d). [9, 10] They can be used for long-term biodistribution studies of pharmaceuticals such as PET and SPECT.[10] Therefore, a handy method for the site-specific iodine labeling of taxoid conjugates is highly desirable for preclinical and clinical use of taxoid-based tumor-targeting drug conjugates.

§ 6.1.4 Biotin as Tumor Targeting Moiety

As described in previous chapter, vitamin is an attractive tumor-targeting moiety. In addition to folic acid, biotin (**Figure 6-3**) is essential for cell division, cell growth, fatty acid production, metabolism of fats and amino acids energy production.[11] Since biotin plays a significant role for rapidly dividing cancer cells, it is recognized as an attractive target for tumor-targeting drug delivery.[12]

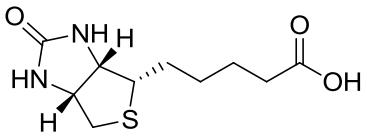

Figure 6- 3: Chemical Structure of Biotin

It has been reported that numerous types of cancer cells overexpressed the biotin receptors by Russell-Jones *et al*. They also reported those cell lines in which folate and vitamin B12 were overexpressed.[13]

§ 6.1.5 3'-Vinyliodo taxoids for PET- and SPECT-Based Theranostics

Iodine is commonly used to via nucleaophillic or electrophilic substitution reactions.[9] In addition, methods have been worked out for the specific labeling.[14]

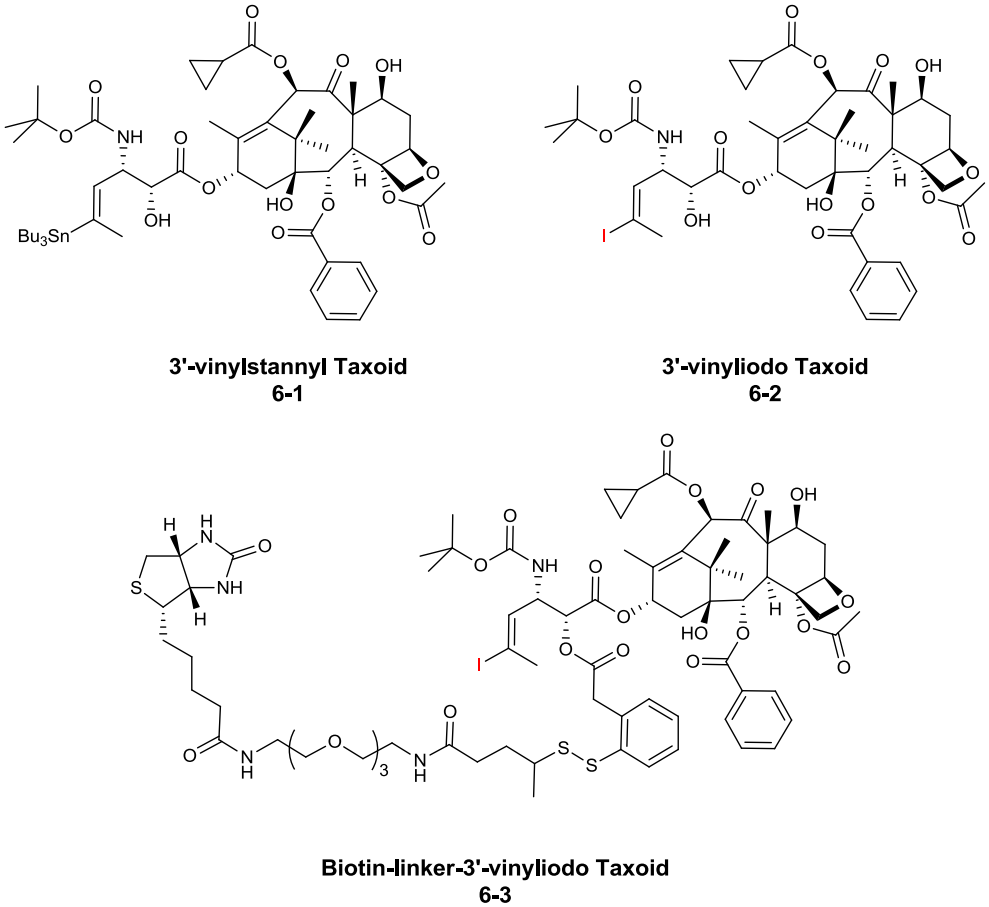

Figure 6- 4: Chemical Structures of

Since electrophillic iodine can react rapidly with organostannanes in a high yielding and highly regioselective manner, it is preferred methods for the radiolabeling of organic compounds. Using this methodology, various molecules have been labeled; morphine (analgesic), purpurinimide (a porpherine derivative) and IML06-08 (EGFR inhibitors).[15-17] It was envisioned that 3'-vinylstannly taxoid **6-1** could be converted to 3'-vinyliodo taxoid **6-2** and synthesized previously in our lab by Dr. Joshua D. Seitz. The detailed method development for synthesis of **6-1**, **6-2** and **6-3** were described previously.[14] Compounds were prepared by Dr. Seitz and used as received.

Preliminary in vitro studies against VERO cells showed that **6-2** possesses cytotoxicity within the same order of magnitude as SB-T-1214. Therefore, it would be worthwhile to test the potency of **6-2** against a small panel of cancer cell lines to assess its potential as a theranostic agent.

§ 6.2 Results and discussion

§ 6.2.1 Biological Evaluation of 3'-vinyliodo taxoid

The potency and efficacy of 3'-vinyliodotaxoid **6-2** was evaluated *in vitro* against various cancer cell lines. The cytotoxicity assays of 3'-vinyliodo taxoid against ID8 and NCI/ADR-RES (murine ovarian carcinoma cell line), HCT-116 (human colon cancer cell line), and MX-1 and MCF-7 (human breast carcinoma cell line) were performed by MTT method. As controls for comparison, paclitaxel and parent taxoid SB-T-1214 were evaluated as well. The results for 72 h drug incubation are given in **Table 6-2**.

Table 6- 2: Cytotoxicities (IC_{50}, nM) of paclitaxel, SB-T-1214, and 3'-vinyliodotaxoid (6-2)

Compound	ID8[a]	NCI/ADR-RES[a]	HCT-116[b]	MX-1[c]	MCF-7[c]
Paclitaxel	**22.9 ± 0.75**	**634 ± 41**	**4.31 ± 0.14**	**1.73 ± 0.42**	**157 ± 6.0**
SB-T-1214	**3.23 ± 0.75**	**10.3 ± 1.35**	**2.41 ± 0.38**	**3.05 ± 0.74**	**7.14 ± 0.18**
6-2	**4.22 ± 0.40**	**15.4 ± 1.60**	**6.58 ± 1.07**	**3.01 ± 0.30**	**12.8 ± 3.33**

[a] murine ovarian carcinoma cell line; [b] human colon cancer cell line; [c] human breast carcinoma cell line; Cells were incubated with drugs at 37 ℃ in a 5% CO_2 atmosphere for 72 h

ID8, NCI/ADR-RES, HCT-116, MX-1 and MCF-7 cancer cell lines were incubated with compound paclitaxel, SB-T-1214 and compound **6-2** for 72 h, and the corresponding IC_{50} values were determined. As **Table 6-2** shows, the cytotoxicity of compound **6-2** exhibited as almost same activity *in vitro* as the parent taxoid SB-T-1214. Compound 6-2 showed single nanomolar scale (3.01 – 6.58 nM) against ID8, HCT-116 and MCF-7 cell lines and it exhibited low double digit nanomolar scale (12.8 – 15.4 nM) against MCI/ADR-RES and MCF-7 cell lines. Since the 3'-vinyliodo taxoid is active, compound **6-2** can be used as imaging agent and provide an excellent clinical theranostic tool for tumor-targeted chemotherapy. Therefore, the attempts to find the condition for labeling compound **6-2** were carried forward.

§ 6.2.2 Cold Labeling of 3'-Vinyliodo taxoid

Compound **6-1** (**Figure 6-5**: A, B) and compound **6-2** (**Figure 6-5**: C, D) were confirmed by LC-HRMS.

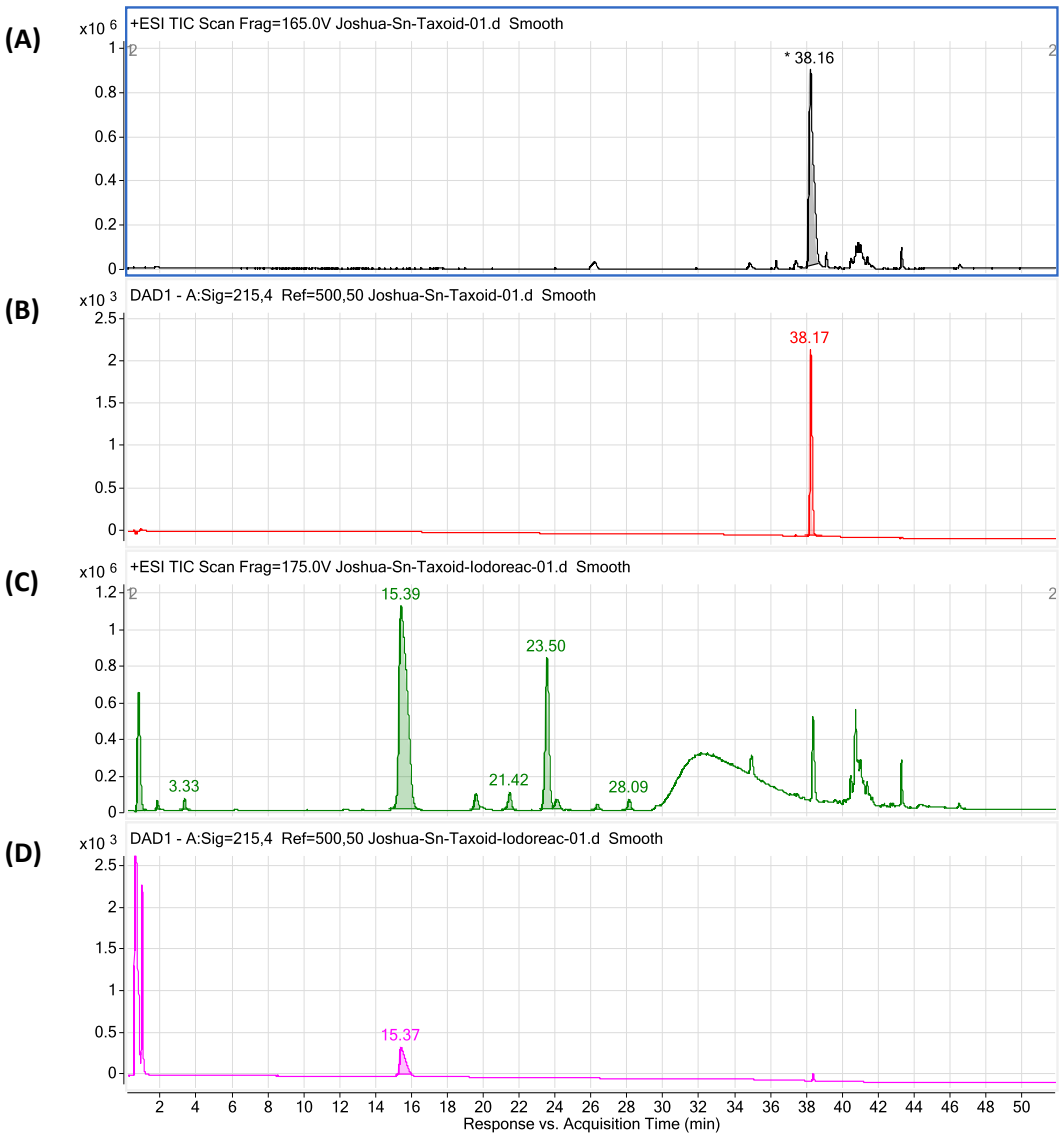

Figure 6- 5: Compound 6-1 and 6-2confirmation by mass chromatogram

(A) and (B) shows mass chromatogram and the UV (@ 215 nm) trace of compound **6-1**. (C) and (D) represent for compound **6-2**, mass trace and UV trace, respectively. The mass chromatogram shows one predominant peak at R_t = 38.16 min with several minor peaks (**Figure 6-5**: (A)). The analysis of compound **6-1** shows one peak, R_t = 38.16 min in the UV-215nm chromatogram (**Figure 6-5**: (A)). Analysis of the extracted mass spectra from R_t = 38.16 min indicates that m/z ions are observed consistent with the target formula (**Figure 6-6**: (A), and (B)).

The TIC mass and UV-@ 215 chromatograms of compound **6-2** are shown **Figure 6**-5: (C) and (D). Analysis of the extracted mass spectra from peak, R_t = 15.38 min indicates that m/z ions are observed consistent with the target formula (**Figure 6-6**: (C), and (D)).

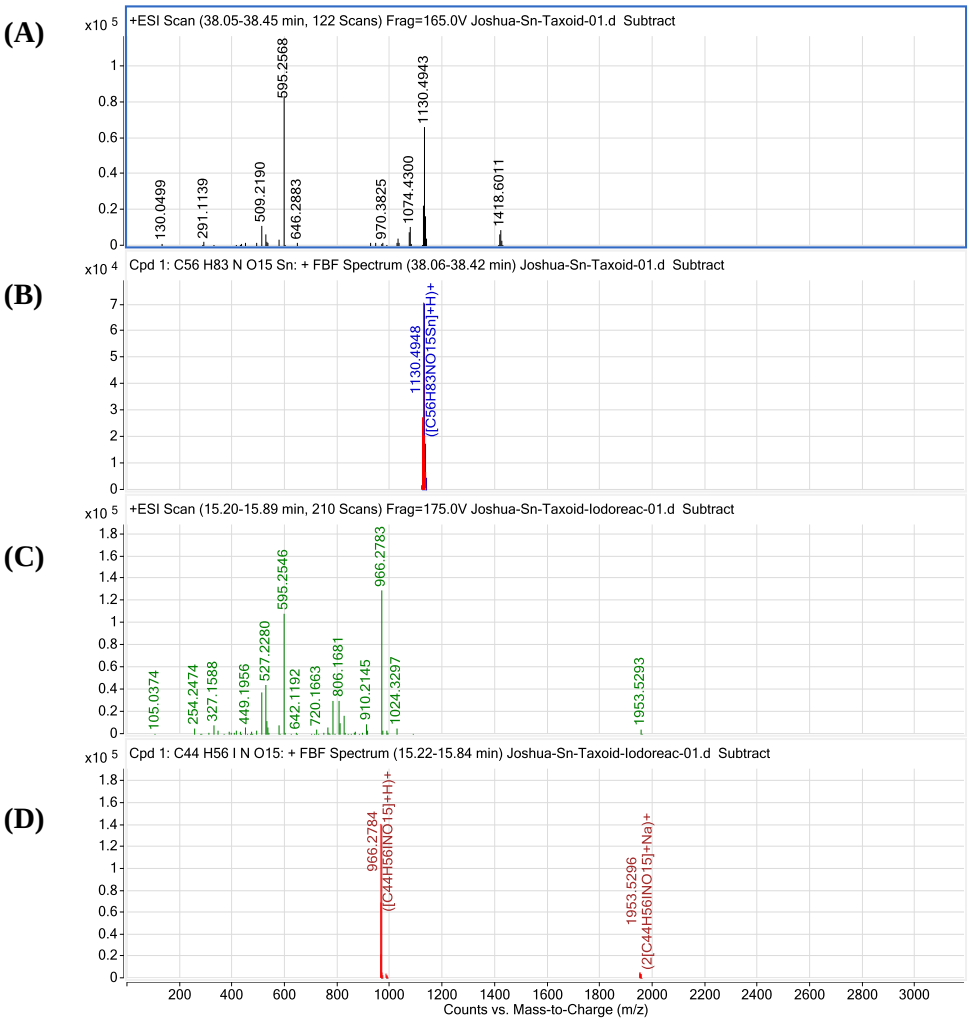

Figure 6- 6: Confirmation of desired product by LC/HRMS

Figure 6-6: (A) shows extracted mass spectra for peak R_t = 38.16 min of compound **6-1** and **Figure 6-6**: (B) m/z ions assigned to target compound, $C_{56}H_{83}NO_{15}Sn$, by Agilent FBF algorithm. Also, **Figure 6-6**: (C) represents extracted mass spectra for peak R_t = 15.39 min of compound 6-2 and **Figure 6-6**: (D) shows m/z ions assigned to target compound, $C_{44}H_{56}INO_{15}$, by Agilent FBF algorithm.

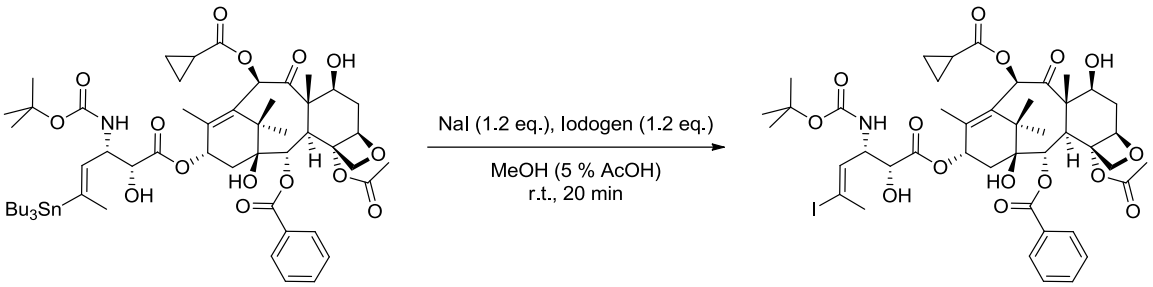

Scheme 6- 1: Cold iodination to form 3'-vinyliodo taxoid (6-2)

Scheme 6-1 shows the cold iodination to for compound **6-2**. In this system, electrophilic iodine is generated in situ using Iodogen® beads as an oxidizing agent.

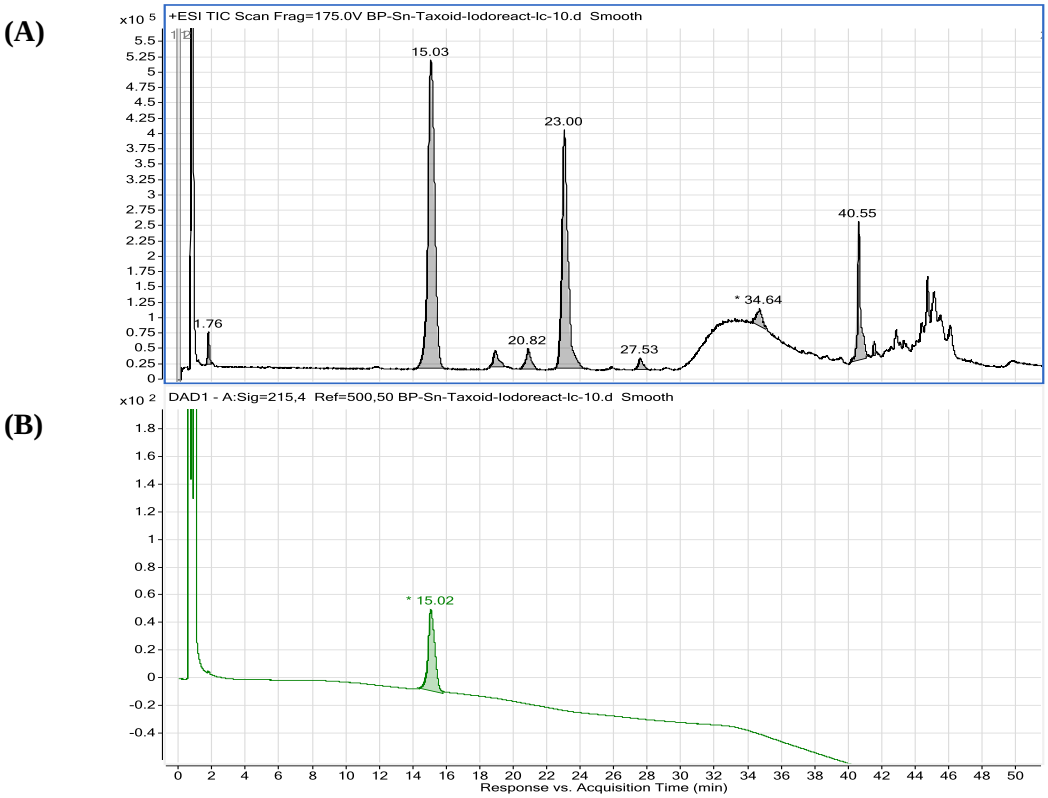

Figure 6- 7: Full HPLC trace of iodination

The TIC mass and UV @215 nm chromatograms of reaction mixture are shown in **Figure 6-7:** (A) and (B), rexpectively. Analysis of the extracted mass spectra from peak, R_t = 15.01 min indicates that m/z ions are observed consistent with the target formula (**Figure 6-8**). It should be noted that there is no evidence of the starting compound **6-1**.

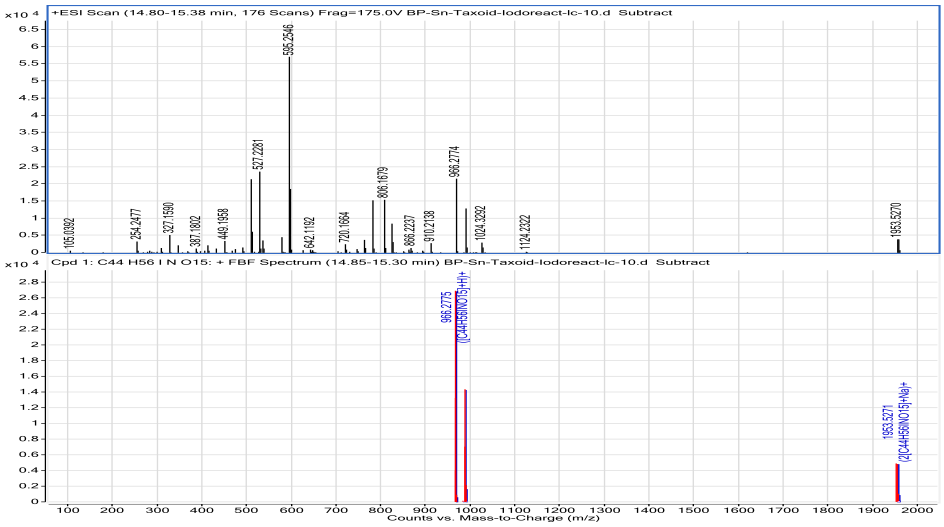

Figure 6- 8: Confirmation of desired product by LC/HRMS of the reaction mixture

Extracted mass was confirmed and the spectra show in Figure 6-8. The desired compound was found at peak R_t = 15.03 min and m/z ions assigned to target compound, $C_{44}H_{56}INO_{15}$, by Agilent FBF algorithm.

Moreover, the biotin linker stannly taxoid, compound **6-3** was determined.

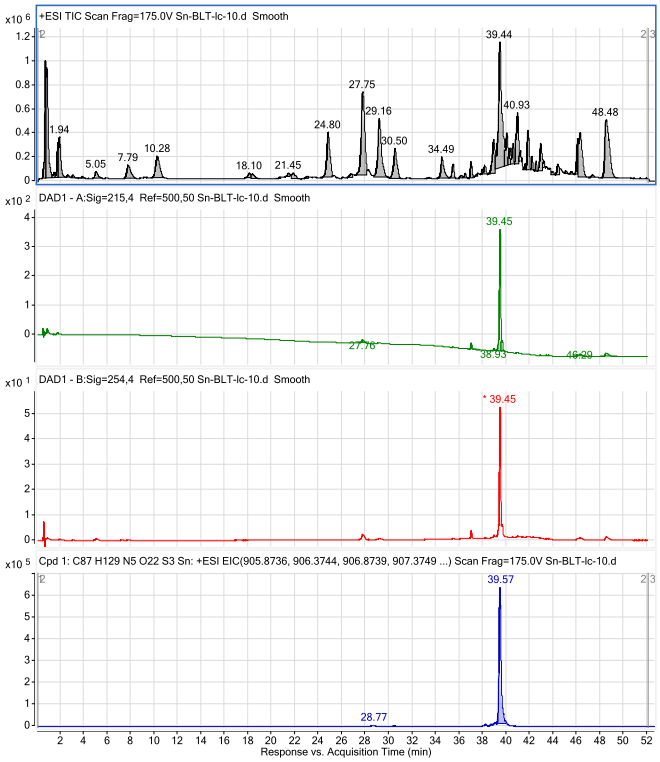

Figure 6- 9: Compound 6-3 confirmation by mass chromatogram

The TIC mass and UV chromatograms of compound **6-3** are shown in **Figure 6-9**. The UV chromatograms show one predominant peak. However, the ESI+ mass chromatogram shows numerous peaks. Analysis of the extracted mass spectra from peak, R_t = 39.45 min indicates that m/z ions are observed consistent with the target formula (**Figure 6-10**). The compound identification is shown below.

(A)

(B)

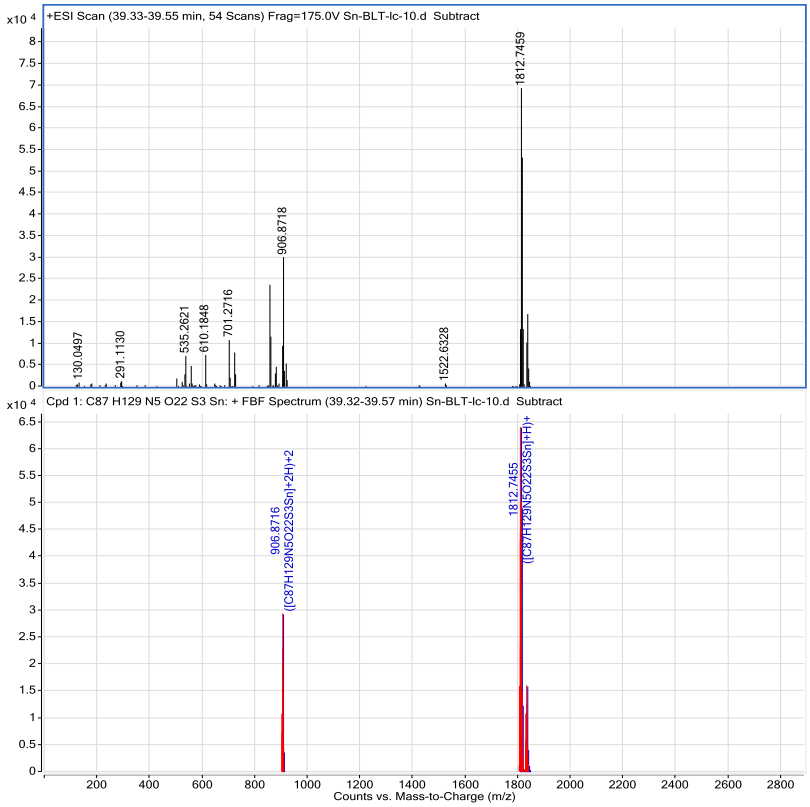

Figure 6- 10: Target confirmation

Extracted mass spectra for peak R_t = 39.45 min of compound 6-3 shown in **Figure 6-10**: (A) and **Figure 6-10**: (B) illustrated Agilent MFE, m/z ions assigned to target formula.

The same condition described in **Scheme 6-1** was applied to the biotin conjugate, **6-3**. However, the desired compound was not found on LC/HRMS, even though the starting material was gone. Further method will be developed for iodination of compound **6-3**.

§ 6.3 Conclusion

Radiolabeling of potent drugs is a extensively used strategy to develop a better understanding of their biodistribution and PK profiles. The radioactive isotopes of ^{123}I and ^{124}I can be used for PET and SPECT studies. A novel taxoid **6-1**, bearing 3'-vinyltrialkylstannanes, 3'-vinyliodo taxoid, **6-2**, and biotin conjugate **6-3**, bearing 3'-vinyltributylstannes, have been designed and synthesized previously (by Dr. Seitz). In addition, biotin conjugates bearing this 3'-vinylstannyl taxoids has been designed and synthesized. 3'-Vinyliodo taxoid, **6-2**, was evaluated *in vitro* against various cancer cell lines, ID8, NCI/ADR-RES, HCT-116, MX-1 and MCF-7. Compound **6-2** exhibited a little less but similar activity compared to the parent taxoid, SB-T-1214. Therefore, 3'-vinyliodo taxoid can be used as imaging agent and also provide an excellent clinical theranostic tool for tumor-targeted chemotherapy. Condition for cold iodination of 3'-stannly taxoid, **6-2** was successfully developed and further optimization for the cold labeling of biotin conjugate is actively on the way in our lab.

§ 6.4 Experimental Section

§ 6.4.1 Caution

Taxoids have been identified as potent cytotoxic agents. Thus, all drugs and structurally related compounds and derivatives must be considered mutagens and potential reproductive hazards for both males and females. All appropriate precautions, such as the use of gloves, goggles, labware, and fume hood, must be taken while handling the compounds at all times.

§ 6.4.2 Materials

The chemicals were purchased from Sigma-Aldrich, Fisher Scientific, and VWR International, and used as received or purified before use by standard methods. Tetrahydrofuran was freshly distilled from sodium and benzophenone. Dichloromethane was also distilled immediately prior to use under nitrogen from calcium hydride. 3-(4,5-Dimethylthiazol-2-yl)-2,5-diphenyltetrazolium bromide (MTT) was obtained from Sigma Chemical Co. Biological materials including RPMI-1640 and DMEM cell culture media, fetal bovine serum, NuSerum, PenStrep, and TrypLE were obtained from Gibco and VWR International, and used as received for cell-based assays.

§ 6.4.3 Cell culture system for MTT assay

All cell lines were obtained from ATCC unless otherwise noted. Cells were cultured in RPMI-1640 cell culture medium (Gibco), supplemented with 10% (v/v) heat-inactivated fetal bovine serum (FBS) and 1% (v/v) penicillin and streptomycin (PenStrep) at 37 ℃ in a humidified atmosphere with 5% CO_2. Murine leukemia cell line L1210FR (a gift from Dr. Gregory Russell-Jones, Access Pharmaceuticals Pty Ltd., Australia) was grown as a suspension in supplemented RPMI-1640. Human breast carcinoma, MX-1 and MFC-7, murine ovarian carcinoma, ID8, and normal lung fibroblast, WI-38, cell lines were cultured as monolayers on 100 mm tissue culture dishes in a supplemented RPMI-1640 cell culture medium. Cells were harvested, collected by centrifugation at 850 rpm for 5 min, and resuspended in fresh culture medium. Cell cultures were routinely divided by treatment with trypsin (TrypLE, Gibco) as needed every 2-4 days and collected by centrifugation at 850 rpm for 5 min, and resuspended in fresh cell culture medium, containing varying cell densities for subsequent biological experiments and analysis.

§ 6.4.4 Single drug MTT assay

The cytotoxicities (IC_{50}, nM) of paclitaxel, SB-T-1214, and 3'-vinyliodo taxoid were evaluated against various cancer cell lines by means of the standard quantitative colorimetric MTT assay. The inhibitory activity of each compound is represented by the IC_{50} value, which is defined as the concentration required for inhibiting 50 % of the cell growth. Cells were harvested, collected, and resuspended in 100 μL cell culture medium (RPMI-1640) at a concentrations ranging from 0.5-1.5 x 10^4 cells per well in a 96-well plate. For adhesive cell types, cells were allowed to descend to the bottom of the wells overnight, and appropriate fresh medium was added to each well upon removal of the old medium.

For the MTT assay of paclitaxel, SB-T-1214, and 3'-vinyliodo taxoid, cells were resuspended in 200 μL medium with 8,000 to 10,000 cells per well of a 96-well plate and incubated at 37 ℃ for 24 h before drug treatment. In DMSO stock solutions, each drug or conjugate was diluted to a series of concentrations in cell culture medium to prepare test solutions. After removing the old medium, these test solutions were added to the wells in the 96-well plate to give the final concentrations ranging from 0.5 to 5,000 nM (100 μL), and the cells were subsequently cultured at 37 ℃ for 48 of 72 h. For the leukemia cell lines, cells were harvested, collected, and resuspended in the test solutions ranging from 0.5 to 5,000 nM (100 μL) at 0.5 to 0.8 x 10^4 cells per well in a 96-well plate and subsequently incubated at 37 ℃ for 72 h. For all experiments, after removing the test medium, fresh solution of MTT in PBS (40 μL of 0.5 mg MTT/mL) was added to the wells, and the cells were incubated at 37 ℃ for 3 h. The MTT solution was then removed, and the resulting insoluble violet formazan crystals were dissolved in 0.1 N HCl in isopropanol with 10% Triton X-100 (40 μL) to give a violet solution.

§ 6.4.5 Data analysis for MTT assay

The spectrophotometric absorbance measurement of each well in the 96-well plate was run at 570 nm using a Labsystems Multiskan Ascent microplate reader. The IC_{50} values and their standard errors were calculated from the viability-concentration curve using Four Parameter Logistic Model of Sigmaplot. The concentration of DMSO per well was ≤ 1% in all cases. Each experiment was run in triplicate.

§ 6.5 References

1. Bergstrom, M.; Grahnen, A.; Langstrom, B., Positron emission tomography microdosing: a new concept with application in tracer and early clinical drug development. *European journal of clinical pharmacology*, **2003,** *59* (5-6), 357-366.
2. Gambhir, S. S., Molecular imaging of cancer with positron emission tomography. *Nature reviews. Cancer,* **2002,** *2* (9), 683-693.
3. Ma, X.; Wang, J.; Cheng, Z., Cerenkov Radiation: A Multi-functional Approach for Biological Sciences. *Frontiers in Physics,* **2014,** *2*.
4. Ravert, H. T.; Klecker, R. W.; Collins, J. M.; Mathews, W. B.; Pomper, M. G.; Wahl, R. L.; Dannals, R. F., Radiosynthesis of [C-11]paclitaxel. *J Labelled Compd Rad,* **2002,** *45* (6), 471-477.
5. Kiesewetter, D. O.; Jagoda, E. M.; Kao, C. H.; Ma, Y.; Ravasi, L.; Shimoji, K.; Szajek, L. P.; Eckelman, W. C., Fluoro-, bromo-, and iodopaclitaxel derivatives: synthesis and biological evaluation. *Nuclear medicine and biology,* **2003,** *30* (1), 11-24.
6. Roh, E. J.; Park, Y. H.; Song, C. E.; Oh, S. J.; Choe, Y. S.; Kim, B. T.; Chi, D. Y.; Kim, D., Radiolabeling of paclitaxel with electrophilic 123I. *Bioorganic & medicinal chemistry,* **2000,** *8* (1), 65-68.
7. E. W. van Tilburg, E. J. F. F., J. J. M. van der Hoeven, M. van der Meij, D. Elshove, A. A. Lammertsma and A. D. Windhorst, Radiosynthesis of [^{11}C]docetaxel. *J Label Compd Radiopharm,* **2004,** *47*, 736-777.
8. van der Veldt, A. A.; Hendrikse, N. H.; Smit, E. F.; Mooijer, M. P.; Rijnders, A. Y.; Gerritsen, W. R.; van der Hoeven, J. J.; Windhorst, A. D.; Lammertsma, A. A.; Lubberink, M., Biodistribution and radiation dosimetry of 11C-labelled docetaxel in cancer patients. *European journal of nuclear medicine and molecular imaging,* **2010,** *37* (10), 1950-1958.
9. Koehler, L.; Gagnon, K.; McQuarrie, S.; Wuest, F., Iodine-124: a promising positron emitter for organic PET chemistry. *Molecules,* **2010,** *15* (4), 2686-2718.
10. Belov, V. V.; Bonab, A. A.; Fischman, A. J.; Heartlein, M.; Calias, P.; Papisov, M. I., Iodine-124 as a label for pharmacological PET imaging. *Molecular pharmaceutics,* **2011,** *8* (3), 736-747.
11. Zempleni, J.; Wijeratne, S. S.; Hassan, Y. I., Biotin. *BioFactors,* **2009,** *35* (1), 36-46.

12. Ojima, I., Guided molecular missiles for tumor-targeting chemotherapy--case studies using the second-generation taxoids as warheads. *Accounts of chemical research,* **2008,** *41* (1), 108-119.
13. Russell-Jones, G.; McTavish, K.; McEwan, J.; Rice, J.; Nowotnik, D., Vitamin-mediated targeting as a potential mechanism to increase drug uptake by tumours. *Journal of inorganic biochemistry,* **2004,** *98* (10), 1625-1633.
14. Seitz, J. D. The design, synthesis and biological evaluation of novel taxoid anticancer agents and their tumor-targeted drug conjugates. Dortoral Dissertation State University of New York at Stony Brook, **2013**.
15. Pandey, S. K.; Sajjad, M.; Chen, Y.; Pandey, A.; Missert, J. R.; Batt, C.; Yao, R.; Nabi, H. A.; Oseroff, A. R.; Pandey, R. K., Compared to purpurinimides, the pyropheophorbide containing an iodobenzyl group showed enhanced PDT efficacy and tumor imaging (124I-PET) ability. *Bioconjugate chemistry,* **2009,** *20* (2), 274-282.
16. Akgun, E.; Portoghese, P. S.; Sajjad, M.; Nabi, H. A., Synthesis and I-124-labeling of m-iodophenylpyrrolomorphinan as a potential PET imaging agent for delta opioid (DOP) receptors. *J Labelled Compd Rad,* **2007,** *50* (3-4), 165-170.
17. Shaul, M.; Abourbeh, G.; Jacobson, O.; Rozen, Y.; Laky, D.; Levitzki, A.; Mishani, E., Novel iodine-124 labeled EGFR inhibitors as potential PET agents for molecular imaging in cancer. *Bioorganic & medicinal chemistry,* **2004,** *12* (13), 3421-3429.

Chapter 7

Combination Chemotherapy

Chapter Contents

§ 7.1 Introduction 139
§ 7.1.1 Cancer Stem Cells 139
§ 7.1.2 Combination Chemotherapy with SB-T-1214 140
§ 7.1.3 Camptothecin (CPT) 141
§ 7.1.4 CMC2.24 142
§ 7.1.5 Epigallocatechin Gallate (EGCG) 143
§ 7.1.6 MMP inhibitors 145
§ 7.2 Results and discussion 147
§ 7.2.1 Synthesis of MMP inhibitors 147
§ 7.2.2 Biological Evaluation of combination therapy 147
§ 7.3 Conclusion 151
§ 7.4 Experimental Section 152
§ 7.4.1 General Methods 152
§ 7.4.2 Materials 152
§ 7.4.3 Experimental Procedures 152
§ 7.4.4 Cell culture system for MTT assay 154
§ 7.4.5 Drug Treatment for MTT assay 154
§ 7.4.6 Data analysis for MTT assay 155
§ 7.5 References 156

§ 7.1 Introduction

§ 7.1.1 Cancer Stem Cells

Stem cells are characterized as cells that can renew themselves and to generate mature cells of a particular tissue through differentiation.[1, 2] In most tissues, stem cells are rare and they divide asymmetrically.[2, 3] When stem cells divide producing two daughter cells, one daughter remains a stem cell and the other becomes a progenitor cell that undergoes differentiation into specialized cells.[3, 4]

Cancer stem cells (CSCs) are very similar to normal stem cells. CSCs can renew themselves and they are built to last a lifetime to be able to slumber for prolonged periods of time and to colonize other parts of the body.[1] CSCs are tumor-initiating cells that possess the capacity to self-renew and differentiate into non-stem cell cancer progeny.[4-6]

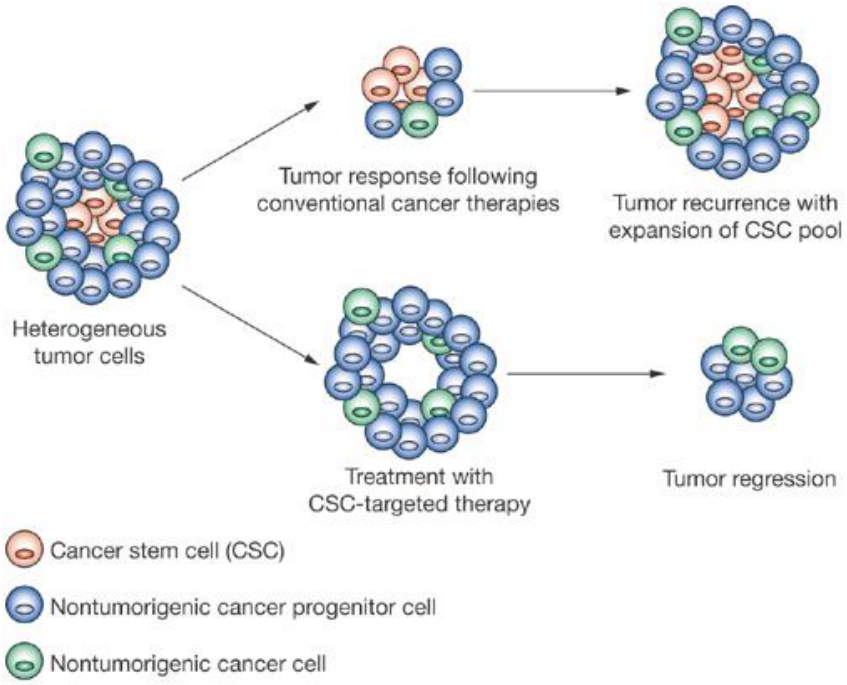

Figure 7- 1: The cancer stem cell hypothesis (adapted from [7])

CSCs have been implicated not only in tumor initiation, but also in tumor recurrence and progression.[7] CSCs are also multipotent and can give rise to the diverse set of cells that make up a given tumor. Inherent within this hypothesis is the assumption that current treatments for cancer can considerably diminish tumor burden, but have a decreased effect on CSCs, which are later capable of driving tumor recurrence and regrowth. Nontumorigenic cancer progenitor cells

are capable of cell division, but their capability to divide is limited, and they are unable to match the rates of tumor cell apoptosis and senescence. To achieve cancer remission or cure, it will be necessary to develop novel therapies that are cytotoxic to CSCs.

§ 7.1.2 Combination Chemotherapy with SB-T-1214

Chemotherapy drugs increase their efficacy when they are given in combination. The rationale for combination chemotherapy is to use drugs that work by different mechanisms, thereby decreasing the likelihood that resistant cancer cells will develop. When drugs with different effects are combined, each drug can be used at its optimal dose, without intolerable side effects. We planned to explore synergistic combinations of new-generation taxoids with other agents to further potentiate the taxoid warheads with lesser amounts and enhance the overall efficacy of chemotherapy.

Table 7- 1: Biological evaluation of chemotherapeutic agents against CSC-enriched cancer cells (adapted from [10])

Drugs	Average IC_{50} (nM)
cisplatin	4540 ± 276
doxorubicin	78.0 ± 28.2
methotrexate	32.7 ± 11.2
paclitaxel	33.8 ± 3.33
topotecan	451 ± 12
SB-T-1214	0.28 ± 0.13

Recently, SB-T-1214 was shown to possess outstanding activity against highly drug resistant CSC-derived tumor spheroids.[8] The surviving cells exhibited compromised clonogenic capacity and significantly impaired ability to generate secondary spheroids. In addition, colon CSC treated with SB-T-1214 showed down-regulation of stem cellrelated genes.[8] As CSCs are considered as important factor for tumor reoccurrence and metastasis,[9] the ability of next generation taxoids such as SB-T-1214 to critically damage CSC populations *in vitro* and *in vivo*. This strongly supports the use of these compounds as efficacious anticancer agents.

To assess the potency of selected next-generation taxoids against CSC-enriched cell populations, they were compared to standard chemotherapeutic agents in an *in vitro* MTT assay against HCT-116++ (CD133+ colon) by Dr. Edison Zuniga in the Ojima laboratory.[10] The screening results are shown in **Table 7-1**. Next-generation taxoids clearly retain their high potency against this CSC-enriched cell population. These next-generation taxoids are two orders of magnitude more active than paclitaxel, methotrexate and doxorubicin.

§ 7.1.3 Camptothecin (CPT)

Camptothecin (CPT) is a quinoline alkaloid that inhibits DNA topoisomerase I by preventing the cleavage and reannealing of single-strand DNA (ssDNA) during replication and transcription.[11] In preliminary clinical trials, CPT showed excellent anticancer activity. However, the compound also showed low solubility and adverse side effects. The anticancer activity of CPT has been attributed to its planar structure (**Figure 7-2**).[12, 13] CPT contains a planar pentacyclic ring structure and one chiral center with (S) configuration. Two camptothecin derivatives, irinotecan and topotecan which have been approved by the FDA for the treatment of cancer, are shown in **Figure 7-2**.

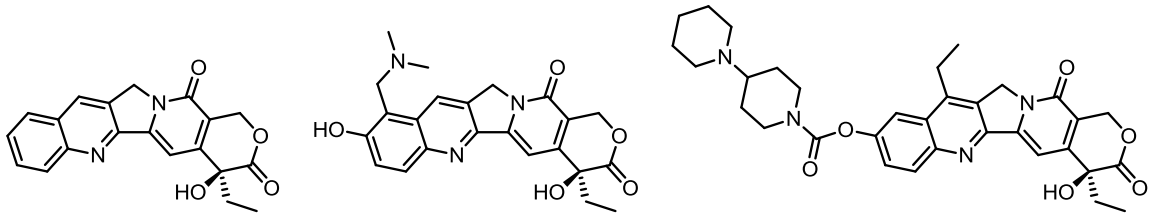

Figure 7- 2: Chemical structures of camptothecin (CPT), topotecan, and irinotecan (CPT-11)

The mechanism of action by camptothecin is highly cell-cycle dependent, rendering cells in S phase 100- to 1000-times more sensitive then those cells in the remaining phases of the cell cycle.[11, 14, 15] Pretreatment *in vitro* with taxanes and other microtubule stabilizing agents can increase the potency of topoisomerase I inhibitors by increasing topoisomerase I levels and the fraction of cells in the S phase, the target phase of the cell cycle by such inhibitors.[16]

§ 7.1.4 CMC2.24

Curcumin is a natural product found in turmeric and it is derived from the perennial herb *Curcuma longa L*. Curcumin has been used as an herbal medicine in various conditions such as, pulmonary, gastrointestinal and liver diseases, and also as a remedy for non-healing wounds and in the treatment of cancer.[17-19] Curcumin was found to possess a variety of therapeutic efficacies including the ability to inhibit proliferation and metastasis of various carcinomas, the down-regulation of transcription factors including nuclear factor kappa-lightchain-enhancer of activated B cells (NF-κB), the down-regulation of the expression of chemokines and cytokines including TNF-α, and the suppression of protein kinases and growth factors.

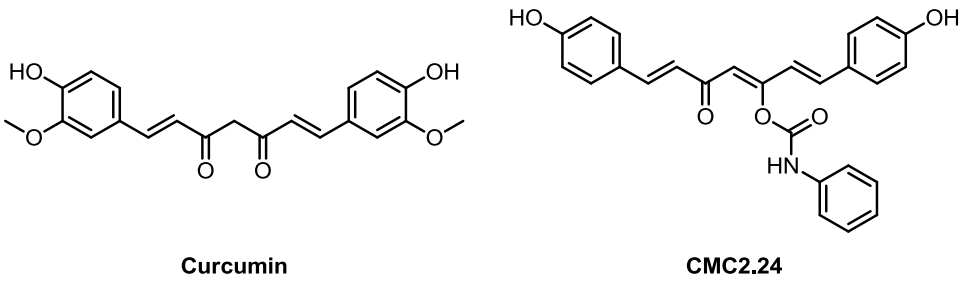

Figure 7- 3: Chemical structure of curcumin and CMC2.24

Since curcumin is highly symmetric and very insoluble, modifications were made to the synthetic method to prepare the unsymmetrical curcumin analogue. Previous studies revealed that chemically modified curcumin 2.24 (CMC2.24) (**Figure 7-3**) is tremendously potent in both *in vitro* and *in vivo*. To study the potential interactions between SB-T-1214 and paclitaxel with CMC2.24, the effectiveness of various drug concentrations and their combination with CMC2.24 was evaluated in the tumorinitiating fractions of the PPT2 and PC3MM2 cell lines.[20] It has been demonstrated that a combination of S-BT-1214 with CMC2.24 exerts more profound pleiotropic, pan-inhibitory effects on a large number of stemness genes and transcription factors.[20] In particular, modulation of multiple stem cell-relevant transcription factors and the pro-apoptotic p21 and p53 "gene wake-up" mechanism can potentially reverse resistance of CSCs to anti-cancer treatment and improve clinical outcome.[20]

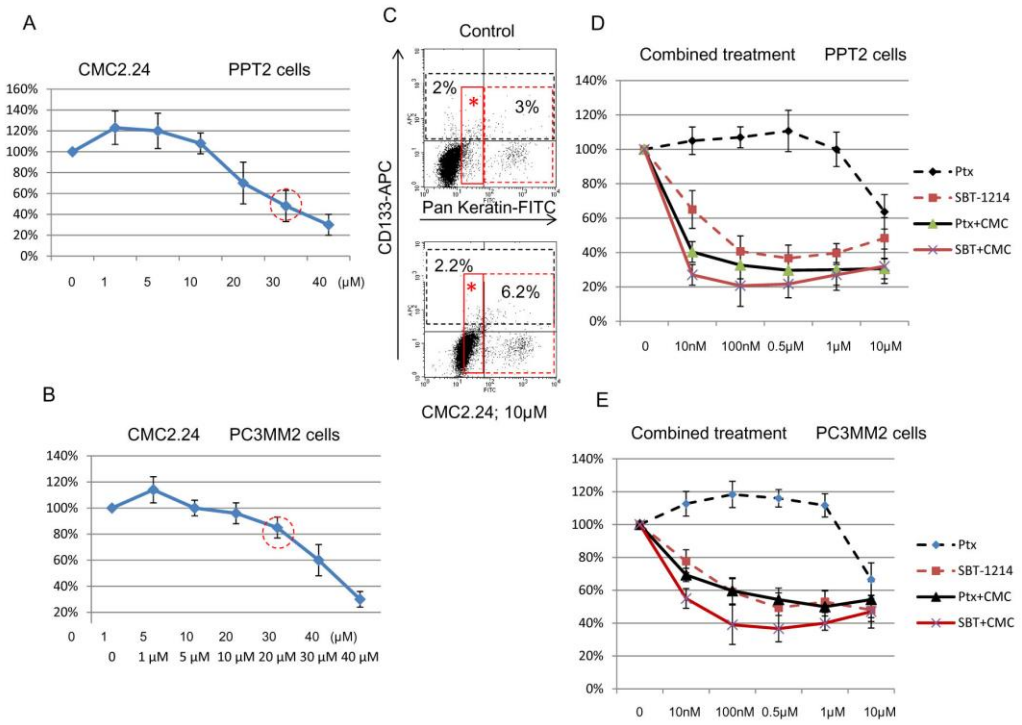

Figure 7- 4: Cytotoxic effects of the SBT-1214/CMC2.24 combination against prostate CD133+ cells (adapted from [20])

As **Figure 5A**, and **B** indicates, CMC2.24 often exerted biphasic effects on prostate CD133+ cells: lower concentrations of it promoted proliferation, whereas higher ones were cytotoxic. FACS analysis revealed that in contrast to SBT-1214, treatment with CMC2.24 did not induce an increase in the ratio of CD133+ cells (**Figure 5C**, black dotted areas), but similarly to SBT-1214, increased expression of the differentiation marker pan-keratin (**Figure 5C**, red dotted areas) and shifted the entire cell population toward differentiation (**Figure 5C**, areas with asterisks). A combination of the two agents induced more significant cell death of the CD133+ PPT2 (**Figure 5D**) and PC3MM2 (**Figure 5E**) cells compared to each compound as a single agent.

§ 7.1.5 Epigallocatechin Gallate (EGCG)

A variety of studies have shown that green tea or its constituents can either inhibit carcinogenesis or the growth of established cancers at various organ sites including the colon.[21] Green tea contains chemicals known as polyphenols, which have antioxidant properties. The major polyphenols in green tea are called catechins, and the most important catechin seems to be

epigallocatechin gallate (EGCG). Studies suggested that EGCG may promote certain types of cancer cells to die in much the same way that normal cells do.[22]

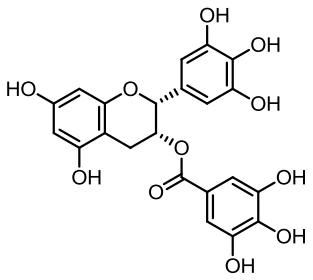

Figure 7- 5: Chemical Structure of Epigallocatechin Gallate (EGCG)

In an attempt to widen the curative therapeutic window of EGCG, researchers explored a combination therapy that consisted of combining EGCG with chemotherapeutic agents. It was found that EGCG in combination with taxanes exert a synergistic effects against human prostate cancer cells (**Figure 7-6**).

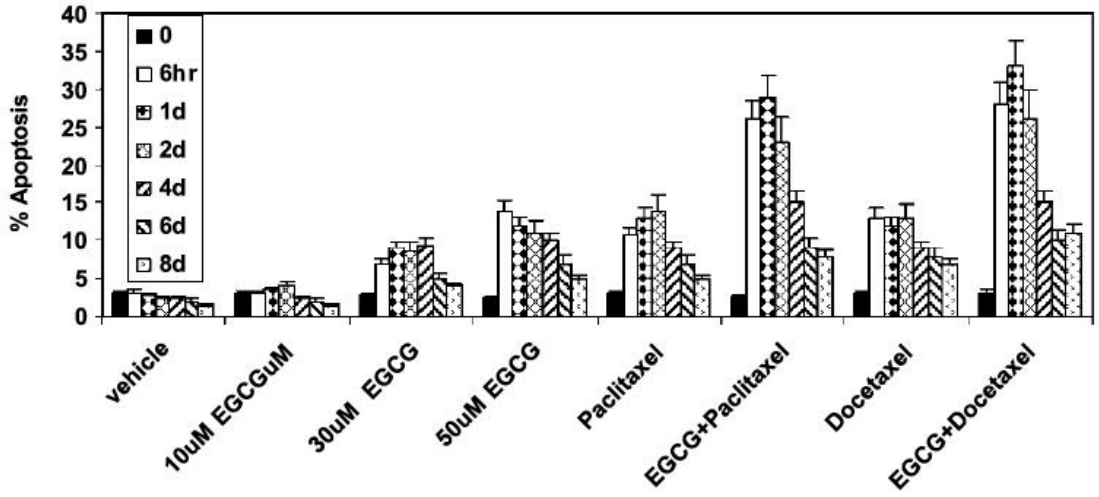

Figure 7- 6: Percent apoptosis by PC-3ML cells (adapted from [22])

As **Figure 7-6** illustrates, treatment with EGCG (30 μM) combined with either paclitaxel (6.25 nM) or docetaxel (3.12 nM) against PC-3ML cell line resulted in more than 25% apoptosis after 6 hours, 1 day, and 2 days compared with ~ 6% to 10% apoptosis in the presence of the individual agents alone. However, the percent apoptosis observed decreased to less than 10% in the presence of EGCG and taxane or the individual agents alone after 6 to 8 days (**Figure 7-6**). Note that higher EGCG levels (50 μM) alone induced more than 10% apoptosis after 6 hours to 4

days compared with less than 8% apoptosis observed in the presence of 30 μM EGCG (**Figure 7-6**), indicating that higher dosages of EGCG may be more efficacious.

§ 7.1.6 MMP inhibitors

Matrix metalloproteinases (MMPs) are a group of more than 25 structurally-related zinc-containing endopeptidases that play an essential role in the degradation of the main components of the extracellular matrix (ECM).[23, 24] MMPs are classified as their different substrate specificities which were observed *in vitro* studies of the individual enzymes. There are five sub-groups of MMPs in total: collagenases, gelatinases, stomelysins, membrane-type, and unclassified.[25-27]

Since MMPs play a crucial role in the degradation of the ECM and are related to a variety of diseases, MMP inhibitors has been an attractive target over the years.[28, 29] Most of the synthetic inhibitors target the zinc ions in the catalytic domains of MMPs, and some of them showed great potency *in vitro*, but failed in clinical trials due to their lack of specificity.[30] To overcome this problem, the development of new-generation inhibitors has to be made with a novel approach. One of very promising approach is to disrupt protease signaling function with binding to the non-catalytic domain of MMPs.

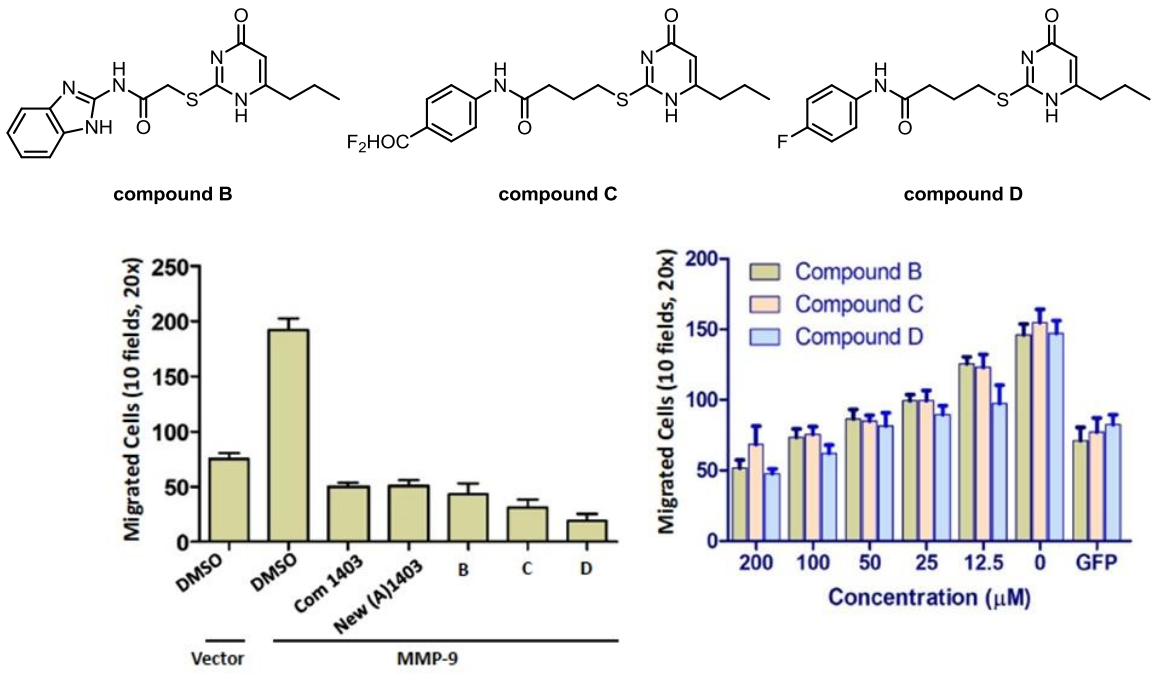

Figure 7- 7: Development of novel MMP-9 inhibitory compounds

Recently, the Cao's laboratory, one of our collaborators, has discovered a new class of MMP inhibitors (MMPi) that interact with the hemopexin (PEX) domain of MMP-9 (**Figure 7-7**).[31] In a tumor xenograft model, this pyrimidinone suppressed MDA-MB-435 tumor growth and inhibited its lung metastasis.[31] Following up this discovery, the optimization of the lead compounds is currently ongoing in our lab for their synergistic effect with SB-T-1214.

§ 7.2 Results and discussion

§ 7.2.1 Synthesis of MMP inhibitors

General procedure for the synthesis of MMP inhibitor (MMPi), **7-4**, is illustrated in **Scheme 7-1.**[32]

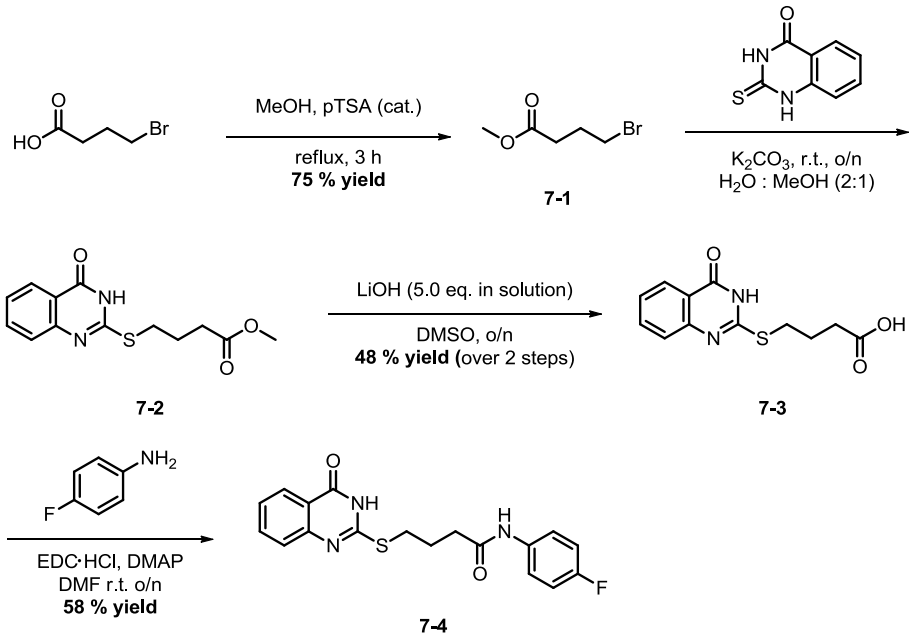

Scheme 7- 1: Synthetic route for MMP inhibitor, 7-4

The first step was methylation of commercially available 4-bromobutanoic acid in the presence of p-toluenesulfonic acid (p-TSA) as a catalyst. Compound **7-1** was obtained by in 75 % yield. A mixture of 2-mercaptoquinazolinone and compound **7-1** in H_2O/MeOH (2:1) mixture was stirred in room temperature in the presence of potassium carbonate to afford the desired compound **7-2**. Compound **7-2** was carried forward with to the next step without further purification. Removal of the methyl group with LiOH gave the corresponding carboxylic acid **7-3** in 48 % yield over two steps. Treatment of carboxylic acid **7-3** with 4-fluoroaniline in the presence of EDC•HCl and DMAP in DMF gave the desired compound **7-4** in 58 % yield.

§ 7.2.2 Biological Evaluation of combination therapy

Next-generation taxoid, SB-T-1214, was selected as the microtubule-stabilizing agent, as it exhibits two to three orders of magnitude greater potency than paclitaxel and docetaxel against multidrug resistant and paclitaxel-resistant cancer cell lines and tumors. The combination with

other agents, CMC2.24, MMP inhibitor and EGCG was performed to explore synergistic combinations of new-generation toxoids, SB-T-1214. The effect of equimolar combinations of SB-T-1214 with other agents was evaluated in single administration as well as combination agents for *in vitro* cytotoxicity studies. Single-drug administrations and combinations were evaluated against HCT-116 and PPT2 cancer initiate cell lines (CICs). The results are summarized in **Table 7-2**.

Table 7- 2: Preliminary screening against CICs

Compound	HCT-116[a]	PPT2[a]
Paclitaxel[b]	13.8 ± 3.0 nM	5.26 ± 0.3 nM
SB-T-1214[b]	31.9 ± 13 nM	4.03 ± 1.9nM
CMC2.24[b]	50.6 ± 4.61 µM	36.5 ± 3.5 µM
MMPi[b]	> 160 µM	> 160 µM
EGCG[b]	> 160 µM	> 160 µM
SB-T-1214 + CMC 2.24[c]	19.1 ± 9.0 nM	1.89 ± 0.75 nM
SB-T-1214 + MMPi[d]	13.6 ± 11 nM	1.49 ± 0.59 nM
SB-T-1214 + EGCG[e]	21.5 ± 7.8 nM	0.21 ± 0.06 nM

[a] Enriched colorectal cancer stem cell; [b] single drug administration; [c] cells were incubated with SB-T-1214 and 40 µM of CMC2.24; [d] cells were incubated with SB-T-1214 and 40 µM of MMPi; [e] cells were incubated with SB-T-1214 and 40 µM of EGCG; All cells were incubated with drugs at 37 °C in a 5% CO_2 atmosphere for 72 h

As **Table 7-2** describes, the cytotoxicity assays of single administration of each drug against HCT-116 and PPT2 were performed by MTT method. As controls for comparison, paclitaxel and parent taxoid SB-T-1214 were evaluated as well. The corresponding cancer cell lines were incubated with each drug for 48 h, and the corresponding IC_{50} values were determined. As **Table 7-2** shows, the cytotoxicity of single administration of CMC2.24 was exhibited IC_{50} value of 50.6 and 36.5 µM against HCT-116 and PPT2, respectively. Interestingly, MMPi and EGCG based on its IC_{50} values were not show appreciate cytotoxicity (IC_{50} > 160 µM). However, when the cells were exposed to an equimolar mixture of the two drugs, the IC_{50} values were lower than as those for the single-drug administration of SB-T-1214 against two prostate CIC

lines. The most exciting data was when SB-T-1214 was treated with EGCG, the cytotoxicity was 20 times more potent than that of SB-T-1214 single administration against PPT2 cell line.

Although there is some questionable point - more effective inhibition of CICs with paclitaxel than SB-T-1214, (we can check more carefully all the dilution steps) - there is a solid biological reason for such a resistance. Since this HCT116 subpopulation represents extremely aggressive, practically purified "educated" CICs, which have produced 3D spheroids even on adherent surfaces. For the future study, we can repeat MTT assay on regular HCT-116 with more gradual increase in drug concentrations. Moreover, molecular biological and functional analyses can be done after drug treatment to determine the shift of stemness gene expression toward differentiation is much more important.

In addition to CSCs, normal cancer cells were included to study combination effects of SB-T-1214 and other agents, CMC2.24, MMPi, and EGCG. Camptothecin, the topoisomerase I inhibitor was also included.

Table 7- 3: Cytotoxicities (IC_{50}) of single and combination administration

Compound	ID8[a]	MX-1[b]
Paclitaxel[c]	42.0 ± 3.79 nM	5.59 ± 2.12 nM
SB-T-1214[c]	2.41 ± 0.08 nM	1.89 ± 0.80 nM
Camptothecin[c]	74.2 ± 5.68 nM	36.3 ± 5.85 nM
CMC2.24[c]	29.7 ± 0.85 µM	14.7 ± 1.28 µM
MMPi[c]	36.1 ± 10.8 µM	> 160 µM
EGCG[c]	36.9 ± 0.76 µM	19.8 ± 1.78 µM
SB-T-1214 + CPT[d]	3.36 ± 0.31 nM	< 500 pM
SB-T-1214 + CMC 2.24[e]	< 500 pM	< 500 pM
SB-T-1214 + MMPi[f]	0.62 ± 0.07 nM	< 500 pM
SB-T-1214 + EGCG[g]	0.37 ± 0.05 nM	< 500 pM

[a] murine ovarian carcinoma cell line; [b] human breast carcinoma cell line Enriched colorectal cancer stem cell; [c] single drug administration; [d] cells were incubated with SB-T-1214 and equimolar of CPT [e] cells were incubated with SB-T-1214 and 40 µM of CMC2.24; [f] cells were incubated with SB-T-1214 and 40 µM of MMPi; [g] cells were incubated with SB-T-1214 and 40 µM of EGCG; All cells were incubated with drugs at 37 °C in a 5% CO_2 atmosphere for 72 h

To evaluate the effects that combination drug administration of SB-T-1214, SB-T-1214 with camptothecin, CMC2.24, MMPi, and EGCG were treated with SB-T-1214 and incubated for 72 hours at 37 ℃. As controls for comparison, single drug administration and paclitaxel were evaluated as well. For these experiments ID8 and MX-1 cancer cell lines were used. These results are listed in **Table 7-3**.

As seen from **Table 7-3**, in general, combinational administration with SB-T-1214 with other agents leads to lower IC_{50} values. Also listed in the table, when the cancer cells are treated with SB-T-1214 and other agents, there is a significant increase in activity against ID8 and MX-1 cancer cell lines compared to treatment with SB-T-1214 as a single agent. In the preliminary *in vitro* results clearly show the benefits of treating cells with an equimolar combination of SB-T-1214 with camptothecin. More importantly when the cells were treated with combination of SB-T-1214 with 40 μM of CMC2.24, MMPi, and EGCG shows a lot higher potency.

§ 7.3 Conclusion

Combination chemotherapy has considered as a major treatment option for many types of cancers. The use of two or more properly selected drugs in combination can lead to a decrease in systemic toxicity and an increase in efficacy, compared to the use of a single cytotoxic agent due to synergistic or cooperative effects of the drugs on tumor eradication. Exploration of synergistic combinations between SB-T-1214 and MMP inhibitors as well as EGCG, CMC2.24 and camptothecin had been done against various cell lines, ID8 and MX-1 including CSCs, HCT-116, PPT2. From the preliminary screening, the combination of a taxoid with other agents was shown promising activity. These findings were shown in an *in vitro* biological evaluation using an MTT assay against a number of cancer cell lines. These experiments demonstrated that the combination of SB-T-1214, a potent new-generation taxoid, and cother agents have increased potent in certain cancer cell lines. Further study on the combination of SB-T-1214 will be carried forward in our laboratory.

§ 7.4 Experimental Section

§ 7.4.1 General Methods

^{1}H and 13C NMR spectra were measured on a Brucker 400 or 500 MHz NMR spectrometer. Melting points were measured on a Thomas Hoover Capillary melting point apparatus and are uncorrected. TLC was performed on Sorbtech with UV254 and column chromatography was carried out on silica gel 60 (Merck; 230-400 mesh ASTM). High- resolution mass spectra were obtained on Agilent-TOF instrument.

§ 7.4.2 Materials

The chemicals were purchased from Sigma Aldrich Co., Synquest Inc., Alfa Aesar and purified before use by standard methods. Tetrahydrofuran was freshly distilled from sodium metal and benzophenone. Dichloromethane was also distilled immediately prior to use under nitrogen from calcium hydride. 3-(4,5-Dimethylthiazol-2-yl)-2,5- diphenyltetrazolium bromide (MTT) was obtained from Sigma Chemical Co. Biological materials including RPMI-1640 and DMEM cell culture media, fetal bovine serum, NuSerum, PenStrep, and TrypLE were obtained from Gibco and VWR International, and used as received for cell-based assays.

§ 7.4.3 Experimental Procedures

Mehyl 4-bromobutanoate (7-1)

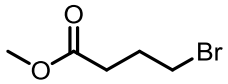

A mixture of 4-bromobutanoic acid (1.47 g, 8.77 mmol) and catalytic amount of p-TSA was stirred in MeOH and refluxed for 6 hours. After the completion of the reaction, the solvent was removed *in vacuo* and the reaction mixture was washed extracted with EA. The organic layer was collected, dried over anhydrous magnesium sulfate and concentrated *in vacuo* to give **7-1** as a colorless oil (1.19 g, 75 % yield): ^{1}H NMR (500 MHz, $CDCl_3$) δ 2.17 (m, 2 H), 2.51 (t, 2 H, *J* = 7.2 Hz), 3.47 (t, 2 H, *J* = 6.6 Hz), 3.69 (s, 3 H); ^{13}C NMR (125 MHz, $CDCl_3$) δ 27.6, 32.0, 32.55, 51.6, 172.7. All data are in agreement with literature values.[33]

Methyl 4-((4-oxo-3,4-dihydroquinazolin-2-yl)thio)butanoate (7-2)

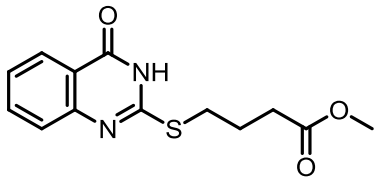

To a mixture of compound **7-1** (1.06 g, 5.84 mmol) and potassium carbonate in H_2O:MeOH (2:1) 2-mercaptoquinazolin-4(3*H*)-one was added. The mixture was stirred in room temperature for 14 hours. After the completion of the reaction, the solvent was removed *in vacuo* and the solid was filtered to provide the desired compound **7-2** as a white solid (807 mg, crude). The crude material was used directly to the further reaction: ^{1}H NMR (500 MHz, $CDCl_3$) δ 1.93 (m, 2 H), 2.38 (t, 2 H, *J* = 7.2 Hz), 3.24 (t, 2 H, *J* = 5.0 Hz), 3.32 (s, 3 H), 7.41 (t, 1 H, *J* = 5.0 Hz), 7.53 (d, 1 H, *J* = 5.0 Hz), 7.75 (t, 1 H, *J* = 5.0 Hz), 8.03 (d, 1 H, *J* = 5.0 Hz), 12.6 (s, 1 H); ^{13}C NMR (125 MHz, $CDCl_3$) δ 24.3, 29.9, 32.1, 51.3, 115.8, 116.2, 124.3, 126.7, 135.4, 140.4, 159.6, 172.7, 174.3.

4-((4-oxo-3,4-dihydroquinazolin-2-yl)thio)butanoic acid (7-3)

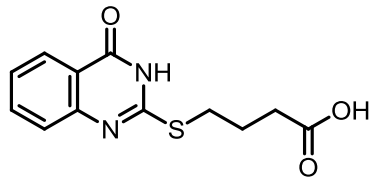

To a mixture of compound **7-2** in DMSO, LiOH (5.0 eq. in solution) was added. The mixture was stirred at room temperature for 12 hours. After the completion of the reaction, the reaction mixture was acidified with 1 M of HCl and the precipitation was filtered and dried to give the desired compound **7-3** as a white solid (747 mg, 48 % yield over two steps): mp 177.5-179 ℃; ^{1}H NMR (500 MHz, $CDCl_3$) δ 1.93 (s, 2 H), 2.39-2.50 (m, 2 H), 3.35-3.49 (m, 2 H), 7.41-7.52 (dd, 2 H), 7.74 (s, 1 H), 8.03 (s, 1 H), 12.1 (s, 1 H), 12.5 (s, 1 H); ^{13}C NMR (125 MHz, $CDCl_3$) δ 24.7, 29.5, 32.9, 120.5, 126.0, 126.4, 126.5, 135.0, 149.9, 155.9, 161.6, 174.3; HRMS (ESI) m/z calcd for $C_{12}H_{13}N_2O_3S^+$ 265.0641 Found: 265.0661 (Δ = 7.5 ppm).

***N*-(4-fluorophenyl)-4-((4-oxo-3,4-dihydroquinazolin-2-yl)thio)butanamide (7-4)**

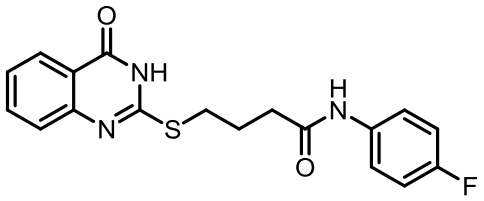

To a mixture of compound **7-3** and EDC•HCl and DMAP in DMF, 4-fluoroaniline (2.0 eq.) was added. The reaction mixture was stirred at room temperature for 16 hours. After completion of the reaction, the reaction mixture was treated with DCM to precipitate and give the desired compound **7-4** as a white solid (97 mg, 58 % yield): mp 217-218 ℃; ^{1}H NMR (500 MHz, $CDCl_3$) δ 2.00-2.05 (m, 2 H), 2.45-2.50 (m, 2 H), 3.29 (t, 2 H, *J* = 7.5 Hz), 7.12 (t, 2 H, *J* = 5.0 Hz), 7.40 (t, 1 H, *J* = 5.0 Hz), 7.45 (d, 1 H, *J* = 5.0 Hz), 7.59 (m, 2 H), 7.71 (t, 1 H, *J* = 5.0 Hz), 8.02 (dd, 1 H), 9.97 (s, 1 H), 12.6 (s, 1 H); ^{13}C NMR (125 MHz, $CDCl_3$) δ 24.7, 29.2, 34.9, 115.1, 115.2, 119.9, 120.7, 125.5, 125.5, 126.0, 134.4, 135.6, 135.7, 149.3, 156.9, 159.7, 161.3, 170.3; HRMS (ESI) m/z calcd for $C_{18}H_{17}FN_3O_2S^+$ 358.1020 Found: 358.1027 (Δ = 1.9 ppm).

§ 7.4.4 Cell culture system for MTT assay

All cell lines were obtained from ATCC unless otherwise noted. Cells were cultured in RPMI-1640 cell culture medium (Gibco), supplemented with 10% (v/v) heat-inactivated fetal bovine serum (FBS) and 1% (v/v) penicillin and streptomycin (PenStrep) at 37 ℃ in a humidified atmosphere with 5% CO_2. CSC-enriched HCT-116 and PPT2 cells were grown as a suspension in supplemented DMEM. Human breast carcinoma, MX-1 and murine ovarian carcinoma, ID8, cell lines were cultured as monolayers on 100 mm tissue culture dishes in a supplemented RPMI-1640 cell culture medium. Cells were harvested, collected by centrifugation at 850 rpm for 5 min, and resuspended in fresh culture medium. Cell cultures were routinely divided by treatment with trypsin (TrypLE, Gibco) as needed every 2-4 days and collected by centrifugation at 850 rpm for 5 min, and resuspended in fresh cell culture medium, containing varying cell densities for subsequent biological experiments and analysis.

§ 7.4.5 Drug Treatment for MTT assay

The cytotoxicities (IC_{50}, nM) of paclitaxel, SB-T-1214, camptothecin and combination of SB-T-1214 and other agents, camptothecin, CMC2.24, MMPi, and EGCG were evaluated

against various cancer cell lines by means of the standard quantitative colorimetric MTT assay. The inhibitory activity of each compound is represented by the IC_{50} value, which is defined as the concentration required for inhibiting 50 % of the cell growth. Cells were harvested, collected, and resuspended in 200 μL cell culture medium (DMEM or RPMI-1640) at a concentrations ranging from 0.5-1.5 x 10^4 cells per well in a 96-well plate at 37 ℃ for 24 h. For adhesive cell types, cells were allowed to descend to the bottom of the wells overnight, and appropriate fresh medium was added to each well upon removal of the old medium.

For single drug administration, each drug was diluted to a series of concentrations in cell culture medium to prepare test solutions. For paclitaxel, SB-T-1214 and camptothecin, after removing the old medium, these test solutions were added to the wells in the 96-well plate to give the final concentrations ranging from 0.5 to 5,000 nM (200 μL). For CMC2.24, MMPi and EGCG, after removing the old medium, these test solutions were added to the wells in the 96-well plate to give the final concentrations ranging from 0.5 to 5,000 nM (200 μL). For the combinational administration, the cells were treated with an equimolar combination of SB-T-1214 with camptothecin in the range from 0.5 to 5,000 nM (total 200 μL) at the final concentration. For the combinational administration of SB-T-1214 with other agents, CMC2.24, MMPi and EGCG, SB-T-1214 was treated in the range from 0.5 to 5,000 nM (100 μL) at the final concentration and the other agents were treated at the 40 μM concentration (100 μL). The cells were cultured at 37 ℃ for 72 h.

For all experiments, after removing the test medium, fresh solution of MTT in PBS (40 μL of 0.5 mg MTT/mL) was added to the wells, and the cells were incubated at 37 ℃ for 3 h. The MTT solution was then removed, and the resulting insoluble violet formazan crystals were dissolved in 0.1 N HCl in isopropanol with 10% Triton X-100 (40 μL) to give a violet solution.

§ 7.4.6 Data analysis for MTT assay

The spectrophotometric absorbance measurement of each well in the 96-well plate was run at 570 nm using a Labsystems Multiskan Ascent microplate reader. The IC_{50} values and their standard errors were calculated from the viability-concentration curve using Four Parameter Logistic Model of Sigmaplot. The concentration of DMSO per well was ≤ 1% in all cases. Each experiment was run in triplicate.

§ 7.5 References

1. Clevers, H., The cancer stem cell: premises, promises and challenges. *Nature medicine,* **2011,** *17* (3), 313-319.
2. Reya, T.; Morrison, S. J.; Clarke, M. F.; Weissman, I. L., Stem cells, cancer, and cancer stem cells. *Nature,* **2001,** *414* (6859), 105-111.
3. Siminovitch, L.; McCulloch, E. A.; Till, J. E., The Distribution of Colony-Forming Cells among Spleen Colonies. *Journal of cellular physiology,* **1963,** *62*, 327-336.
4. Becker, A. J.; Mc, C. E.; Till, J. E., Cytological demonstration of the clonal nature of spleen colonies derived from transplanted mouse marrow cells. *Nature,* **1963,** *197*, 452-454.
5. Al-Hajj, M.; Clarke, M. F., Self-renewal and solid tumor stem cells. *Oncogene,* **2004,** *23* (43), 7274-7282.
6. Al-Hajj, M.; Wicha, M. S.; Benito-Hernandez, A.; Morrison, S. J.; Clarke, M. F., Prospective identification of tumorigenic breast cancer cells. *Proceedings of the National Academy of Sciences of the United States of America,* **2003,** *100* (7), 3983-3988.
7. Das, S.; Srikanth, M.; Kessler, J. A., Cancer stem cells and glioma. *Nature clinical practice. Neurology,* **2008,** *4* (8), 427-435.
8. Botchkina, G. I.; Zuniga, E. S.; Das, M.; Wang, Y.; Wang, H.; Zhu, S.; Savitt, A. G.; Rowehl, R. A.; Leyfman, Y.; Ju, J.; Shroyer, K.; Ojima, I., New-generation taxoid SB-T-1214 inhibits stem cell-related gene expression in 3D cancer spheroids induced by purified colon tumor-initiating cells. *Molecular cancer,* **2010,** *9*, 192.
9. Li, F.; Tiede, B.; Massague, J.; Kang, Y., Beyond tumorigenesis: cancer stem cells in metastasis. *Cell research,* **2007,** *17* (1), 3-14.
10. Zuniga, E. S. Design, synthesis and biological evaluation of new-generation taxoid-based tumor-targeting drug conjugates. Stony Brook University **2012**.
11. Murren, J. R.; Peccerillo, K.; DiStasio, S. A.; Li, X.; Leffert, J. J.; Pizzorno, G.; Burtness, B. A.; McKeon, A.; Cheng, Y., Dose escalation and pharmacokinetic study of irinotecan in combination with paclitaxel in patients with advanced cancer. *Cancer chemotherapy and pharmacology,* **2000,** *46* (1), 43-50.

12. Ulukan, H.; Swaan, P. W., Camptothecins: a review of their chemotherapeutic potential. *Drugs,* **2002,** *62* (14), 2039-2057.
13. Lu, A. J.; Zhang, Z. S.; Zheng, M. Y.; Zou, H. J.; Luo, X. M.; Jiang, H. L., 3D-QSAR study of 20 (S)-camptothecin analogs. *Acta pharmacologica Sinica,* **2007,** *28* (2), 307-314.
14. Li, L. H.; Fraser, T. J.; Olin, E. J.; Bhuyan, B. K., Action of camptothecin on mammalian cells in culture. *Cancer research,* **1972,** *32* (12), 2643-2650.
15. Horwitz, S. B.; Horwitz, M. S., Effects of camptothecin on the breakage and repair of DNA during the cell cycle. *Cancer research,* **1973,** *33* (11), 2834-2836.
16. Bahadori, H. R.; Green, M. R.; Catapano, C. V., Synergistic interaction between topotecan and microtubule-interfering agents. *Cancer chemotherapy and pharmacology,* **2001,** *48* (3), 188-196.
17. Sharma, O. P., Antioxidant activity of curcumin and related compounds. *Biochemical pharmacology,* **1976,** *25* (15), 1811-1812.
18. Ruby, A. J.; Kuttan, G.; Babu, K. D.; Rajasekharan, K. N.; Kuttan, R., Anti-tumour and antioxidant activity of natural curcuminoids. *Cancer letters,* **1995,** *94* (1), 79-83.
19. Aggarwal, B. B.; Kumar, A.; Bharti, A. C., Anticancer potential of curcumin: preclinical and clinical studies. *Anticancer research,* **2003,** *23* (1A), 363-398.
20. Botchkina, G. I.; Zuniga, E. S.; Rowehl, R. H.; Park, R.; Bhalla, R.; Bialkowska, A. B.; Johnson, F.; Golub, L. M.; Zhang, Y.; Ojima, I.; Shroyer, K. R., Prostate cancer stem cell-targeted efficacy of a new-generation taxoid, SBT-1214 and novel polyenolic zinc-binding curcuminoid, CMC2.24. *PloS one,* **2013,** *8* (9), e69884.
21. Shimizu, M.; Deguchi, A.; Lim, J. T.; Moriwaki, H.; Kopelovich, L.; Weinstein, I. B., (-)-Epigallocatechin gallate and polyphenon E inhibit growth and activation of the epidermal growth factor receptor and human epidermal growth factor receptor-2 signaling pathways in human colon cancer cells. *Clinical cancer research : an official journal of the American Association for Cancer Research,* **2005,** *11* (7), 2735-2746.
22. American Cancer Society, Find Support & Treatment. *http://www.cancer.org*, **2012**.
23. Egeblad, M.; Werb, Z., New functions for the matrix metalloproteinases in cancer progression. *Nature reviews. Cancer,* **2002,** *2* (3), 161-174.

24. Hojilla, C. V.; Mohammed, F. F.; Khokha, R., Matrix metalloproteinases and their tissue inhibitors direct cell fate during cancer development. *British journal of cancer,* **2003,** *89* (10), 1817-1821.

25. Whittaker, M.; Floyd, C. D.; Brown, P.; Gearing, A. J., Design and therapeutic application of matrix metalloproteinase inhibitors. *Chemical reviews,* **1999,** *99* (9), 2735-2776.

26. Dove, A., MMP inhibitors: glimmers of hope amidst clinical failures. *Nature medicine,* **2002,** *8* (2), 95.

27. Visse, R.; Nagase, H., Matrix metalloproteinases and tissue inhibitors of metalloproteinases: structure, function, and biochemistry. *Circulation research,* **2003,** *92* (8), 827-839.

28. Wojtowicz-Praga, S.; Torri, J.; Johnson, M.; Steen, V.; Marshall, J.; Ness, E.; Dickson, R.; Sale, M.; Rasmussen, H. S.; Chiodo, T. A.; Hawkins, M. J., Phase I trial of Marimastat, a novel matrix metalloproteinase inhibitor, administered orally to patients with advanced lung cancer. *Journal of clinical oncology : official journal of the American Society of Clinical Oncology,* **1998,** *16* (6), 2150-2156.

29. Coussens, L. M.; Fingleton, B.; Matrisian, L. M., Matrix metalloproteinase inhibitors and cancer: trials and tribulations. *Science,* **2002,** *295* (5564), 2387-2392.

30. Overall, C. M.; Lopez-Otin, C., Strategies for MMP inhibition in cancer: innovations for the post-trial era. *Nature reviews. Cancer,* **2002,** *2* (9), 657-672.

31. Dufour, A.; Sampson, N. S.; Li, J.; Kuscu, C.; Rizzo, R. C.; Deleon, J. L.; Zhi, J.; Jaber, N.; Liu, E.; Zucker, S.; Cao, J., Small-molecule anticancer compounds selectively target the hemopexin domain of matrix metalloproteinase-9. *Cancer research,* **2011,** *71* (14), 4977-4988.

32. Hua, Z.; Bregman, H.; Buchanan, J. L.; Chakka, N.; Guzman-Perez, A.; Gunaydin, H.; Huang, X.; Gu, Y.; Berry, V.; Liu, J.; Teffera, Y.; Huang, L.; Egge, B.; Emkey, R.; Mullady, E. L.; Schneider, S.; Andrews, P. S.; Acquaviva, L.; Dovey, J.; Mishra, A.; Newcomb, J.; Saffran, D.; Serafino, R.; Strathdee, C. A.; Turci, S. M.; Stanton, M.; Wilson, C.; Dimauro, E. F., Development of novel dual binders as potent, selective, and orally bioavailable tankyrase inhibitors. *Journal of medicinal chemistry,* **2013,** *56* (24), 10003-10015.

33. Hu, M.; Li, L.; Wu, H.; Su, Y.; Yang, P. Y.; Uttamchandani, M.; Xu, Q. H.; Yao, S. Q., Multicolor, one- and two-photon imaging of enzymatic activities in live cells with fluorescently Quenched Activity-Based Probes (qABPs). *Journal of the American Chemical Society*, **2011,** *133* (31), 12009-12020.

References

References for Chapter 1:

1. Global tuberculosis report 2013, World Health Organization. *http://apps.who.int/iris/bitstream/10665/75938/10661/9789241564502_eng.pdf*, **2013**.
2. Pasqualoto, K. F.; Ferreira, E. I., An approach for the rational design of new antituberculosis agents. *Current drug targets,* **2001,** *2* (4), 427-437.
3. Gill, W. P.; Harik, N. S.; Whiddon, M. R.; Liao, R. P.; Mittler, J. E.; Sherman, D. R., A replication clock for Mycobacterium tuberculosis. *Nature medicine,* **2009,** *15* (2), 211-214.
4. Schluger, N. W.; Rom, W. N., The host immune response to tuberculosis. *American journal of respiratory and critical care medicine,* **1998,** *157* (3 Pt 1), 679-691.
5. Bishai, W., Lipid lunch for persistent pathogen. *Nature,* **2000,** *406* (6797), 683-685.
6. Huang, Q.; Tonge, P. J.; Slayden, R. A.; Kirikae, T.; Ojima, I., FtsZ: a novel target for tuberculosis drug discovery. *Curr. Top. Med. Chem.,* **2007,** *7* (5), 527-543.
7. Gandhi, N. R.; Moll, A.; Sturm, A. W.; Pawinski, R.; Govender, T.; Lalloo, U.; Zeller, K.; Andrews, J.; Friedland, G., Extensively drug-resistant tuberculosis as a cause of death in patients co-infected with tuberculosis and HIV in a rural area of South Africa. *Lancet,* **2006,** *368* (9547), 1575-1580.
8. Raviglione, M. C., Issues facing TB control (7). Multiple drug-resistant tuberculosis. *Scott. Med. J.,* **2000,** *45*, 52-55.
9. Haile, M.; Kallenius, G., Recent developments in tuberculosis vaccines. *Current opinion in infectious diseases,* **2005,** *18* (3), 211-215.
10. Ducati, R. G.; Ruffino-Netto, A.; Basso, L. A.; Santos, D. S., The resumption of consumption -- a review on tuberculosis. *Memorias do Instituto Oswaldo Cruz,* **2006,** *101* (7), 697-714.
11. Ormerod, L. P., Multidrug-resistant tuberculosis (MDR-TB): epidemiology, prevention and treatment. *British medical bulletin,* **2005,** *73-74*, 17-24.

12. Almeida Da Silva, P. E.; Palomino, J. C., Molecular basis and mechanisms of drug resistance in Mycobacterium tuberculosis: classical and new drugs. *The Journal of antimicrobial chemotherapy,* **2011,** *66* (7), 1417-1430.
13. Ramaswamy, S.; Musser, J. M., Molecular genetic basis of antimicrobial agent resistance in Mycobacterium tuberculosis: 1998 update. *Tubercle and lung disease : the official journal of the International Union against Tuberculosis and Lung Disease,* **1998,** *79* (1), 3-29.
14. Jarlier, V.; Nikaido, H., Mycobacterial cell wall: structure and role in natural resistance to antibiotics. *FEMS microbiology letters,* **1994,** *123* (1-2), 11-18.
15. Kochi, A.; Vareldzis, B.; Styblo, K., Multidrug-resistant tuberculosis and its control. *Research in microbiology,* **1993,** *144* (2), 104-110.
16. Rawat, R.; Whitty, A.; Tonge, P. J., The isoniazid-NAD adduct is a slow, tight-binding inhibitor of InhA, the Mycobacterium tuberculosis enoyl reductase: adduct affinity and drug resistance. *Proceedings of the National Academy of Sciences of the United States of America,* **2003,** *100* (24), 13881-13886.
17. Zhang, Y.; Heym, B.; Allen, B.; Young, D.; Cole, S., The catalase-peroxidase gene and isoniazid resistance of Mycobacterium tuberculosis. *Nature,* **1992,** *358* (6387), 591-593.
18. Telenti, A.; Imboden, P.; Marchesi, F.; Schmidheini, T.; Bodmer, T., Direct, automated detection of rifampin-resistant Mycobacterium tuberculosis by polymerase chain reaction and single-strand conformation polymorphism analysis. *Antimicrobial agents and chemotherapy,* **1993,** *37* (10), 2054-2058.
19. Takiff, H. E.; Salazar, L.; Guerrero, C.; Philipp, W.; Huang, W. M.; Kreiswirth, B.; Cole, S. T.; Jacobs, W. R., Jr.; Telenti, A., Cloning and nucleotide sequence of Mycobacterium tuberculosis gyrA and gyrB genes and detection of quinolone resistance mutations. *Antimicrobial agents and chemotherapy,* **1994,** *38* (4), 773-780.
20. Johansen, S. K.; Maus, C. E.; Plikaytis, B. B.; Douthwaite, S., Capreomycin binds across the ribosomal subunit interface using tlyA-encoded 2'-O-methylations in 16S and 23S rRNAs. *Molecular cell,* **2006,** *23* (2), 173-182.
21. Kumar, K.; Awasthi, D.; Berger, W. T.; Tonge, P. J.; Slayden, R. A.; Ojima, I., Discovery of anti-TB agents that target the cell-division protein FtsZ. *Future medicinal chemistry,* **2010,** *2* (8), 1305-1323.

22. Bi, E. F.; Lutkenhaus, J., FtsZ ring structure associated with division in Escherichia coli. *Nature,* **1991,** *354* (6349), 161-164.
23. van den Ent, F.; Amos, L.; Lowe, J., Bacterial ancestry of actin and tubulin. *Current opinion in microbiology,* **2001,** *4* (6), 634-638.
24. Oliva, M. A.; Cordell, S. C.; Lowe, J., Structural insights into FtsZ protofilament formation. *Nature structural & molecular biology,* **2004,** *11* (12), 1243-1250.
25. Ben-Yehuda, S.; Losick, R., Asymmetric cell division in B. subtilis involves a spiral-like intermediate of the cytokinetic protein FtsZ. *Cell,* **2002,** *109* (2), 257-266.
26. Errington, J.; Daniel, R. A.; Scheffers, D. J., Cytokinesis in bacteria. *Microbiology and molecular biology reviews : MMBR,* **2003,** *67* (1), 52-65, table of contents.
27. Ojima, I.; Kumar, K.; Awasthi, D.; Vineberg, J. G., Drug discovery targeting cell division proteins, microtubules and FtsZ. *Bioorganic & medicinal chemistry,* **2014,** *22* (18), 5060-5077.
28. Slayden, R. A.; Knudson, D. L.; Belisle, J. T., Identification of cell cycle regulators in Mycobacterium tuberculosis by inhibition of septum formation and global transcriptional analysis. *Microbiology,* **2006,** *152* (Pt 6), 1789-1797.
29. Respicio, L.; Nair, P. A.; Huang, Q.; Anil, B.; Tracz, S.; Truglio, J. J.; Kisker, C.; Raleigh, D. P.; Ojima, I.; Knudson, D. L.; Tonge, P. J.; Slayden, R. A., Characterizing septum inhibition in Mycobacterium tuberculosis for novel drug discovery. *Tuberculosis,* **2008,** *88* (5), 420-429.
30. Romberg, L.; Levin, P. A., Assembly dynamics of the bacterial cell division protein FTSZ: poised at the edge of stability. *Annual review of microbiology,* **2003,** *57,* 125-154.
31. de Pereda, J. M.; Leynadier, D.; Evangelio, J. A.; Chacon, P.; Andreu, J. M., Tubulin secondary structure analysis, limited proteolysis sites, and homology to FtsZ. *Biochemistry,* **1996,** *35* (45), 14203-14215.
32. Reynolds, R. C.; Srivastava, S.; Ross, L. J.; Suling, W. J.; White, E. L., A new 2-carbamoyl pteridine that inhibits mycobacterial FtsZ. *Bioorganic & medicinal chemistry letters,* **2004,** *14* (12), 3161-3164.
33. White, E. L.; Suling, W. J.; Ross, L. J.; Seitz, L. E.; Reynolds, R. C., 2-Alkoxycarbonylaminopyridines: inhibitors of Mycobacterium tuberculosis FtsZ. *The Journal of antimicrobial chemotherapy,* **2002,** *50* (1), 111-114.

34. Sarcina, M.; Mullineaux, C. W., Effects of tubulin assembly inhibitors on cell division in prokaryotes in vivo. *FEMS microbiology letters,* **2000,** *191* (1), 25-29.
35. Awasthi, D.; Kumar, K.; Ojima, I., Therapeutic potential of FtsZ inhibition: a patent perspective. *Expert opinion on therapeutic patents,* **2011,** *21* (5), 657-679.
36. Kumar, K.; Awasthi, D.; Lee, S. Y.; Zanardi, I.; Ruzsicska, B.; Knudson, S.; Tonge, P. J.; Slayden, R. A.; Ojima, I., Novel trisubstituted benzimidazoles, targeting Mtb FtsZ, as a new class of antitubercular agents. *Journal of medicinal chemistry,* **2011,** *54* (1), 374-381.
37. Awasthi, D.; Kumar, K.; Knudson, S. E.; Slayden, R. A.; Ojima, I., SAR studies on trisubstituted benzimidazoles as inhibitors of Mtb FtsZ for the development of novel antitubercular agents. *Journal of medicinal chemistry,* **2013,** *56* (23), 9756-9770.
38. Mukherjee, A.; Lutkenhaus, J., Analysis of FtsZ assembly by light scattering and determination of the role of divalent metal cations. *Journal of bacteriology,* **1999,** *181* (3), 823-832.
39. Collins, L.; Franzblau, S. G., Microplate alamar blue assay versus BACTEC 460 system for high-throughput screening of compounds against Mycobacterium tuberculosis and Mycobacterium avium. *Antimicrobial agents and chemotherapy,* **1997,** *41* (5), 1004-1009.
40. Park, B.; Awasthi, D.; Chowdhury, S. R.; Melief, E. H.; Kumar, K.; Knudson, S. E.; Slayden, R. A.; Ojima, I., Design, synthesis and evaluation of novel 2,5,6-trisubstituted benzimidazoles targeting FtsZ as antitubercular agents. *Bioorganic & medicinal chemistry,* **2014,** *22* (9), 2602-2612.

References for Chapter 2:

1. Bi, E. F.; Lutkenhaus, J., FtsZ ring structure associated with division in Escherichia coli. *Nature* **1991,** *354* (6349), 161-164.
2. Schaffner-Barbero, C.; Martin-Fontecha, M.; Chacon, P.; Andreu, J. M., Targeting the assembly of bacterial cell division protein FtsZ with small molecules. *ACS chemical biology* **2012,** *7* (2), 269-277.
3. Adams, D. W.; Wu, L. J.; Czaplewski, L. G.; Errington, J., Multiple effects of benzamide antibiotics on FtsZ function. *Molecular microbiology* **2011,** *80* (1), 68-84.

4. Kumar, K.; Awasthi, D.; Berger, W. T.; Tonge, P. J.; Slayden, R. A.; Ojima, I., Discovery of anti-TB agents that target the cell-division protein FtsZ. *Future medicinal chemistry* **2010,** *2* (8), 1305-1323.
5. Kaur, S.; Modi, N. H.; Panda, D.; Roy, N., Probing the binding site of curcumin in Escherichia coli and Bacillus subtilis FtsZ--a structural insight to unveil antibacterial activity of curcumin. *European journal of medicinal chemistry* **2010,** *45* (9), 4209-4214.
6. Li, Z.; Trimble, M. J.; Brun, Y. V.; Jensen, G. J., The structure of FtsZ filaments in vivo suggests a force-generating role in cell division. *The EMBO journal* **2007,** *26* (22), 4694-4708.
7. Kumar, K.; Awasthi, D.; Lee, S. Y.; Zanardi, I.; Ruzsicska, B.; Knudson, S.; Tonge, P. J.; Slayden, R. A.; Ojima, I., Novel trisubstituted benzimidazoles, targeting Mtb FtsZ, as a new class of antitubercular agents. *Journal of medicinal chemistry* **2011,** *54* (1), 374-381.
8. Kelley, C.; Zhang, Y.; Parhi, A.; Kaul, M.; Pilch, D. S.; LaVoie, E. J., 3-Phenyl substituted 6,7-dimethoxyisoquinoline derivatives as FtsZ-targeting antibacterial agents. *Bioorganic & medicinal chemistry* **2012,** *20* (24), 7012-7029.
9. Chen, S.; Zhao, X.; Chen, J.; Chen, J.; Kuznetsova, L.; Wong, S. S.; Ojima, I., Mechanism-based tumor-targeting drug delivery system. Validation of efficient vitamin receptor-mediated endocytosis and drug release. *Bioconjugate chemistry* **2010,** *21* (5), 979-987.
10. Mosmann, T., Rapid colorimetric assay for cellular growth and survival: application to proliferation and cytotoxicity assays. *Journal of immunological methods* **1983,** *65* (1-2), 55-63.

References for Chapter 3:

1. Awasthi, D.; Kumar, K.; Knudson, S. E.; Slayden, R. A.; Ojima, I., SAR studies on trisubstituted benzimidazoles as inhibitors of Mtb FtsZ for the development of novel antitubercular agents. *Journal of medicinal chemistry* **2013,** *56* (23), 9756-9770.
2. Kumar, K.; Awasthi, D.; Lee, S. Y.; Zanardi, I.; Ruzsicska, B.; Knudson, S.; Tonge, P. J.; Slayden, R. A.; Ojima, I., Novel trisubstituted benzimidazoles, targeting Mtb FtsZ, as

a new class of antitubercular agents. *Journal of medicinal chemistry* **2011,** *54* (1), 374-381.

3. Park, B.; Awasthi, D.; Chowdhury, S. R.; Melief, E. H.; Kumar, K.; Knudson, S. E.; Slayden, R. A.; Ojima, I., Design, synthesis and evaluation of novel 2,5,6-trisubstituted benzimidazoles targeting FtsZ as antitubercular agents. *Bioorganic & medicinal chemistry* **2014,** *22* (9), 2602-2612.
4. Collins, L.; Franzblau, S. G., Microplate alamar blue assay versus BACTEC 460 system for high-throughput screening of compounds against Mycobacterium tuberculosis and Mycobacterium avium. *Antimicrobial agents and chemotherapy* **1997,** *41* (5), 1004-1009.

References for Chapter 4:

1. Gill, W. P.; Harik, N. S.; Whiddon, M. R.; Liao, R. P.; Mittler, J. E.; Sherman, D. R., A replication clock for Mycobacterium tuberculosis. *Nature medicine,* **2009,** *15* (2), 211-214.
2. Klevens, R. M.; Morrison, M. A.; Nadle, J.; Petit, S.; Gershman, K.; Ray, S.; Harrison, L. H.; Lynfield, R.; Dumyati, G.; Townes, J. M.; Craig, A. S.; Zell, E. R.; Fosheim, G. E.; McDougal, L. K.; Carey, R. B.; Fridkin, S. K.; Active Bacterial Core surveillance, M. I., Invasive methicillin-resistant Staphylococcus aureus infections in the United States. *Jama,* **2007,** *298* (15), 1763-1771.
3. Raviglione, M. C., Issues facing TB control (7). Multiple drug-resistant tuberculosis. *Scottish medical journal,* **2000,** *45* (5 Suppl), 52-55; discussion 56.
4. Branda, J. A.; Ruoff, K., Bioterrorism. Clinical recognition and primary management. *American journal of clinical pathology,* **2002,** *117 Suppl,* S116-123.
5. Chaturvedi, V.; Dwivedi, N.; Tripathi, R. P.; Sinha, S., Evaluation of Mycobacterium smegmatis as a possible surrogate screen for selecting molecules active against multi-drug resistant Mycobacterium tuberculosis. *The Journal of general and applied microbiology,* **2007,** *53* (6), 333-337.
6. Meyer, C. G.; May, J., [Germs employed as biological weapons]. *Anasthesiologie, Intensivmedizin, Notfallmedizin, Schmerztherapie : AINS,* **2002,** *37* (9), 538-546.

7. Pohanka, M.; Skladal, P., Bacillus anthracis, Francisella tularensis and Yersinia pestis. The most important bacterial warfare agents - review. *Folia microbiologica,* **2009,** *54* (4), 263-272.
8. Warren, D. K.; Nitin, A.; Hill, C.; Fraser, V. J.; Kollef, M. H., Occurrence of co-colonization or co-infection with vancomycin-resistant enterococci and methicillin-resistant Staphylococcus aureus in a medical intensive care unit. *Infection control and hospital epidemiology : the official journal of the Society of Hospital Epidemiologists of America,* **2004,** *25* (2), 99-104.
9. Konno, K.; Oizumi, K.; Oka, S., Mode of action of rifampin on mycobacteria. II. Biosynthetic studies on the inhibition of ribonucleic acid polymerase of Mycobacterium bovis BCG by rifampin and uptake of rifampin- 14 C by Mycobacterium phlei. *The American review of respiratory disease,* **1973,** *107* (6), 1006-1012.
10. Zhang, Y.; Dhandayuthapani, S.; Deretic, V., Molecular basis for the exquisite sensitivity of Mycobacterium tuberculosis to isoniazid. *Proceedings of the National Academy of Sciences of the United States of America,* **1996,** *93* (23), 13212-13216.
11. Birosova, L.; Mikulasova, M., The mechanism of ciprofloxacin resistance in dihydrogen peroxide-induced mutants of Salmonella enterica subsp. enterica serovar typhimurium consists mainly in mutations in gyrA gene and less in mutations affecting ciprofloxacin uptake. *Folia microbiologica,* **2008,** *53* (4), 368-372.
12. Huang, Q.; Kirikae, F.; Kirikae, T.; Pepe, A.; Amin, A.; Respicio, L.; Slayden, R. A.; Tonge, P. J.; Ojima, I., Targeting FtsZ for antituberculosis drug discovery: noncytotoxic taxanes as novel antituberculosis agents. *Journal of medicinal chemistry,* **2006,** *49* (2), 463-466.
13. Huang, Q.; Tonge, P. J.; Slayden, R. A.; Kirikae, T.; Ojima, I., FtsZ: a novel target for tuberculosis drug discovery. *Current topics in medicinal chemistry,* **2007,** *7* (5), 527-543.
14. Kumar, K.; Awasthi, D.; Berger, W. T.; Tonge, P. J.; Slayden, R. A.; Ojima, I., Discovery of anti-TB agents that target the cell-division protein FtsZ. *Future medicinal chemistry,* **2010,** *2* (8), 1305-1323.
15. Awasthi, D.; Kumar, K.; Ojima, I., Therapeutic potential of FtsZ inhibition: a patent perspective. *Expert opinion on therapeutic patents,* **2011,** *21* (5), 657-679.

16. Kumar, K.; Awasthi, D.; Lee, S. Y.; Zanardi, I.; Ruzsicska, B.; Knudson, S.; Tonge, P. J.; Slayden, R. A.; Ojima, I., Novel trisubstituted benzimidazoles, targeting Mtb FtsZ, as a new class of antitubercular agents. *Journal of medicinal chemistry*, **2011,** *54* (1), 374-381.
17. Awasthi, D.; Kumar, K.; Knudson, S. E.; Slayden, R. A.; Ojima, I., SAR studies on trisubstituted benzimidazoles as inhibitors of Mtb FtsZ for the development of novel antitubercular agents. *Journal of medicinal chemistry*, **2013,** *56* (23), 9756-9770.
18. Ojima, I.; Kumar, K.; Awasthi, D.; Vineberg, J. G., Drug discovery targeting cell division proteins, microtubules and FtsZ. *Bioorganic & medicinal chemistry*, **2014,** *22* (18), 5060-5077.
19. Park, B.; Awasthi, D.; Chowdhury, S. R.; Melief, E. H.; Kumar, K.; Knudson, S. E.; Slayden, R. A.; Ojima, I., Design, synthesis and evaluation of novel 2,5,6-trisubstituted benzimidazoles targeting FtsZ as antitubercular agents. *Bioorganic & medicinal chemistry*, **2014,** *22* (9), 2602-2612.
20. Romberg, L.; Levin, P. A., Assembly dynamics of the bacterial cell division protein FTSZ: poised at the edge of stability. *Annual review of microbiology*, **2003,** *57*, 125-154.
21. Tyagi, J. S.; Sharma, D., Mycobacterium smegmatis and tuberculosis. *Trends in microbiology*, **2002,** *10* (2), 68-69.
22. Bercovier, H.; Vincent, V., Mycobacterial infections in domestic and wild animals due to Mycobacterium marinum, M. fortuitum, M. chelonae, M. porcinum, M. farcinogenes, M. smegmatis, M. scrofulaceum, M. xenopi, M. kansasii, M. simiae and M. genavense. *Revue scientifique et technique*, **2001,** *20* (1), 265-290.
23. Cole, S. T.; Brosch, R.; Parkhill, J.; Garnier, T.; Churcher, C.; Harris, D.; Gordon, S. V.; Eiglmeier, K.; Gas, S.; Barry, C. E., 3rd; Tekaia, F.; Badcock, K.; Basham, D.; Brown, D.; Chillingworth, T.; Connor, R.; Davies, R.; Devlin, K.; Feltwell, T.; Gentles, S.; Hamlin, N.; Holroyd, S.; Hornsby, T.; Jagels, K.; Krogh, A.; McLean, J.; Moule, S.; Murphy, L.; Oliver, K.; Osborne, J.; Quail, M. A.; Rajandream, M. A.; Rogers, J.; Rutter, S.; Seeger, K.; Skelton, J.; Squares, R.; Squares, S.; Sulston, J. E.; Taylor, K.; Whitehead, S.; Barrell, B. G., Deciphering the biology of Mycobacterium tuberculosis from the complete genome sequence. *Nature*, **1998,** *393* (6685), 537-544.

24. Zahrt, T. C.; Deretic, V., Mycobacterium tuberculosis signal transduction system required for persistent infections. *Proceedings of the National Academy of Sciences of the United States of America*, **2001,** *98* (22), 12706-12711.
25. Collins, L.; Franzblau, S. G., Microplate alamar blue assay versus BACTEC 460 system for high-throughput screening of compounds against Mycobacterium tuberculosis and Mycobacterium avium. *Antimicrobial agents and chemotherapy*, **1997,** *41* (5), 1004-1009.
26. Pasca, M. R.; Guglierame, P.; De Rossi, E.; Zara, F.; Riccardi, G., mmpL7 gene of Mycobacterium tuberculosis is responsible for isoniazid efflux in Mycobacterium smegmatis. *Antimicrobial agents and chemotherapy,* **2005,** *49* (11), 4775-4777.
27. Stephan, J.; Mailaender, C.; Etienne, G.; Daffe, M.; Niederweis, M., Multidrug resistance of a porin deletion mutant of Mycobacterium smegmatis. *Antimicrobial agents and chemotherapy,* **2004,** *48* (11), 4163-4170.
28. Alexander, D. C.; Jones, J. R.; Liu, J., A rifampin-hypersensitive mutant reveals differences between strains of Mycobacterium smegmatis and presence of a novel transposon, IS1623. *Antimicrobial agents and chemotherapy,* **2003,** *47* (10), 3208-3213.
29. Piddock, L. J.; Williams, K. J.; Ricci, V., Accumulation of rifampicin by Mycobacterium aurum, Mycobacterium smegmatis and Mycobacterium tuberculosis. *The Journal of antimicrobial chemotherapy,* **2000,** *45* (2), 159-165.

References for Chapter 5:

1. Cancer Facts & Figures 2014. *American Cancer Society* **2014**.
2. Worldwide cancer Key Facts. *Cancer Research UK*, **2012**.
3. Goodman, L. S.; Wintrobe, M. M.; et al., Nitrogen mustard therapy; use of methyl-bis (beta-chloroethyl) amine hydrochloride and tris (beta-chloroethyl) amine hydrochloride for Hodgkin's disease, lymphosarcoma, leukemia and certain allied and miscellaneous disorders. *Journal of the American Medical Association,* **1946,** *132*, 126-132.
4. Farber, S.; Diamond, L. K., Temporary remissions in acute leukemia in children produced by folic acid antagonist, 4-aminopteroyl-glutamic acid. *The New England journal of medicine,* **1948,** *238* (23), 787-793.

5. DeVita, V. T., Jr.; Chu, E., A history of cancer chemotherapy. *Cancer research,* **2008,** *68* (21), 8643-8653.
6. Park, S. J.; Wu, C. H.; Gordon, J. D.; Zhong, X.; Emami, A.; Safa, A. R., Taxol induces caspase-10-dependent apoptosis. *The Journal of biological chemistry,* **2004,** *279* (49), 51057-51067.
7. Wall, M. E.; Wani, M. C., Camptothecin and taxol: discovery to clinic--thirteenth Bruce F. Cain Memorial Award Lecture. *Cancer research,* **1995,** *55* (4), 753-760.
8. Fu, Y.; Li, S.; Zu, Y.; Yang, G.; Yang, Z.; Luo, M.; Jiang, S.; Wink, M.; Efferth, T., Medicinal chemistry of paclitaxel and its analogues. *Current medicinal chemistry,* **2009,** *16* (30), 3966-3985.
9. Ojima, I.; Duclos, O.; Zucco, M.; Bissery, M. C.; Combeau, C.; Vrignaud, P.; Riou, J. F.; Lavelle, F., Synthesis and structure-activity relationships of new antitumor taxoids. Effects of cyclohexyl substitution at the C-3' and/or C-2 of taxotere (docetaxel). *Journal of medicinal chemistry,* **1994,** *37* (16), 2602-2608.
10. Ojima, I.; Slater, J. C.; Kuduk, S. D.; Takeuchi, C. S.; Gimi, R. H.; Sun, C. M.; Park, Y. H.; Pera, P.; Veith, J. M.; Bernacki, R. J., Syntheses and structure-activity relationships of taxoids derived from 14 beta-hydroxy-10-deacetylbaccatin III. *Journal of medicinal chemistry,* **1997,** *40* (3), 267-278.
11. Ojima, I.; Geng, X.; Lin, S.; Pera, P.; Bernacki, R. J., Design, synthesis and biological activity of novel C2-C3' N-Linked macrocyclic taxoids. *Bioorganic & medicinal chemistry letters,* **2002,** *12* (3), 349-352.
12. Ojima, I.; Fumero-Oderda, C. L.; Kuduk, S. D.; Ma, Z.; Kirikae, F.; Kirikae, T., Structure-activity relationship study of taxoids for their ability to activate murine macrophages as well as inhibit the growth of macrophage-like cells. *Bioorganic & medicinal chemistry,* **2003,** *11* (13), 2867-2888.
13. Ojima, I.; Zuniga, E. S.; Berger, W. T.; Seitz, J. D., Tumor-targeting drug delivery of new-generation taxoids. *Future medicinal chemistry,* **2012,** *4* (1), 33-50.
14. Ojima, I., Guided molecular missiles for tumor-targeting chemotherapy--case studies using the second-generation taxoids as warheads. *Accounts of chemical research,* **2008,** *41* (1), 108-119.

15. Ojima, I.; Chen, J.; Sun, L.; Borella, C. P.; Wang, T.; Miller, M. L.; Lin, S.; Geng, X.; Kuznetsova, L.; Qu, C.; Gallager, D.; Zhao, X.; Zanardi, I.; Xia, S.; Horwitz, S. B.; Mallen-St Clair, J.; Guerriero, J. L.; Bar-Sagi, D.; Veith, J. M.; Pera, P.; Bernacki, R. J., Design, synthesis, and biological evaluation of new-generation taxoids. *Journal of medicinal chemistry,* **2008,** *51* (11), 3203-3221.

16. Chen, S.; Zhao, X.; Chen, J.; Chen, J.; Kuznetsova, L.; Wong, S. S.; Ojima, I., Mechanism-based tumor-targeting drug delivery system. Validation of efficient vitamin receptor-mediated endocytosis and drug release. *Bioconjugate chemistry,* **2010,** *21* (5), 979-987.

17. Wind, N. S.; Holen, I., Multidrug resistance in breast cancer: from in vitro models to clinical studies. *International journal of breast cancer,* **2011,** *2011,* 967419.

18. Gottesman, M. M.; Pastan, I., Biochemistry of multidrug resistance mediated by the multidrug transporter. *Annual review of biochemistry,* **1993,** *62,* 385-427.

19. Ferlini, C.; Distefano, M.; Pignatelli, F.; Lin, S.; Riva, A.; Bombardelli, E.; Mancuso, S.; Ojima, I.; Scambia, G., Antitumour activity of novel taxanes that act at the same time as cytotoxic agents and P-glycoprotein inhibitors. *British journal of cancer,* **2000,** *83* (12), 1762-1768.

20. Russell-Jones, G.; McTavish, K.; McEwan, J.; Rice, J.; Nowotnik, D., Vitamin-mediated targeting as a potential mechanism to increase drug uptake by tumours. *Journal of inorganic biochemistry,* **2004,** *98* (10), 1625-1633.

21. Weinstein, S. J.; Hartman, T. J.; Stolzenberg-Solomon, R.; Pietinen, P.; Barrett, M. J.; Taylor, P. R.; Virtamo, J.; Albanes, D., Null association between prostate cancer and serum folate, vitamin B(6), vitamin B(12), and homocysteine. *Cancer epidemiology, biomarkers & prevention : a publication of the American Association for Cancer Research, cosponsored by the American Society of Preventive Oncology,* **2003,** *12* (11 Pt 1), 1271-1272.

22. Vlahov, I. R.; Leamon, C. P., Engineering folate-drug conjugates to target cancer: from chemistry to clinic. *Bioconjugate chemistry,* **2012,** *23* (7), 1357-1369.

23. Lu, Y.; Sega, E.; Leamon, C. P.; Low, P. S., Folate receptor-targeted immunotherapy of cancer: mechanism and therapeutic potential. *Advanced drug delivery reviews,* **2004,** *56* (8), 1161-1176.

24. Xia, W.; Low, P. S., Folate-targeted therapies for cancer. *Journal of medicinal chemistry,* **2010,** *53* (19), 6811-6824.
25. Leamon, C. P.; Reddy, J. A., Folate-targeted chemotherapy. *Advanced drug delivery reviews,* **2004,** *56* (8), 1127-1141.
26. Kigawa, J.; Minagawa, Y.; Kanamori, Y.; Itamochi, H.; Cheng, X.; Okada, M.; Oishi, T.; Terakawa, N., Glutathione concentration may be a useful predictor of response to second-line chemotherapy in patients with ovarian cancer. *Cancer,* **1998,** *82* (4), 697-702.
27. Hussain, S. P.; Hofseth, L. J.; Harris, C. C., Radical causes of cancer. *Nature reviews. Cancer,* **2003,** *3* (4), 276-285.
28. Sies, H., Glutathione and its role in cellular functions. *Free radical biology & medicine,* **1999,** *27* (9-10), 916-921.
29. Meister, A., Glutathione metabolism. *Methods in enzymology,* **1995,** *251*, 3-7.
30. Estrela, J. M.; Ortega, A.; Obrador, E., Glutathione in cancer biology and therapy. *Critical reviews in clinical laboratory sciences,* **2006,** *43* (2), 143-181.
31. Calvert, P.; Yao, K. S.; Hamilton, T. C.; O'Dwyer, P. J., Clinical studies of reversal of drug resistance based on glutathione. *Chemico-biological interactions,* **1998,** *111-112*, 213-224.
32. Traverso, N.; Ricciarelli, R.; Nitti, M.; Marengo, B.; Furfaro, A. L.; Pronzato, M. A.; Marinari, U. M.; Domenicotti, C., Role of glutathione in cancer progression and chemoresistance. *Oxidative medicine and cellular longevity,* **2013,** *2013*, 972913.
33. Lu, S. C., Regulation of hepatic glutathione synthesis: current concepts and controversies. *FASEB journal : official publication of the Federation of American Societies for Experimental Biology,* **1999,** *13* (10), 1169-1183.
34. Zheng, Z. B.; Zhu, G.; Tak, H.; Joseph, E.; Eiseman, J. L.; Creighton, D. J., N-(2-hydroxypropyl)methacrylamide copolymers of a glutathione (GSH)-activated glyoxalase i inhibitor and DNA alkylating agent: synthesis, reaction kinetics with GSH, and in vitro antitumor activities. *Bioconjugate chemistry,* **2005,** *16* (3), 598-607.
35. O'Brien, M. L.; Tew, K. D., Glutathione and related enzymes in multidrug resistance. *European journal of cancer,* **1996,** *32A* (6), 967-978.
36. Wu, X.; Ojima, I., Tumor specific novel taxoid-monoclonal antibody conjugates. *Current medicinal chemistry,* **2004,** *11* (4), 429-438.

37. Seitz, J. D. The design, synthesis and biological evaluation of novel taxoid anticancer agents and their tumor-targeted drug conjugates. Dortoral Dissertation State University of New York at Stony Brook, **2013**.

References for Chapter 6:

1. Bergstrom, M.; Grahnen, A.; Langstrom, B., Positron emission tomography microdosing: a new concept with application in tracer and early clinical drug development. *European journal of clinical pharmacology,* **2003,** *59* (5-6), 357-366.
2. Gambhir, S. S., Molecular imaging of cancer with positron emission tomography. *Nature reviews. Cancer,* **2002,** *2* (9), 683-693.
3. Ma, X.; Wang, J.; Cheng, Z., Cerenkov Radiation: A Multi-functional Approach for Biological Sciences. *Frontiers in Physics,* **2014,** *2*.
4. Ravert, H. T.; Klecker, R. W.; Collins, J. M.; Mathews, W. B.; Pomper, M. G.; Wahl, R. L.; Dannals, R. F., Radiosynthesis of [C-11]paclitaxel. *J Labelled Compd Rad,* **2002,** *45* (6), 471-477.
5. Kiesewetter, D. O.; Jagoda, E. M.; Kao, C. H.; Ma, Y.; Ravasi, L.; Shimoji, K.; Szajek, L. P.; Eckelman, W. C., Fluoro-, bromo-, and iodopaclitaxel derivatives: synthesis and biological evaluation. *Nuclear medicine and biology,* **2003,** *30* (1), 11-24.
6. Roh, E. J.; Park, Y. H.; Song, C. E.; Oh, S. J.; Choe, Y. S.; Kim, B. T.; Chi, D. Y.; Kim, D., Radiolabeling of paclitaxel with electrophilic 123I. *Bioorganic & medicinal chemistry,* **2000,** *8* (1), 65-68.
7. E. W. van Tilburg, E. J. F. F., J. J. M. van der Hoeven, M. van der Meij, D. Elshove, A. A. Lammertsma and A. D. Windhorst, Radiosynthesis of [^{11}C]docetaxel. *J Label Compd Radiopharm,* **2004,** *47*, 736-777.
8. van der Veldt, A. A.; Hendrikse, N. H.; Smit, E. F.; Mooijer, M. P.; Rijnders, A. Y.; Gerritsen, W. R.; van der Hoeven, J. J.; Windhorst, A. D.; Lammertsma, A. A.; Lubberink, M., Biodistribution and radiation dosimetry of 11C-labelled docetaxel in cancer patients. *European journal of nuclear medicine and molecular imaging,* **2010,** *37* (10), 1950-1958.

9. Koehler, L.; Gagnon, K.; McQuarrie, S.; Wuest, F., Iodine-124: a promising positron emitter for organic PET chemistry. *Molecules,* **2010,** *15* (4), 2686-2718.
10. Belov, V. V.; Bonab, A. A.; Fischman, A. J.; Heartlein, M.; Calias, P.; Papisov, M. I., Iodine-124 as a label for pharmacological PET imaging. *Molecular pharmaceutics,* **2011,** *8* (3), 736-747.
11. Zempleni, J.; Wijeratne, S. S.; Hassan, Y. I., Biotin. *BioFactors,* **2009,** *35* (1), 36-46.
12. Ojima, I., Guided molecular missiles for tumor-targeting chemotherapy--case studies using the second-generation taxoids as warheads. *Accounts of chemical research,* **2008,** *41* (1), 108-119.
13. Russell-Jones, G.; McTavish, K.; McEwan, J.; Rice, J.; Nowotnik, D., Vitamin-mediated targeting as a potential mechanism to increase drug uptake by tumours. *Journal of inorganic biochemistry,* **2004,** *98* (10), 1625-1633.
14. Seitz, J. D. The design, synthesis and biological evaluation of novel taxoid anticancer agents and their tumor-targeted drug conjugates. Dortoral Dissertation State University of New York at Stony Brook, **2013**.
15. Pandey, S. K.; Sajjad, M.; Chen, Y.; Pandey, A.; Missert, J. R.; Batt, C.; Yao, R.; Nabi, H. A.; Oseroff, A. R.; Pandey, R. K., Compared to purpurinimides, the pyropheophorbide containing an iodobenzyl group showed enhanced PDT efficacy and tumor imaging (124I-PET) ability. *Bioconjugate chemistry,* **2009,** *20* (2), 274-282.
16. Akgun, E.; Portoghese, P. S.; Sajjad, M.; Nabi, H. A., Synthesis and I-124-labeling of m-iodophenylpyrrolomorphinan as a potential PET imaging agent for delta opioid (DOP) receptors. *J Labelled Compd Rad,* **2007**, *50* (3-4), 165-170.
17. Shaul, M.; Abourbeh, G.; Jacobson, O.; Rozen, Y.; Laky, D.; Levitzki, A.; Mishani, E., Novel iodine-124 labeled EGFR inhibitors as potential PET agents for molecular imaging in cancer. *Bioorganic & medicinal chemistry,* **2004**, *12* (13), 3421-3429.

References for Chapter 7:

1. Clevers, H., The cancer stem cell: premises, promises and challenges. *Nature medicine,* **2011,** *17* (3), 313-319.
2. Reya, T.; Morrison, S. J.; Clarke, M. F.; Weissman, I. L., Stem cells, cancer, and cancer stem cells. *Nature,* **2001,** *414* (6859), 105-111.

3. Siminovitch, L.; McCulloch, E. A.; Till, J. E., The Distribution of Colony-Forming Cells among Spleen Colonies. *Journal of cellular physiology,* **1963,** *62,* 327-336.
4. Becker, A. J.; Mc, C. E.; Till, J. E., Cytological demonstration of the clonal nature of spleen colonies derived from transplanted mouse marrow cells. *Nature,* **1963,** *197,* 452-454.
5. Al-Hajj, M.; Clarke, M. F., Self-renewal and solid tumor stem cells. *Oncogene,* **2004,** *23* (43), 7274-7282.
6. Al-Hajj, M.; Wicha, M. S.; Benito-Hernandez, A.; Morrison, S. J.; Clarke, M. F., Prospective identification of tumorigenic breast cancer cells. *Proceedings of the National Academy of Sciences of the United States of America,* **2003,** *100* (7), 3983-3988.
7. Das, S.; Srikanth, M.; Kessler, J. A., Cancer stem cells and glioma. *Nature clinical practice. Neurology,* **2008,** *4* (8), 427-435.
8. Botchkina, G. I.; Zuniga, E. S.; Das, M.; Wang, Y.; Wang, H.; Zhu, S.; Savitt, A. G.; Rowehl, R. A.; Leyfman, Y.; Ju, J.; Shroyer, K.; Ojima, I., New-generation taxoid SB-T-1214 inhibits stem cell-related gene expression in 3D cancer spheroids induced by purified colon tumor-initiating cells. *Molecular cancer,* **2010,** *9,* 192.
9. Li, F.; Tiede, B.; Massague, J.; Kang, Y., Beyond tumorigenesis: cancer stem cells in metastasis. *Cell research,* **2007,** *17* (1), 3-14.
10. Zuniga, E. S. Design, synthesis and biological evaluation of new-generation taxoid-based tumor-targeting drug conjugates. Stony Brook University **2012**.
11. Murren, J. R.; Peccerillo, K.; DiStasio, S. A.; Li, X.; Leffert, J. J.; Pizzorno, G.; Burtness, B. A.; McKeon, A.; Cheng, Y., Dose escalation and pharmacokinetic study of irinotecan in combination with paclitaxel in patients with advanced cancer. *Cancer chemotherapy and pharmacology,* **2000,** *46* (1), 43-50.
12. Ulukan, H.; Swaan, P. W., Camptothecins: a review of their chemotherapeutic potential. *Drugs,* **2002,** *62* (14), 2039-2057.
13. Lu, A. J.; Zhang, Z. S.; Zheng, M. Y.; Zou, H. J.; Luo, X. M.; Jiang, H. L., 3D-QSAR study of 20 (S)-camptothecin analogs. *Acta pharmacologica Sinica,* **2007,** *28* (2), 307-314.

14. Li, L. H.; Fraser, T. J.; Olin, E. J.; Bhuyan, B. K., Action of camptothecin on mammalian cells in culture. *Cancer research,* **1972,** *32* (12), 2643-2650.
15. Horwitz, S. B.; Horwitz, M. S., Effects of camptothecin on the breakage and repair of DNA during the cell cycle. *Cancer research,* **1973,** *33* (11), 2834-2836.
16. Bahadori, H. R.; Green, M. R.; Catapano, C. V., Synergistic interaction between topotecan and microtubule-interfering agents. *Cancer chemotherapy and pharmacology,* **2001,** *48* (3), 188-196.
17. Sharma, O. P., Antioxidant activity of curcumin and related compounds. *Biochemical pharmacology,* **1976,** *25* (15), 1811-1812.
18. Ruby, A. J.; Kuttan, G.; Babu, K. D.; Rajasekharan, K. N.; Kuttan, R., Anti-tumour and antioxidant activity of natural curcuminoids. *Cancer letters,* **1995,** *94* (1), 79-83.
19. Aggarwal, B. B.; Kumar, A.; Bharti, A. C., Anticancer potential of curcumin: preclinical and clinical studies. *Anticancer research,* **2003,** *23* (1A), 363-398.
20. Botchkina, G. I.; Zuniga, E. S.; Rowehl, R. H.; Park, R.; Bhalla, R.; Bialkowska, A. B.; Johnson, F.; Golub, L. M.; Zhang, Y.; Ojima, I.; Shroyer, K. R., Prostate cancer stem cell-targeted efficacy of a new-generation taxoid, SBT-1214 and novel polyenolic zinc-binding curcuminoid, CMC2.24. *PloS one,* **2013,** *8* (9), e69884.
21. Shimizu, M.; Deguchi, A.; Lim, J. T.; Moriwaki, H.; Kopelovich, L.; Weinstein, I. B., (-)-Epigallocatechin gallate and polyphenon E inhibit growth and activation of the epidermal growth factor receptor and human epidermal growth factor receptor-2 signaling pathways in human colon cancer cells. *Clinical cancer research : an official journal of the American Association for Cancer Research,* **2005,** *11* (7), 2735-2746.
22. American Cancer Society, Find Support & Treatment. *http://www.cancer.org*, **2012**.
23. Egeblad, M.; Werb, Z., New functions for the matrix metalloproteinases in cancer progression. *Nature reviews. Cancer,* **2002,** *2* (3), 161-174.
24. Hojilla, C. V.; Mohammed, F. F.; Khokha, R., Matrix metalloproteinases and their tissue inhibitors direct cell fate during cancer development. *British journal of cancer,* **2003,** *89* (10), 1817-1821.
25. Whittaker, M.; Floyd, C. D.; Brown, P.; Gearing, A. J., Design and therapeutic application of matrix metalloproteinase inhibitors. *Chemical reviews,* **1999,** *99* (9), 2735-2776.

26. Dove, A., MMP inhibitors: glimmers of hope amidst clinical failures. *Nature medicine,* **2002,** *8* (2), 95.

27. Visse, R.; Nagase, H., Matrix metalloproteinases and tissue inhibitors of metalloproteinases: structure, function, and biochemistry. *Circulation research,* **2003,** *92* (8), 827-839.

28. Wojtowicz-Praga, S.; Torri, J.; Johnson, M.; Steen, V.; Marshall, J.; Ness, E.; Dickson, R.; Sale, M.; Rasmussen, H. S.; Chiodo, T. A.; Hawkins, M. J., Phase I trial of Marimastat, a novel matrix metalloproteinase inhibitor, administered orally to patients with advanced lung cancer. *Journal of clinical oncology : official journal of the American Society of Clinical Oncology,* **1998,** *16* (6), 2150-2156.

29. Coussens, L. M.; Fingleton, B.; Matrisian, L. M., Matrix metalloproteinase inhibitors and cancer: trials and tribulations. *Science,* **2002,** *295* (5564), 2387-2392.

30. Overall, C. M.; Lopez-Otin, C., Strategies for MMP inhibition in cancer: innovations for the post-trial era. *Nature reviews. Cancer,* **2002,** *2* (9), 657-672.

31. Dufour, A.; Sampson, N. S.; Li, J.; Kuscu, C.; Rizzo, R. C.; Deleon, J. L.; Zhi, J.; Jaber, N.; Liu, E.; Zucker, S.; Cao, J., Small-molecule anticancer compounds selectively target the hemopexin domain of matrix metalloproteinase-9. *Cancer research,* **2011,** *71* (14), 4977-4988.

32. Hua, Z.; Bregman, H.; Buchanan, J. L.; Chakka, N.; Guzman-Perez, A.; Gunaydin, H.; Huang, X.; Gu, Y.; Berry, V.; Liu, J.; Teffera, Y.; Huang, L.; Egge, B.; Emkey, R.; Mullady, E. L.; Schneider, S.; Andrews, P. S.; Acquaviva, L.; Dovey, J.; Mishra, A.; Newcomb, J.; Saffran, D.; Serafino, R.; Strathdee, C. A.; Turci, S. M.; Stanton, M.; Wilson, C.; Dimauro, E. F., Development of novel dual binders as potent, selective, and orally bioavailable tankyrase inhibitors. *Journal of medicinal chemistry,* **2013,** *56* (24), 10003-10015.

33. Hu, M.; Li, L.; Wu, H.; Su, Y.; Yang, P. Y.; Uttamchandani, M.; Xu, Q. H.; Yao, S. Q., Multicolor, one- and two-photon imaging of enzymatic activities in live cells with fluorescently Quenched Activity-Based Probes (qABPs). *Journal of the American Chemical Society,* **2011,** *133* (31), 12009-12020.

Chapter 1

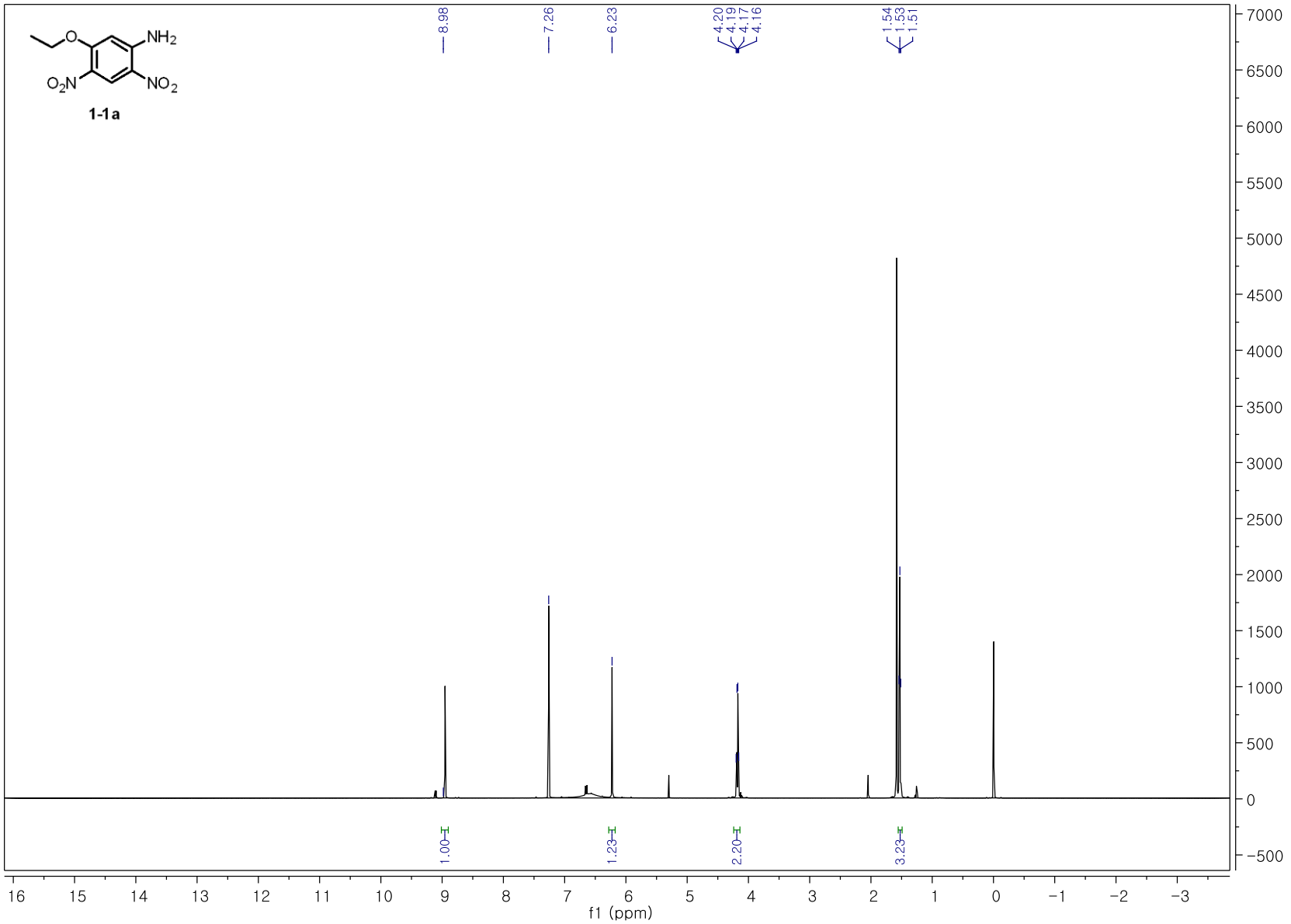
1-1a
8.98
7.26
6.23
4.20
4.19
4.17
4.16
1.54
1.53
1.51
1.00
1.23
2.20
3.23
f1 (ppm)

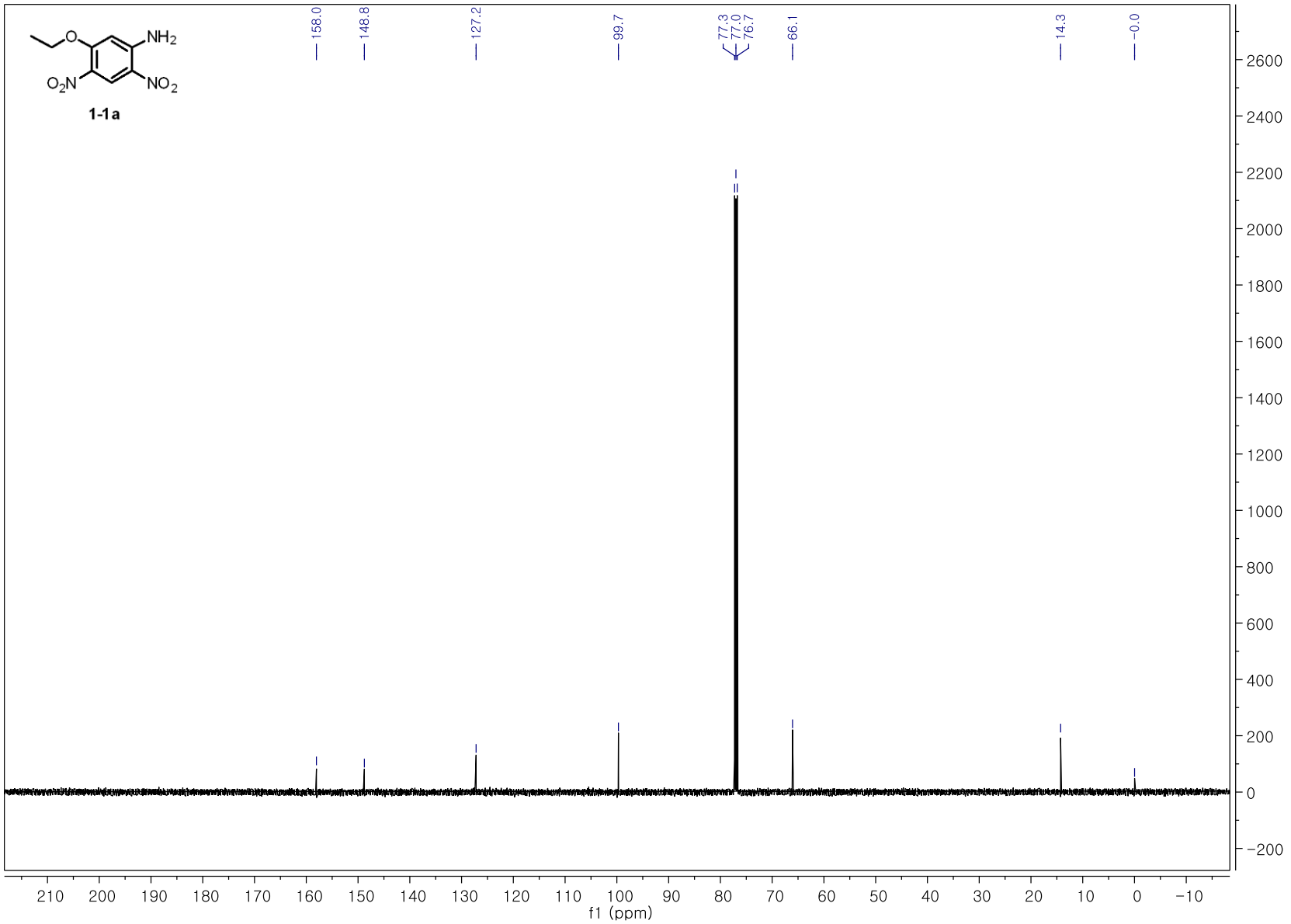
1-1a
158.0
148.8
127.2
99.7
77.3
77.0
76.7
66.1
14.3
0.0
f1 (ppm)

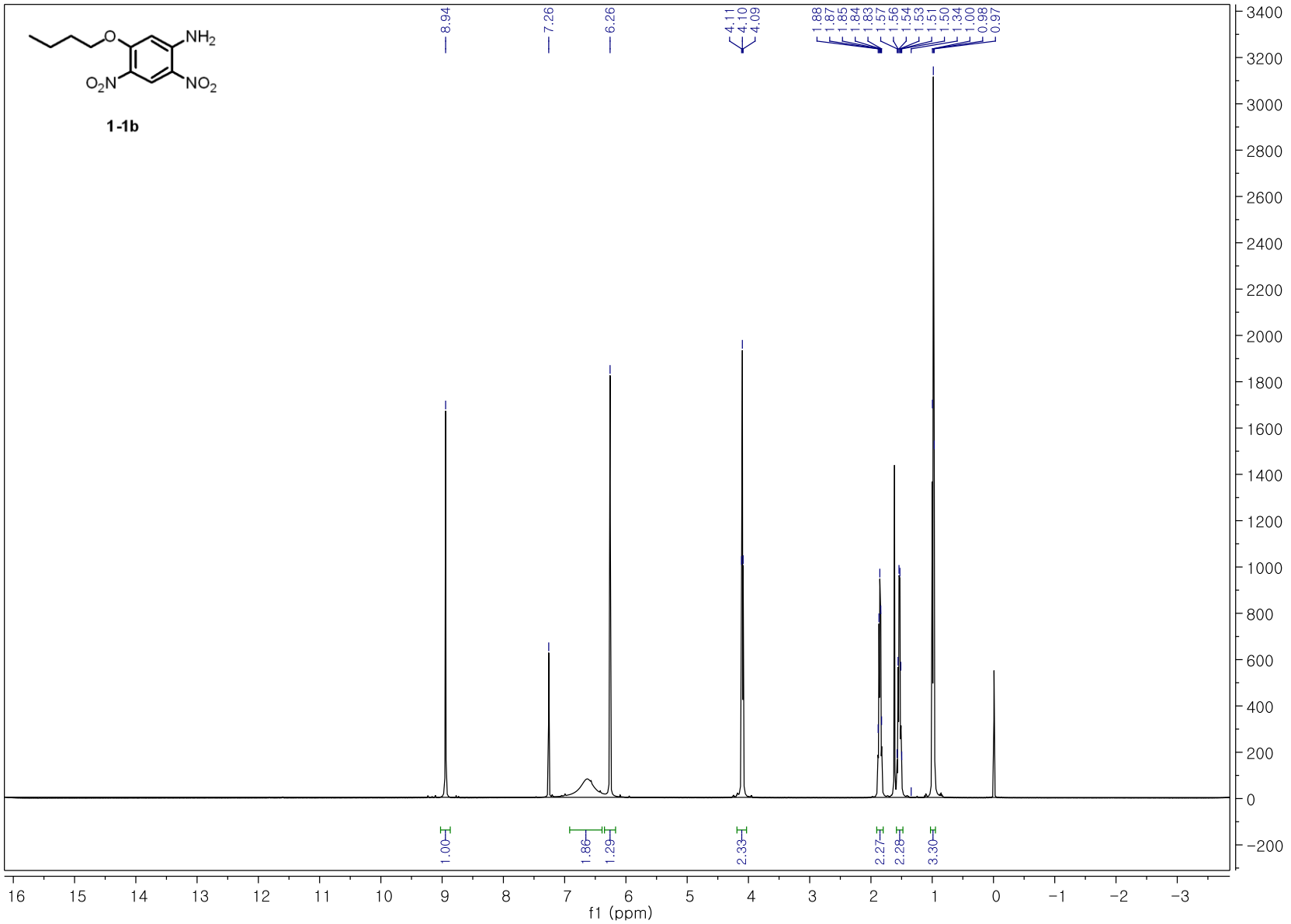
1-1b
8.94
7.26
6.26
4.11
4.10
4.09
1.88
1.87
1.85
1.84
1.83
1.57
1.56
1.54
1.53
1.51
1.50
1.34
1.00
0.98
0.97
1.00
1.86
1.29
2.33
2.27
2.28
3.30
f1 (ppm)

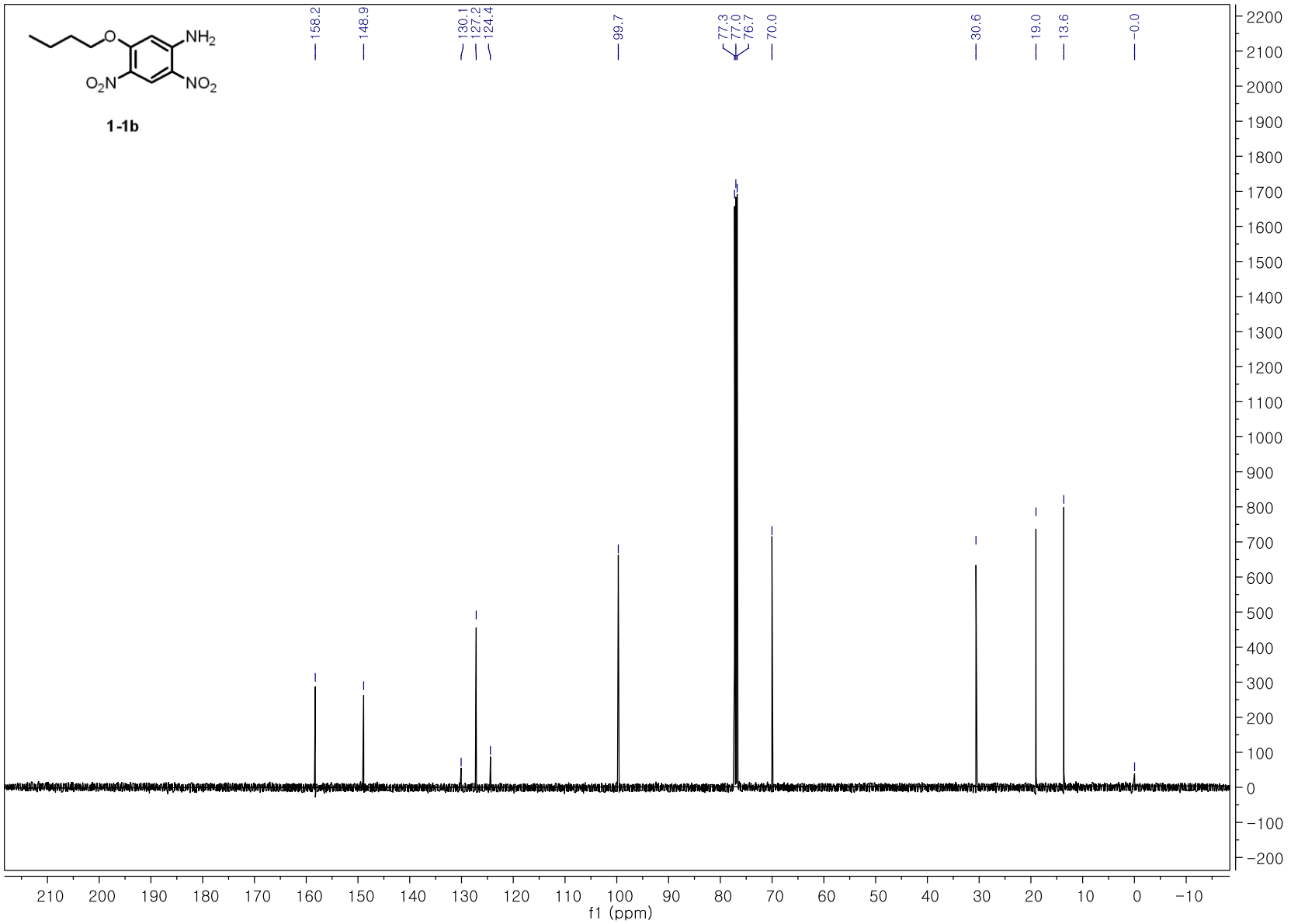
1-1b
158.2
148.9
130.1
127.2
124.4
99.7
77.3
77.0
76.7
70.0
30.6
19.0
13.6
-0.0
f1 (ppm)

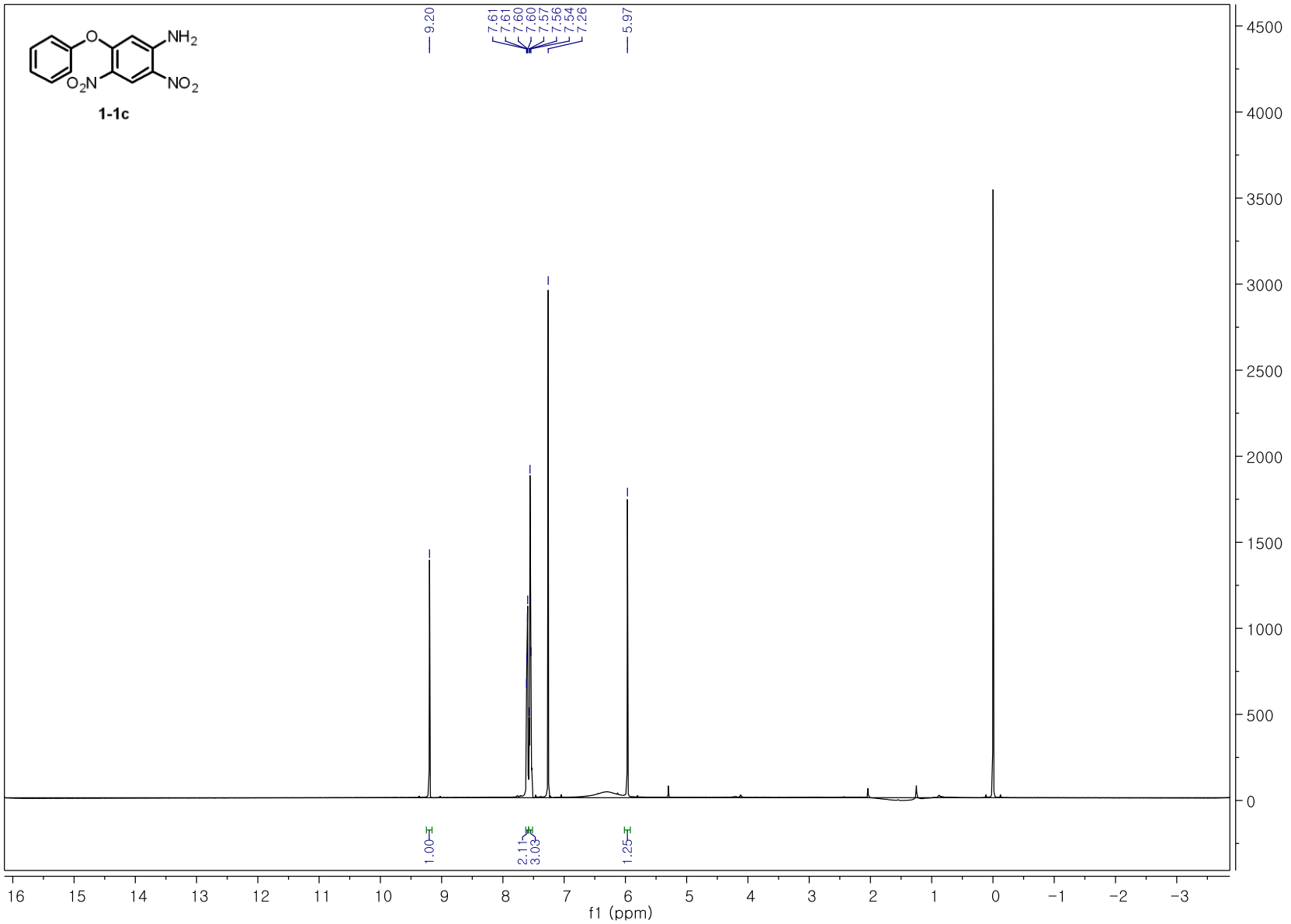
1-1c
9.20
7.61
7.61
7.60
7.60
7.57
7.56
7.54
7.26
5.97
1.00
2.11
3.03
1.25
f1 (ppm)

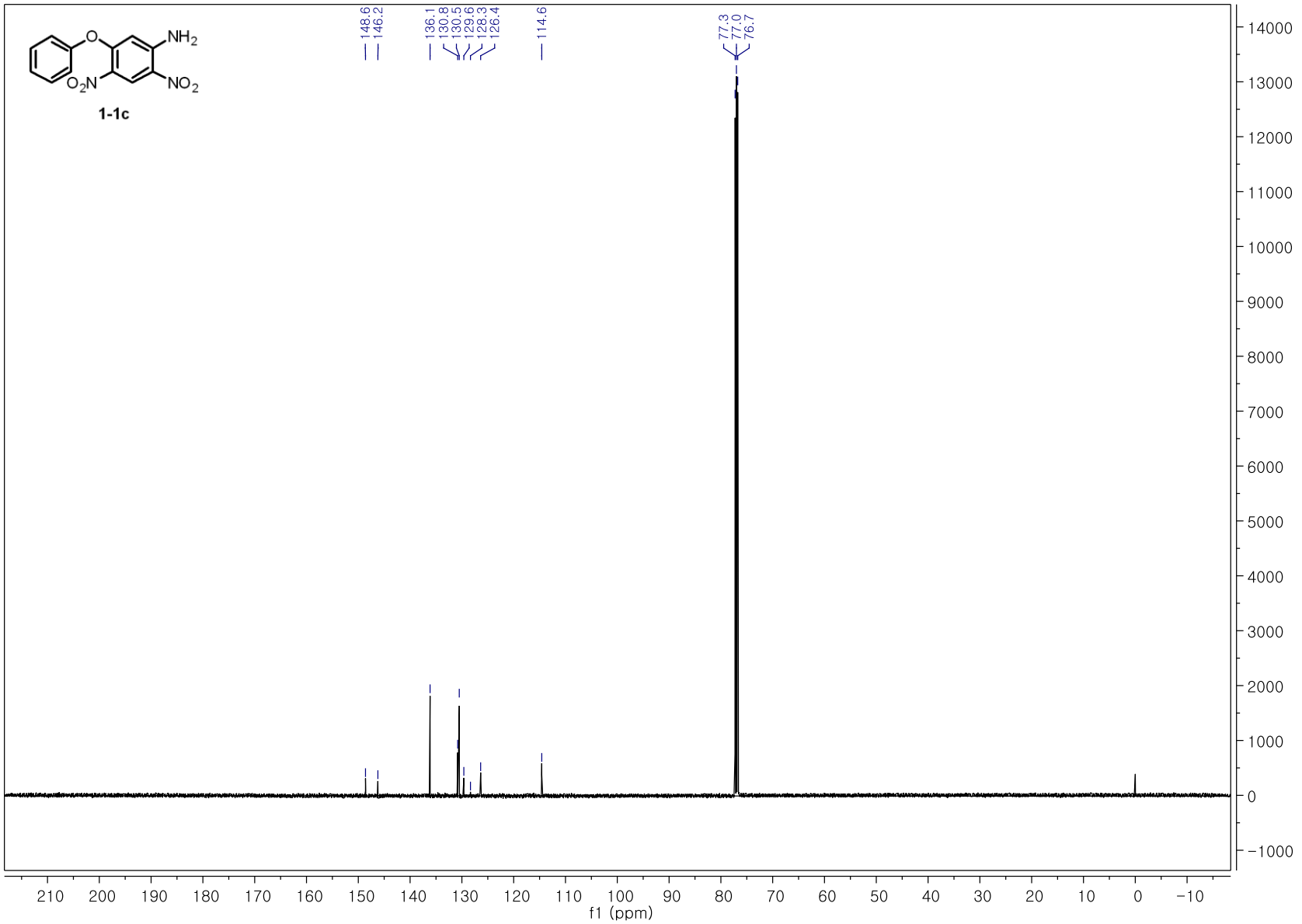
148.6
146.2
136.1
130.8
130.5
129.6
128.3
126.4
114.6
77.3
77.0
76.7
NH2
O
O2N
NO2
1-1c
14000
13000
12000
11000
10000
9000
8000
7000
6000
5000
4000
3000
2000
1000
0
-1000
210 200 190 180 170 160 150 140 130 120 110 100 90 80 70 60 50 40 30 20 10 0 -10
f1 (ppm)

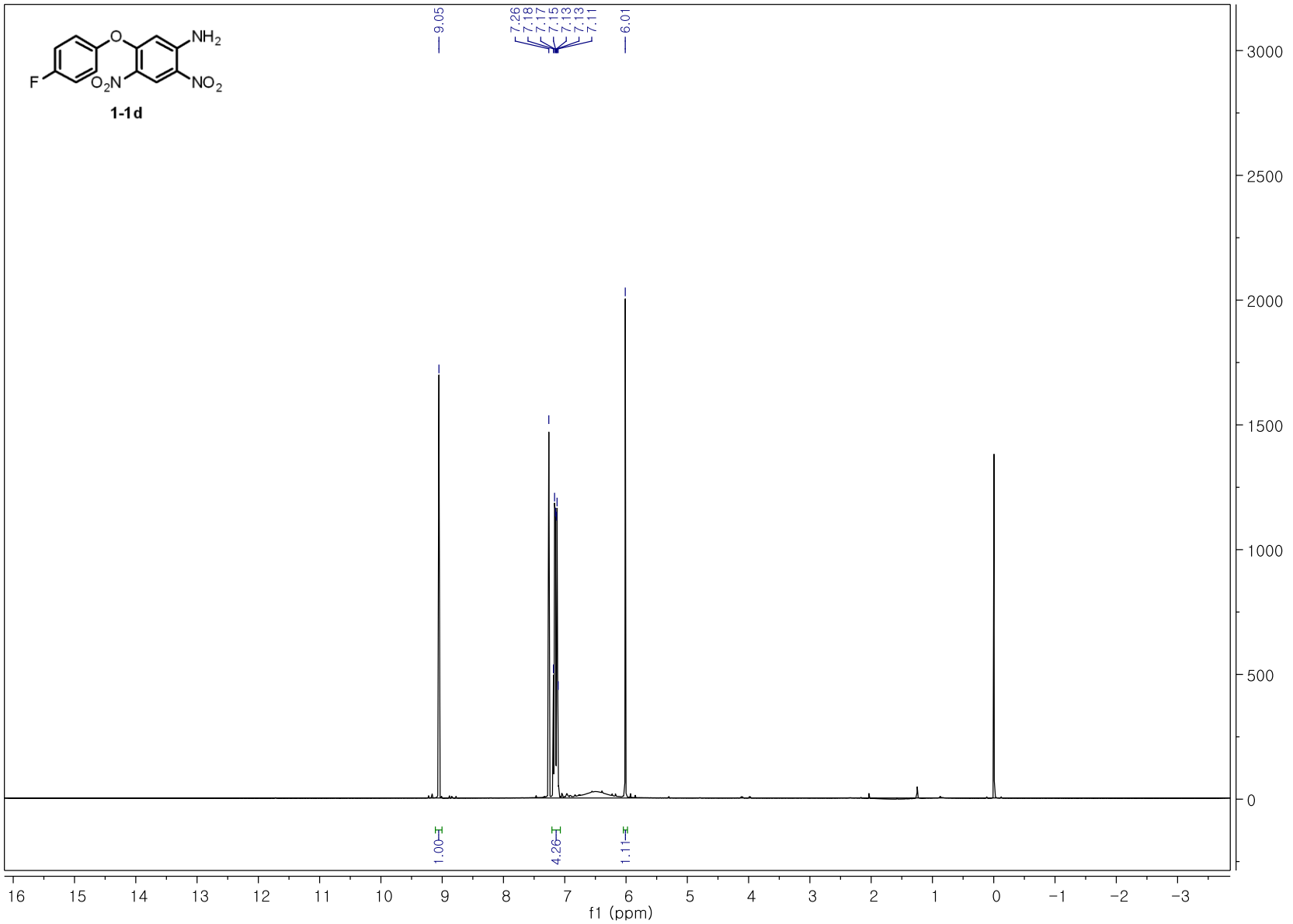
1-1d
9.05
7.26
7.18
7.17
7.15
7.13
7.11
6.01
1.00
4.26
1.11
f1 (ppm)

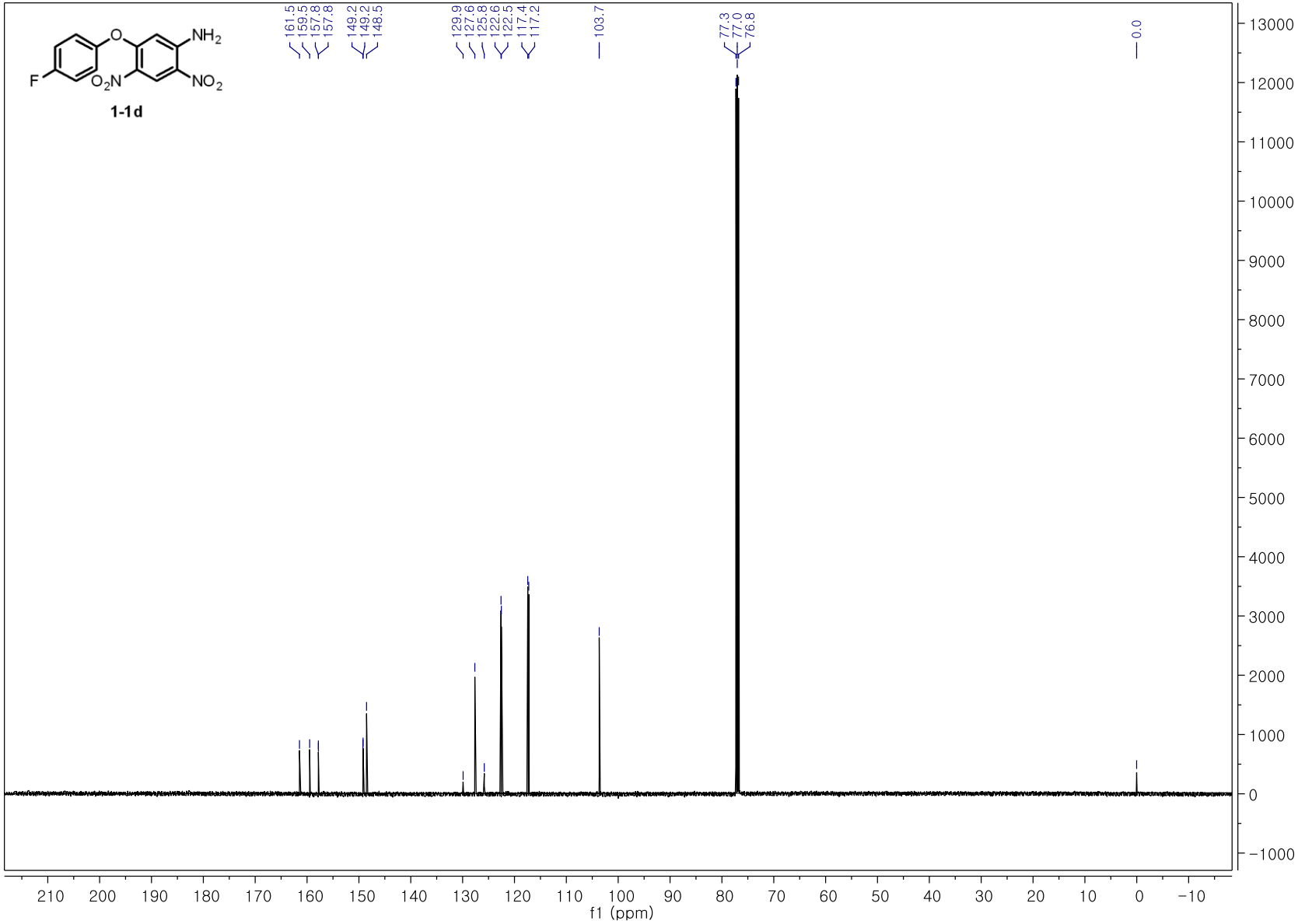
1-1d
161.5
159.5
157.8
157.8
149.2
149.2
148.5
129.9
127.6
125.8
122.6
122.5
117.4
117.2
103.7
77.3
77.0
76.8
0.0
f1 (ppm)

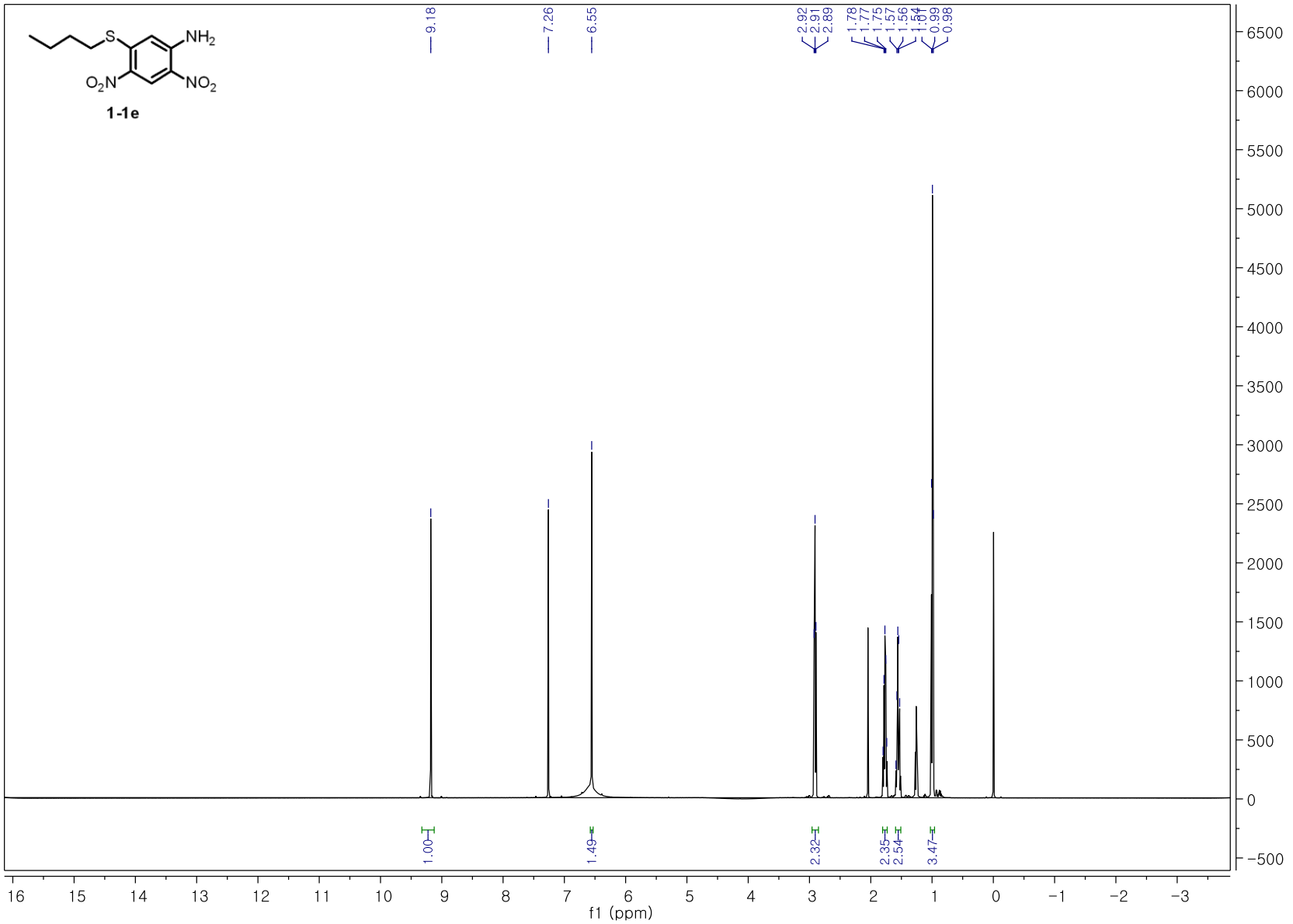
1-1e
9.18
7.26
6.55
2.92
2.91
2.89
1.78
1.77
1.75
1.57
1.56
1.54
1.51
0.99
0.98
1.00
1.49
2.32
2.35
2.54
3.47
f1 (ppm)

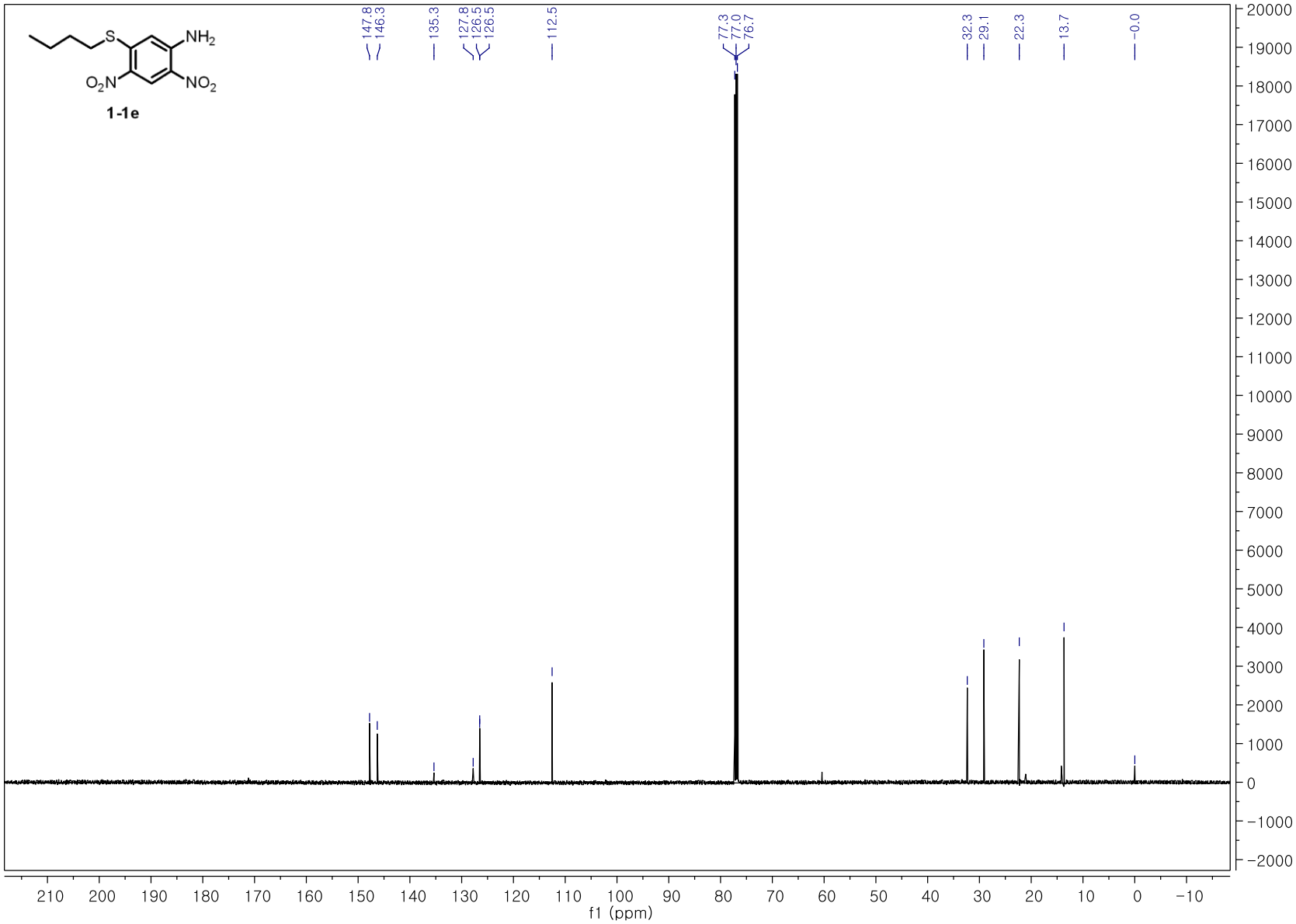
1-1e
147.8
146.3
135.3
127.8
126.5
126.5
112.5
77.3
77.0
76.7
32.3
29.1
22.3
13.7
0.0
f1 (ppm)

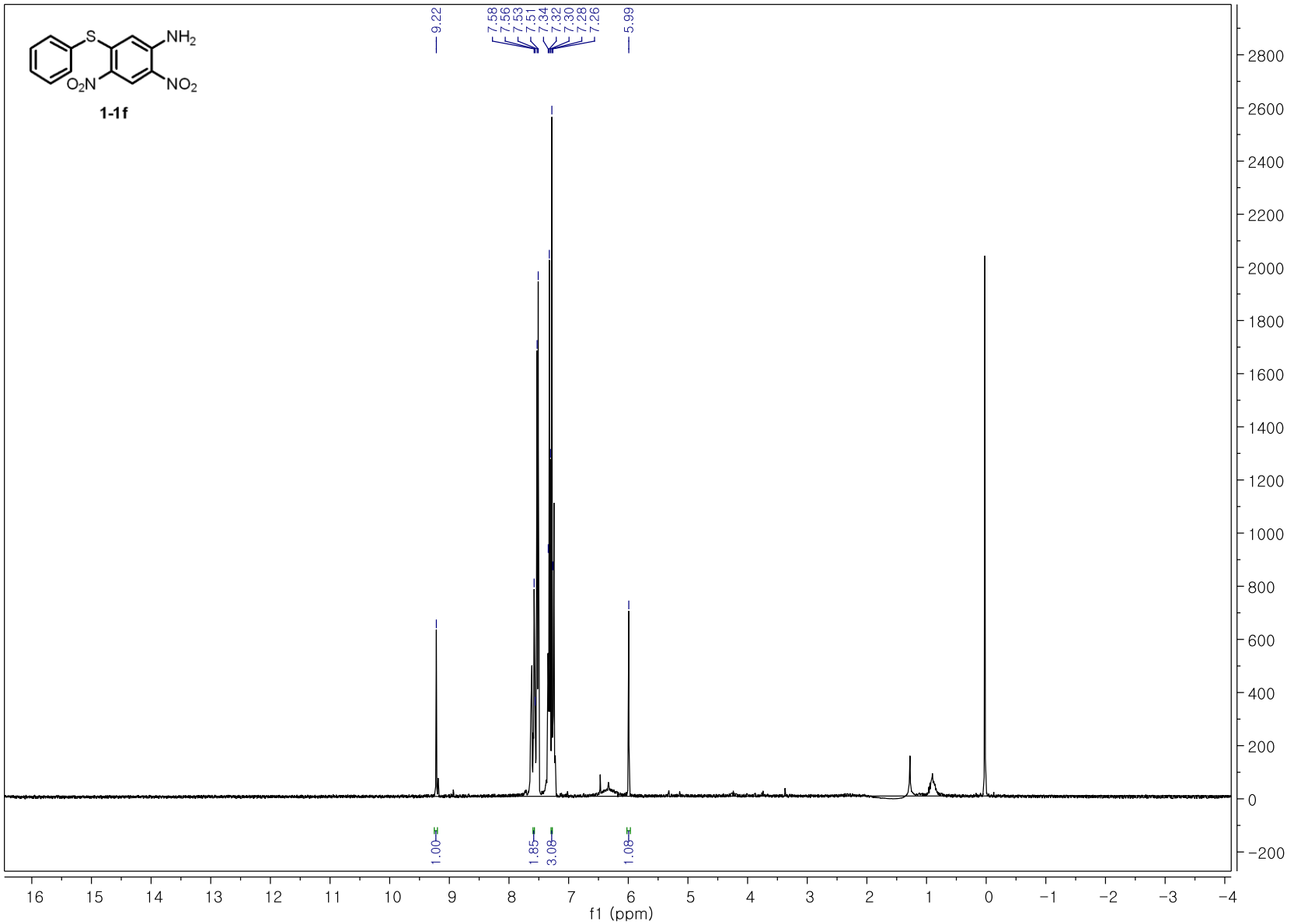
1-1f
9.22
7.58
7.56
7.53
7.51
7.34
7.32
7.30
7.28
7.26
5.99
1.00
1.85
3.08
1.08
f1 (ppm)

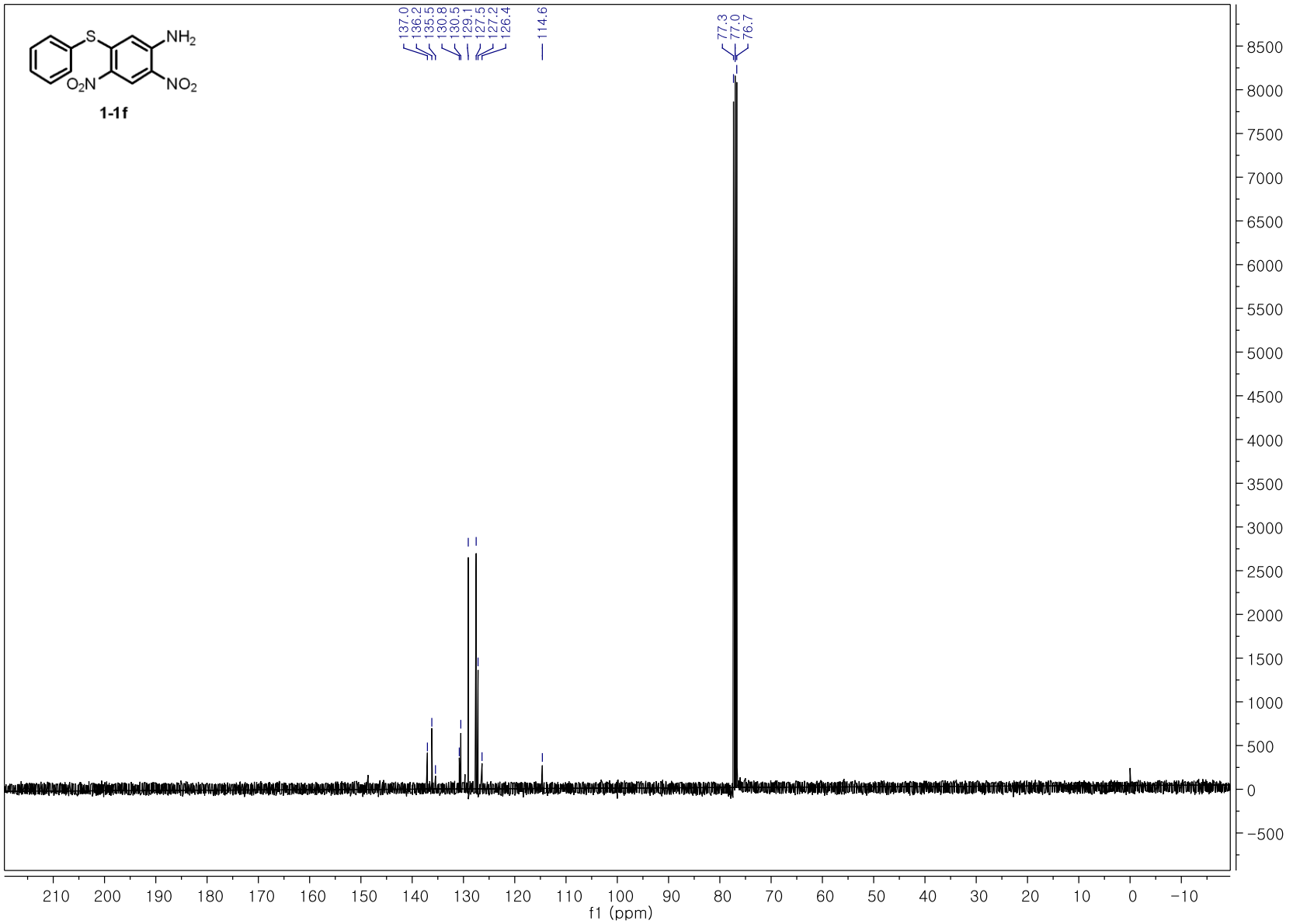
1-1f
137.0
136.2
135.5
130.8
130.5
129.1
127.5
127.2
126.4
114.6
77.3
77.0
76.7
f1 (ppm)

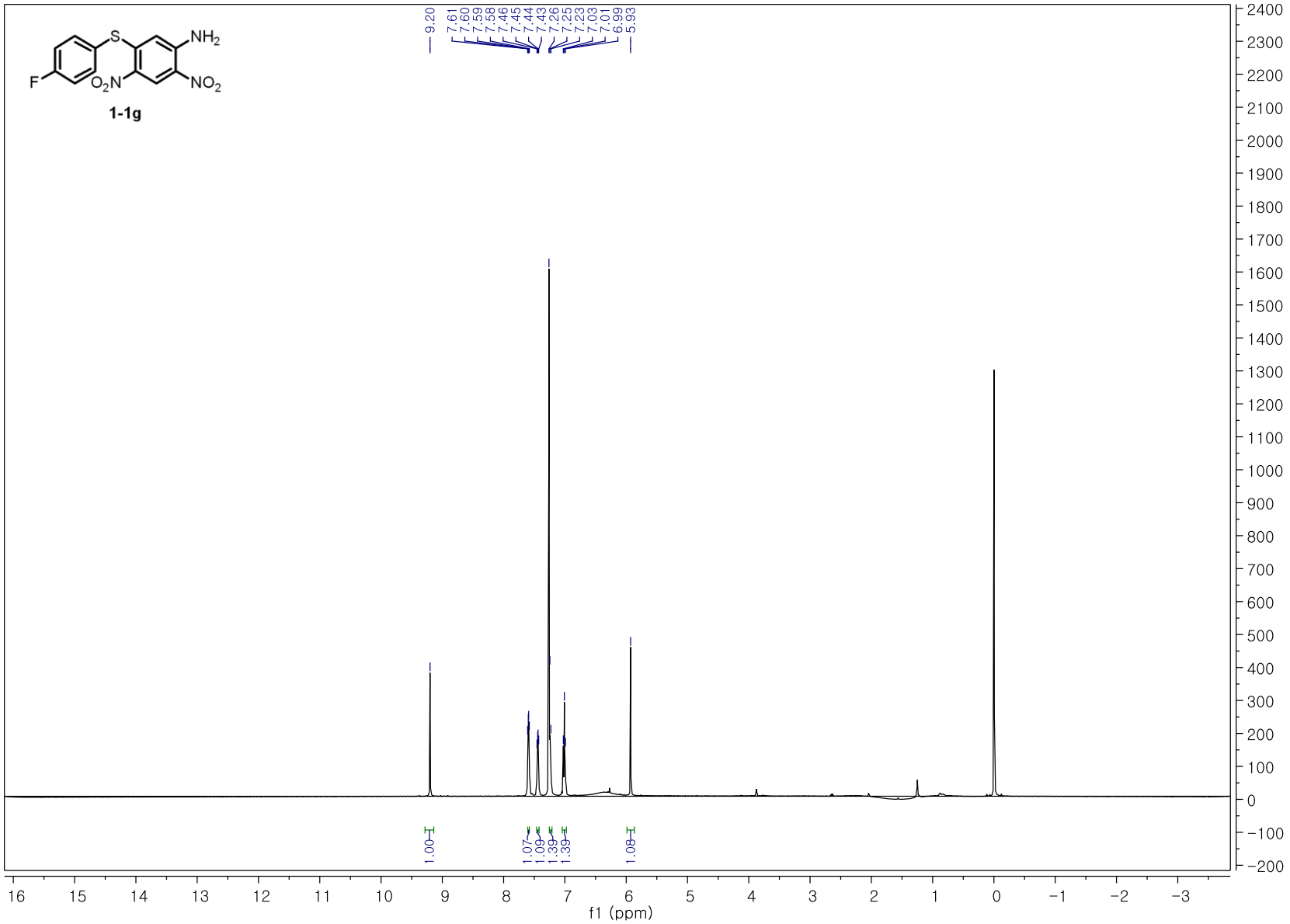
1-1g
9.20
7.61
7.60
7.59
7.58
7.46
7.45
7.44
7.43
7.26
7.25
7.23
7.03
7.01
6.99
5.93
1.00
1.07
1.09
1.39
1.39
1.08
f1 (ppm)

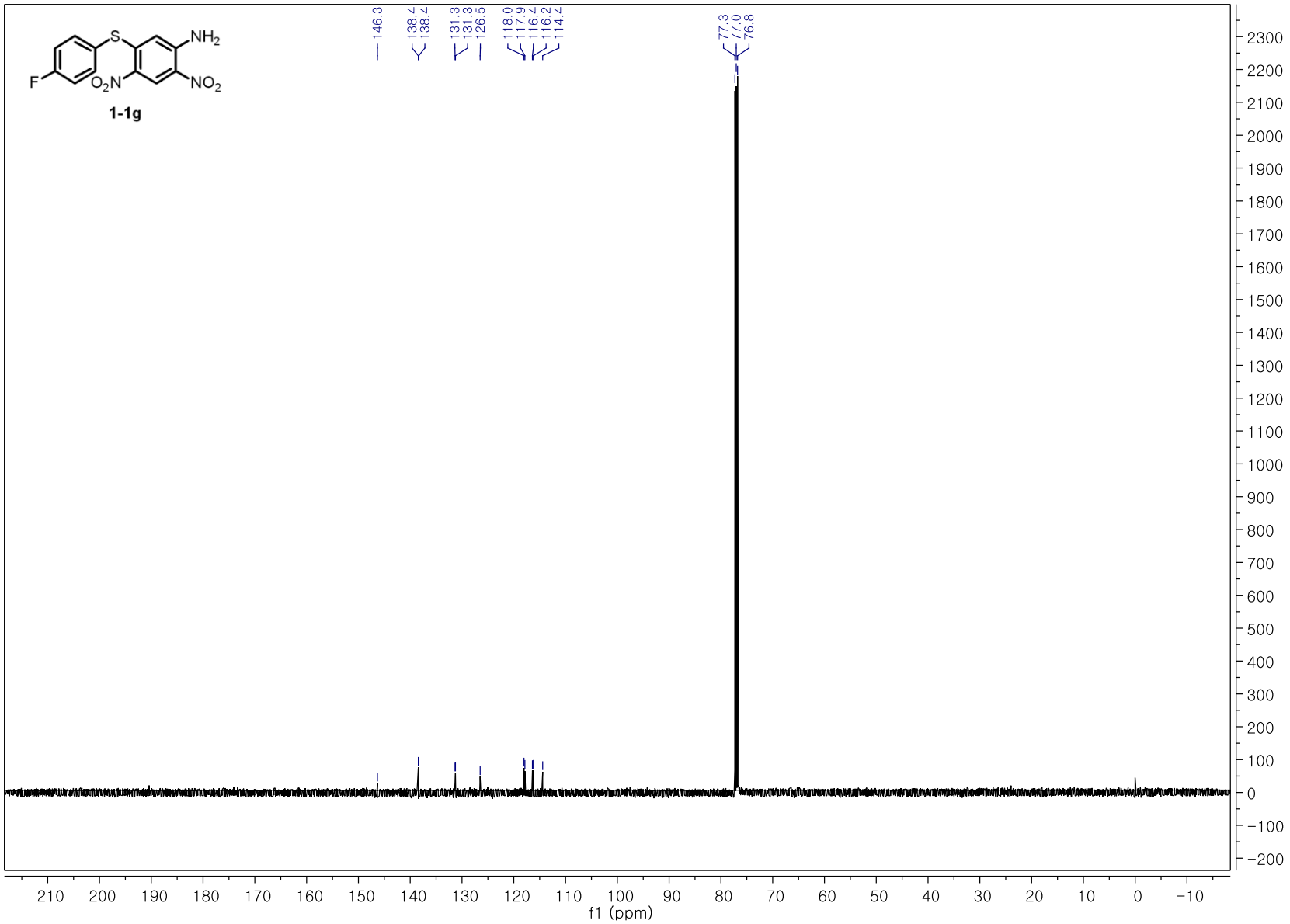
1-1g
146.3
138.4
138.4
131.3
131.3
126.5
118.0
117.9
116.4
116.2
114.4
77.3
77.0
76.8
f1 (ppm)

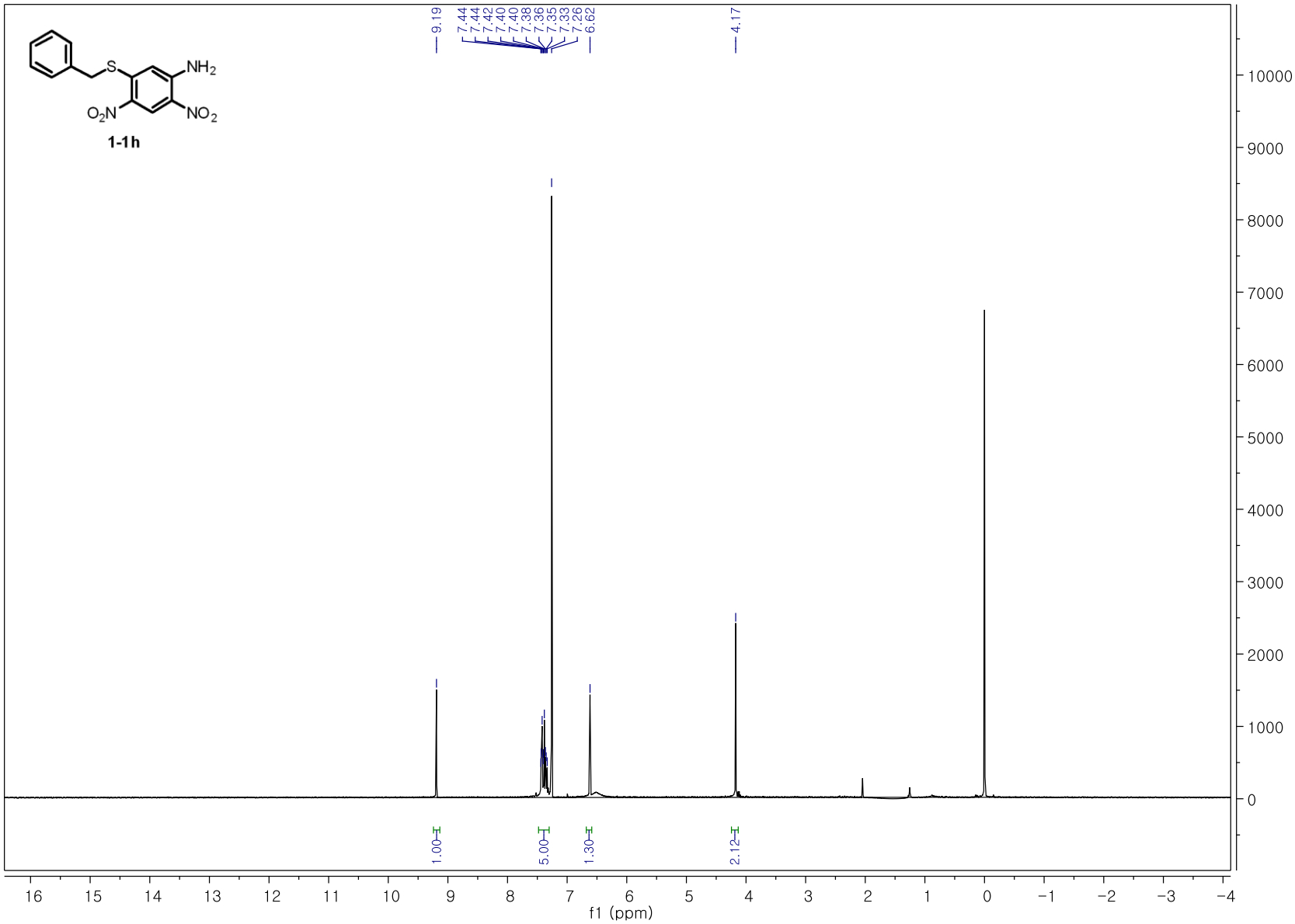
1-1h
9.19
7.44
7.44
7.42
7.40
7.40
7.38
7.36
7.35
7.33
7.26
6.62
4.17
1.00
5.00
1.30
2.12
f1 (ppm)

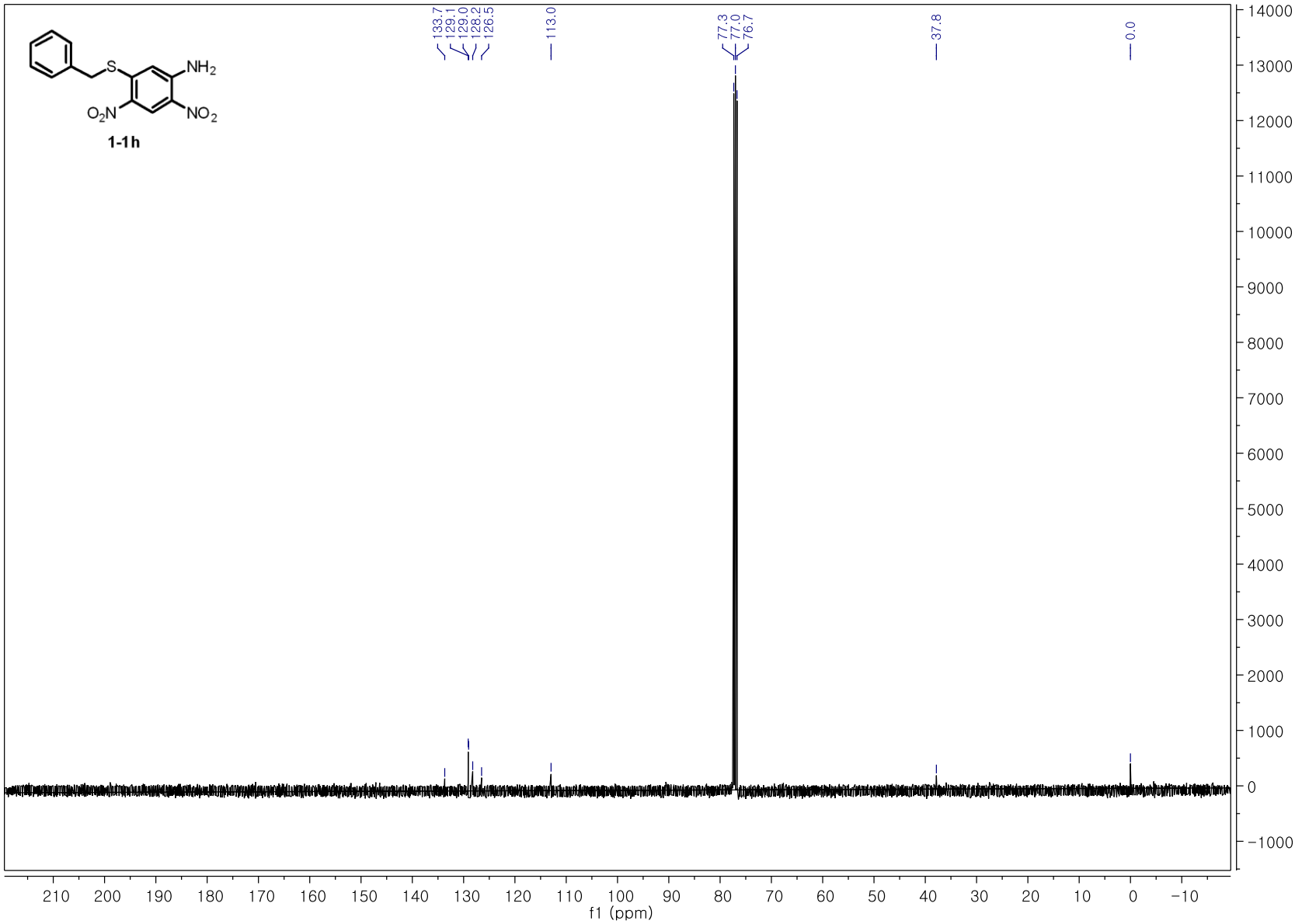
1-1h
133.7
129.1
129.0
128.2
126.5
113.0
77.3
77.0
76.7
37.8
0.0
f1 (ppm)

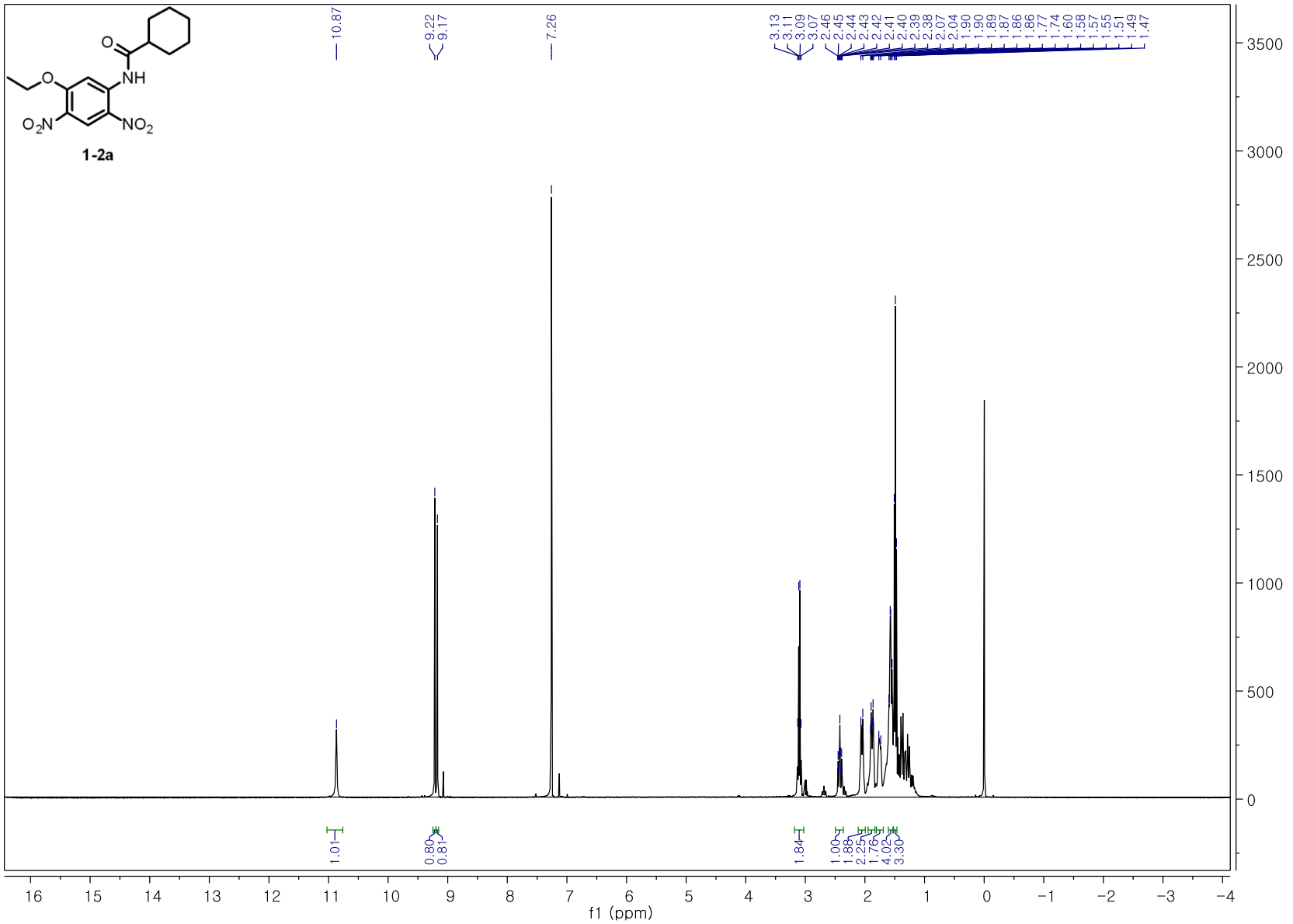
1-2a
10.87
9.22
9.17
7.26
3.13
3.11
3.09
3.07
2.46
2.45
2.44
2.43
2.42
2.41
2.40
2.39
2.38
2.07
2.04
1.90
1.90
1.89
1.87
1.86
1.86
1.77
1.74
1.60
1.58
1.57
1.55
1.51
1.49
1.47
1.01
0.80
0.81
1.84
1.00
1.88
2.25
1.76
4.02
3.30
f1 (ppm)

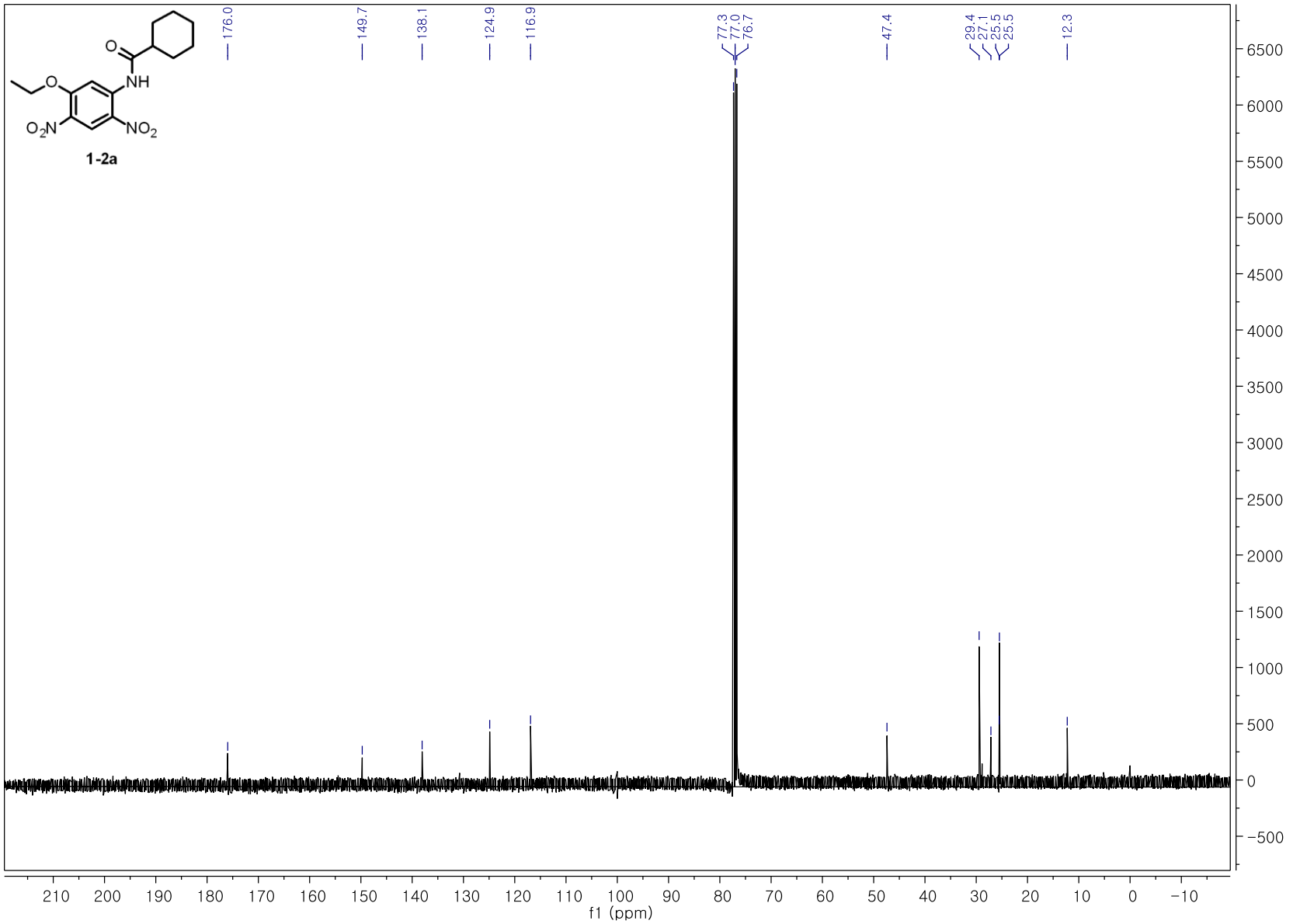
1-2a
176.0
149.7
138.1
124.9
116.9
77.3
77.0
76.7
47.4
29.4
27.1
25.5
25.5
12.3
f1 (ppm)

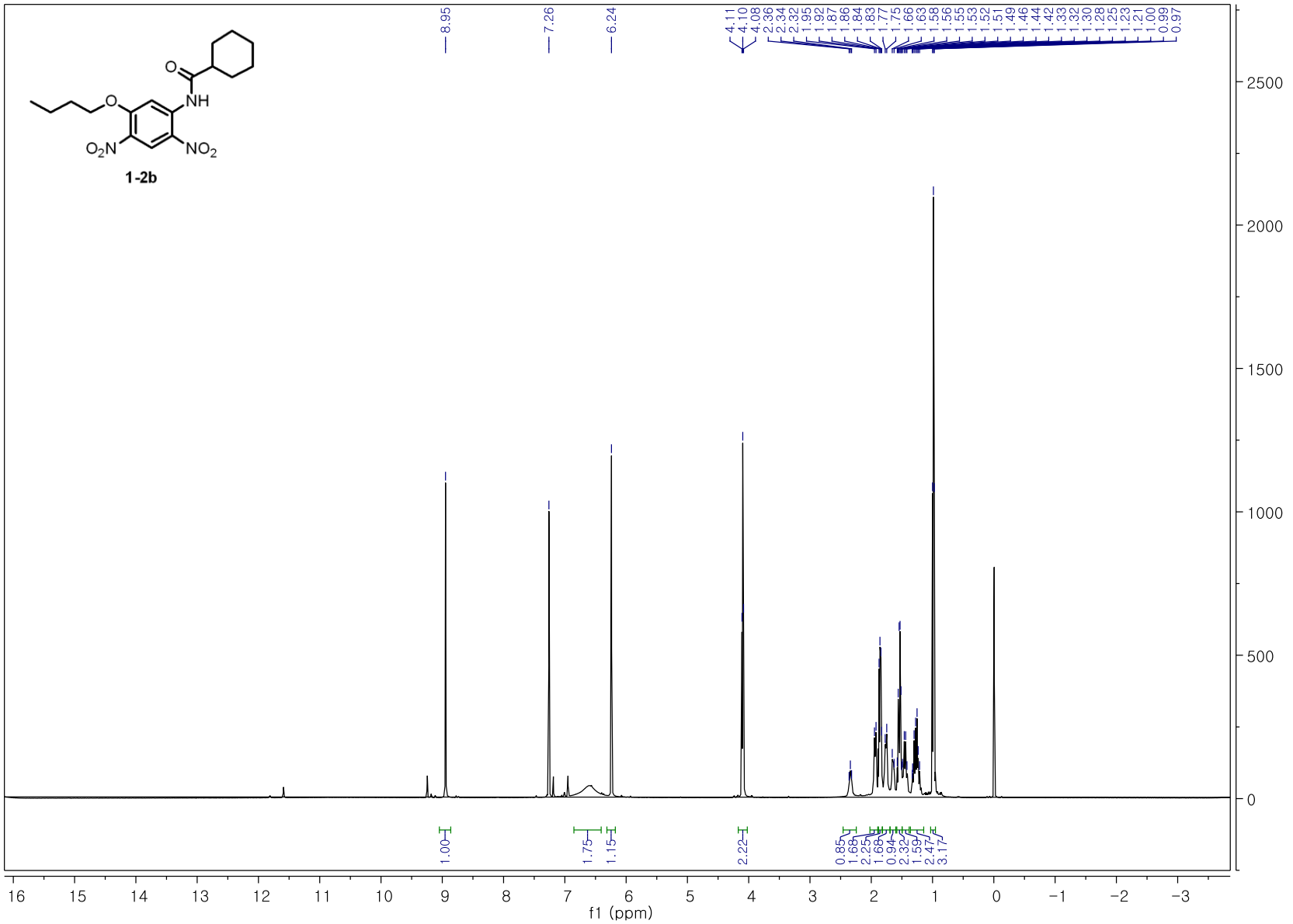
1-2b
8.95
7.26
6.24
4.11
4.10
4.08
2.36
2.34
2.32
1.95
1.92
1.87
1.86
1.84
1.83
1.77
1.75
1.66
1.63
1.58
1.56
1.55
1.53
1.52
1.51
1.49
1.46
1.44
1.42
1.33
1.32
1.30
1.28
1.25
1.23
1.21
1.00
0.99
0.97
2500
2000
1500
1000
500
0
1.00
1.75
1.15
2.22
0.85
1.68
2.25
1.68
0.94
2.32
1.59
2.47
3.17
16
15
14
13
12
11
10
9
8
7
6
5
4
3
2
1
0
−1
−2
−3
f1 (ppm)

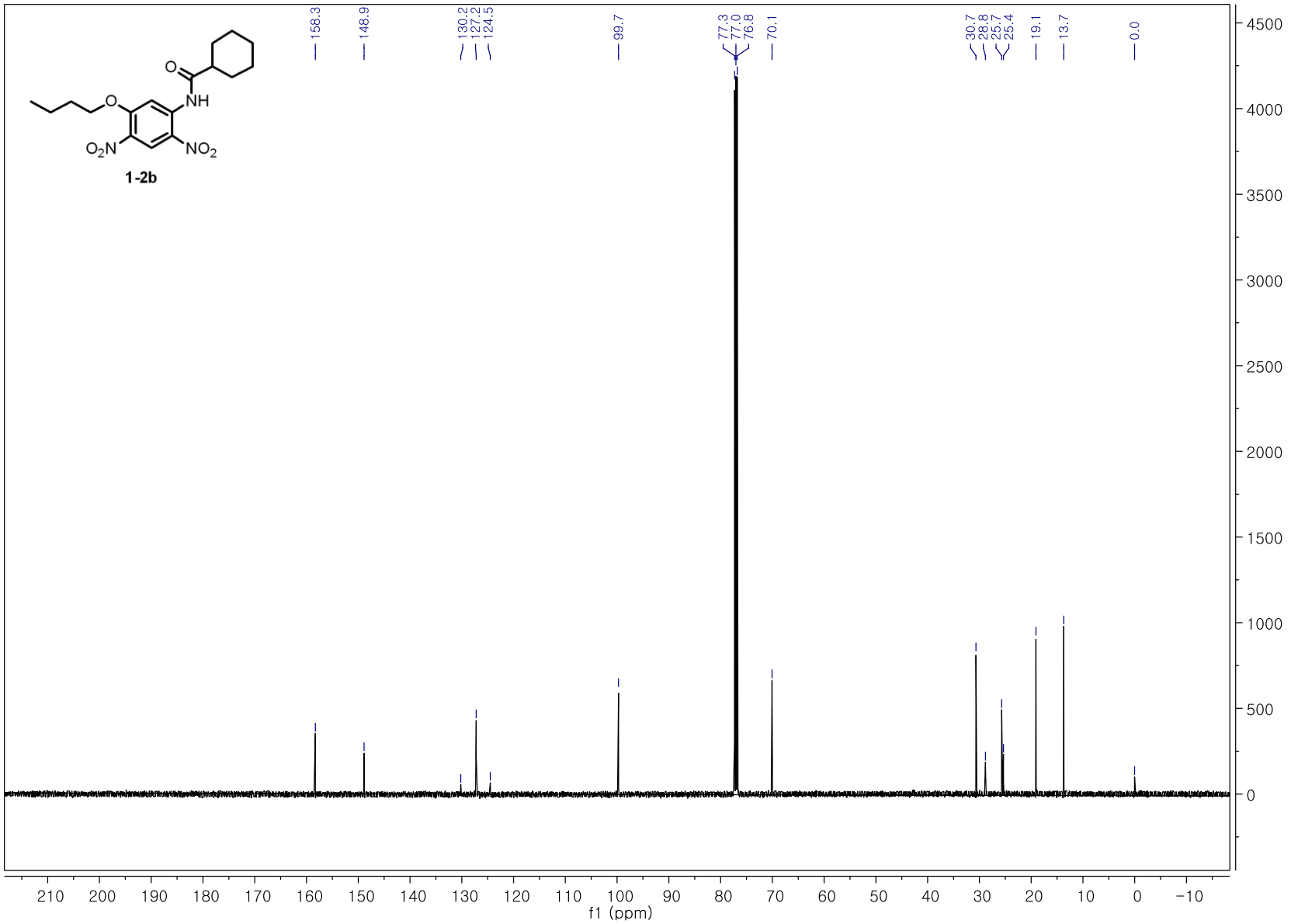
158.3
148.9
130.2
127.2
124.5
99.7
77.3
77.0
76.8
70.1
30.7
28.8
25.7
25.4
19.1
13.7
0.0
O
NH
O
O_2N
NO_2
1-2b
4500
4000
3500
3000
2500
2000
1500
1000
500
0
210 200 190 180 170 160 150 140 130 120 110 100 90 80 70 60 50 40 30 20 10 0 −10
f1 (ppm)

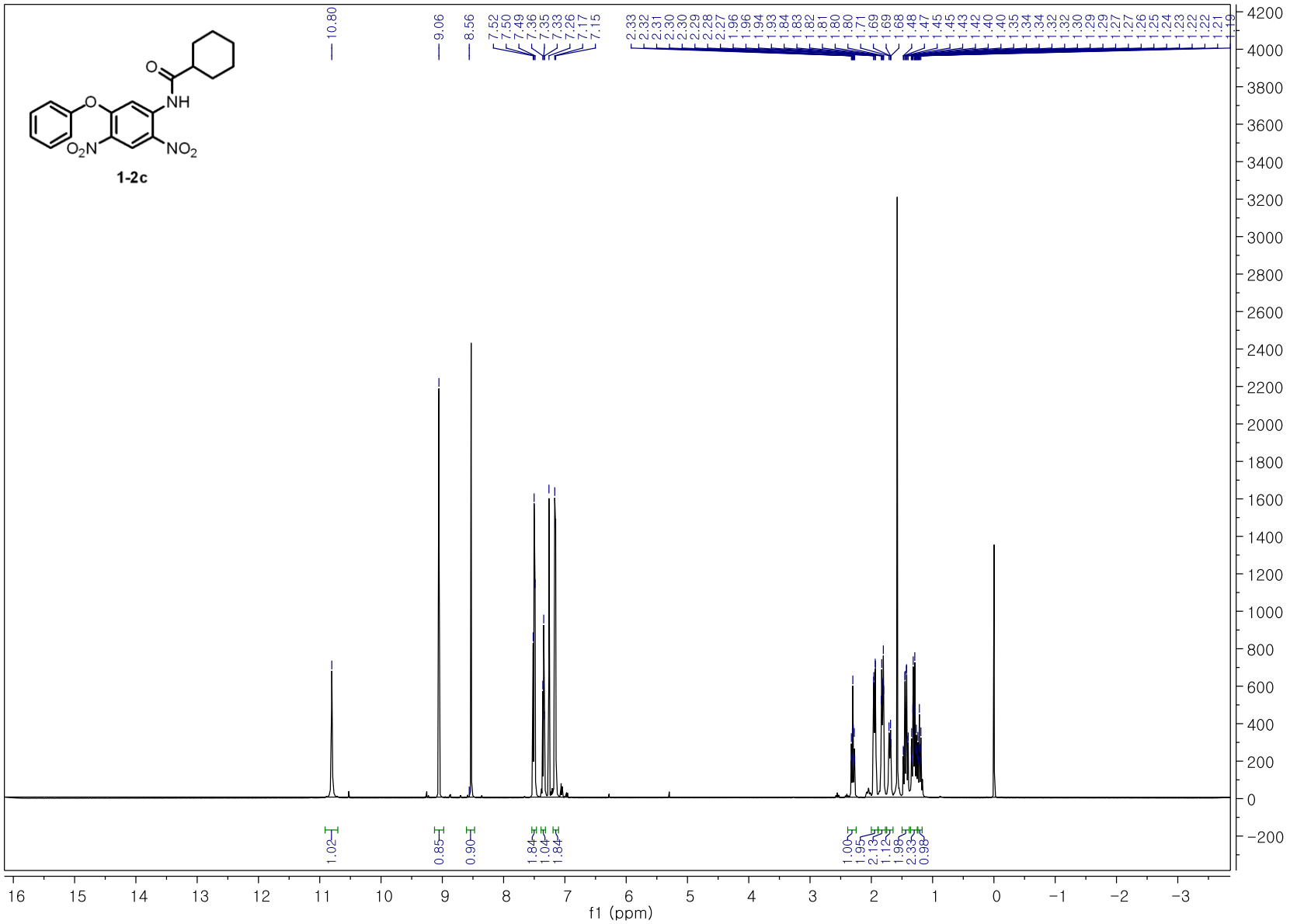
1-2c
10.80
9.06
8.56
7.52
7.50
7.49
7.36
7.35
7.33
7.26
7.17
7.15
2.33
2.32
2.31
2.30
2.30
2.29
2.28
2.27
1.96
1.96
1.94
1.93
1.84
1.83
1.82
1.81
1.80
1.80
1.71
1.69
1.69
1.68
1.48
1.47
1.45
1.45
1.43
1.42
1.40
1.40
1.35
1.34
1.34
1.32
1.32
1.30
1.29
1.27
1.27
1.26
1.25
1.24
1.23
1.22
1.22
1.21
1.19
1.02
0.85
0.90
1.84
1.04
1.84
1.00
1.95
2.13
1.12
1.96
2.33
0.98
f1 (ppm)

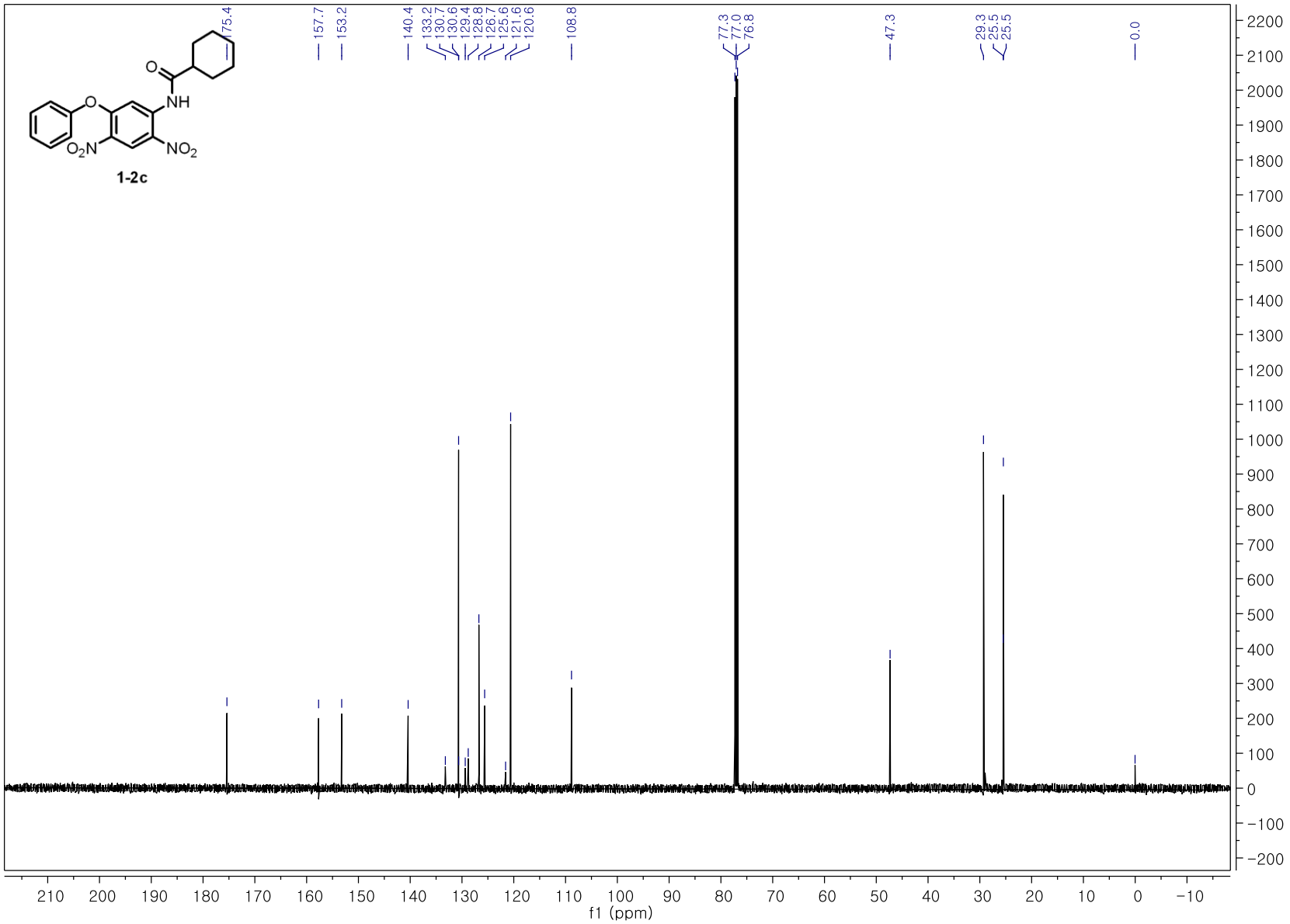
1-2c
O
NH
O
O2N
NO2
175.4
157.7
153.2
140.4
133.2
130.7
130.6
129.4
128.8
126.7
125.6
121.6
120.6
108.8
77.3
77.0
76.8
47.3
29.3
25.5
25.5
0.0
f1 (ppm)

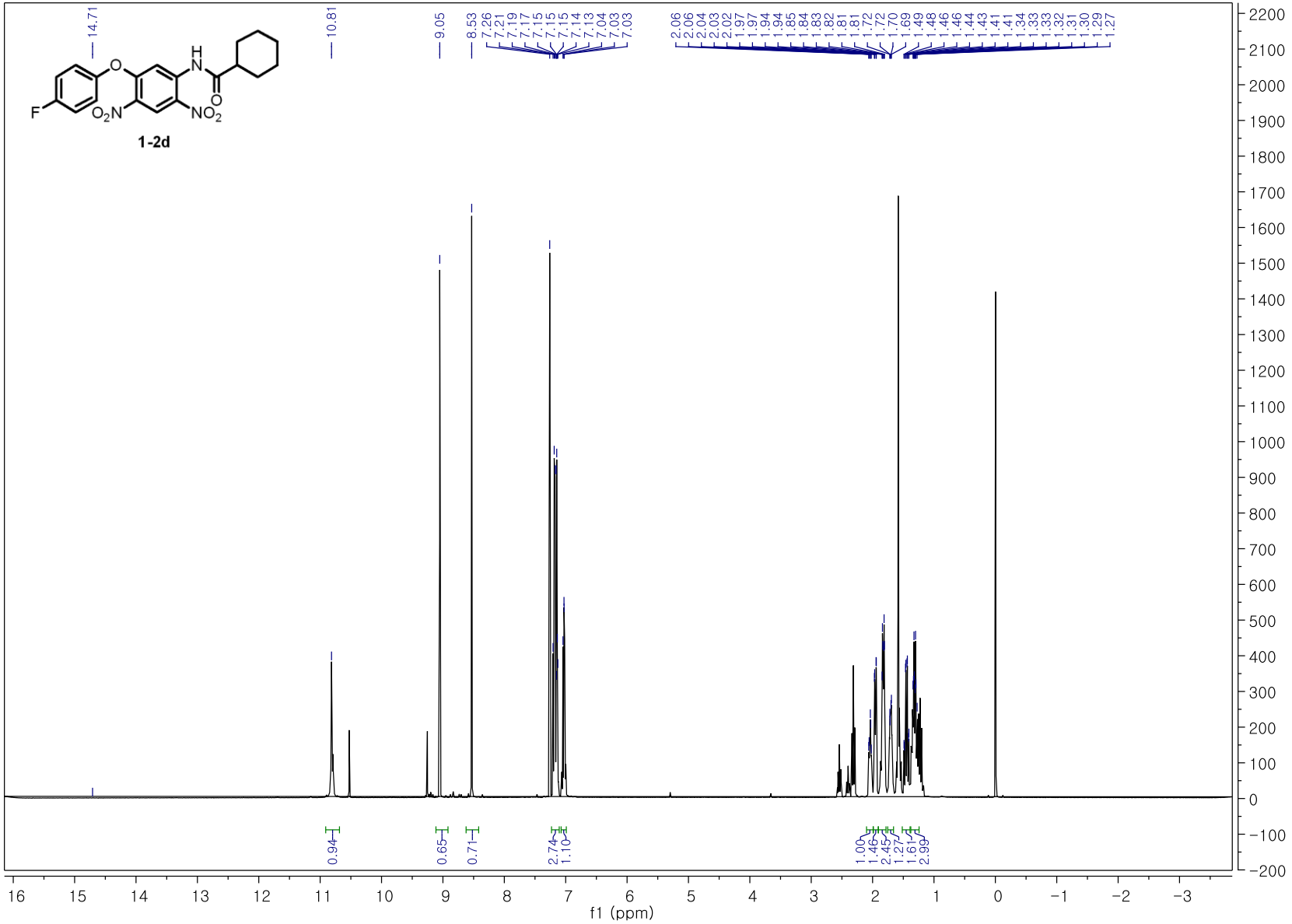
14.71
10.81
9.05
8.53
7.26
7.21
7.19
7.17
7.15
7.15
7.15
7.14
7.13
7.04
7.03
7.03
2.06
2.06
2.04
2.03
2.02
1.97
1.97
1.94
1.94
1.85
1.84
1.83
1.82
1.81
1.81
1.72
1.72
1.70
1.69
1.49
1.48
1.46
1.46
1.44
1.43
1.41
1.41
1.34
1.33
1.33
1.32
1.31
1.30
1.29
1.27
1-2d
0.94
0.65
0.71
2.74
1.10
1.00
1.46
2.45
1.27
1.61
2.99
f1 (ppm)

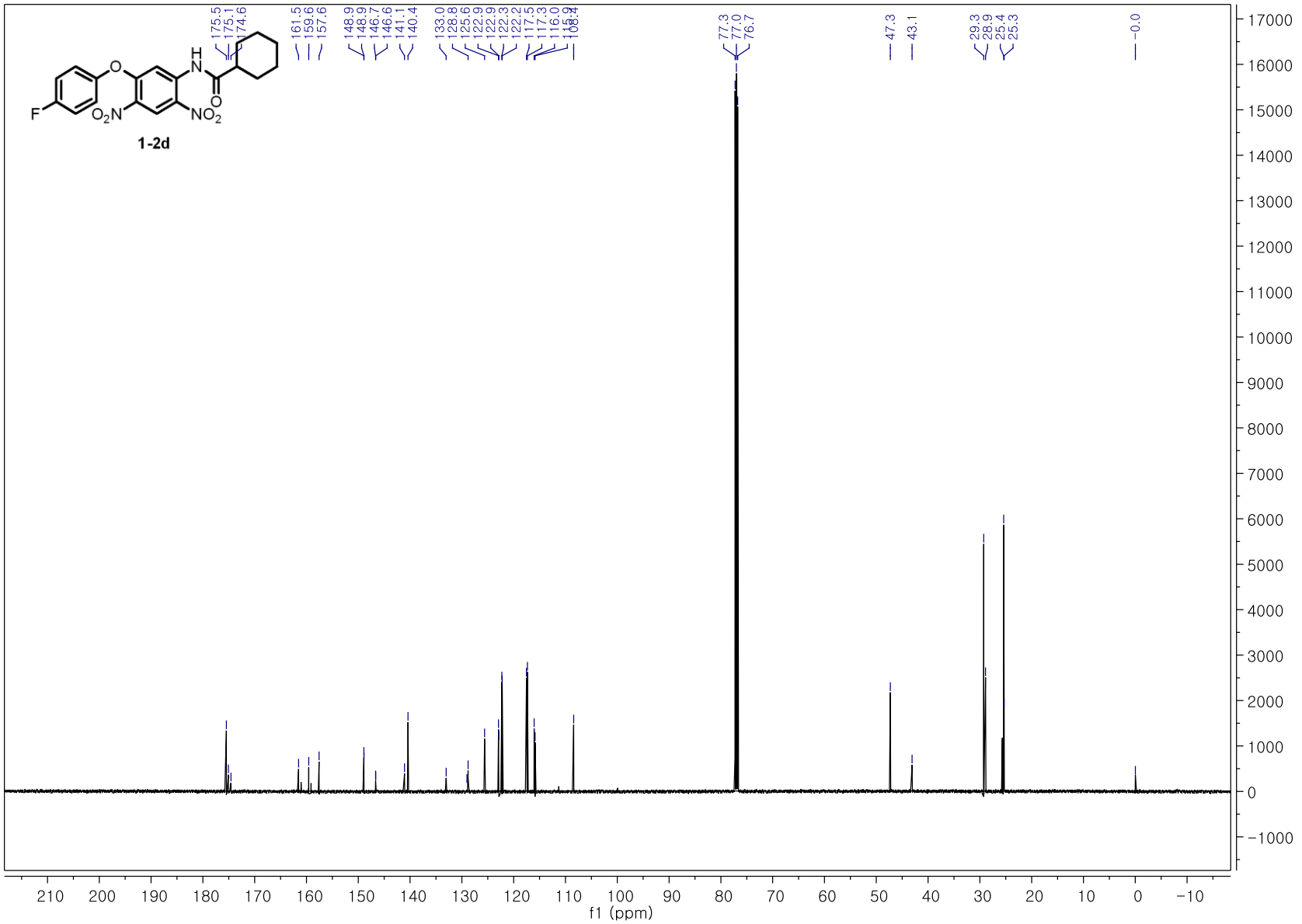
1-2d
175.5
175.1
174.6
161.5
159.6
157.6
148.9
148.9
146.7
146.6
141.1
140.4
133.0
128.8
125.6
122.9
122.9
122.3
122.2
117.5
117.3
116.0
77.3
77.0
76.7
47.3
43.1
29.3
28.9
25.4
25.3
0.0
f1 (ppm)

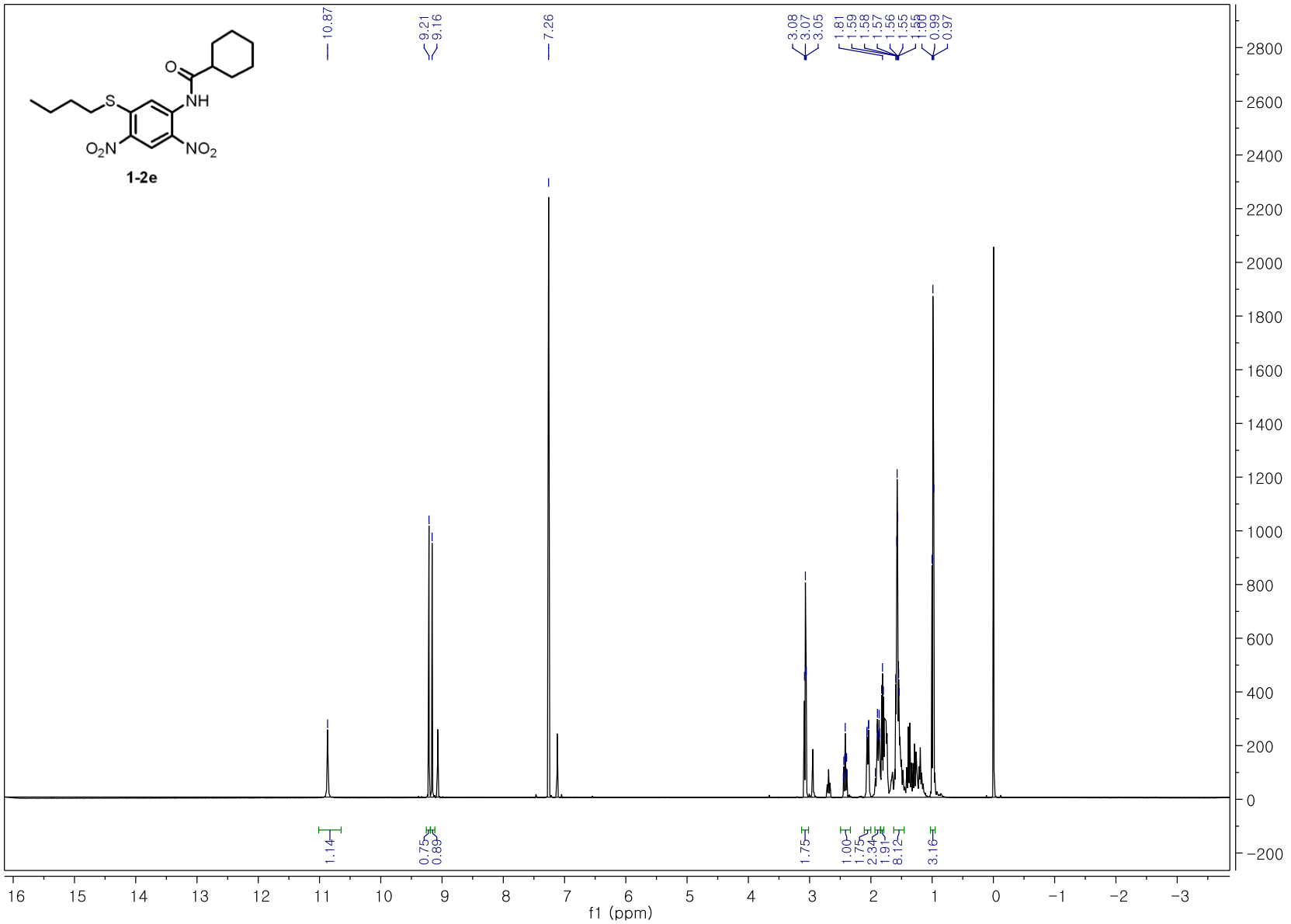
10.87
9.21
9.16
7.26
3.08
3.07
3.05
1.81
1.59
1.58
1.57
1.56
1.55
1.00
0.99
0.97
1.14
0.75
0.89
1.75
1.00
1.75
2.34
1.91
8.12
3.16
f1 (ppm)
1-2e

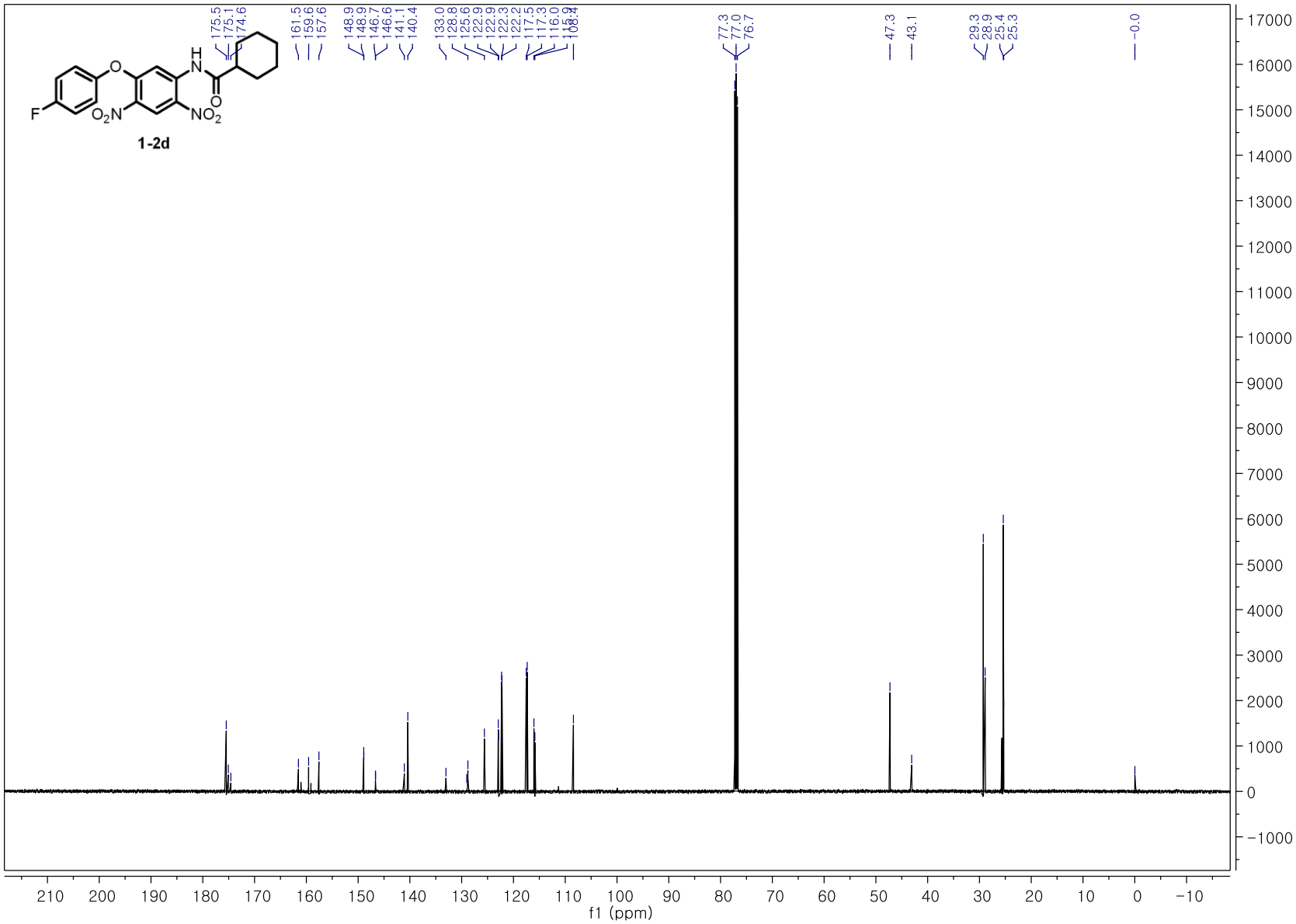
1-2d
175.5
175.1
174.6
161.5
159.6
157.6
148.9
148.9
146.7
146.6
141.1
140.4
133.0
128.8
125.6
122.9
122.9
122.3
122.2
117.5
117.3
116.0
77.3
77.0
76.7
47.3
43.1
29.3
28.9
25.4
25.3
0.0
f1 (ppm)

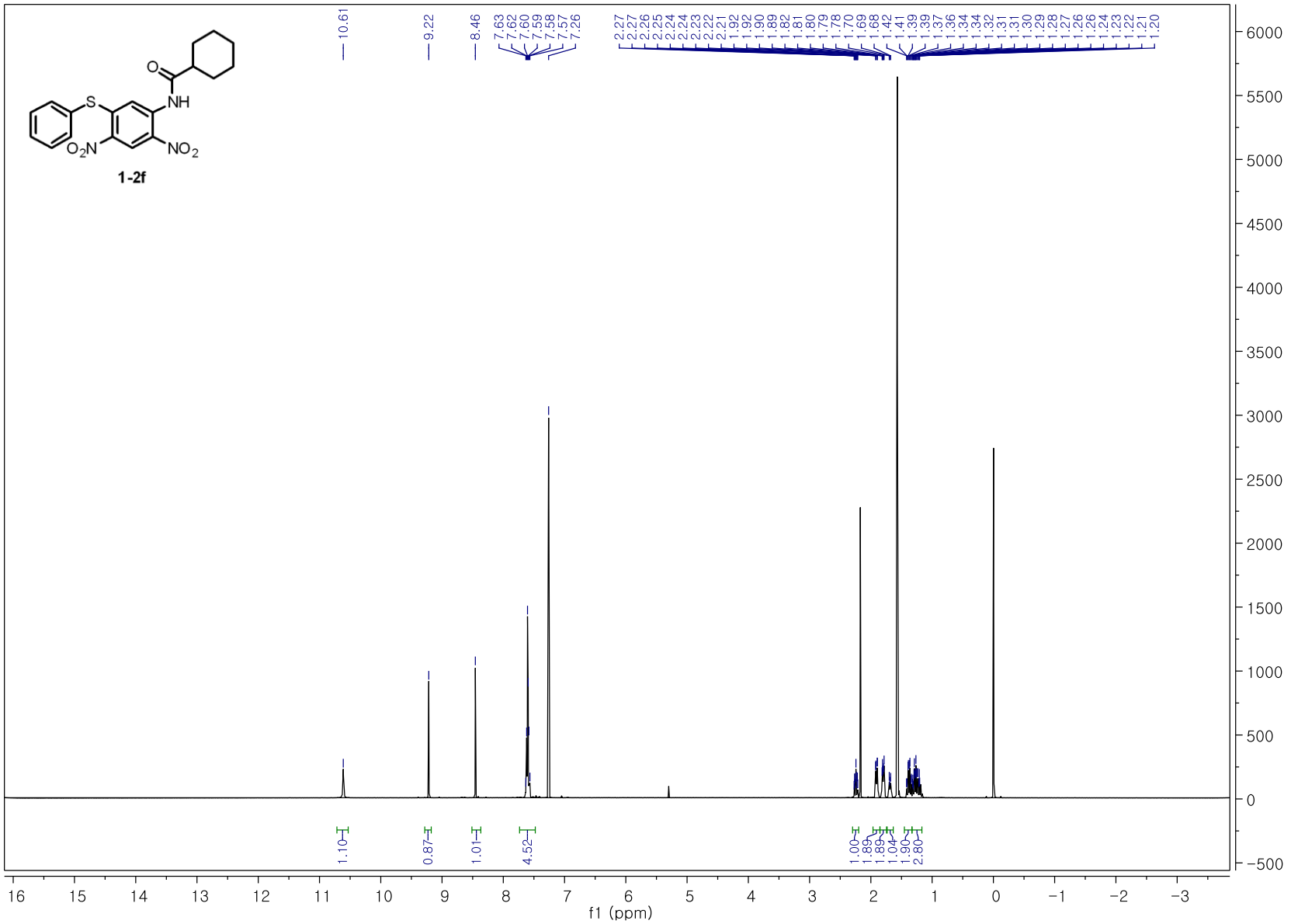
10.61
9.22
8.46
7.63
7.62
7.60
7.59
7.58
7.57
7.26
2.27
2.27
2.26
2.25
2.24
2.24
2.23
2.22
2.21
1.92
1.90
1.89
1.82
1.81
1.80
1.79
1.78
1.70
1.69
1.68
1.42
1.41
1.39
1.39
1.37
1.36
1.34
1.34
1.32
1.31
1.31
1.30
1.29
1.28
1.27
1.26
1.26
1.24
1.23
1.22
1.21
1.20
O
NH
S
O2N
NO2
1-2f
1.10
0.87
1.01
4.52
1.00
1.85
1.89
1.04
1.90
2.80
f1 (ppm)

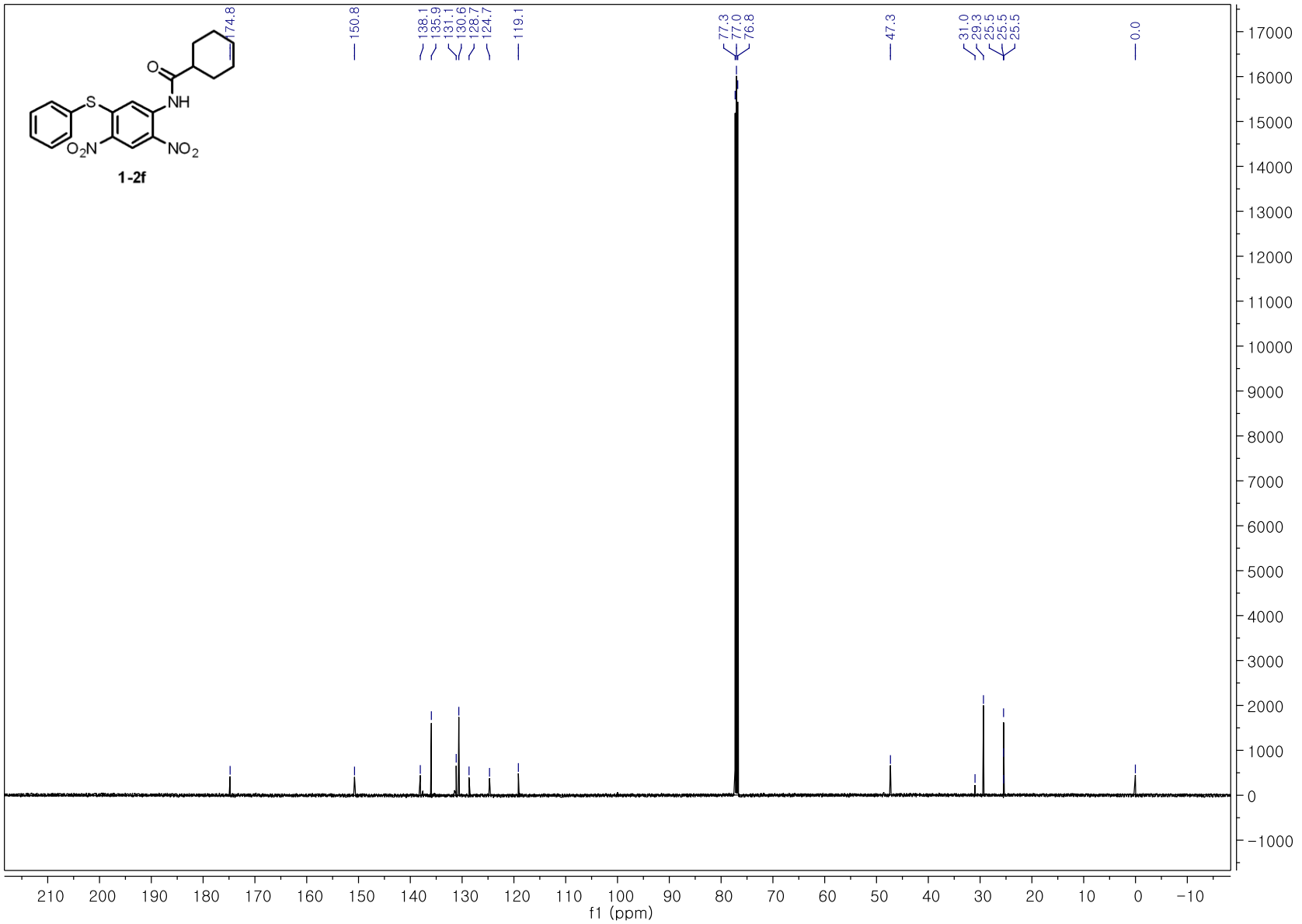
174.8
150.8
138.1
135.9
131.1
130.6
128.7
124.7
119.1
77.3
77.0
76.8
47.3
31.0
29.3
25.5
25.5
25.5
0.0
O
NH
S
O2N
NO2
1-2f
f1 (ppm)

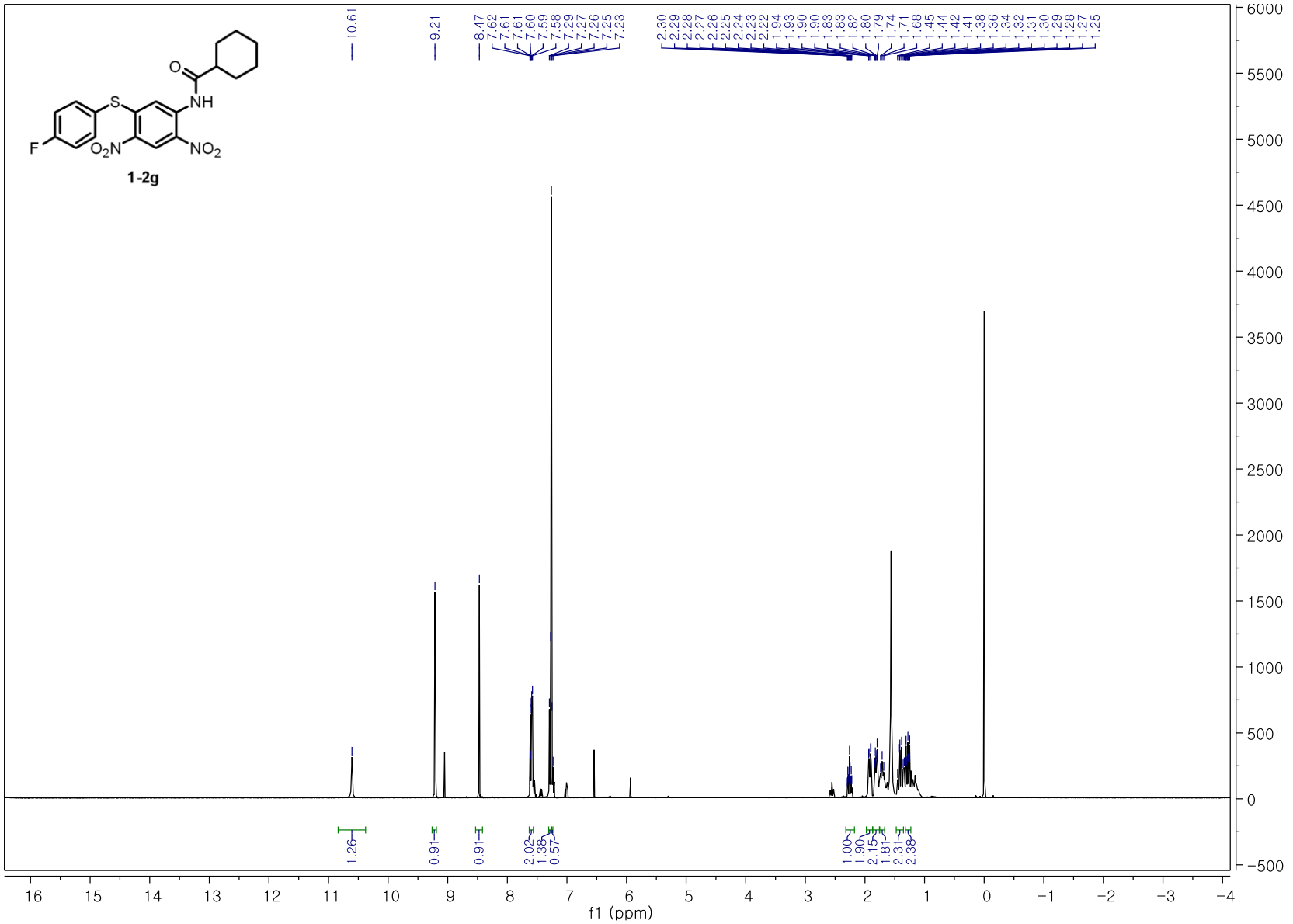
1-2g
10.61
9.21
8.47
7.62
7.61
7.61
7.60
7.59
7.58
7.29
7.27
7.26
7.25
7.23
2.30
2.29
2.28
2.27
2.26
2.25
2.24
2.23
2.22
1.94
1.93
1.90
1.90
1.83
1.83
1.82
1.80
1.79
1.74
1.71
1.68
1.45
1.44
1.42
1.41
1.38
1.36
1.34
1.32
1.31
1.30
1.29
1.28
1.27
1.25
1.26
0.91
0.91
2.02
1.38
0.57
1.00
1.90
2.15
1.81
2.31
2.38
f1 (ppm)

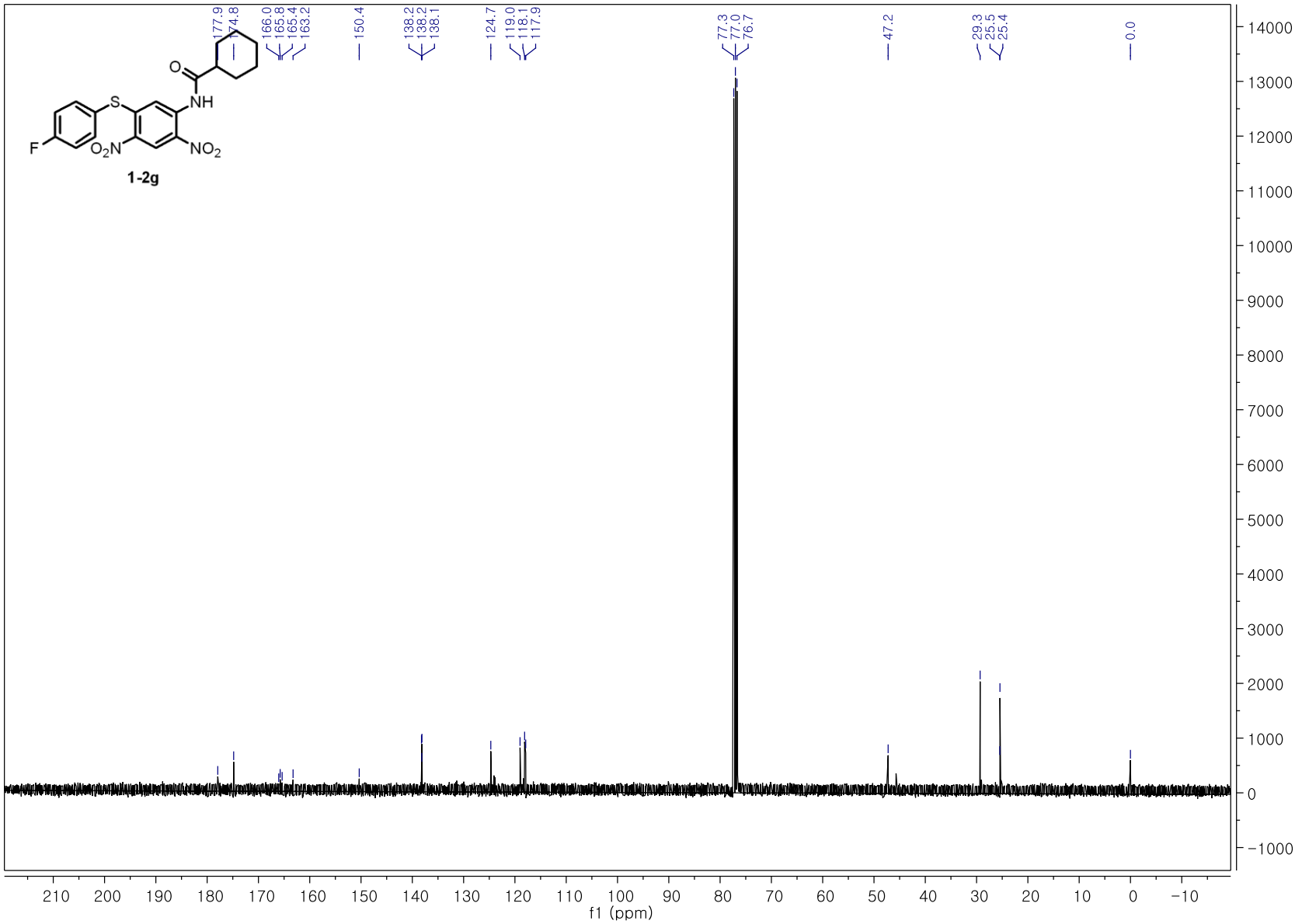
177.9
174.8
166.0
165.8
165.4
163.2
150.4
138.2
138.2
138.1
124.7
119.0
118.1
117.9
77.3
77.0
76.7
47.2
29.3
25.5
25.4
0.0
O
NH
S
F
O2N
NO2
1-2g
14000
13000
12000
11000
10000
9000
8000
7000
6000
5000
4000
3000
2000
1000
0
−1000
210 200 190 180 170 160 150 140 130 120 110 100 90 80 70 60 50 40 30 20 10 0 −10
f1 (ppm)

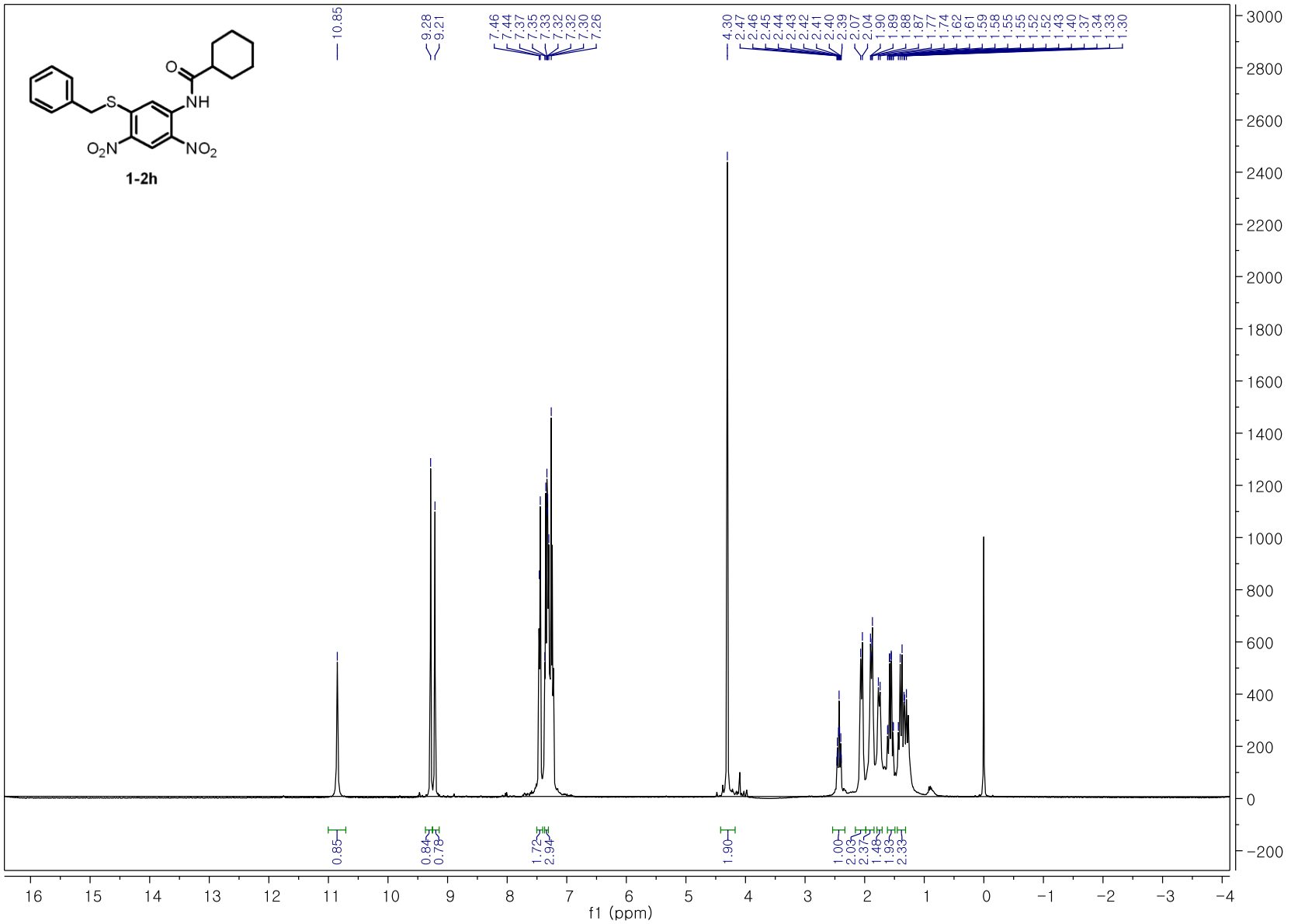
1-2h
10.85
9.28
9.21
7.46
7.44
7.37
7.35
7.33
7.32
7.32
7.30
7.26
4.30
2.47
2.46
2.45
2.44
2.43
2.42
2.41
2.40
2.39
2.07
2.04
1.90
1.89
1.88
1.87
1.77
1.74
1.62
1.61
1.59
1.58
1.55
1.55
1.52
1.52
1.43
1.40
1.37
1.34
1.33
1.30
0.85
0.84
0.78
1.72
2.94
1.90
1.00
2.03
2.37
1.46
1.93
2.33
f1 (ppm)

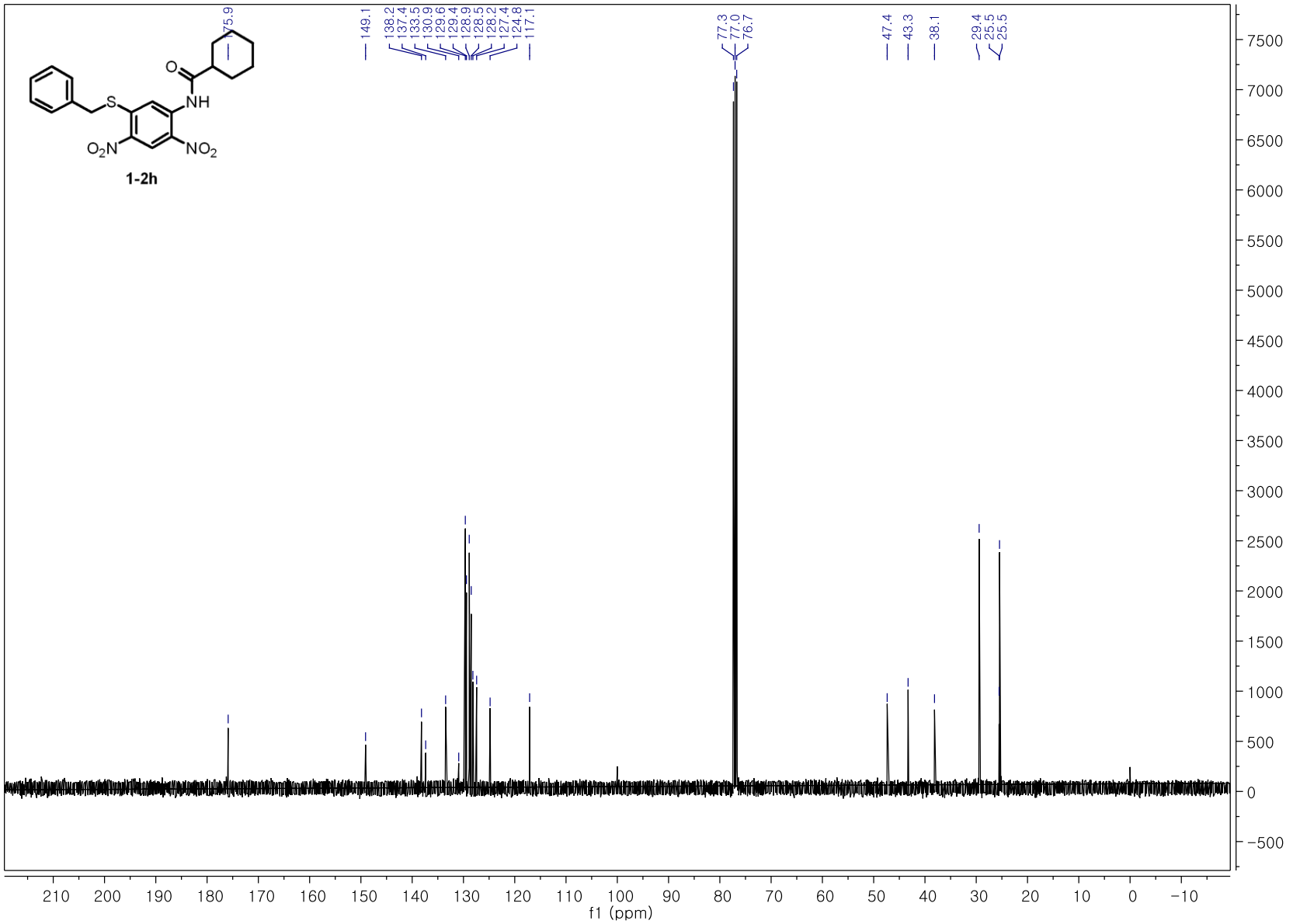
175.9
149.1
138.2
137.4
133.5
130.9
129.6
129.4
128.9
128.5
128.2
127.4
124.8
117.1
77.3
77.0
76.7
47.4
43.3
38.1
29.4
25.5
25.5
O
NH
S
O_2N
NO_2
1-2h
f1 (ppm)

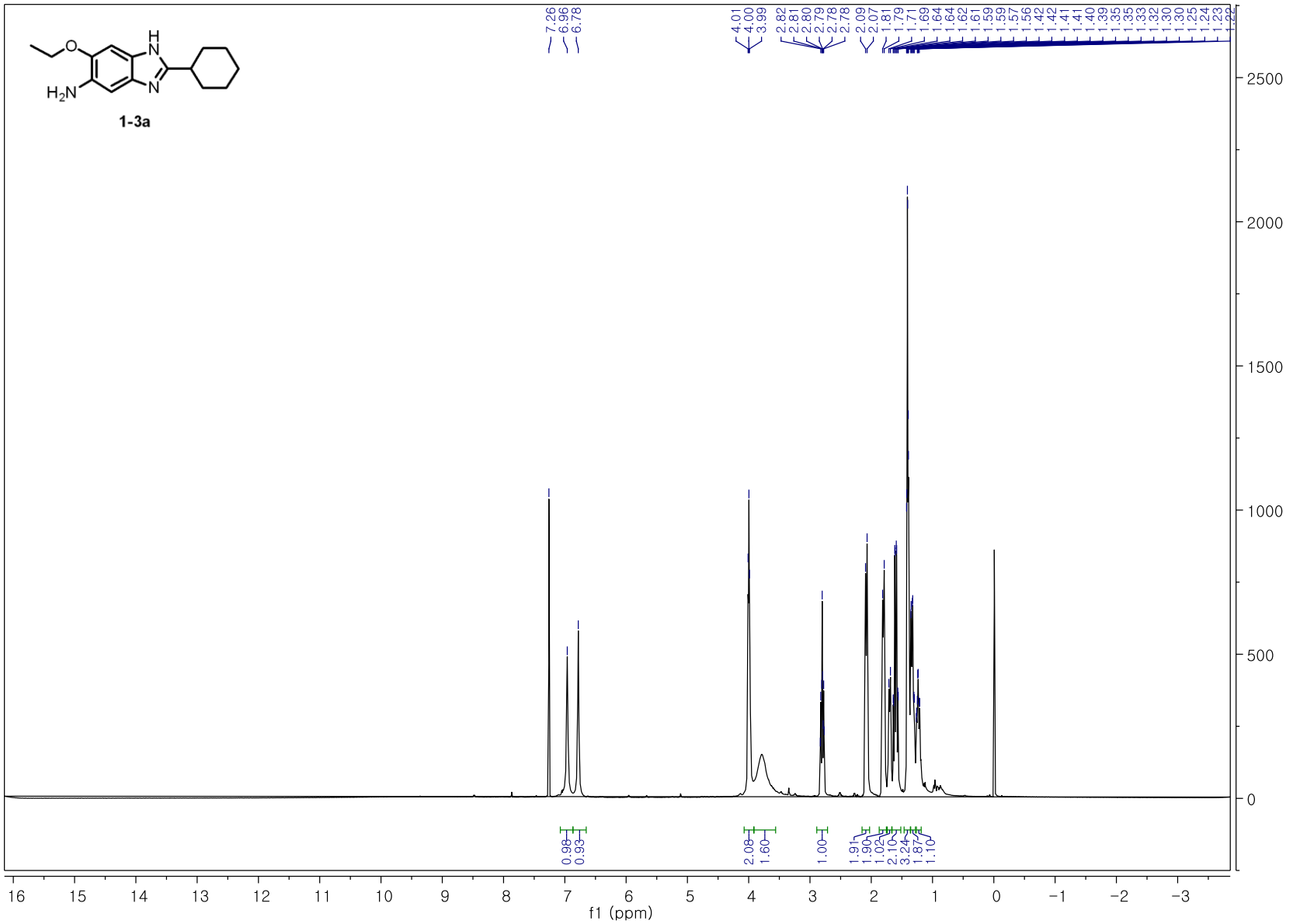
1-3a
7.26
6.96
6.78
4.01
4.00
3.99
2.82
2.81
2.80
2.79
2.78
2.78
2.09
2.07
1.81
1.79
1.71
1.69
1.64
1.64
1.62
1.61
1.59
1.59
1.57
1.56
1.42
1.42
1.41
1.41
1.40
1.39
1.35
1.35
1.33
1.32
1.30
1.30
1.25
1.24
1.23
1.22
0.98
0.93
2.08
1.60
1.00
1.91
1.90
1.02
2.10
3.24
1.87
1.10
f1 (ppm)

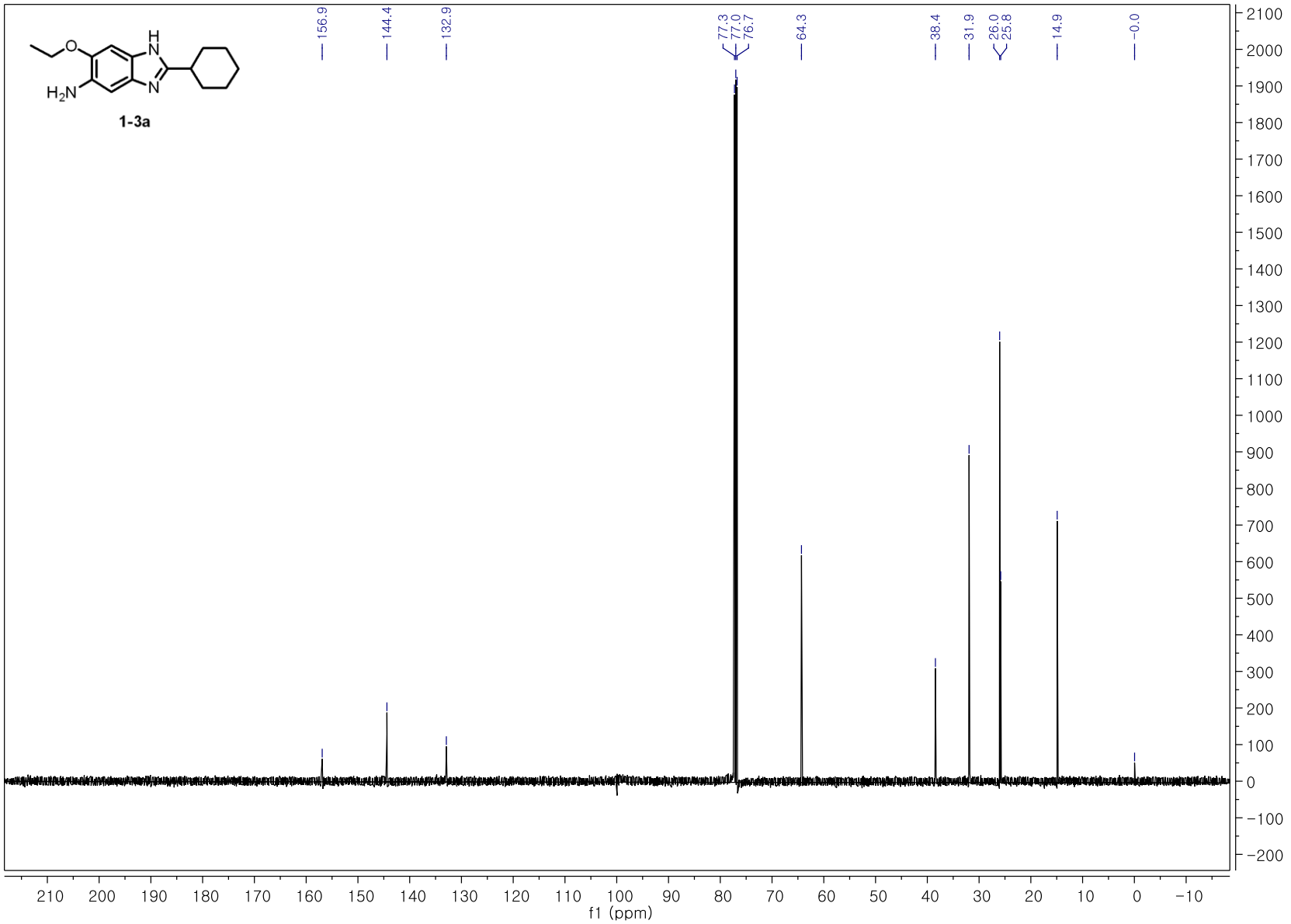
1-3a
156.9
144.4
132.9
77.3
77.0
76.7
64.3
38.4
31.9
26.0
25.8
14.9
0.0
f1 (ppm)

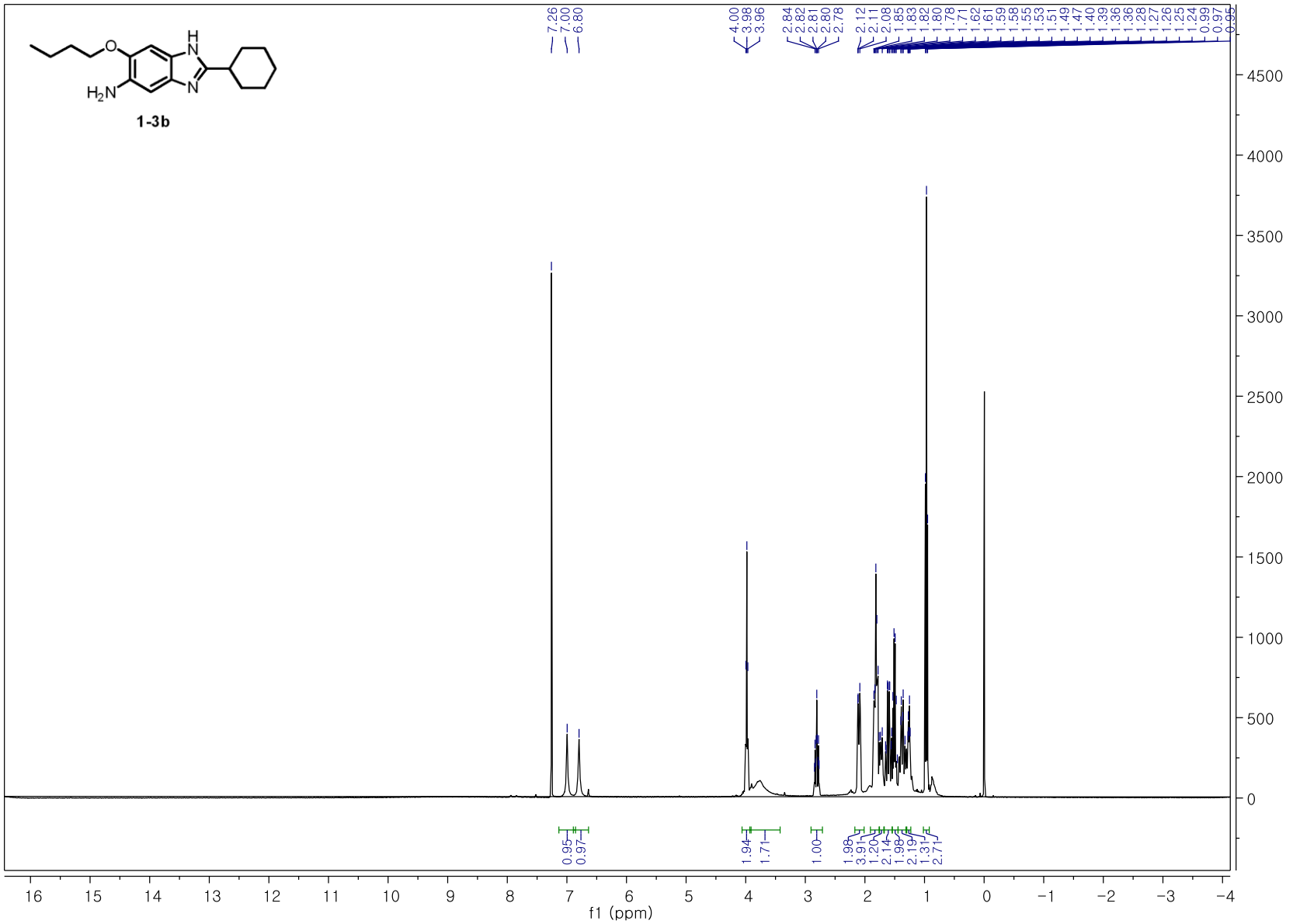
1-3b
7.26
7.00
6.80
4.00
3.98
3.96
2.84
2.82
2.81
2.80
2.78
2.12
2.11
2.08
1.85
1.83
1.82
1.80
1.78
1.71
1.62
1.61
1.59
1.58
1.55
1.53
1.51
1.49
1.47
1.40
1.39
1.36
1.36
1.28
1.27
1.26
1.25
1.24
0.99
0.97
0.95
0.95
0.97
1.94
1.71
1.00
1.98
3.91
1.20
2.14
1.98
2.19
1.31
2.71
f1 (ppm)

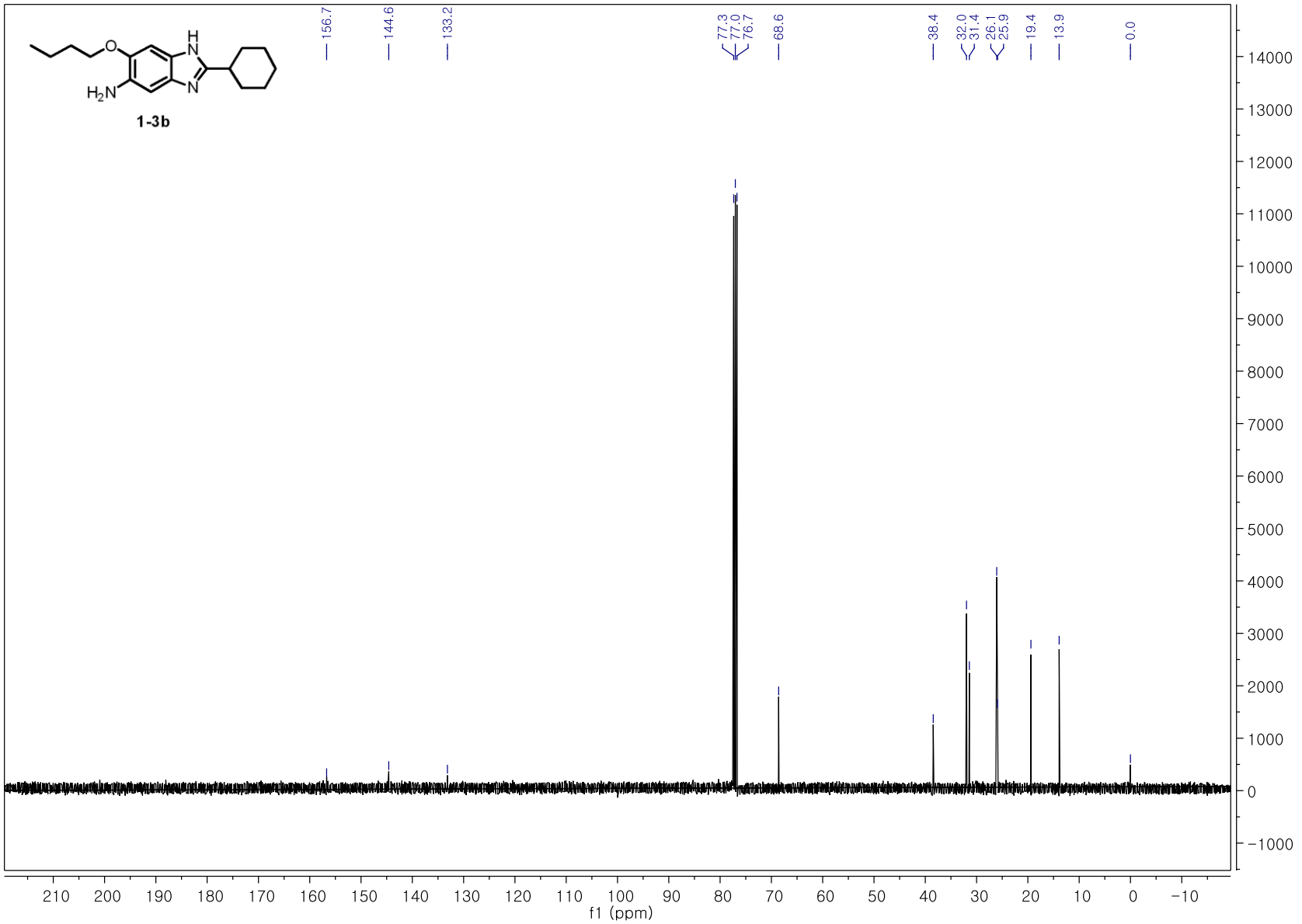
1-3b
156.7
144.6
133.2
77.3
77.0
76.7
68.6
38.4
32.0
31.4
26.1
25.9
19.4
13.9
0.0
f1 (ppm)

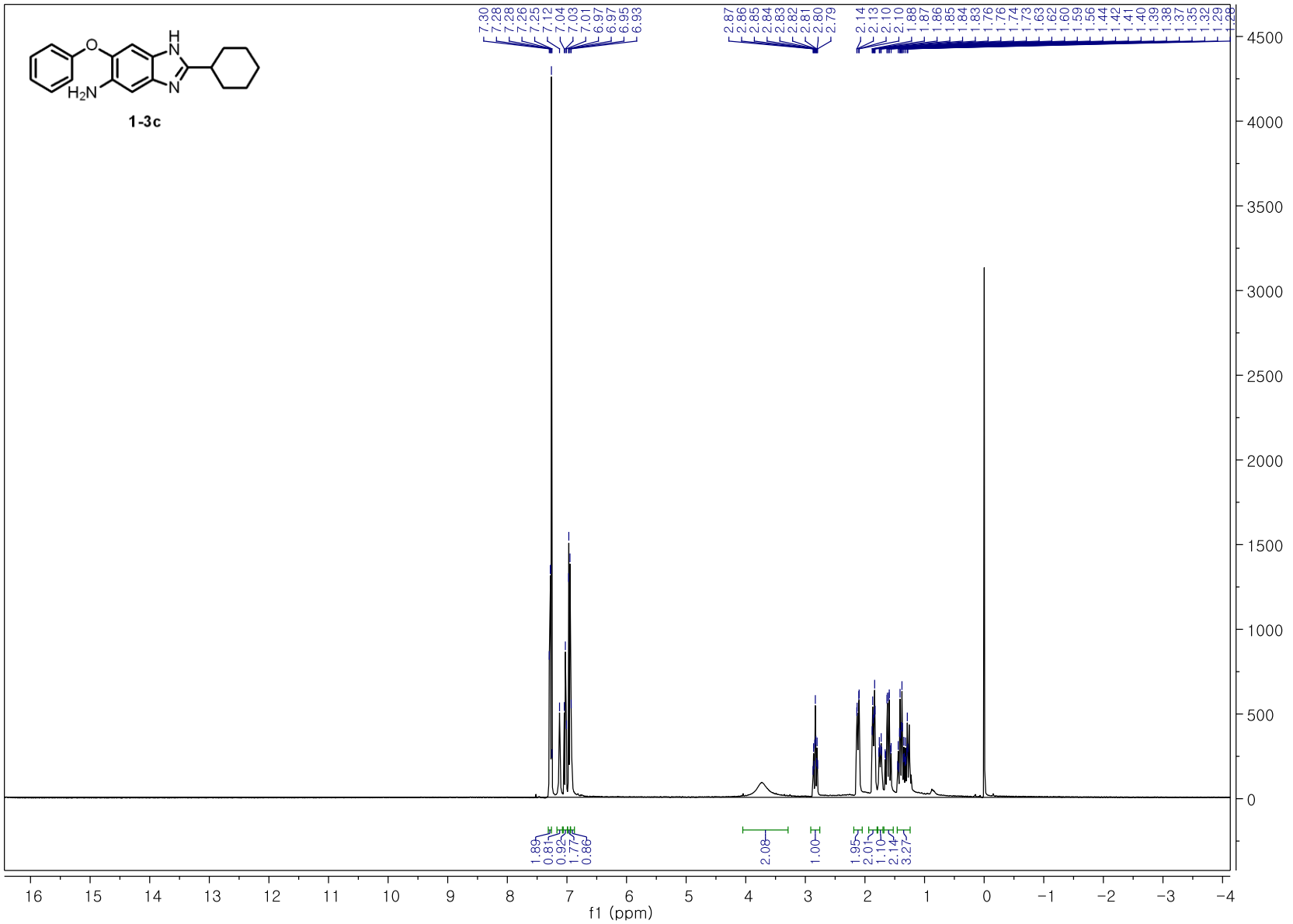
1-3c
7.30
7.28
7.28
7.26
7.25
7.12
7.04
7.03
7.01
6.97
6.95
6.93
2.87
2.86
2.85
2.84
2.83
2.82
2.81
2.80
2.79
2.14
2.13
2.10
2.10
1.88
1.87
1.86
1.85
1.84
1.83
1.76
1.76
1.74
1.73
1.63
1.62
1.60
1.59
1.56
1.44
1.42
1.41
1.40
1.39
1.38
1.37
1.35
1.32
1.29
1.28
1.89
0.81
0.92
1.77
0.86
2.08
1.00
1.95
2.01
1.10
2.14
3.27
f1 (ppm)

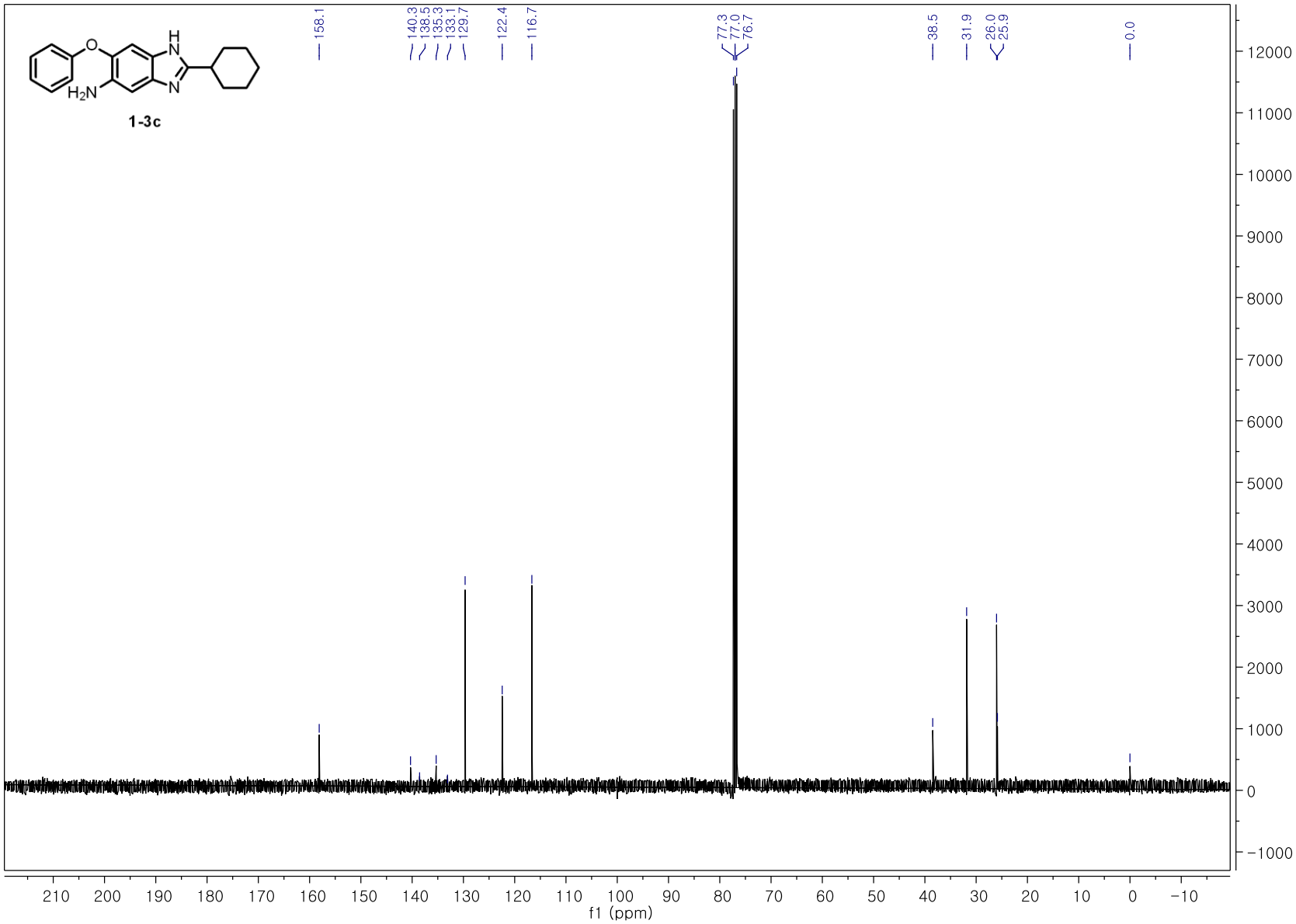
1-3c
158.1
140.3
138.5
135.3
133.1
129.7
122.4
116.7
77.3
77.0
76.7
38.5
31.9
26.0
25.9
0.0
f1 (ppm)

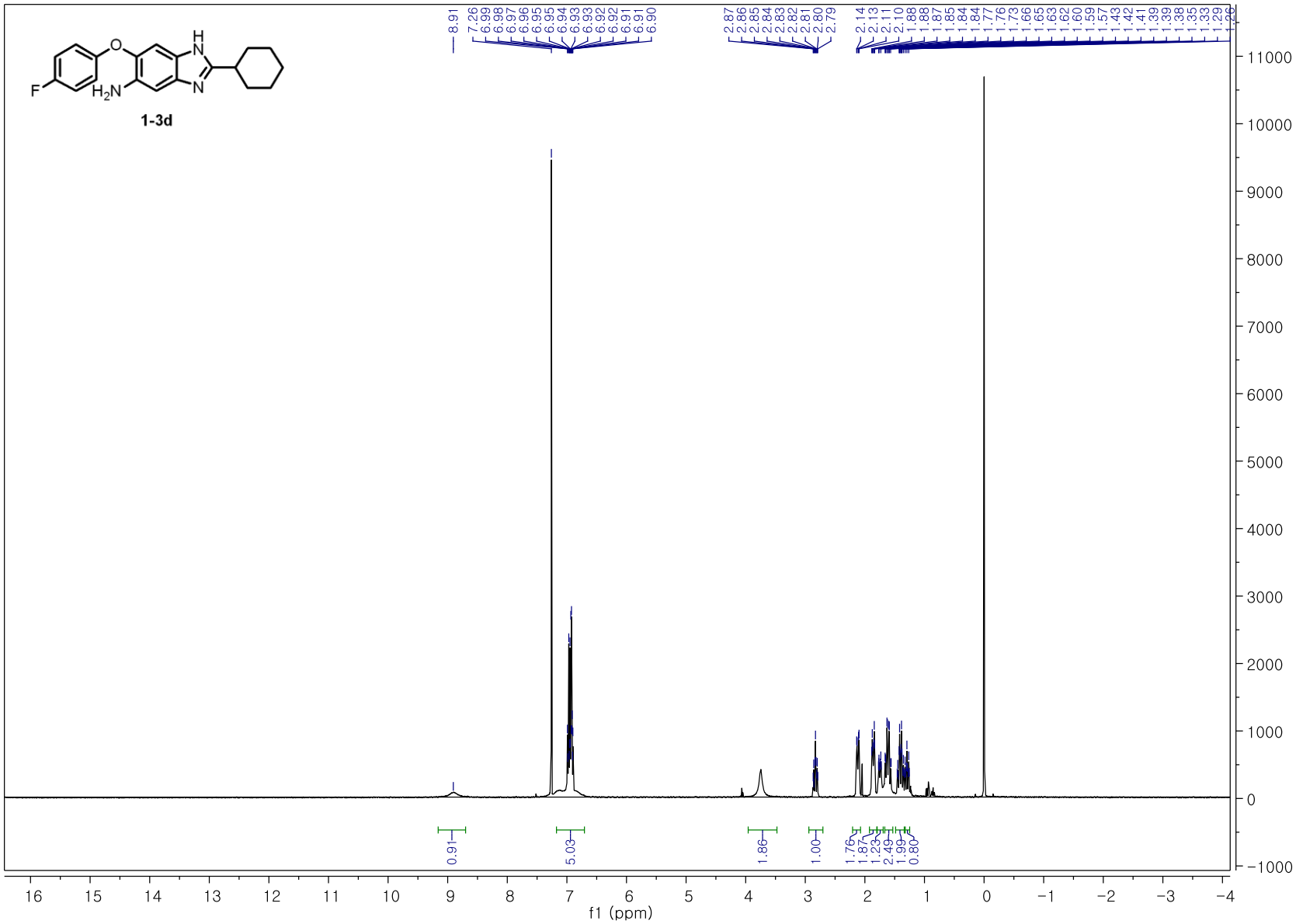
1-3d
f1 (ppm)

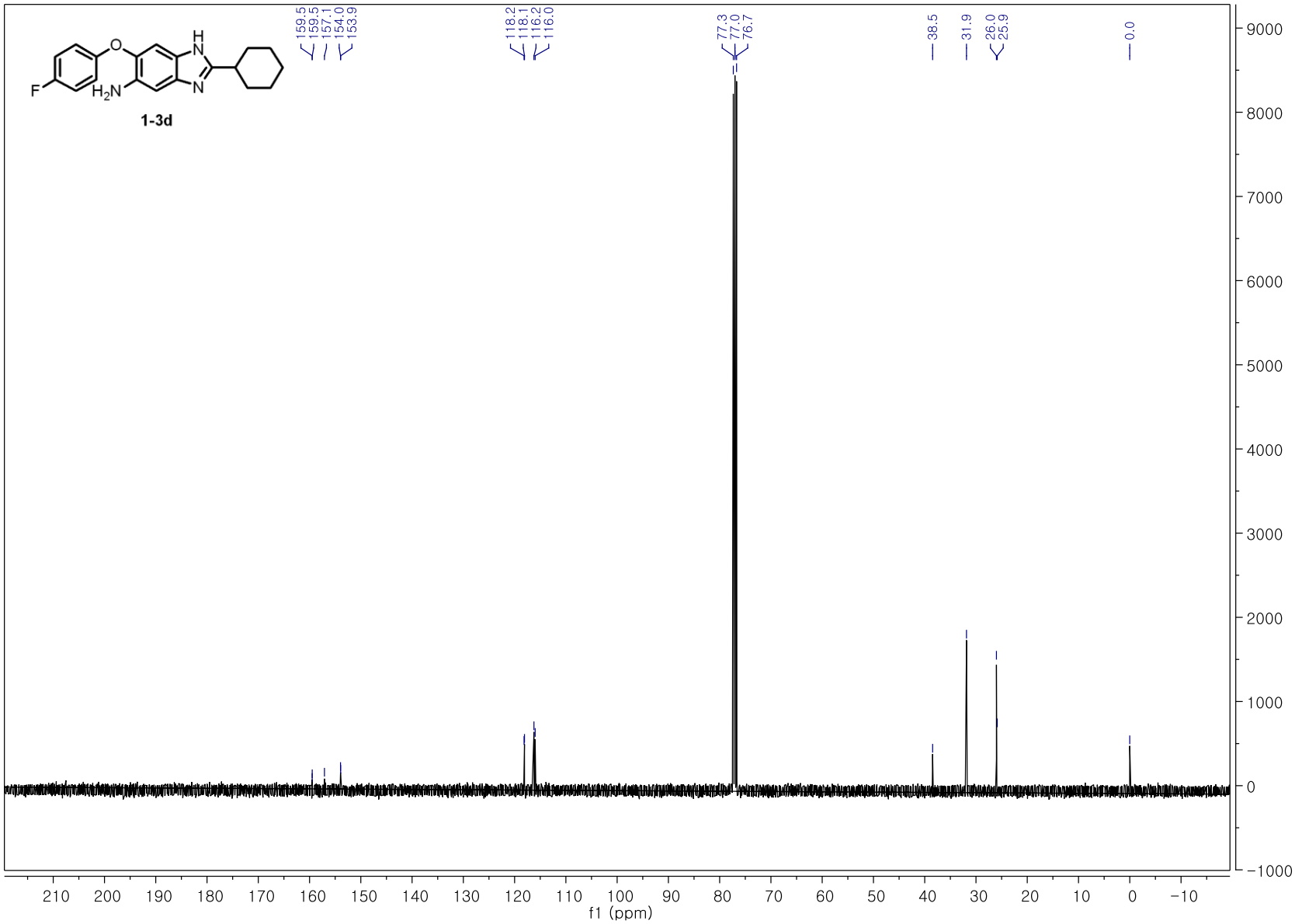
1-3d
159.5
159.5
157.1
154.0
153.9
118.2
118.1
116.2
116.0
77.3
77.0
76.7
38.5
31.9
26.0
25.9
0.0
f1 (ppm)

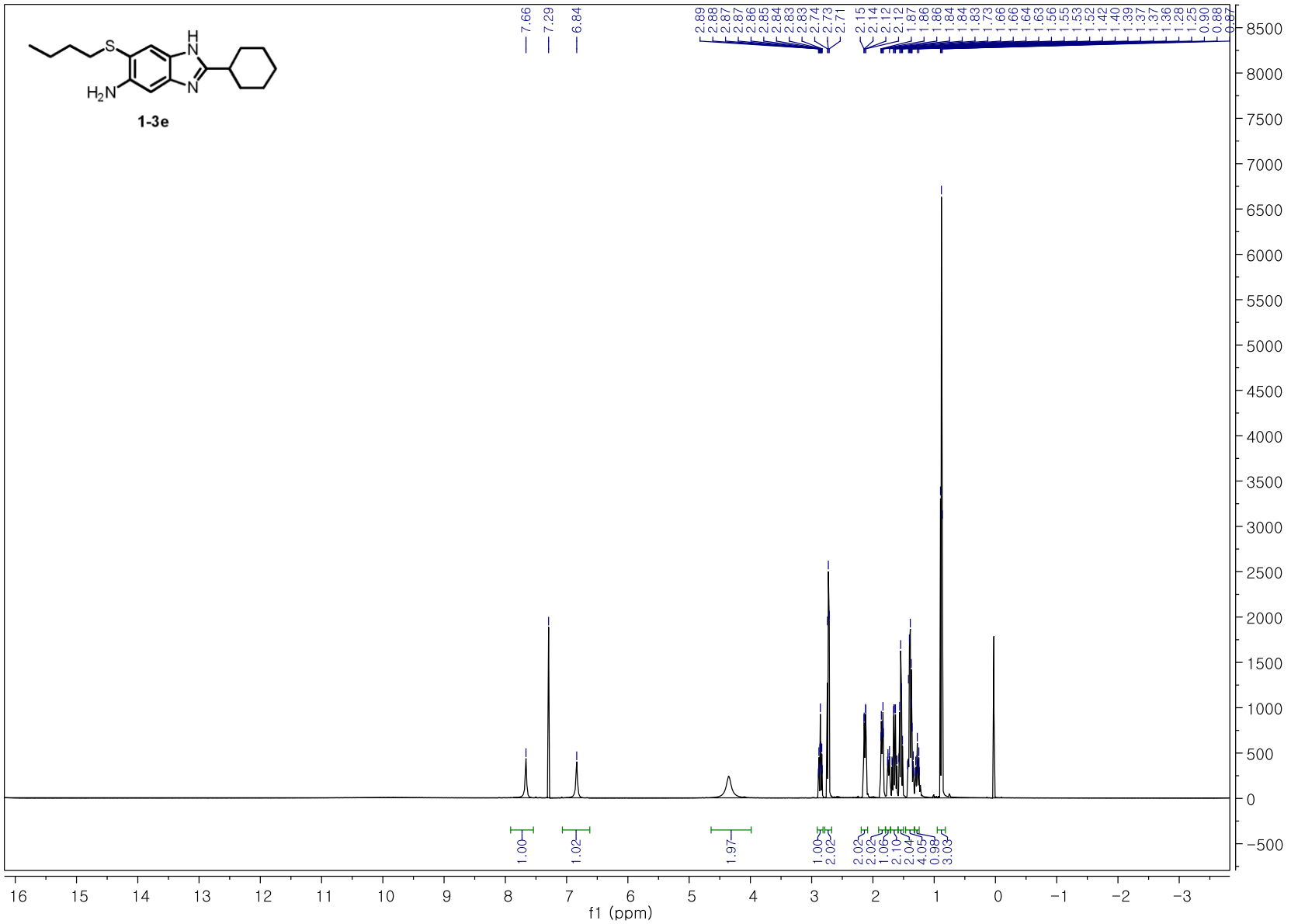
1-3e
7.66
7.29
6.84
2.89
2.88
2.87
2.87
2.86
2.85
2.84
2.83
2.83
2.74
2.73
2.71
2.15
2.14
2.12
2.12
1.87
1.86
1.86
1.84
1.84
1.83
1.73
1.66
1.66
1.64
1.63
1.56
1.55
1.53
1.52
1.42
1.40
1.39
1.37
1.37
1.36
1.28
1.25
0.90
0.88
0.87
1.00
1.02
1.97
1.00
2.02
2.02
2.02
1.06
2.10
2.04
4.05
0.98
3.03
f1 (ppm)

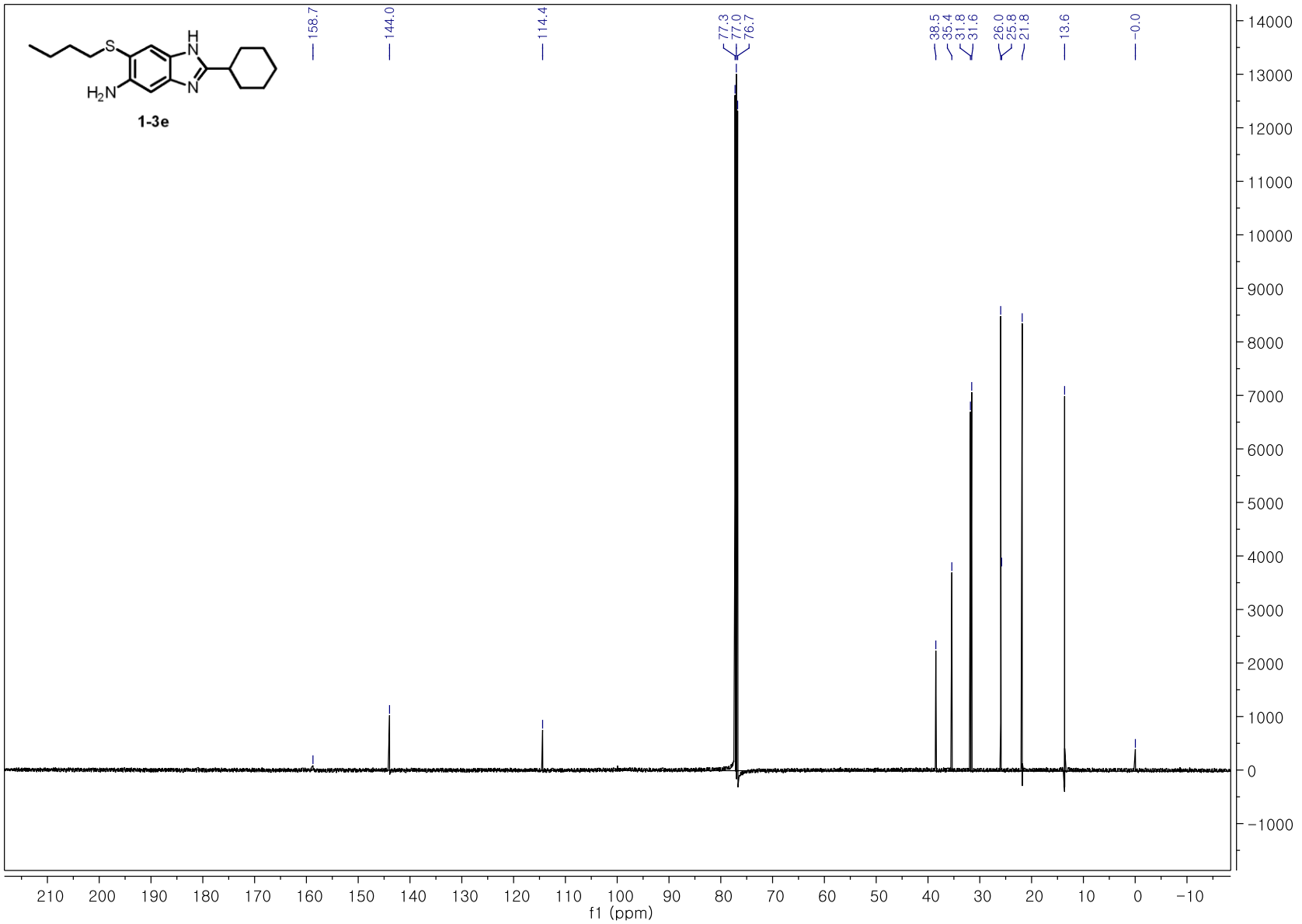
1-3e
158.7
144.0
114.4
77.3
77.0
76.7
38.5
35.4
31.8
31.6
26.0
25.8
21.8
13.6
0.0
f1 (ppm)

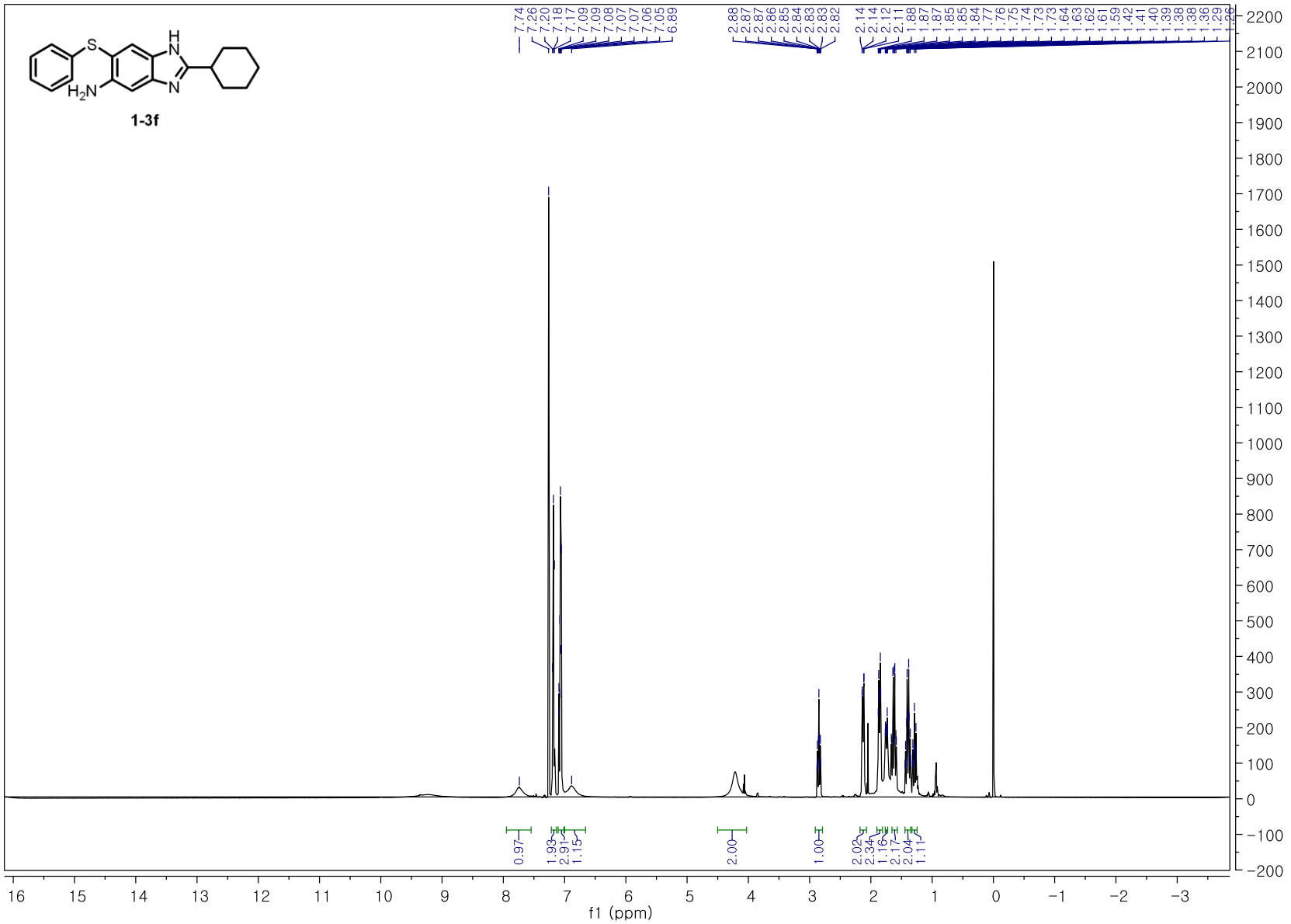
1-3f
7.74
7.26
7.20
7.18
7.17
7.09
7.09
7.08
7.07
7.07
7.06
7.05
6.89
2.88
2.87
2.87
2.86
2.85
2.84
2.83
2.83
2.82
2.14
2.14
2.12
2.11
1.88
1.87
1.87
1.85
1.85
1.84
1.77
1.76
1.75
1.74
1.73
1.64
1.63
1.62
1.61
1.59
1.42
1.41
1.40
1.39
1.38
1.38
1.36
1.29
0.97
1.93
2.91
1.15
2.00
1.00
2.02
2.34
1.16
2.17
2.04
1.11
f1 (ppm)

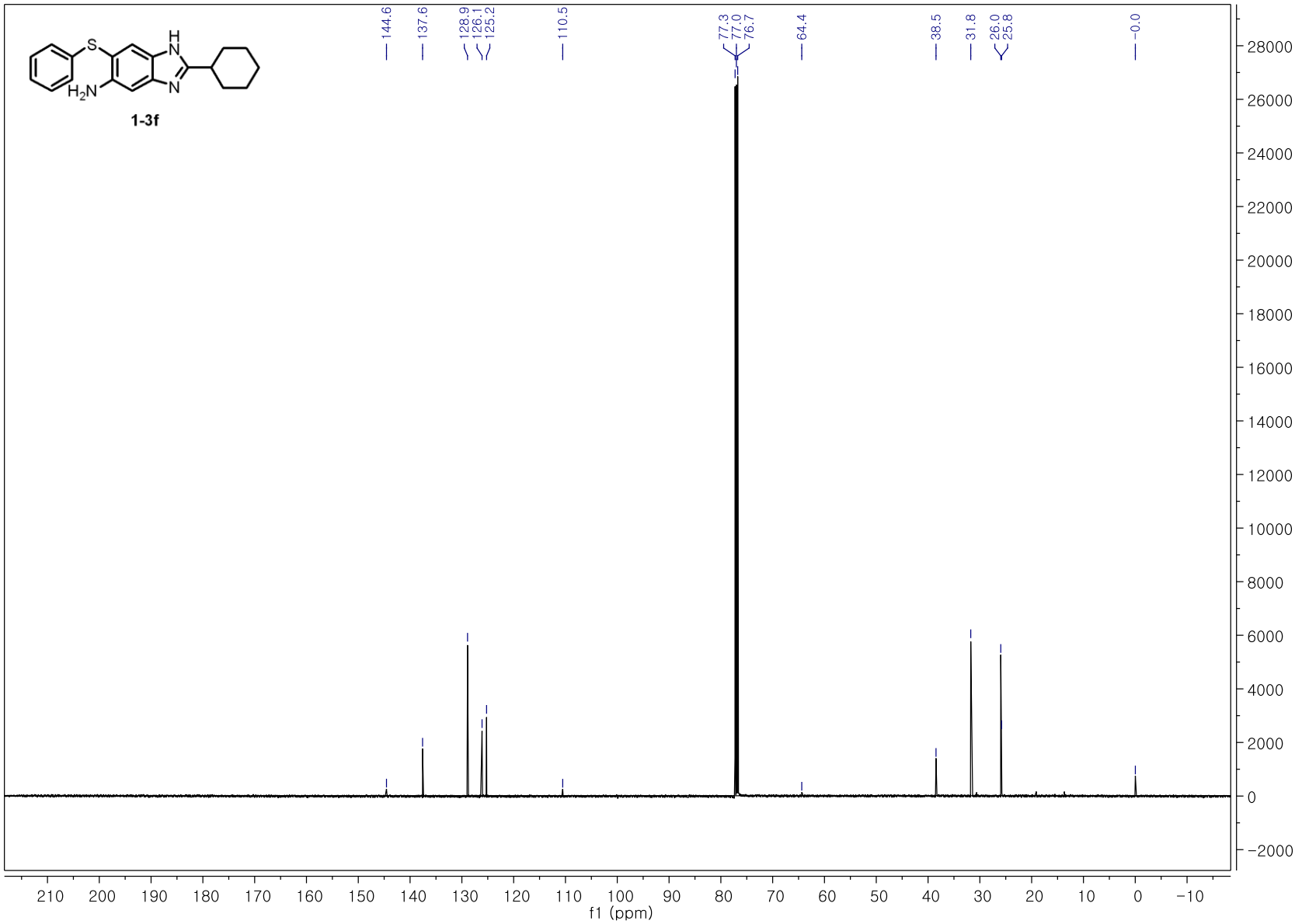
1-3f
144.6
137.6
128.9
126.1
125.2
110.5
77.3
77.0
76.7
64.4
38.5
31.8
26.0
25.8
0.0
f1 (ppm)

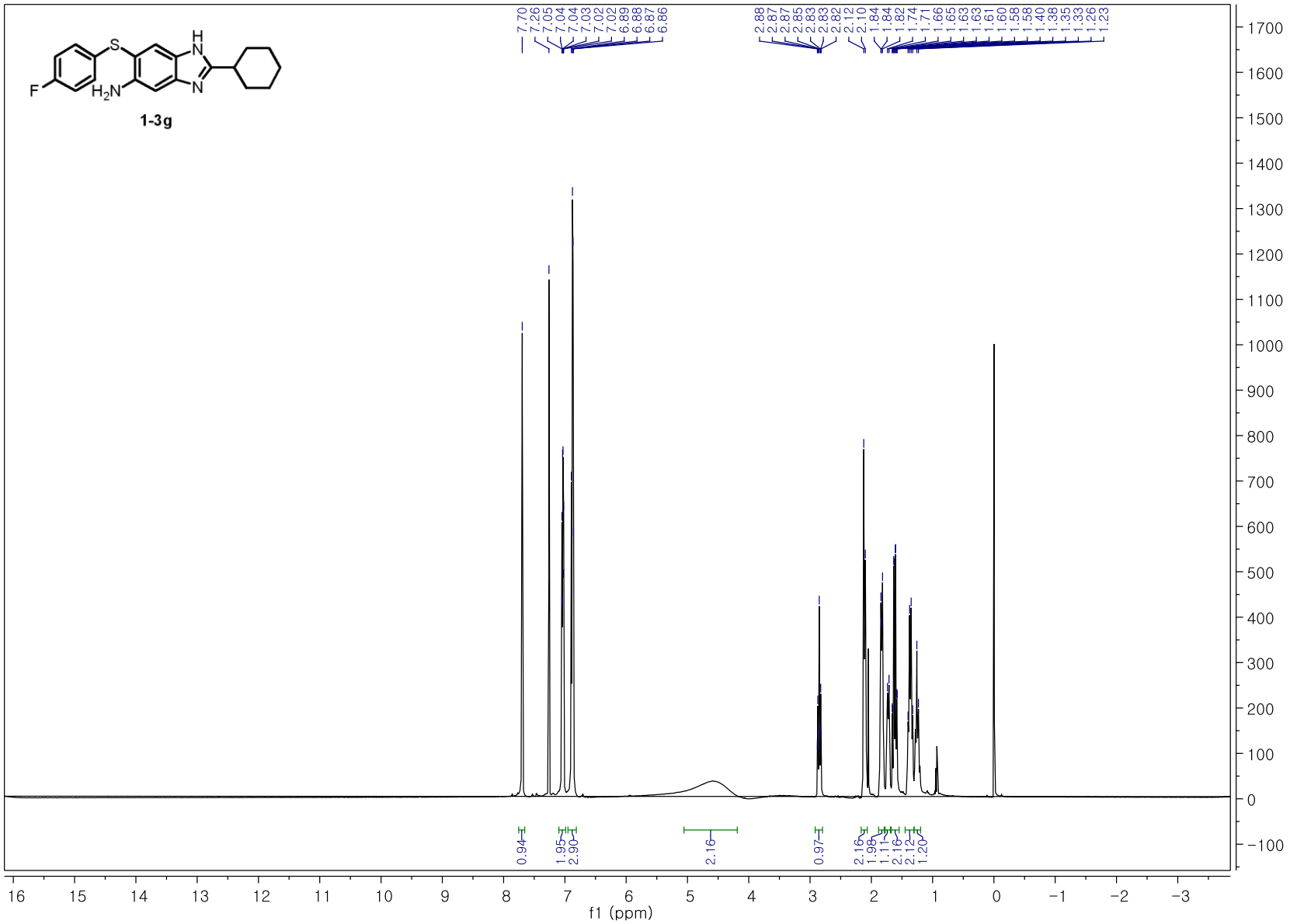
1-3g
7.70
7.26
7.05
7.04
7.04
7.03
7.02
7.02
6.89
6.88
6.87
6.86
2.88
2.87
2.87
2.85
2.83
2.83
2.82
2.12
2.10
1.84
1.84
1.82
1.74
1.71
1.66
1.65
1.63
1.63
1.61
1.60
1.58
1.58
1.40
1.38
1.35
1.33
1.26
1.23
0.94
1.95
2.90
2.16
0.97
2.16
1.98
1.11
2.16
2.12
1.20
f1 (ppm)

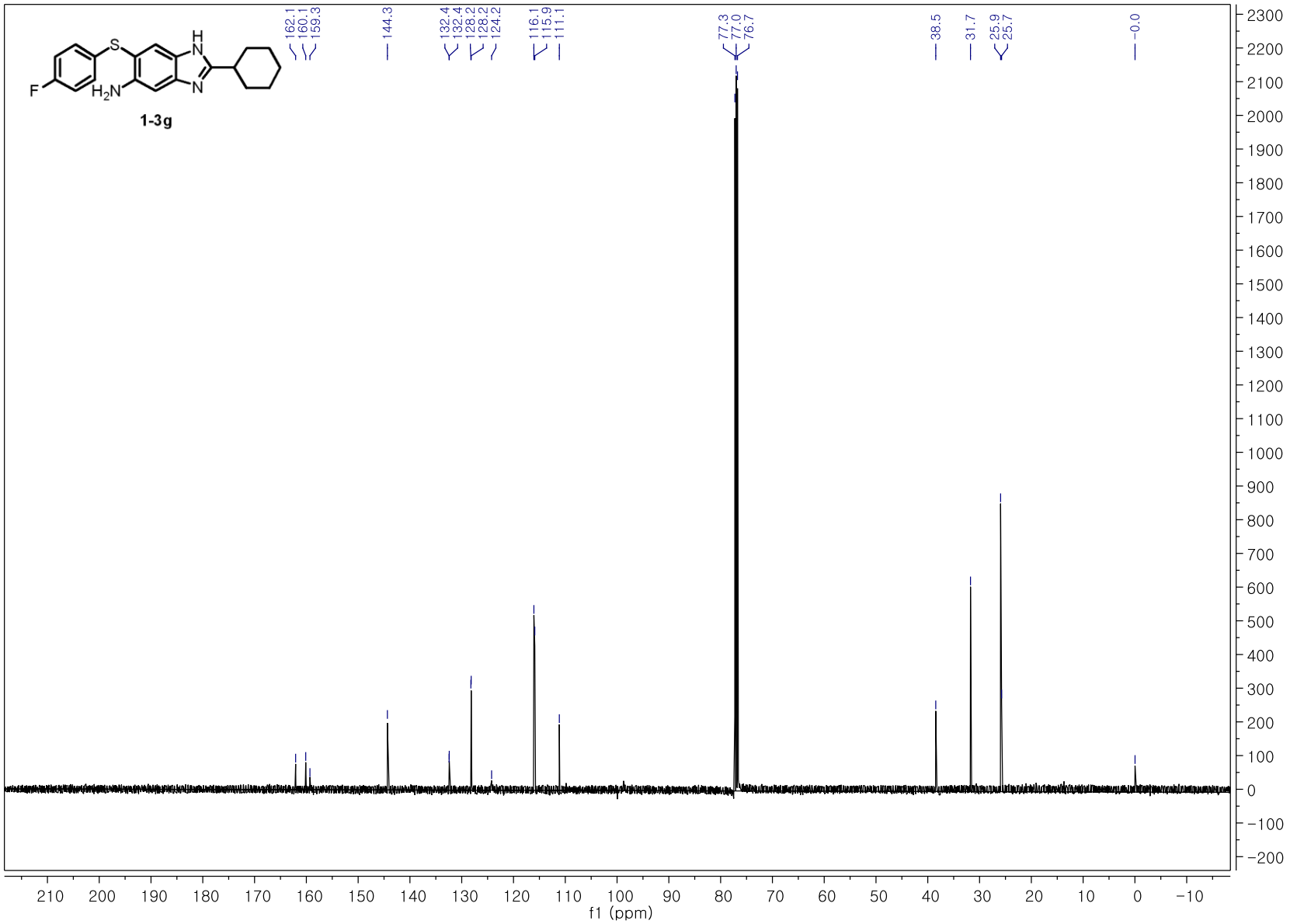
1-3g
162.1
160.1
159.3
144.3
132.4
132.4
128.2
128.2
124.2
116.1
115.9
111.1
77.3
77.0
76.7
38.5
31.7
25.9
25.7
0.0
f1 (ppm)

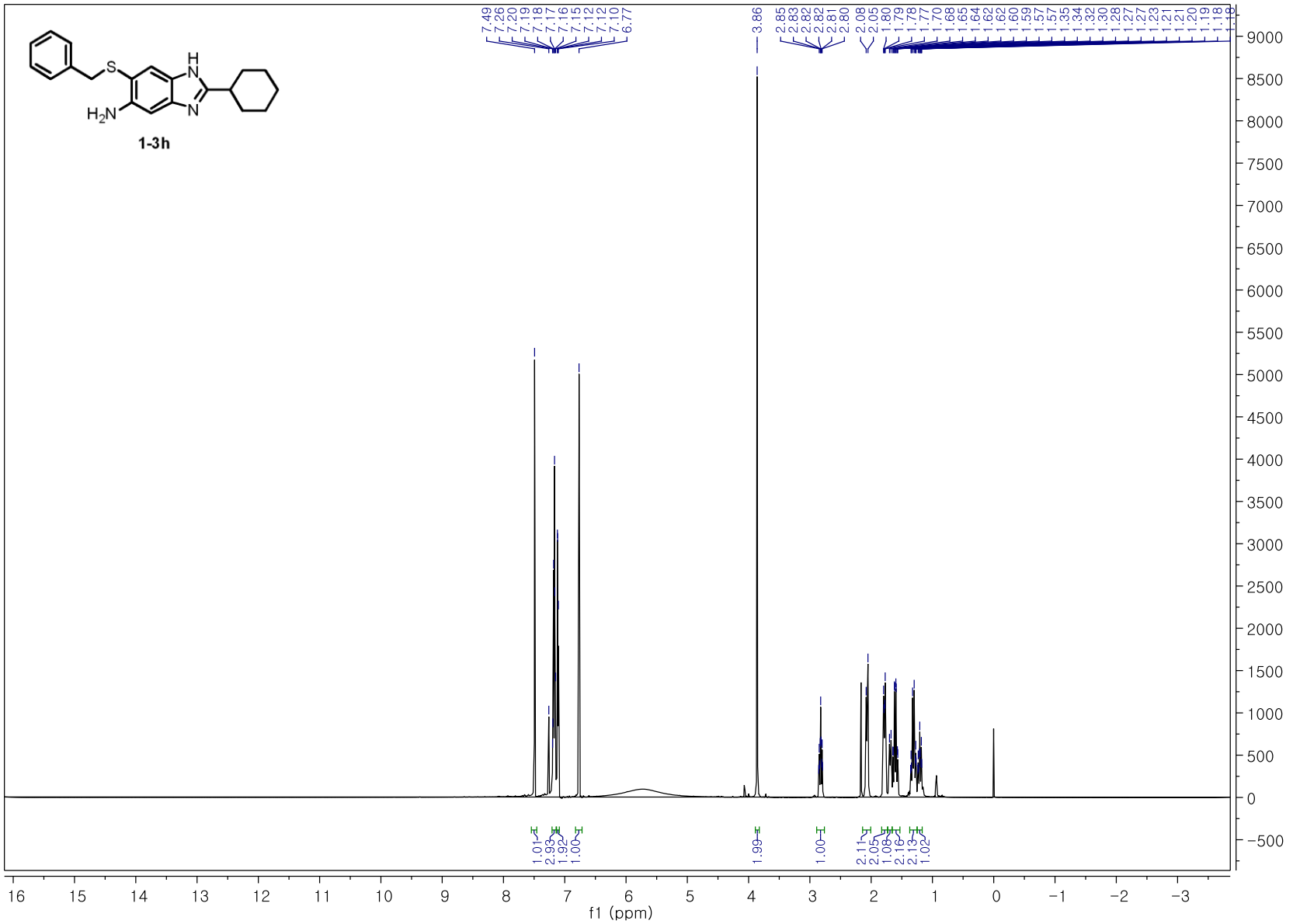
1-3h
f1 (ppm)

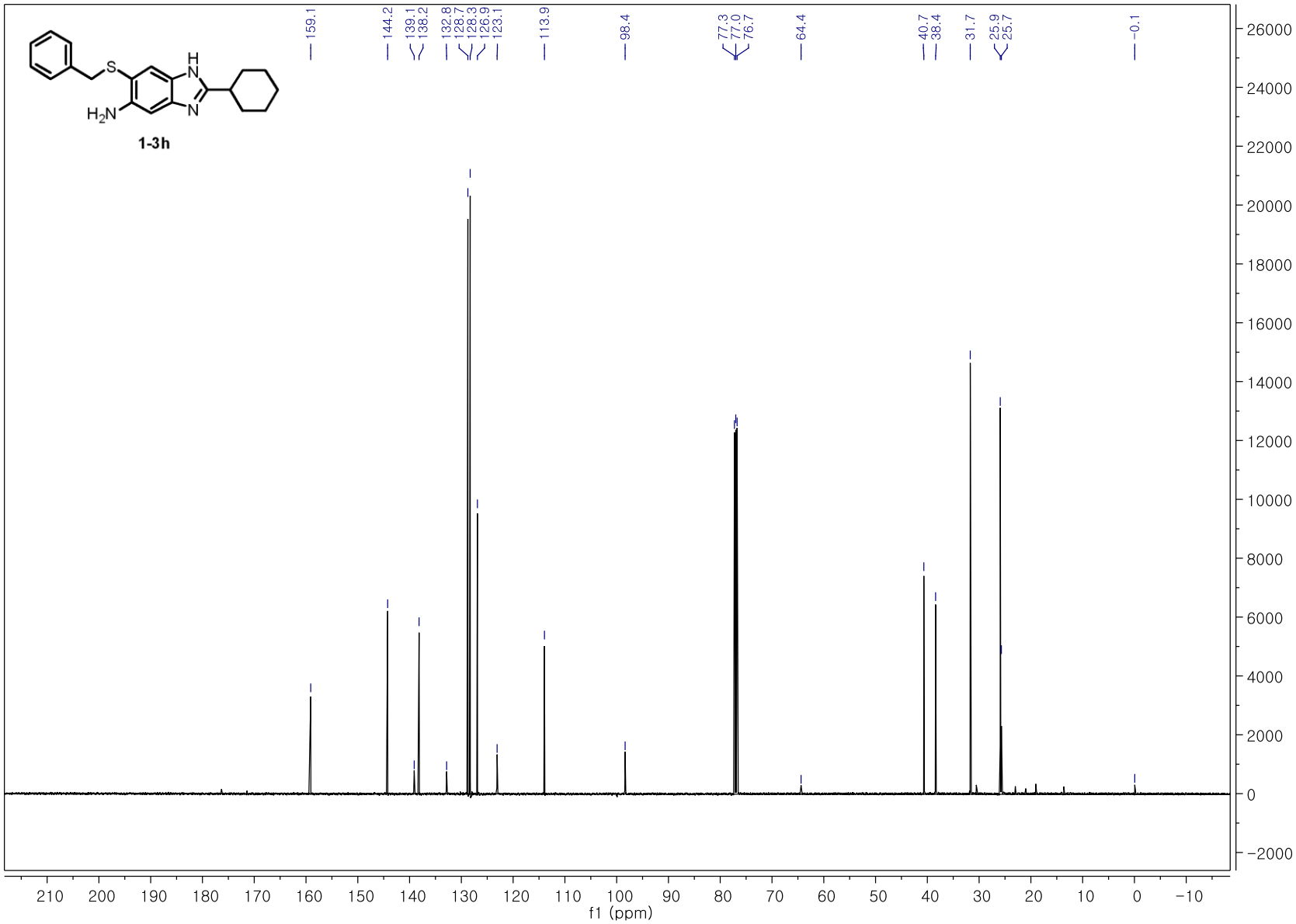
1-3h
159.1
144.2
139.1
138.2
132.8
128.7
128.3
126.9
123.1
113.9
98.4
77.3
77.0
76.7
64.4
40.7
38.4
31.7
25.9
25.7
-0.1
f1 (ppm)

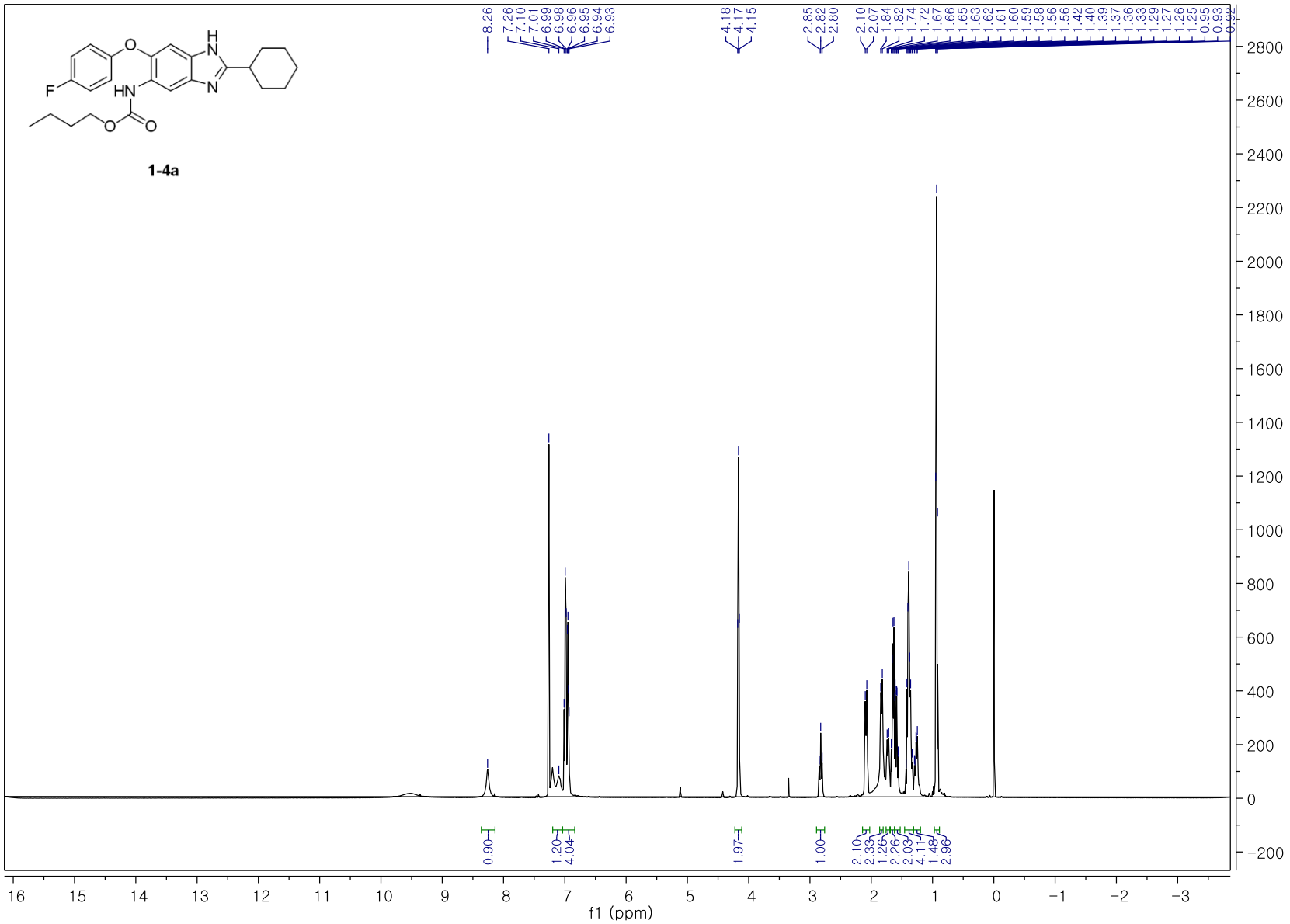
1-4a
f1 (ppm)

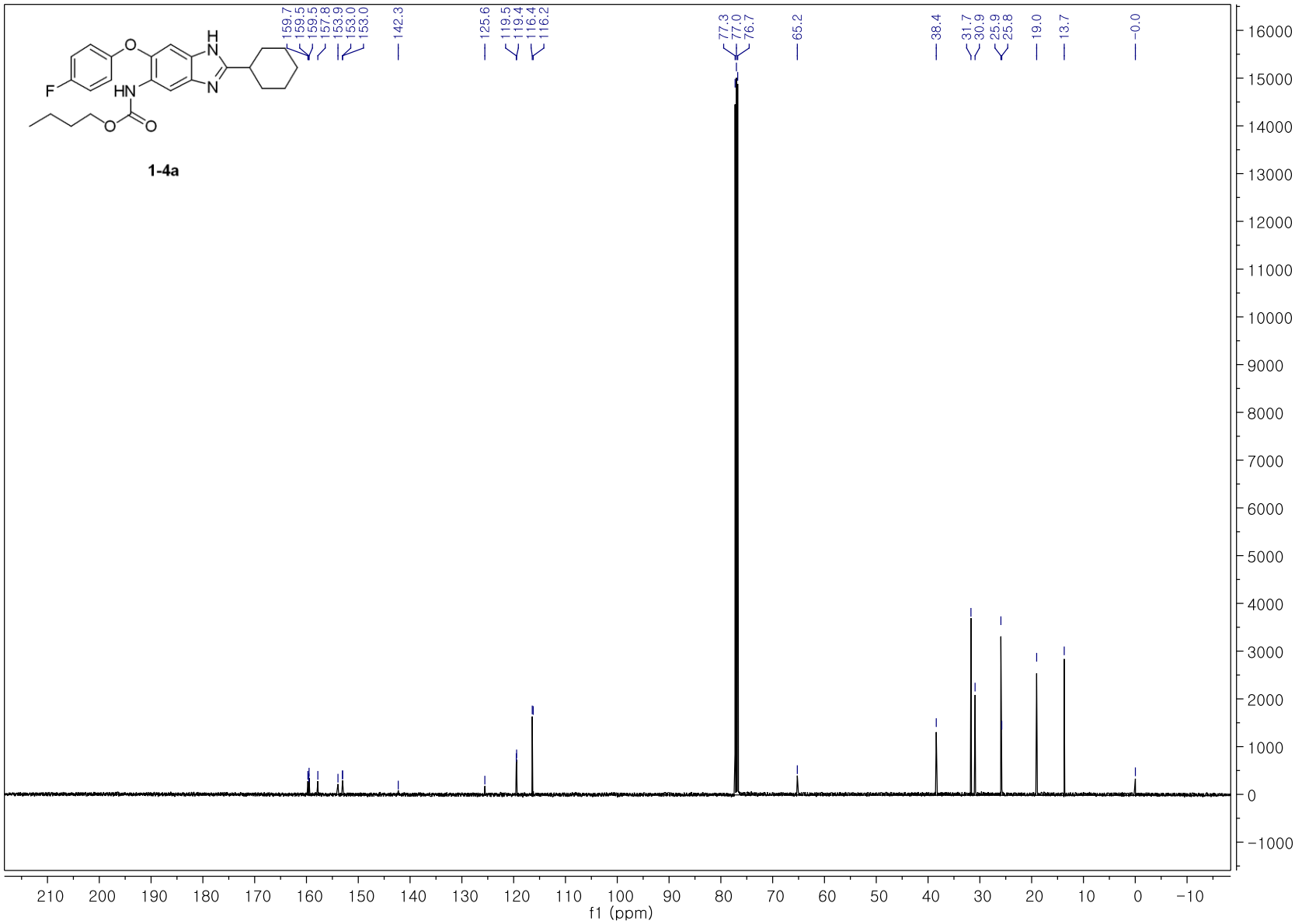
1-4a
159.7
159.5
159.5
157.8
153.9
153.0
153.0
142.3
125.6
119.5
119.4
116.4
116.2
77.3
77.0
76.7
65.2
38.4
31.7
30.9
25.9
25.8
19.0
13.7
-0.0
f1 (ppm)

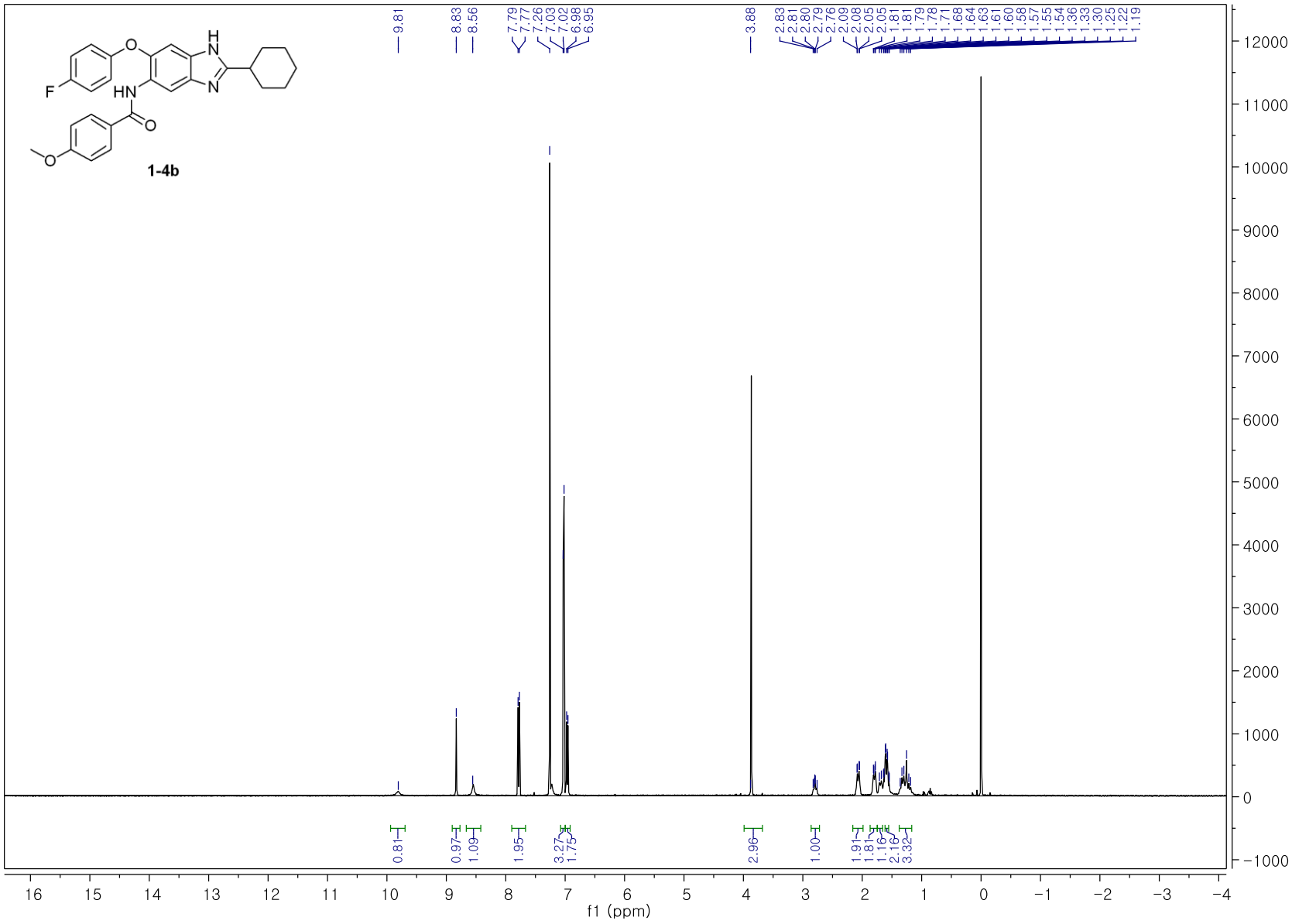
1-4b
9.81
8.83
8.56
7.79
7.77
7.26
7.03
7.02
6.98
6.95
3.88
2.83
2.81
2.80
2.79
2.76
2.09
2.08
2.05
2.05
1.81
1.81
1.79
1.78
1.71
1.68
1.64
1.63
1.61
1.60
1.58
1.57
1.55
1.54
1.36
1.33
1.30
1.25
1.22
1.19
0.81
0.97
1.09
1.95
3.27
1.75
2.96
1.00
1.91
1.81
1.16
2.16
3.32
f1 (ppm)

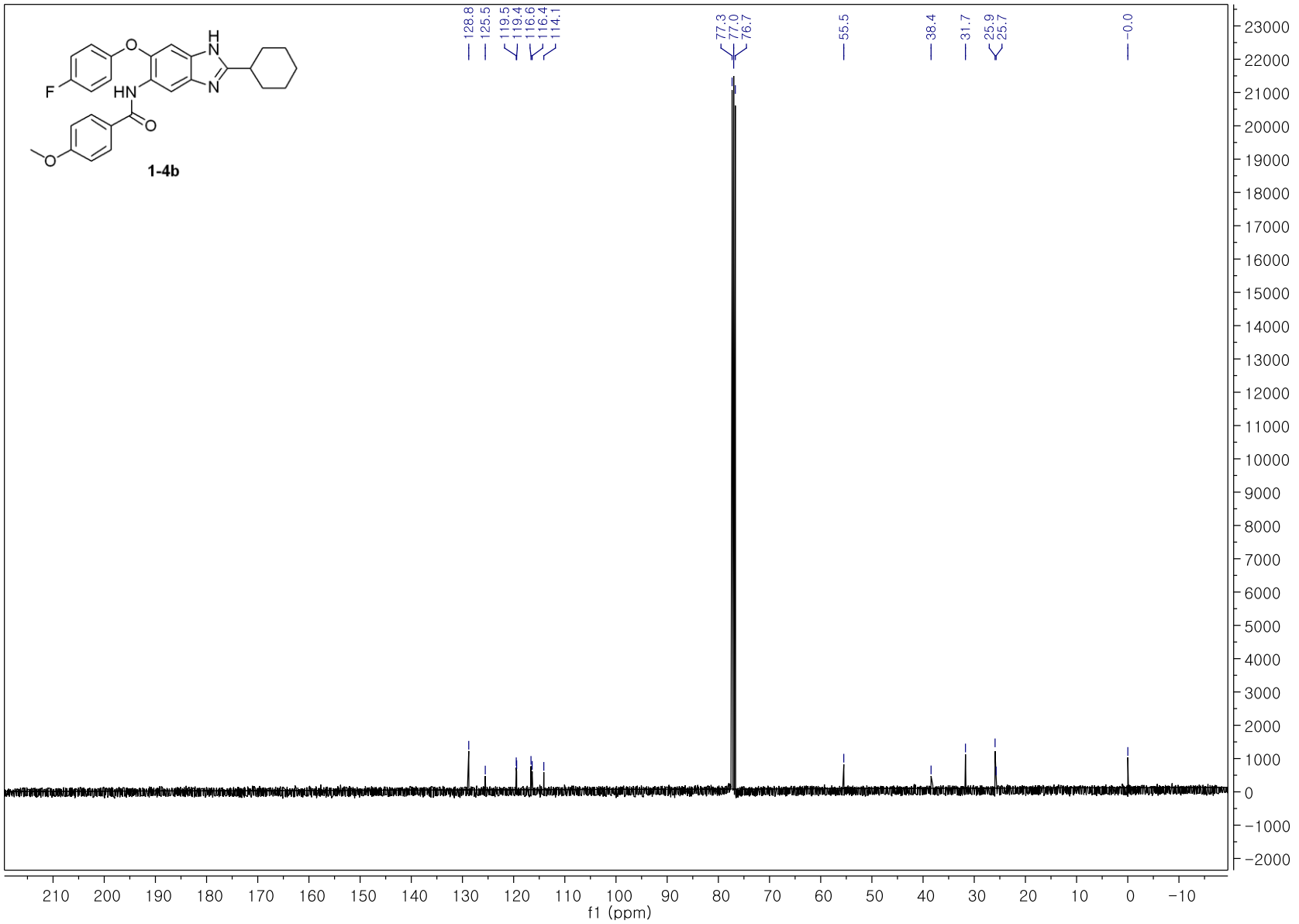
1-4b
128.8
125.5
119.5
119.4
116.6
116.4
114.1
77.3
77.0
76.7
55.5
38.4
31.7
25.9
25.7
0.0
f1 (ppm)

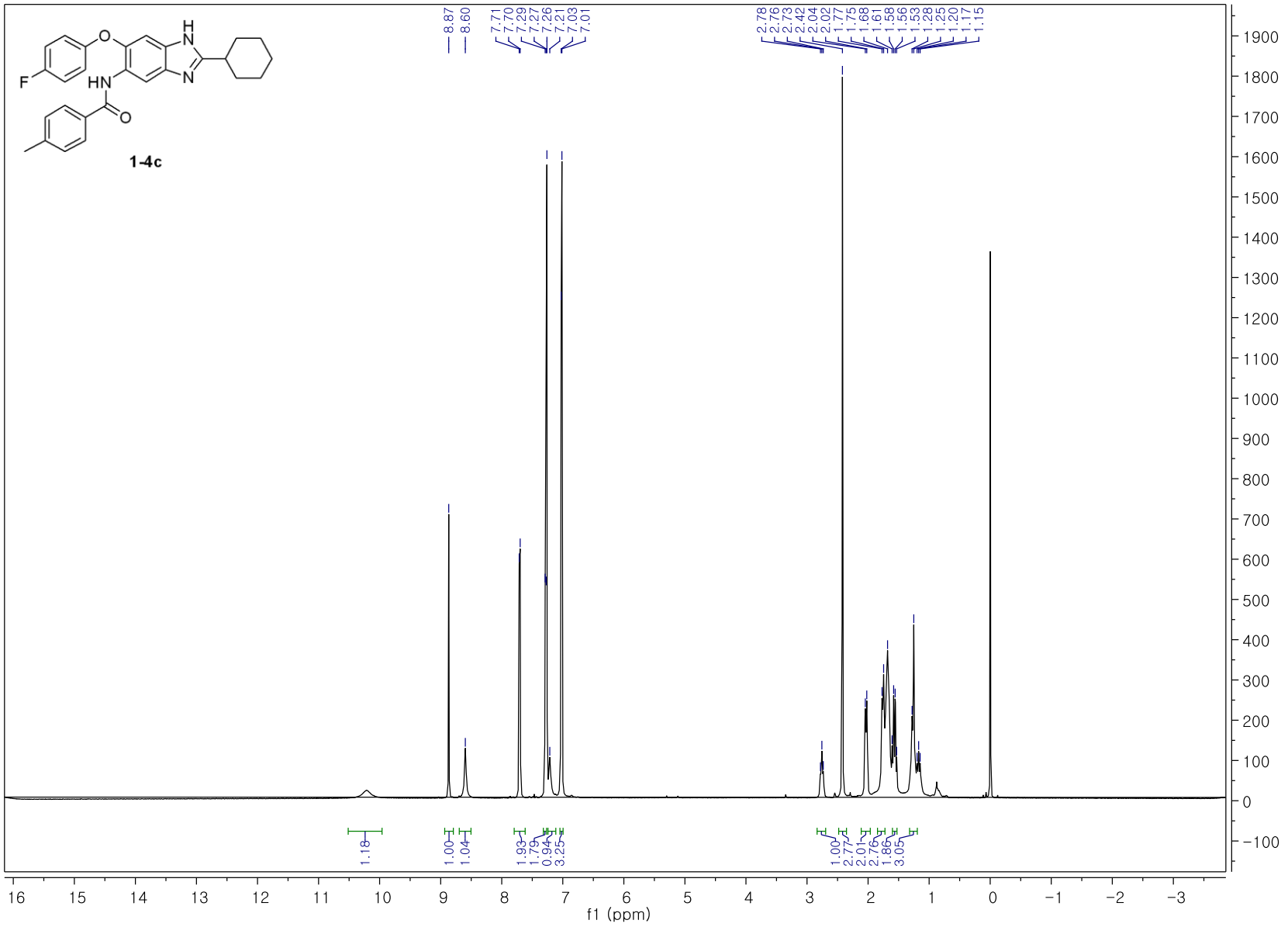
1-4c
8.87
8.60
7.71
7.70
7.29
7.27
7.26
7.21
7.03
7.01
2.78
2.76
2.73
2.42
2.04
2.02
1.77
1.75
1.68
1.61
1.58
1.56
1.53
1.28
1.25
1.20
1.17
1.15
1.18
1.00
1.04
1.93
1.79
0.94
3.25
1.00
2.77
2.01
2.76
1.86
3.05
f1 (ppm)

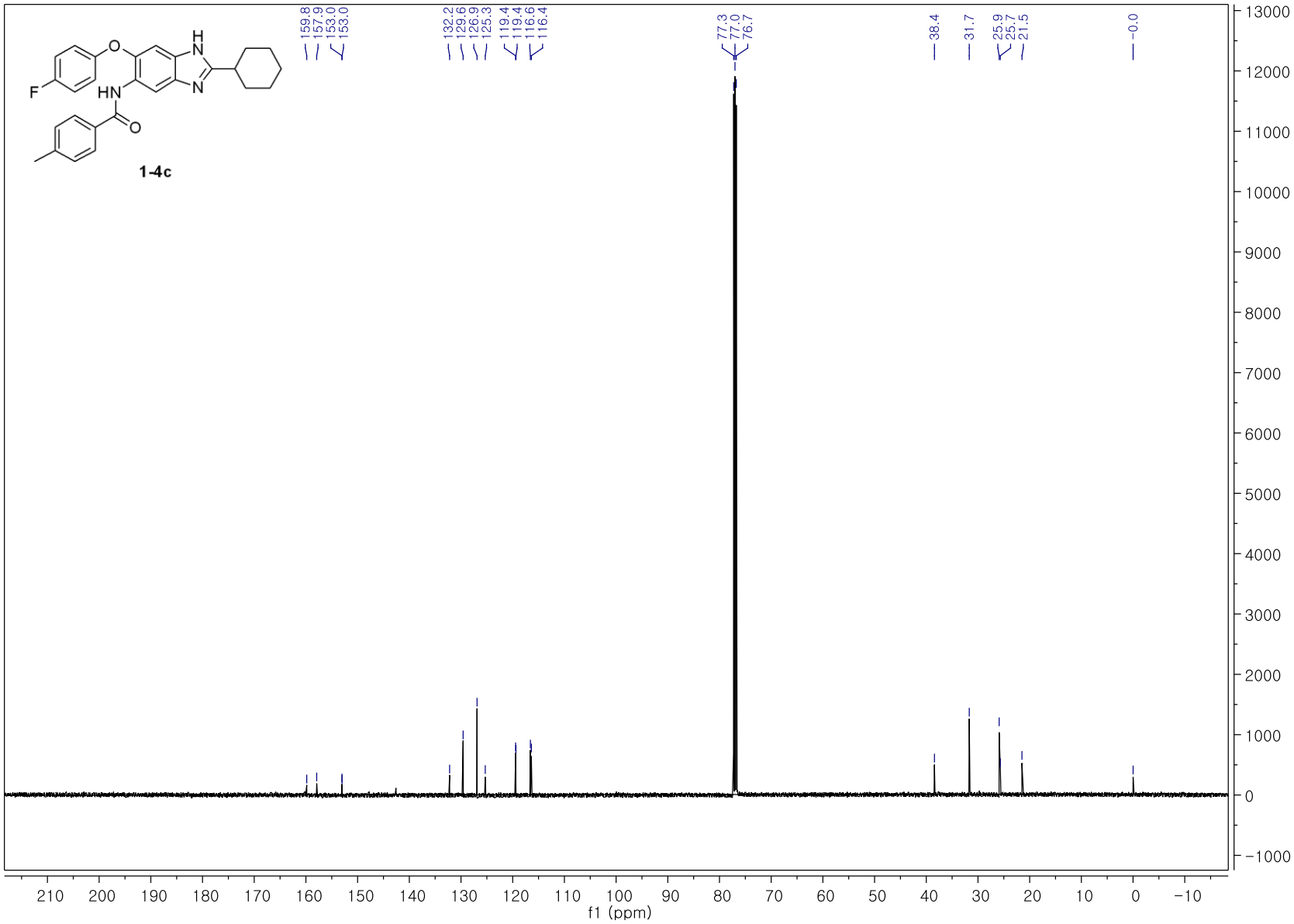
1-4c
159.8
157.9
153.0
153.0
132.2
129.6
126.9
125.3
119.4
119.4
116.6
116.4
77.3
77.0
76.7
38.4
31.7
25.9
25.7
21.5
0.0
f1 (ppm)

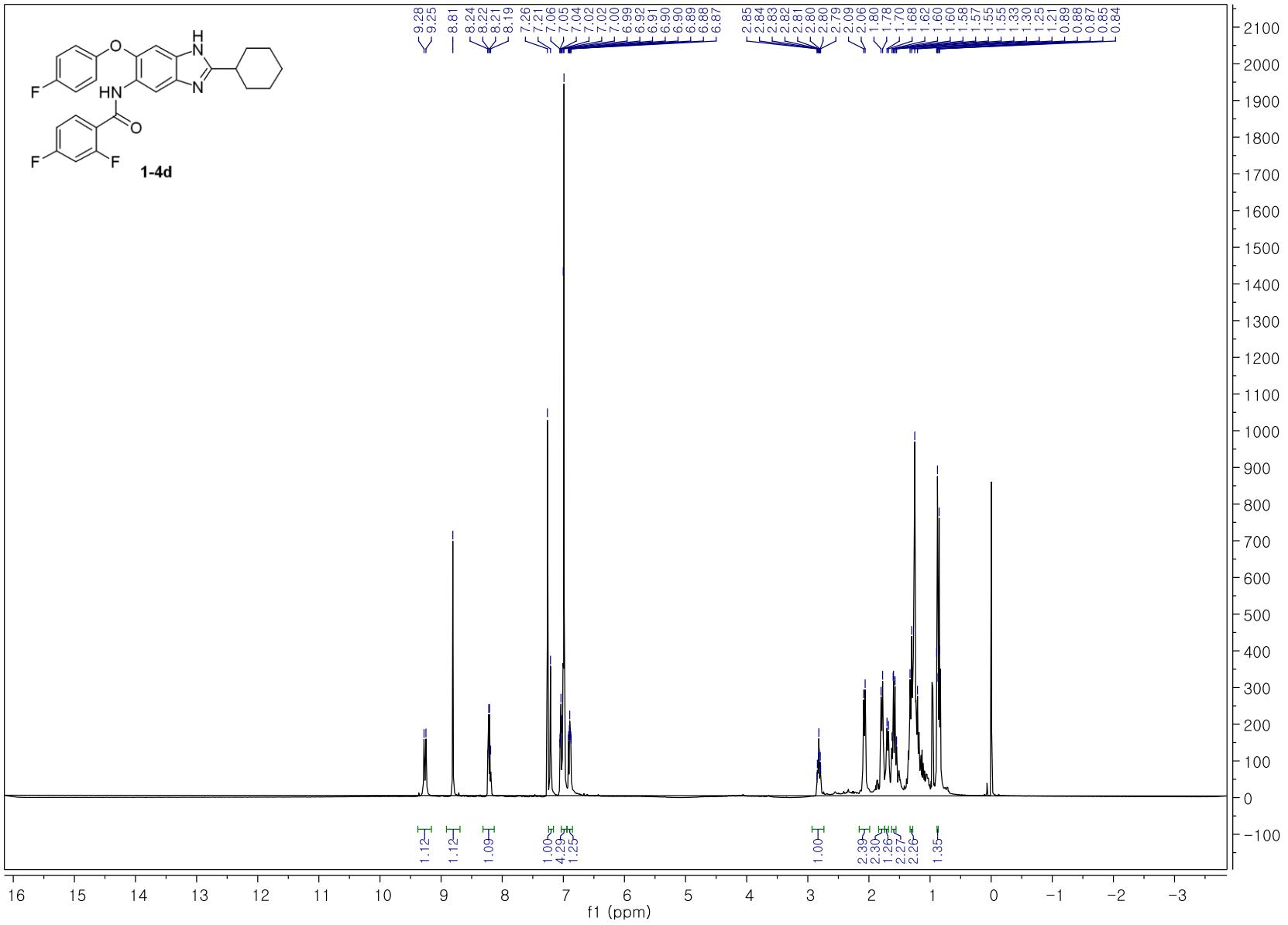
1-4d
f1 (ppm)

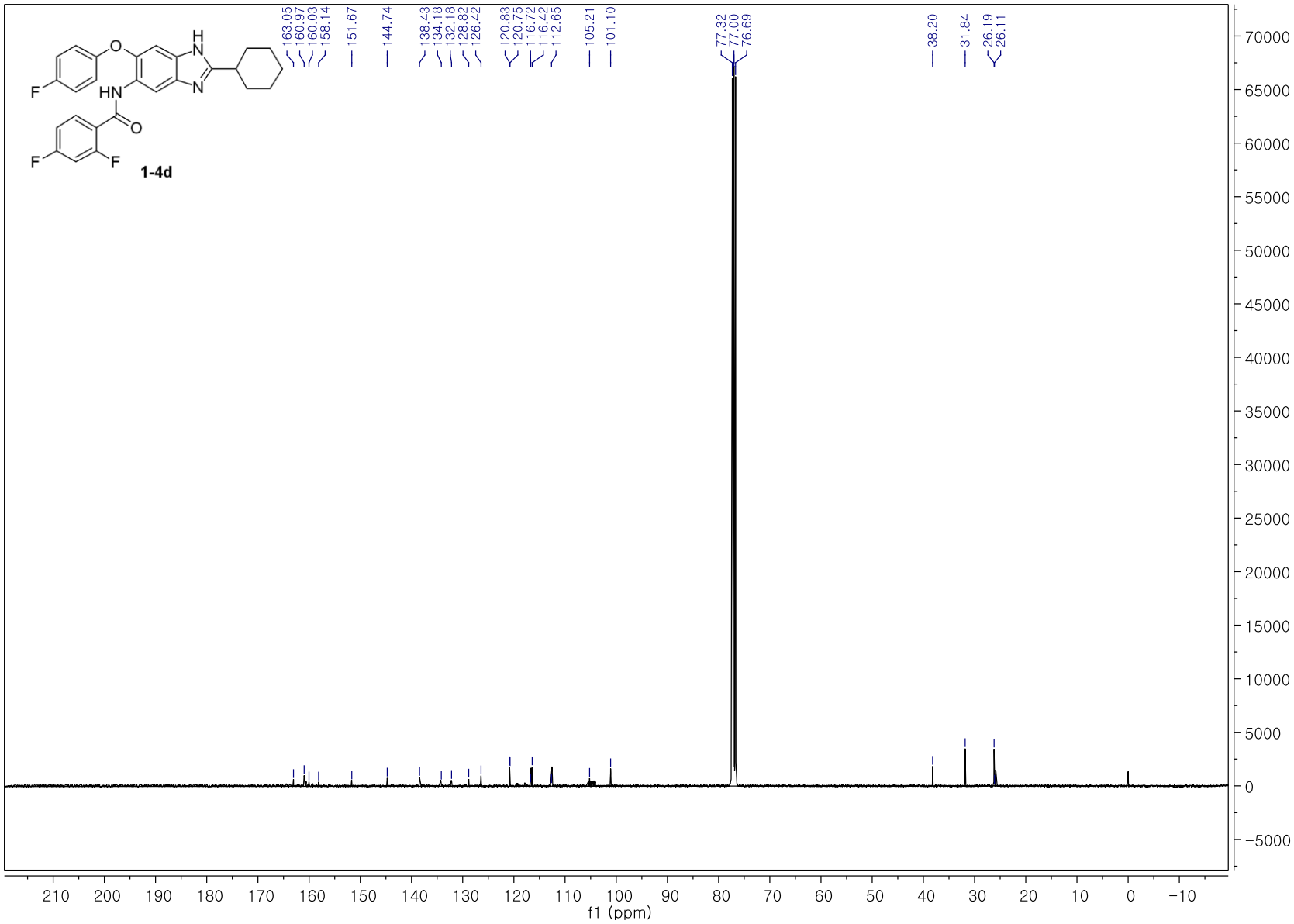
1-4d
163.05
160.97
160.03
158.14
151.67
144.74
138.43
134.18
132.18
128.82
126.42
120.83
120.75
116.72
116.42
112.65
105.21
101.10
77.32
77.00
76.69
38.20
31.84
26.19
26.11
f1 (ppm)

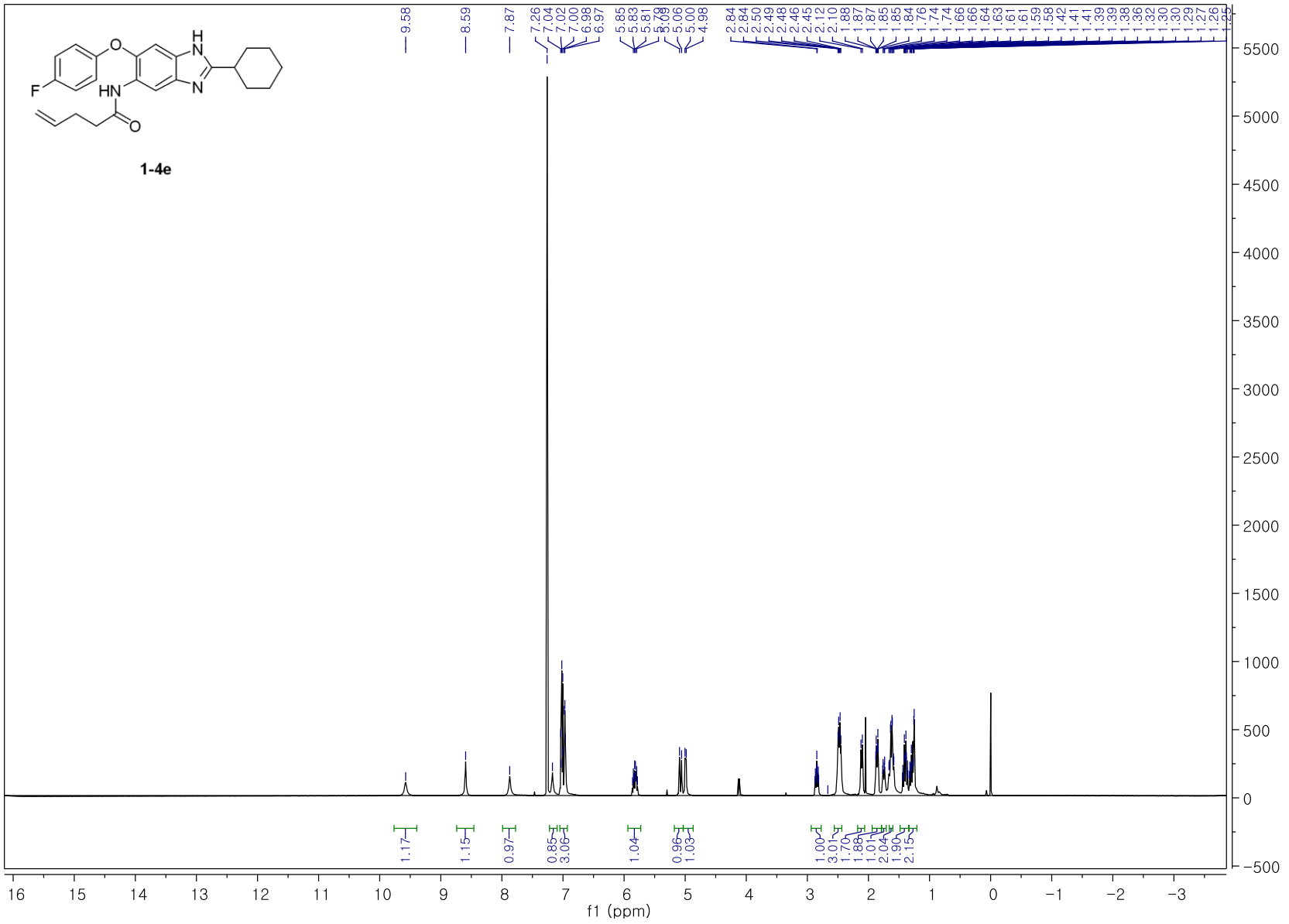
1-4e
f1 (ppm)

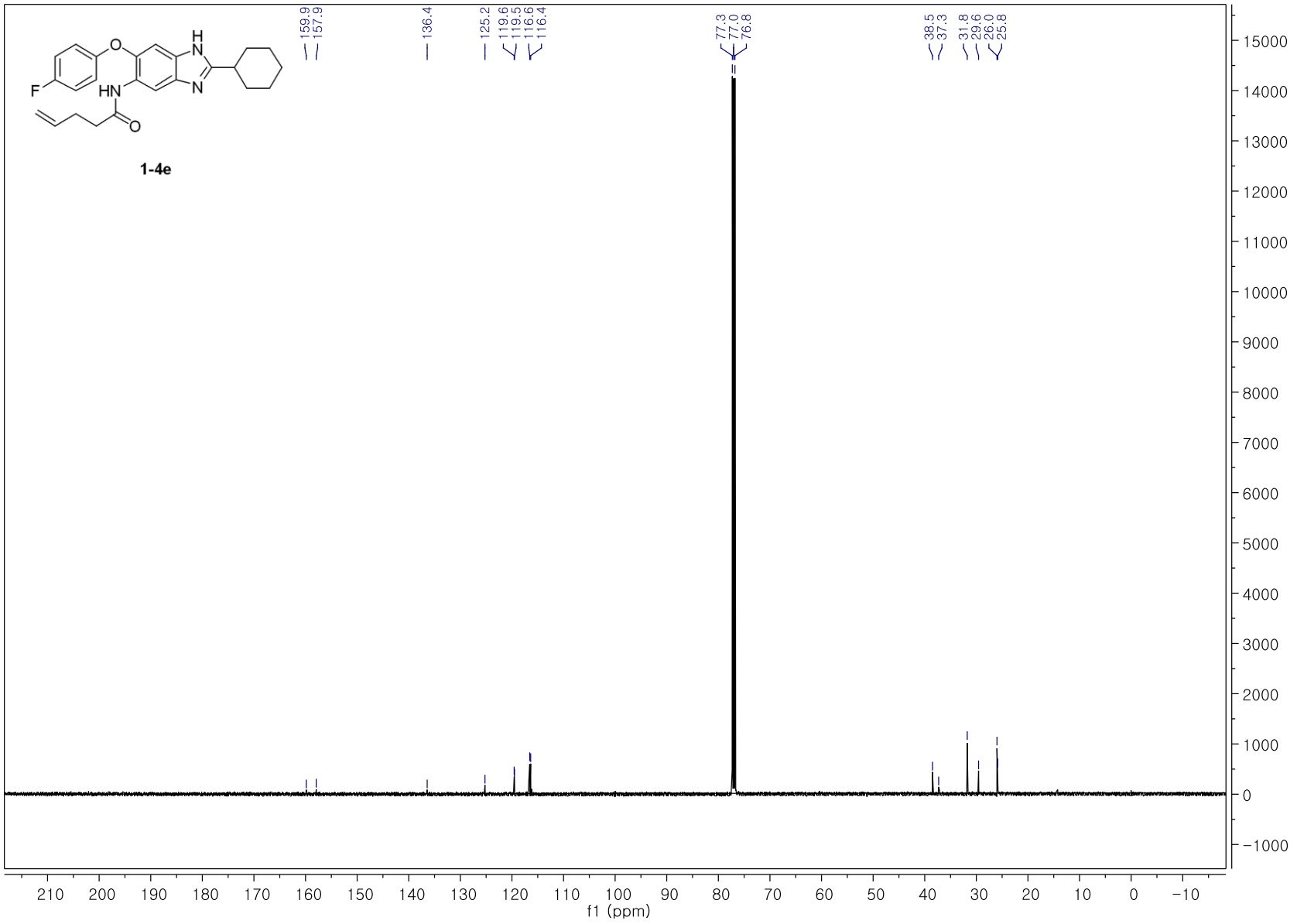
159.9
157.9
136.4
125.2
119.6
119.5
116.6
116.4
77.3
77.0
76.8
38.5
37.3
31.8
29.6
26.0
25.8
F
O
HN
N
H
N
O
1-4e
15000
14000
13000
12000
11000
10000
9000
8000
7000
6000
5000
4000
3000
2000
1000
0
-1000
210
200
190
180
170
160
150
140
130
120
110
100
90
80
70
60
50
40
30
20
10
0
-10
f1 (ppm)

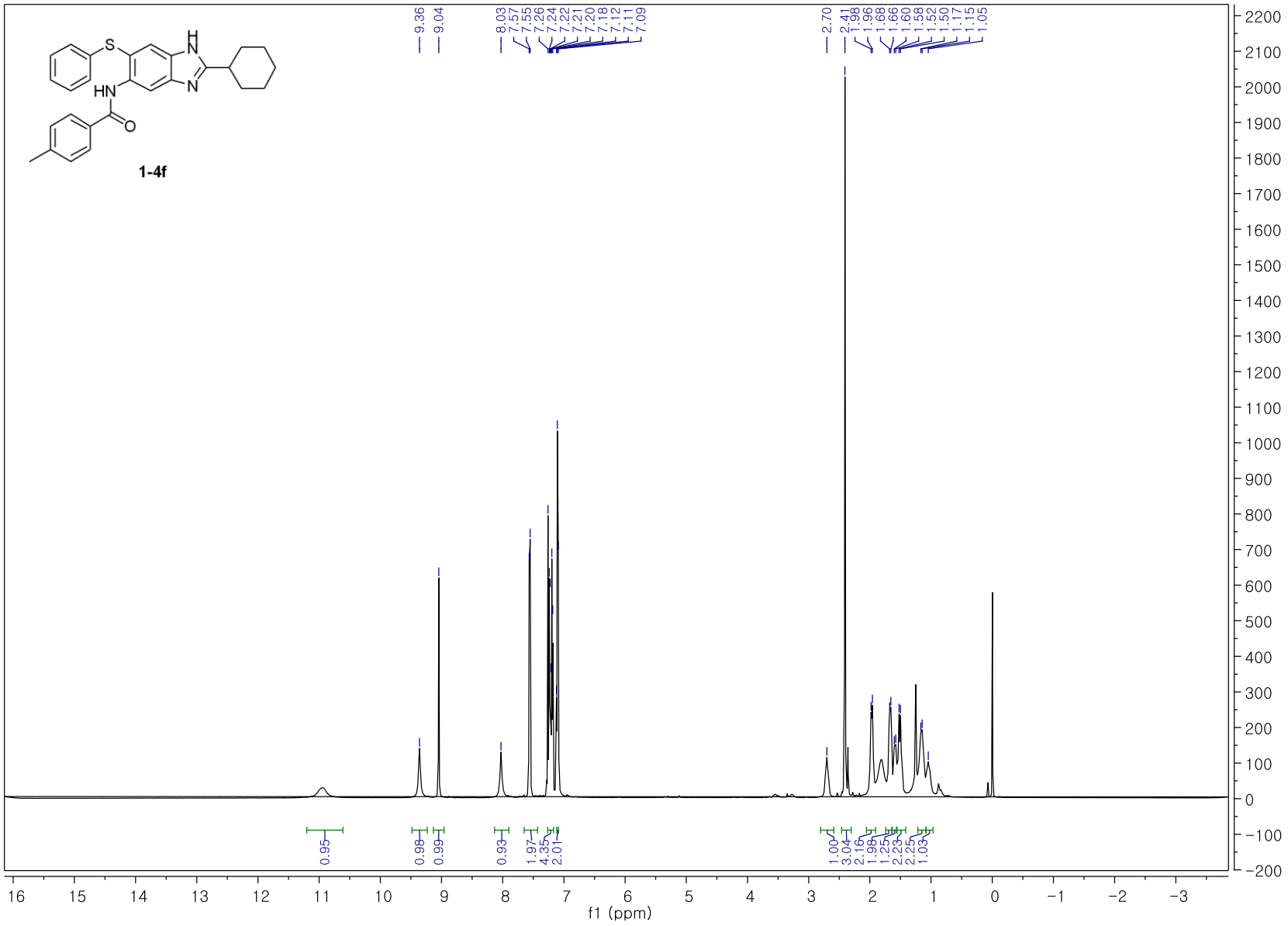
1-4f
9.36
9.04
8.03
7.57
7.55
7.26
7.24
7.22
7.21
7.20
7.18
7.12
7.11
7.09
2.70
2.41
1.98
1.96
1.68
1.66
1.60
1.58
1.52
1.50
1.17
1.15
1.05
0.95
0.98
0.99
0.93
1.97
4.35
2.01
1.00
3.04
2.16
1.98
1.25
2.23
2.25
1.03
f1 (ppm)

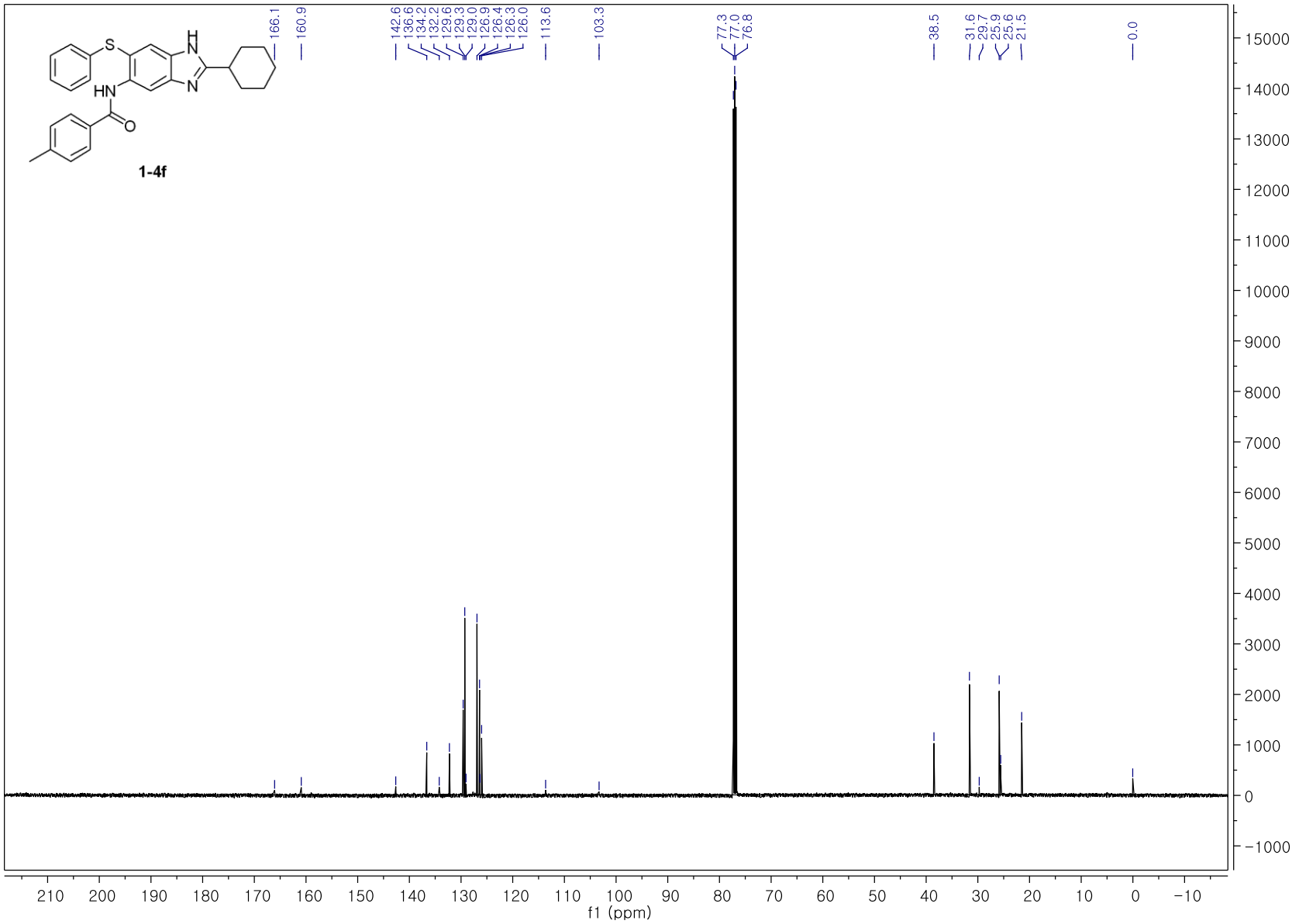
166.1
160.9
142.6
136.6
134.2
132.2
129.6
129.3
129.0
126.9
126.4
126.3
126.0
113.6
103.3
77.3
77.0
76.8
38.5
31.6
29.7
25.9
25.6
21.5
0.0
1-4f
f1 (ppm)

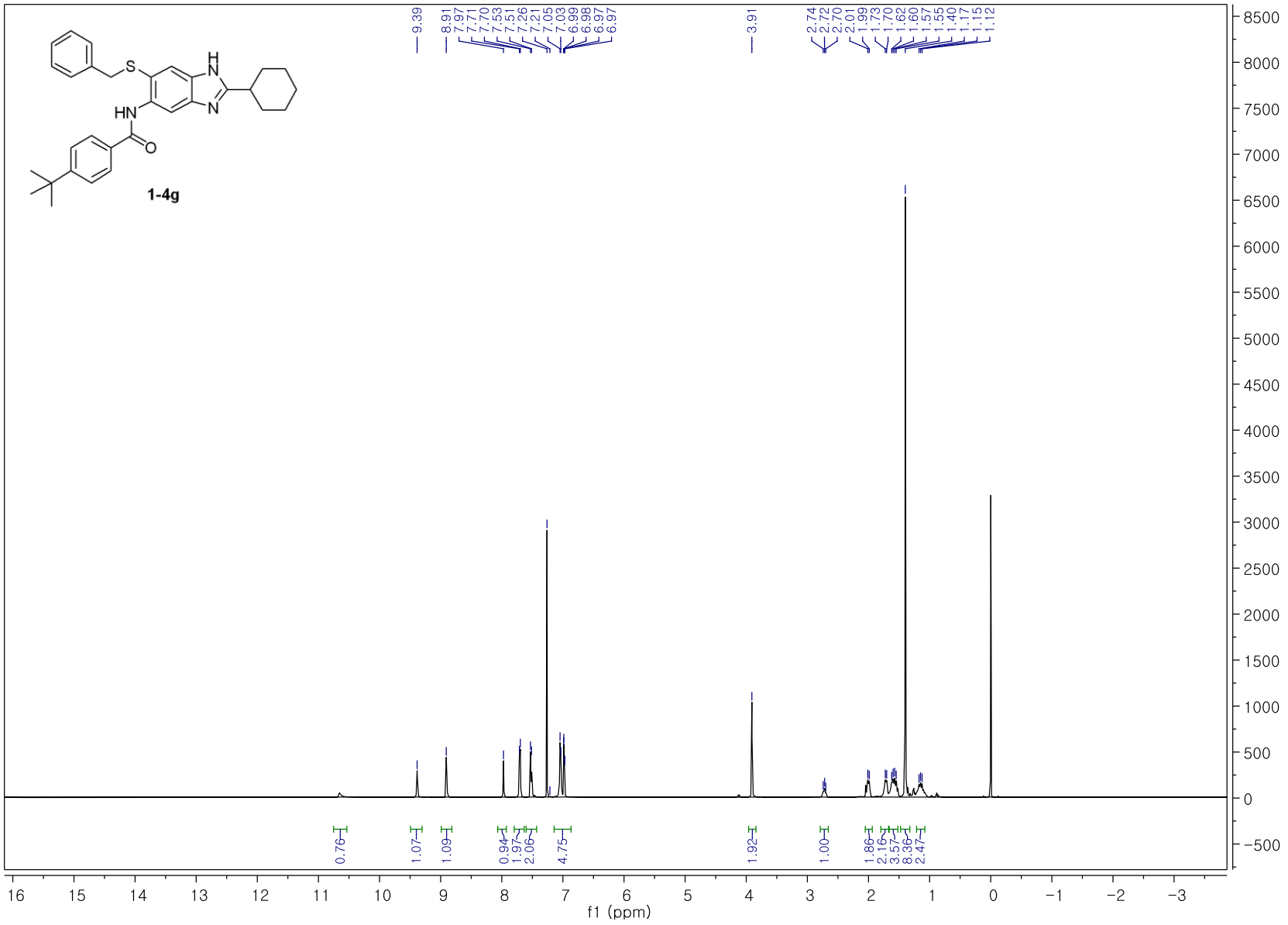
1-4g
9.39
8.91
7.97
7.71
7.70
7.53
7.51
7.26
7.21
7.05
7.03
6.99
6.98
6.97
6.97
3.91
2.74
2.72
2.70
2.01
1.99
1.73
1.70
1.62
1.60
1.57
1.55
1.40
1.17
1.15
1.12
0.76
1.07
1.09
0.94
1.97
2.06
4.75
1.92
1.00
1.86
2.16
3.57
8.36
2.47
f1 (ppm)

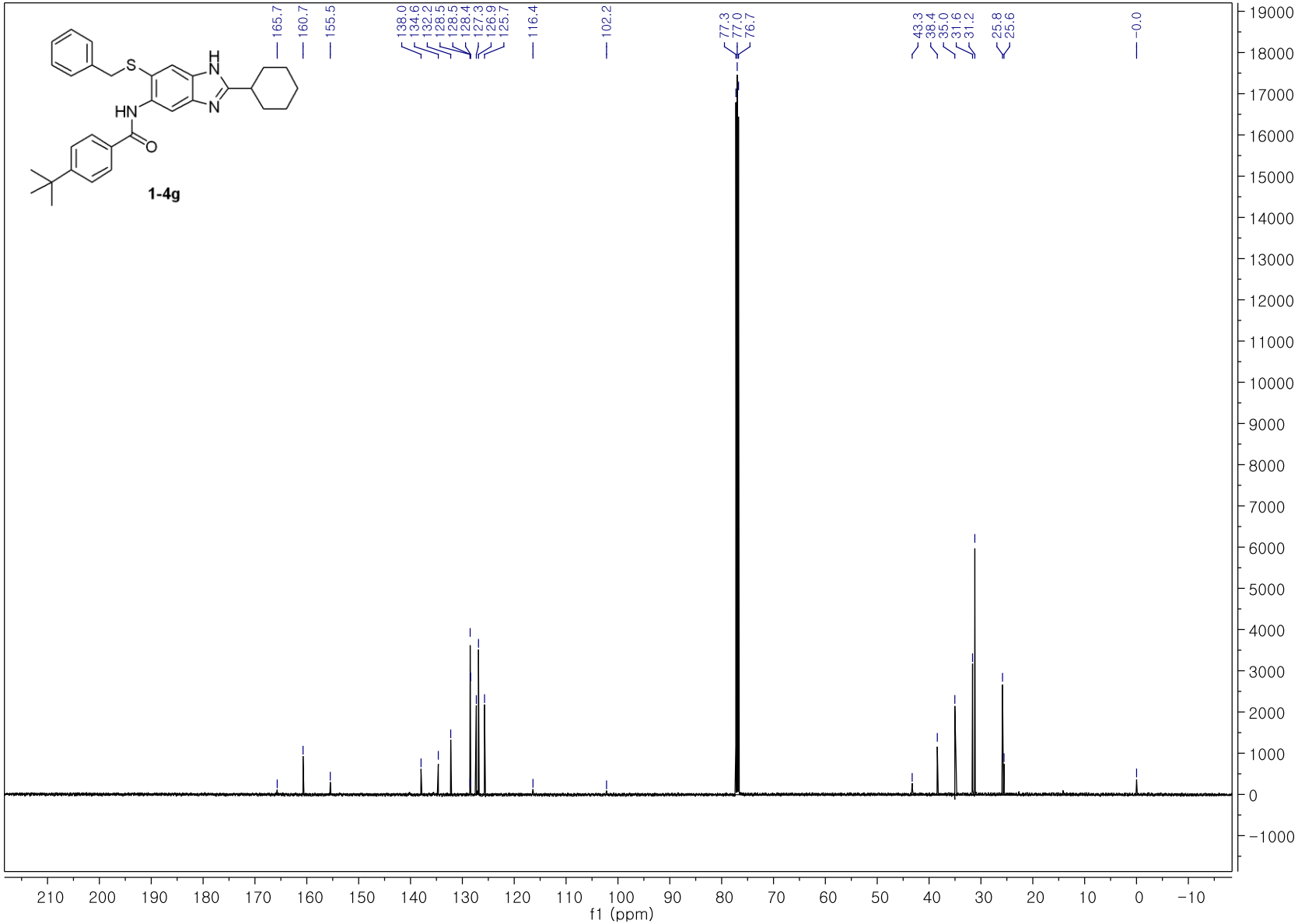
1-4g
165.7
160.7
155.5
138.0
134.6
132.2
128.5
128.5
128.4
127.3
126.9
125.7
116.4
102.2
77.3
77.0
76.7
43.3
38.4
35.0
31.6
31.2
25.8
25.6
0.0
f1 (ppm)

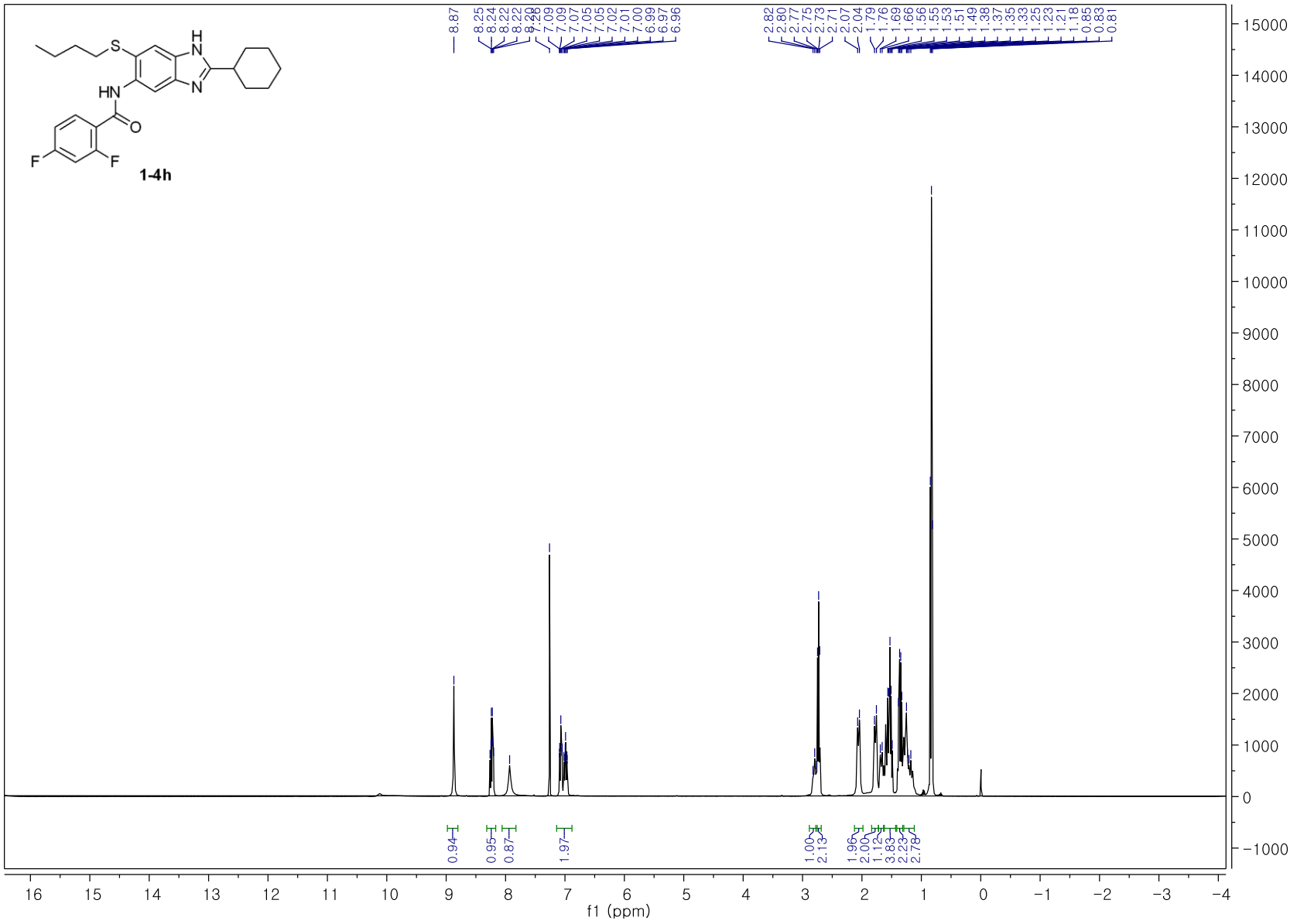
1-4h
f1 (ppm)

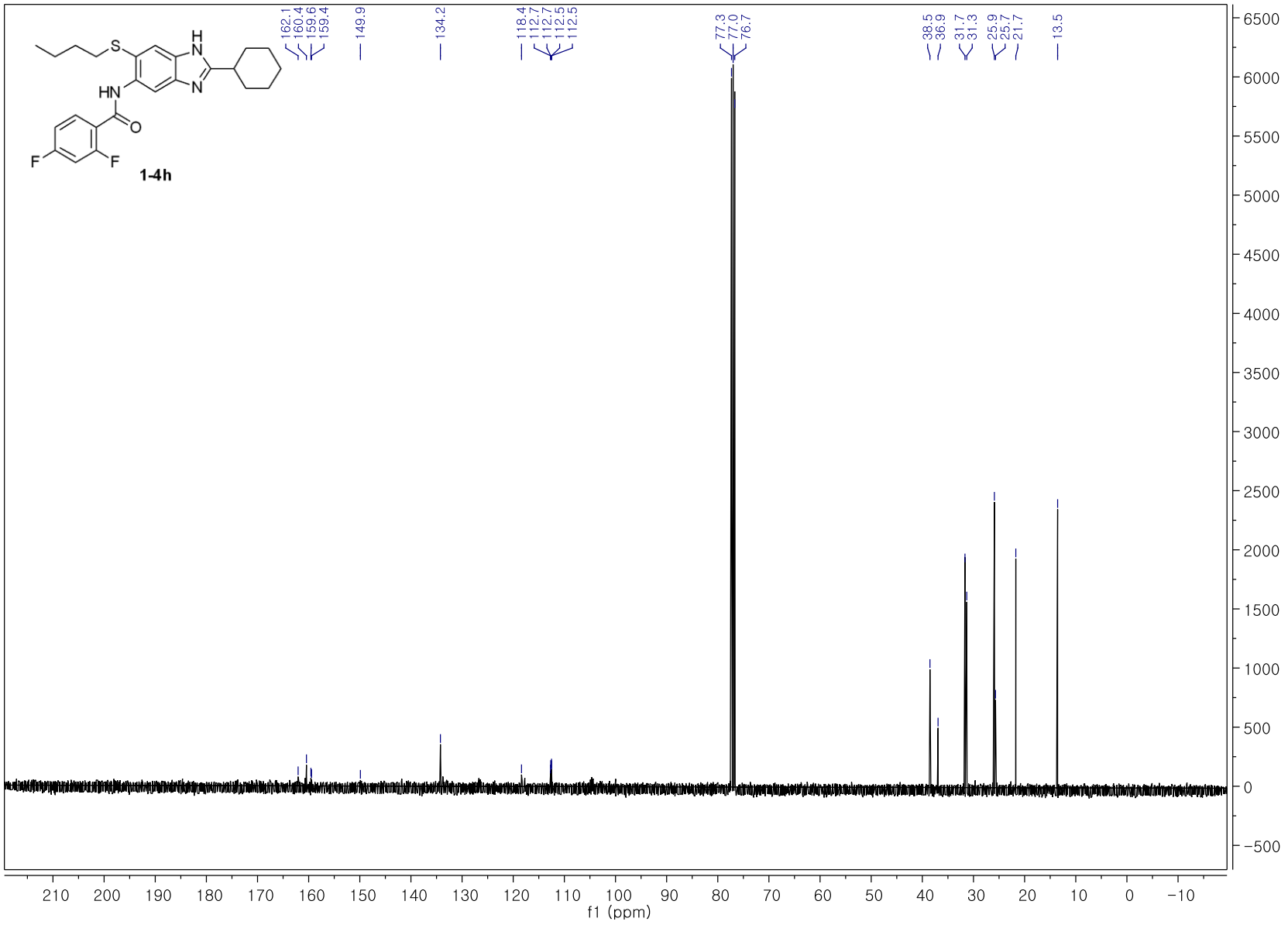
1-4h
162.1
160.4
159.6
159.4
149.9
134.2
118.4
112.7
112.7
112.5
112.5
77.3
77.0
76.7
38.5
36.9
31.7
31.3
25.9
25.7
21.7
13.5
f1 (ppm)

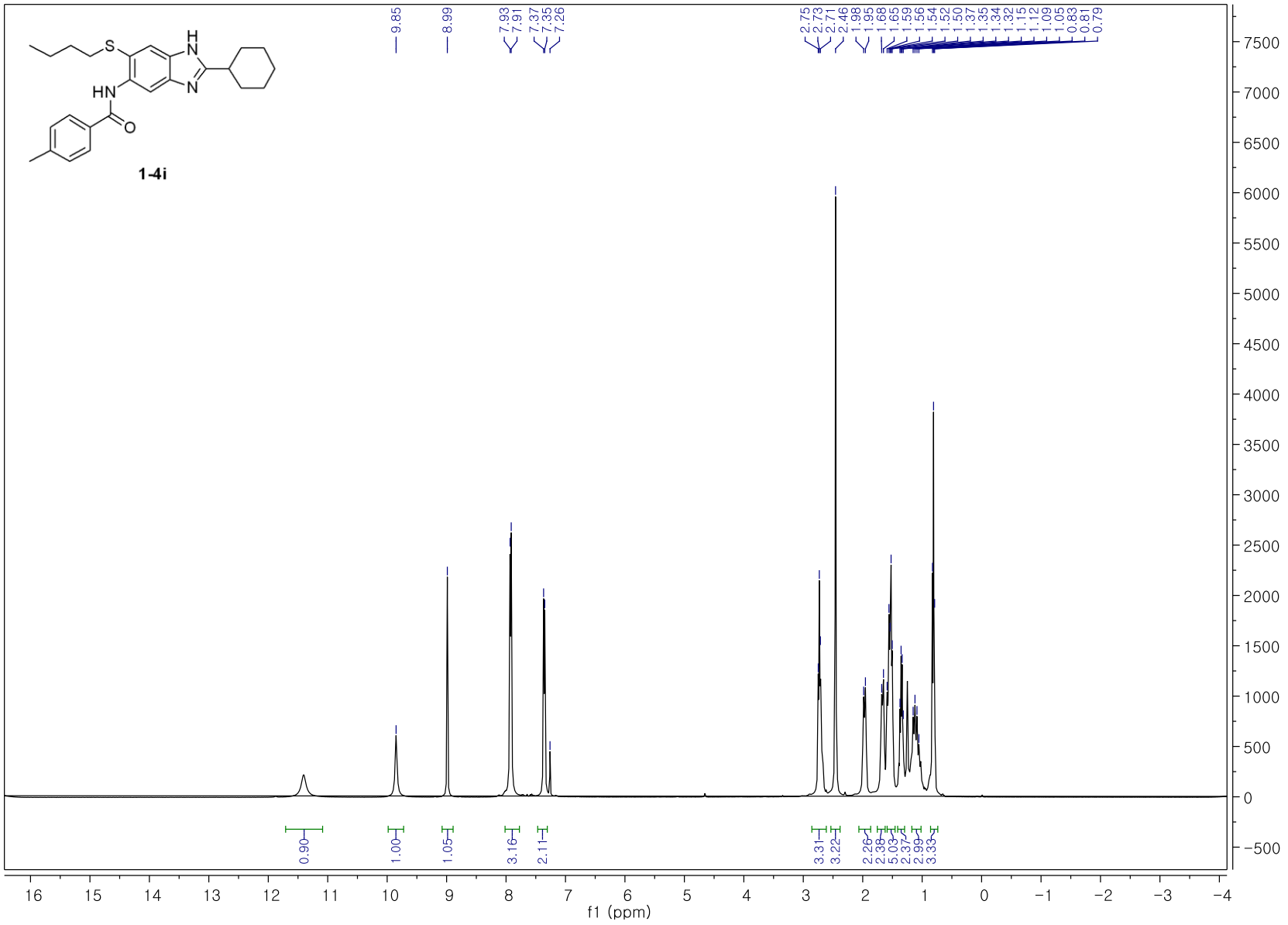
1-4i
9.85
8.99
7.93
7.91
7.37
7.35
7.26
2.75
2.73
2.71
2.46
1.98
1.95
1.68
1.65
1.59
1.56
1.54
1.52
1.50
1.37
1.35
1.34
1.32
1.15
1.12
1.09
1.05
0.83
0.81
0.79
0.90
1.00
1.05
3.16
2.11
3.31
3.22
2.26
2.38
5.03
2.37
2.99
3.33
f1 (ppm)

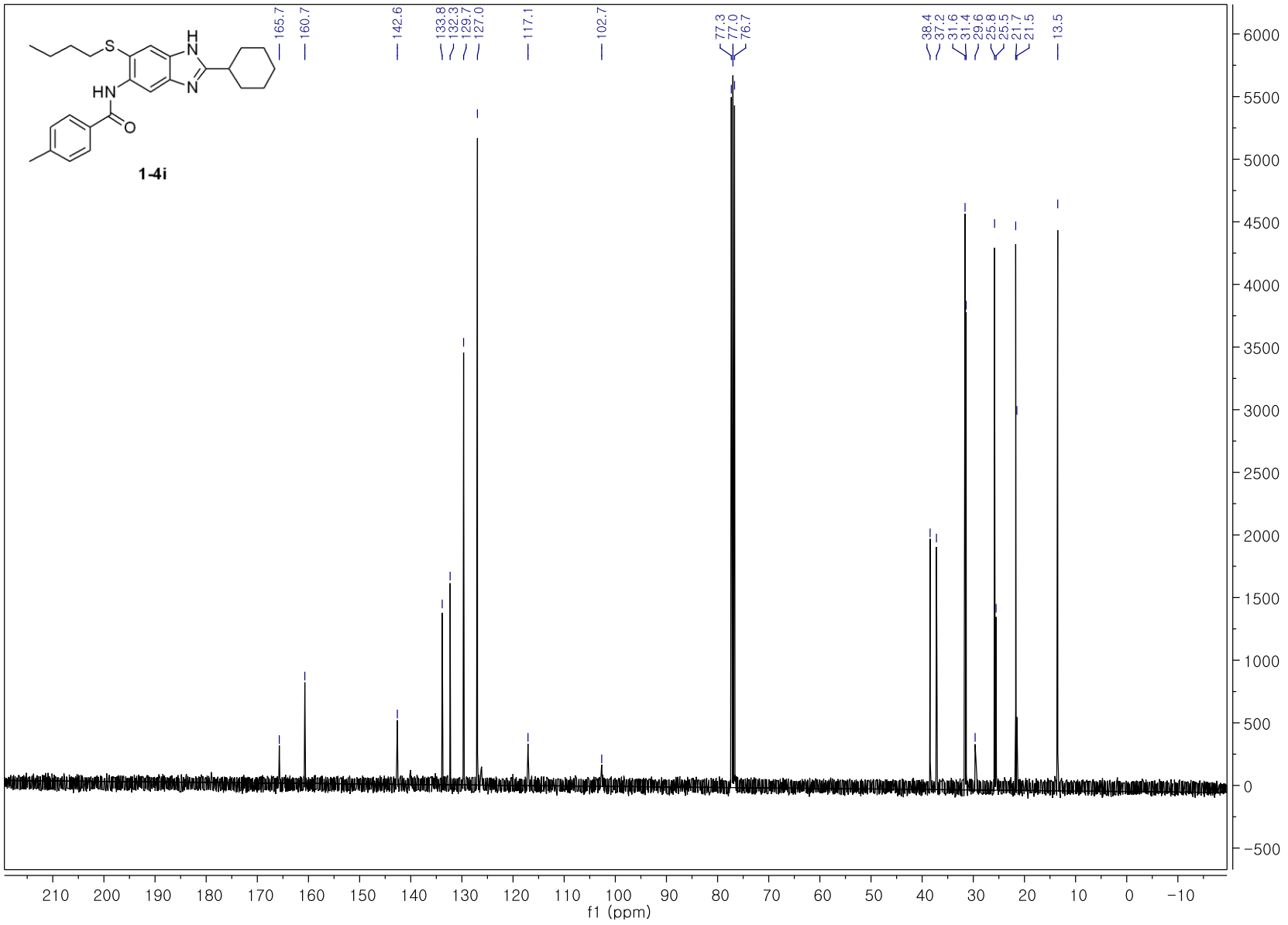
1-4i
165.7
160.7
142.6
133.8
132.3
129.7
127.0
117.1
102.7
77.3
77.0
76.7
38.4
37.2
31.6
31.4
29.6
25.8
25.5
21.7
21.5
13.5
f1 (ppm)

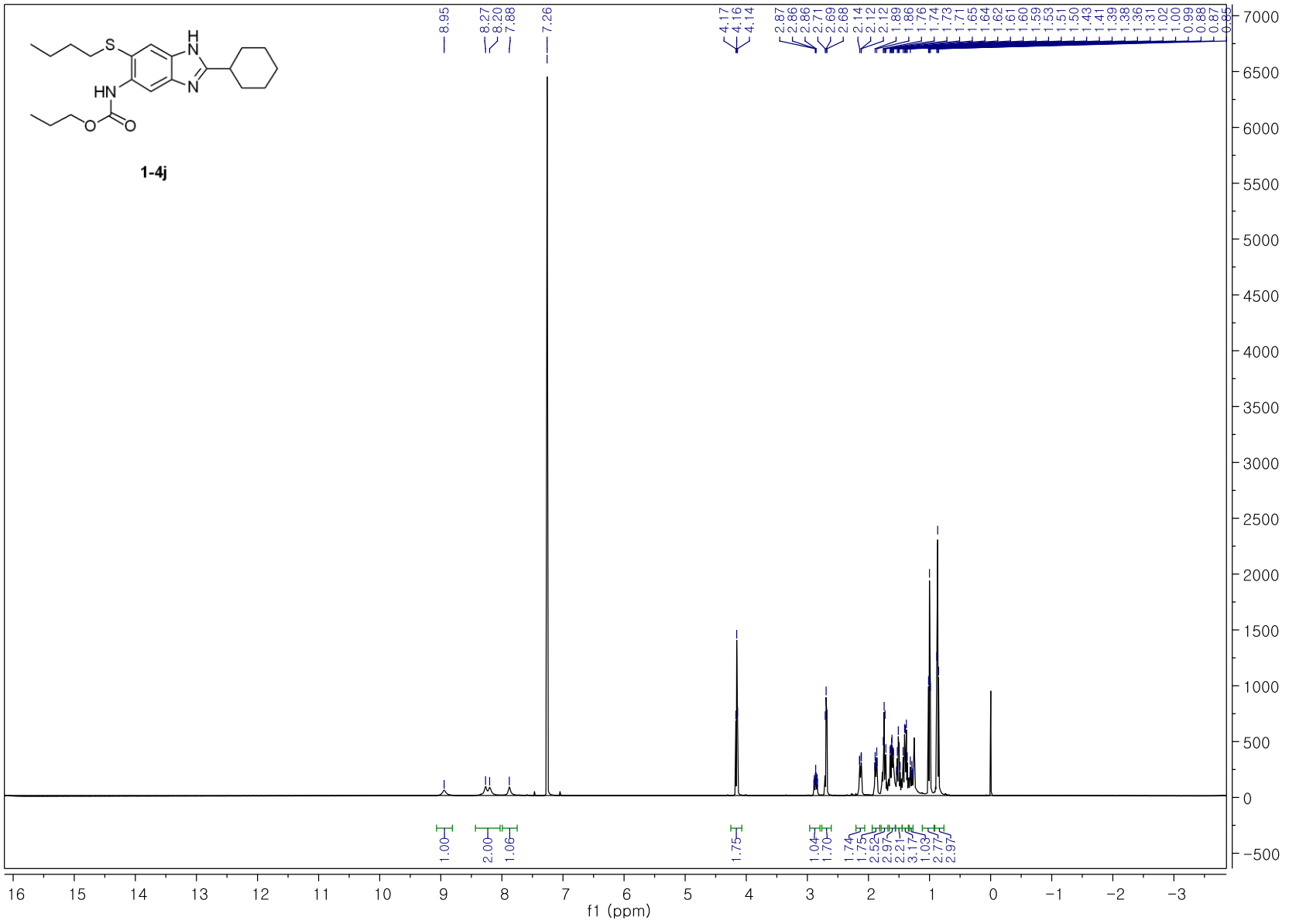
1-4j
8.95
8.27
8.20
7.88
7.26
4.17
4.16
4.14
2.87
2.86
2.86
2.71
2.69
2.68
2.14
2.12
2.12
1.89
1.86
1.76
1.74
1.73
1.71
1.65
1.64
1.62
1.61
1.60
1.59
1.53
1.51
1.50
1.43
1.41
1.39
1.38
1.36
1.31
1.02
1.00
0.99
0.88
0.87
0.85
1.00
2.00
1.06
1.75
1.04
1.70
1.74
1.75
2.52
2.97
2.21
3.17
1.03
2.77
2.97
f1 (ppm)

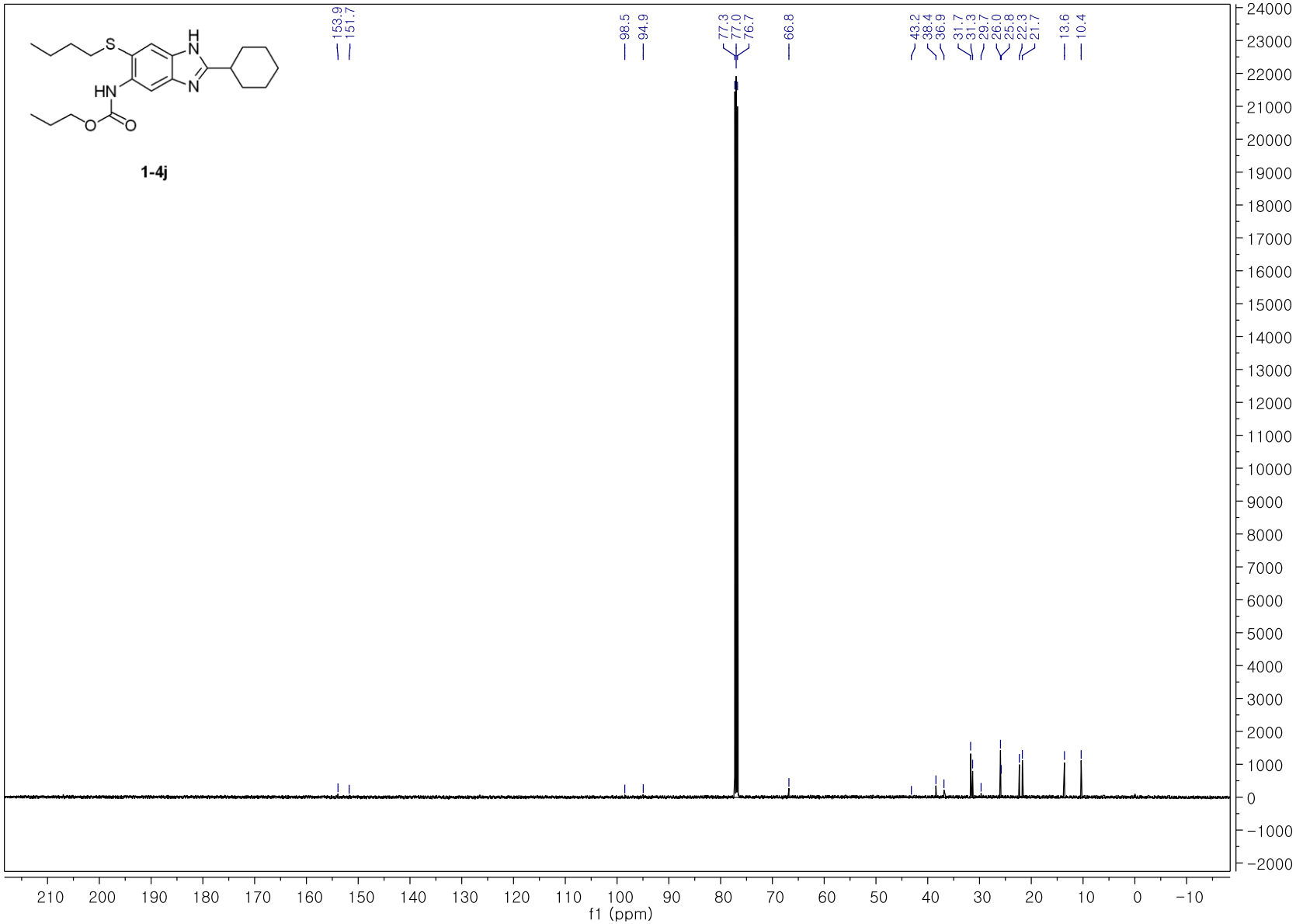
1-4j
153.9
151.7
98.5
94.9
77.3
77.0
76.7
66.8
43.2
38.4
36.9
31.7
31.3
29.7
26.0
25.8
22.3
21.7
13.6
10.4
f1 (ppm)

Chapter 2

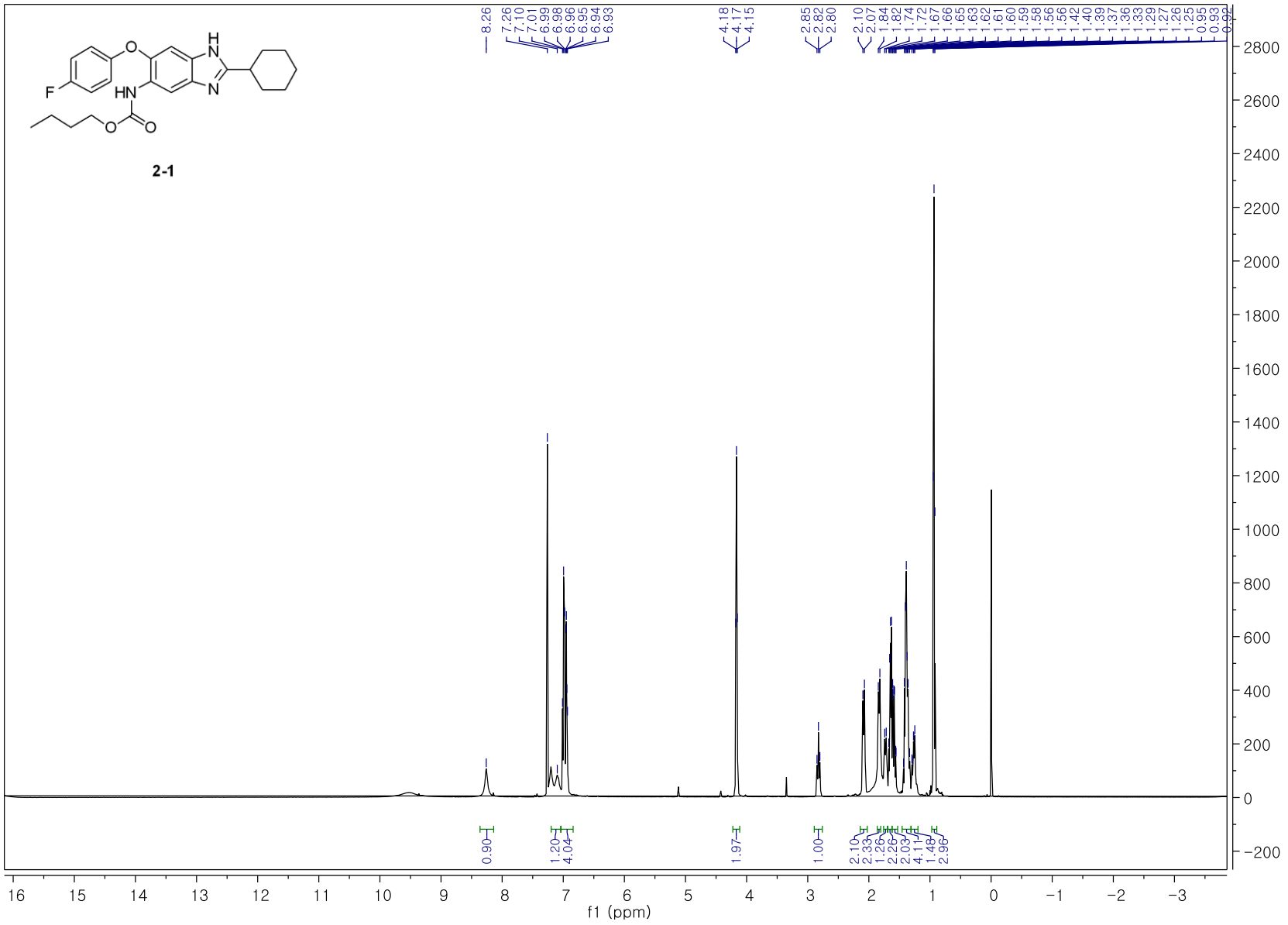
2-1
8.26
7.26
7.10
7.01
6.99
6.98
6.96
6.95
6.94
6.93
4.18
4.17
4.15
2.85
2.82
2.80
2.10
2.07
1.84
1.82
1.74
1.72
1.67
1.66
1.65
1.63
1.62
1.61
1.60
1.59
1.58
1.56
1.42
1.40
1.39
1.37
1.36
1.33
1.29
1.27
1.26
1.25
0.95
0.93
0.92
0.90
1.20
4.04
1.97
1.00
2.10
2.33
1.25
2.26
2.03
4.11
1.48
2.96
f1 (ppm)

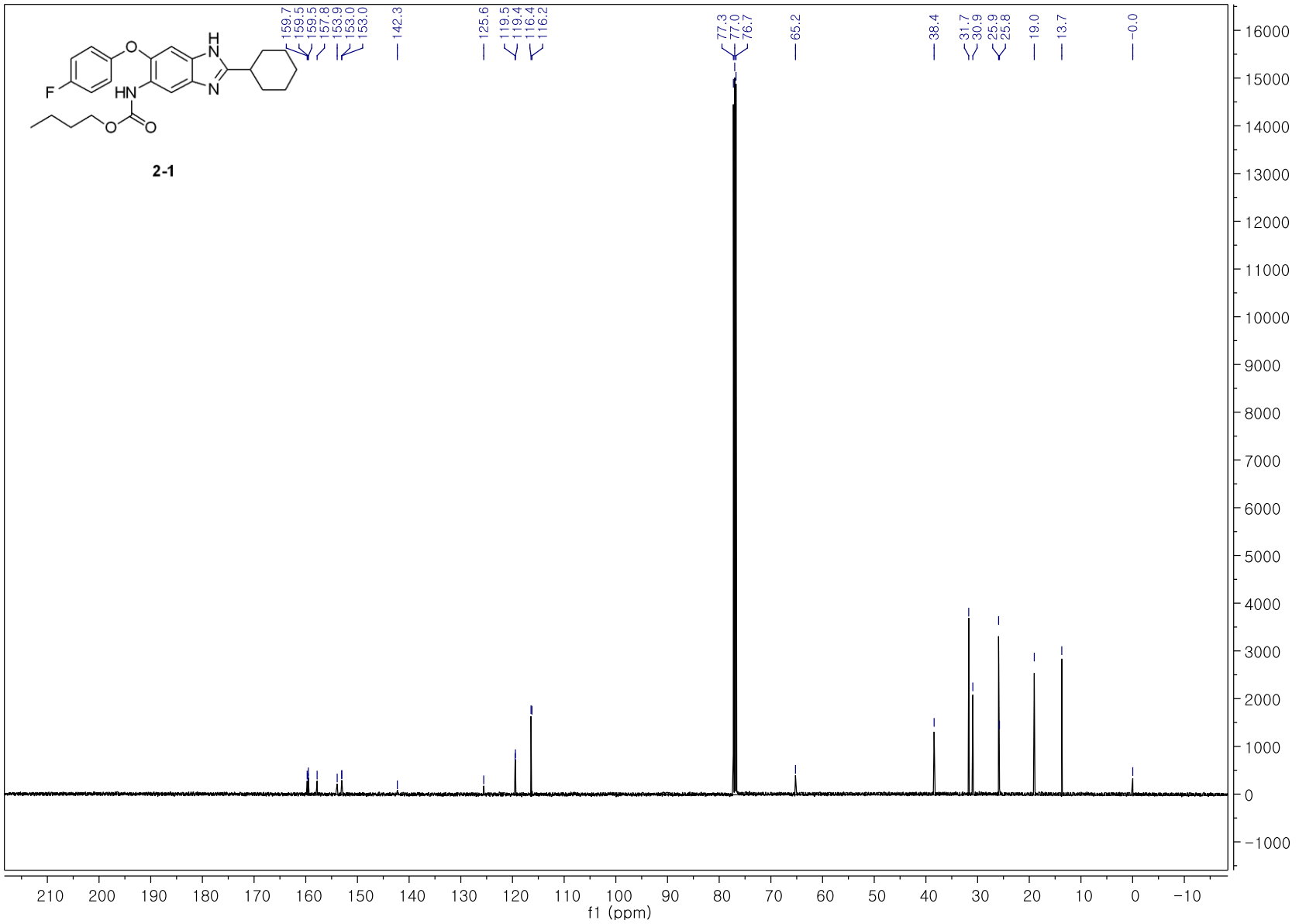
2-1
159.7
159.5
159.5
157.8
153.9
153.0
153.0
142.3
125.6
119.5
119.4
116.4
116.2
77.3
77.0
76.7
65.2
38.4
31.7
30.9
25.9
25.8
19.0
13.7
0.0
f1 (ppm)

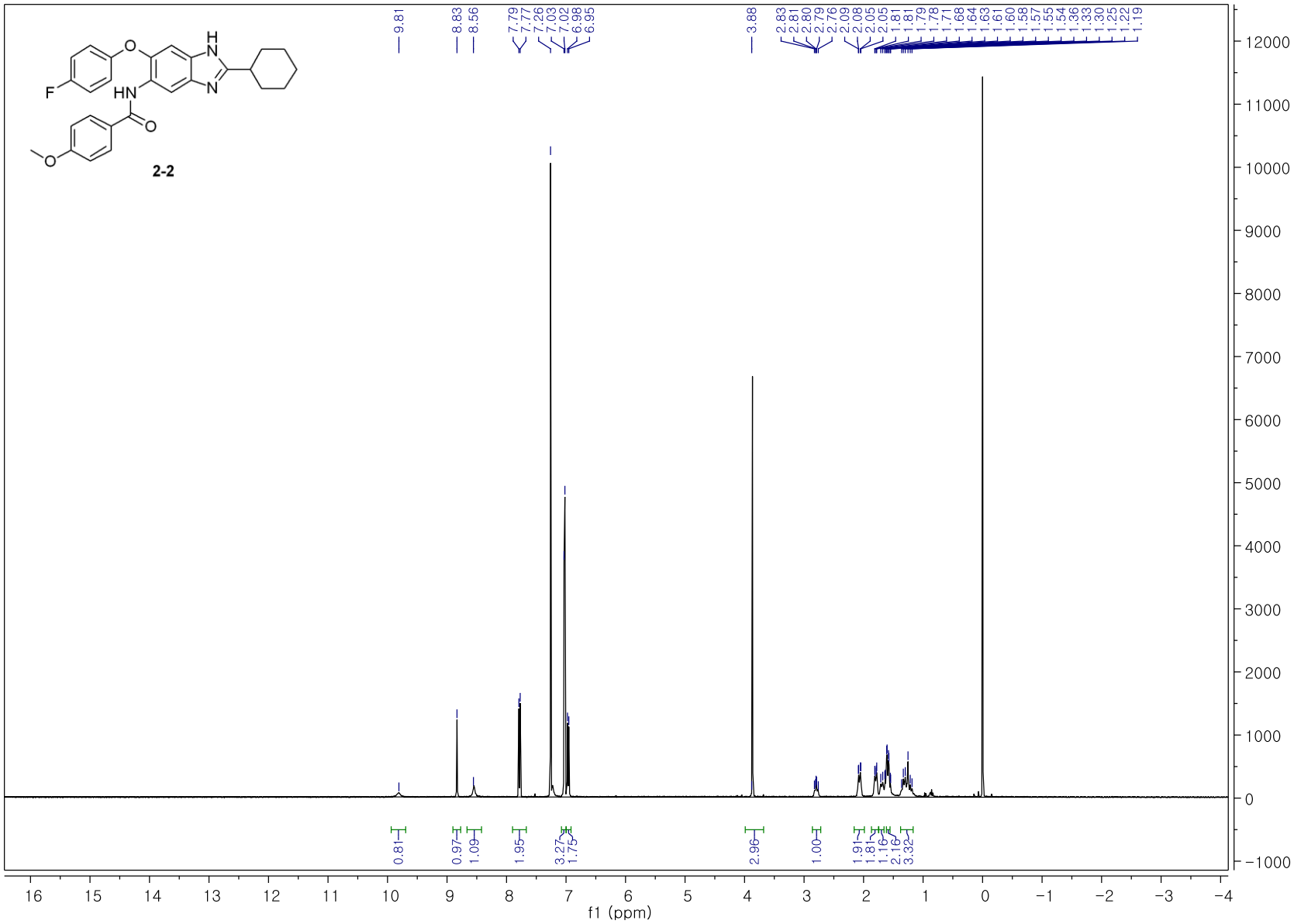
2-2
9.81
8.83
8.56
7.79
7.77
7.26
7.03
7.02
6.98
6.95
3.88
2.83
2.81
2.80
2.79
2.76
2.09
2.08
2.05
2.05
1.81
1.81
1.79
1.78
1.71
1.68
1.64
1.63
1.61
1.60
1.58
1.57
1.55
1.54
1.36
1.33
1.30
1.25
1.22
1.19
0.81
0.97
1.09
1.95
3.27
1.75
2.96
1.00
1.91
1.81
1.16
2.16
3.32
f1 (ppm)

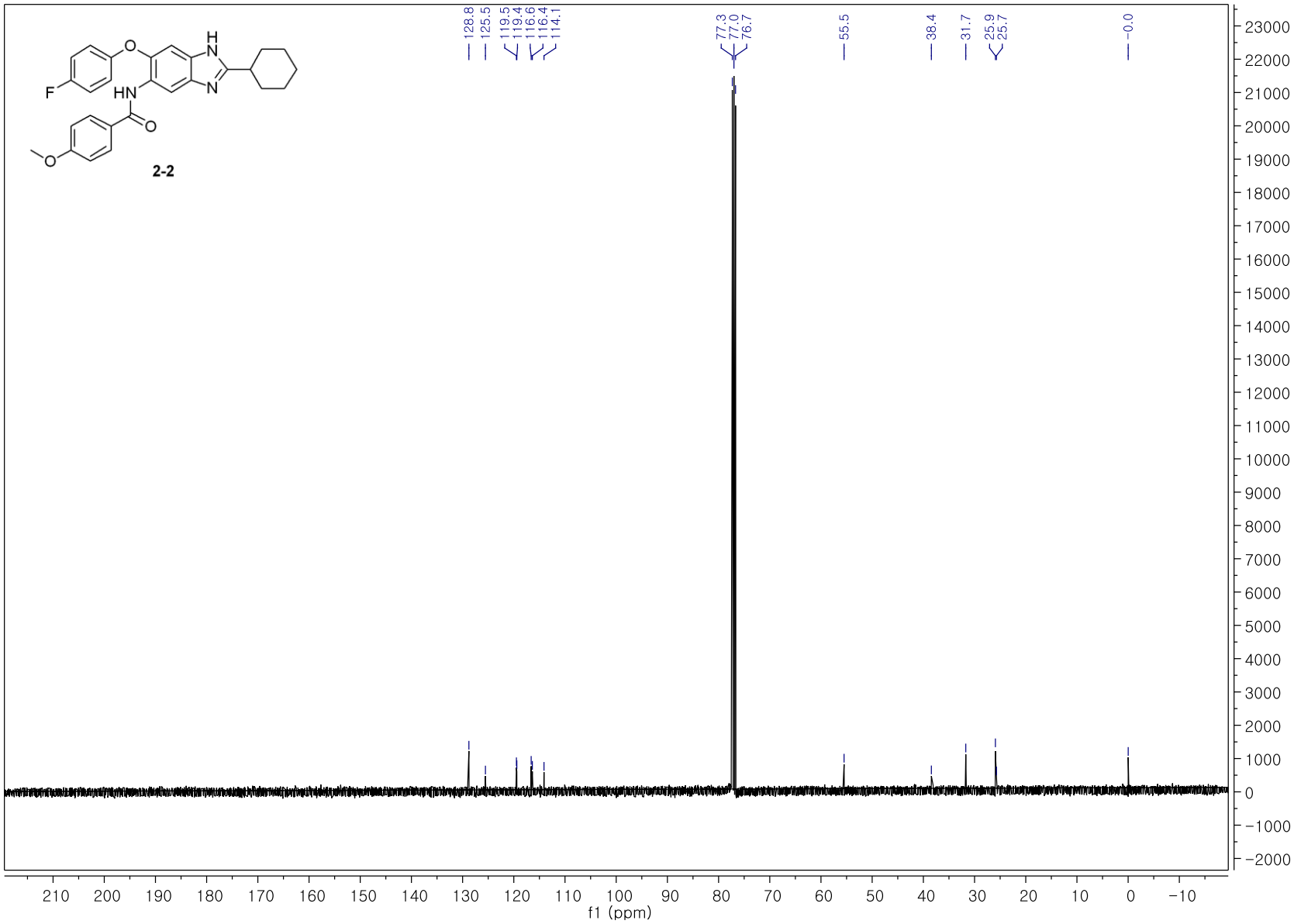
2-2
128.8
125.5
119.5
119.4
116.6
116.4
114.1
77.3
77.0
76.7
55.5
38.4
31.7
25.9
25.7
0.0
f1 (ppm)

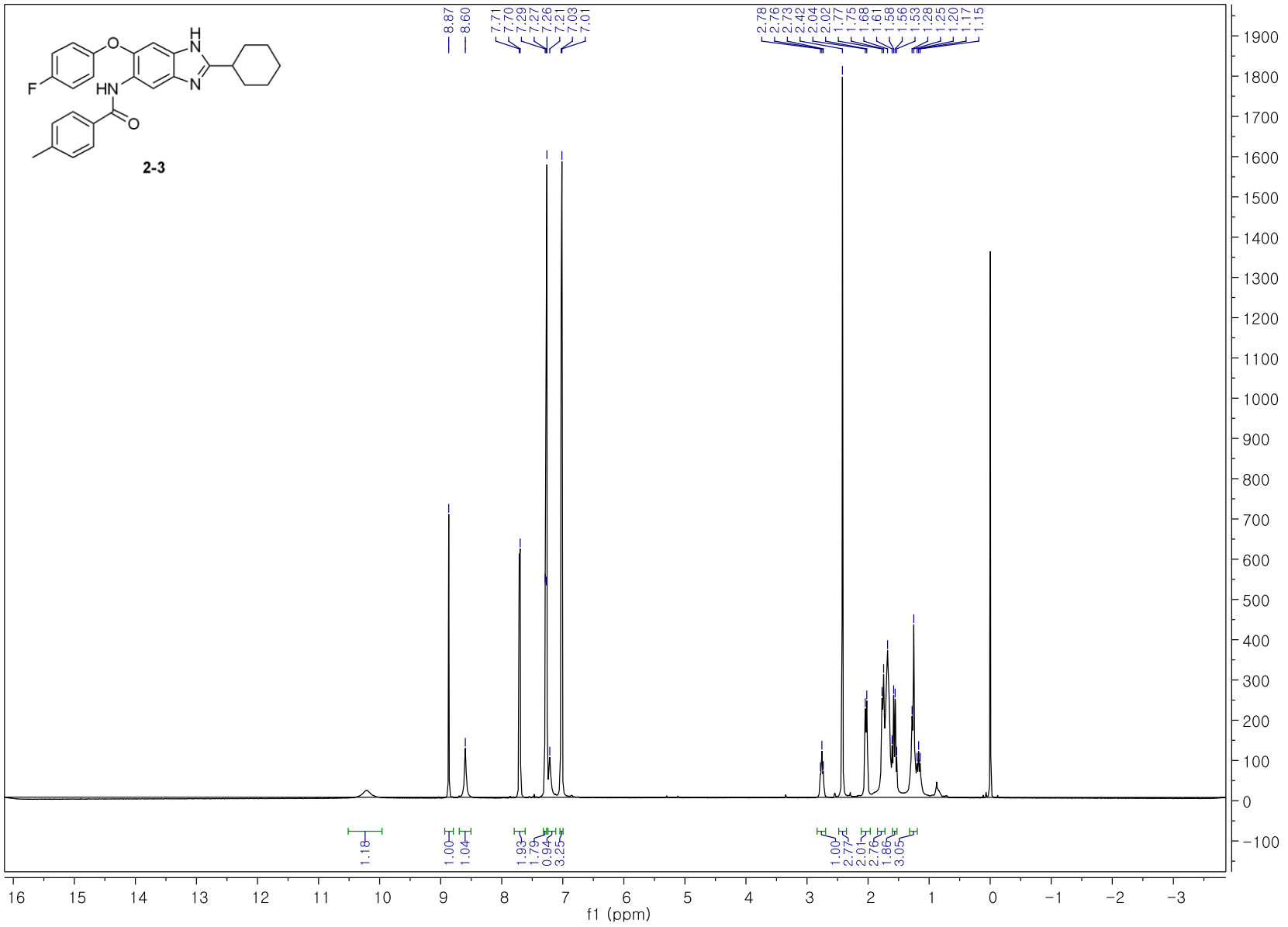
2-3
8.87
8.60
7.71
7.70
7.29
7.27
7.26
7.21
7.03
7.01
2.78
2.76
2.73
2.42
2.04
2.02
1.77
1.75
1.68
1.61
1.58
1.56
1.53
1.28
1.25
1.20
1.17
1.15
1.18
1.00
1.04
1.93
1.79
0.94
3.25
1.00
2.77
2.01
2.76
1.86
3.05
f1 (ppm)

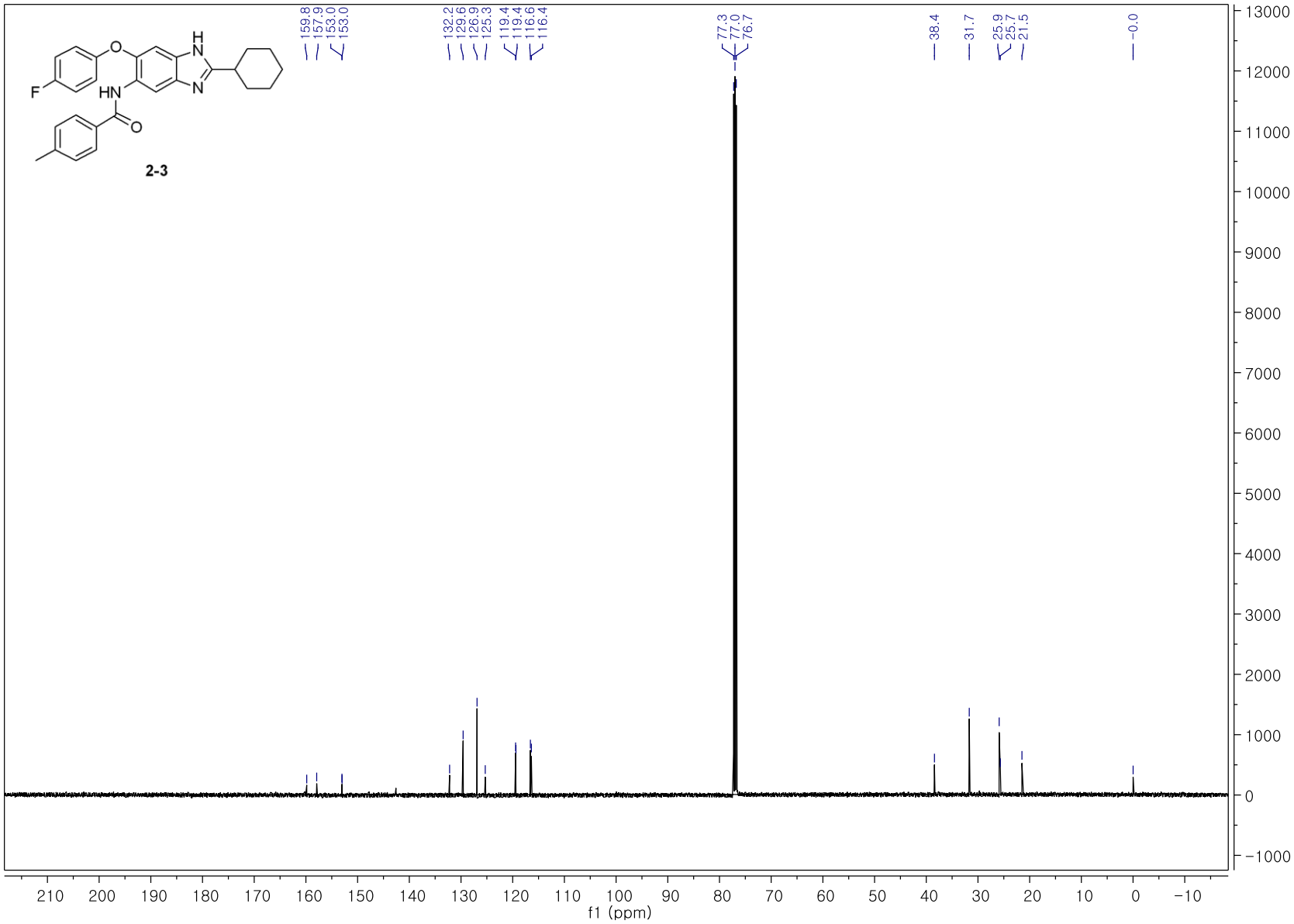
2-3
159.8
157.9
153.0
153.0
132.2
129.6
126.9
125.3
119.4
119.4
116.6
116.4
77.3
77.0
76.7
38.4
31.7
25.9
25.7
21.5
0.0
f1 (ppm)

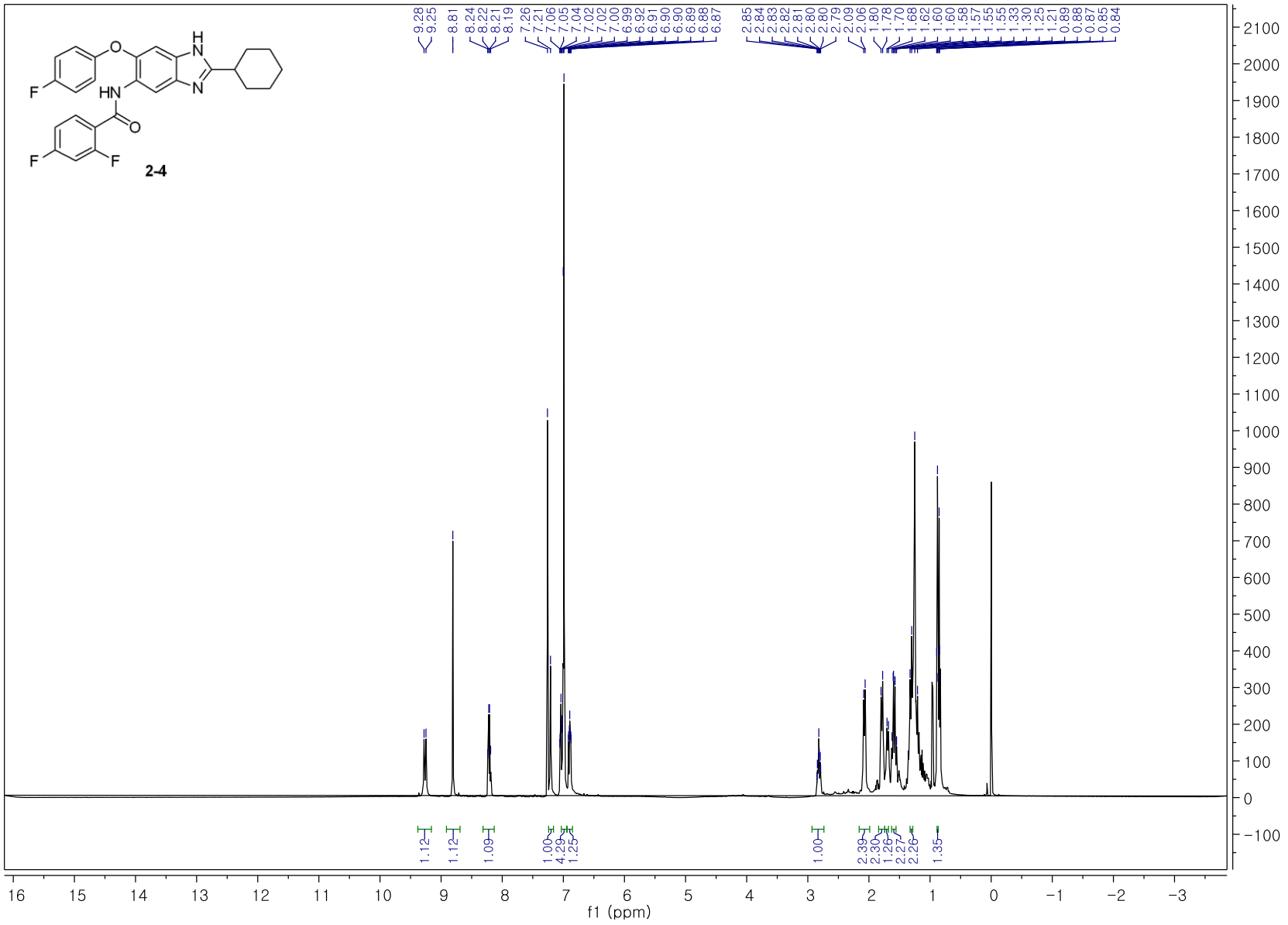
2-4
f1 (ppm)

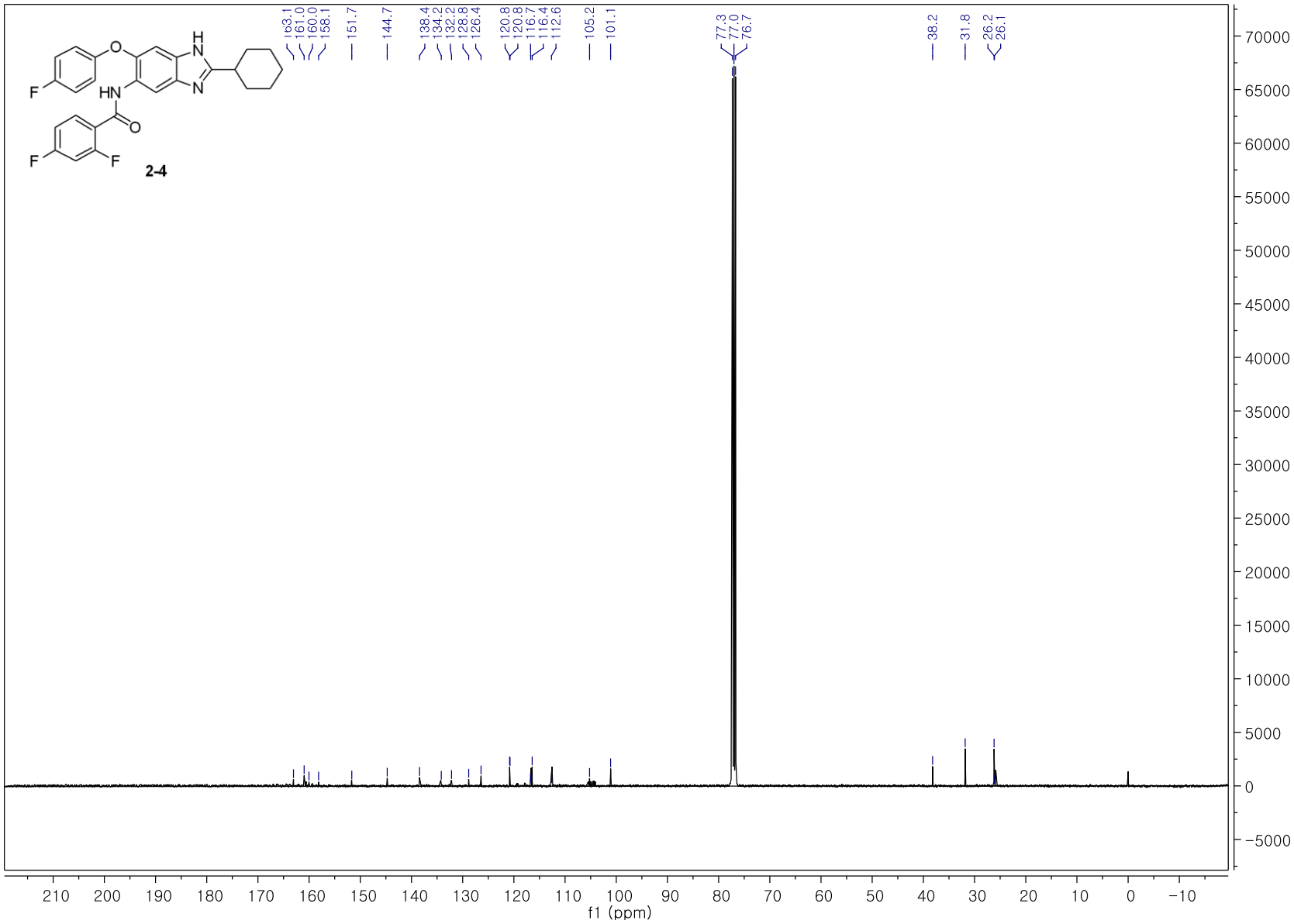
2-4
163.1
161.0
160.0
158.1
151.7
144.7
138.4
134.2
132.2
128.8
126.4
120.8
120.8
116.7
116.4
112.6
105.2
101.1
77.3
77.0
76.7
38.2
31.8
26.2
26.1
f1 (ppm)

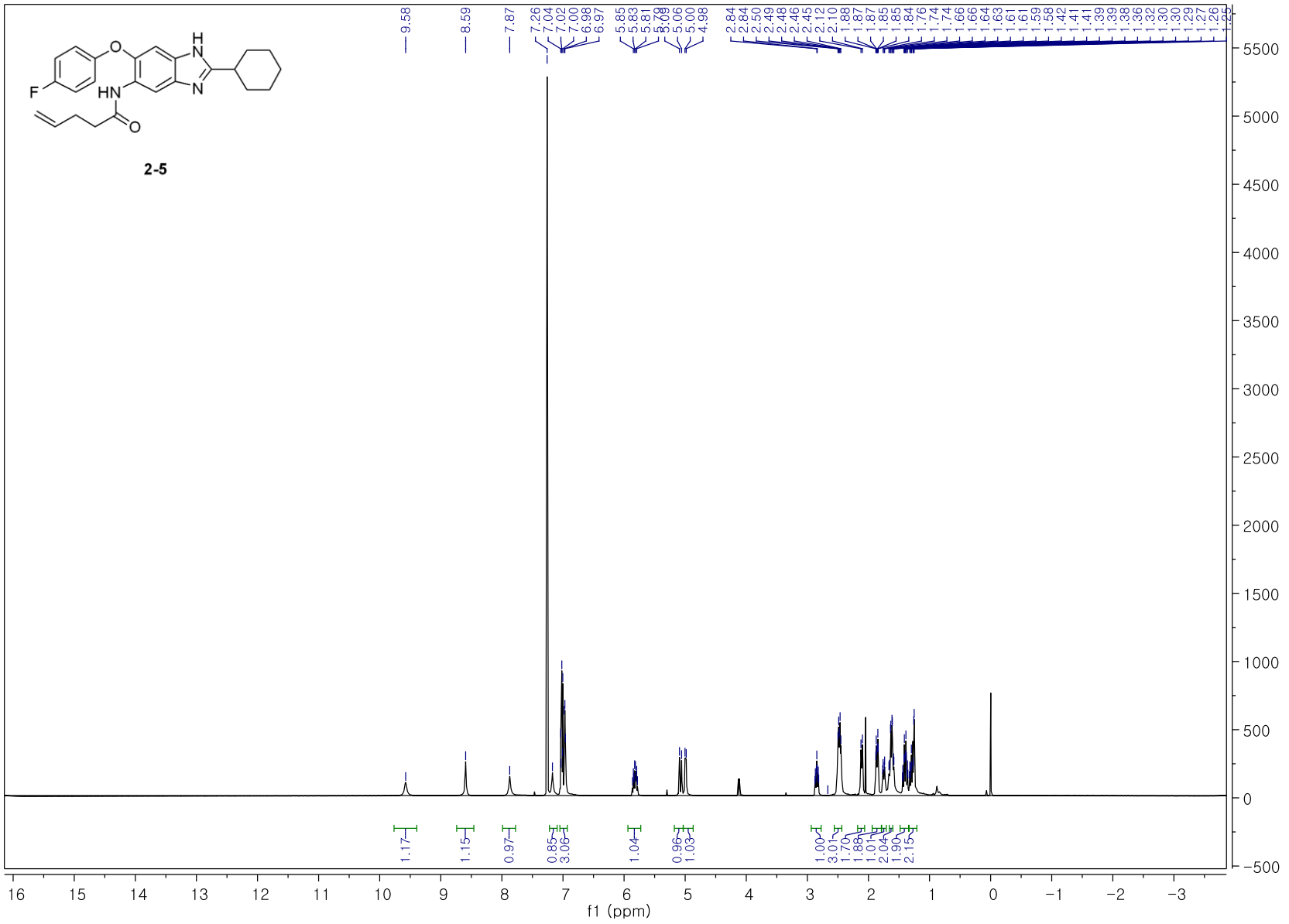
2-5
f1 (ppm)

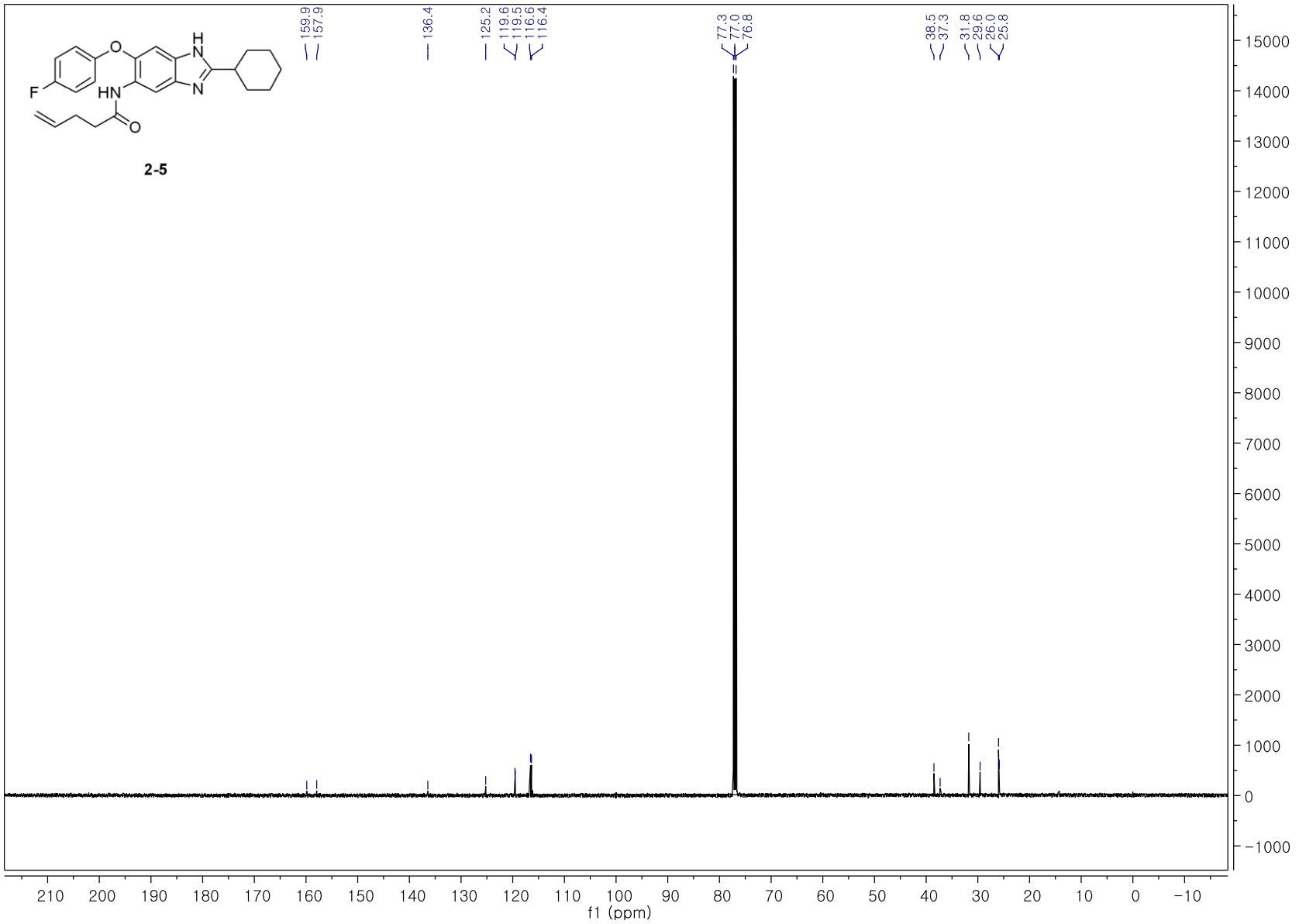
159.9
157.9
136.4
125.2
119.6
119.5
116.6
116.4
77.3
77.0
76.8
38.5
37.3
31.8
29.6
26.0
25.8
F
O
HN
H
N
N
O
2-5
15000
14000
13000
12000
11000
10000
9000
8000
7000
6000
5000
4000
3000
2000
1000
0
-1000
210 200 190 180 170 160 150 140 130 120 110 100 90 80 70 60 50 40 30 20 10 0 -10
f1 (ppm)

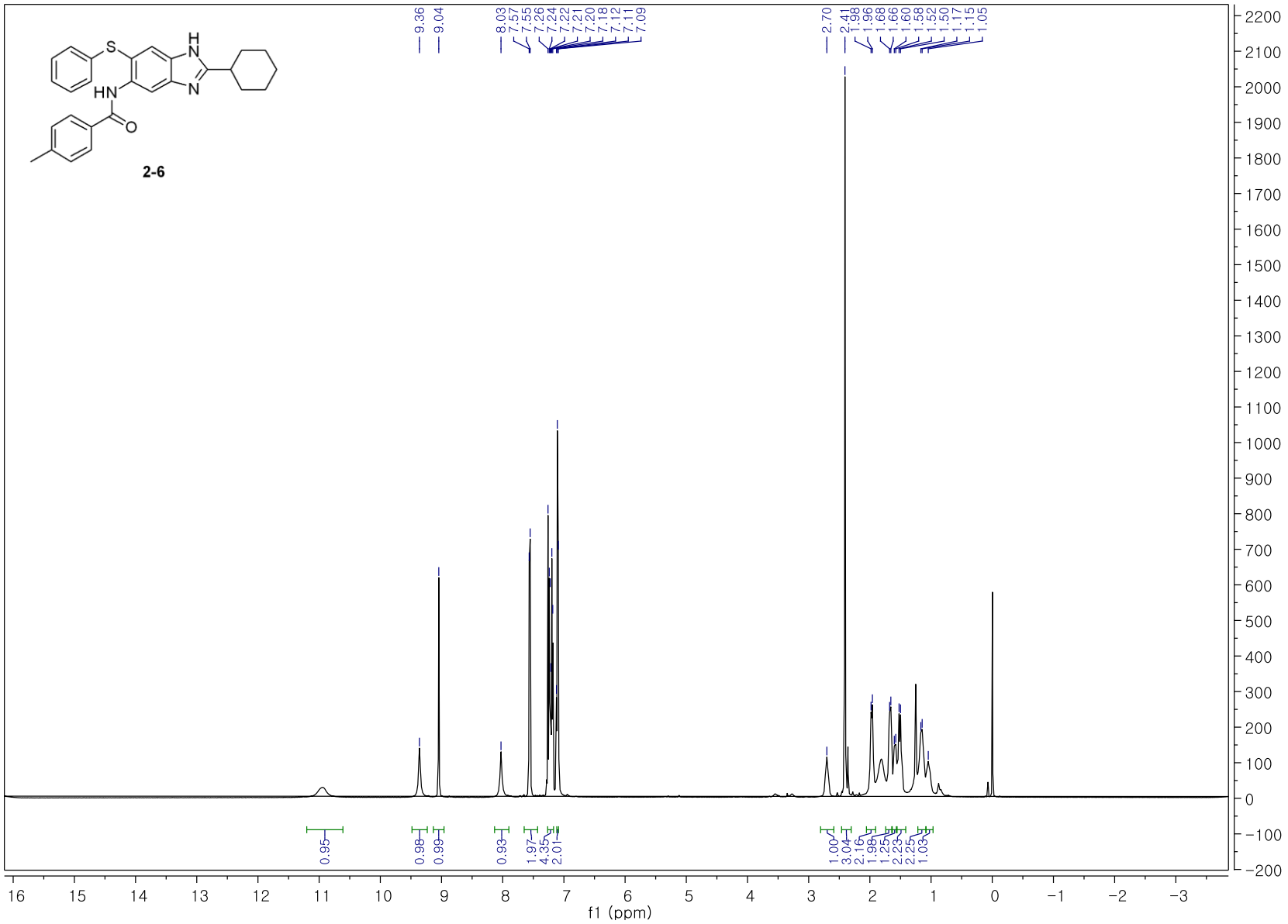
2-6
9.36
9.04
8.03
7.57
7.55
7.26
7.24
7.22
7.21
7.20
7.18
7.12
7.11
7.09
2.70
2.41
1.98
1.96
1.68
1.66
1.60
1.58
1.52
1.50
1.17
1.15
1.05
0.95
0.98
0.99
0.93
1.97
4.35
2.01
1.00
3.04
2.16
1.98
1.25
2.23
2.25
1.03
f1 (ppm)

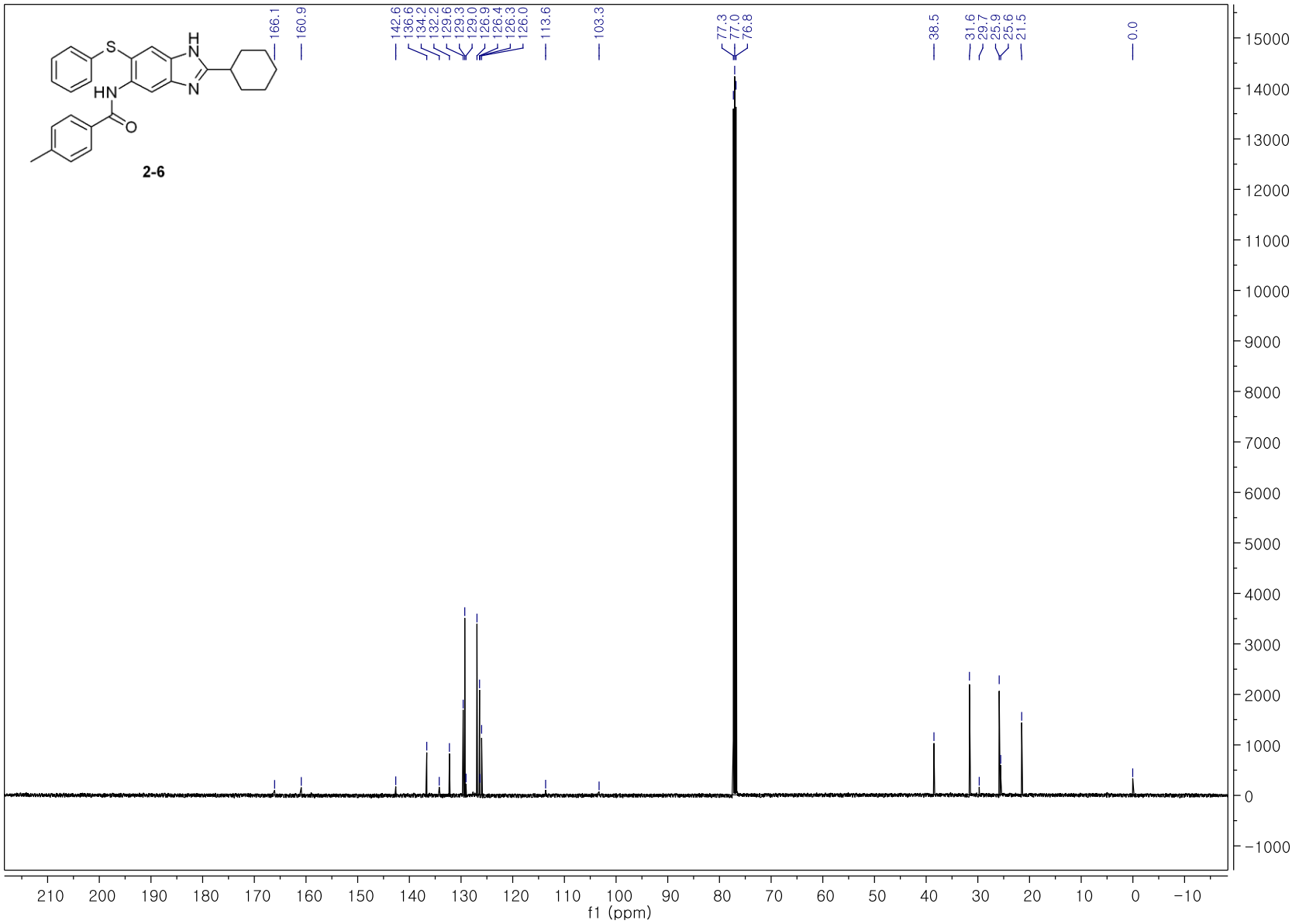
2-6
166.1
160.9
142.6
136.6
134.2
132.2
129.6
129.3
129.0
126.9
126.4
126.3
126.0
113.6
103.3
77.3
77.0
76.8
38.5
31.6
29.7
25.9
25.6
21.5
0.0
f1 (ppm)

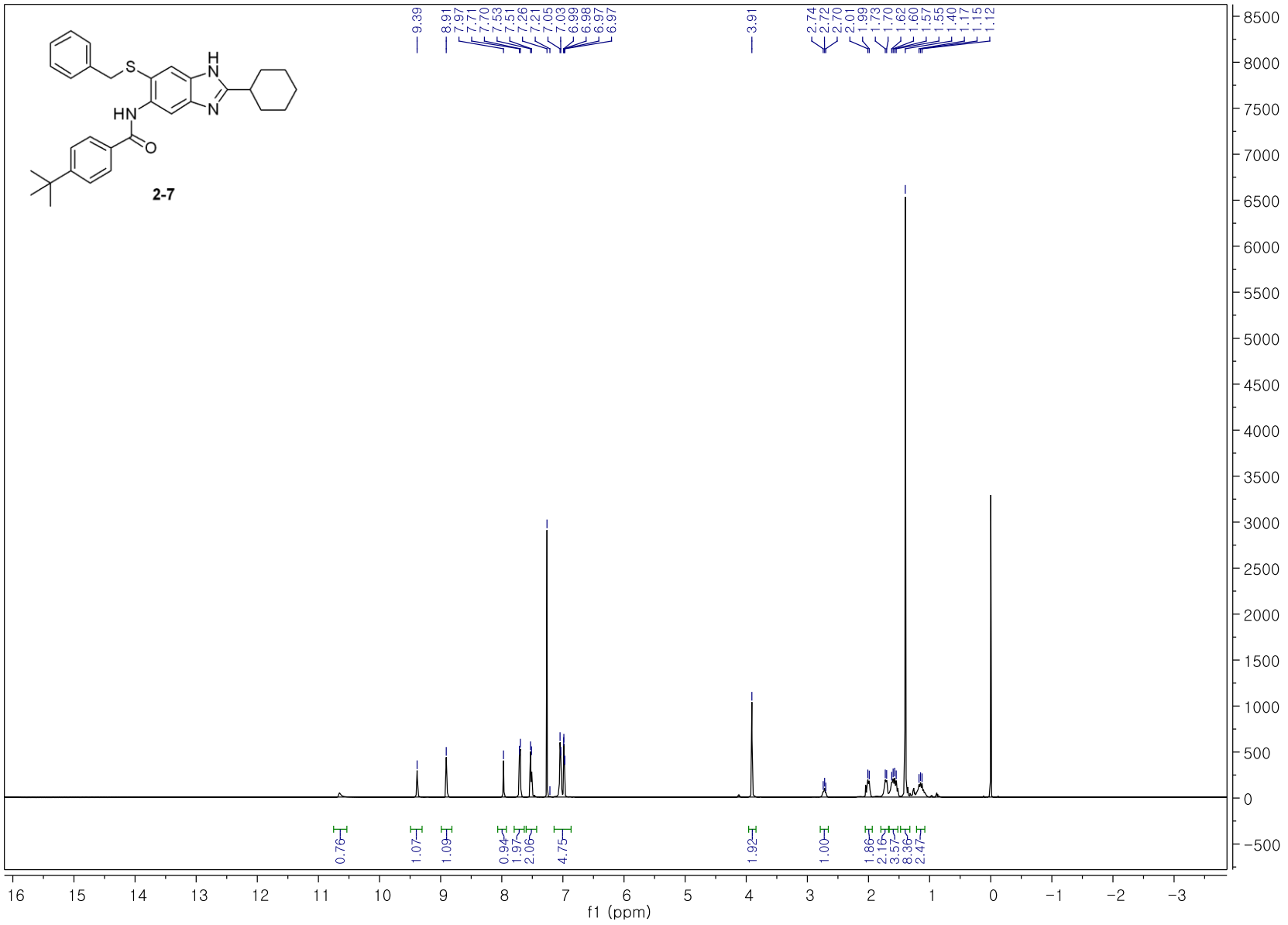
2-7
9.39
8.91
7.97
7.71
7.70
7.53
7.51
7.26
7.21
7.05
7.03
6.99
6.98
6.97
6.97
3.91
2.74
2.72
2.70
2.01
1.99
1.73
1.70
1.62
1.60
1.57
1.55
1.40
1.17
1.15
1.12
0.76
1.07
1.09
0.94
1.97
2.06
4.75
1.92
1.00
1.86
2.16
3.57
8.36
2.47
f1 (ppm)

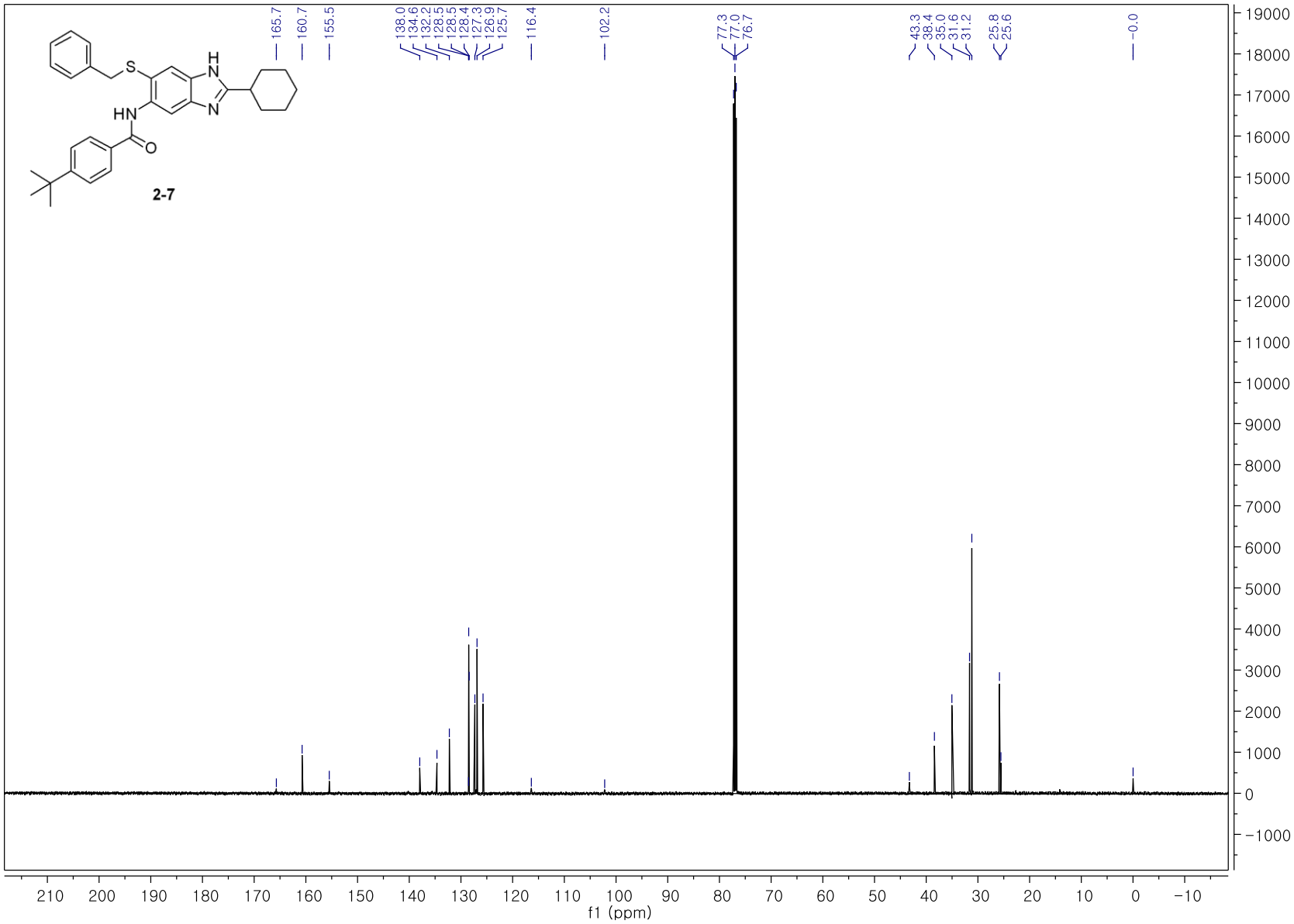
2-7
165.7
160.7
155.5
138.0
134.6
132.2
128.5
128.5
128.4
127.3
126.9
125.7
116.4
102.2
77.3
77.0
76.7
43.3
38.4
35.0
31.6
31.2
25.8
25.6
0.0
f1 (ppm)

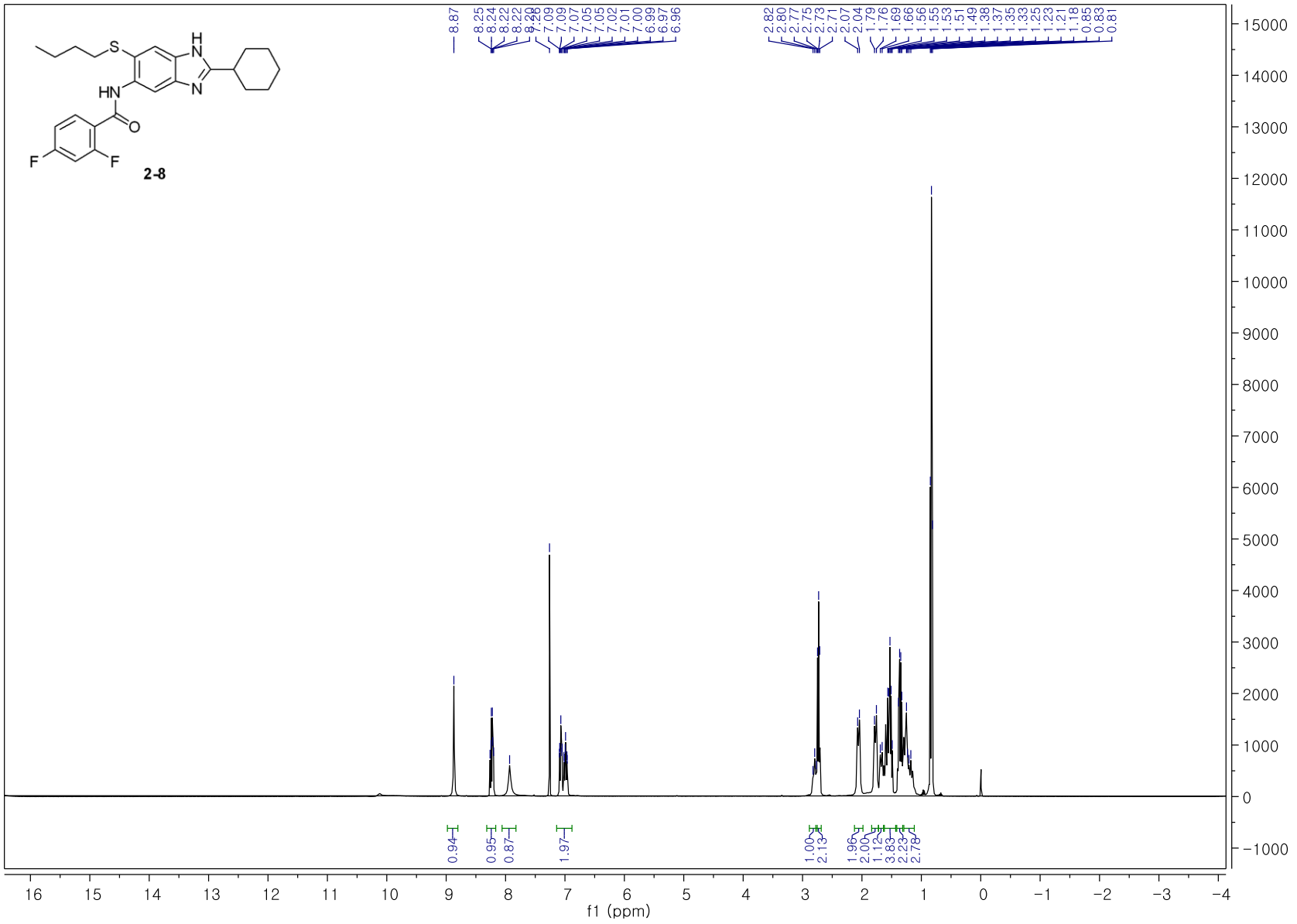
2-8
8.87
8.25
8.24
8.22
8.22
7.09
7.09
7.07
7.05
7.05
7.02
7.01
7.00
6.99
6.97
6.96
2.82
2.80
2.77
2.75
2.73
2.71
2.07
2.04
1.79
1.76
1.69
1.66
1.56
1.55
1.53
1.51
1.49
1.38
1.37
1.35
1.33
1.25
1.23
1.21
1.18
0.85
0.83
0.81
0.94
0.95
0.87
1.97
1.00
2.13
1.96
2.00
1.12
3.83
2.23
2.78
f1 (ppm)

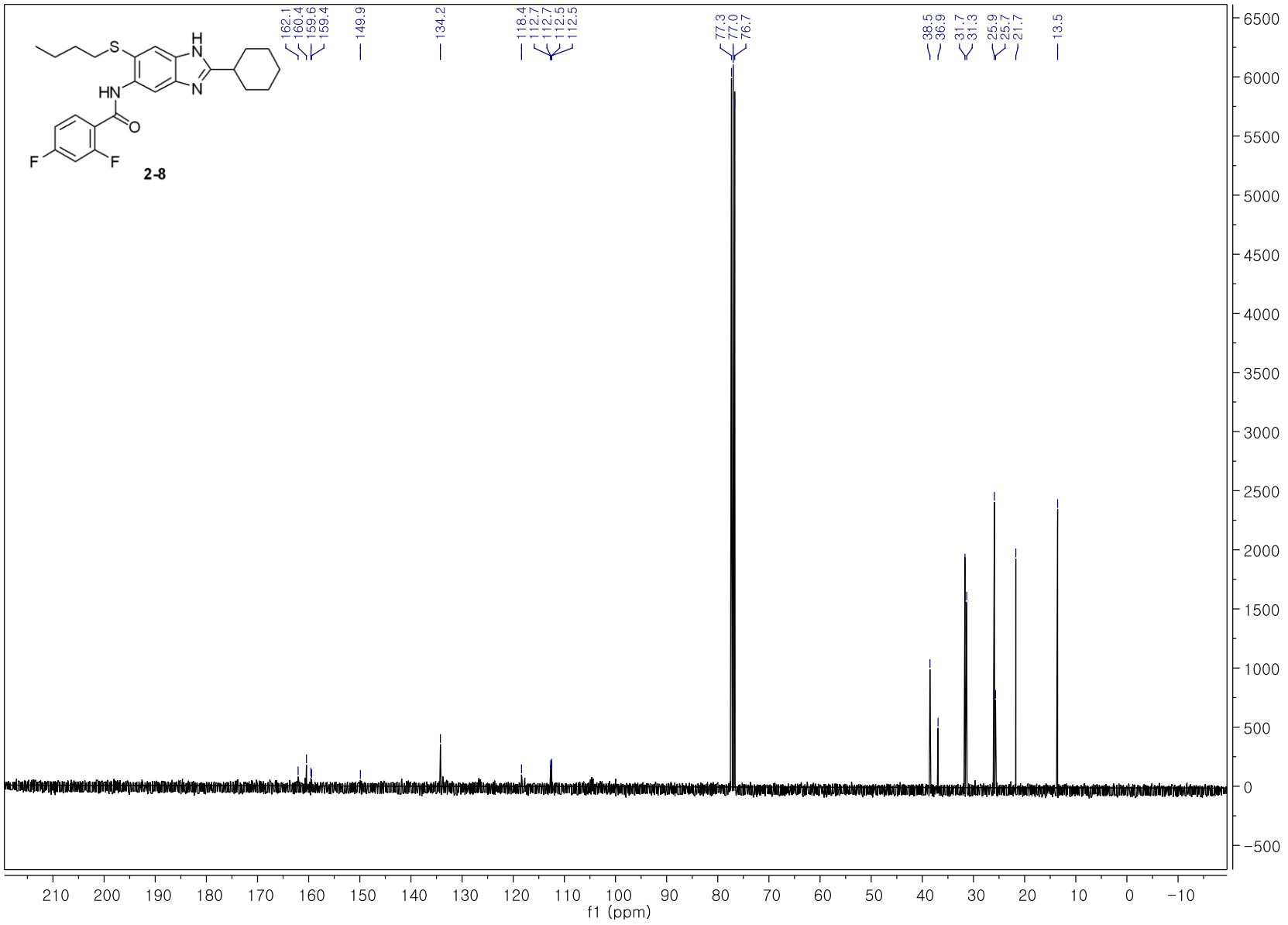
2-8
162.1
160.4
159.6
159.4
149.9
134.2
118.4
112.7
112.7
112.5
112.5
77.3
77.0
76.7
38.5
36.9
31.7
31.3
25.9
25.7
21.7
13.5
f1 (ppm)

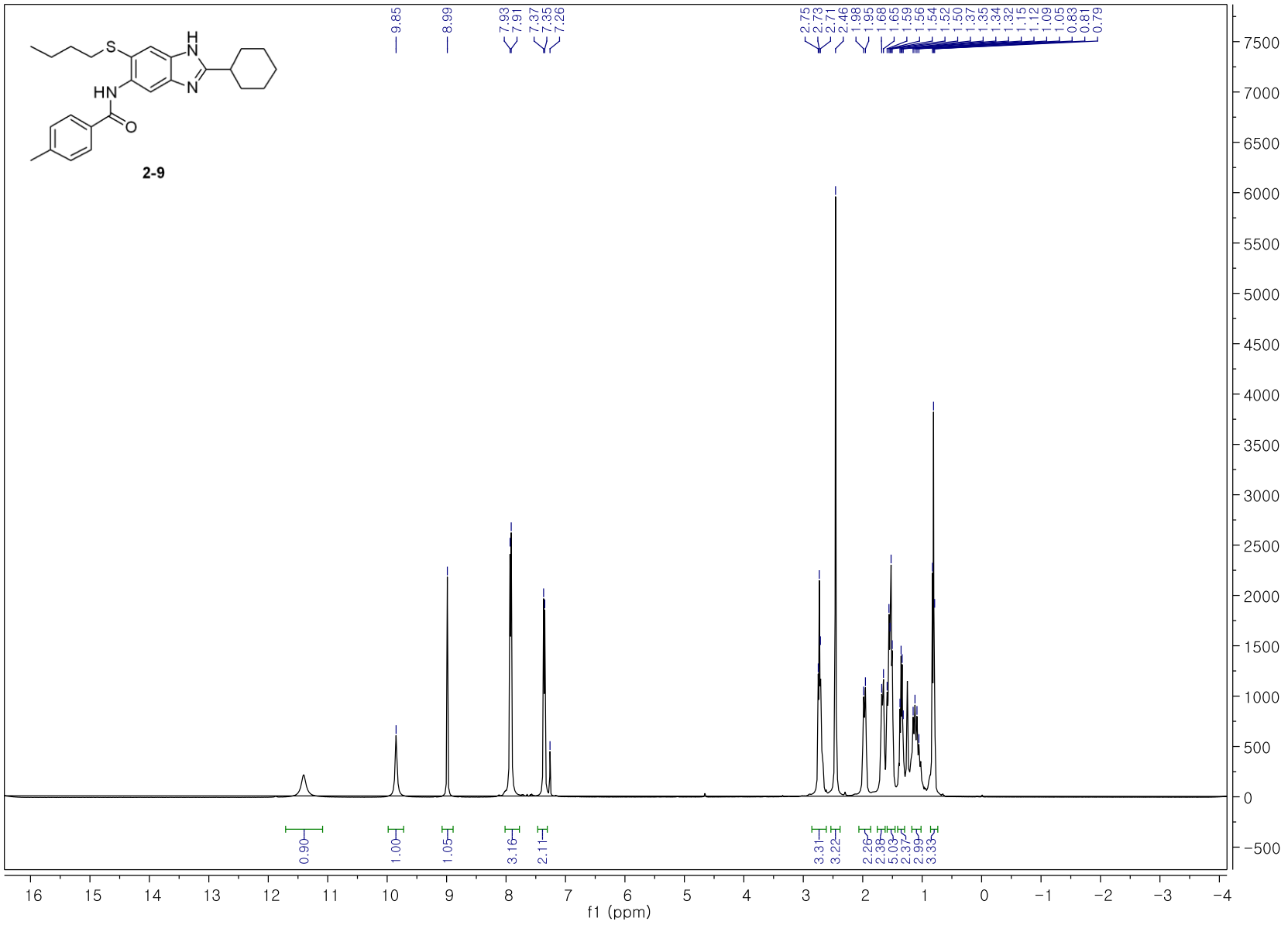
2-9
9.85
8.99
7.93
7.91
7.37
7.35
7.26
2.75
2.73
2.71
2.46
1.98
1.95
1.68
1.65
1.59
1.56
1.54
1.52
1.50
1.37
1.35
1.34
1.32
1.15
1.12
1.09
1.05
0.83
0.81
0.79
0.90
1.00
1.05
3.16
2.11
3.31
3.22
2.26
2.38
5.03
2.37
2.99
3.33
f1 (ppm)

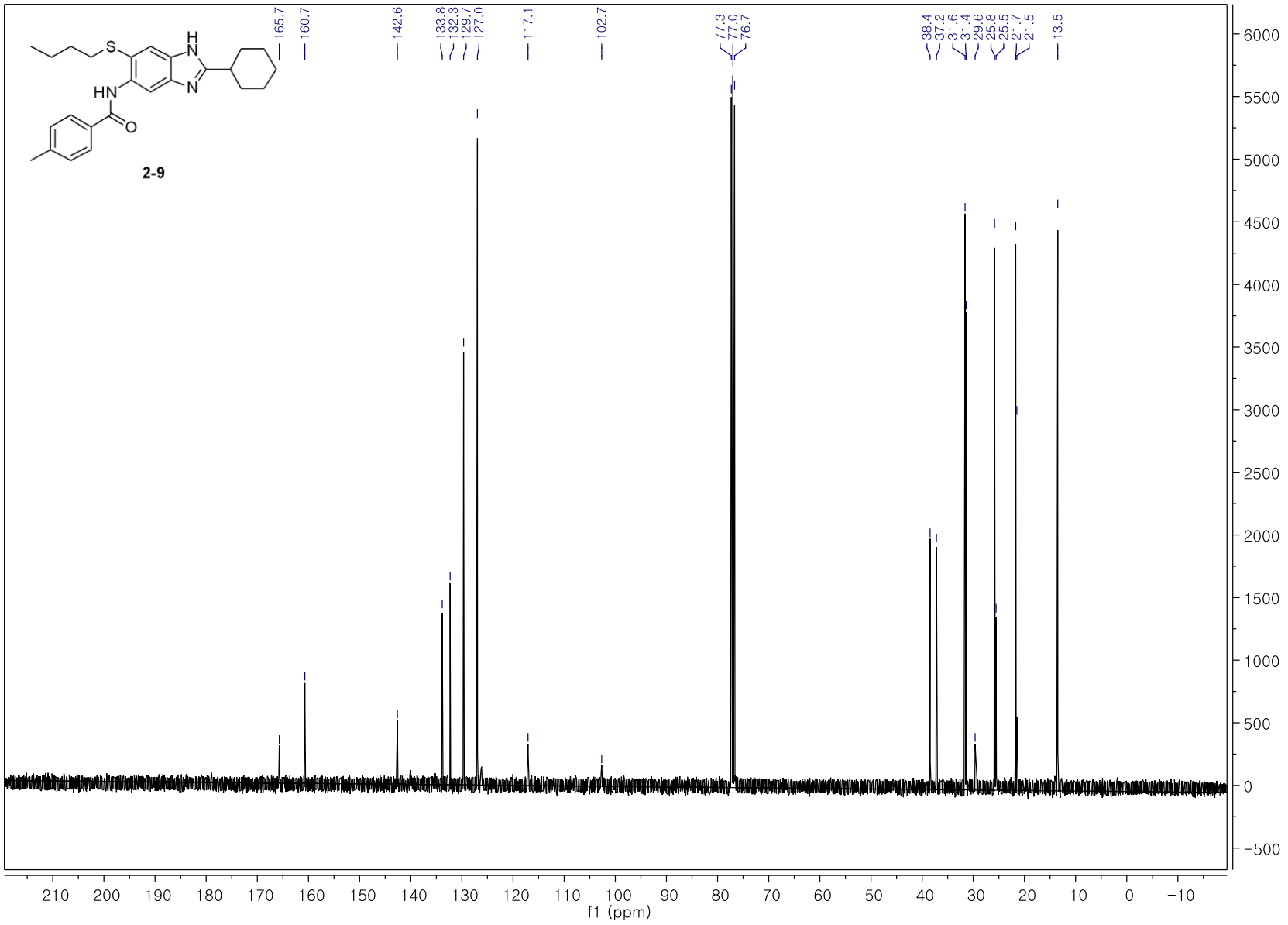
2-9
165.7
160.7
142.6
133.8
132.3
129.7
127.0
117.1
102.7
77.3
77.0
76.7
38.4
37.2
31.6
31.4
29.6
25.8
25.5
21.7
21.5
13.5
f1 (ppm)

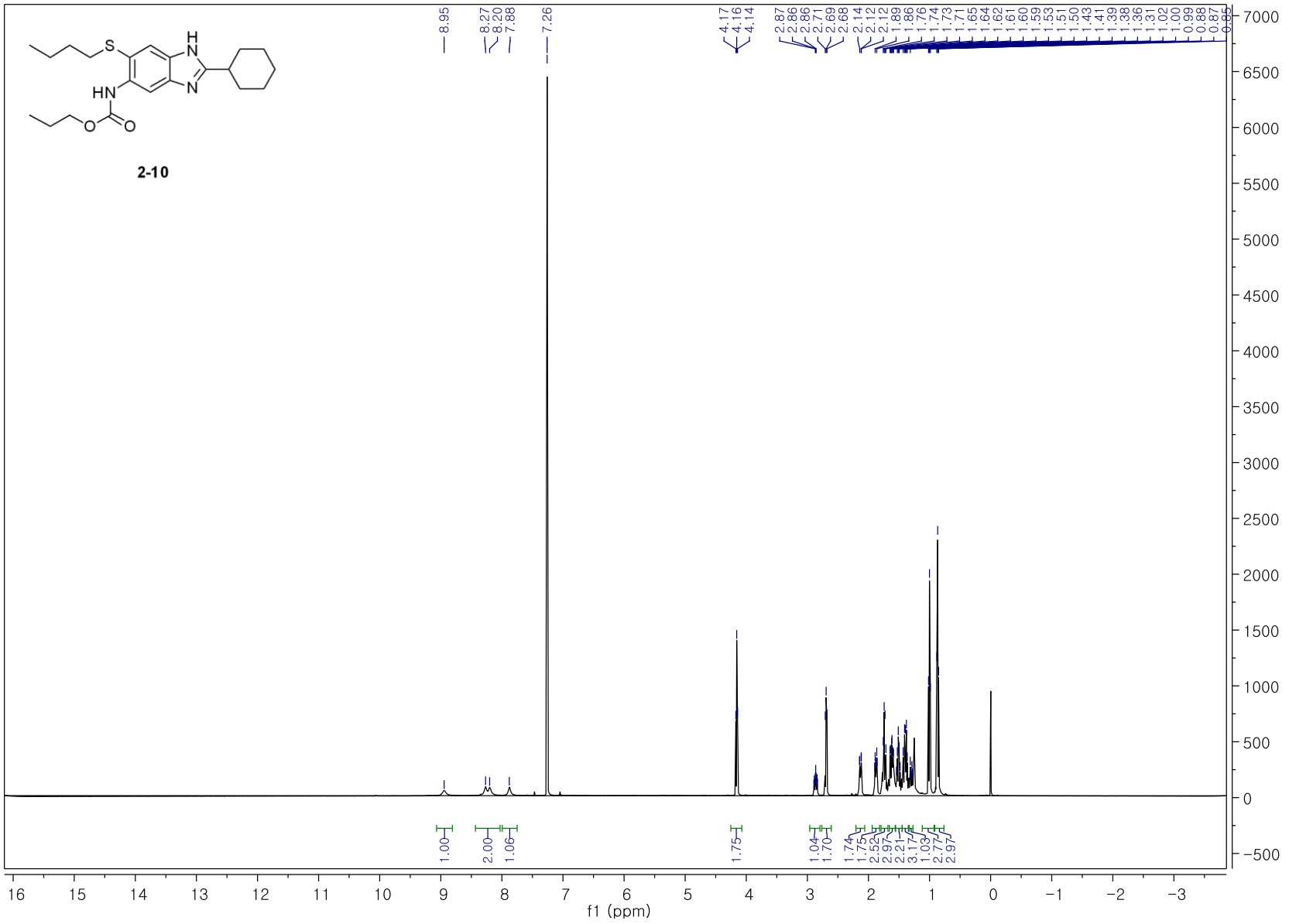
2-10
8.95
8.27
8.20
7.88
7.26
4.17
4.16
4.14
2.87
2.86
2.86
2.71
2.69
2.68
2.14
2.12
2.12
1.89
1.86
1.76
1.74
1.73
1.71
1.65
1.64
1.62
1.61
1.60
1.59
1.53
1.51
1.50
1.43
1.41
1.39
1.38
1.36
1.31
1.02
1.00
0.99
0.88
0.87
0.85
1.00
2.00
1.06
1.75
1.04
1.70
1.74
1.75
2.52
2.97
2.21
3.17
1.03
2.77
2.97
f1 (ppm)

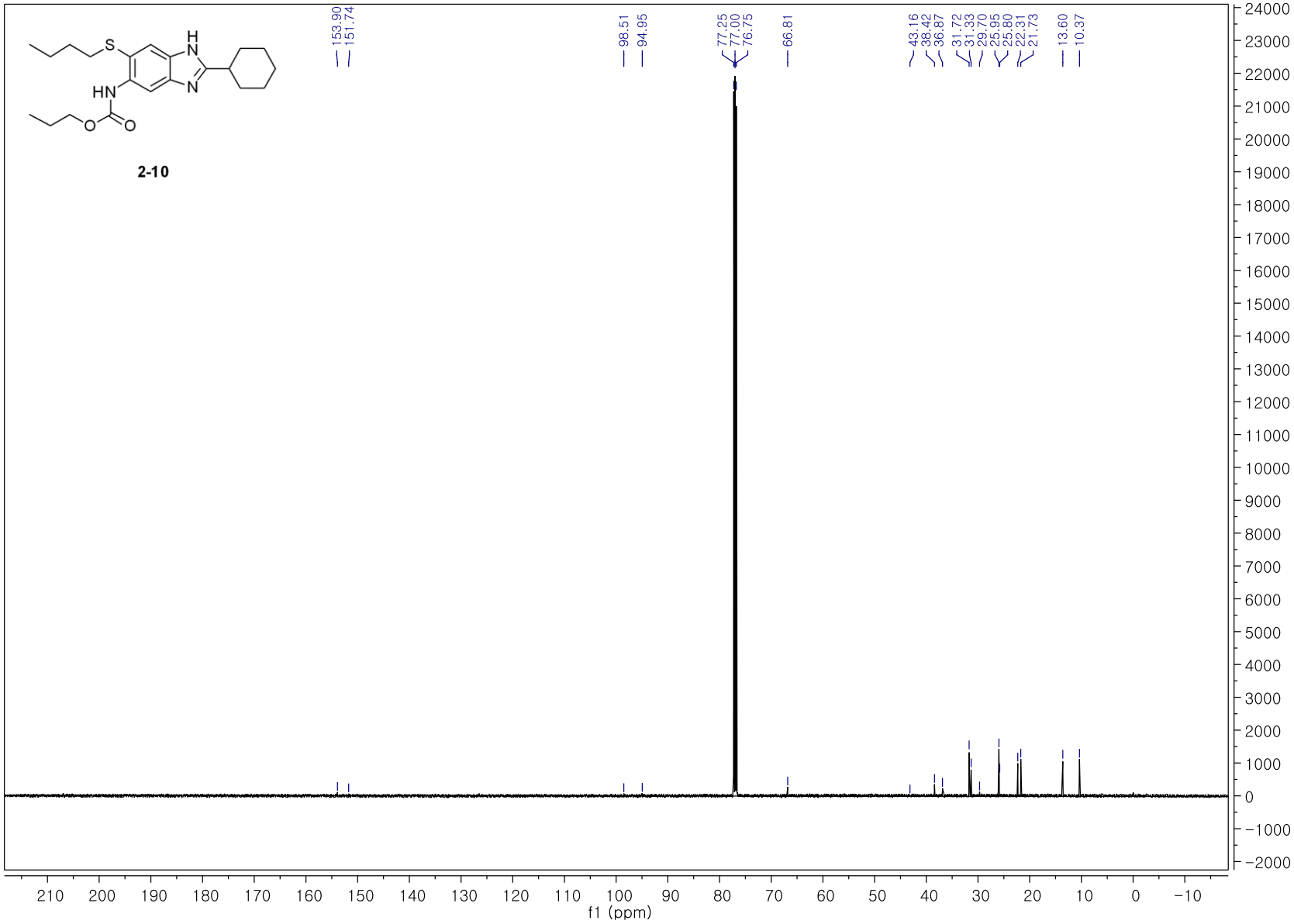
2-10
153.90
151.74
98.51
94.95
77.25
77.00
76.75
66.81
43.16
38.42
36.87
31.72
31.33
29.70
25.95
25.80
22.31
21.73
13.60
10.37
f1 (ppm)

Chapter 3

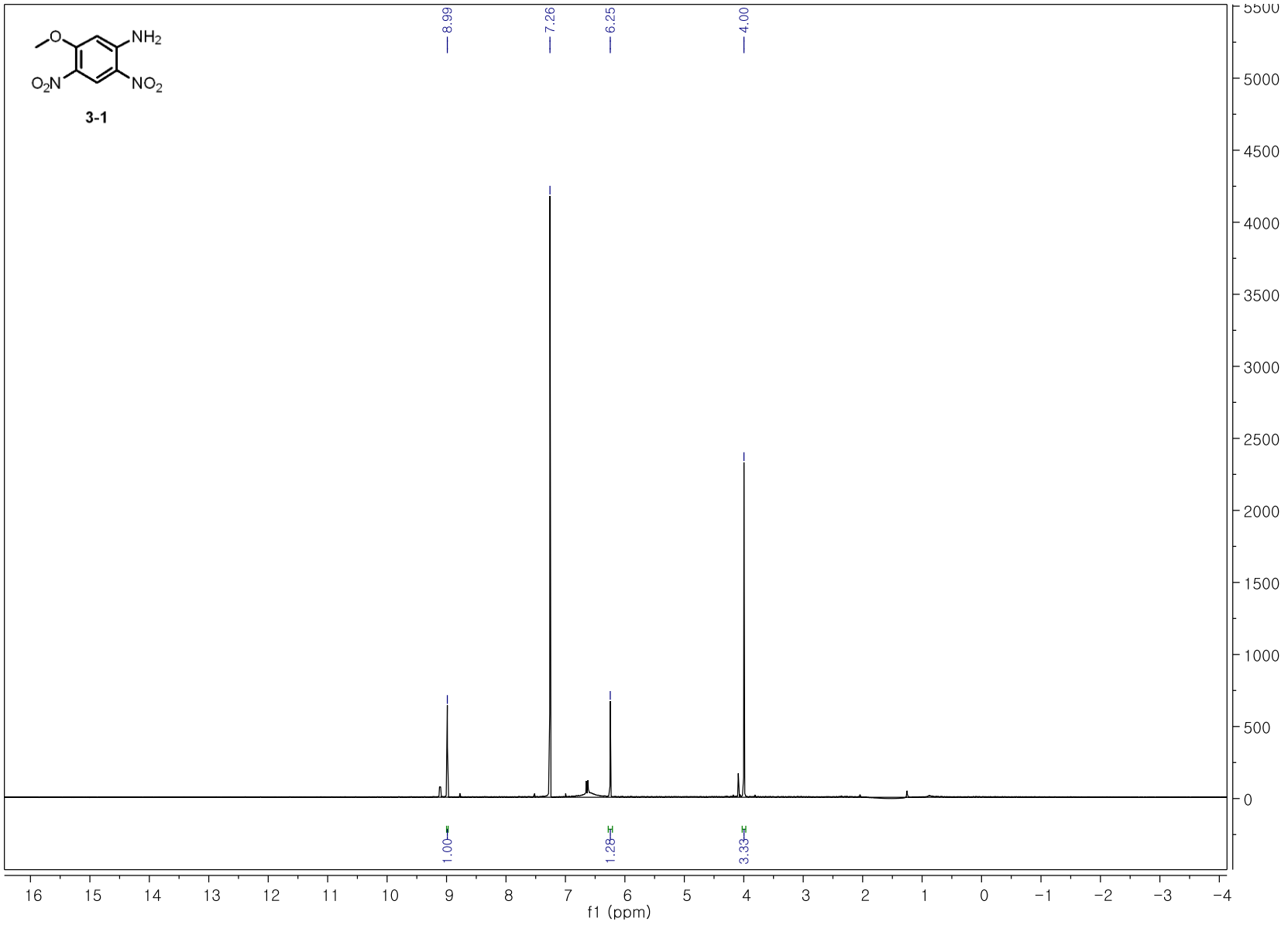
3-1
8.99
7.26
6.25
4.00
1.00
1.28
3.33
f1 (ppm)

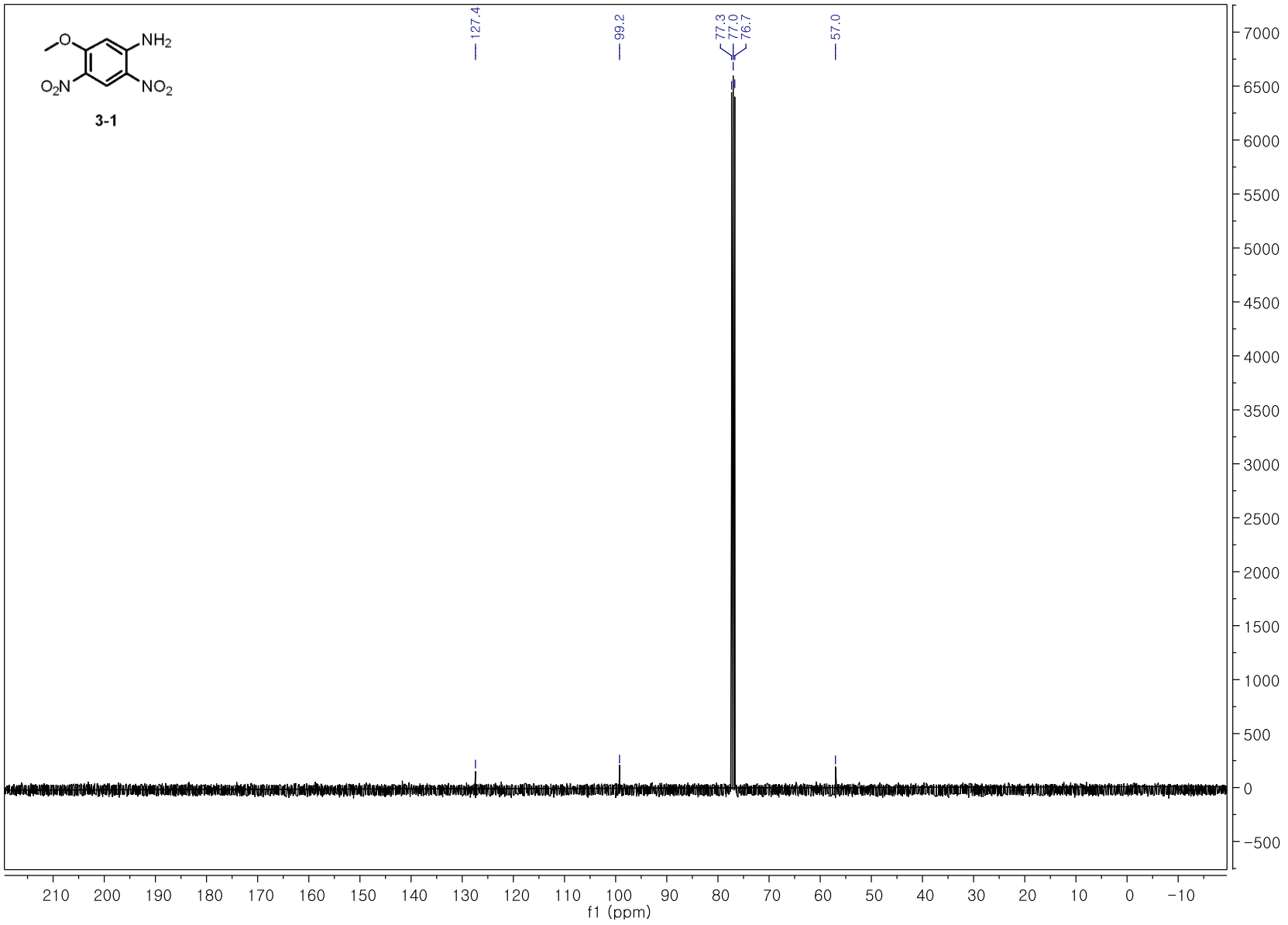
O
NH2
O2N
NO2
3-1
127.4
99.2
77.3
77.0
76.7
57.0
7000
6500
6000
5500
5000
4500
4000
3500
3000
2500
2000
1500
1000
500
0
−500
210 200 190 180 170 160 150 140 130 120 110 100 90 80 70 60 50 40 30 20 10 0 −10
f1 (ppm)

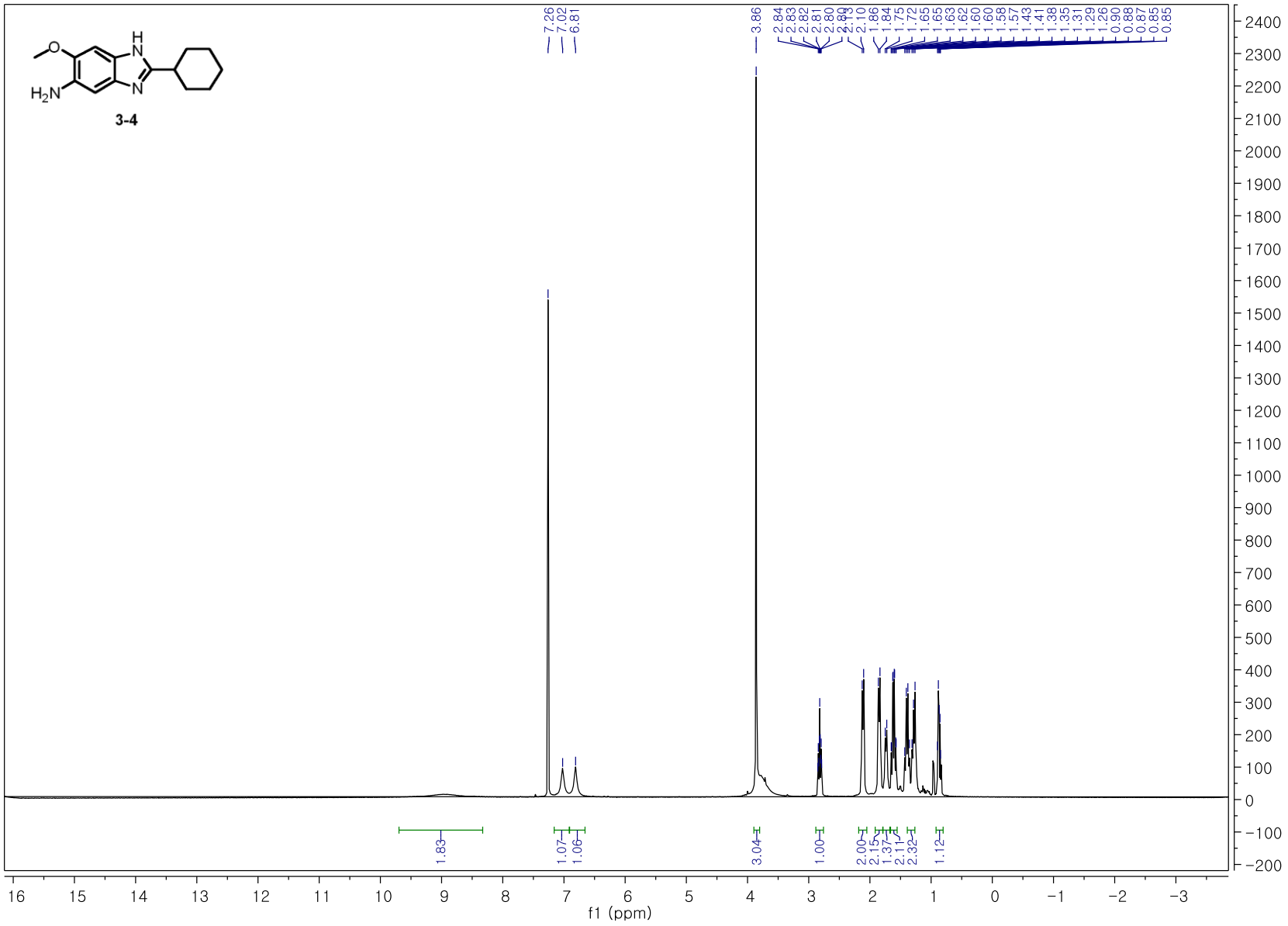
3-4
7.26
7.02
6.81
3.86
2.84
2.83
2.82
2.81
2.80
2.10
1.86
1.84
1.75
1.72
1.65
1.63
1.62
1.60
1.58
1.57
1.43
1.41
1.38
1.35
1.31
1.29
1.26
0.90
0.88
0.87
0.85
0.85
1.83
1.07
1.06
3.04
1.00
2.00
2.15
1.37
2.11
2.32
1.12
f1 (ppm)

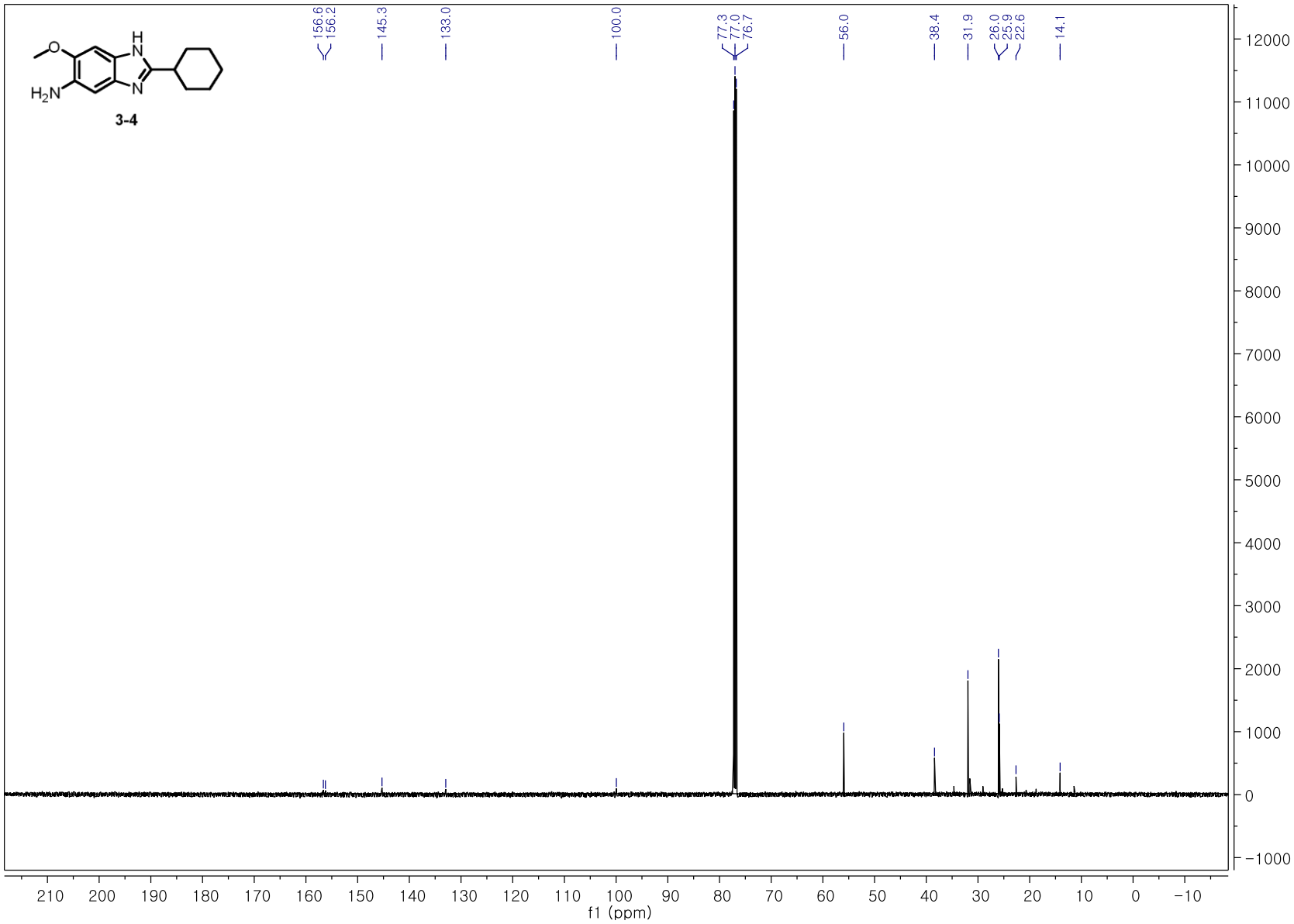
3-4
156.6
156.2
145.3
133.0
100.0
77.3
77.0
76.7
56.0
38.4
31.9
26.0
25.9
22.6
14.1
f1 (ppm)

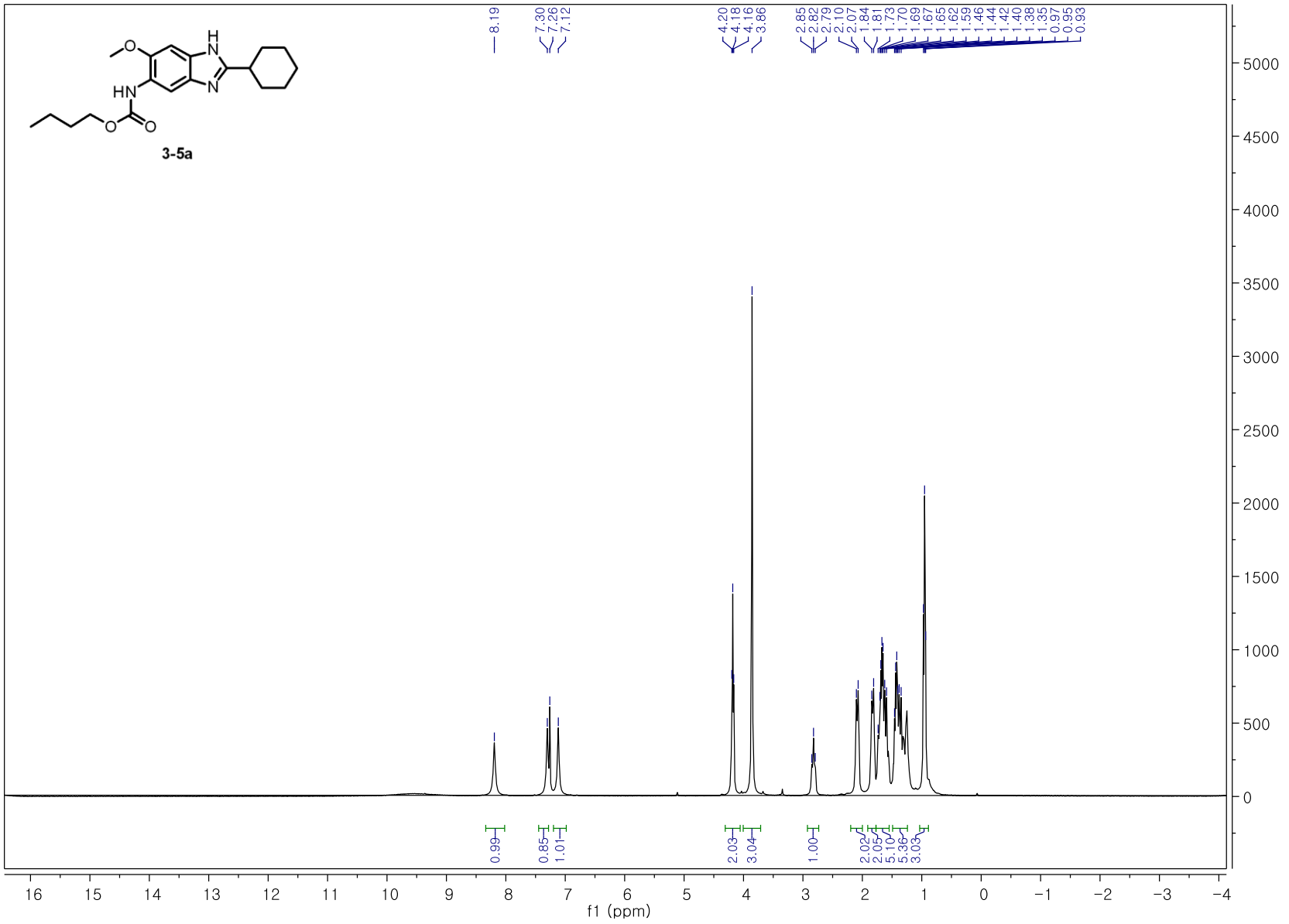
3-5a
8.19
7.30
7.26
7.12
4.20
4.18
4.16
3.86
2.85
2.82
2.79
2.10
2.07
1.84
1.81
1.73
1.70
1.69
1.67
1.65
1.62
1.59
1.46
1.44
1.42
1.40
1.38
1.35
0.97
0.95
0.93
0.99
0.85
1.01
2.03
3.04
1.00
2.02
2.05
5.10
5.36
3.03
f1 (ppm)

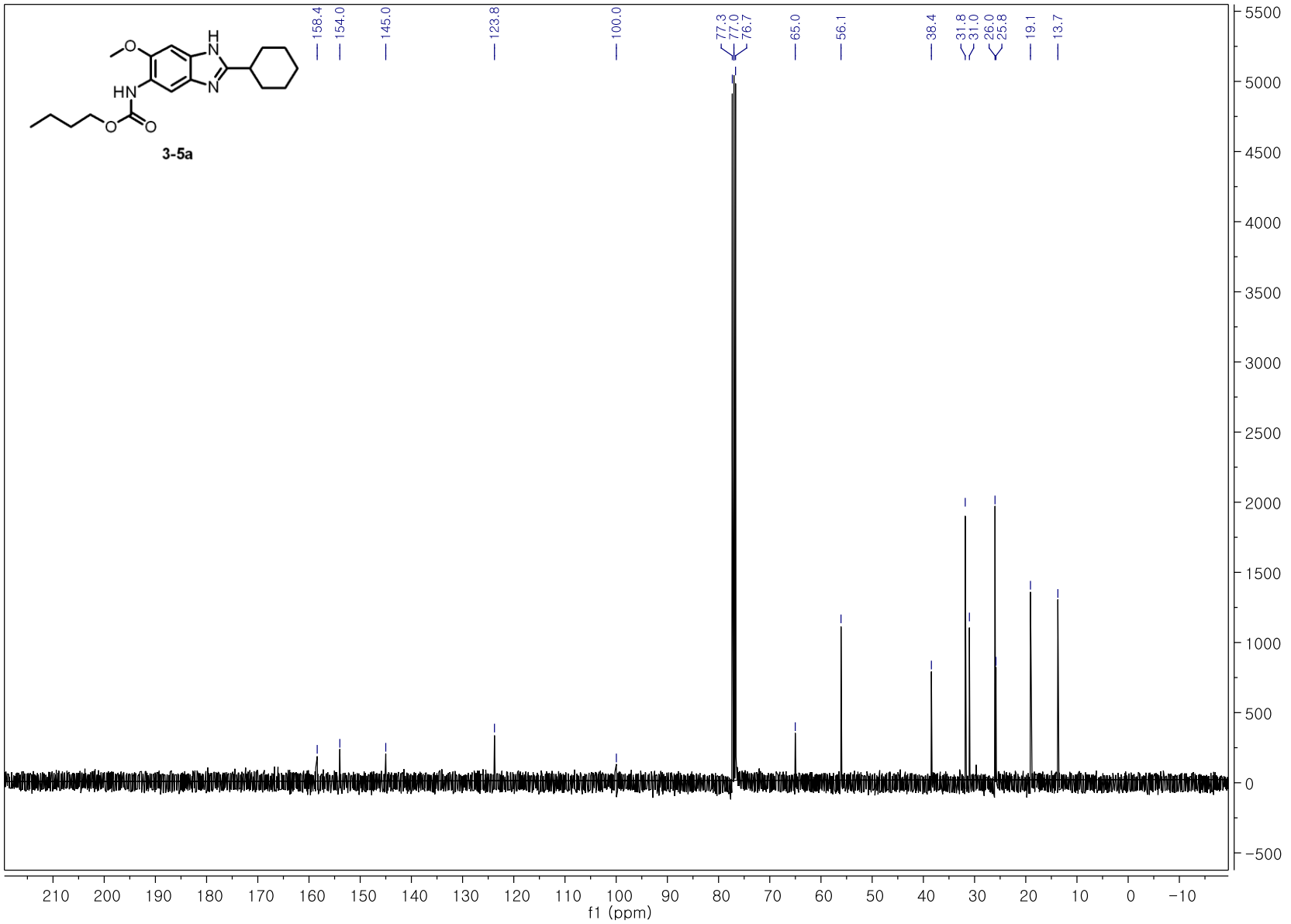
3-5a
158.4
154.0
145.0
123.8
100.0
77.3
77.0
76.7
65.0
56.1
38.4
31.8
31.0
26.0
25.8
19.1
13.7
f1 (ppm)

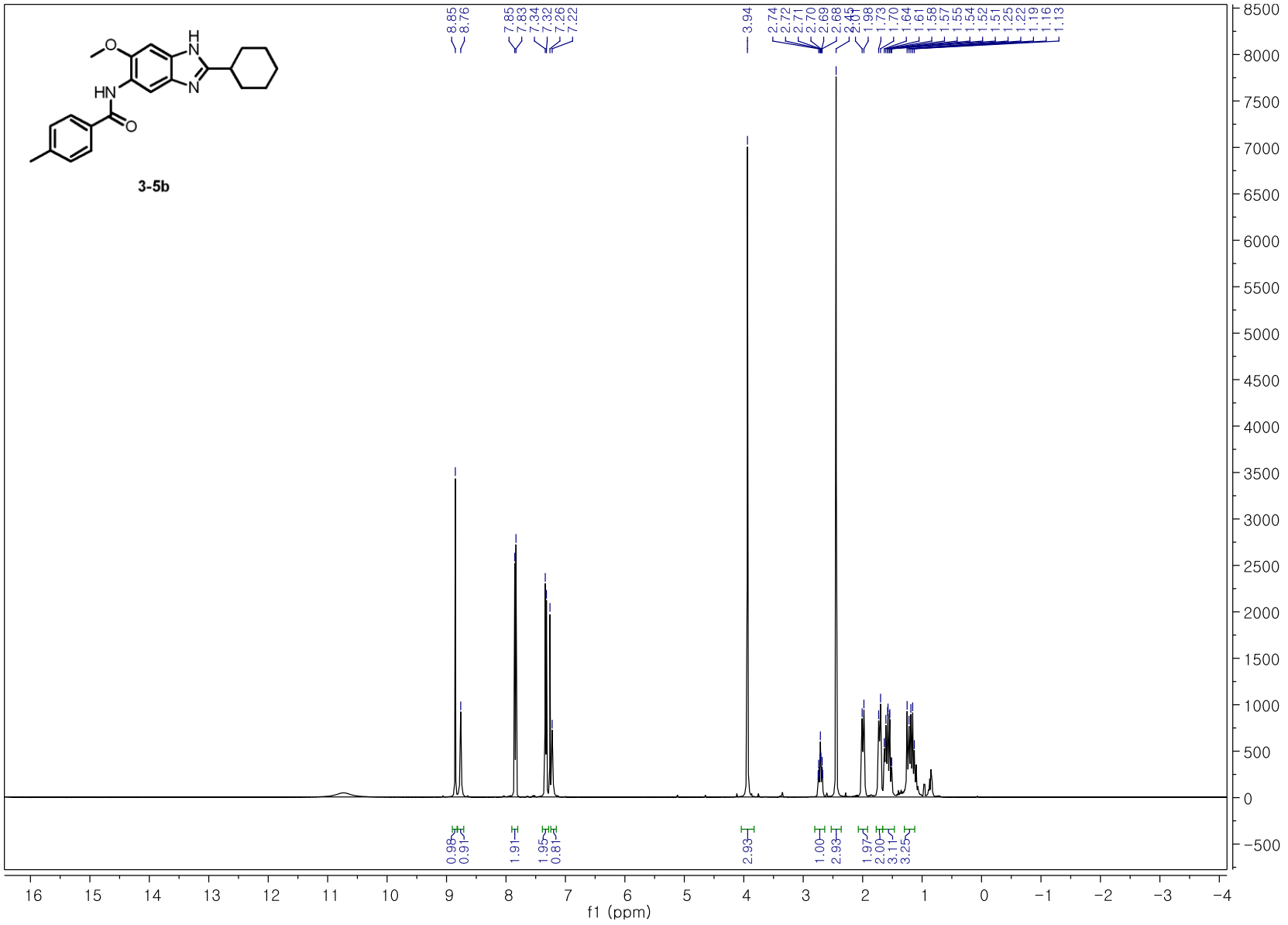
3-5b
8.85
8.76
7.85
7.83
7.34
7.32
7.26
7.22
3.94
2.74
2.72
2.71
2.70
2.69
2.68
2.45
2.01
1.98
1.73
1.70
1.64
1.61
1.58
1.57
1.55
1.54
1.52
1.51
1.25
1.22
1.19
1.16
1.13
0.98
0.91
1.91
1.95
0.81
2.93
1.00
2.93
1.97
2.00
3.11
3.25
f1 (ppm)

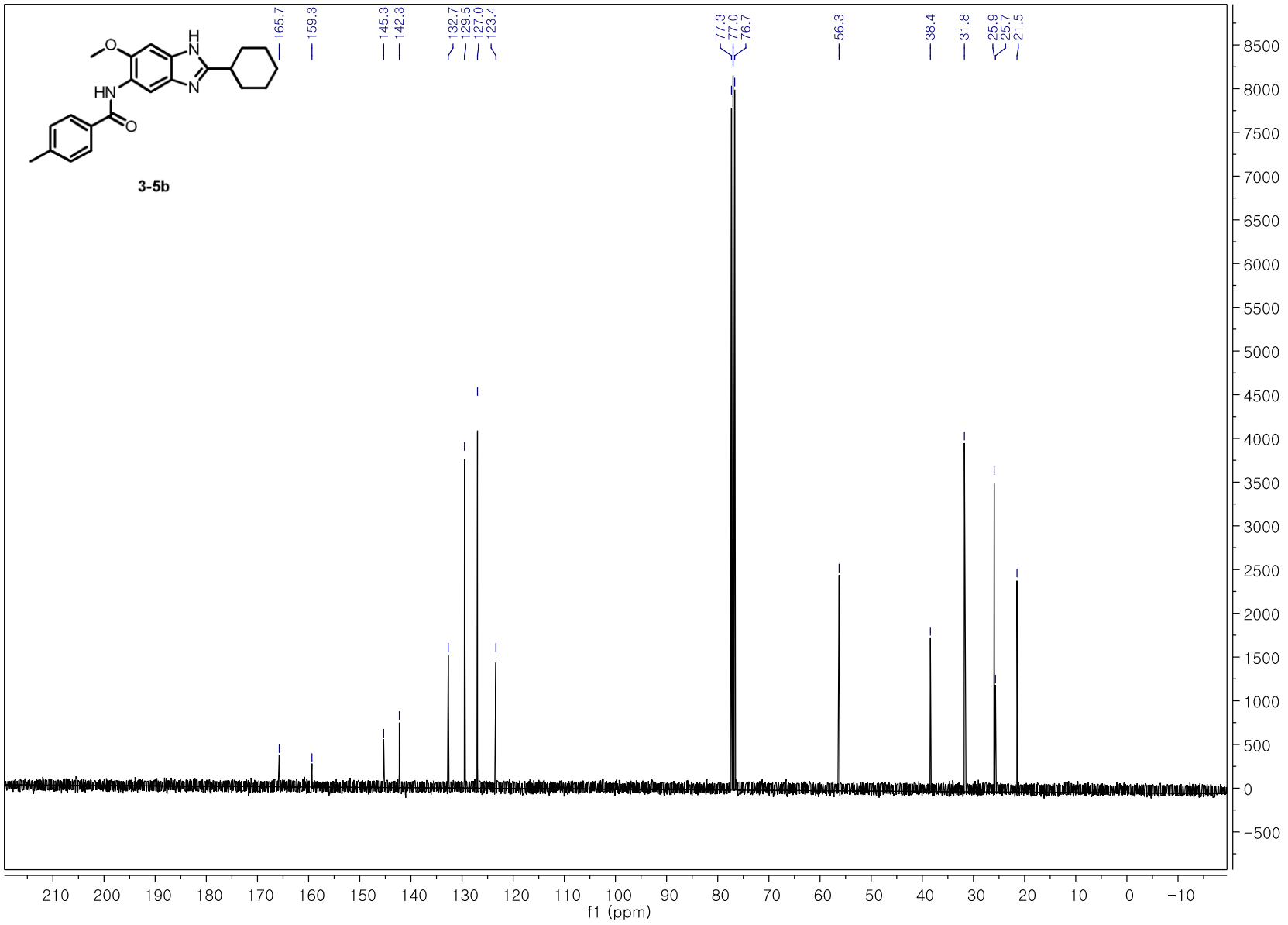
3-5b
165.7
159.3
145.3
142.3
132.7
129.5
127.0
123.4
77.3
77.0
76.7
56.3
38.4
31.8
25.9
25.7
21.5
f1 (ppm)

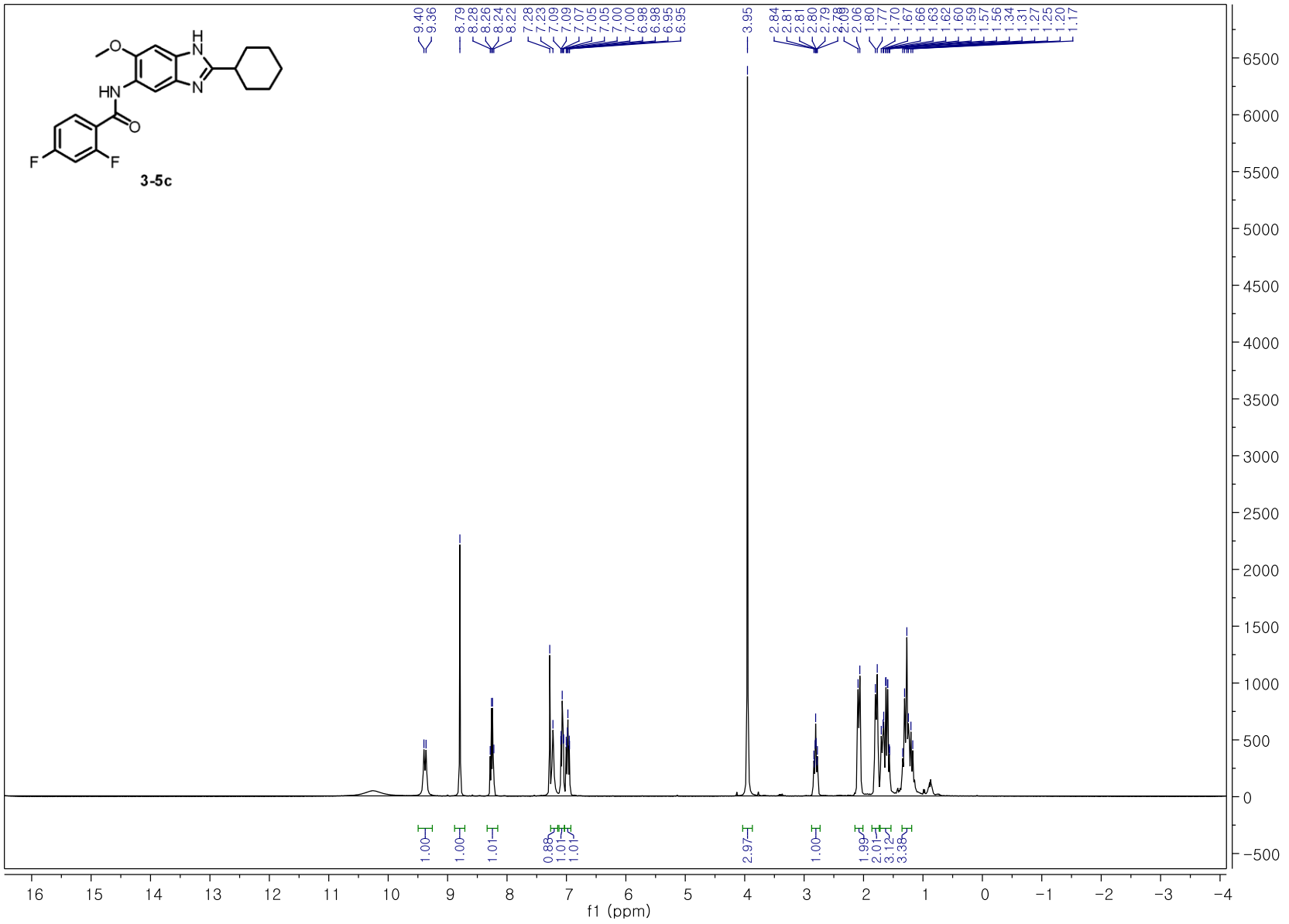
3-5c
f1 (ppm)

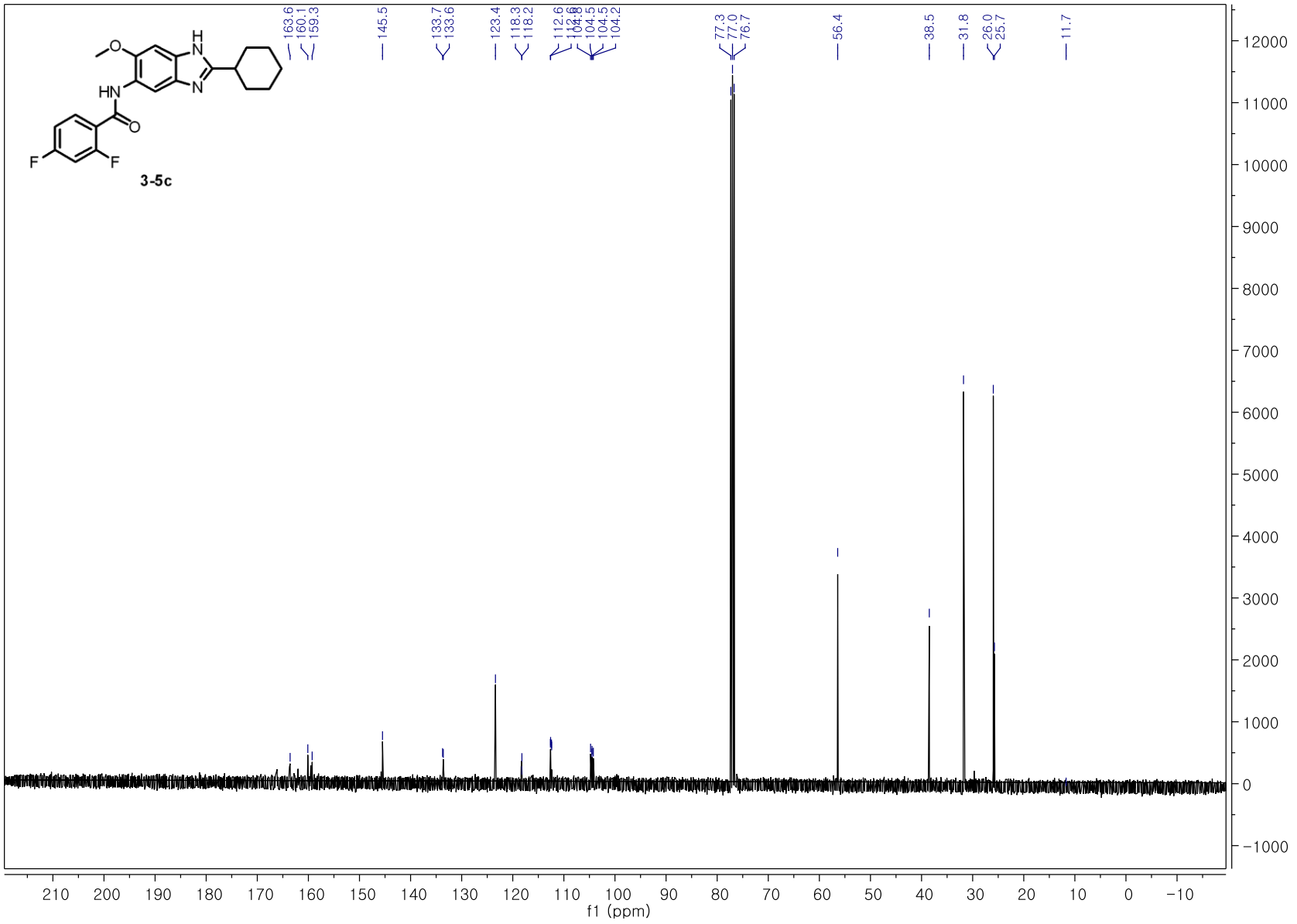
3-5c
163.6
160.1
159.3
145.5
133.7
133.6
123.4
118.3
118.2
112.6
104.5
104.5
104.2
77.3
77.0
76.7
56.4
38.5
31.8
26.0
25.7
11.7
f1 (ppm)

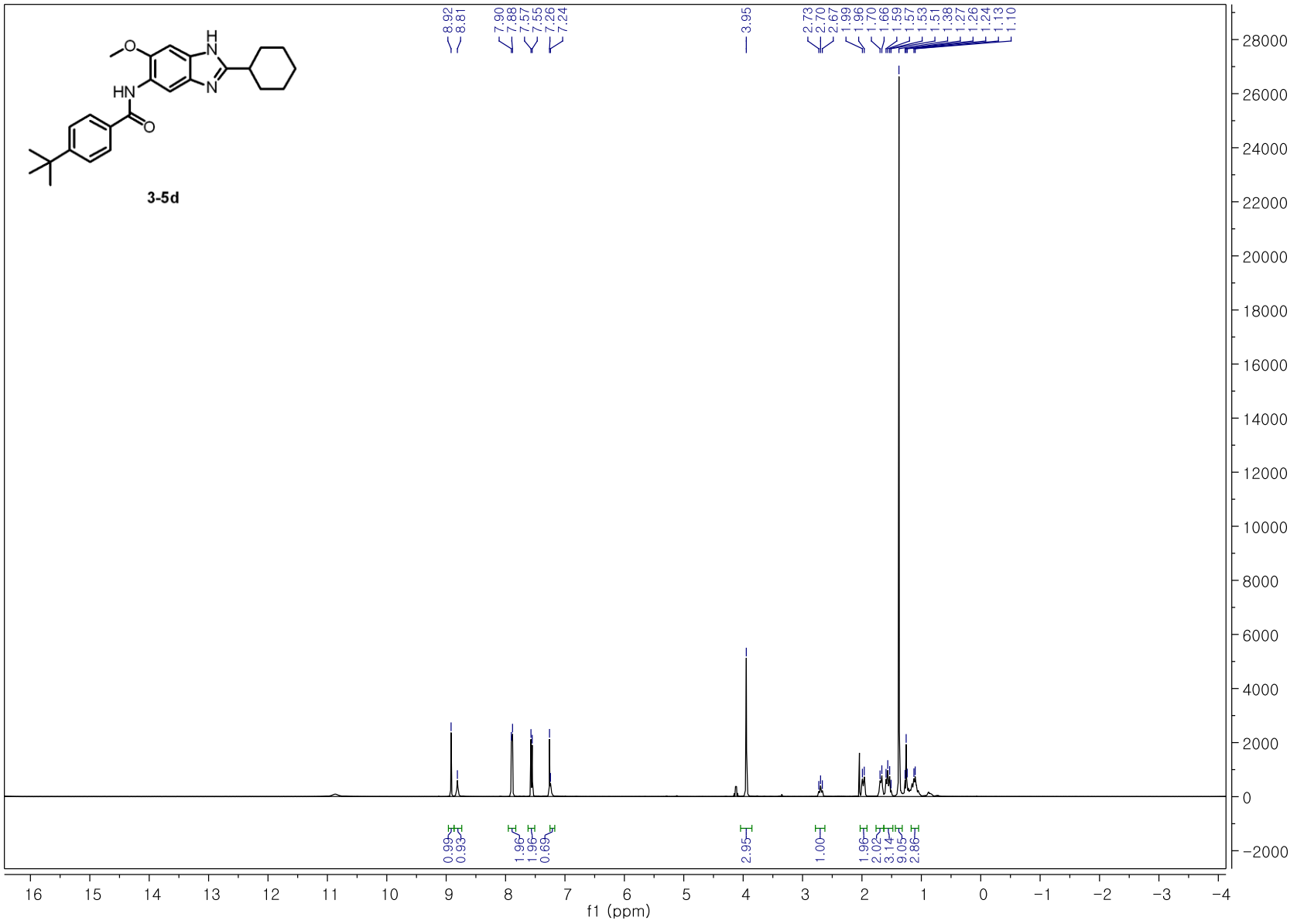
3-5d
8.92
8.81
7.90
7.88
7.57
7.55
7.26
7.24
3.95
2.73
2.70
2.67
1.99
1.96
1.70
1.66
1.59
1.57
1.53
1.51
1.38
1.27
1.26
1.24
1.13
1.10
0.99
0.93
1.96
1.96
0.69
2.95
1.00
1.96
2.02
3.14
9.05
2.86
f1 (ppm)

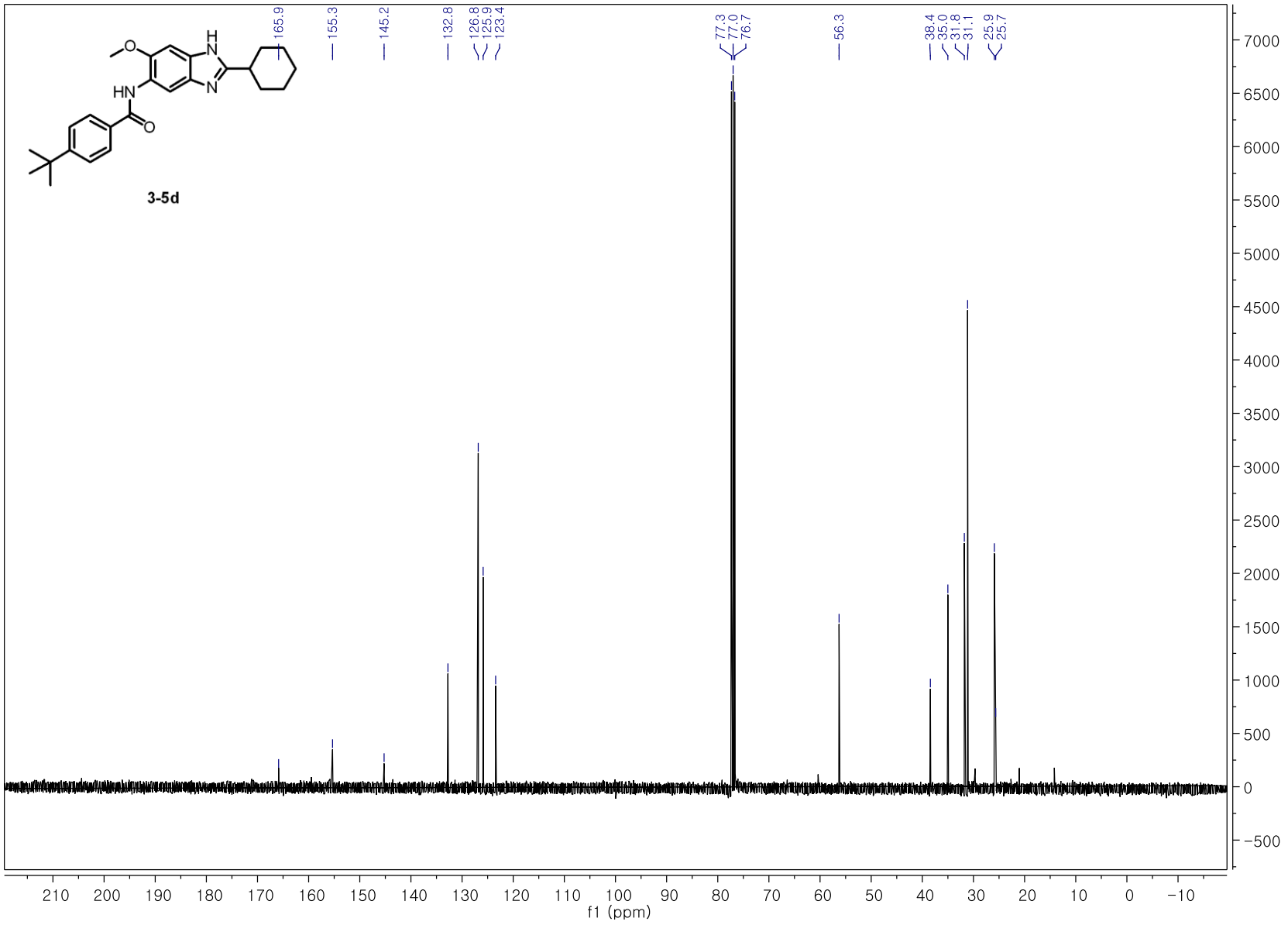
3-5d
165.9
155.3
145.2
132.8
126.8
125.9
123.4
77.3
77.0
76.7
56.3
38.4
35.0
31.8
31.1
25.9
25.7
f1 (ppm)

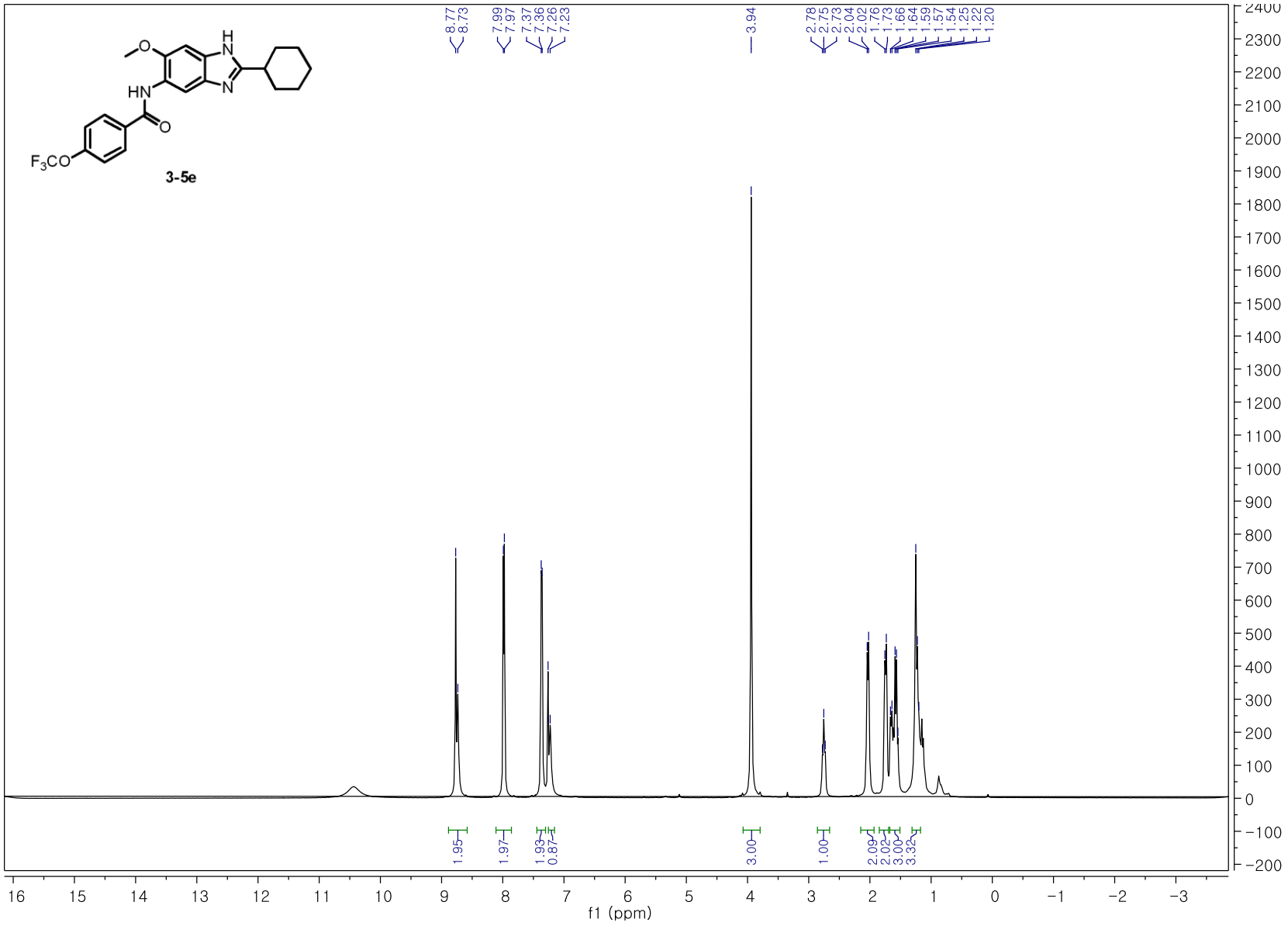
3-5e
8.77
8.73
7.99
7.97
7.37
7.36
7.26
7.23
3.94
2.78
2.75
2.73
2.04
2.02
1.76
1.73
1.66
1.64
1.59
1.57
1.54
1.25
1.22
1.20
1.95
1.97
1.99
0.87
3.00
1.00
2.09
2.02
3.00
3.32
f1 (ppm)

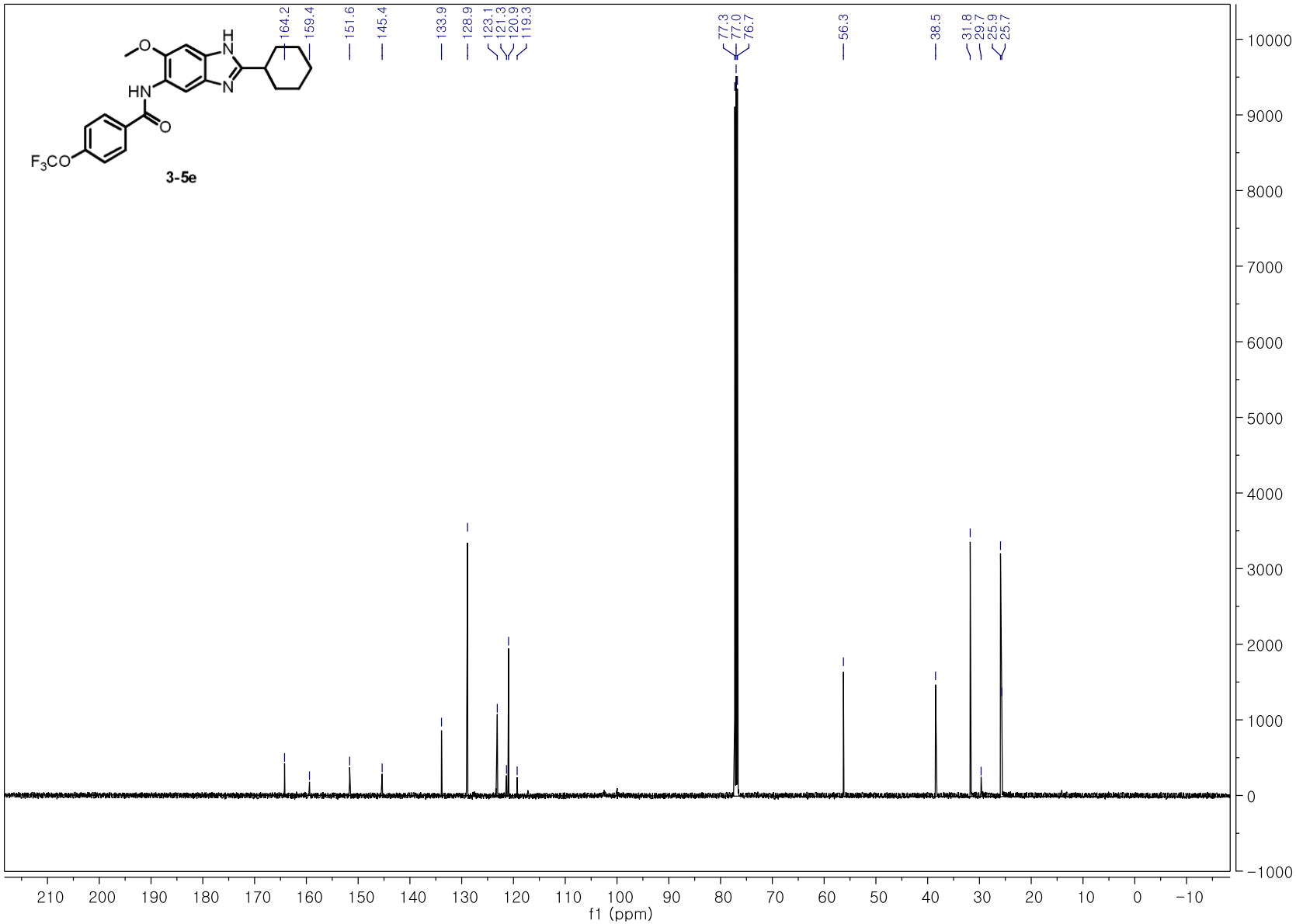
3-5e
164.2
159.4
151.6
145.4
133.9
128.9
123.1
121.3
120.9
119.3
77.3
77.0
76.7
56.3
38.5
31.8
29.7
25.9
25.7
f1 (ppm)

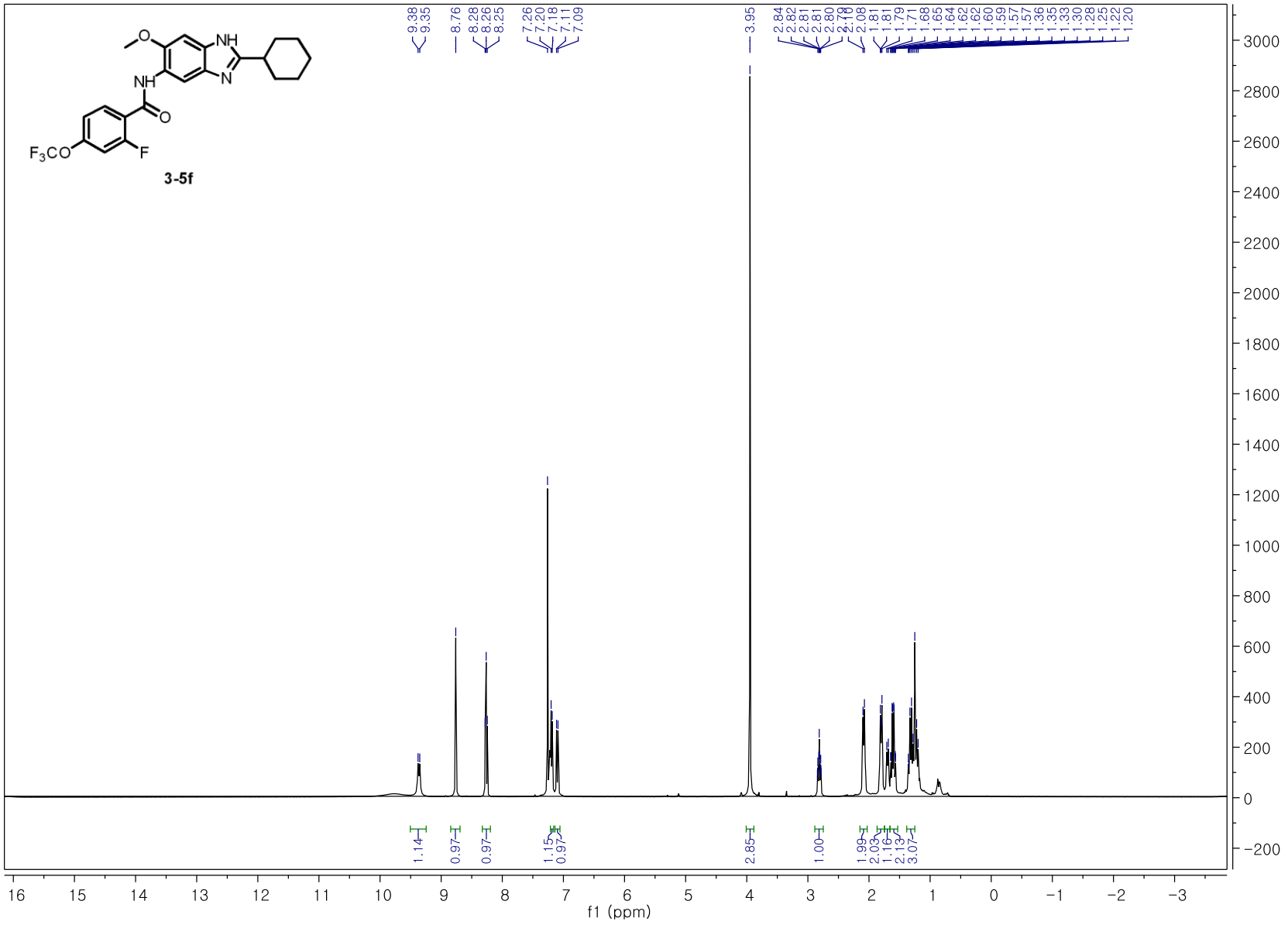
3-5f
f1 (ppm)

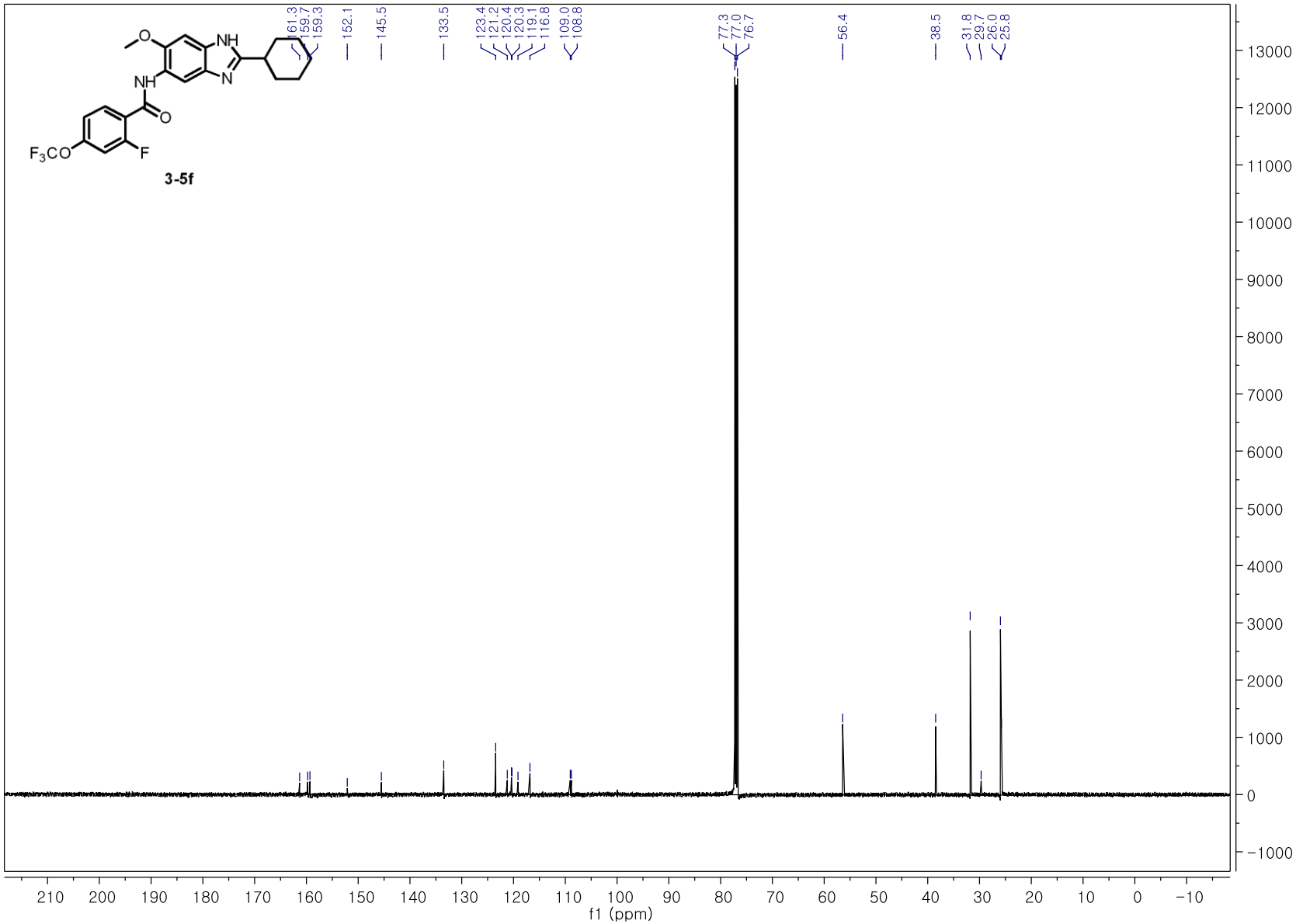
161.3
159.7
159.3
152.1
145.5
133.5
123.4
121.2
120.4
120.3
119.1
116.8
109.0
108.8
77.3
77.0
76.7
56.4
38.5
31.8
29.7
26.0
25.8
3-5f
f1 (ppm)

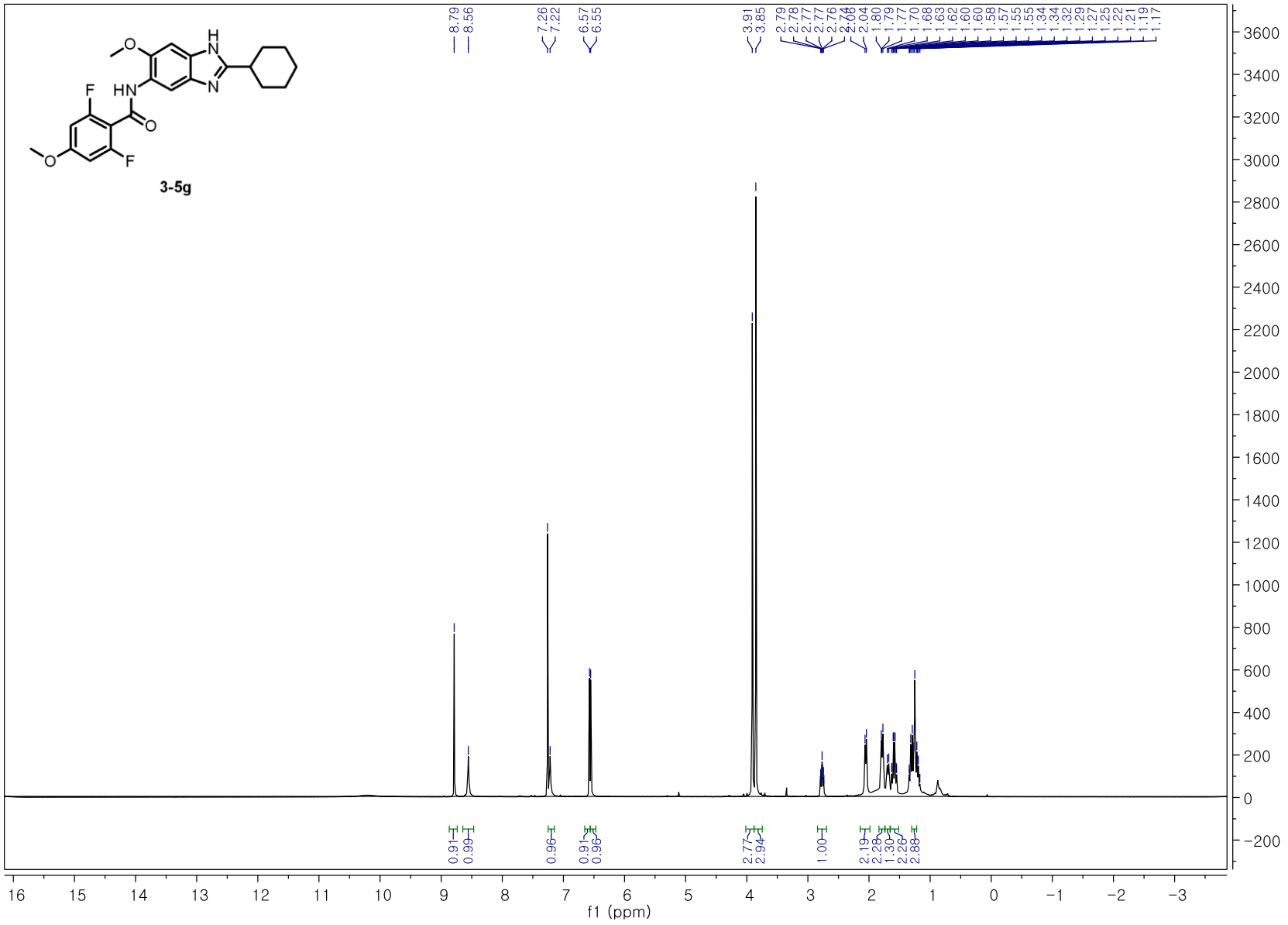
3-5g
8.79
8.56
7.26
7.22
6.57
6.55
3.91
3.85
2.79
2.78
2.77
2.77
2.76
2.04
2.04
1.80
1.79
1.77
1.70
1.68
1.63
1.62
1.60
1.60
1.58
1.57
1.55
1.55
1.34
1.34
1.32
1.29
1.27
1.25
1.22
1.21
1.19
1.17
0.91
0.99
0.96
0.91
0.96
2.77
2.94
1.00
2.19
2.29
1.30
2.26
2.88
f1 (ppm)

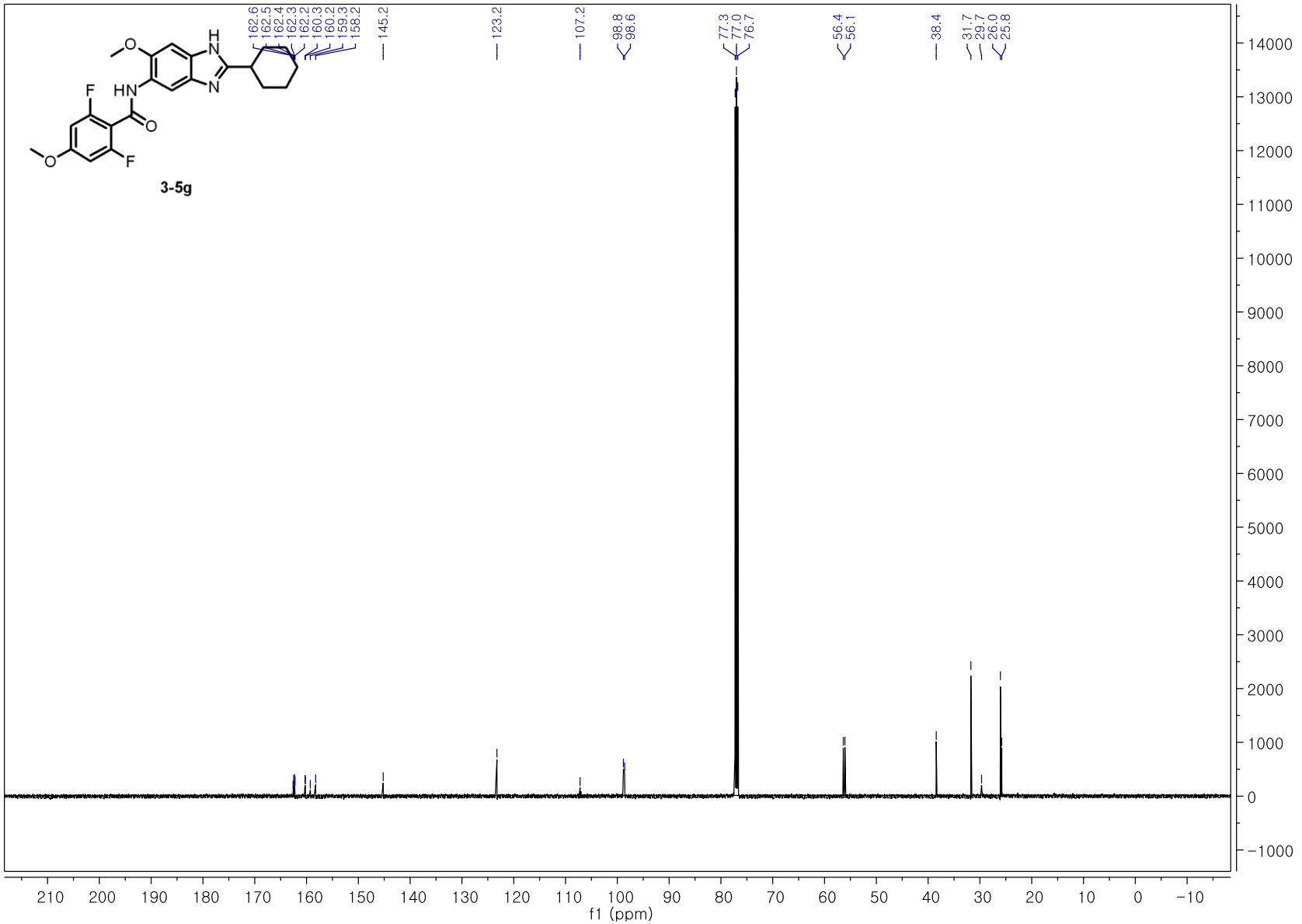
3-5g
162.6
162.5
162.4
162.3
162.2
160.3
160.2
159.3
158.2
145.2
123.2
107.2
98.8
98.6
77.3
77.0
76.7
56.4
56.1
38.4
31.7
29.7
26.0
25.8
f1 (ppm)

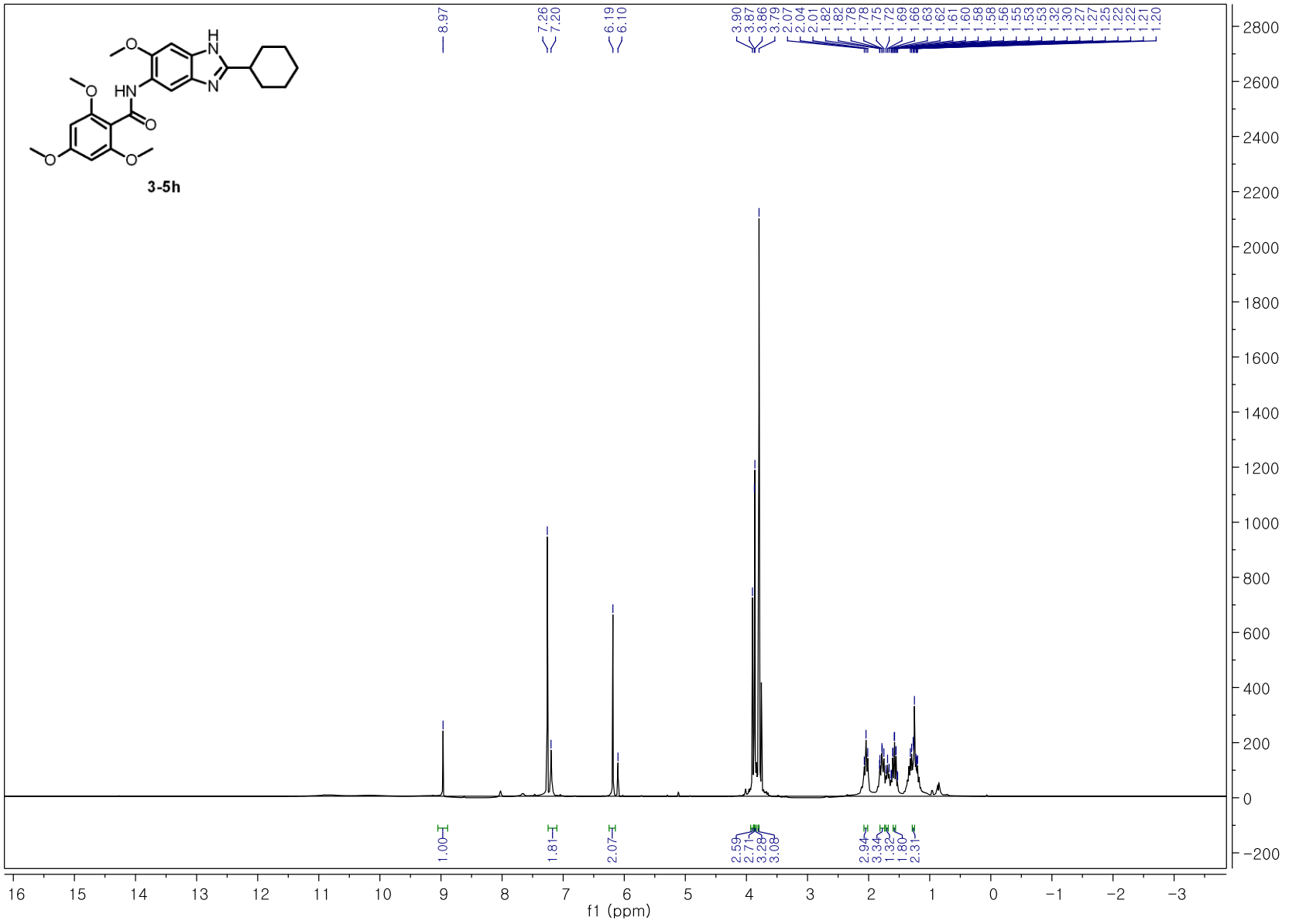
3-5h
8.97
7.26
7.20
6.19
6.10
3.90
3.87
3.86
3.79
2.07
2.04
2.01
1.82
1.82
1.78
1.78
1.75
1.72
1.69
1.66
1.63
1.62
1.61
1.60
1.58
1.58
1.56
1.55
1.53
1.53
1.32
1.30
1.27
1.27
1.25
1.22
1.22
1.21
1.20
1.00
1.81
2.07
2.59
2.71
3.28
3.08
2.94
3.34
1.32
1.80
2.31
f1 (ppm)

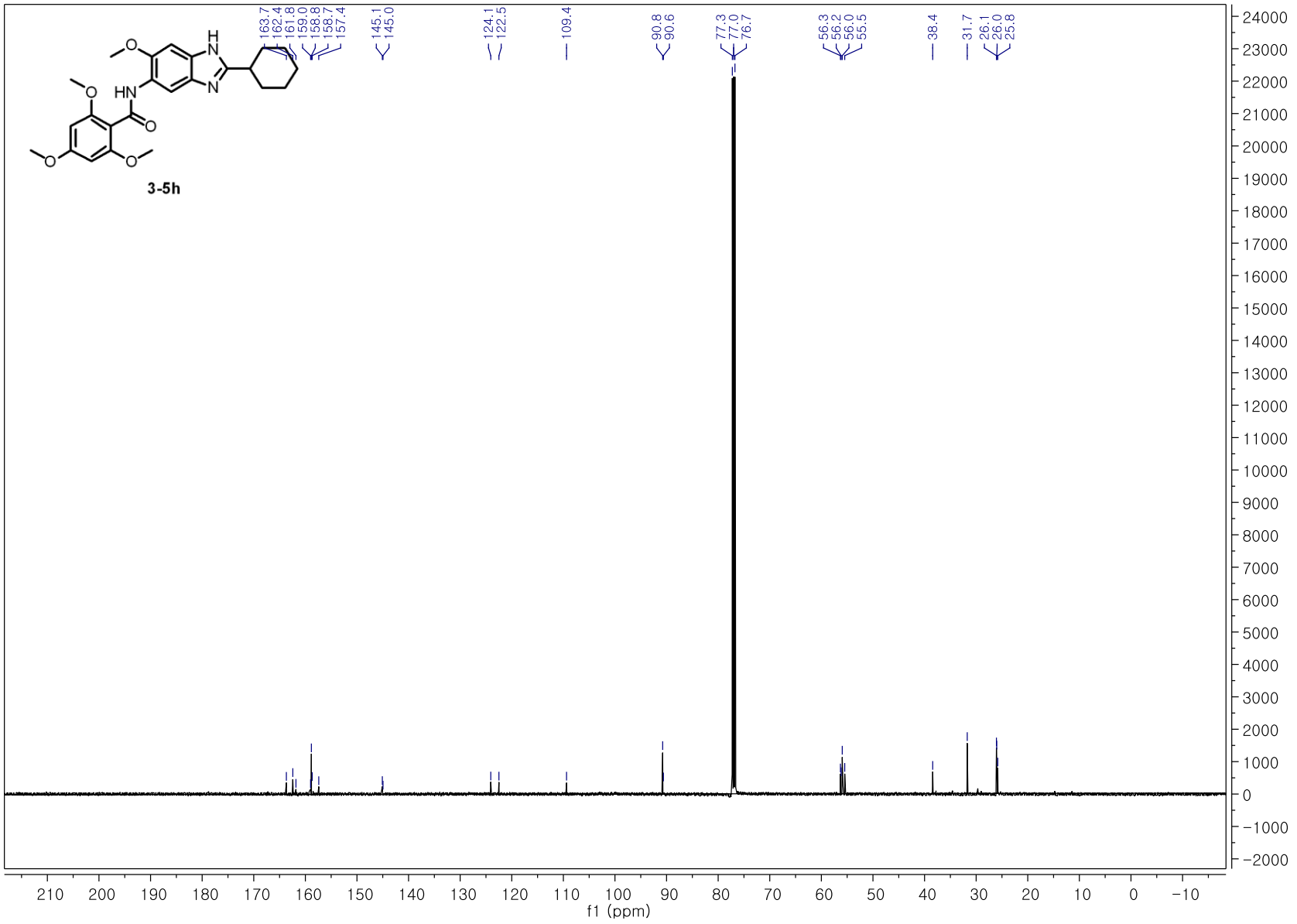
3-5h
163.7
162.4
161.8
159.0
158.8
158.7
157.4
145.1
145.0
124.1
122.5
109.4
90.8
90.6
77.3
77.0
76.7
56.3
56.2
56.0
55.5
38.4
31.7
26.1
26.0
25.8
f1 (ppm)

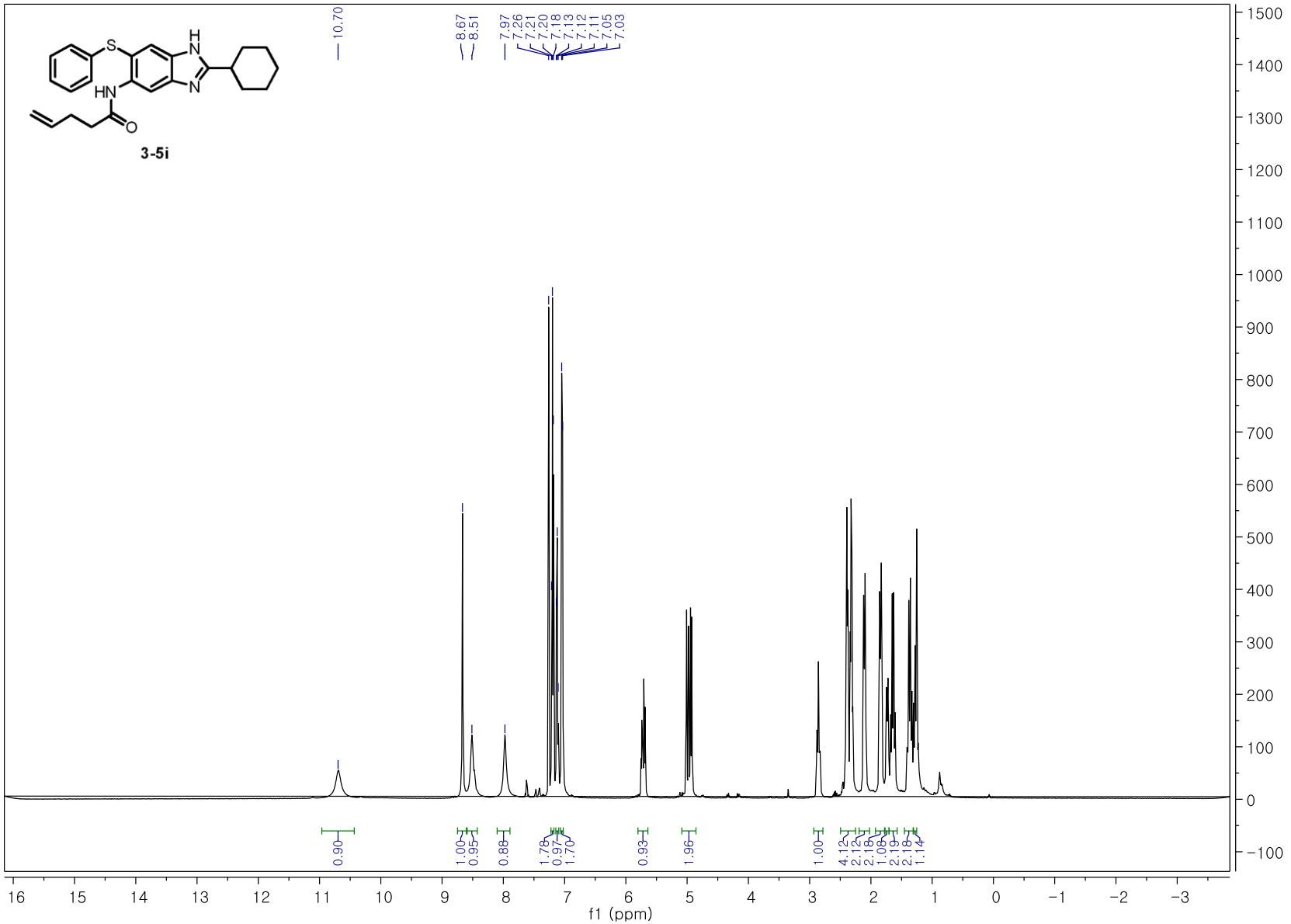
3-5i
10.70
8.67
8.51
7.97
7.26
7.21
7.20
7.18
7.13
7.12
7.11
7.05
7.03
0.90
1.00
0.95
0.88
1.78
0.97
1.70
0.93
1.96
1.00
4.12
2.12
2.18
1.08
2.19
2.18
1.14
f1 (ppm)

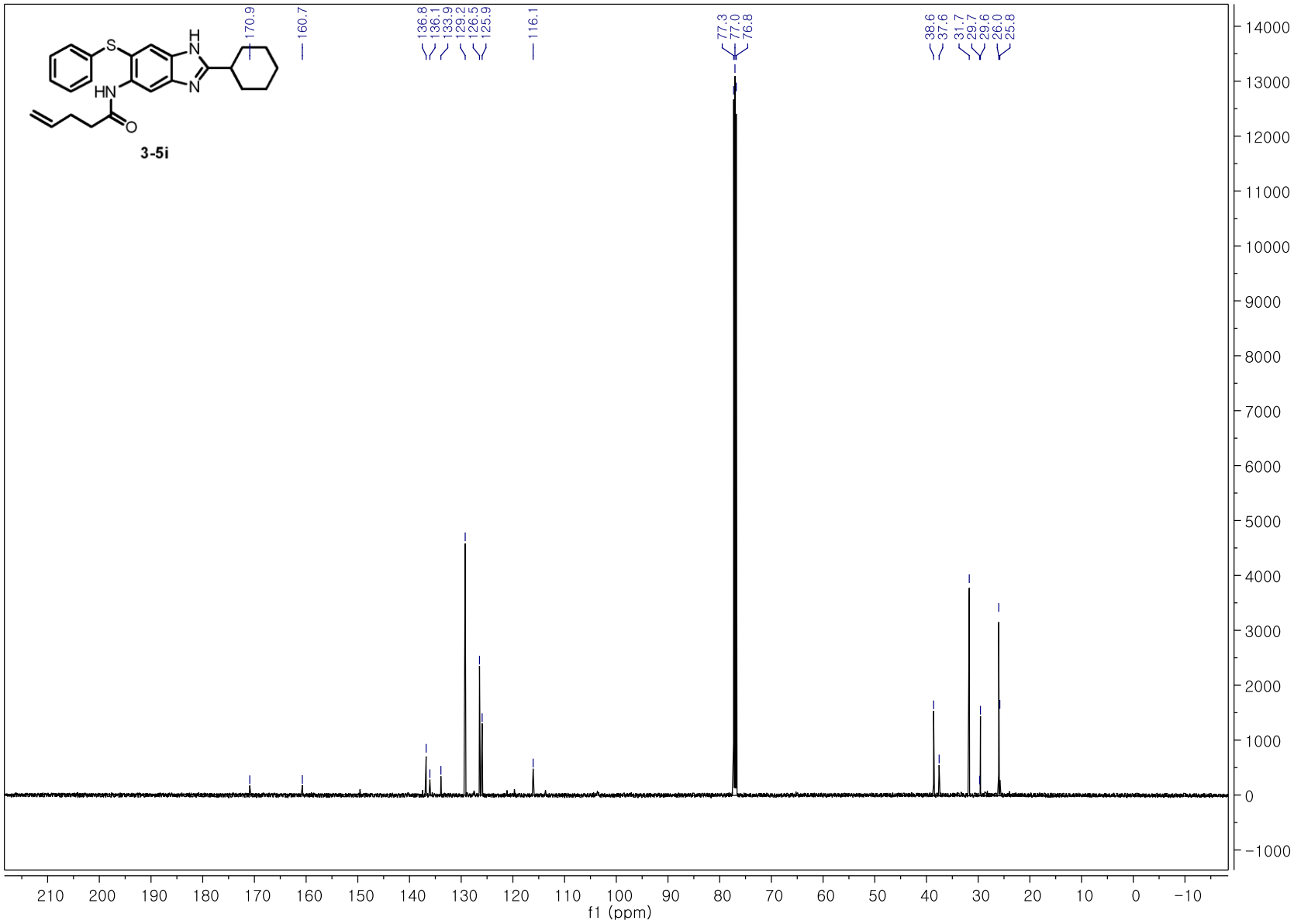
3-5i
170.9
160.7
136.8
136.1
133.9
129.2
126.5
125.9
116.1
77.3
77.0
76.8
38.6
37.6
31.7
29.7
29.6
26.0
25.8
f1 (ppm)

Chapter 4

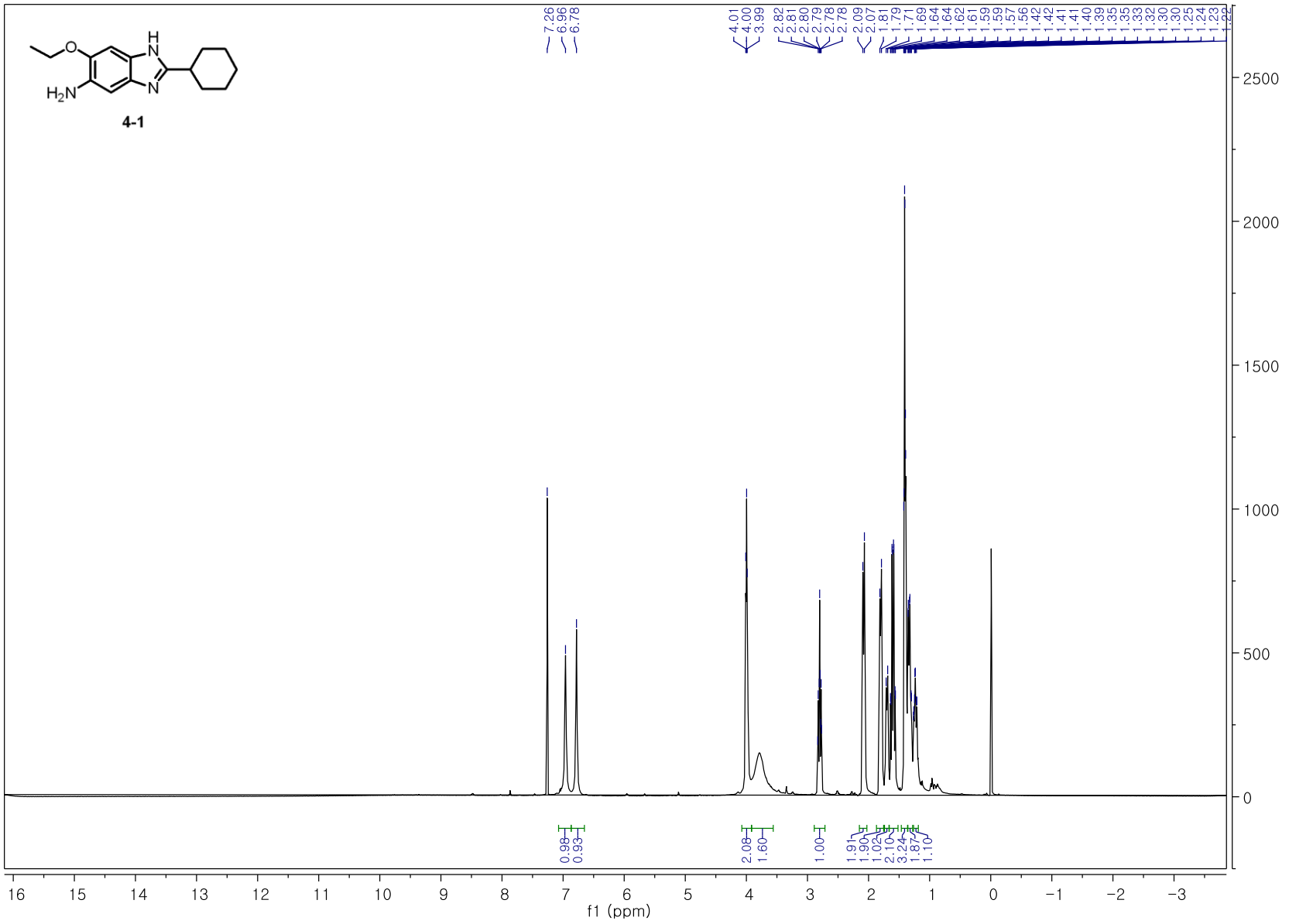
4-1
7.26
6.96
6.78
4.01
4.00
3.99
2.82
2.81
2.80
2.79
2.78
2.78
2.09
2.07
1.81
1.79
1.71
1.69
1.64
1.64
1.62
1.61
1.59
1.59
1.57
1.56
1.42
1.42
1.41
1.41
1.40
1.39
1.35
1.35
1.33
1.32
1.30
1.30
1.25
1.24
1.23
1.22
2500
2000
1500
1000
500
0
0.98
0.93
2.08
1.60
1.00
1.91
1.90
1.02
2.10
3.24
1.87
1.10
16
15
14
13
12
11
10
9
8
7
6
5
4
3
2
1
0
−1
−2
−3
f1 (ppm)

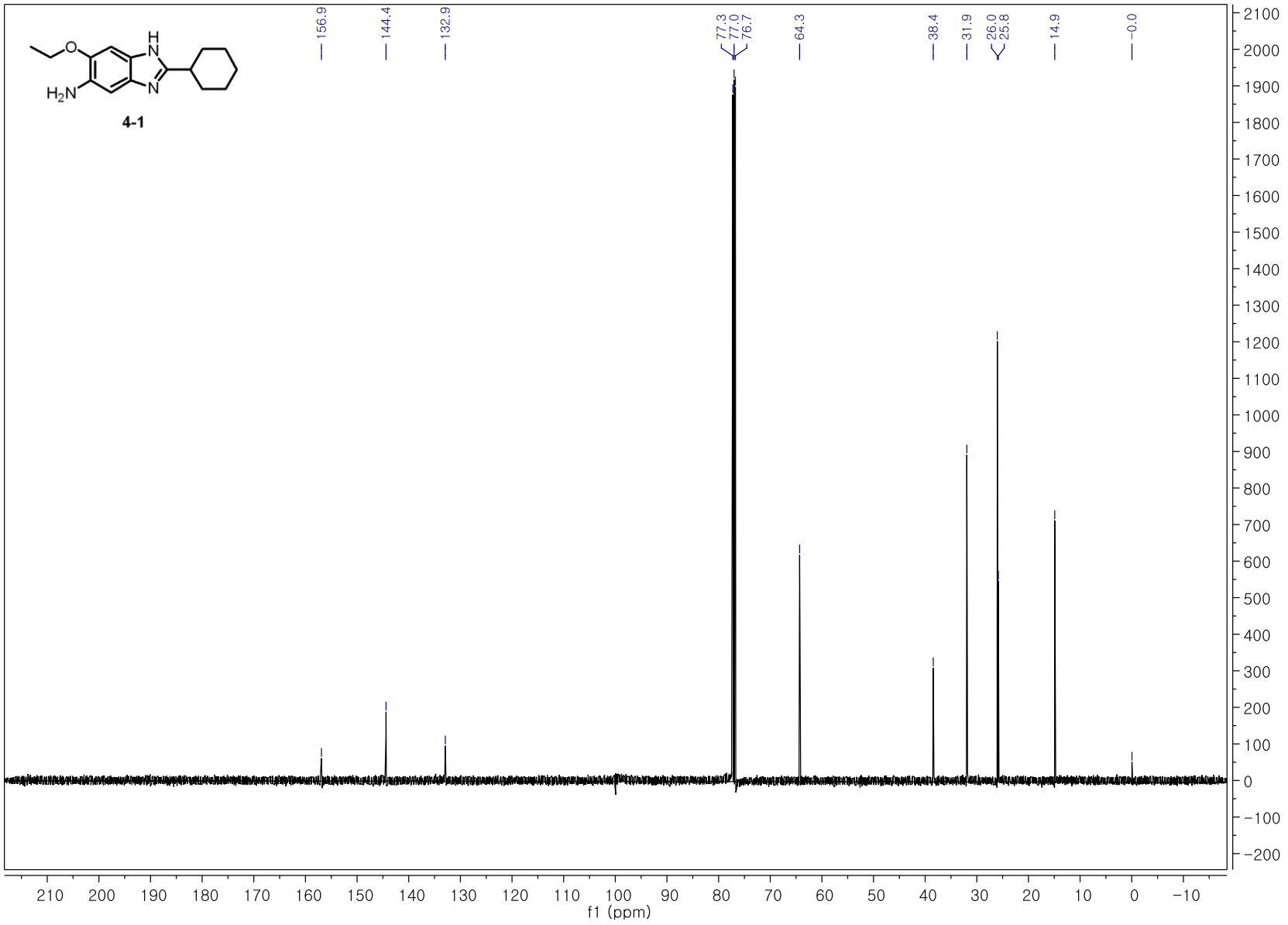
4-1
156.9
144.4
132.9
77.3
77.0
76.7
64.3
38.4
31.9
26.0
25.8
14.9
0.0
f1 (ppm)

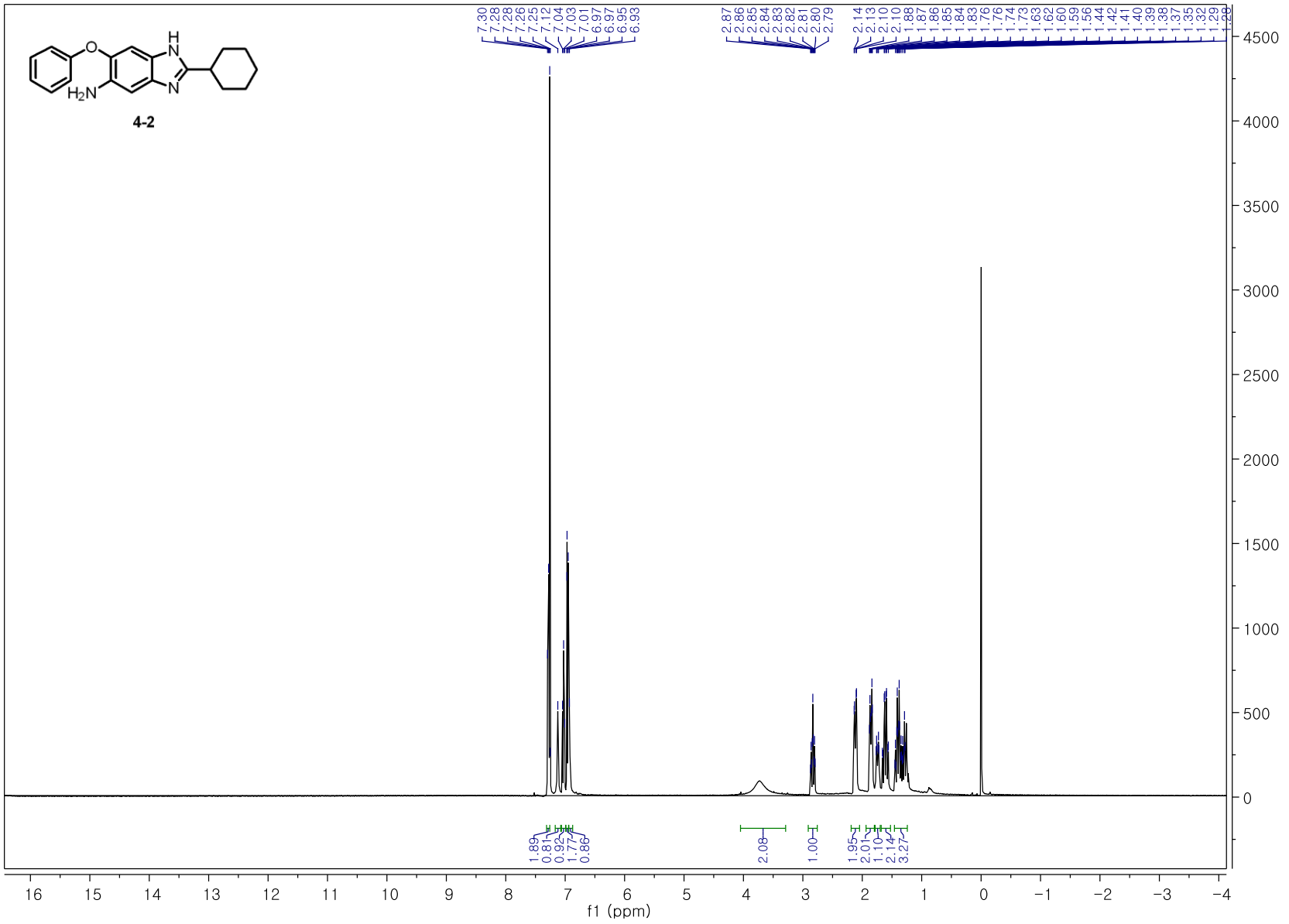
4-2
f1 (ppm)

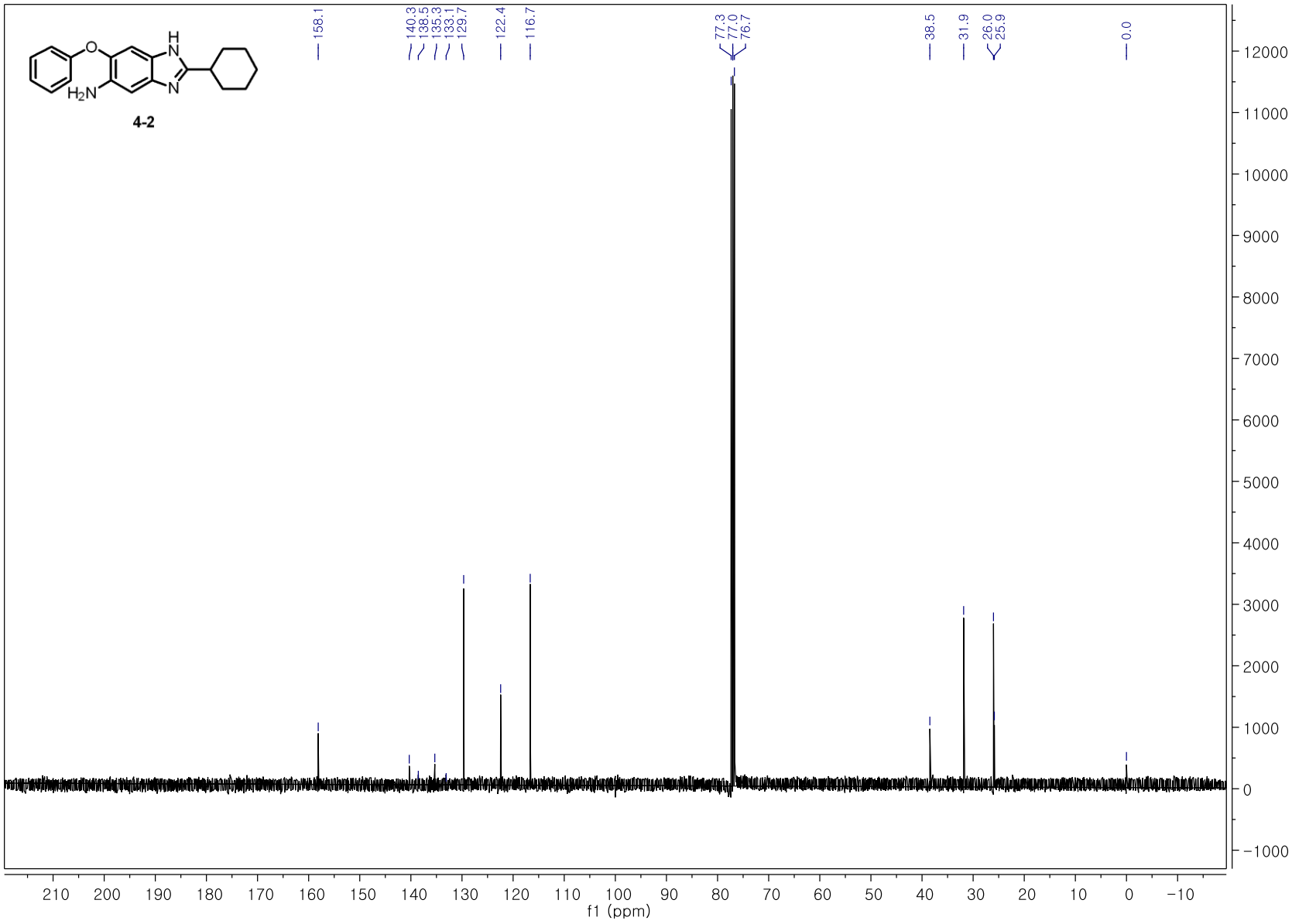
4-2
158.1
140.3
138.5
135.3
133.1
129.7
122.4
116.7
77.3
77.0
76.7
38.5
31.9
26.0
25.9
0.0
f1 (ppm)

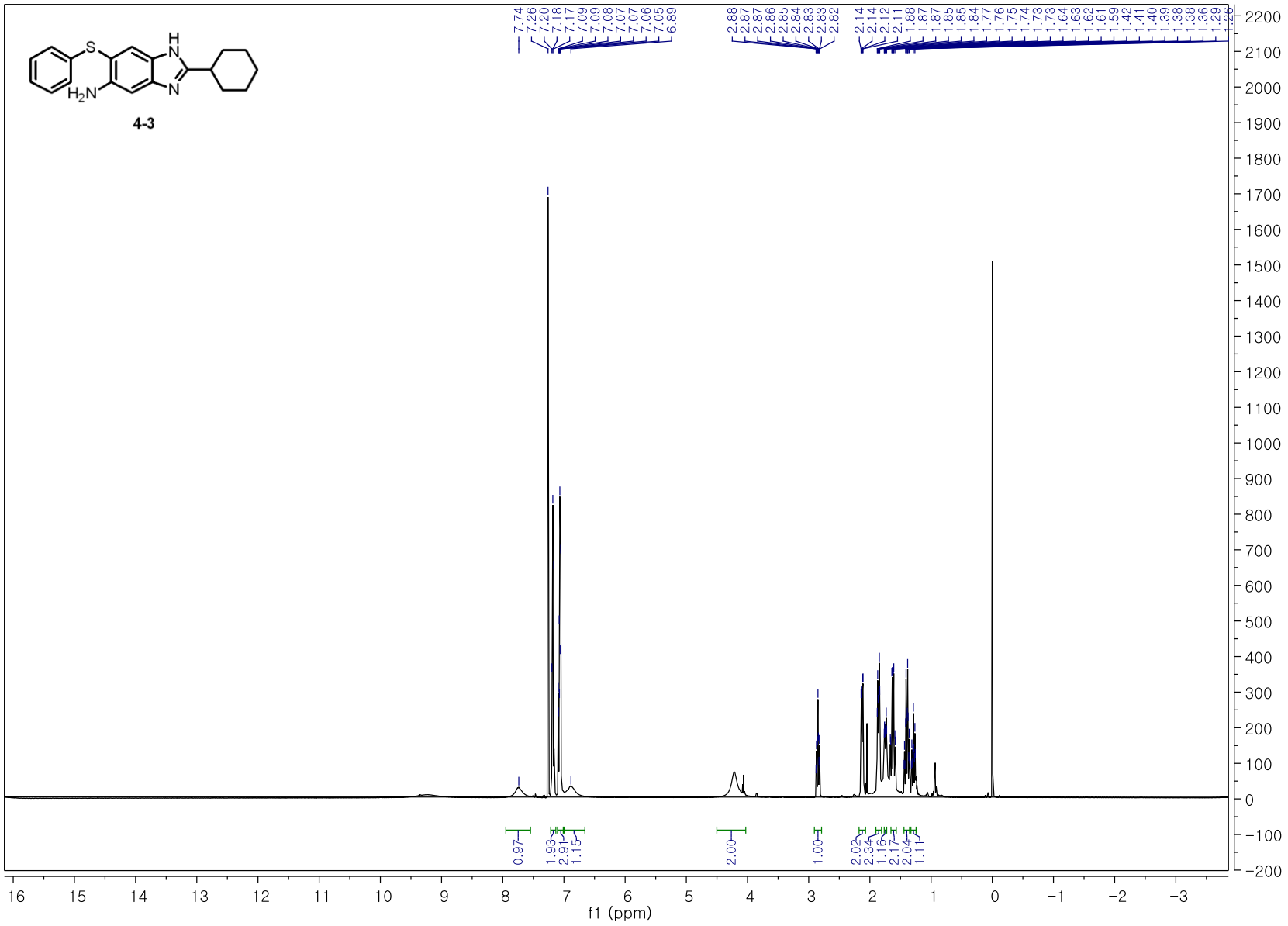
4-3
7.74
7.26
7.20
7.18
7.17
7.09
7.09
7.08
7.07
7.07
7.06
7.05
6.89
2.88
2.87
2.87
2.86
2.85
2.84
2.83
2.83
2.82
2.14
2.14
2.12
2.11
1.88
1.87
1.87
1.85
1.85
1.84
1.77
1.76
1.75
1.74
1.73
1.64
1.63
1.62
1.61
1.59
1.42
1.41
1.40
1.39
1.38
1.38
1.36
1.29
0.97
1.99
2.91
1.15
2.00
1.00
2.02
2.34
1.16
2.17
2.04
1.11
f1 (ppm)

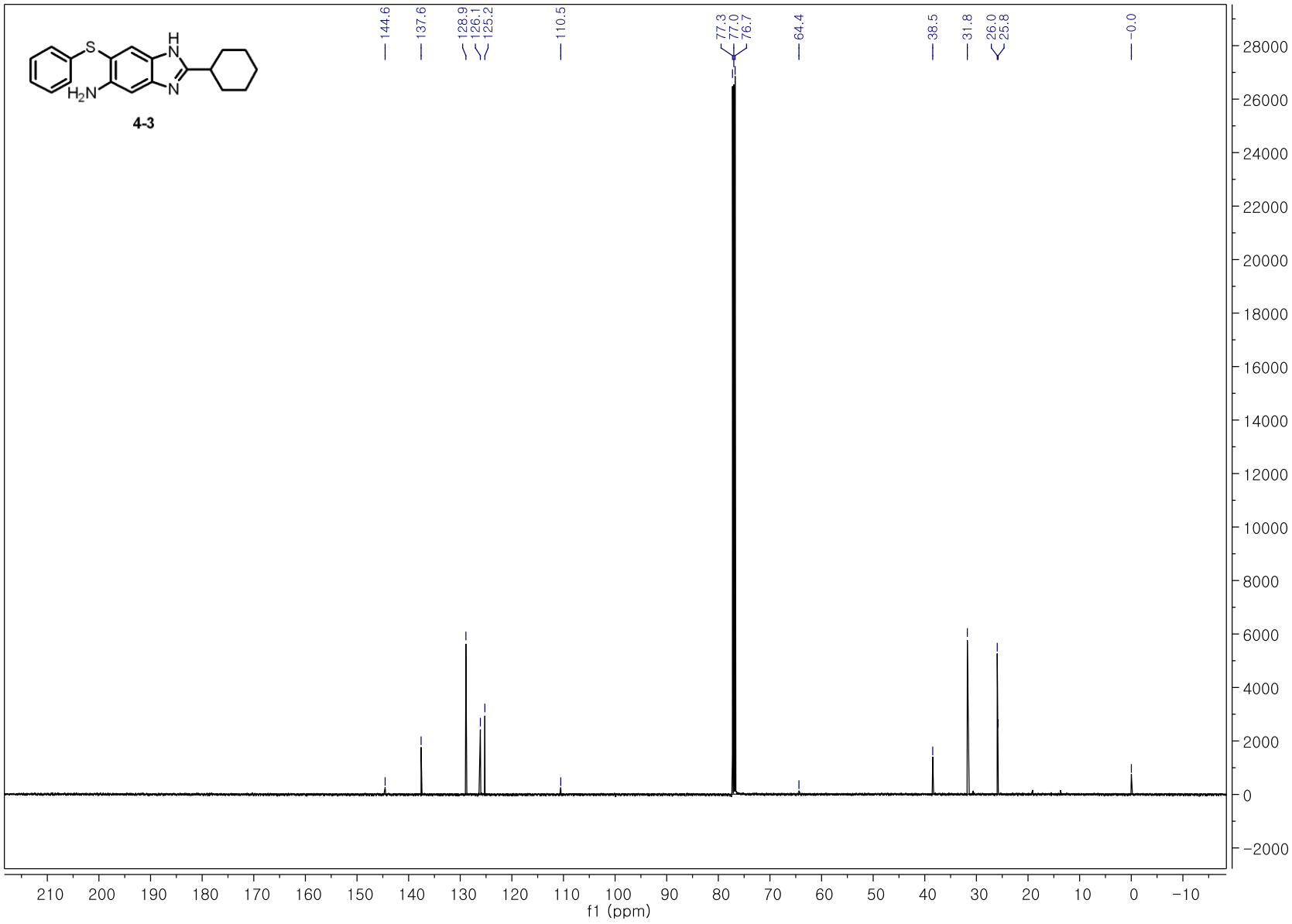
4-3
144.6
137.6
128.9
126.1
125.2
110.5
77.3
77.0
76.7
64.4
38.5
31.8
26.0
25.8
0.0
f1 (ppm)

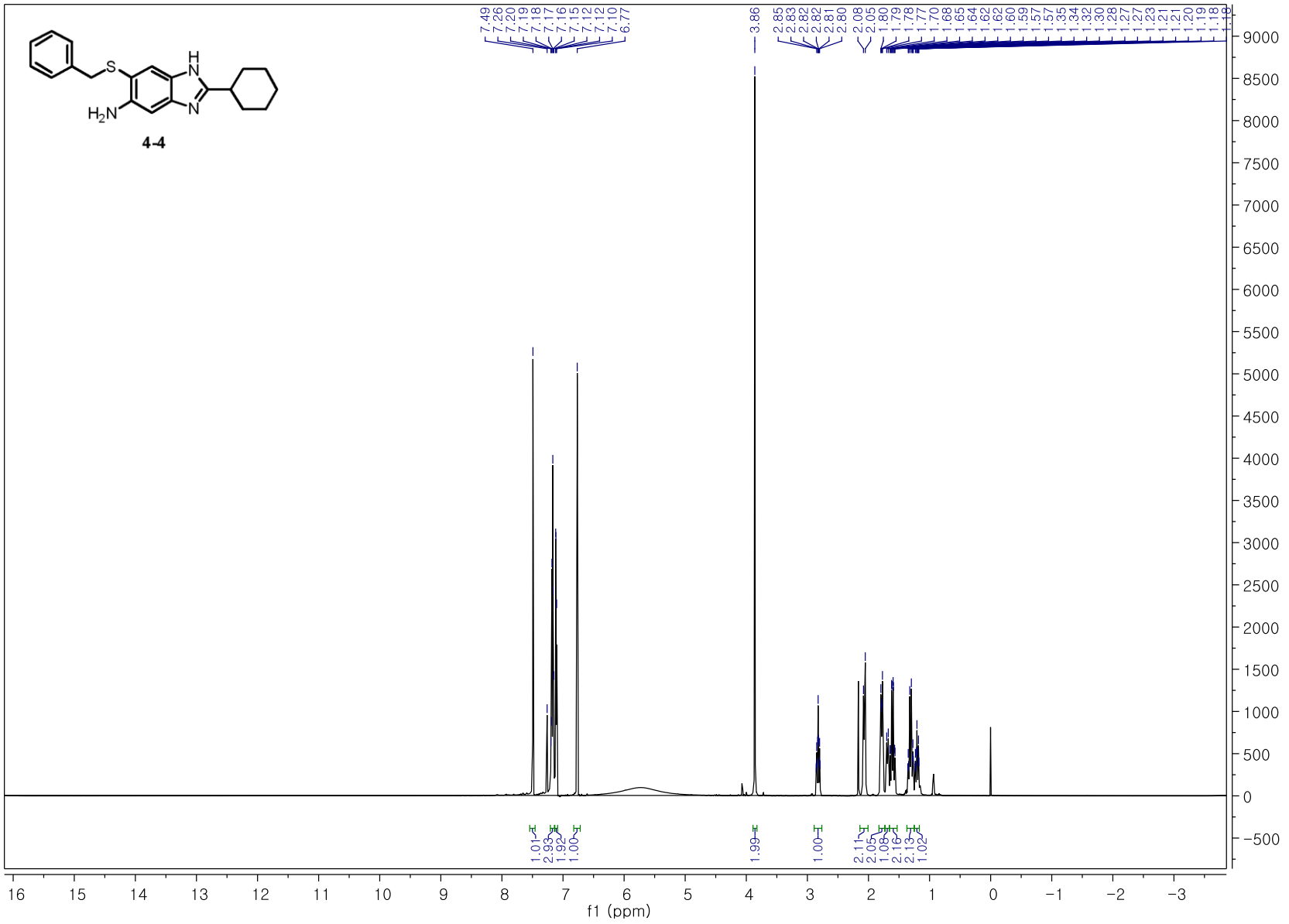
4-4
7.49
7.26
7.20
7.19
7.18
7.17
7.16
7.15
7.12
7.12
7.10
6.77
3.86
2.85
2.83
2.82
2.82
2.81
2.80
2.08
2.05
1.80
1.79
1.78
1.77
1.70
1.68
1.65
1.64
1.62
1.62
1.60
1.59
1.57
1.57
1.35
1.34
1.32
1.30
1.28
1.27
1.27
1.23
1.21
1.21
1.20
1.19
1.18
1.18
1.01
2.93
1.92
1.00
1.99
1.00
2.11
2.05
1.08
2.16
2.13
1.02
f1 (ppm)

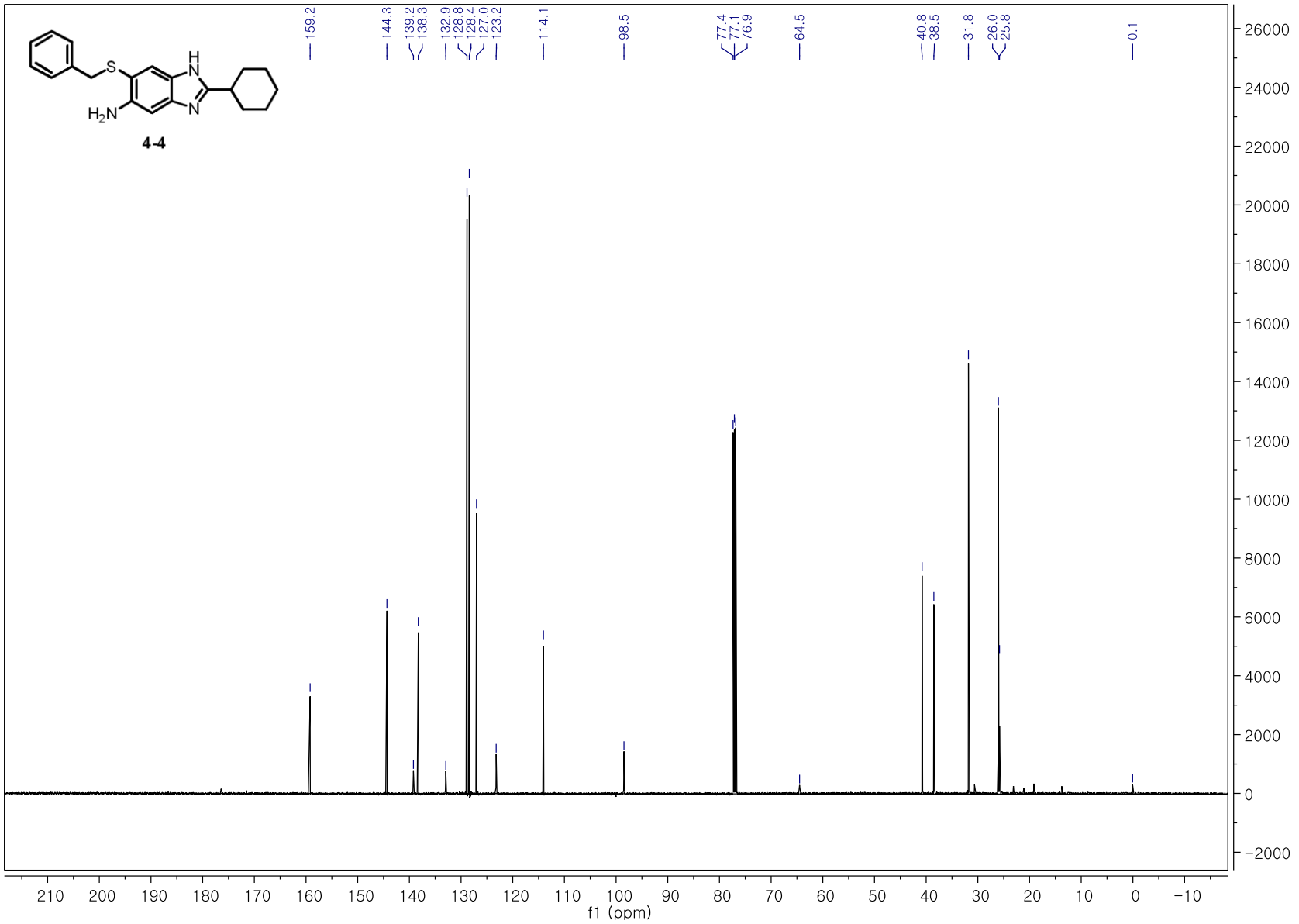
4-4
159.2
144.3
139.2
138.3
132.9
128.8
128.4
127.0
123.2
114.1
98.5
77.4
77.1
76.9
64.5
40.8
38.5
31.8
26.0
25.8
0.1
f1 (ppm)

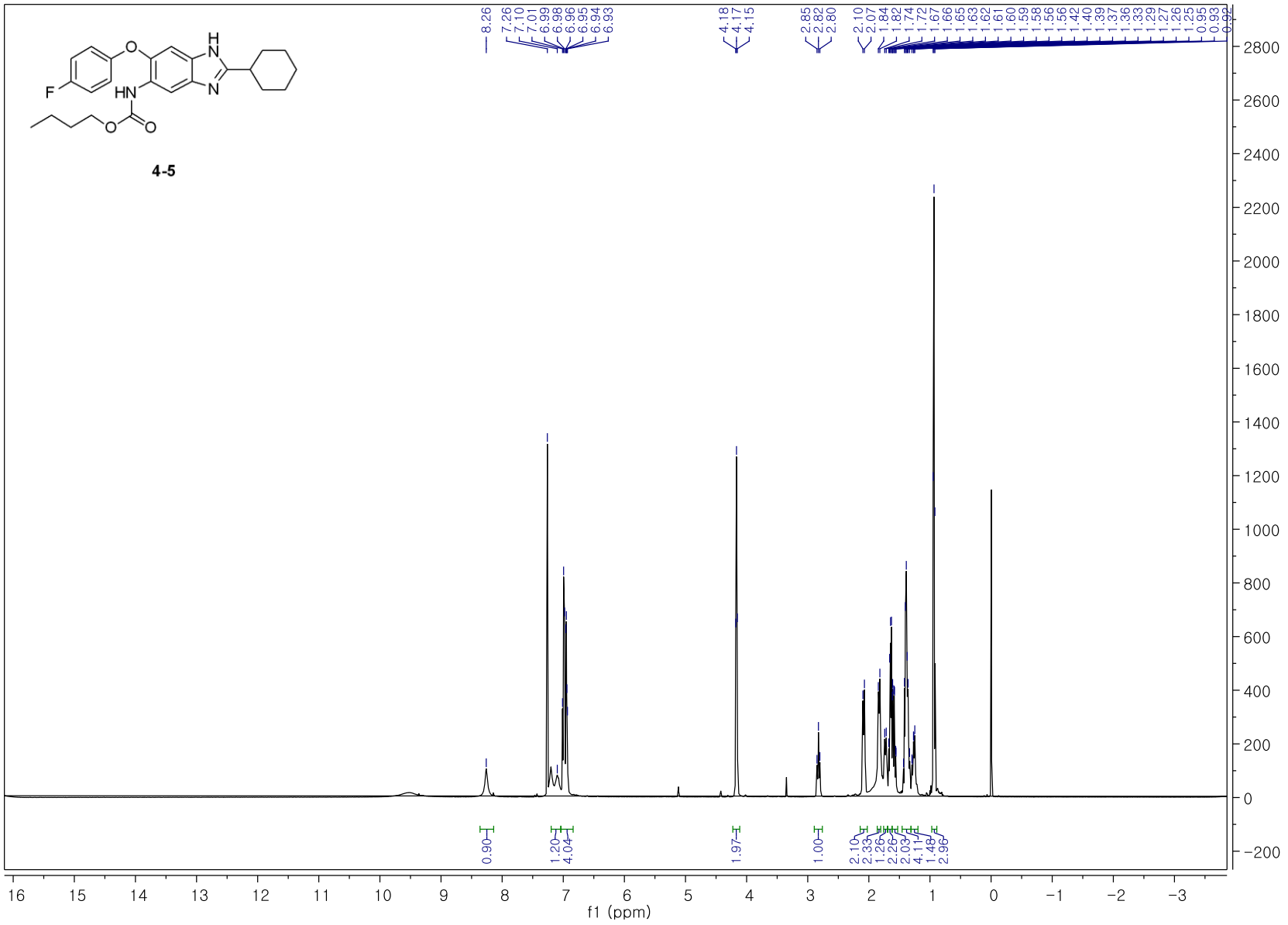
4-5
8.26
7.26
7.10
7.01
6.99
6.98
6.96
6.95
6.94
6.93
4.18
4.17
4.15
2.85
2.82
2.80
2.10
2.07
1.84
1.82
1.74
1.72
1.67
1.66
1.65
1.63
1.62
1.61
1.60
1.59
1.58
1.56
1.56
1.42
1.40
1.39
1.37
1.36
1.33
1.29
1.27
1.26
1.25
0.95
0.93
0.92
0.90
1.20
4.04
1.97
1.00
2.10
2.33
1.25
2.26
2.03
4.11
1.48
2.96
f1 (ppm)

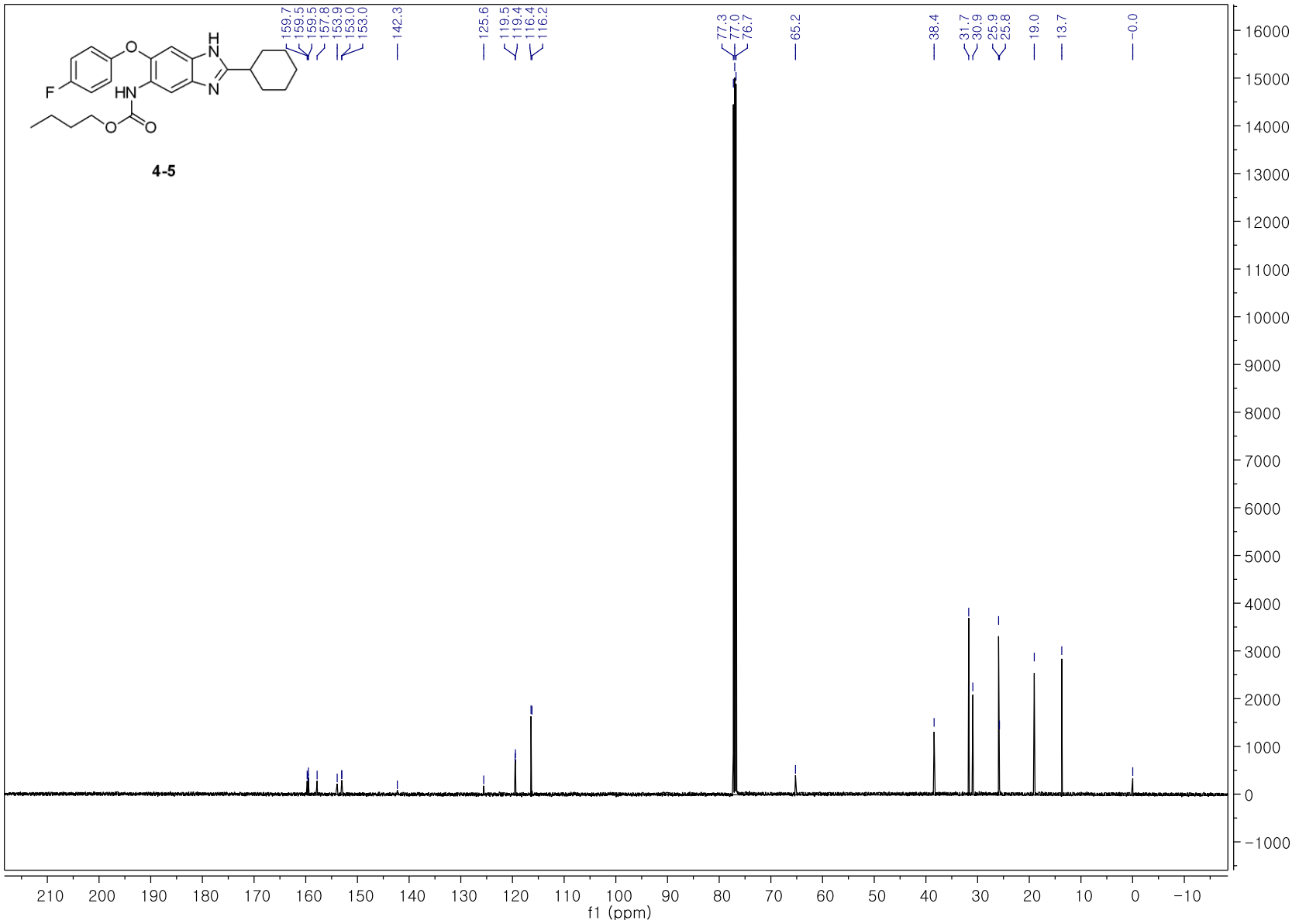
4-5
159.7
159.5
159.5
157.8
153.9
153.0
153.0
142.3
125.6
119.5
119.4
116.4
116.2
77.3
77.0
76.7
65.2
38.4
31.7
30.9
25.9
25.8
19.0
13.7
-0.0
f1 (ppm)

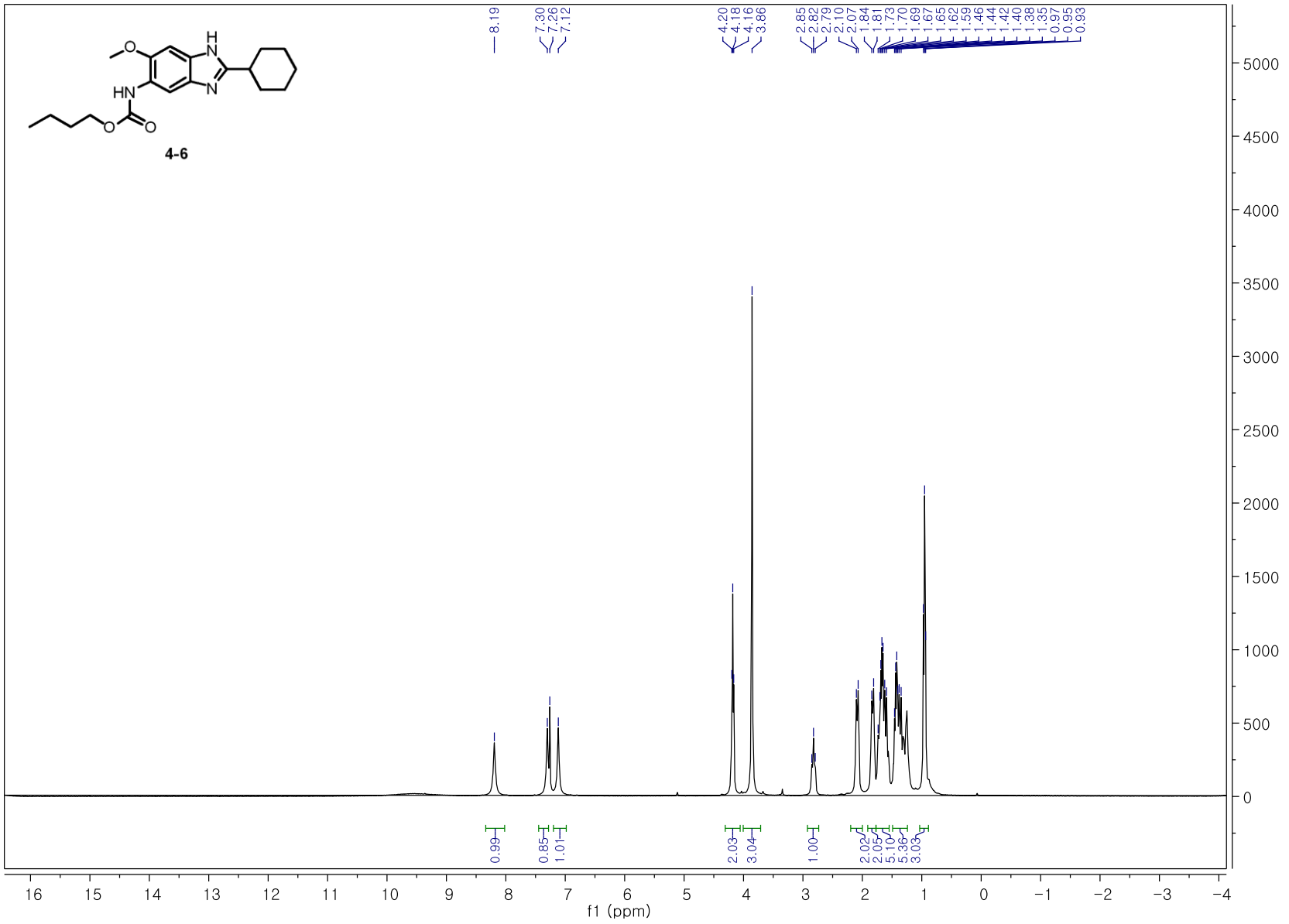
4-6
8.19
7.30
7.26
7.12
4.20
4.18
4.16
3.86
2.85
2.82
2.79
2.10
2.07
1.84
1.81
1.73
1.70
1.69
1.67
1.65
1.62
1.59
1.46
1.44
1.42
1.40
1.38
1.35
0.97
0.95
0.93
0.99
0.85
1.01
2.03
3.04
1.00
2.02
2.05
5.10
5.36
3.03
f1 (ppm)

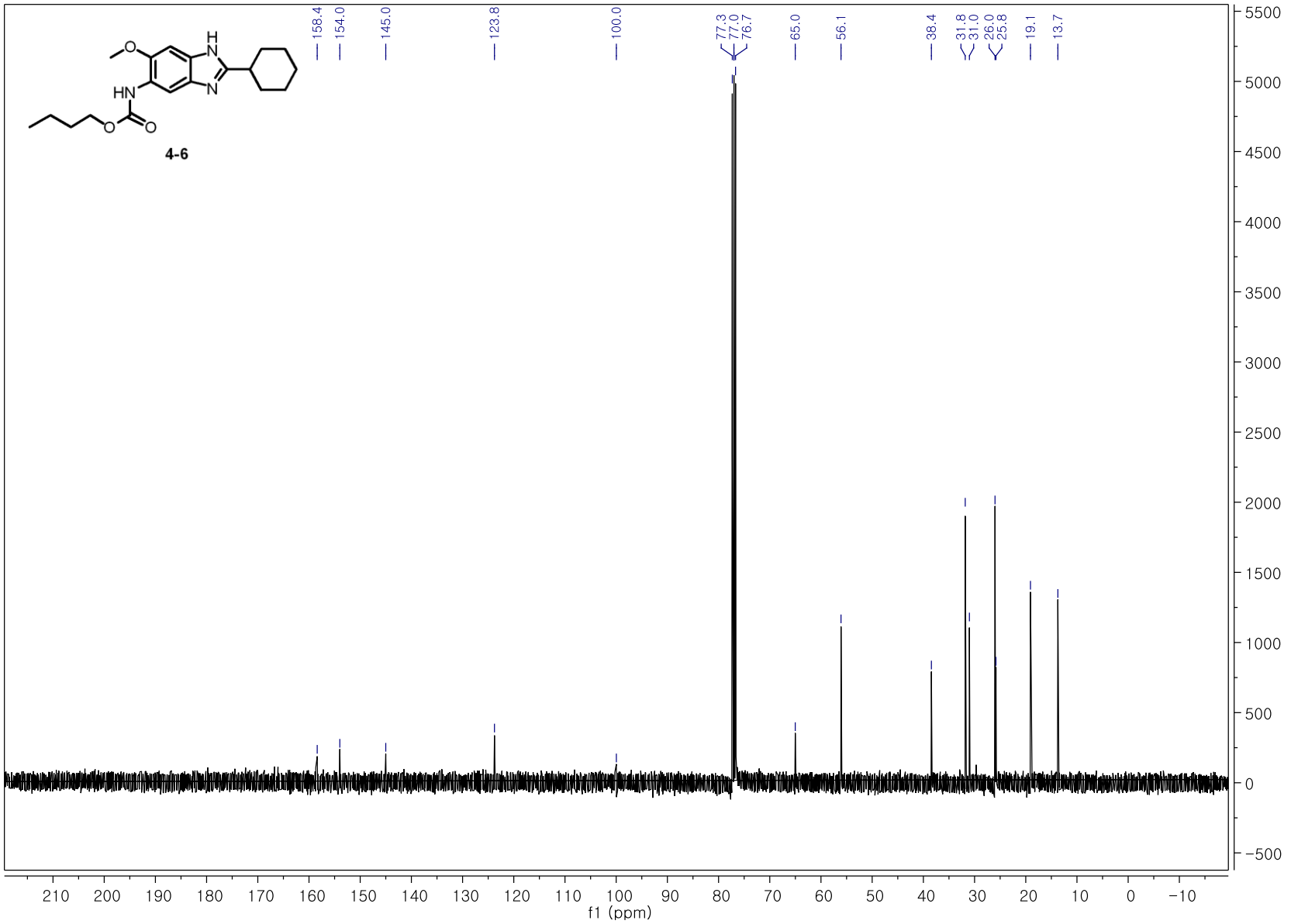
4-6
158.4
154.0
145.0
123.8
100.0
77.3
77.0
76.7
65.0
56.1
38.4
31.8
31.0
26.0
25.8
19.1
13.7
f1 (ppm)

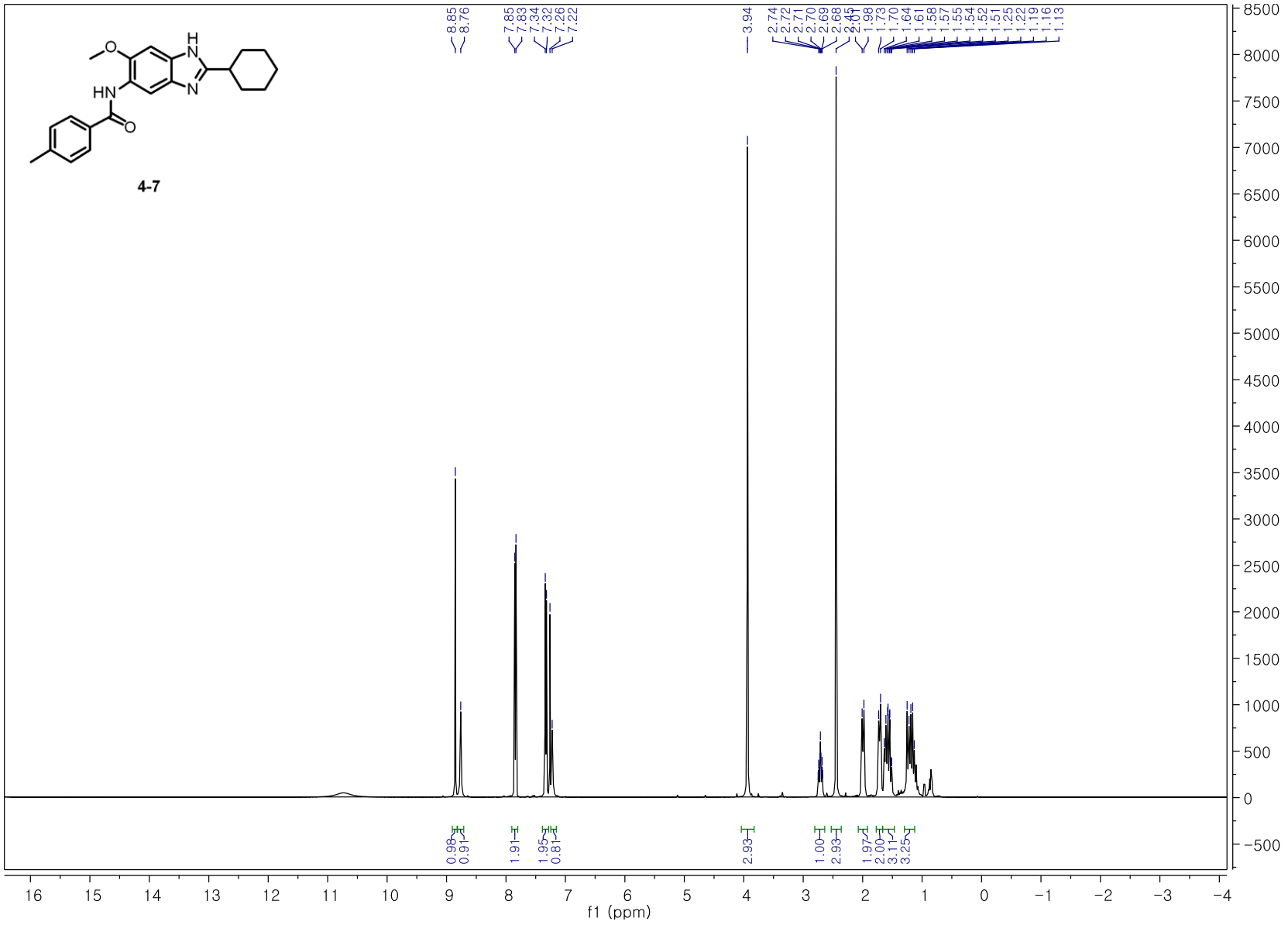
4-7
8.85
8.76
7.85
7.83
7.34
7.32
7.26
7.22
3.94
2.74
2.72
2.71
2.70
2.69
2.68
2.45
2.01
1.98
1.73
1.70
1.64
1.61
1.58
1.57
1.55
1.54
1.52
1.51
1.25
1.22
1.19
1.16
1.13
0.98
0.91
1.91
1.95
0.81
2.93
1.00
2.93
1.97
2.00
3.11
3.25
f1 (ppm)

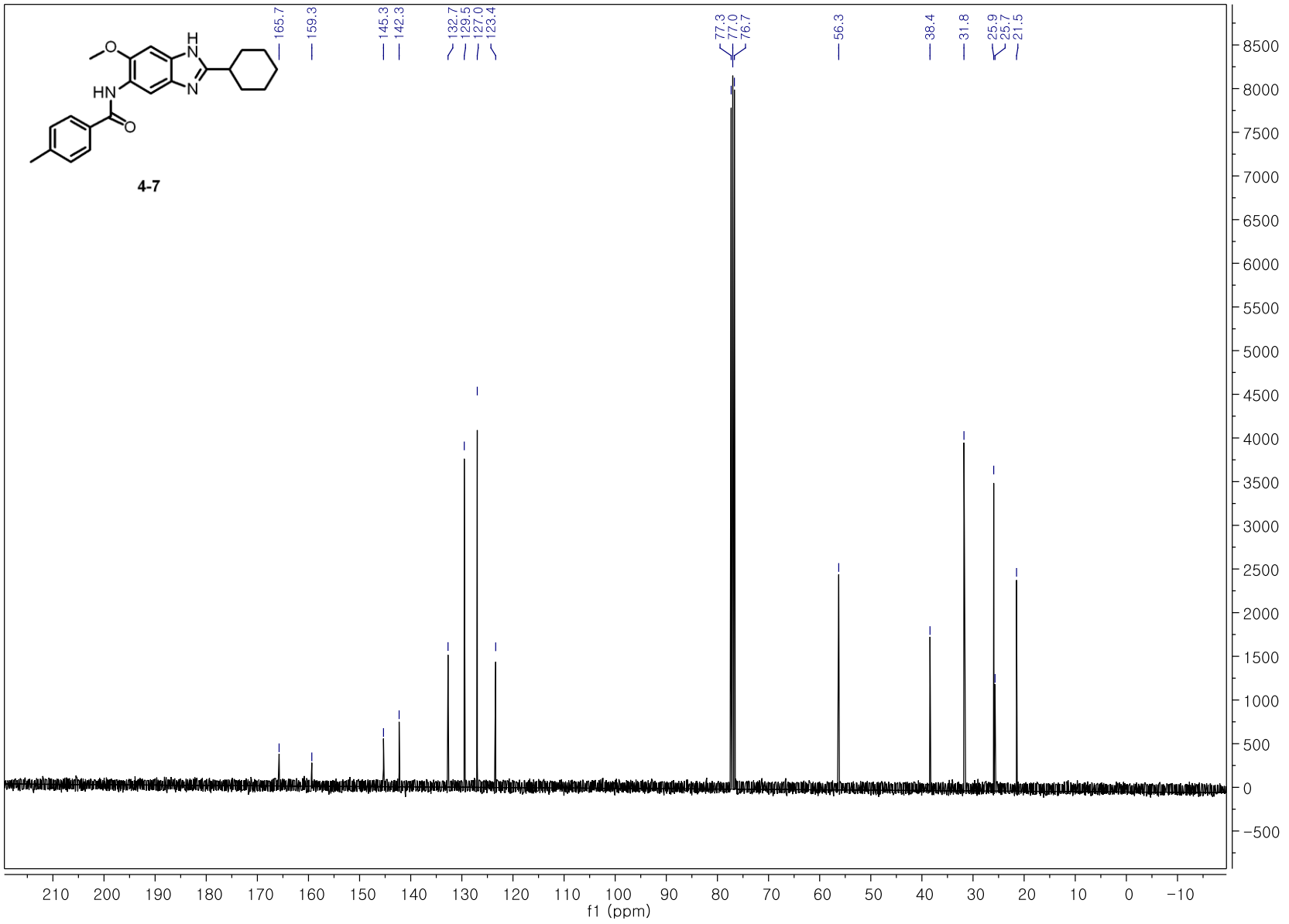
4-7
165.7
159.3
145.3
142.3
132.7
129.5
127.0
123.4
77.3
77.0
76.7
56.3
38.4
31.8
25.9
25.7
21.5
f1 (ppm)

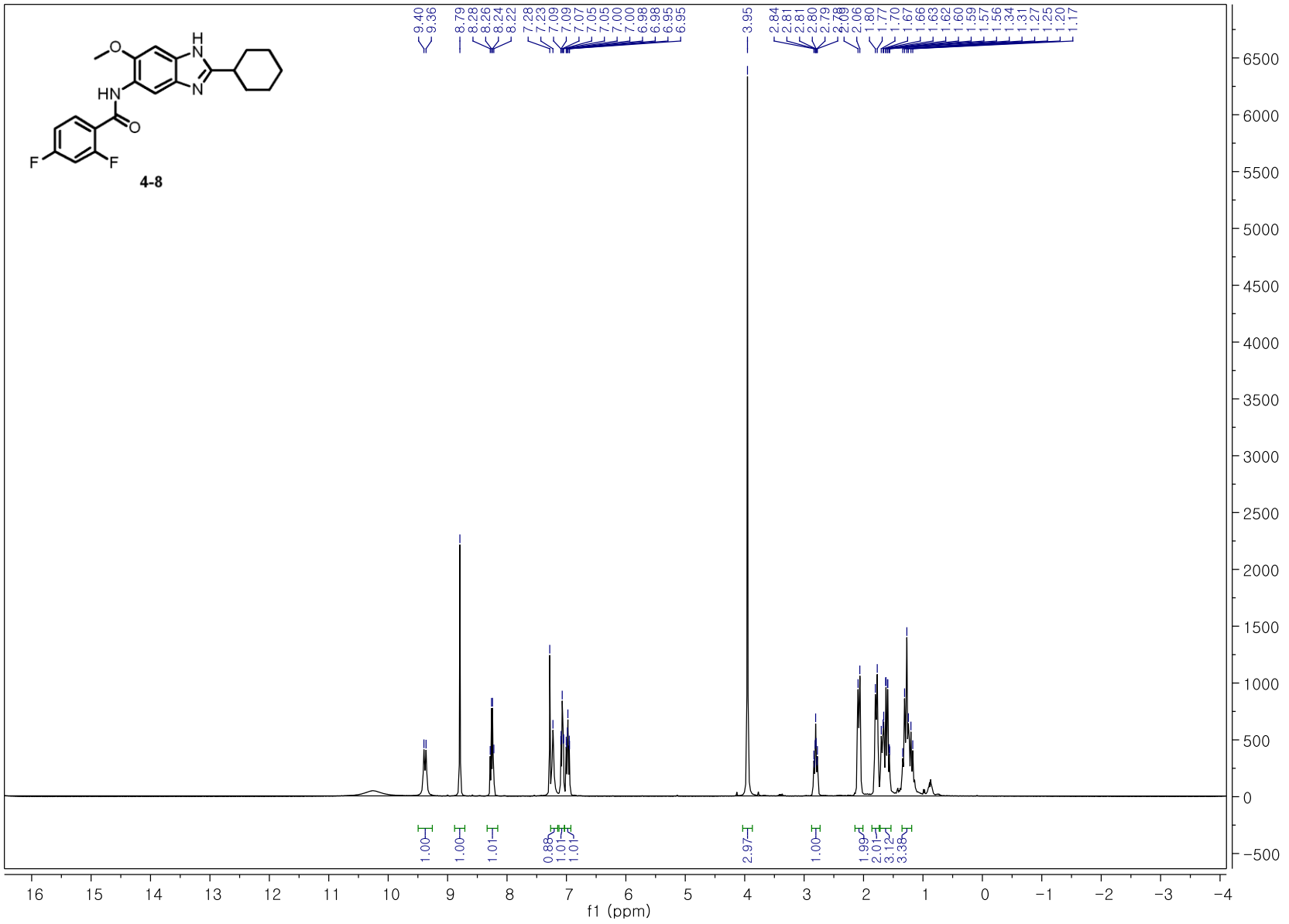
4-8
9.40
9.36
8.79
8.28
8.26
8.24
8.22
7.28
7.23
7.09
7.09
7.07
7.05
7.05
7.00
7.00
6.98
6.98
6.95
6.95
3.95
2.84
2.81
2.81
2.80
2.79
2.06
1.80
1.77
1.70
1.67
1.66
1.63
1.62
1.60
1.59
1.57
1.56
1.34
1.31
1.27
1.25
1.20
1.17
1.00
1.00
1.01
0.88
1.01
1.01
2.97
1.00
1.99
2.01
3.12
3.38
f1 (ppm)

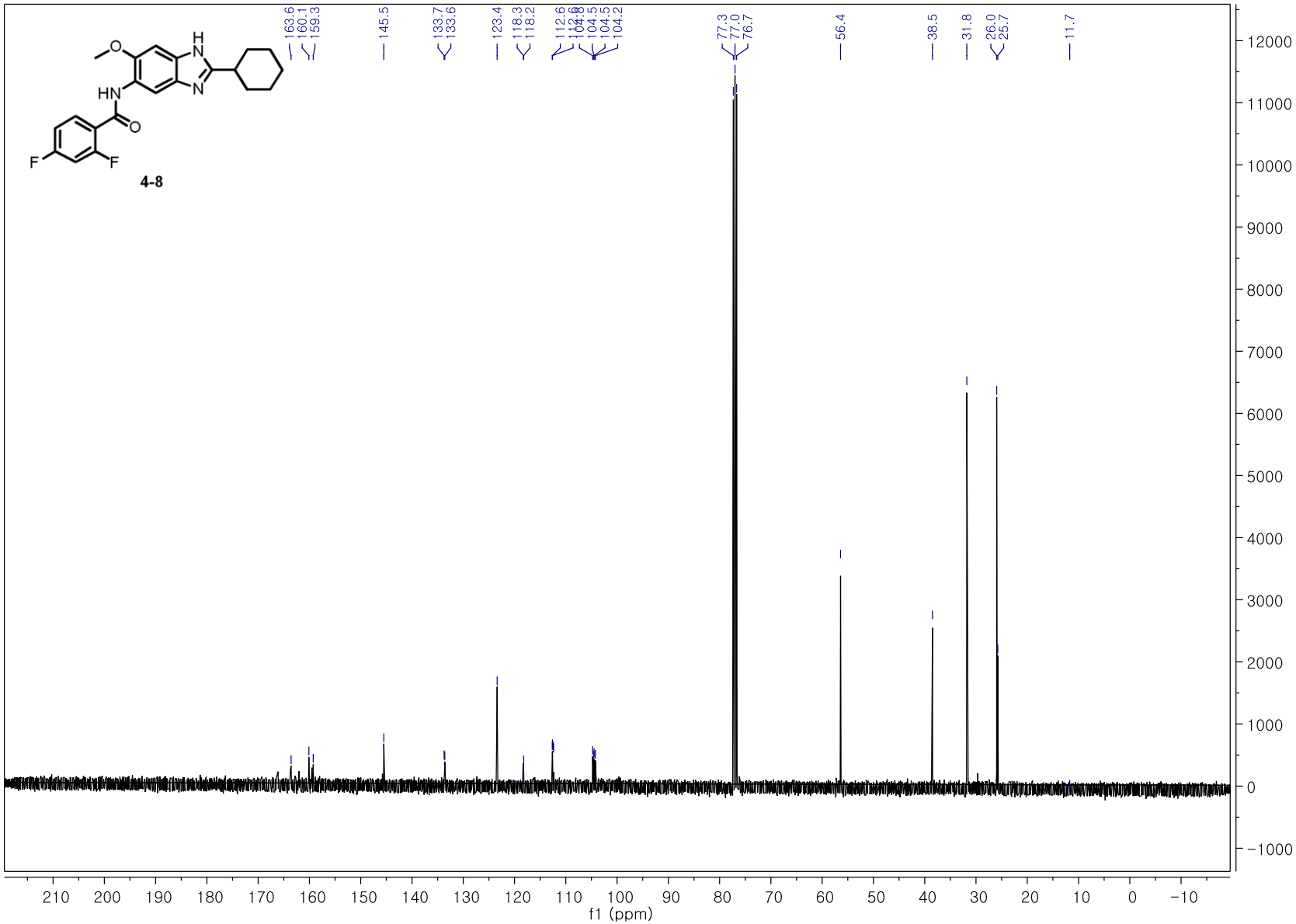
4-8
163.6
160.1
159.3
145.5
133.7
133.6
123.4
118.3
118.2
112.6
112.4
104.8
104.5
104.5
104.2
77.3
77.0
76.7
56.4
38.5
31.8
26.0
25.7
11.7
f1 (ppm)

Chapter 7

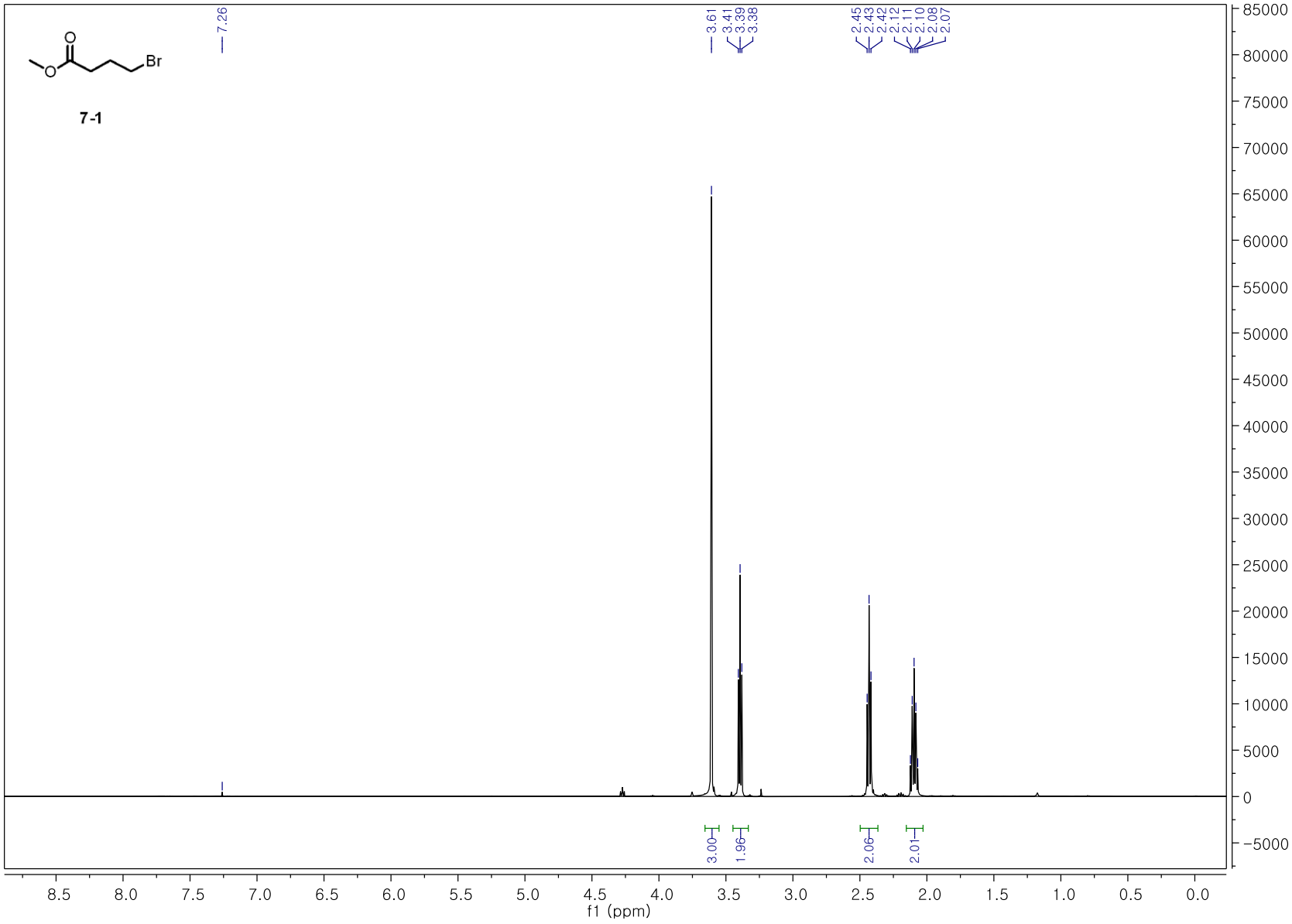
7-1
Br
O
O
7.26
3.61
3.41
3.39
3.38
2.45
2.43
2.42
2.12
2.11
2.10
2.08
2.07
3.00
1.96
2.06
2.01
f1 (ppm)

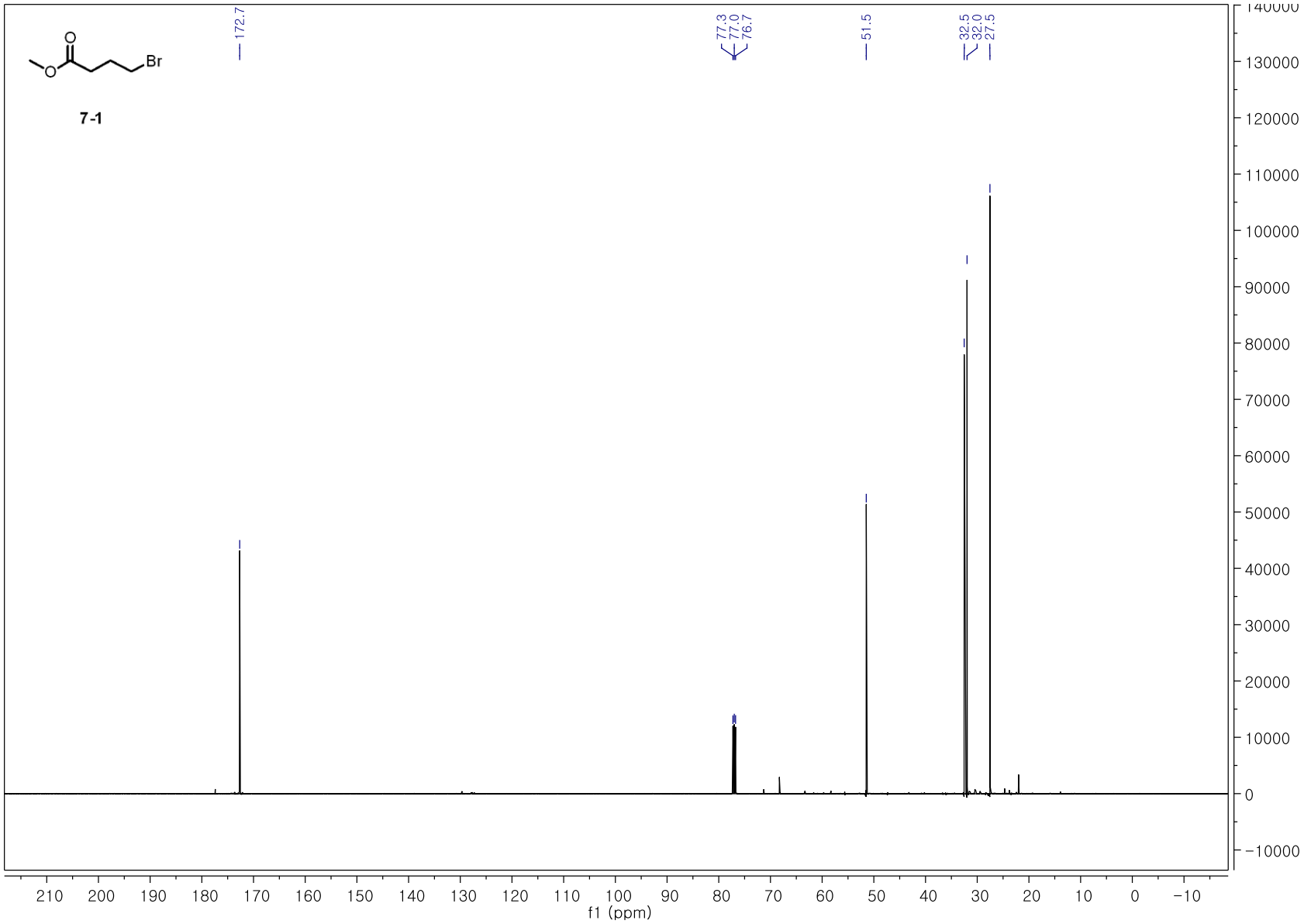
7-1
172.7
77.3
77.0
76.7
51.5
32.5
32.0
27.5
f1 (ppm)

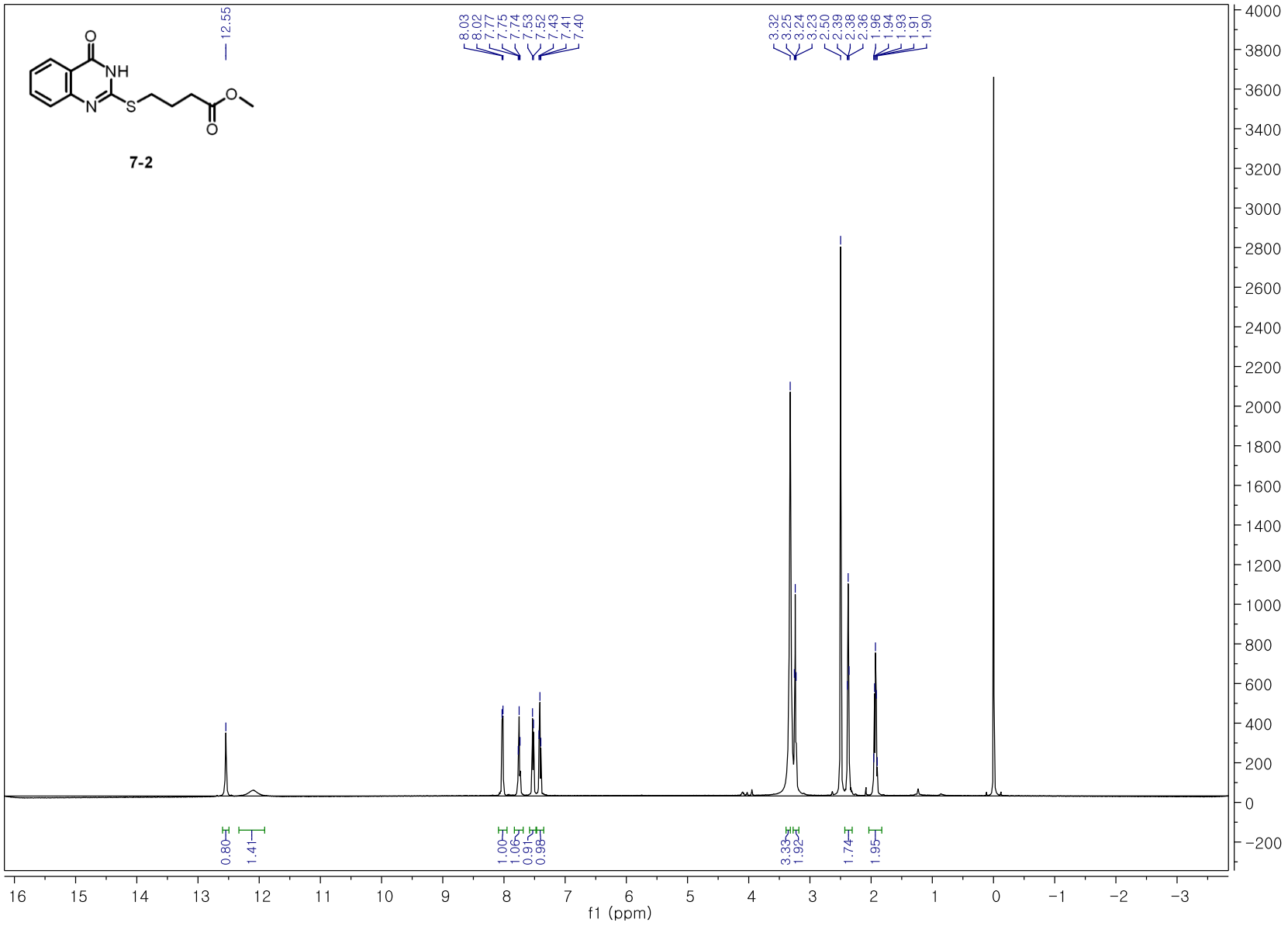
12.55
8.03
8.02
7.77
7.75
7.74
7.53
7.52
7.43
7.41
7.40
3.32
3.25
3.24
3.23
2.50
2.39
2.38
2.36
1.96
1.94
1.93
1.91
1.90
7-2
0.80
1.41
1.00
1.06
0.91
0.98
3.33
1.92
1.74
1.95
f1 (ppm)

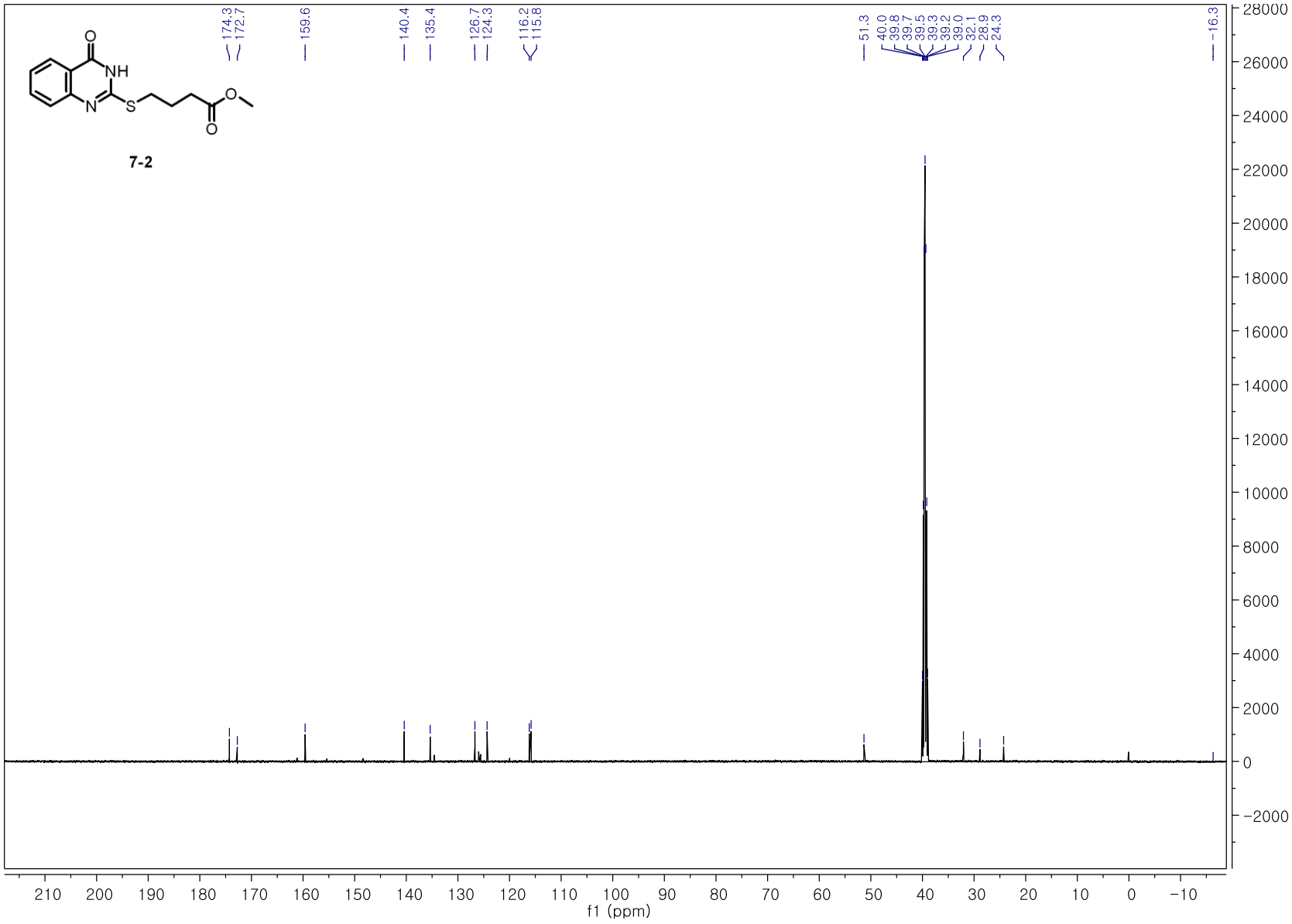
7-2
174.3
172.7
159.6
140.4
135.4
126.7
124.3
116.2
115.8
51.3
40.0
39.8
39.7
39.5
39.3
39.2
39.0
32.1
28.9
24.3
16.3
f1 (ppm)

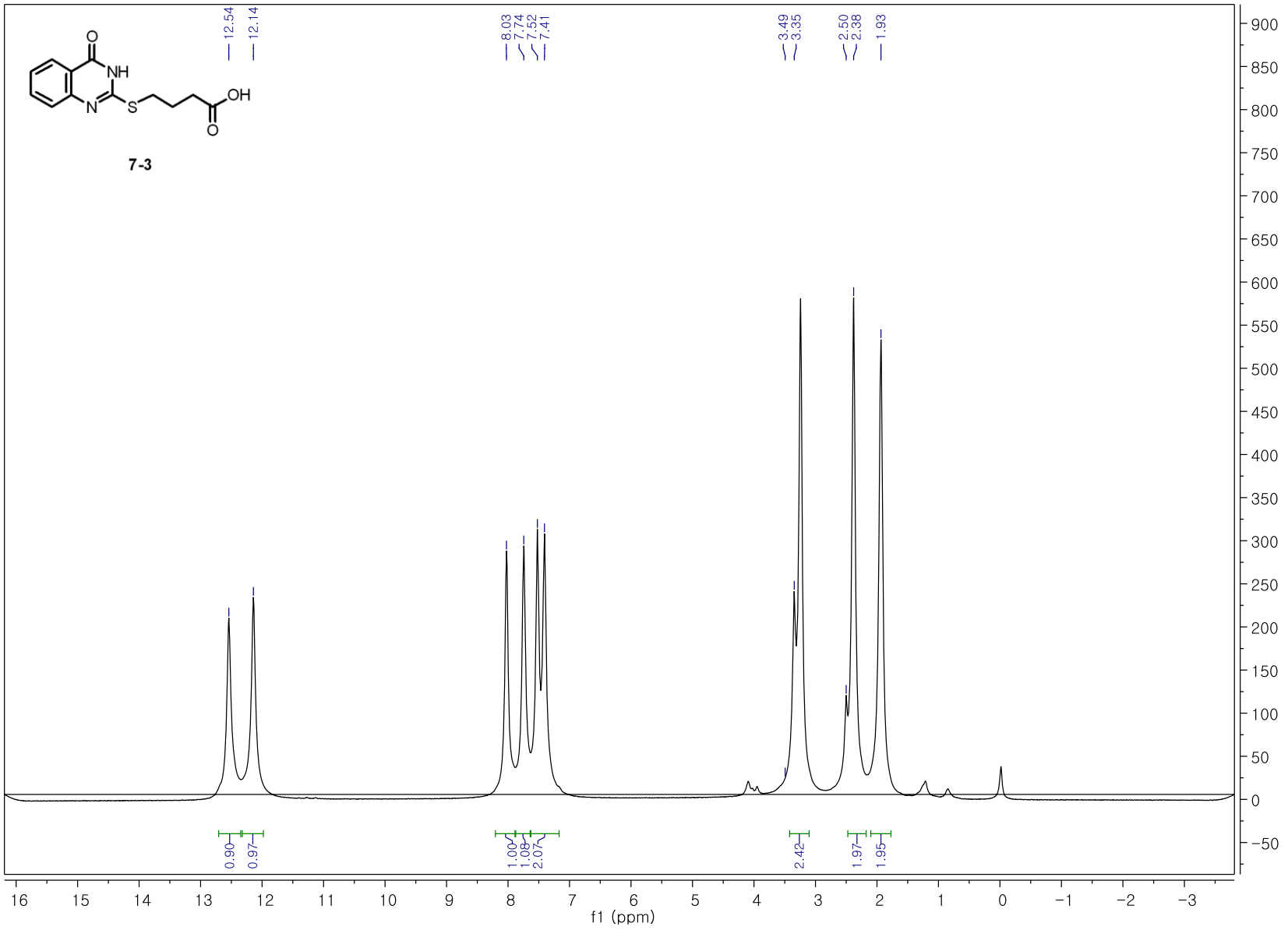
12.54
12.14
8.03
7.74
7.52
7.41
3.49
3.35
2.50
2.38
1.93
NH
N
S
OH
O
O
7-3
0.90
0.97
1.00
1.08
2.07
2.42
1.97
1.95
f1 (ppm)

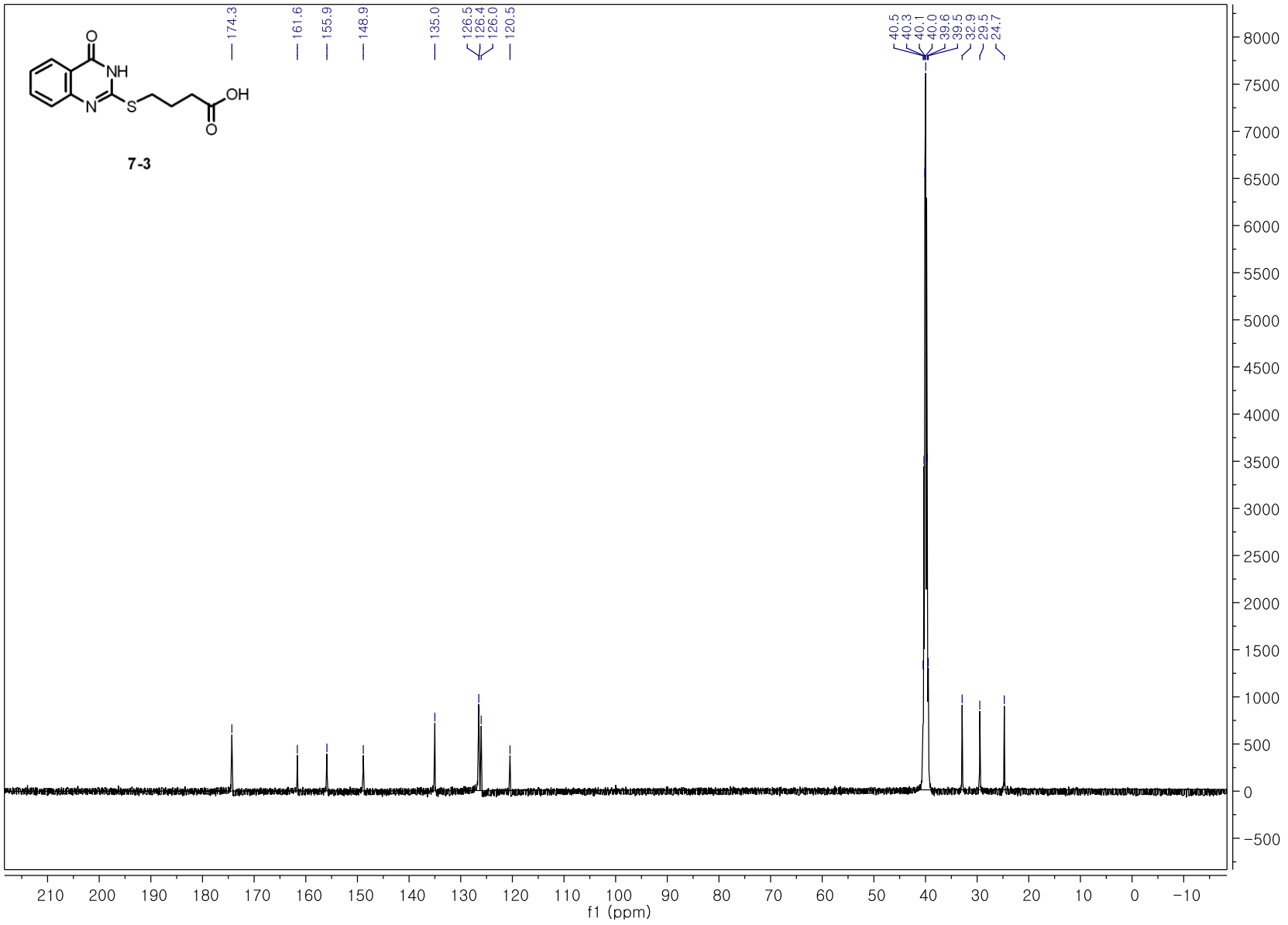
174.3
161.6
155.9
148.9
135.0
126.5
126.4
126.0
120.5
40.5
40.3
40.1
40.0
39.6
39.5
32.9
29.5
24.7
NH
N
S
OH
O
O
7-3
f1 (ppm)

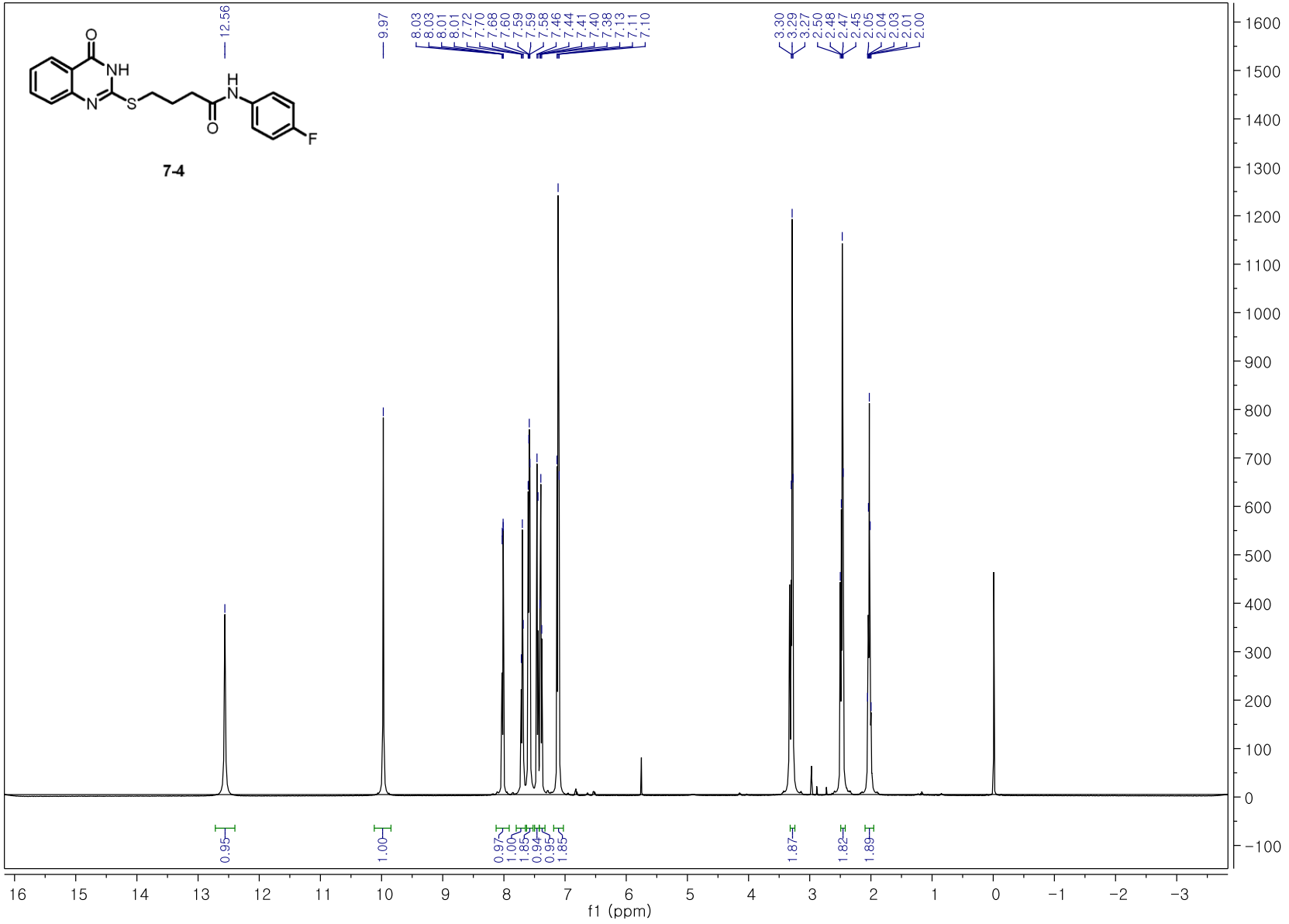
12.56
9.97
8.03
8.03
8.01
8.01
7.72
7.70
7.68
7.60
7.59
7.59
7.58
7.46
7.44
7.41
7.40
7.38
7.13
7.11
7.10
3.30
3.29
3.27
2.50
2.48
2.47
2.45
2.05
2.04
2.03
2.01
2.00
7-4
0.95
1.00
0.97
1.00
1.85
0.94
0.95
1.85
1.87
1.82
1.89
f1 (ppm)

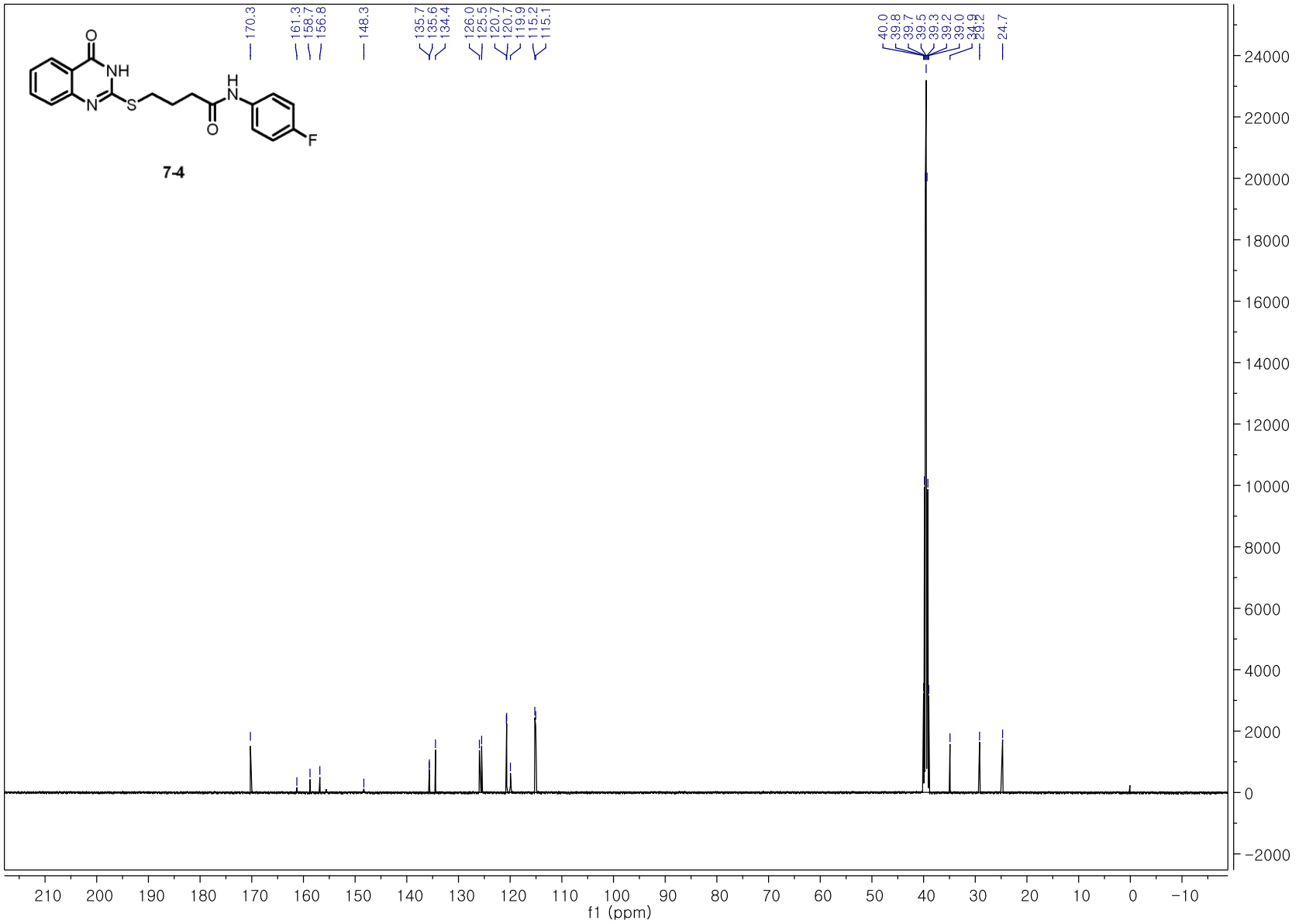
7-4
170.3
161.3
158.7
156.8
148.3
135.7
135.6
134.4
126.0
125.5
120.7
120.7
119.9
115.2
115.1
40.0
39.8
39.7
39.5
39.3
39.2
39.0
24.9
24.2
24.7
f1 (ppm)